INVESTIGATION OF THE FLEXURAL PROPERTIES OF REINFORCED CONCRETE BEAMS STRENGTHENED BY EXTERNALLY BONDED STEEL PLATES

by

John W. Bloxham. A.C.G.I., B.Sc.Eng., C.Eng., M.I.C.E.

Thesis submitted to the University of Sheffield
for the Degree of Doctor of Philosophy in
the Faculty of Engineering

September 1980

Dedicated to my parents.

SUMMARY

It is sometimes necessary to strengthen in situ concrete structures. Externally bonded plate reinforcement has been successfully applied to structures with subsequent satisfactory performance. However, little research has been reported, especially in respect to long term behaviour.

The present study investigated the flexural behaviour of normal under-reinforced concrete beams with plate reinforcement bonded to their tensile face. Furthermore, long term studies of loaded and unloaded plated beams were initiated for testing after exposure to natural weathering conditions. The parameters under investigation were adhesive and steel plate thickness, the degree of cracking in the beam prior to bonding on the plates, multiple plate layers and plate jointing techniques.

Test results showed that although the increase in ultimate load produced by the bonded plates was only 17%, the service loads were increased up to 90%. The deformations at service loads were reduced up to 65%. In general, the deformations decreased for an increase in adhesive or plate thickness, the latter having the larger effect. The maximum crack widths in the plated beams were up to 63% lower than those in the unplated beam. The ACI and CP 110 crack width prediction formulae overestimated the measured values. Within the limitations of the present test series, empirical formulae were derived for calculating rotations, crack widths, crack spacings and concrete surface strains. Tests on specimens after 18 months weathering showed no loss of flexural performance nor any visual deterioration of the adhesive or adhesive/steel interface. Further tests will be reported.

Bonded plate reinforcement can only enhance the ultimate strength of a beam to limited extent. More important are the decrease in deformations and consequently the increase in service loads, thus making it a viable technique for up-rating the load carrying capacity of existing structures.

ACKNOWLEDGEMENTS

The author wishes to thank his Supervisors, Dr. R. N. Swamy and Mr. R. Jones, for their guidance, assistance and helpful advice throughout the research and for their help during the presentation of this thesis.

Professors D. Bond and T. H. Hanna of the Department of Civil and Structural Engineering are also to be thanked for their assistance.

Thanks are due to McCall and Company (Sheffield) Ltd., the Associated Portand Cement Manufacturers Ltd., and Colebrand Ltd. for their generous supply of materials.

The author also acknowledges the assistance of the Technical and Secretarial staff of the Department, in particular Mr. R. Newman.

Finally the author wishes to thank Linda Bell and Chris Harrison for so patiently typing the text of this thesis.

CONTENTS

LIST OF FIGURES

LIST OF TABLES

LIST OF PLATES

NOTATIONS

a	Deflection
$\bar{a}$	Distance from compression face to point of measurement
a_{cr}	Distance from point considered to the surface of the nearest reinforcing bar
A	Area, as defined
b	Width of section
b_p	Width of plate
c_{min}	Minimum cover to the main reinforcing bars
C	Coefficient or constant, as defined
d	Effective depth to centroid of reinforcement
d^1	Thickness of adhesive
E	Youngs Modulus, as defined
f_{bs}	Local bond stress due to ultimate load
f_{bsa}	Anchorage bond stress due to ultimate load
f_{bsd}	Local bond stress due to service load
f_{bsda}	Anchorage bond stress due to service load
f_{cu}	Concrete cube strength
f_{cg}	Compressive strength of glue
f_p	Stress in plate
f_r	Stress in reinforcing bars
f_{tg}	Tensile strength of glue
f_{yp}	Yield stress of plate
f_{yr}	Yield stress of reinforcing bars
G	Modulus of rigidity
h	Overall depth of section
h_1	Distance from neutral axis to tension steel
h_2	Distance from neutral axis to tension face
I	Moment of inertia, as defined
k, K	Coefficient or constant, as defined
l, L	Span
M	Bending moment, as defined
M_{cr}	Cracking moment for concrete
P	Axial force
r	Correlation coefficient
S	Slope, as defined
S_u, S_{rm}	Ultimate mean crack spacing
t	Thickness of adherend
t_b	Bottom cover to the centre of longitudinal reinforcing bar
t_g	Glue thickness

t_p	Plate thickness
t_s	Side cover to the centre of longitudinal reinforcing bar
u	Axial deformation
V	Shear force
W, W_m	Mean crack width
W_{cr}	Maximum crack width
W_k	Characteristic crack width
x	Neutral axis depth
$\bar{x}$	Mean value
z	Lever arm
α_e	Modular ratio
γ	Angular deformation
γ_m	Partial safety factor for materials
ε	Strain, as defined
ϕ	Curvature
ρ	Proportion of tension reinforcement
σ	Standard deviation
σ_f	Tensile stress in the concrete
τ	Shear stress in the glue

CHAPTER 1

INTRODUCTION AND OUTLINE OF THESIS

1.1 GENERAL INTRODUCTION

In practice, situations can often arise when the behaviour of a conventional reinforced or prestressed concrete beam is found to be inadequate, and replacement or strengthening then becomes necessary. Such inadequacy may be related to the ultimate strength of the member or to its behaviour under service loading. The cause may be inferior materials, design or constructional faults, external damage or deterioration. Alternatively it may arise from requirements to increase the imposed loading above the original design load. When such situations arise, it has to be considered whether it is more economical to strengthen the existing member or to replace it.

Unless additional supports can be provided, any attempt to strengthen an existing structure is generally a difficult operation because of the fact that its strength properties are essentially determined during construction. The main problem in strengthening techniques is that of ensuring adequate connection and composite action between the reinforcing element and the existing structure. Methods of strengthening are generally straightforward to carry out, but may need great care and control. However, when extensive strengthening is required, there is generally a great deal of labour, plant and disruption involved whether the structure be steel or concrete.

Strengthening of concrete structures can be carried out by several techniques. Provision of additional reinforcement along with guniting and external prestressing have been successfully used. More recently polymer impregnation techniques have been successfully used to restore a severely disintegrated reinforced concrete slab at a cost of about £35 per sq m (75). The development of glues based on synthetic resins has, on the other hand, opened up another method of structural repair in which steel plates are bonded to the structural element with epoxy glue. These glues have adequate bonding strength and it has been shown that they provide effective composite action between the steel plate and the concrete element to be strengthened. However, careful attention is necessary at all stages of the strengthening operation to ensure adequate interaction.

The method has been used to strengthen a variety of existing structures including: bridges in France (55), Japan (51) and England (53), a concrete crane gantry in France (54) and floor slabs of a telephone exchange in Zurich (56).

Despite the advantages and future potential of the technique only a limited amount of systematic research has so far been reported. A review of the literature which has been published on this subject is given in Chapter 2. In concrete joints (4) shear strengths in the glue can reach 7 N/mm^2 without much difficulty, so that failure would occur by shearing of the concrete. Although great emphasis has been placed on the considerable care needed in preparing the adherend surfaces, there is a degree of latitude which should allow satisfactory bonding when prepared to the tolerances attainable on site.

1.2 OUTLINE OF THESIS

The purpose of the present work is to investigate the static flexural behaviour, in both long and short term, of reinforced concrete beams strengthened by externally bonded steel plates glued to their tension faces. The tests were carried out to investigate the effects of varying:

(a) thickness of the glue layer

(b) thickness of the reinforcing plate

(c) number of layers of plate

(d) plate lapping techniques

(e) degree of cracking prior to bonding on the plates.

Points of stress concentration were formed in some beams by cutting notches in their tension faces.

The aims of the study were:

(i) To investigate the deformation behaviour, i.e. load-deflection and moment rotation characteristics.

(ii) To determine the internal bar strains, external plate strains, and concrete strains through the elastic, inelastic and ultimate regions.

(iii) To determine the first crack load in the concrete and study crack propagation and distribution.

(iv) To investigate interfacial stress properties.

(v) To compare theoretical analysis with experimental results.

The properties mentioned above were studied (a) in beams tested approximately 14 days after bonding on the plates and (b) in similar beams tested 18 months after plating.

(vi) To study the durability of the concrete/epoxy/steel bond.

Before studying the technique of externally bonded plate reinforcement an appraisal of the materials involved was made. Chapter 3 reports the tests carried out on the materials used in the manufacture of the beams, i.e. concrete, epoxy resin, steel plates and bars.

Chapter 4 gives details of some preliminary testing on plain, unreinforced concrete beams which was performed to gain experience in the plating technique. This testing was made up of series A and B. Altogether eighteen beams were tested; two sizes of beams 150 x 150 x 710 mm (Series A) and 100 x 150 x 1200 mm (Series B) were used. Two epoxy resin systems were used in both series. The steel plates were of the same material for both series.

In series A the effects of uniform and tapering glue thickness were studied. In series B the provision of steps in the tension face of a beam forming stress concentrations was studied, together with lapping techniques. All the beams were tested under centre point loading over a single span.

The major testing programme was performed on reinforced concrete beams 155 x 255 x 2500 mm loaded at the 1/3 points of the span, which was 2300 mm. Firstly, the long term testing programme was started.

Concrete and epoxy resins are both susceptible to time dependent deformation due to shrinkage and creep. These deformations may be critical to the serviceability and sometimes to the safety of structural elements, particularly if accompanied by a reduction in cohesive or adhesive strength of the epoxy resin.

Eight beams, all of which have identical internal reinforcement are being subjected to sustained loading. The parameters under investigation are:

(a) glue layer constant - 3 mm

(b) glue layer constant - 6 mm

(c) glue layer variable - 3 mm to 8 mm

(d) glue layer variable - 25 mm x 25 mm notches at load points

(e) single plate layer, central lap

(f) single plate layer, laps at the 1/3 points of span

(g) two layers of plate, central lap in outer layer

(h) two layers of plate, laps at 1/3 points of the span in the outer layer.

All beams have plates 1.5 mm thick, yield stress 250 N/mm^2, with internal reinforcement 3 x 20 mm diameter bars, 0.2% proof stress 470 N/mm^2. There are two unloaded beams corresponding to each loaded beam. All the beams were left outside open to the weathering effects of the elements. Eight unloaded beams were to be returned for testing after eighteen months. These results are given in Chapter 8. The remaining eight unloaded beams and the eight loaded specimens will be tested, in due course after 5 years exposure.

The short term test series of twenty four beams was performed on beams identical to those described above for the long term tests with these additional parameters under investigation:

(a) plate thicknesses 3 mm and 6 mm, glue thicknesses 1.5, 3 and 6 mm

(b) plate thickness 1.5 mm, glue thickness 1.5 mm

(c) plate and glue thickness 3 mm, central lap

(d) glue thickness 3 mm, no plate

(e) plate thickness 3 mm, glue thickness 3 mm, beam loaded to 50% theoretical ultimate load prior to plating

(f) plate thickness 1.5 mm, glue thickness 3 mm, beams loaded to 50% and 90% theoretical ultimate load prior to plating.

An unplated control beam was also tested. 6 mm diameter stirrups were provided at 75 mm centres in the shear spans of all these beams, to prevent shear failure.

The results from the tests were reported as follows:

Chapter 5 - strength characteristics.

Chapter 6 - load-strain; load-deflection and moment rotation characteristics.

Chapter 7 - cracking characteristics.

In most environments the hardened epoxy resins will undergo both heat variation and moisture changes, but unlike many other adhesives, cured epoxies are said to be very resistant to water. However, moisture will eventually penetrate most epoxies and the bond between the resin and steel or concrete may be weakened. This problem was investigated using small concrete prisms 100 x 100 x 500 mm plated on one face. The plate and glue layer were coated with different sealing agents to prevent the ingress of moisture. The specimens were then placed in a fog chamber at 100% relative humidity for 18 months prior to testing. Control beams with no sealant were also kept in the fog chamber and in dry conditions for comparison. These prisms, were tested with a single, central point load over a span of 450 mm. The results are given in Chapter 8.

Wherever possible, the results of the present investigation are compared with those found by others.

Lastly Chapter 9 concerns the limitations of the present work, the overall conclusions, design recommendations and proposals for future work.

Appendix 1 gives a glossary of terms used in adhesives technology. Appendix 2 outlines the calculation of the theoretical stress distribution in a bonded lap joint under compression. Appendix 3 gives the methods of calculation of the first crack and ultimate loads for the preliminary test beams A and B. Appendix 4 gives the calculations of ultimate load for the main series of 24 beams. Appendix 5 gives calculations of the deflections of these 24 beams by methods recommended by CP110, CEB and ACI. Appendix 6 gives calculations for rotations. Appendix 7 discusses the interfacial stresses between the glue and steel or concrete. Appendix 8 outlines the calculations for crack widths and Appendix 9 gives a brief outline of the statistical methods used in the analyses.

CHAPTER 2

REVIEW OF LITERATURE

2.1 EPOXY RESINS

(Appendix 1 gives a glossary of terms relating to adhesive technology.)

2.1.1 General Introduction (1-5)

The use of adhesive materials to join two or more objects together can be traced back for centuries. The Ancient Egyptians used a type of glue to stick decorations onto their coffins. The Phonecians used bitumen as a crude jointing for their boat timbers and for sealing purposes. By the Middle Ages the art of making adhesives had made little progress, glues being made from animal bones and blood. From these cases it can be seen that the materials used for bonding were all obtained from natural products and no real progress was made until the nineteenth century.

The advent of systematic chemistry, particularly in respect of physical and organic chemistry, has led to an attempt by scientists to understand the process of adhesion. This in turn has led to the development of synthetic adhesives. A change in intellectual approach, rather than any specific invention, has given adhesives a new dimension: adhesives are now engineering materials. A tremendous impetus was given to the research, by the need to form high strength bonds or joints, especially in the lightweight structures of the aircraft industry.

The first practical application of epoxy resins took place in Germany and Switzerland in the 1930's, although their basic chemistry had been known for several decades. Limited production of epoxy resins started in the late 1940's and they became available in the early 1950's on a commercial scale.

Epoxy formulations developed until there were available systems with a combination of properties which made them suitable for use as an adhesive with concrete. Epoxy resin systems cure without release of water or other by-products of a condensation reaction, and can consequently have low autogenous shrinkage (3). Because of the high degree of cross linking between long chain epoxide molecules there is little tendency to creep under sustained loading and moisture resistance is good.

The confusingly large variety of available products has hindered the progress of the use of epoxy resins for structural uses in the construction industry. The engineer requires the resin to have a consistency such that it allows ease of application and satisfactory curing under the prevailing weather conditions found on site. The bond thus formed must show little or no loss in adhesion as a function of time, or on exposure to moisture, sustained load and temperature variations. With these properties in mind the resin manufacturers should be able to formulate satisfactory structural engineering materials.

2.1.2 Materials and Mixes

A single epoxy resin system cannot be found to suit all applications. It is for this reason that epoxy resin systems which are sold commercially are generally the products of formulators who specialise in modifying the system with flexibilisers, extenders, diluents and fillers to meet specific end-use requirements. It logically follows that it is important to follow the manufacturers recommendations for use.

Conversely, the successful use of a resin system depends on the preparation of an adequate specification which must include such requirements as; adherend material, mixing/application temperatures and techniques, curing temperatures, surface preparation techniques, thermal expansion, creep properties, abrasion and chemical resistance etc. The specification should be so worded as to avoid any misunderstanding in these provisions for anyone concerned in the design, manufacture and application of the resin system from the formulating chemist to the site labourer.

2.1.3 Mixing

The accuracy of the required proportioning of resin and hardener is very important and a tolerance of plus or minus 2% is desirable. Some compounds can tolerate a wider variation but such variations should only be allowed if the manufacturer has test data available which show the complete effect of the variation on both mechanical and chemical resistance properties of the cured compound. The most accurate method of proportioning is by the use of pre-proportioned units supplied by the manufacturer so that the contents of one component container can be emptied into the other, usually hardener into resin, and then mixed together.

A low speed electric drill with a mixing paddle may be used with the caution that paddle type mixers can introduce air which can reduce adhesive and cohesive strengths if the system cures with the air entrapped. Mixing should continue until the mixture is homogeneous. The manufacturers often facilitate this by giving the resin and hardener two distinct colours which merge to form one colour when mixing is complete.

2.1.4. Temperature

Most epoxy resin formulations available today react favourably in the temperature range 40 - 150°F, although below 60°F mixing usually becomes difficult, and above 100°F the pot life may be shortened too much. In Great Britain, temperatures are often below 40°F so it is helpful to raise the temperature of the resin system prior to mixing. This reduces the viscosity of the resin system which in turn reduces the tendency to whip air into the compound during mixing. It may also be necessary to heat the adhered surfaces. Direct flame heating of concrete surfaces is difficult to control and warm air circulation heating or radiant heaters are preferable.

2.1.5 Surface Preparation

The strength of a bonded joint depends on the degree of adhesion to the adherends as well as the cohesive strength of the resin. The aim of surface preparation is to ensure that adhesion develops to the extent that the cohesion is the weaker link in the system.

2.1.5.1 Concrete

Concrete surfaces must be cleared to remove all substances detrimental to bond of epoxy compounds such as laitance, curing compounds, dust, dirt and other debris resulting from surface preparation operations. The simplest method of achieving this is to shotblast the surface and then remove dust and debris by jetting with compressed air. The result should be a surface abraded to the extent that large aggregate particles are exposed and free from dust and contaminants. Care should be taken to ensure that good water and oil traps are incorporated in the compressed air system to prevent contamination after shotblasting is completed.

2.1.5.2 Steel

As rolled, metals have a contaminated surface layer, which is usually so thick that the metal surface exhibits the properties of the layer and not the metal itself. There are three methods which can be used to remove these surface contaminants: solvent cleaning or degreasing; mechanical abrasion; or chemical etching.

For site applications in the construction industry it is unlikely that chemical treatments would be used on a large scale. Cleaning and degreasing using solvents is practical, but adequate time must be allowed for their evaporation before mechanical treatment, otherwise they can be forced deeper into the metal causing weakening of the adhesive bond. The only practical, consistent field method of assuring an adequate bonding surface is shotblasting. After solvent cleaning and shotblasting any dust created by the mechanical cleaning must be removed by jetting with compressed air. A cleaned metal surface is very susceptible to corrosion, particularly in a humid atmosphere, so the work should be planned to permit the epoxy application as soon as possible after cleaning.

2.1.6 Bonding

In its broadest sense adhesive bonding includes the application of the adhesive to the adherends and holding them in position until the joint acquires some strength.

The applicator should ensure that the epoxy is applied at a rate compatible with the pot life and rate of hardening of the system. Both are affected by the temperature at which the epoxy is applied.

Intimate contact is essential and all measures should be taken to ensure complete wetting. This is often more difficult to achieve with higher viscosity systems or when fillers are present.

The application process applies a certain amount of pressure to assist the resin penetration of the adherend surface. This penetration can be increased by applying pressure to the closed joint during the curing process.

In the region of the adherend surface the adhesive hardly moves when pressure is applied, but further away the glue is squeezed out taking unwanted air bubbles with it. For this reason it is usual to apply more adhesive than is necessary in the completed joint and squeeze out the excess under pressure to remove air bubbles. This also gives an indication of how even the pressure was by inspecting the amount of resin pressed out along the joint.

2.1.7 Curing

To cure an epoxy resin system means to alter the physical properties by chemical change. This usually means polymerisation brought about by either heating or the use of a catalyst. This causes the union of adjacent molecules of adhesive, often existing as long chains, to form a tough solid resin. The interaction of such long chain molecules is known as cross-linking.

During curing the joint must not be moved otherwise cracks can develop at the interface which could lead to loss of bond by the ingress of moisture.

As curing progresses, strains are set up due to the differential expansion of the resin and adherends, and also due to polymerisation. Initially the resin is a liquid or paste, and as polymerisation starts it becomes a gel. During this period autogenous shrinkage is not important as both liquid and gel can accommodate volume change by flowing. The process continues and results in a hard polymer. At some point its strength increases so that shrinkage cannot be accommodated without producing internal stresses. These observations have led to the development of compounds in which most shrinkage occurs during the gel stage. Fillers can be used to reduce shrinkage but do not adversely affect adhesion when used in normal amounts.

2.1.8 Safety and Health Provisions

Just as there are proper, safe practices for handling acids, portland cement, etc., there are also precautions which should be observed when handling epoxy resins and materials used with them.

Two typical health problems encountered with epoxy materials when carelessly handled are skin irritations, such as burns and rashes, and skin sensitisation, which is an allergic reaction.

Safe handling can be accomplished by working in a well ventilated area and using disposable equipment whenever possible. Disposable suits and gloves are readily available. Goggles are strongly recommended, and involuntary habits such as eyeglass adjustment should be avoided. In the case of direct skin contact solvents other than soap and water should not be used. Most solvents merely dilute the epoxy compound, aiding their penetration into the skin.

The solvents used for precleaning and equipment cleaning require additional precautions. Many have low flash points and these should be avoided. Ketones are a fire hazard and if used good ventilation is required. Smoking and other fire initiating devices should be barred from the area of use.

Chlorinated solvents, while not presenting a fire hazard, will present a toxicological problem if smoking takes place in the area or if a fire occurs in the immediate area. Many can be toxic when inhaled.

No amount of equipment will substitute for worker education. Those involved with the use of epoxy materials should be informed of the hazards of the particular materials they must handle. The handling of epoxy materials is not dangerous as long as reasonable care is taken and personnel and equipment are kept clean.

Instances of sensitisation are rare but the possibility of burns, loss of an eye and other time losing accidents makes knowledge and observance of safe handling practices absolutely essential.

2.2 GLUED JOINTS IN CONCRETE

2.2.1 General Uses

Epoxy resins have been used in concrete repair work since the 1950's. Tremper (7) describes the use of epoxies in repairing concrete highways; Gaul and Apton (9) for repair of runways and roads; Wakeman, Stover and Blye (10) and Ciesielski (11) describe resin injection of cracked pile caps and beams; and Levy (14) reports their use in the repair of precast elements. In general (8) it was found that bond strengths were greater than concrete strength in flexure, shear and direct tension.

2.2.2 Surface Preparation

The generally accepted methods of concrete surface preparation are discussed by Batchelar (21) and Moar (22). The relative convenience of these methods will vary with location of construction site and availability of equipment. Moar found that mechanical treatment was less important for short term strength, which depended mainly on the adequate removal of dirt, grease and laitance. For long term strength the amount of mechanically exposed aggregate greatly increased the durability of the joint.

Gorgol (23) considered concrete surfaces to be adequate, "as stripped", but he was only working with compression joints.

Hallquist (24) found wire brushing to be inadequate but does not compare this with other preparations, nor does he make any positive recommendations.

Lee and Neville (6), state that porous surfaces such as concrete require no special surface treatment. This has been shown to be incorrect by many other researchers.

Guttman (12) tabulated the properties of 26 adhesives suitable for structural bonding. Skin grease deposits on the surfaces led to 75% reduction in bond strength in some cases, minute quantities of solvents used for cleaning were found to inhibit curing in most of the adhesives.

Johnson (13) suggested the surfaces should be cleaned by sand blasting and then air blown, followed by degreasing and flushing. It would seem more sensible to degrease and remove dirt before shotblasting as this operation would tend to force the contaminants deeper into the surface.

2.2.3 Moisture Effects

Lee and Neville (6) state that moisture accelerates the curing process in agreement with the findings of Caron (29) who also found water reduced the mechanical properties.

Hallquist (24) tested epoxies after exposure to humidities ranging from 30 - 85% and found no significant effect on 7 day strength.

Ciba Geigy (25) state that certain resins, containing polyamides exhibit comparitively high water absorption, which can reduce joint strengths.

Shue Fai (26) and Batchelar (21) tested mixes in both wet and dry conditions. The ultimate strength was not affected, but the curing rate was slower in water, contradicting the opinion of Caron, Lee and Neville.

Shaw (27) describes the use of three different epoxy resins. The strength of wet joints varied from 16 - 65% of the dry joints in the short term and 24 - 75% in the long term.

Moar (22) found moisture to have no apparent affect on initial strength but to be beneficial for long term strength.

Cusens and Smith (28) tested concrete prisms, with 45° glued scarf joints, to compare the water resistance of four adhesive systems. Three resins gave only 25% of the strength of dry prisms after only 8 weeks immersion in water, whereas the fourth resin showed an increase in strength.

Some of these apparent disagreements can be accounted for by the different chemical compositions of the resins used. A full comparison of the conclusions drawn by individual researchers could only be made considering this factor and also the surface preparation techniques used. The various fillers, flexibilisers, dilutents etc. that can be added to the basic resin can all affect the behaviour of the resin system in relation to moisture.

2.2.4 Miscellaneous

O'Brien (18) stated that the lack of knowledge of the long term behaviour of bonded joints is the main factor restricting their use to gap filling compression joints.

Johnson (15) performed a series of tests on glued lap joints which showed the long term strength to be only 50% of the short term strength. He suggested that vibrations may also cause creep.

Taylor (16) investigated long term vibration of concrete scarf joints under compression and found the creep to be no greater than in control specimens.

Kreigh (17) reports tests on composite beams using epoxy mortar as a shear connector. No debonding was evident after seven million cycles. The shear stress was a maximum of $2N/mm^2$ which is approximately only 50% of the failure stress, but is still significant as it is approximately the working stress.

Johnson (20) formulated an epoxy suitable for structural joints transmitting loads by shear and compression. Flexibility and creep were little greater than in concrete, and in order of magnitude less than in his earlier tests. No shear or tensile test results were given for the glue so its use in anything but compression joints is not clear.

2.2.5 Summary

Lee and Neville (6), and Gorgol (23) found no special surface preparation to be required, contrary to the conclusions of Batchelar (21), Moar (22), Hallquist (24), Guttman (12), Johnson (13) and Cusens and Smith (28).

Lee and Neville (6), Caron (29), Moar (22) and in one system Cusens and Smith (28) found moisture to be advantageous to curing and in some cases joint strength. Hallquist (24), Shue Fai (26) and Batchelar (21) found moisture had no effect on joint strength whereas Shaw (27), Ciba Geigy (25) and Cusens and Smith (28) found that moisture reduced joint strengths considerably.

Johnson (15) (20) tested various resin systems to produce one with creep properties with the same order of magnitude as concrete. However, to what extent this affects its ability to resist moisture, temperature cycling etc., is not reported.

It can be seen that there is a great deal of contradictory information available and comparisons could only be made when all the facts, involving glue chemistry; surface preparation; application; curing method and test technique; are known.

2.3 STRESS DISTRIBUTION IN LAP JOINTS

External forces seldom produce a uniform field of stress, even in an homogeneous body. When a body consists of two or more materials joined together a uniform stress is even less likely. The stress concentration, (ratio of highest to mean stress), depends on many factors including the elastic moduli of adherends and adhesive, and the shape and size of the specimen. The more highly stressed areas fail first and a progressive failure of the joint follows.

The earliest theoretical analysis of lap joints due to Volkersen (30), considered the distribution of shear forces, in the adhesive layer, for the case of very stiff adherends which do not bend on loading. It was soon recognised that the loading of a lap joint gives rise to bending, tending to peel the adherends apart.

Goland and Reissner (31) formulated a theory, taking these stresses into account, considering two distinct cases. Firstly, a thin stiff layer of adhesive is assumed to bond flexible adherends, and secondly vice-versa.

Cornell (32) varied this theory by assuming the adherends behave like simple beams and the adhesive is represented by shear and tension springs.

Wooley and Carver (33), and Amijima, Fujii and Yashida (34) carried out finite element analyses to investigate stress concentrations in lap joints. Many other theories have been suggested and are critically compared by Mylonas (35).

Bresson (54) gives a theory for stress distributions in bonded steel/concrete joints in both tension and compression.

2.4 GLUED JOINTS IN METALS

2.4.1 General

Gilibert, Delmas and Collot (36, 37) studied the fabrication of test specimens and apparatus to ensure good reproducibility of tests for comparing different glue systems. The fact that there was little scatter in their results should facilitate research into long term properties.

Allen (38) states that a primary loss of bond strength is due to the failure of molecules to achieve full cross linking due to poor batching and mixing.

2.4.2 Surface Preparation

Gagle (39) states that the service environment and life expectancy play the most important role in the selection of surface preparation techniques. This would seem to assume a greater understanding of the bonding process than is generally accepted.

Smith (40) and Olsen (41) both criticise mechanical abrasion prior to solvent cleaning as contaminants can be driven deeper into the metal.

Shields (42) recommends sharp jagged grits as round shots produce a peened surface consisting of many loose pieces of metal bent over each other resulting in a weak surface layer.

Jennings (43), and Delmas and Collot (36) (37) showed optimum adhesion is achieved by shotblasting. However, different resins, temperatures and humidities would most likely give different optimum grit size for the same metal adherend. It should also be remembered that the fluid properties of a resin change with time during curing. The rate of displacement of air from the surface pockets is essentially controlled by viscosity, and so the application of resin to a rough surface can trap air, causing stress concentrations. Thus a rough surface does not necessarily mean a high specific contact area. If heavily filled resins are used, displacement of air may be incomplete due to the increased viscosity of the resin system.

Ramel (44) found that rusting had little effect on bonding for various resins. Some could withstand 40 - 50% rusting. De Lollis (45), on the other hand, stated that corrosion was an important factor in loss of bond, soon after surface preparation.

Shields (42) found that in addition to their cleaning action, chemicals modify the surface physically and chemically.

Ciba Geigy (25) point out that chemicals can lead to inferior bond strengths if not used in the correct strength, or for the right duration. Flushing after treatment to remove all traces of chemical is also very important. Chemical treatment is unlikely to be used in the construction industry, however.

2.4.3 Moisture Effects

Buck and Hockney (46) immersed lap shear specimens for up to 1000 hours in water and water vapour. It was found that at 20°C the joint strength was not affected. At 45°C there was a 25% reduction.

Kinloch and Gledhill (47) exposed lap joints in distilled water at 20, 40, 60 and 90°C and control 20°C; 56% relative humidity. They considered that immersion in water reduced the strength considerably, particularly at high temperature.

2.4.4 Miscellaneous

Tests (48) have been carried out on joints which had been held together at pressures ranging from 2 - 400 lb/in^2 during curing. There was no effect on joint strength, except when the joints were placed in natural weathering conditions when the low pressure bonded joints were adversely affected. In another series the rate of loading was varied from 0.35 to 26.5 tons/minute. In the limited number of tests no significant change in strength was observed. However, McNicholas (49) performed tests which showed that the high loading rates produced premature failure.

Delmas and Collot (37) varied the joint thickness from 0.05 mm to 1.5 mm and the optimum was found to be 0.5 mm. As the thickness increased the failure was due to a combination of adhesive and cohesive failure, i.e. a fracture plane which passed partly along the interface between adherend and adhesive, and partly through the body of the glue. In thinner joints failure was completely adhesive. It was concluded from this that the joint became brittle when thicker. Theoretically, the mean stress in a joint should increase with joint thickness, but practically thicker joints are more likely to have air bubbles, flaws and internal stresses. In filled resins the shrinkage and temperature stresses are much lower so that a filled thick joint could possibly be stronger than a thinner unfilled one.

Cusens and Smith (28) have performed comparative tests on four resin systems in steel/steel lap joints under static and cyclic loading. The effects of curing at elevated temperature and of temperature cycling were included. It was found that shear strengths increased with the roughness of the blasted surface, and slightly with increase in curing temperature. Temperature cycling between $-7^{\circ}C$ and $+35^{\circ}C$ had little effect on joint strength. There was satisfactory fatigue performance, with all specimens sustaining a stress range of 4.5 N/mm^2 for 10^7 cycles. It was found that slight contamination with dust or water was not harmful.

The practical application of all these findings to predict breaking loads is very difficult. It is easy to control the surface preparation and application/curing techniques in small test specimens, but more difficult in actual site applications.

2.4.5 Summary

There is general agreement that the best surface preparation is shot-blasting. However, differentresins, temperatures and humidities give different optimum grit sizes for the same metal adherend. Various glue thicknesses are recommended but these again would depend on the type of glue etc. for optimum strength.

Smith (40), Olsen (41), Shields (42) and Ciba Geigy (25), all agree that cleaning solvents and chemical treatments can lead to loss of bond if not removed completely from the surface prior to bonding. The use of chemicals prior to mechanical blasting is not recommended as this would lead to the solvents being driven deeper into the metal surface.

Buck and Hockney (46), and Kinloch and Gledhill (67) found water immersion to produce a loss in joint strength, which increased with temperature.

McNicholas (49) and others (48) give contradictory results on the effect of varying the loading rate.

Again, it is almost impossible to compare the different author's findings without knowing the resin chemistry; the exact surface preparation, loading techniques etc.

2.5 GLUED JOINTS BETWEEN STEEL AND CONCRETE

2.5.1 General

The application of epoxy resins to civil engineering structures may be classified under two main headings:

(a) resin used as a filler

(b) applications which depend on the shear strength of adhesive.

Tabor (50) gives examples of type (a) uses in his general review of the uses of epoxies in civil engineering.

Type (b) applications still remain rare and are largely confined to repair and/or strengthening of bridges. In Japan (51), by 1975, some 240 bridges had been strengthened, against increased vehicle loading, by the addition of steel plates glued to their upper and lower surfaces. In South Africa 11 bridges have been similarly strengthened and in Britain the technique has been used at Quinton (52) and Swanley (53). In France (54) (55) the technique has been used to strengthen a travelling crane and a motorway bridge, and in Switzerland (56) telephone exchange floors. Franke (57) describes the use of reinforcing bars bonded with epoxy to strengthen a spherical prefabricated concrete tank.

2.5.2 L'Hermite and Bresson (54, 55, 58, 59)

From L'Hermite's first experiments he concluded that the metal surface must be freed from contaminants and surface oxidation, and to prevent oxides reforming the joint must be bonded quickly, or alternatively a primer applied.

Beams with tension reinforcing plates all failed by concrete crushing or shearing, not by debonding. They behaved as normal reinforced concrete beams, with regard to failure load, however, the onset of cracking was delayed and crack propagation reduced indicating a close combined action between the steel plate and concrete beam.

Beams with plate reinforcement on their sides, to increase shear capacity, also behaved well and both types of beam, under cyclic loading, sustained half their ultimate loads for one million cycles without failure.

It is stated that after one year long term deflections increased by 20% but no information is given on stress level, glue type, surface preparation, etc.

In tests on plated slabs it was found indispensible to secure the edges of the plates with bonded angles to prevent premature and sudden failure.

2.5.3 Transport and Road Research Laboratories (60) (61) (62)

Flexural Tests have been reported on six reinforced concrete beams. The specimens used were in fact I shaped columns with a corbel towards one end which had a considerable local stiffening effect. However, useful information was obtained from observations of the beams away from the corbel. The columns, 4.9 m long, were positioned horizontally so that they could be regarded as under reinforced concrete beams.

The tests were used to study the effects of changes in type of adhesive, plate thickness, a joint in the external reinforcement and load cycling. In all cases full composite action was developed between the steel, resin and concrete. Failure occurred by horizontal shear in the concrete adjacent to the glue layer. The main structural benefits were:

(a) For a given crack width, the applied load for the plated beam was nearly double that for an unplated beam.

(b) The post cracking stiffness was increased by 35 - 105%.

(c) There was an increase in failure load ranging from 12 - 24%.

A seventh beam has since been tested which was cracked under flexural loading before the plate was bonded to it. The results from this indicate that immediately prior to failure the strain in the plate was considerably less than in a similar beam that was not precracked.

Long term exposure tests are being carried out on small concrete prisms, 500 x 100 x 100 mm, reinforced with epoxy-bonded steel plates, in marine, industrial and high rainfall sites for periods of 1, 2, 5 and 10 years. Half the prisms are subject to sustained loading during their exposure period.

The results to date from 1 and 2 year tests, have shown that the failure loads were slightly lower for high rainfall and marine sites. On the whole, the beams under sustained load during exposure were stronger.

All the beams from the exposure sites showed varying amounts of steel corrosion, which had been in contact with the adhesive, and become partially debonded. The control beams kept in the laboratory showed no signs of corrosion.

If such corrosion occurred on full scale bridge structures failure may occur after only a few years. Methods of preventing corrosion, and surface priming techniques are being investigated and checked with additional exposure tests.

Beams of 3.5 m length are at present being used to investigate:

(a) Four different resin systems.

(b) Four different glue line thicknesses.

(c) Different concrete strengths.

(d) Jointing, end bolting and multiple plate layers.

2.5.4 Dundee University (28) (44) (63) (70)

Development work at the Wolfson Bridge Research Unit, Dundee, is investigating the practical feasibility of two main forms of decking for medium and long span bridges. Both forms consist of concrete slabs reinforced with epoxy bonded steel plates. In each case the concrete is cast directly on to the steel plate which has been coated with epoxy resin. Thus the plate serves both as formwork and reinforcement.

Solomon (63) used this method of bonding steel plates on to hardened concrete. He found a lack of ductility in the mode of failure which was probably due to the plate thickness used.

For these purposes a resin which retains its strength in the presence of prolonged damp is required and which also has a rust inhibiting quality. The problem of aggregate particles penetrating the glue line during compaction would seem to be most important as this could facilitate permeation of water through the concrete and glue to cause steel corrosion and bond degradation, as well as forming points of weakness in the glue layer.

Cusens and Smith (28) report on the behaviour of concrete beams of 2.0 m and 344 mm length. Cusens' earlier tests with Solomon confirmed the feasibility of using a steel plate as external reinforcement, with the procedure of casting fresh concrete onto the plate coated with epoxy. In more recent tests (28), beams 2 m long have been used to study the ductility and the effects of adhesive type and thickness on the static flexural behaviour. It was found that a minimum glue thickness of 1 mm was required to ensure bond between concrete and steel and that ductility was good, especially for thicker glue layers.

The smaller beams, 344 mm long, were used to investigate the effect of curing temperature, cyclic loading and immersion in water. In both static and fatigue tests the type of adhesive seemed to have little significance. The majority of beams survived 1.5 million cycles having a load range between 52 and 70% of their static failure load. Water immersion of beam specimens sealed on all surfaces except the top causes serious loss of flexural strength (> 33%) with some adhesives, mainly due to corrosion on the plate surface indicating ingress of moisture at the interface.

Solomon and Gopalani (70) report tests on beams similarly formed by pouring wet concrete onto the fresh adhesive applied to the steel sheet, which acts as formwork to the beam soffit. The tests were part of a feasibility study for a new type of concrete floor for buildings. All the beams failed in flexure and showed good ductility. No mention, however, is made of durability tests. All the beams mentioned in this section had the reinforcing plates along their entire length. The loading rig supports would therefore hold the plate ends onto the beam under testing conditions.

2.5.5 Warwick University

This work concerns the strengthening of a concrete bridge by epoxy bonding plates, to the top surface, above supports. The beams used were subject to a combination of longitudinal tension, bending and vertical shear. Most beams failed by a crack forming at the end of the plate and spreading towards the central section at the level of the internal reinforcement. The results shows that the stress concentration at the end of the plate produces a shear/bond failure and thus prevents the concrete member from achieving its full flexural strength. This effect is probably greater in these specimens, which resisted longitudinal tension as well as bending and shear, than it would be in a beam, where the deeper compression zone would provide additional stiffness.

2.5.6 Miscellaneous

Lerchenthal (65) carried out tests on model slabs 300 x 300 x 30 mm reinforced with 0.25 mm sheets. Simultaneously, tests were carried out on slabs reinforced with strips, in both directions, cut from the sheets. For the same quantity of steel the slab with a complete sheet had almost twice the capacity, showing the exploitation of the biaxial strength of the sheet. Three methods of bonding were used; bonding onto cured concrete; pouring fresh concrete onto sheets with resin applied; and fresh concrete poured onto a sheet with a grip layer of grit and sand glued to it. No significant difference was found, and all failures were by rupture of sheet or concrete, not by debonding. The sheet reduced the depth and spacing of cracks, relative to slabs reinforced conventionally with the same area of reinforcement. Because thin sheets were used no problem of the edges lifting was encountered as found by Bresson, who had to hold the edges down with bonded angle plates.

Cirodde (66) describes beam tests with steel and aluminium plates bonded to concrete. The resin used showed a large amount of creep.

Fleming and King (67) plated beams 150 x 150 x 1680 mm with no internal reinforcement. Failure occurred in the concrete along a plane parallel to the adhesive layer.

Kaifasz (68) describes tests carried out on rectangular and T section concrete beams having externally bonded bars and plates. Except in the case of reinforcing bars simply glued to the underside of the beam, where debonding occurred, satisfactory results were obtained with good agreement with theoretical predictions.

2.5.7 E.M.P.A. Swiss Federal Laboratories for Testing Materials and Research (56) (69)

Tests were carried out at E.M.P.A. to investigate the bonding properties of a steel/epoxy/concrete joint. The tests studied ways of anchoring the plate ends and the effects of long term fatigue loading. The technique of plated concrete as applied to floor slabs in a Zurich telephone exchange is reported.

The first short term static tests indicated that special attention should be given to anchor the plate ends. A second series of tests on plated Tee beams, subjected to both static and dynamic loading showed an 85% increase of static deflection after two million load cycles between 0.8 and 1.2 times the working load. No details are given of surface preparation, glue thickness and formulation.

The efficiency of the floor slab strengthening was checked by field measurements. Deflections were measured before, during and after strengthening, for different loadings. It was concluded that the strengthening had provided an increase in bending stiffness thereby reducing deflections and crack widths.

At present there is an extensive series of long and short term testing in progress, investigating different glue types, steel quality and thickness and lapping techniques. So far no report has been published on these.

2.5.8 Sheffield University

Bouderbalah (71) used reinforced concrete beams 100 x 150 x 1200 mm to investigate the adhesive type, glue thickness, plate lapping and precracking prior to plating. Beams were tested in flexural and shear modes and it was found that the addition of the steel plate increased the ultimate flexural capacity and the serviceability range, but had no effect on the shear capacity. The variation of glue thickness from 1.6 mm to 8 mm had no significant effect. The application of bonded plates to a precracked beam, and lapping of bonded plates were shown to be successful.

Reinforced concrete beams 100 x 150 x 2400 mm were used by Ang (72) to investigate the effects of plate thickness. Five beams were under-reinforced and three over reinforced, before plating. For the under-reinforced beams the plates increased bending stiffness and flexural capacity and reduced crack widths. The beams with 1.6 mm, 3 mm and 5 mm thick plates failed in a flexural mode by yielding of the steel followed by local crushing of concrete. The beam with 10 mm thick plate failed due to plate separation at its end.

One over-reinforced beam was plated on its tension face and the other on the compression face. Both gave an increase in capacity of approximately 22%. The mode of failure was by debonding at the plate ends followed by shearing of the concrete.

The failure loads of all the plated beams could be satisfactorily predicted by CP 110 methods.

A limited series of tests (73) was performed to study the effect of cyclic loading during glue curing. The results showed no adverse effects on flexural capacity when compared with control beams which were not loaded during the curing period.

2.6 CONCLUSIONS

It is apparent that many factors affecting the behaviour of bonded joints are still not fully understood, and consequently not fully controlled. As is evident from the published literature there is some degree of disagreement and lack of detail in the information given on the following:

(a) glue composition and thickness

(b) plate thickness, lapping techniques, end anchorage

(c) behaviour of precracked beams

(d) long term behaviour under sustained load

(e) durability of epoxy resin bonded joints exposed to moisture.

CHAPTER 3

MATERIAL PROPERTIES

Practical experience and test results such as were outlined in Chapter 2 illustrate that the properties of epoxy adhesives are retained under varying conditions. The possibility of reinforcing concrete structures simply and effectively using epoxies could be of particular interest to the civil engineer. Nevertheless, efficient use of the adhesives will depend on the engineer having confidence in their properties and knowing their limitations.

Similarly, the properties of steel and concrete, involved in such strengthening operations, are of considerable importance. The resistance to cracking of concrete depends on its tensile strength and the control of cracking is important in maintaining the continuity of a structure; in many cases in the prevention of corrosion of reinforcement and in this application to minimise the degradation of the concrete/epoxy/steel bond. Modulus of elasticity is of importance in controlling the deflection of members, and in addition to the tensile and compressive strengths of the steel and concrete respectively, in the analysis of structural members.

3.1 CONCRETE

3.1.1 Experimental Procedure

A trial mix was performed to assess the workability and strength properties of the concrete, which was consistent with that used in precast prestressed beams used in bridge construction. Bearing in mind that in practice strengthening is often carried out after several years in service, the concrete would have matured and acquired substantial increase in strength.

The proportions of the concrete constituents were approximately 1 : 1.05 : 2.45, with a water/cement ratio of 0.4 and plasticised by the use of Febflow. The quantities for $1m^3$ are given below.

sand	480 kg
19 mm aggregate	1124 kg
cement	450 kg

water	177 kg
Febflow	140 cc/50 kg cement

Rapid hardening cement, Ferrocrete, was used. The coarse aggregate was 19 mm maximum, uncrushed gravel and the fine aggregate was natural river sand. The gradings for these are shown in Fig. 3.1.

The mixing of concrete was carried out in a non tilting pan type mixer with 0.127 m^3 capacity. The materials were dry mixed for two minutes, and after the addition of water, for a further two minutes. A poker vibrator was used for compaction and the specimens were cast in steel moulds as follows,

(a) 26 - 100 mm cubes for compressive strength

(b) 12 - 500 x 100 x 100 mm prisms for modulus of rupture

(c) 4 - 300 x 100 x 100 mm prisms for modulus of elasticity.

The moulds were stripped after 24 hours and the specimens were then placed in a mist room at 21°C and 100% relative humidity, until required for testing.

Compressive strength, modulus of rupture and Young's modulus tests were carried out in accordance with the recommendations of British Standards.

3.1.2 Results

Table 3.1 shows the compressive strength results. The mean strength at 28 days was 69.5 N/mm^2.

Table 3.2 shows the modulus of elasticity results. The mean Young's Modulus at 28 days was 36.0 kN/mm^2 with a Poisson's ratio of 0.16.

Table 3.3 shows the modulus of rupture results. The mean value at 28 days was 5.59 N/mm^2.

3.1.3 Conclusions

The results for mean compressive strength modulus of rupture and Young's Modulus were consistent and their standard deviations fell within acceptable limits.

3.2 EPOXY RESINS

In the preliminary test series, two types of adhesive were used.

Type A CIBA GEIGY XD 808

Type B COLEBRAND CXL 194

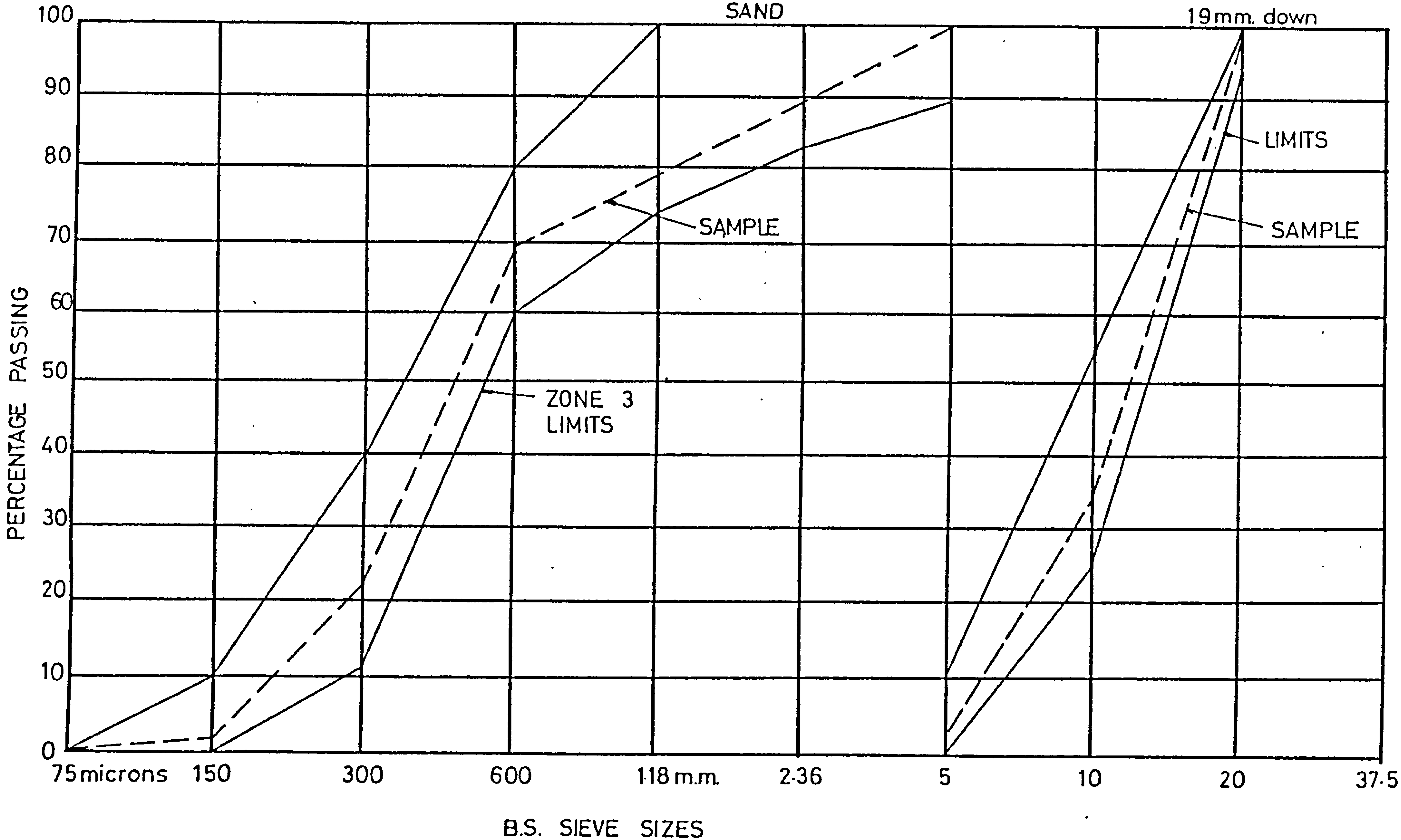

FIGURE 3.1 GRADING OF AGGREGATES

TABLE 3·1 CONCRETE COMPRESSIVE STRENGTH

3 DAYS		7 DAYS		14 DAYS		28 DAYS	
N/mm²	mean	N /mm²	mean	N/mm²	mean	N/mm²	mean
47·6		60·3					
48·0		64·1					
46·0		62·4		70·1			
48·4		61·4		64·4		70·4	
46·7	47·2	62·4	60·6	64·8	64·7	69·6	69·5
43·5		52·3		65·2		68·4	
47·0		55·0		56·8			
47·6		63·0					
50·2		64·5					

TABLE 3·2 MODULUS OF ELASTICITY

28 DAYS		
kN/mm²	mean	Poissons ratio
36·2		
35·7	36·0	0·16
37·7		
34·5		

TABLE 3·3 MODULUS OF RUPTURE

28 DAYS				
N /mm²	N /mm²	N /mm²	mean	coeff. of variation
5·71	5·52	5·64		
5·21	5·82	5·37	5·59	4 %
5·33	5·47	5·65		
6·00	5·31	5·91		

In the main series of long and short term tests only glue type A was used.

3.2.1 Lap Shear Tests - Steel/Steel in Tension

A qualitative series of lap-shear tests was carried out to find the optimum glue thickness to be used when lapping two layers of plate, as judged by the average shear strength of the various glue thicknesses used.

3.2.1.1 Experimental Procedure

Double lap specimens were prepared, as shown in Fig. 3.2 cut from the same sheets of steel used as external reinforcement in the preliminary series of tests. The steel was shotblasted prior to bonding using steel grit with a mean particle size of 340 microns at a pressure of 0.55 - 0.75 N/mm^2. The steel pieces were then bonded together within one hour after shotblasting.

The glue was mixed using a low speed drill, operating at 280 rpm fitted with a paddle, for at least two minutes, but no more than three minutes. Bonding took place under controlled conditions at 15°C and 56% relative humidity. The central lapping plates were slightly offset to induce failure in the shorter side. The specimens were allowed to cure for ten days before testing. Four thicknesses of glue were used for each glue type, and two specimens for each thickness.

3.2.1.2 Results

Fig. 3.3 shows the results of the lap shear tests. The value of average shear stress was found for each glue and plotted against glue thickness.

These tests showed an almost linear reduction in strength over the range of thicknesses used, 0.5 mm - 3.5 mm. This series was very limited in scope, and the results should be treated qualitatively. The control was sufficient to enable a choice of 0.5 mm joint thickness between lapping plates.

3.2.1.3 Conclusions

The alignment of all the pieces in the lap joint is very important so as not to induce peeling stresses in the glue when load is applied. The co-efficient of variation for any batch varied from 1 to 24% and this would suggest that some specimens had better alignment than others, rather than any

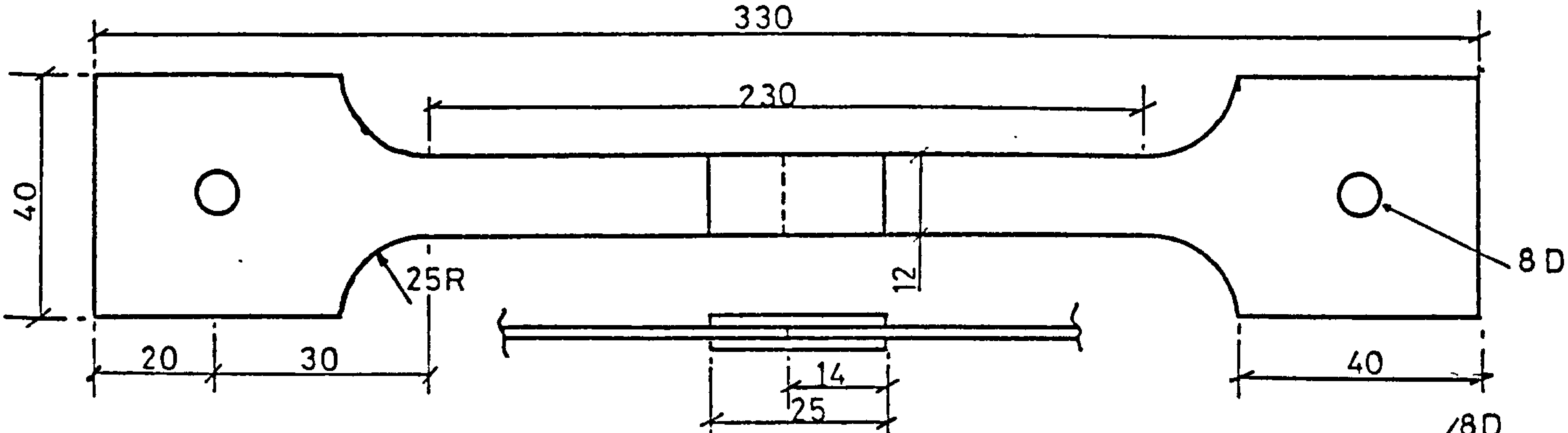

DOUBLE LAP SHEAR SPECIMEN

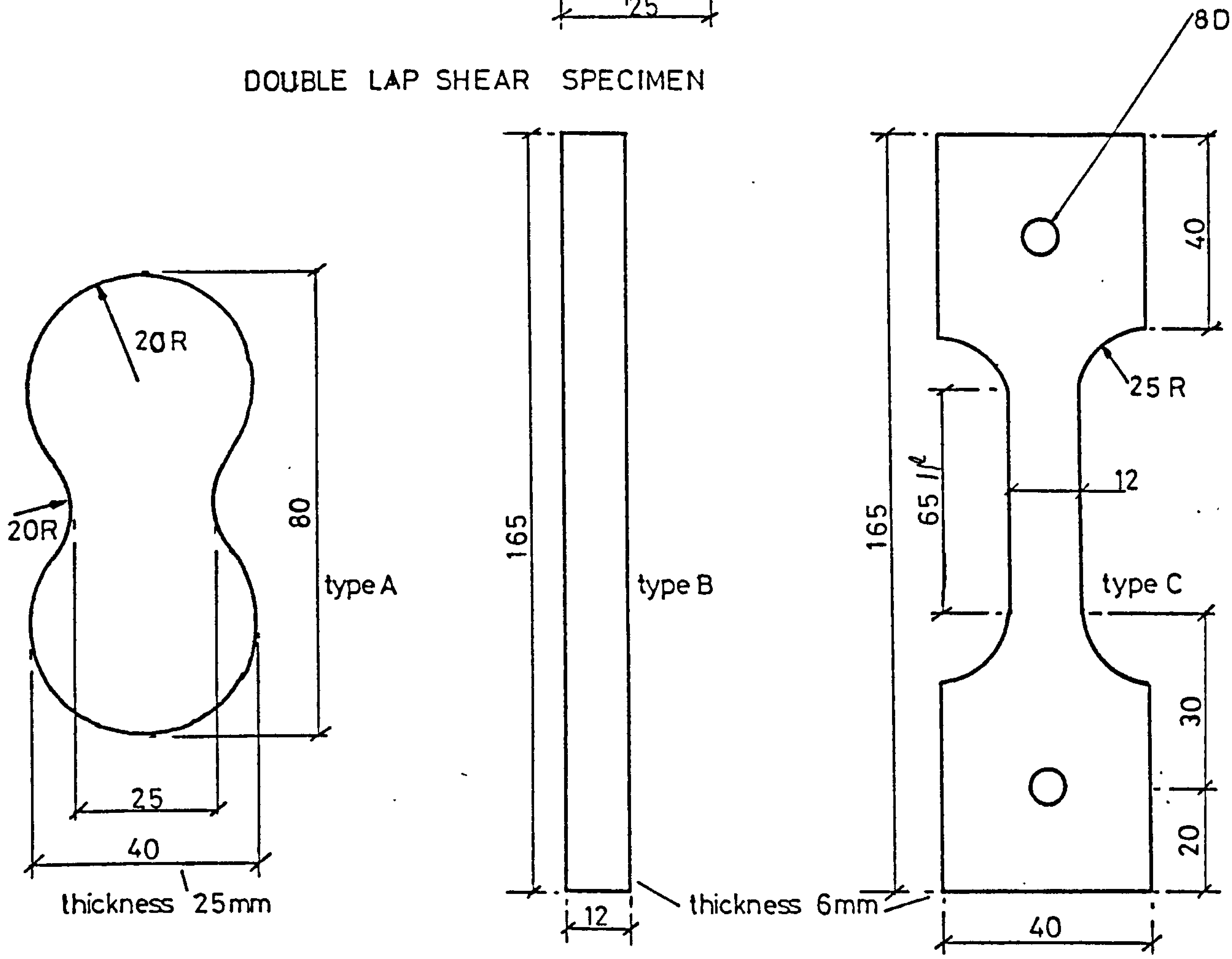

TENSILE SPECIMENS

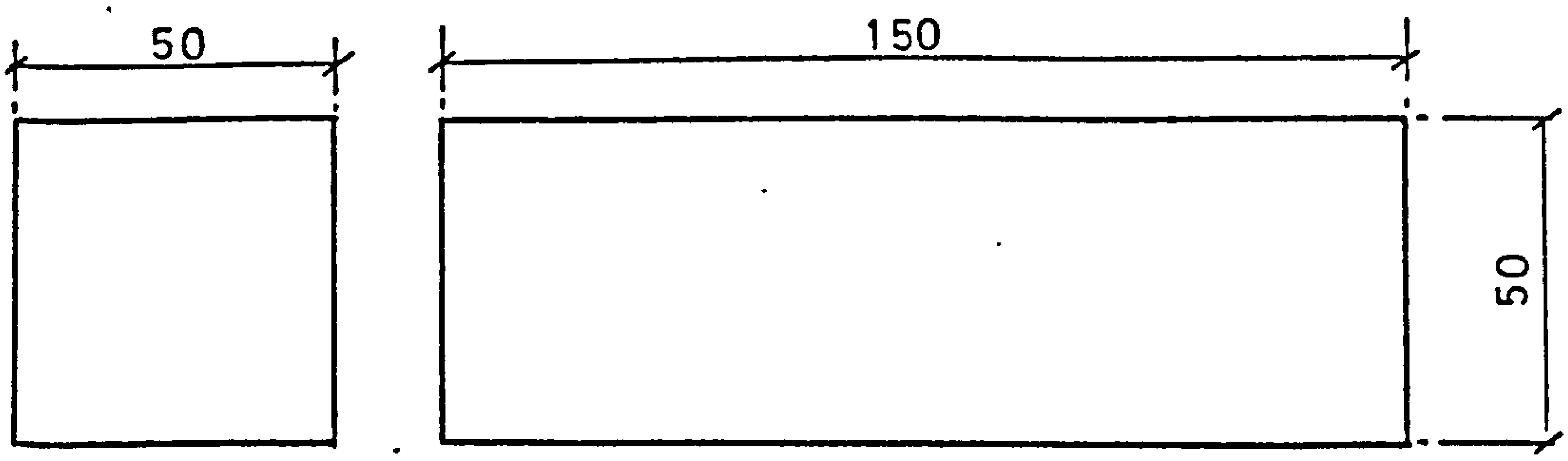

COMPRESSION SPECIMEN

FIGURE 3.2 DETAILS OF ADHESIVE TEST SPECIMENS

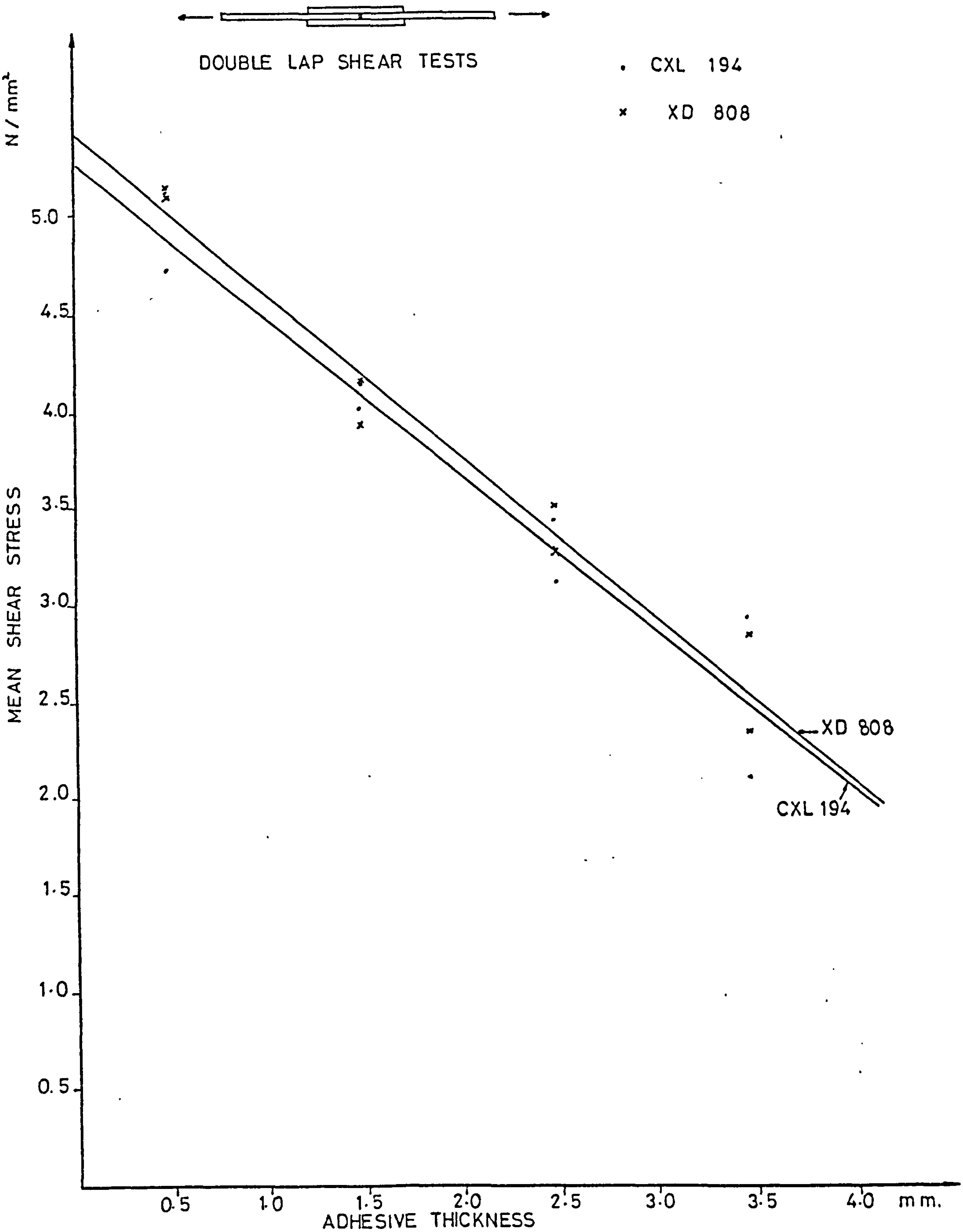

FIGURE 3.3 MEAN SHEAR STRESS v ADHESIVE THICKNESS

fault in the resin itself.

The general conclusions seemed to be in agreement with the findings of others (37) who tested lap shear joints with glue thicknesses ranging from 0.05 mm - 1.5 mm and found 0.5 mm as the optimum. However, the fact that 0.5 mm is the optimum in both cases seems to be coincidental as the resin formulation, grit size for blasting and chemical treatments, were different.

3.2.2 Tension Tests

Tensile tests were performed for adhesive CXL 194 only.

3.2.2.1 Experimental Procedure

Three types of specimen were used as shown in Fig. 3.2. Type (A) was cast in steel moulds of the required shape; types (B) and (C) were made from prisms, which were cast in steel moulds, and subsequently milled and cut to shape after curing. A total of 6 type (A) specimens; 24 type (B) and 12 type (C), were made. Histograms were drawn for each type as shown in Fig. 3.4.

Three type (C) specimens from each casting were fitted with 2 mm gauge length electrical resistance strain gauges, set at right angles to obtain Poisson's ratio. To determine the stress-strain curve, demec points were also fitted for strain readings over a gauge length of 50 mm. The test results are shown in Fig. 3.4. Type (C) specimens are shown in Plate 3.1.

3.2.2.2 Results

(a) Tensile strength (f_{tg})

Type (A) specimens gave a mean value of 13.2 N/mm^2 and a standard deviation of 0.92 N/mm^2, coefficient of variation of 7%.

Type (B) gave corresponding values of 14.7 N/mm^2, 0.77 N/mm^2 and 5%.

Type (C) gave corresponding values of 16.6 N/mm^2, 0.79 N/mm^2 and 5%.

(b) Modulus of elasticity (E_{tg})

Young's Modulus varied considerably with the stress range as shown in Fig. 3.4. Between zero and 2500 microstrain E_{tg} was 2060 N/mm^2 and between 2500 and 7000 microstrain it was 1650 N/mm^2; these values are the average of three specimens.

(c) Poisson's ratio (ν_{tg})

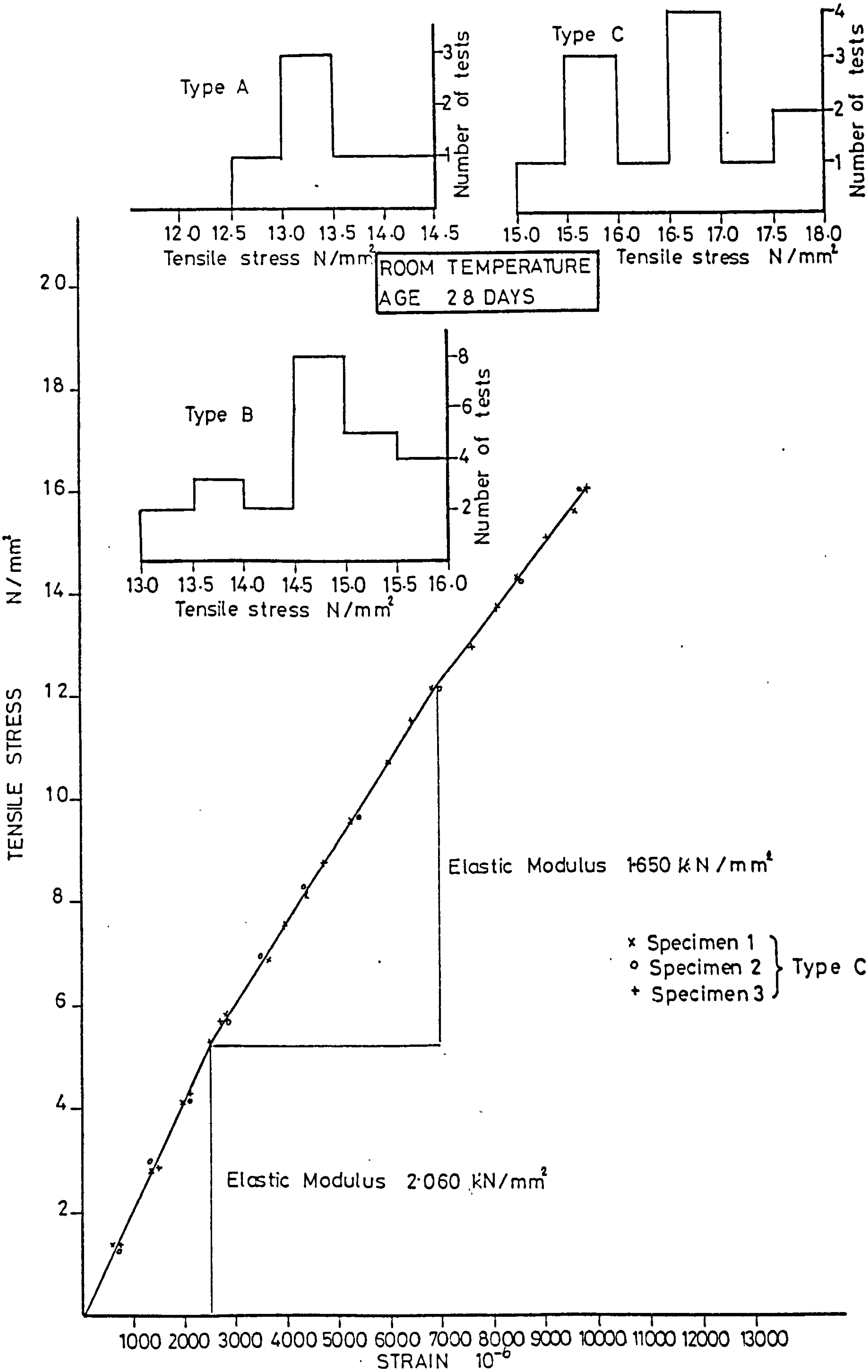

FIGURE 3.4 TENSILE STRESS STRAIN CURVE FOR EPOXY ADHESIVE CXL 194

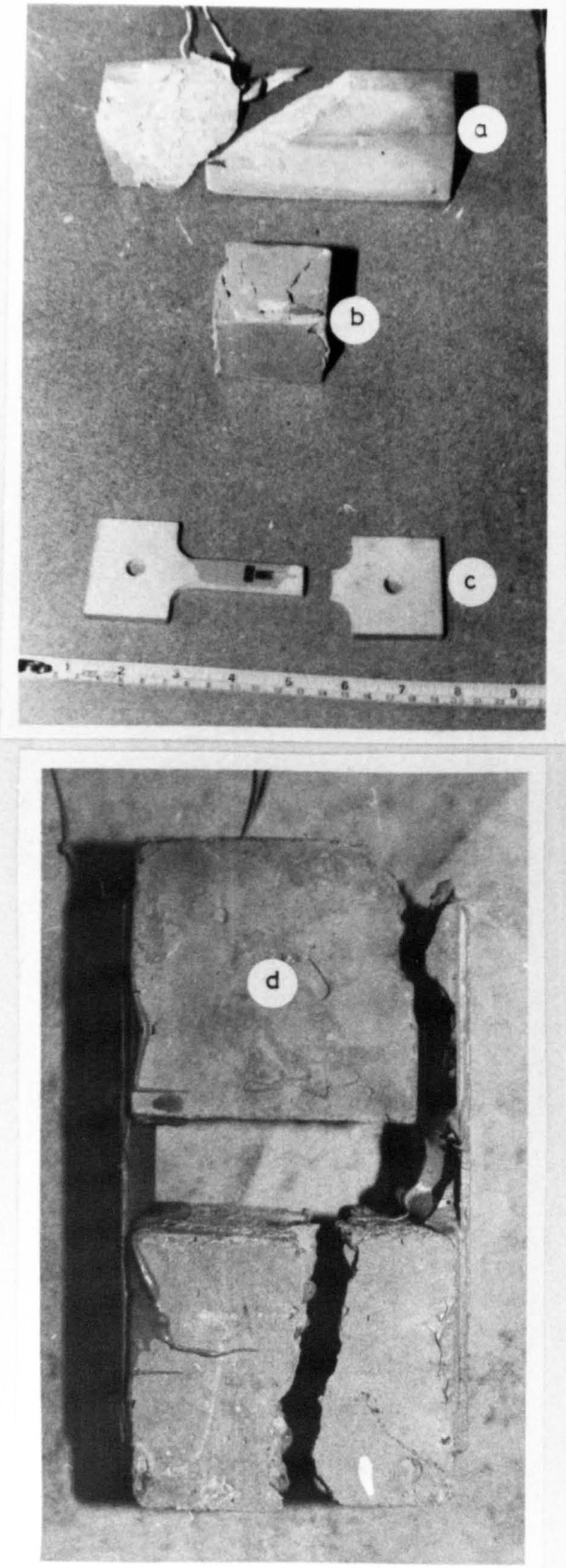

a - compressive Youngs modulus

b - compressive strength

c - tensile strength and Youngs modulus

d compressive lap shear

PLATE 3·1 GLUE TEST SPECIMENS

The average value from three specimens over the range zero to 7000 microstrain was 0.33.

3.2.2.3 Conclusions

For calculation purposes the values of the tensile properties of the epoxy adhesive system CXL 194 were taken as:

$$E_{tg} = 2000 \text{ N/mm}^2$$

$$\nu_{tg} = 0.33$$

$$f_{tg} = 16 \text{ N/mm}^2$$

The coefficients of variation were of the order expected when testing polymers and the different types of specimen gave mean values varying by 12%. The value chosen from type (C) specimens seems realistic because there was considerable deformation of type (A) specimens within the testing machine's jaws, and in type (B) specimen fracture sometimes occurred at the jaws.

3.2.3 Compression Tests

Compression tests were carried out for glue type CXL 194 only.

3.2.3.1 Experimental Procedure

The type of test pieces used is shown in Fig. 3.2. The prisms were fitted with 2 mm gauge length electrical resistance strain gauges for determining Poisson's ratio, and demec points on a gauge length of 50 mm for determining the stress strain curve. A histogram was drawn for the compressive strength results, from tests on 50 mm cubes, as shown in Fig. 3.5, together with the stress strain curve from the prisms. Plate 3.1 shows the compressive specimens after failure.

3.2.3.2 Results

(a) Compressive strength (f_{cg})

The mean compressive strength from eighteen cubes was 40 N/mm^2 with a standard deviation of 2.27 N/mm^2, coefficient of variation 6%.

(b) Modulus of Elasticity (E_{cg})

The mean value from three specimens was 3050 N/mm^2 between zero and 2500 microstrain and 2200 N/mm^2 between 2500 and 7000 microstrain.

(c) Poisson's ratio (ν_{cg})

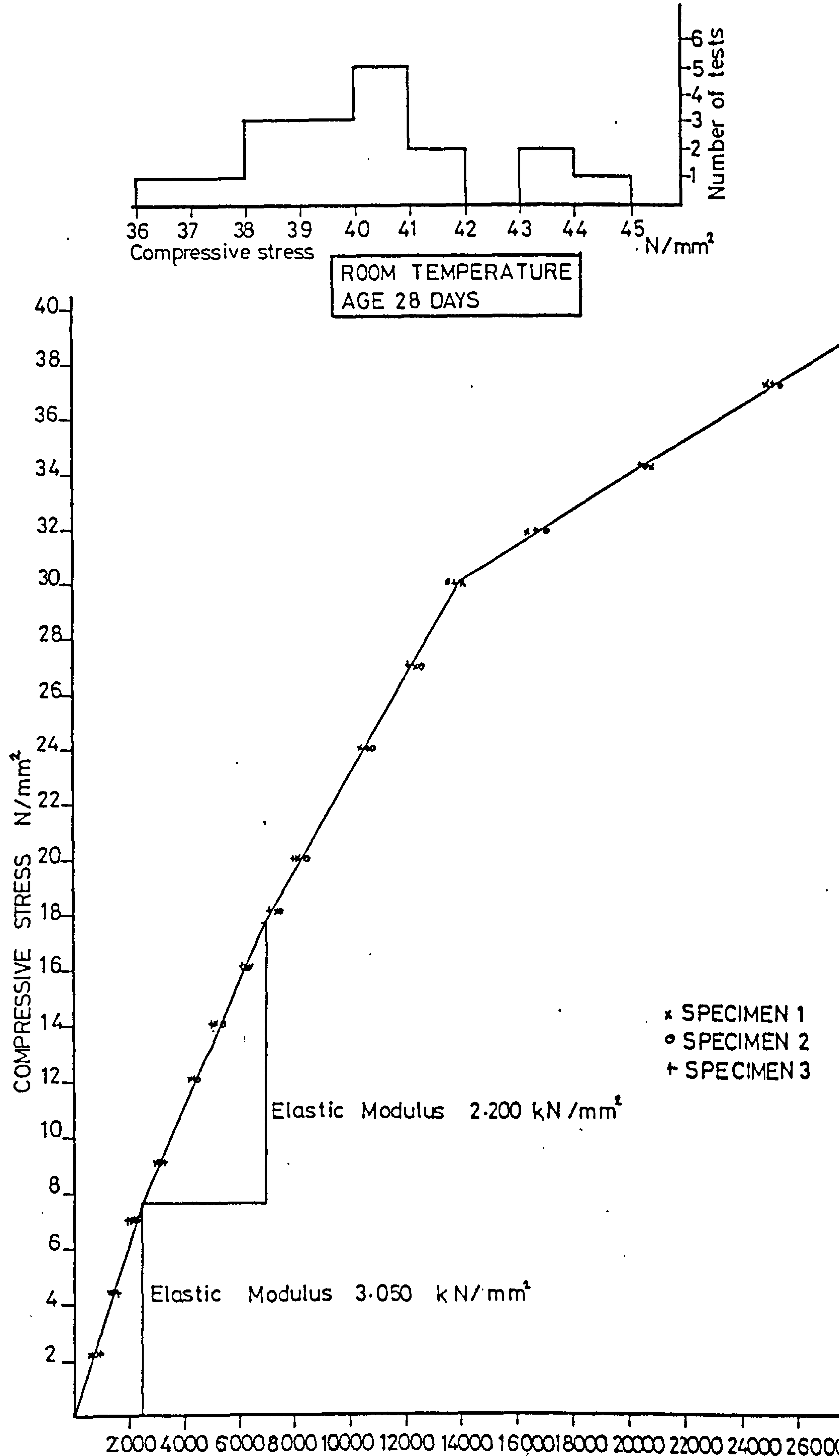

FIGURE 3·5 COMPRESSIVE STRESS STRAIN CURVE FOR EPOXY ADHESIVE CXL 194

The mean value from three specimens was 0.36 over the range zero to 7000 microstrain.

3.2.3.3 Conclusions

For calculation purposes the compressive strength properties found from the tests were taken as:

$$E_{cg} = 3050 \text{ N/mm}^2$$

$$\nu_{cg} = 0.36$$

$$f_{cg} = 40 \text{ N/mm}^2$$

3.2.4 Lap Shear Tests - Steel/Concrete in Compression

Shear tests were carried out for glue type CXL 194 only.

3.2.4.1 Experimental Procedure

Three shear specimens were made up from two 100 mm concrete cubes and two 3 mm thick steel plates, 80 mm x 180 mm, with a 3 mm thick glue layer as shown in Fig. 3.6. Great care had to be taken to ensure the two ends which would be loaded were parallel to each other and at right angles to the axis of the plates. The surface preparation of the steel was as described in 3.2.1.1 and the concrete surface was abraded with a disc grinder, then hand sanded and blown with nitrogen to remove all loose particles and dust. The bonding took place within two hours of surface preparation. After twenty-eight days the specimens were tested in a compression machine at a loading rate of 4 kN/minute, up to failure. Readings of plate strains were taken at five stages during loading, at the locations shown on Fig. 3.6. The mode of failure was by shearing off one of the concrete faces very close to the adhesive layer as shown in Plate 3.1.

3.2.4.2 Results

The mean shear stress at failure was calculated by dividing the failure load by the total area of glue being sheared. (80×80 mm $\times 4 = 2{\cdot}56.10^4$ mm^2). The average value from the three test specimens was 2.87 N/mm^2, with a coefficient of variation of 6%.

The theoretical stress distribution is derived in Appendix 2 and shown in Fig. 3.7 for both the axial stress in the plate and the shear stress in the

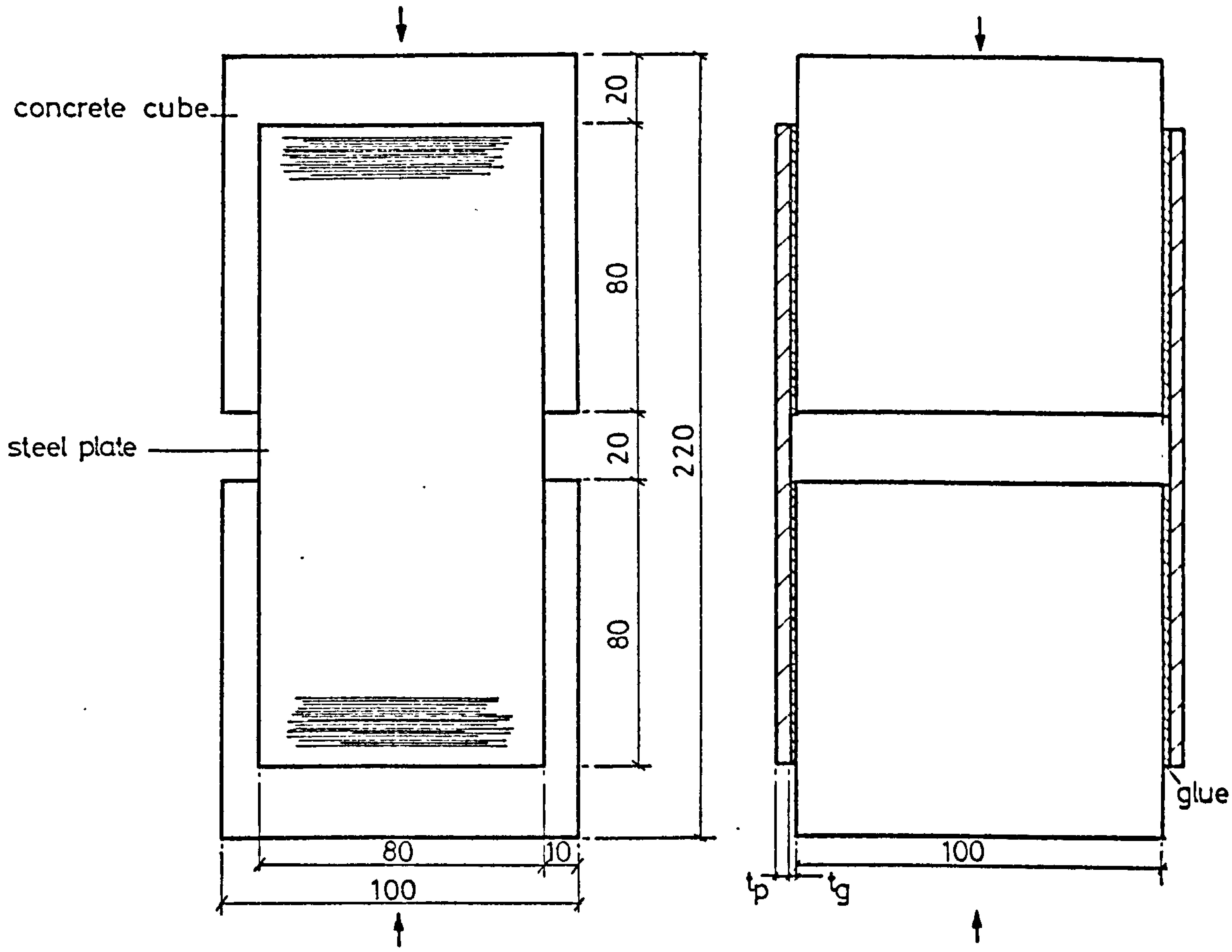

SIDE ELEVATIONS OF TEST SPECIMEN

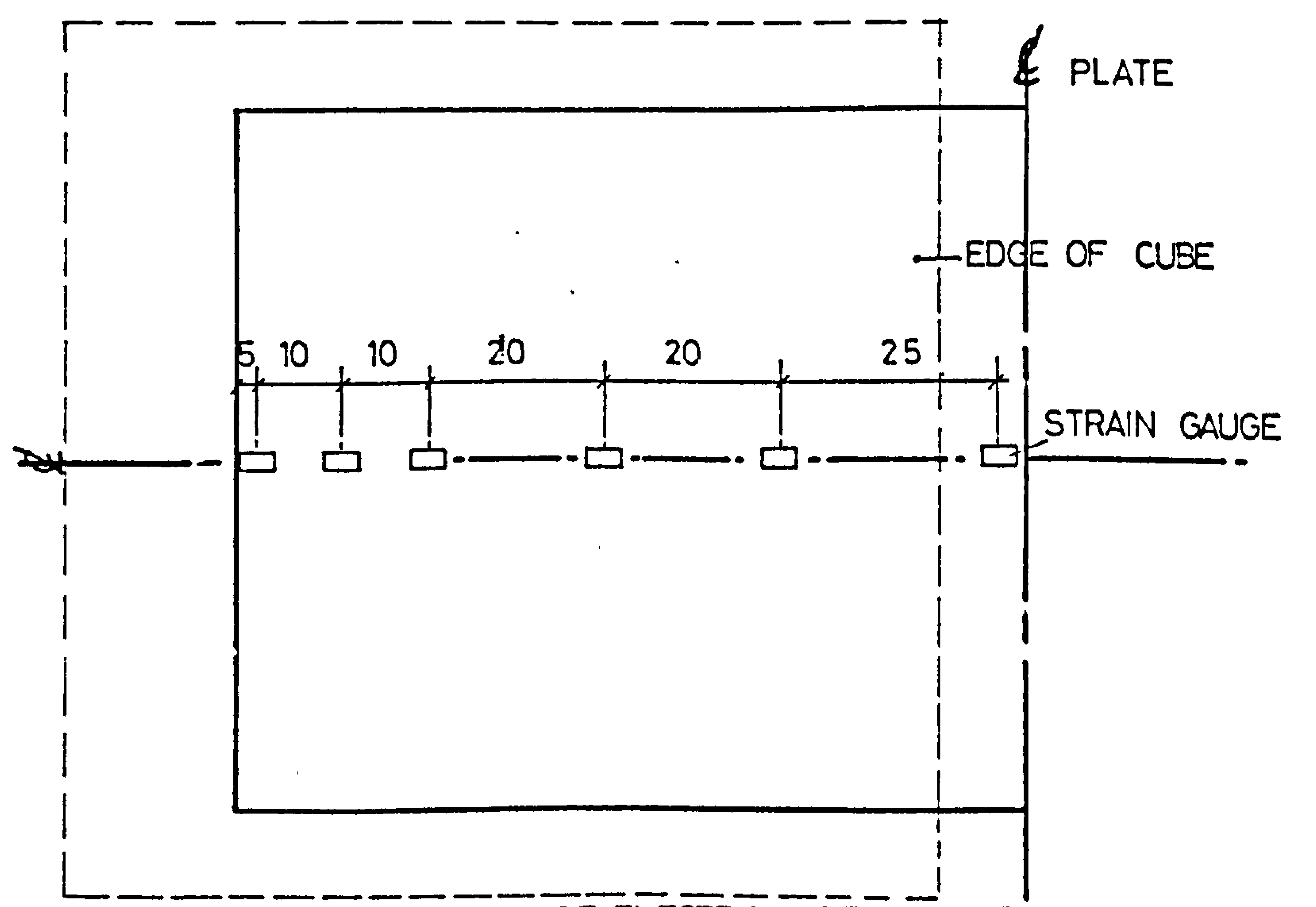

LOCATIONS OF ELECTRICAL RESISTANCE STRAIN GAUGES

FIGURE 3·6 DETAILS OF SHEAR SPECIMEN

glue. The theoretical distribution of shear stress gives a stress intensity factor (maximum stress to mean stress) of 1.82 for the concrete, glue and plate properties used. Assuming this value and applying it to the mean experimental shear stress gives a value of 5.2 N/mm^2 for the maximum shear stress in the glue at failure.

The experimental and theoretical values of axial stress in the plate show good agreement as shown in Fig. 3.7. The experimental values were obtained from electrical resistance strain gauges of 2 mm gauge length.

3.2.4.3 Conclusion

The theoretical distribution of axial stress proposed by Bresson (54) was confirmed. The assessed value of maximum shear stress in the glue, 5.2 N/mm^2 seems reasonable as the tensile shear strength of the concrete is approximately 5 N/mm^2.

3.3 REINFORCEMENT

Prior to manufacturing the preliminary beams, the stress-strain behaviour, of the steel reinforcing bars and plates, was investigated.

3.3.1 Bars

3.3.1.1 Experimental Procedure

Two specimens from each bar diameter, 6 mm and 20 mm, were used to determine the Young's Modulus, yield strength and ultimate tensile strength. The tensile tests on the 6 mm standard round bar specimens were carried out as recommended in BS 18: Part 2, 1970. To eliminate any initial lack of straightness, the specimens were first loaded to about 25% of the nominal yield stress, as specified by the manufacturer, and then released. The initial readings were then taken. The strains were measured using an extensometer of 50 mm gauge length. The 20 mm diameter high yield steel bars were tested in the same manner, but without any initial "straightening". The results for both bar diameters are shown in Fig. 3.8.

3.3.1.2 Results

The high tensile steel, unlike the mild steel, had no definite yield point. The elastic modulus for both steels was 200 kN/mm^2. The yield stress

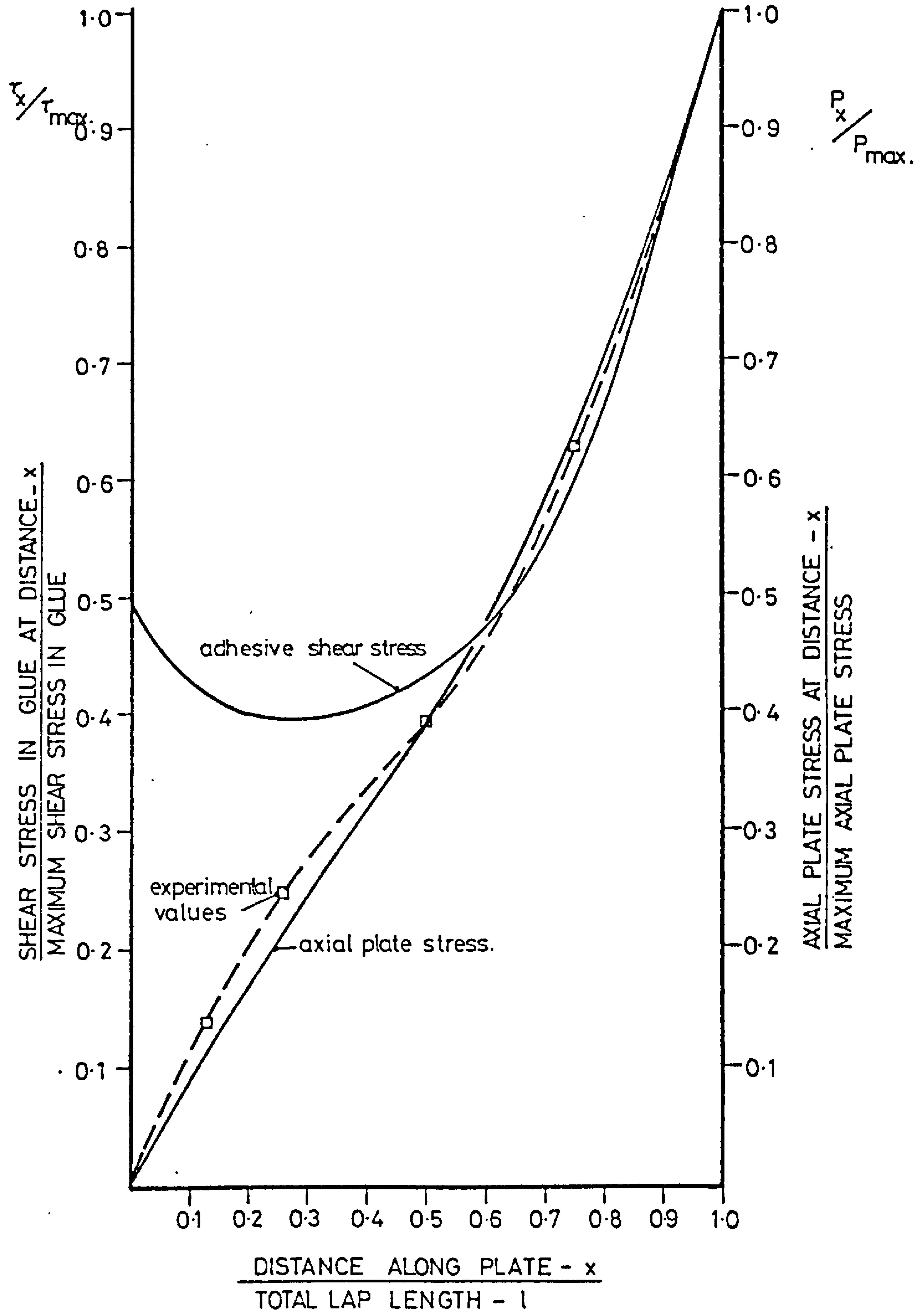

FIGURE 3·7 EXPERIMENTAL AND THEORETICAL STRESS DISTRIBUTIONS IN A BONDED STEEL/CONCRETE LAP JOINT UNDER COMPRESSIVE SHEAR LOADING

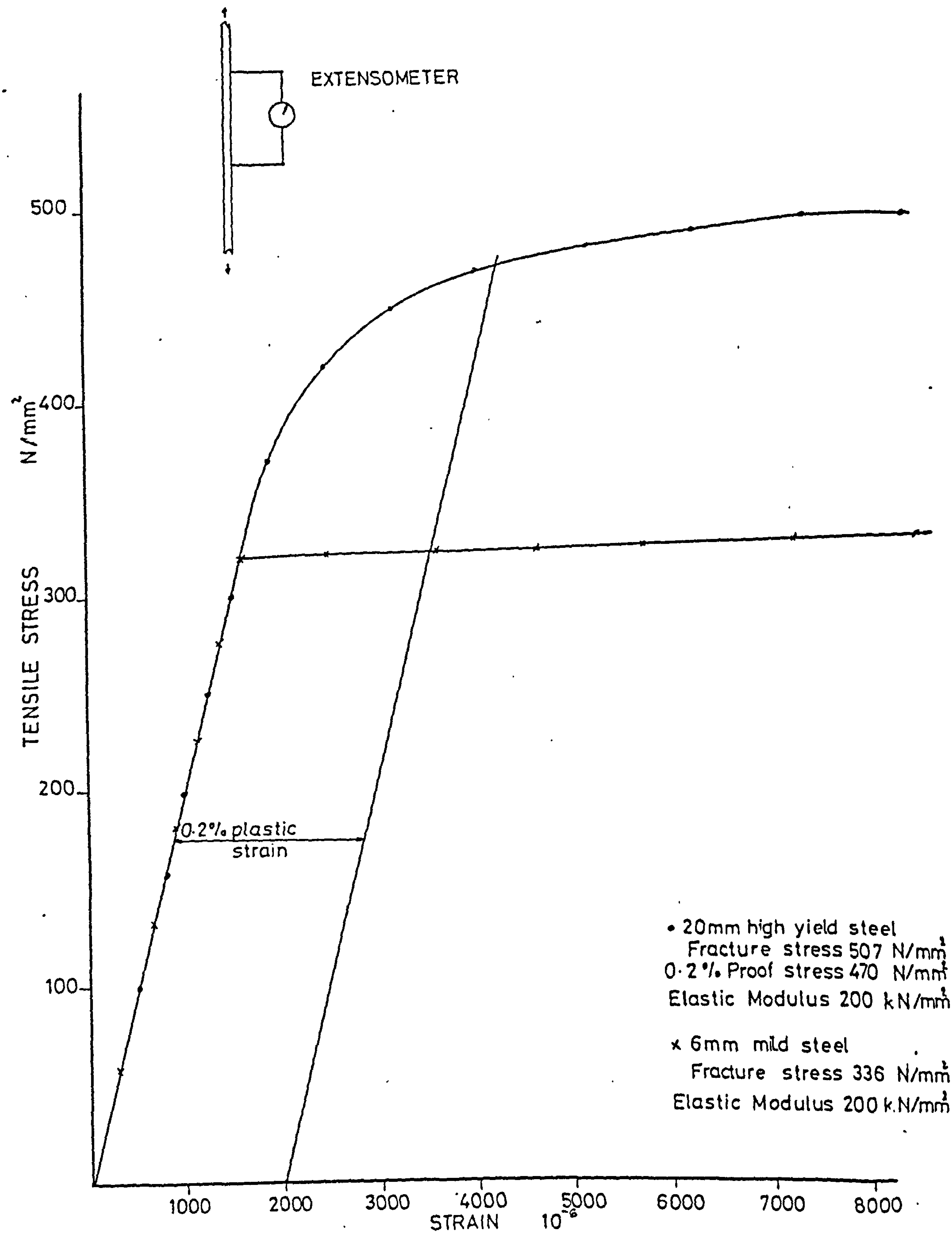

FIGURE 3.8 TENSILE STRESS STRAIN CURVES FOR 6mm & 20 mm BARS

of the 6 mm bar was 320 N/mm^2 and for the 20 mm bar the proof stress was 470 N/mm^2.

3.3.1.3 Conclusions

The samples of steel which were tested behaved as expected and satisfied the requirements of British Standards.

3.3.2 Plates

3.3.2.1 Experimental Procedure

The external reinforcement was in the form of mild steel plates of three different thicknesses i.e. 1.5 mm, 3 mm and 6 mm. Two specimens from each thickness of steel plate were used to determine their Young's Modulus, yield strength and ultimate tensile strength. The tests were carried out as recommended in BS 18: Part 3, 1970. The strains were measured by demountable mechanical extensometer of 50 mm gauge length. The results are shown in Fig. 3.9.

3.3.2.2 Results

The elastic modulus was 200 kN/mm^2, and the yield stresses for 1.5 mm, 3 mm and 6 mm thicknesses were 236 N/mm^2, 258 N/mm^2 and 248 N/mm^2 respectively. The respective fracture stresses were 310 N/mm^2, 316 N/mm^2 and 308 N/mm^2.

3.3.2.3 Conclusions

The samples of mild steel plate behaved as expected and were satisfactory for use as the external reinforcement to the plated beams.

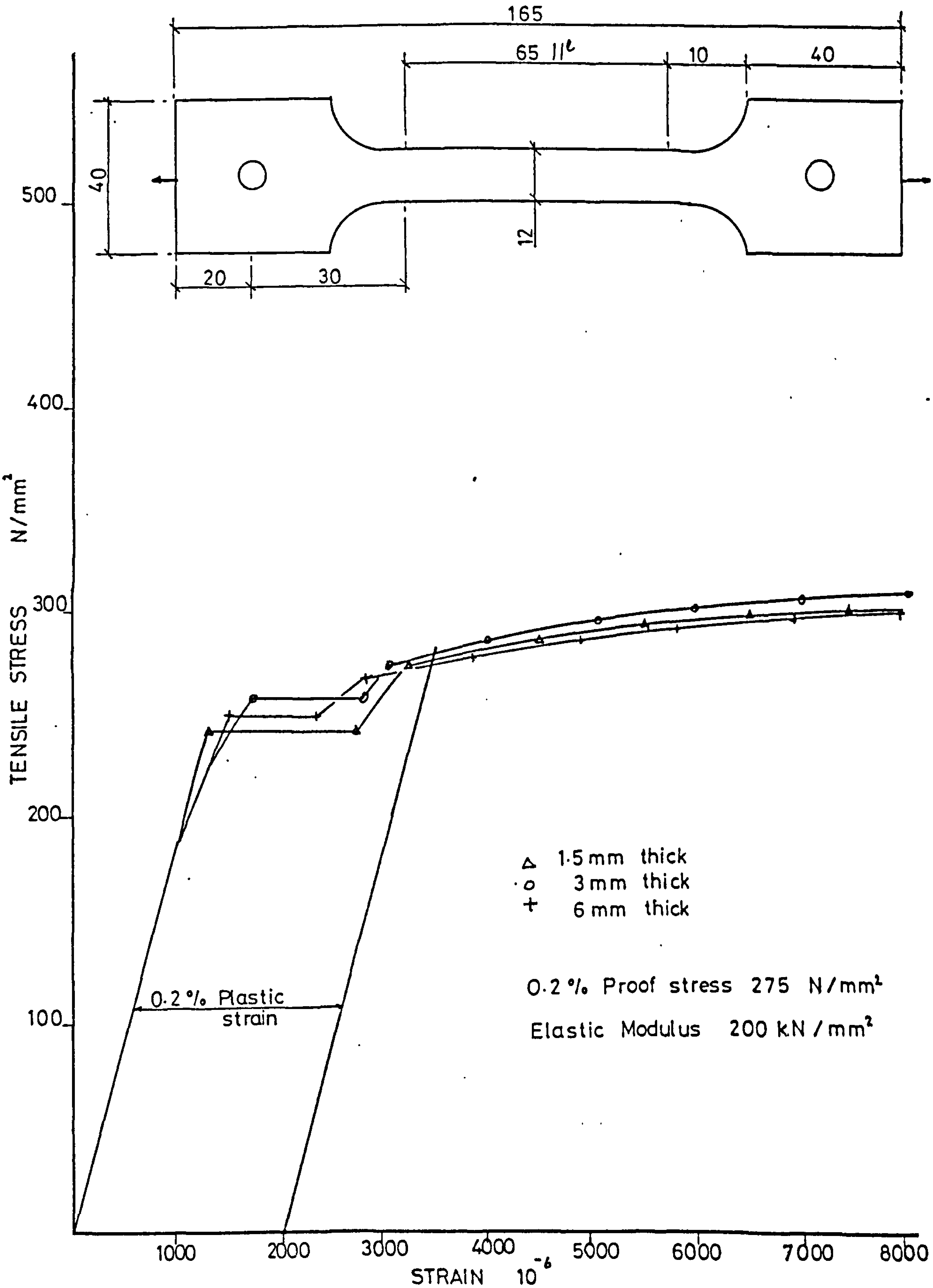

FIGURE 3.9 TENSILE STRESS STRAIN CURVES FOR STEEL PLATES

CHAPTER 4

PRELIMINARY SERIES OF TESTS

INTRODUCTION

Since so many factors affecting the behaviour of bonded joints are still not fully understood, and consequently not fully controlled, it was decided that a preliminary series of tests would be performed for two main reasons:

(a) to gain some knowledge of the properties of the epoxy resin systems used

(b) to investigate methods of surface preparation and resin application in strengthening simple unreinforced concrete beams.

It was felt that this would ensure that the main series of large test beams would have less variation in results and that wastage of materials would be reduced to a minimum.

The preliminary testing was made up of two series - A and B.

4.1 EXPERIMENTAL PROGRAMME

4.1.1 Beam Details

In series A and B plated and unplated plain concrete beams with no tension bar reinforcement were tested. Altogether eighteen beams were tested; two sizes of beams, 150 x 150 x 710 mm (Series A) and 100 x 150 x 1200 mm (Series B) were used. Two epoxy resin systems were used in both series A and series B. The steel plates used for strengthening were the same material for both series.

4.1.1.1 Series A

The beams designated A1, 3, 5, 7 (Table 4.1) were bonded with type A resin and were tested on a loading rig which had no roller support. The friction force at the supports would therefore cause a relative increase in the applied load to produce a particular bending moment.

The beams designated A2, 4, 6, 8 were bonded with type B resin and tested with a roller support.

In this series the effects of uniform and tapering glue thickness were studied. Eight beams were tested. Beams A1 and A2 had no internal reinforcement at all. The other beams had shear reinforcement at the supports, to avoid shear

TABLE 4·1 DETAILS OF PLAIN CONCRETE TEST BEAMS : SERIES A

BEAM MK. NO.	CONCRETE AGE AT TESTING days	ADHESIVE		
		TYPE	THICKNESS* mm	PROFILE
A1	86	A	4·0	Uniform glue thickness
A2	114	B	4·5	= = =
A3	85	A	3·5	= = =
A4	114	B	5·0	= = =
A5	88	A	3·8	Tapering glue thickness
A6	114	B	4·0	= = =
A7	84	-	-	Unplated beam
A8	114	-	-	= =

TABLE 4·2 DETAILS OF PLAIN CONCRETE TEST BEAMS : SERIES B

BEAM MK. NO.	CONCRETE AGE AT TESTING days	ADHESIVE		
		TYPE	THICKNESS* mm	PROFILE
B1	83	A	3·5	Uniform glue thickness.
B2	108	B	3·0	= = =
B3	83	A	5·0	Uniform glue, lapped plates.
B4	108	B	3·0	= = = =
B5	77	-	-	Unplated beam.
B6	106	-	-	= =
B7	77	-	-	Unplated, notched beam.
B8	106	-	-	= = =
B9	85	A	3·5	Plated, notched beam.
B10	100	B	3·0	= = =

* average thickness at midspan.

failure outside the plated length. Beams A1, A2, A3 and A4 had uniform glue thickness, whereas beams A5 and A6 had tapering glue thickness as shown in Fig. 4.1. Beams A7 and A8 were unplated control beams.

In beams A1 to A5, the steel plates were 100 x 500 x 1 mm thick, and were stopped short of the supports by about 50 mm. The beams were tested under centre point loading, over an effective span of 610 mm.

4.1.1.2 Series B

Series B consisted of the beams in which the effects of uniform glue thickness, lapping of plates and the provision of steps on the soffit of the beam were studied. The steps were cast into the beam's tension face as shown in Fig. 4.2 and detailed in Table 4.2.

All the beams in this series had shear reinforcement at the supports and the steel plates were 75 x 1000 x 1 mm thick, again stopped short of the supports. Beams B1 and B2 had uniform glue thickness whilst B3 and B4 had lapped plates. For these latter beams, two 500 mm long plates were used, butting each other, with a cover plate 75 x 400 x 1 mm thick. The cover plate was bonded with a glue thickness of approximately 0.5 mm. Beams B9 and B10 had tapered, stepped glue lines. This was intended to simulate the soffit of a bridge deck consisting of precast, prestressed box beams spanning longitudinally. Beams B5 and B8 were unplated control beams. Beams B7 and B8 were stepped as beams B9 and B10.

As in series A the beams with even numbered marks, i.e. B2, 4, 6, 8, 10 were bonded with type B resin and tested with a roller support. Beams with odd numbered marks, i.e. B1, 3, 5, 7, 9 were bonded with type A resin and were tested without a roller support. All the beams were tested under central point loading over an effective span of 1100 mm.

4.1.2 Material Properties

4.1.2.1 Concrete

The concrete chosen for the beams was designed to be consistent with that used in bridge construction using precast prestressed beams as detailed in Section 3.1.

The concrete properties for the two series of tests were as follows. For

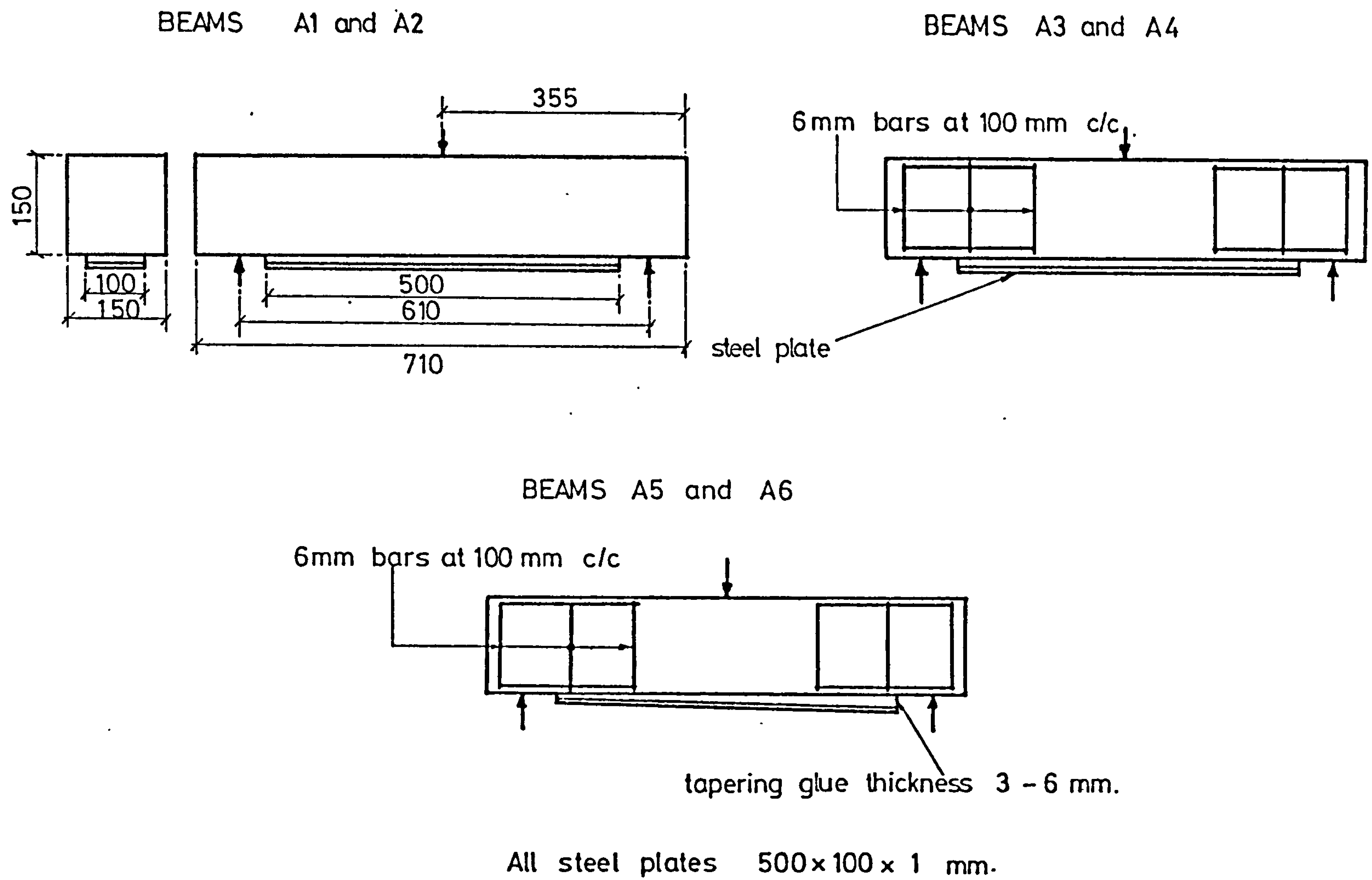

FIGURE 4·1 DETAILS OF TEST BEAMS : SERIES A

BEAMS B1 and B2 UNIFORM GLUE THICKNESS

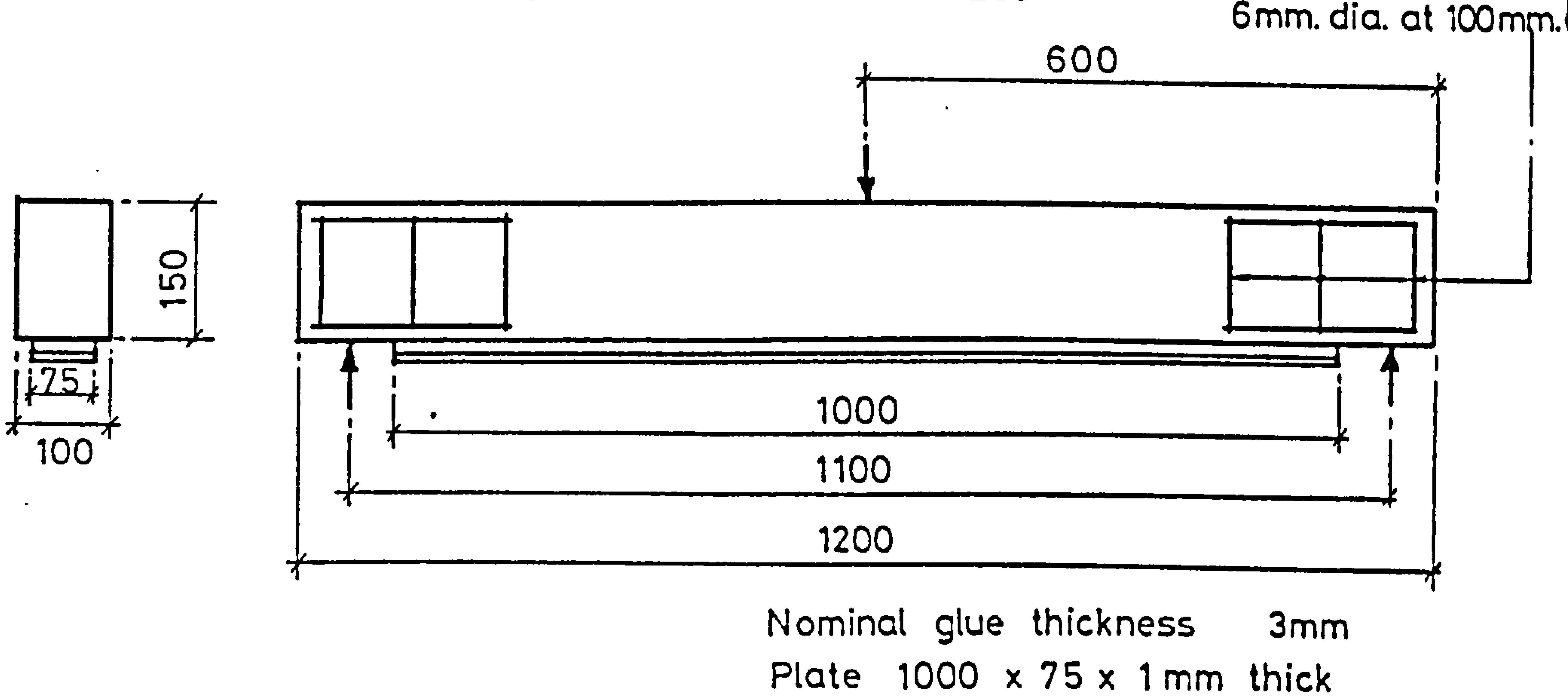

BEAMS B9 and B10 NOTCHED BEAM

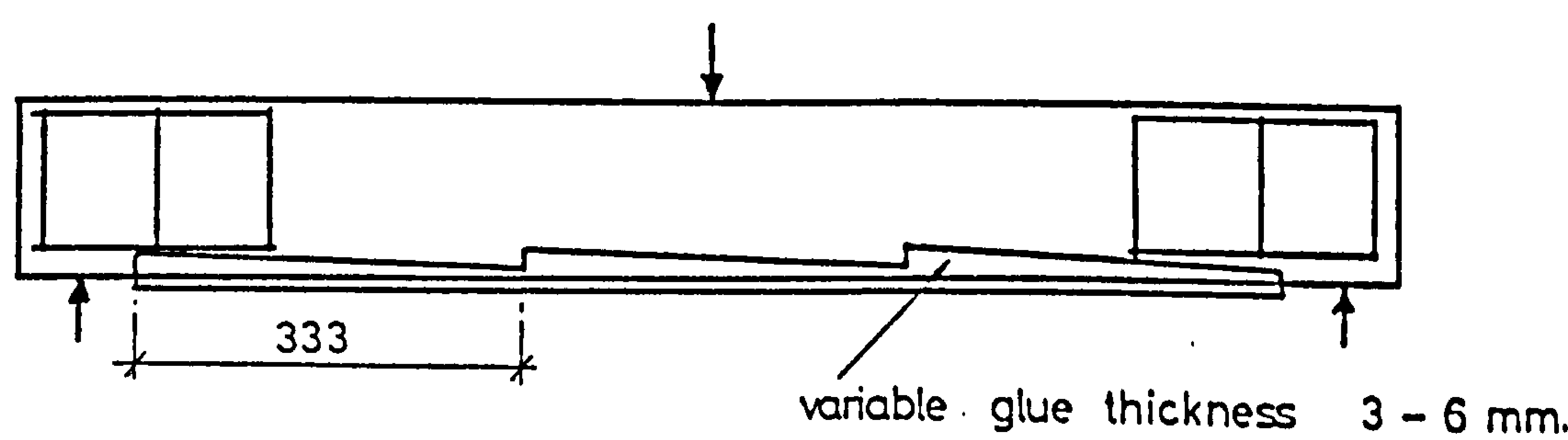

BEAMS B3andB4 LAPPED PLATES

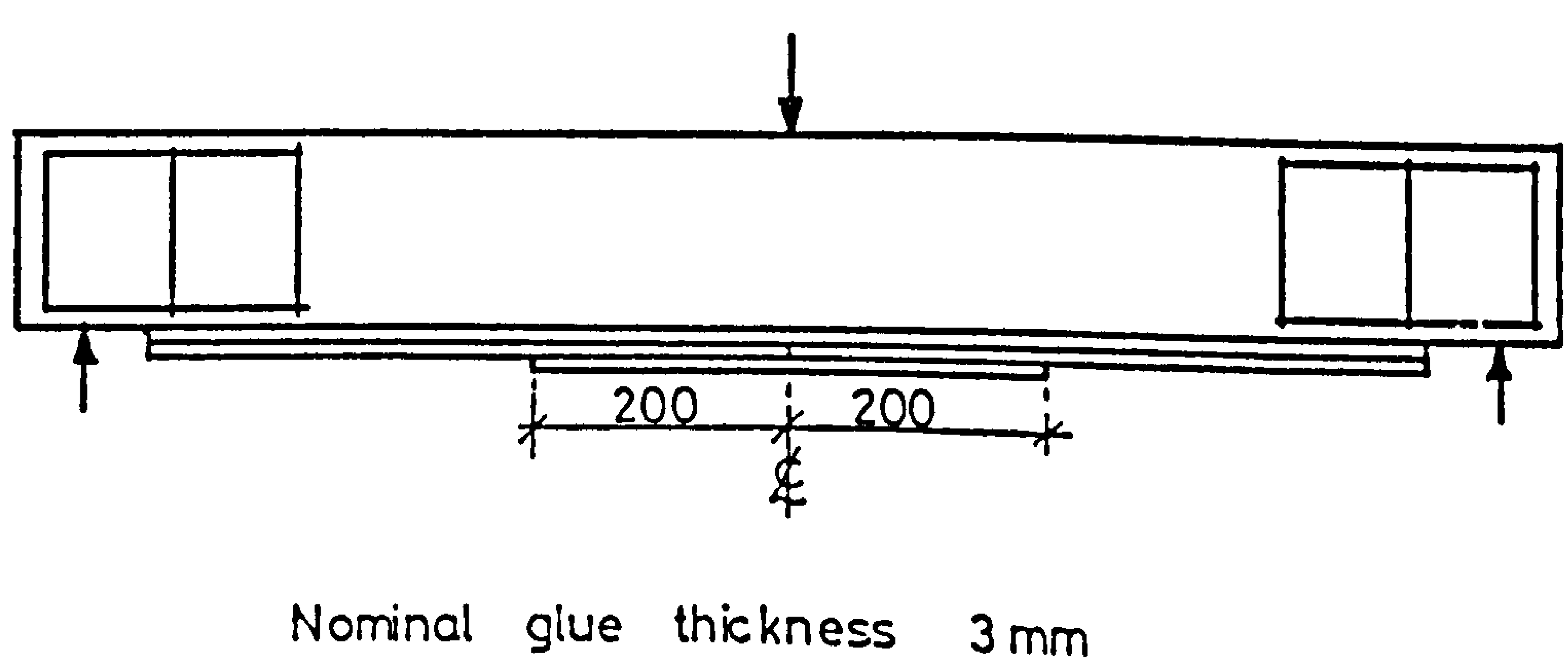

FIGURE 4·2 DETAILS OF TEST BEAMS : SERIES B beams of series A, the cube strength at 28 days varied from 56-60 N/mm^2 with a mean value of 58.3 N/mm^2. The cube strength at the age of testing of the beams varied from 64 to 66 N/mm^2 with a mean value of 65.5 N/mm^2. The modulus of rupture of the beams at testing varied between 4.37 and 4.94 N/mm^2 with a mean value of 4.65 N/mm^2.

For the beams of series B, the 28 day cube strength varied from 67.2 to 75.2 N/mm^2 with a mean value of 70.6 N/mm^2. The cube strength when the beams were tested varied from 71.9 to 82.7 N/mm^2 with a mean value of 76.7 N/mm^2. The modulus of rupture at this age varied from 5.1 to 5.35 N/mm^2 with a mean value of 5.22 N/mm^2.

The two concretes had an average elastic modulus of 36 kN/mm^2 at 3 months, a Poisson's ratio of 0.16 and an average shrinkage of 280 x 10^{-6} m/m.

4.1.2.2 Steel

The 6 mm diameter steel reinforcing bars used for stirrups and hanger bars at top and bottom in the two series were as detailed in Section 3.3.1 with a yield stress of 320 N/mm^2.

Tensile tests were carried out on standard tensile specimens cut from the steel plates to determine the tensile strength. The average yield stress and elastic modulus were 125 N/mm^2 and 200 kN/mm^2 respectively. The ultimate tensile strength of the plates was 132 N/mm^2. This plate was not the same as used for the main test series, as detailed in Section 3.3.2.

4.1.2.3 Adhesives

Two epoxy adhesives, both filled systems, were used in series A and B. Glue A was a 2 part liquid system manufactured by Ciba Geigy Ltd. and designated XD 808. Glue B was also a 2 part system but with a paste consistency, manufactured by Colebrand Ltd. and designated CXL 194.

To determine the shear strength of the glue, and hence the best thickness to use when lapping plates, double lap shear tests on specimens cut from the same sheet as the tensile specimens were carried out, as detailed in Section 3.2.1. Based on these results, 0.5 mm thickness was chosen for plate lapping. The other glue properties were detailed in Section 3.2.

4.1.3 Preparation of Test Specimens

All the test beams were made in four castings. The beams and control specimens were stripped after 24 hours and then cured in a fog room at 21°C, 100% relative humidity, until required for plating or testing. After removal from the fog room, the beams were kept in a warm dry atmosphere for 24 hours prior to surface preparation.

The surface preparation of the beams consisted of the following operations. The beams were abraded, on the tension face, with a disc grinder to remove laitance and expose the aggregates. They were then wire brushed to remove all loose particles. Finally they were sanded, by hand, with 100 grit emery cloth. All remaining dust and debris were removed by blowing with nitrogen.

The steel plates were gritblasted, as for the lap shear tests, under pressure to a uniform grade, as judged visually. Mixing and bonding operations were performed as described in Section 3.2.1.1. The glue was applied to both the steel plate and the prepared surface of the beam. Small pieces of hardened epoxy resin were used as spacers to control the glue thickness. The plate was then applied and held in position by weights.

Using this technique, any entrapped air would generally be restricted to the body of the glue layer, and not to the glue/concrete or glue/steel interface, where its effect on bond is greatest. The weights were generally left for four days after which the beams were left for at least another ten days to allow the glue to cure.

4.1.4 Testing Procedure

All the beams were tested under a single central point load. The beams were loaded in stages. At each stage central deflection, concrete strain distribution, strain in the steel plate and the state of cracking were noted. The concrete and steel strains were measured at mid-span using a demountable mechanical extensometer on a 100 mm gauge length. The concrete strains were measured at the compression face and over the depth of the beam. The beams were tested at ages varying between 77 and 114 days (at ages from 14 to 30 days after gluing). The concrete cube strength and the flexural strength at the age of testing were given in Section 4.1.2.1.

4.2 TEST RESULTS AND DISCUSSION

The load-deflection curves are shown in Figs. 4.3 to 4.6 and 4.7 shows two typical strain distributions across the concrete section. Figs. 4.8 to 4.11 show the load-strain curves. Plates 4.1 and 4.2 show typical beams after failure and Tables 4.3 to 4.6 show the test results. The properties are discussed below under the relevant sections.

4.2.1 Deflections and Strains

The load-deflection curves are shown in Figs. 4.3 and 4.4 for beams of series A and in Figs. 4.5 and 4.6 for beams of series B. These results show that glued reinforcement has four distinct effects:

1. It increases the range of elastic behaviour.
2. It increases the stiffness of the beam.
3. It increases the ultimate flexural capacity of the beam, and
4. It makes the beams more ductile.

Considering beams of series A (Figs. 4.3 and 4.4), it is seen that beam A4 with shear reinforcement at supports showed better performance than the comparable beam A2 without shear reinforcement. Beam A6 with a tapering glue thickness of 3 to 6 mm, on the other hand, showed initially higher stiffness than beam A2 with uniform glue thickness, but with cracking at higher loads this stiffness became less than that of beam A2.

In beams of series B, the presence of notches showed no adverse effects on the unplated beams; with plated beams, the notched beam B10 showed marginally better behaviour than the beam B2 with uniform glue thickness. Beam A4 with lapped plates also showed marginally better performance than beams B2 and B10 (Fig. 4.6).

The measured strain distribution over the depth of the beams is shown in Fig. 4.7 for two typical beams A2 and B5. These diagrams show that the strain distribution remained approximately linear in the compression zone throughout the loading range whereas in the tensile zone the strain distribution, approximately

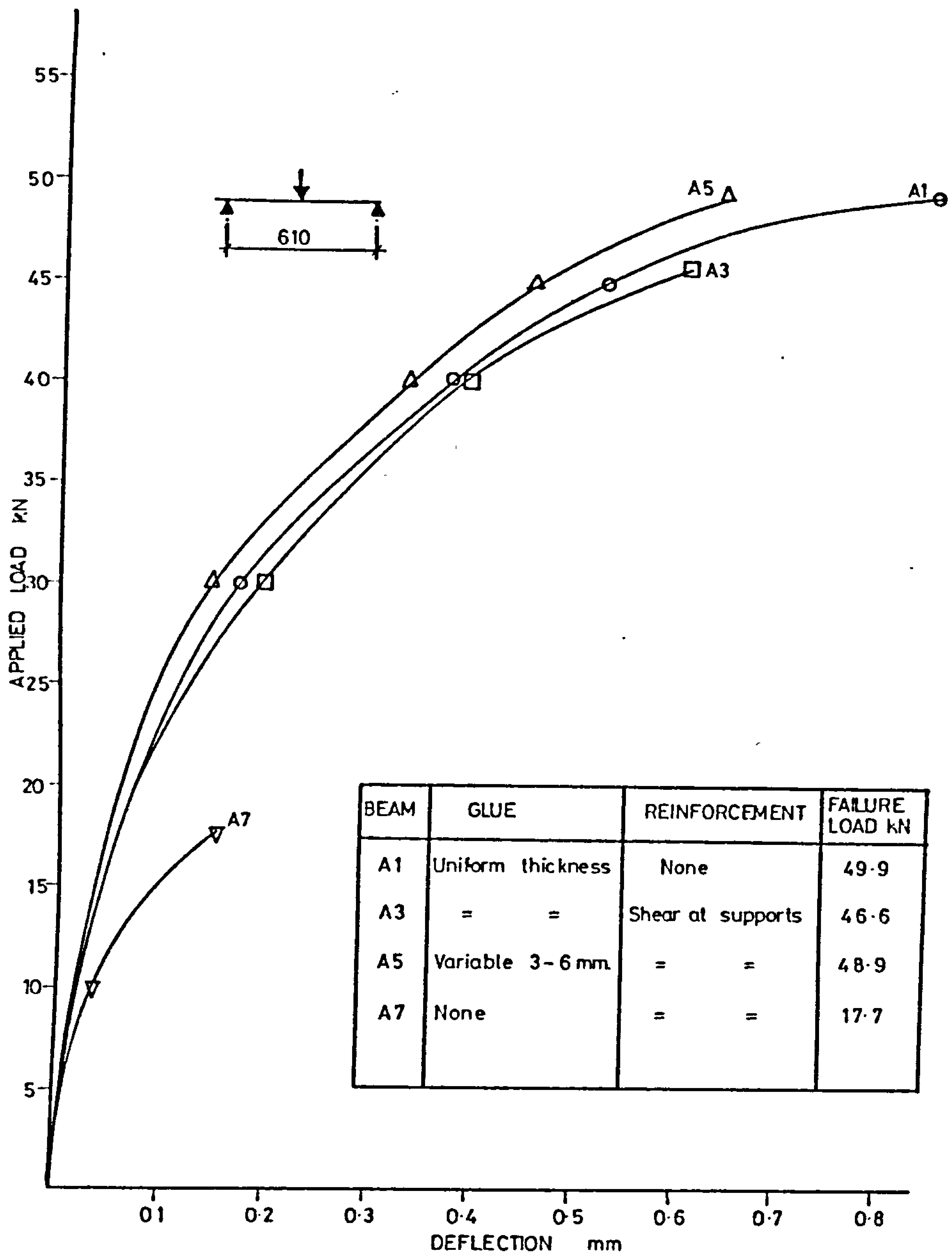

BEAM	GLUE	REINFORCEMENT	FAILURE LOAD kN
A1	Uniform thickness	None	49·9
A3	= =	Shear at supports	46·6
A5	Variable 3 – 6 mm.	= =	48·9
A7	None	= =	17·7

FIGURE 4·3 LOAD-DEFLECTION CURVES : SERIES A

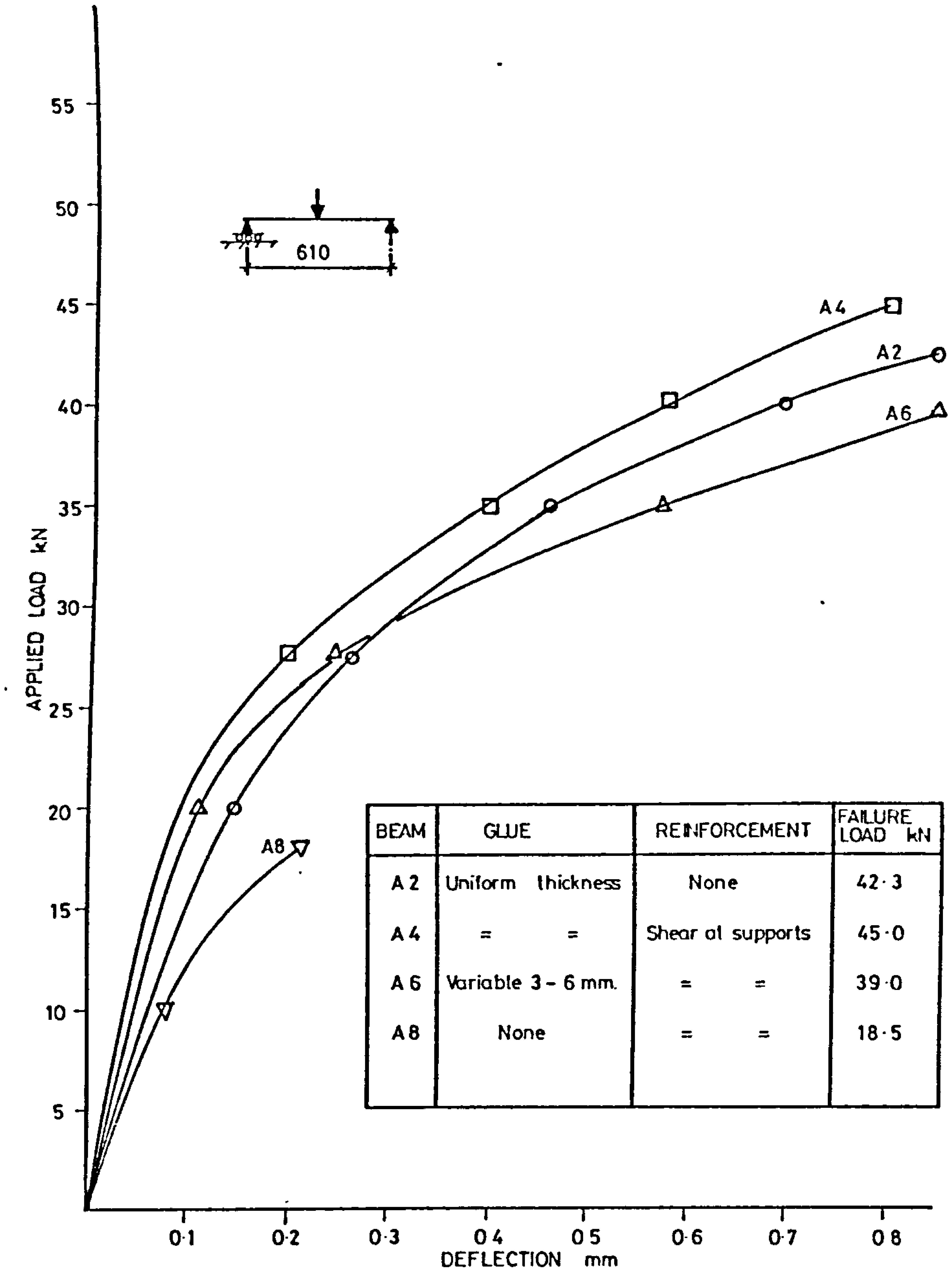

BEAM	GLUE	REINFORCEMENT	FAILURE LOAD kN
A 2	Uniform thickness	None	42·3
A 4	= =	Shear at supports	45·0
A 6	Variable 3 – 6 mm.	= =	39·0
A 8	None	= =	18·5

FIGURE 4·4 LOAD-DEFLECTION CURVES : SERIES A.

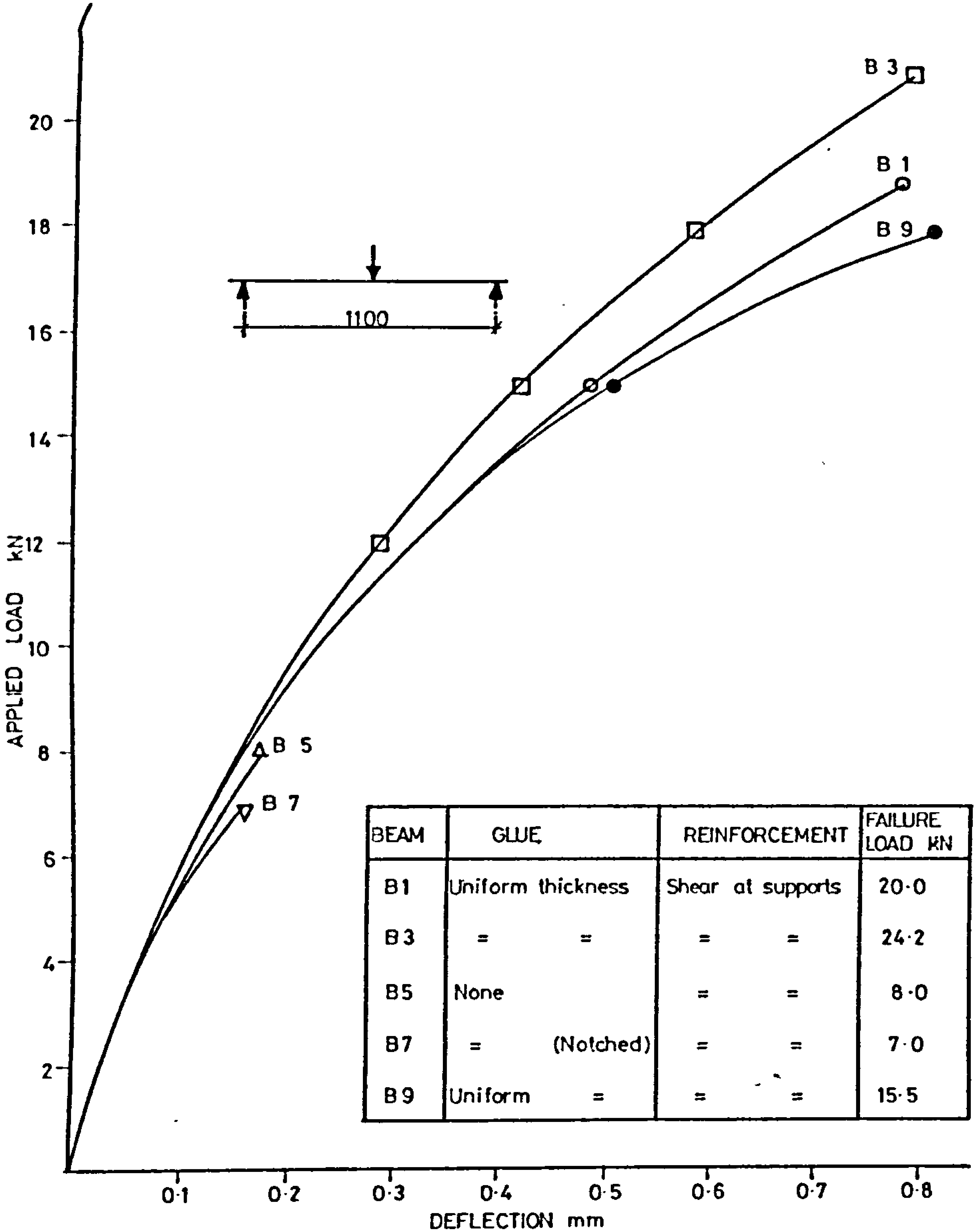

BEAM	GLUE	REINFORCEMENT	FAILURE LOAD kN
B1	Uniform thickness	Shear at supports	20·0
B3	= =	= =	24·2
B5	None	= =	8·0
B7	= (Notched)	= =	7·0
B9	Uniform =	= =	15·5

FIGURE 4·5 LOAD-DEFLECTION CURVES : SERIES B

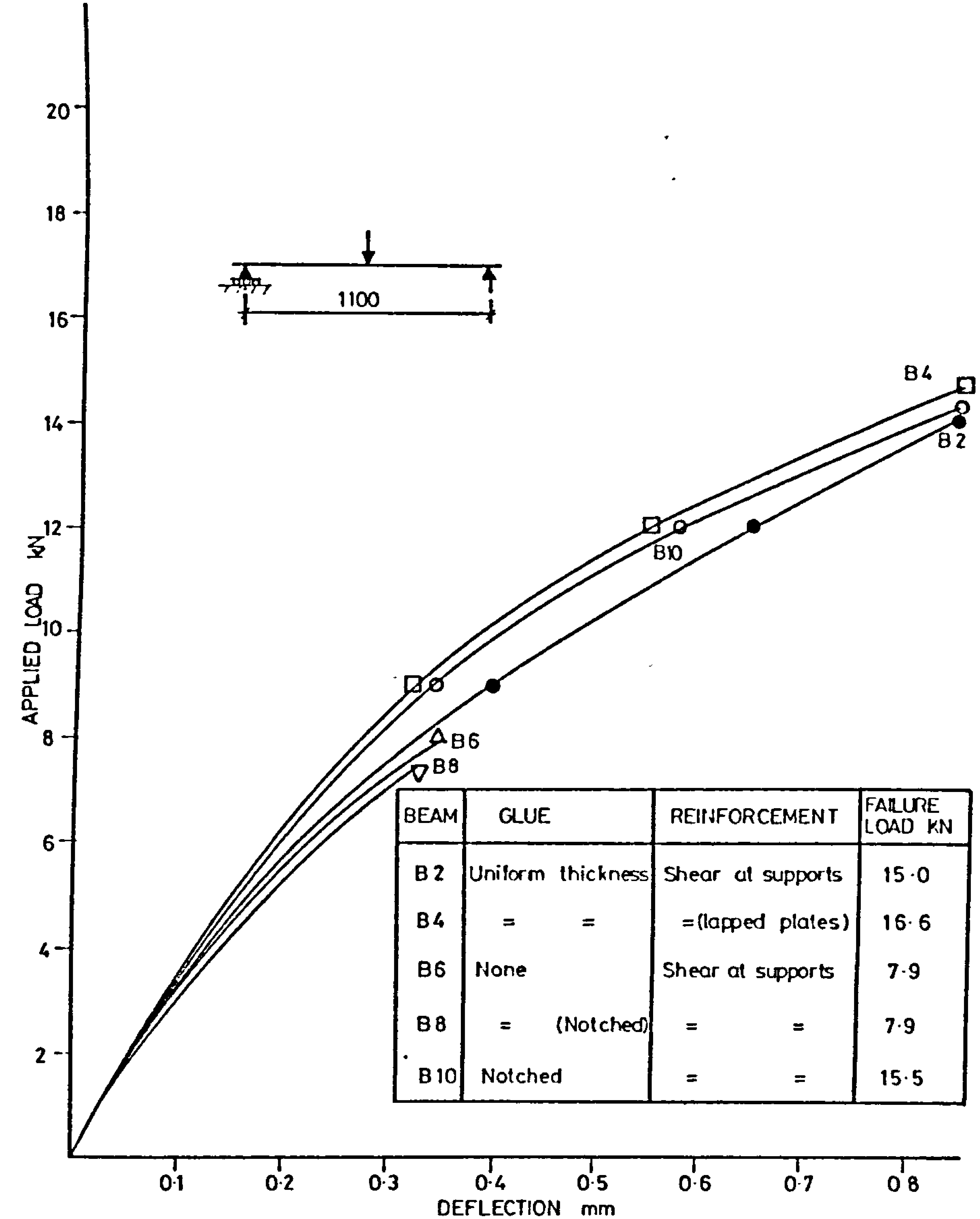

BEAM	GLUE	REINFORCEMENT	FAILURE LOAD kN
B 2	Uniform thickness	Shear at supports	15·0
B 4	= =	=(lapped plates)	16·6
B 6	None	Shear at supports	7·9
B 8	= (Notched)	= =	7·9
B 10	Notched	= =	15·5

FIGURE 4·6 LOAD-DEFLECTION CURVES : SERIES B

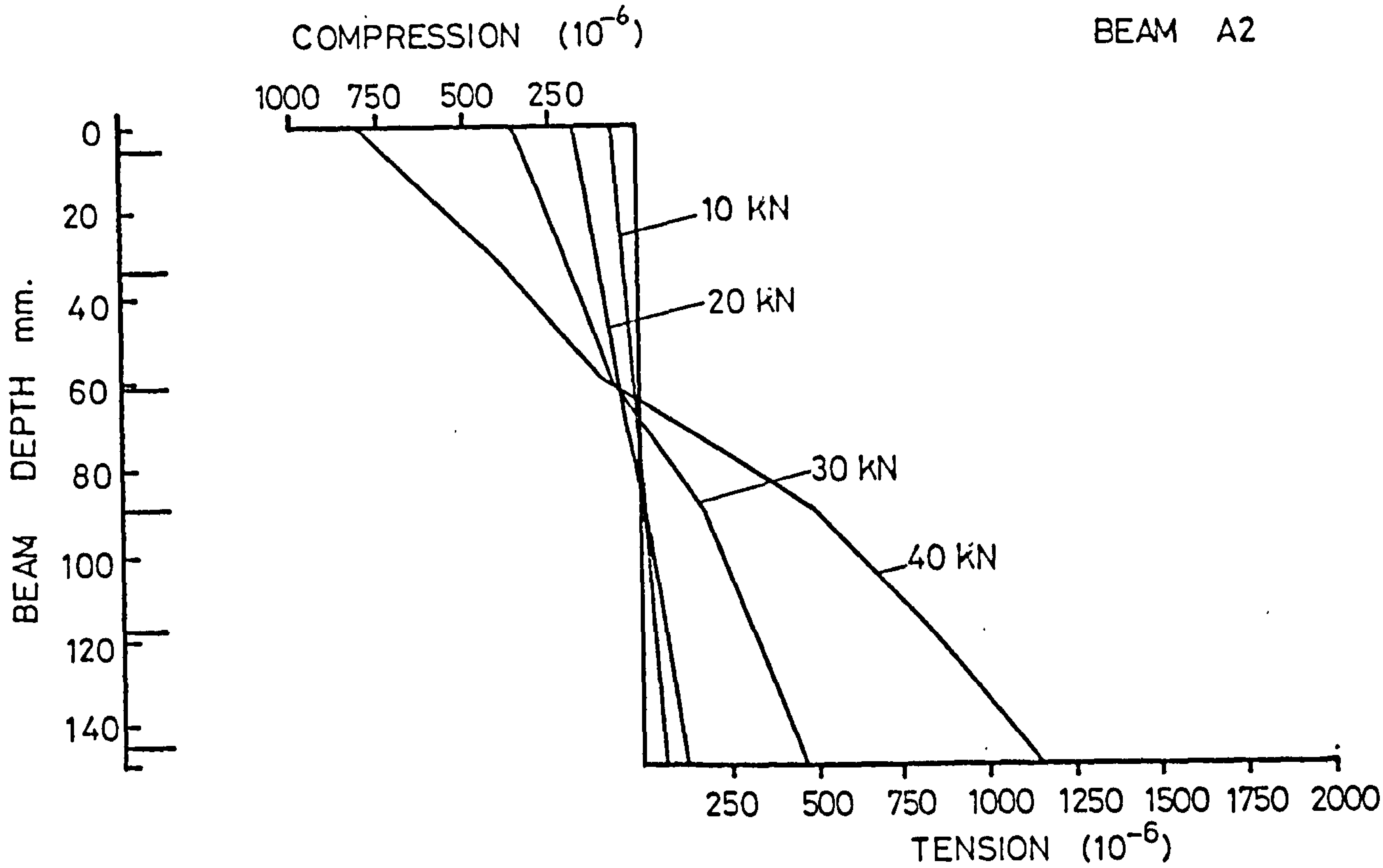

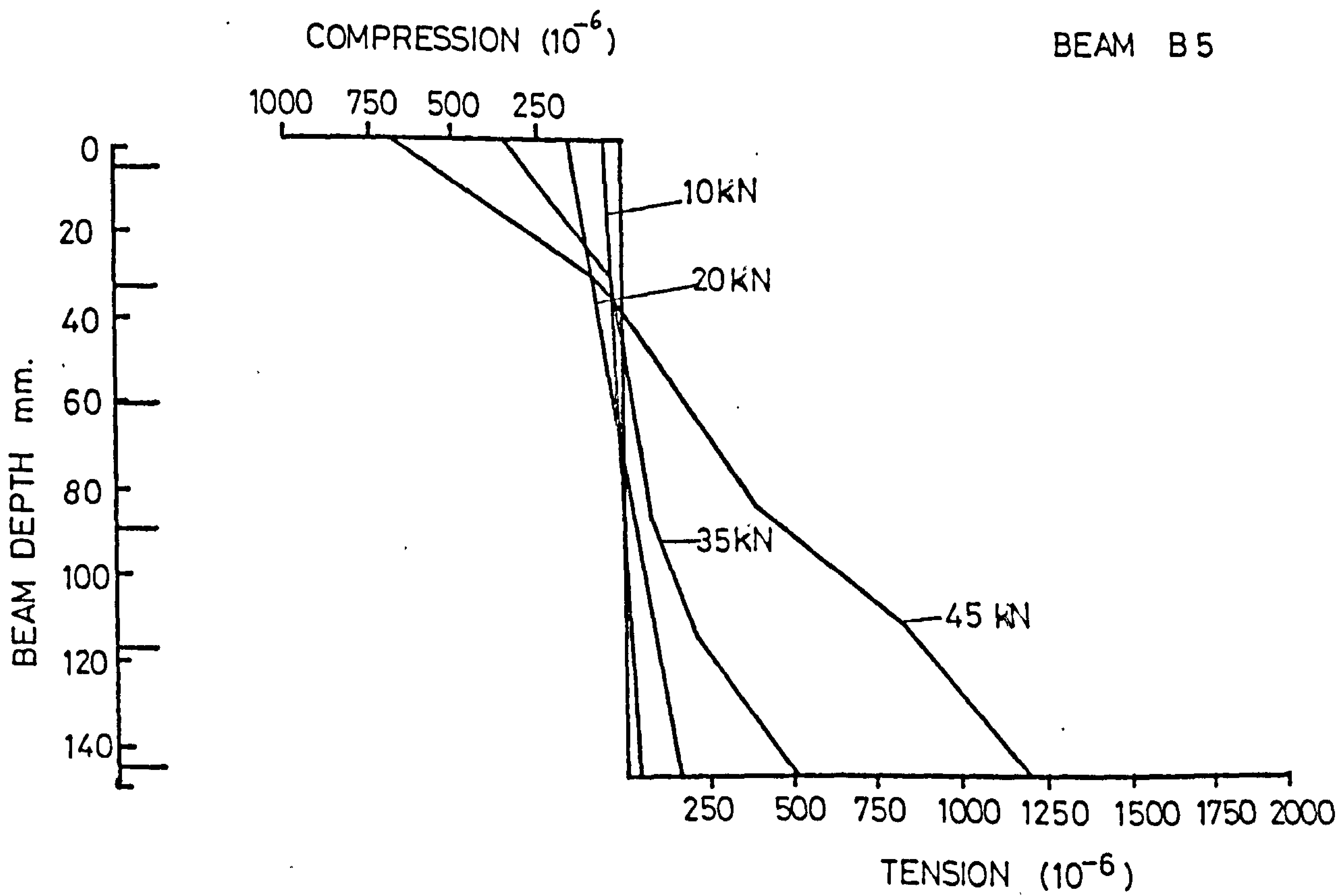

FIGURE 4·7 TYPICAL STRAIN DISTRIBUTIONS

linear at low loads, became increasingly non-linear at higher loads due to cracking. Within the limits of experimentation, Fig. 4.7 confirms that the assumption that plane sections remain plane is valid for plated beams as well. As expected, the strain distributions showed a movement of the neutral axis towards the compression face as the loading approached failure.

The variation of strain in the steel plate at mid-span is shown in Figs. 4.8 and 4.9 for series A and Figs. 4.10 and 4.11 for series B. Bearing in mind that the steel plates used for the series A and B are of low yield strength (125 N/mm^2), Figs. 4.8 - 4.11 show that the plates were well past the yielding stage, at failure, in all the beams tested in the two series. The steel strains in beams A2, A4 and A6 showed trends similar to the deflection curves shown in Fig. 4.4 and confirm the behaviour discussed earlier. In the series B, the beam B10 with notches on the tension side showed better behaviour than beams B2 and B4 (cf. Fig. 4.6).

4.2.2 Modes of Failure

The first crack in all the beams occurred in the concrete in the tension zone above the glue and the plate. With increase in load, additional cracks formed but only one major crack extended into the compression zone. Because of the lack of internal tensile reinforcement, no extensive tensile concrete cracking was observed. Generally two or three cracks formed in the shorter beams of series A, whereas in the longer beams of series B, only one or two cracks were in evidence; in all cases only one major crack developed leading to a simple tensile failure.

All the beams, except beam A3, failed by tensile yielding of the steel sheet followed by vertical (or nearly vertical) crack propagation towards the central loading point (Plates 4.1 and 4.2). Failure in all the beams was initiated by vertical cracking of the glue layer at a position coincident with the largest concrete crack. Yielding then commenced and local debonding of the plate occurred in the vicinity of the failure plane and the concrete crack propagated up to the load point leading to failure.

In the shorter beams the failure plane sometimes developed along a shear

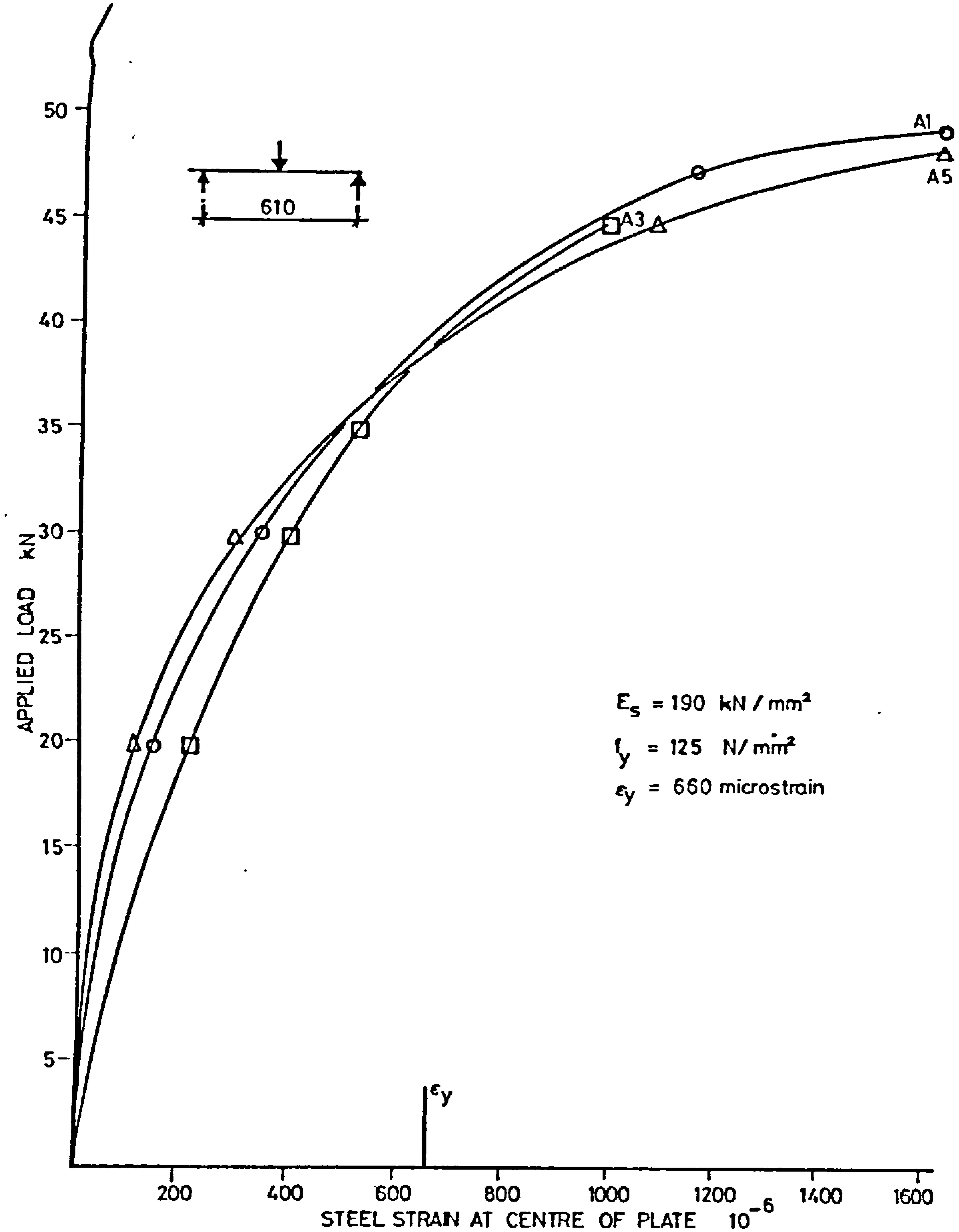

FIGURE 4·8 LOAD-STRAIN CURVES : SERIES A

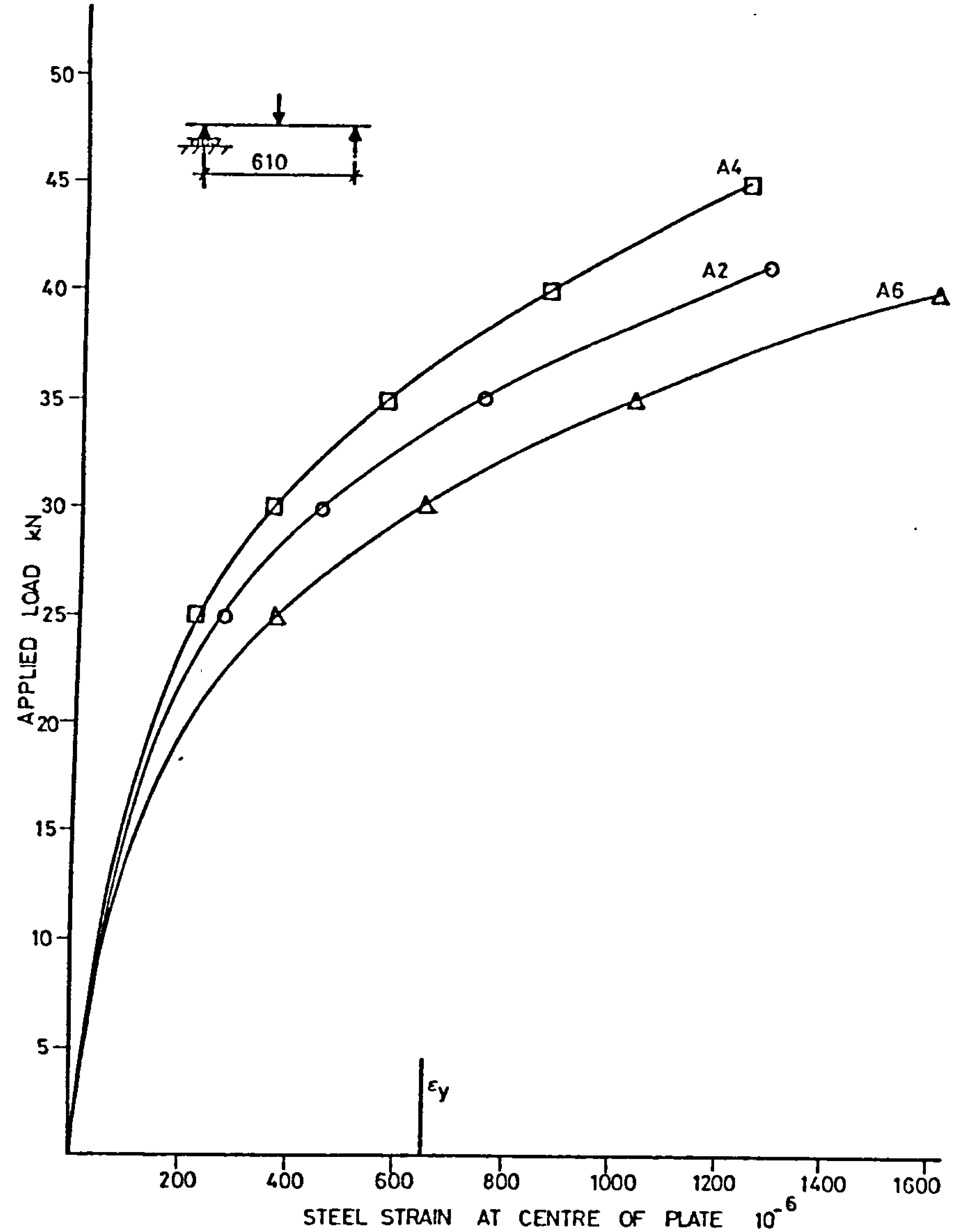

FIGURE 4·9 LOAD - STRAIN CURVES : SERIES A

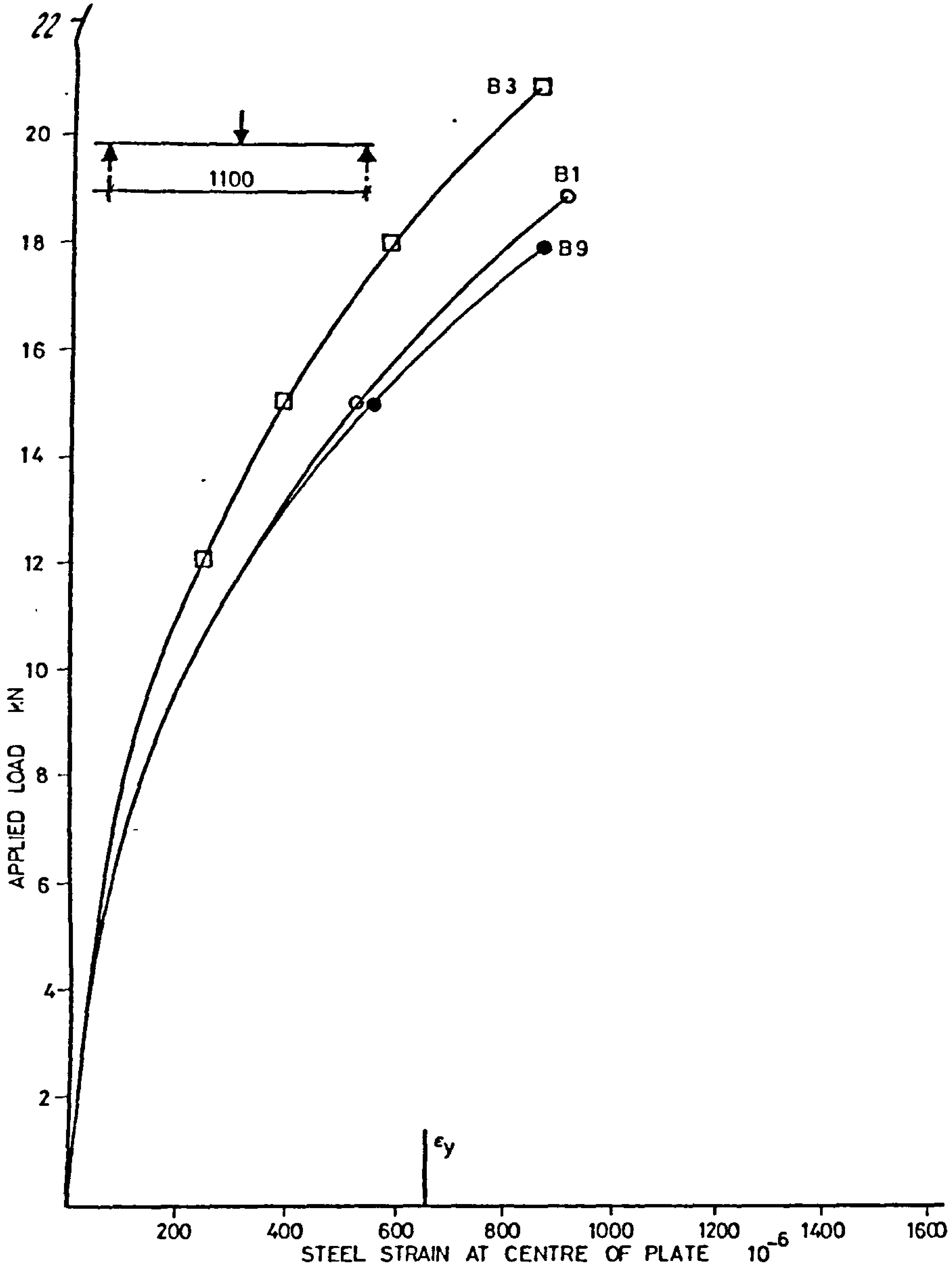

FIGURE 4·10 LOAD - STRAIN CURVES : SERIES B

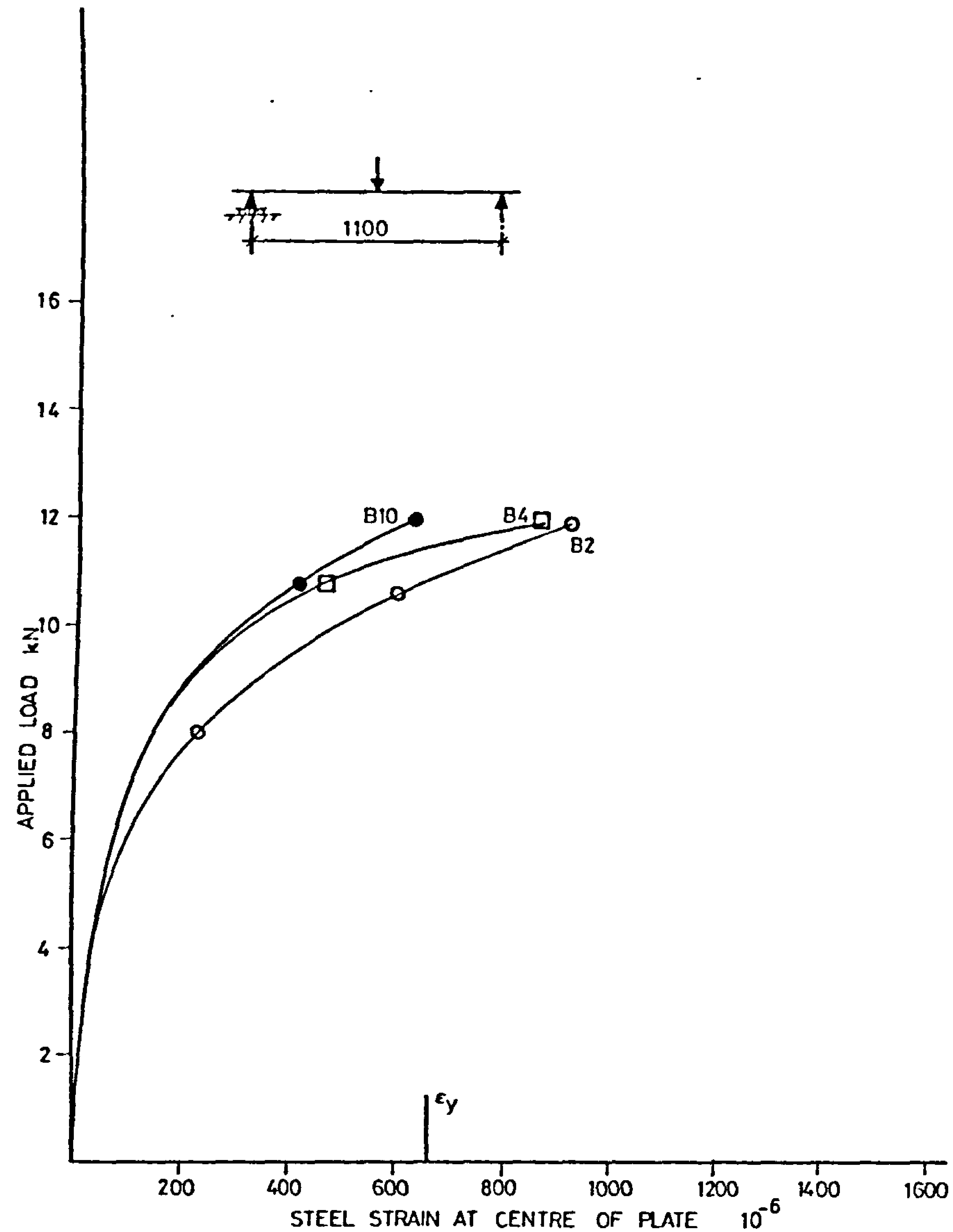

FIGURE 4·11 LOAD - STRAIN CURVES : SERIES B crack (due to short shear span), whereas in the longer beams, the cracks were generally vertical. Extensive concrete crushing never occurred, and although the strains, recorded at about 80-95% of the ultimate load, were only about 600-800 x 10^{-6} m/m, severe strain concentration and signs of crushing occurred locally above the failure crack.

Beam A3 showed extensive debonding of the plate (Plate 4.1), and this was found to be due to the presence of large air voids in the glue line, which had reduced the bonded cross-section by about 50%. However, the beam failed at 94% of the ultimate load for a similar correctly bonded beam.

4.2.3 First Crack and Ultimate Loads

Tables 4.3 and 4.4 show the theoretical and experimental first crack and ultimate loads of all the beams tested in series A and B respectively.

The experimental first crack loads relate to the visually observed cracks both in concrete and in the glue. The latter is necessarily more approximate as the observation is confined to a thin strip equal to the glue thickness. The theoretical first crack load in concrete is based on an uncracked transformed (composite) section with an E value for the glue of 6 kN/mm^2. The theoretical first crack load in the glue is based on a cracked transformed (composite) section, assuming a tensile strength of 60 N/mm^2 in the glue. These values were as supplied by the manufacturer. After the preliminary test series was complete further tests were performed on the glue as described in Chapter 3. Tables 4.5 and 4.6 show the corresponding values to Tables 4.3 and 4.4, but using the values of E = 2 kN/mm^2 and tensile strength of 16 N/mm^2 as determined experimentally. Sample calculations for first crack and failure loads are given in Appendix 3.

The results show that the theoretically predicted first crack loads in the concrete consistently underestimate the experimental loads. It is likely that the latter is slightly overestimated as they are based on visual examination, but even then the composite effect on delaying the formation of the first crack in the concrete is clear. The theoretical first crack loads in the glue show good agreement with experimental values when assuming 60 N/mm^2 for the glue's

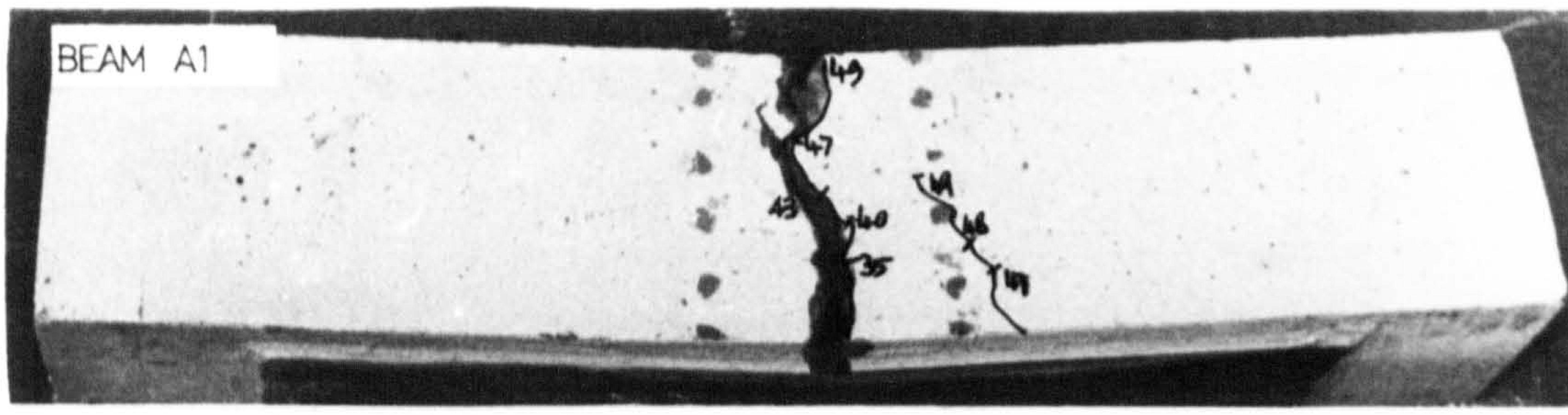

uniform glue (A) thickness, no shear reinforcement.

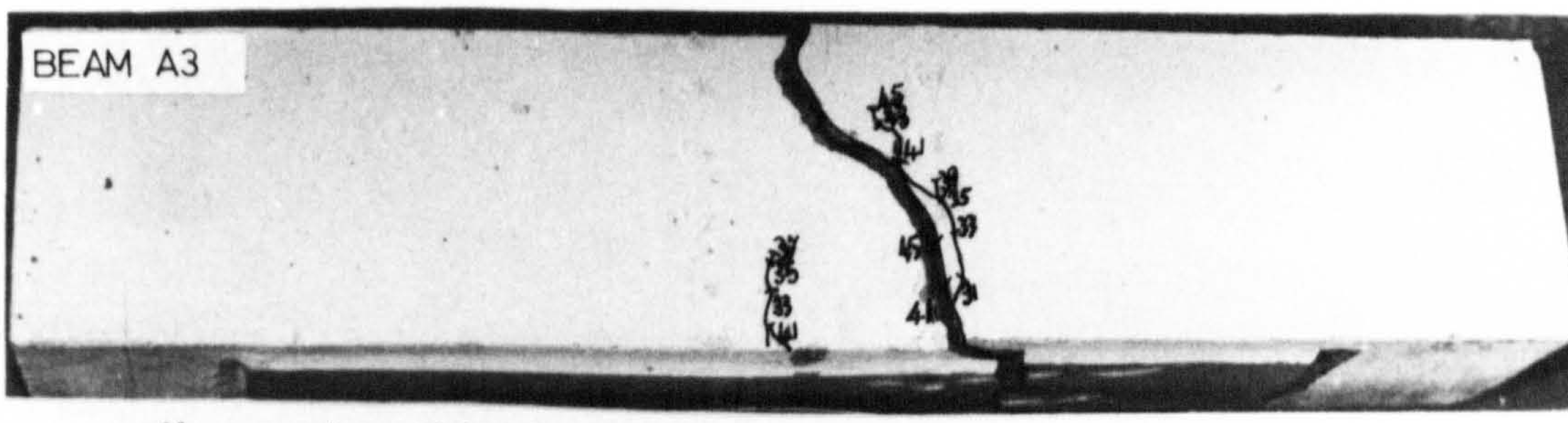

uniform glue (A) thickness, shear reinforcement at supports.

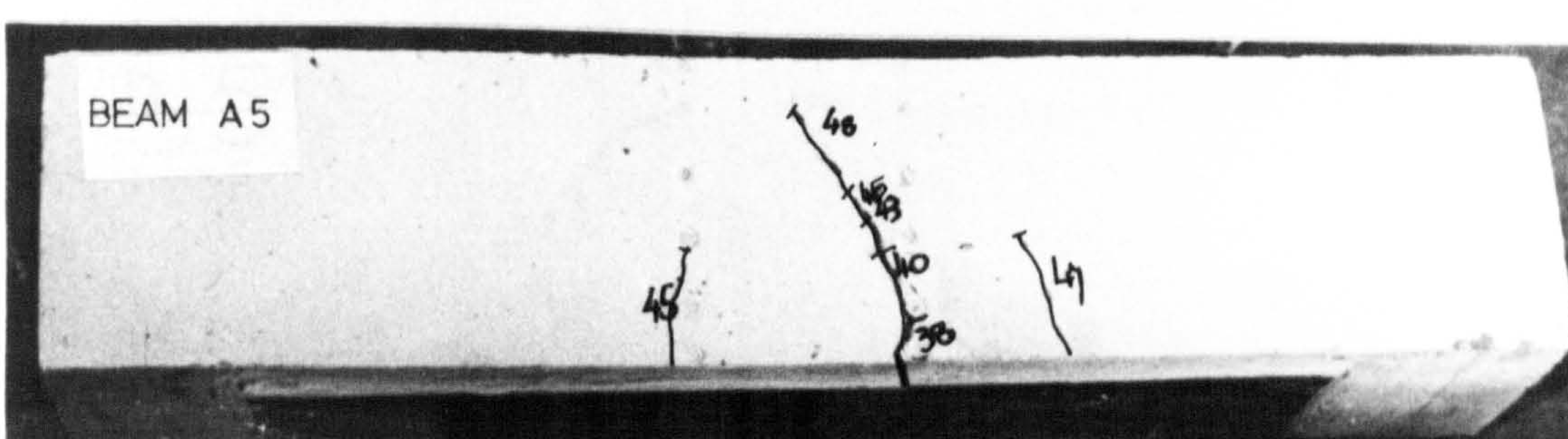

tapering glue (A) thickness, shear reinforcement at supports.

PLATE 4.1 TYPICAL BEAMS AFTER FAILURE : SERIES A

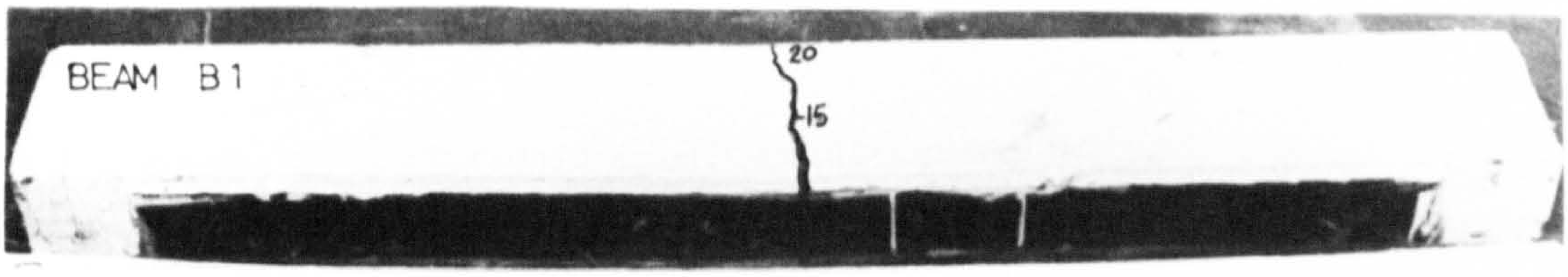

uniform glue (A) thickness,

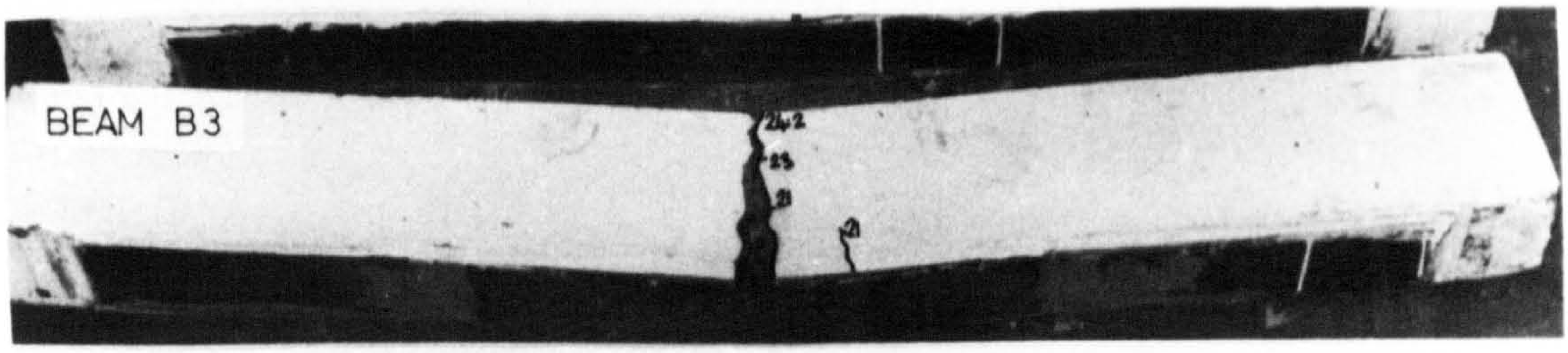

uniform glue (A) thickness, lapped plates.

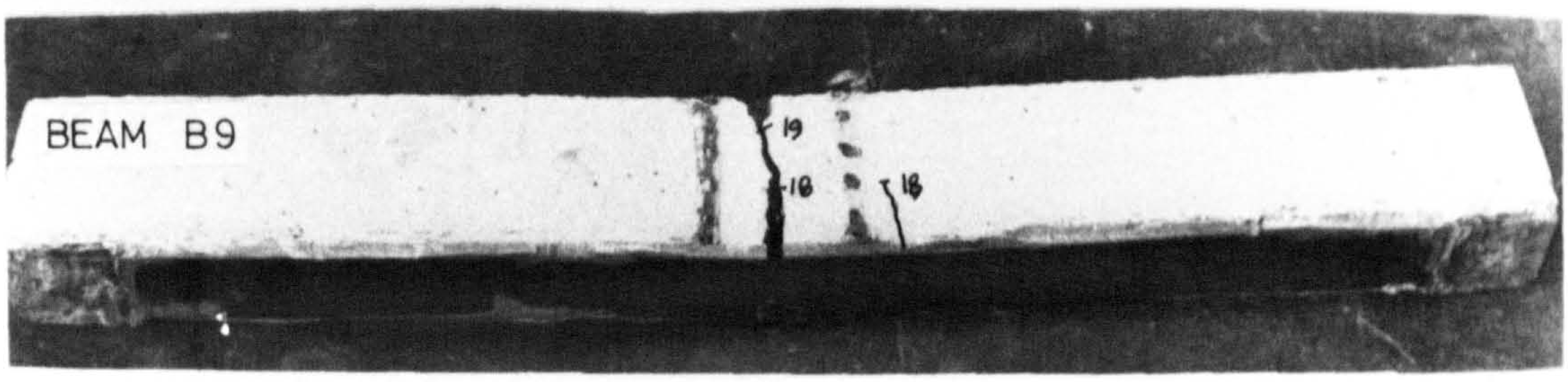

glue (A) thickness varies, notched beam.

PLATE 4·2 TYPICAL BEAMS AFTER FAILURE : SERIES B

TABLE 4·3 TEST RESULTS FOR PLAIN CONCRETE BEAMS : SERIES A

BEAM MK. No.	CONCRETE FIRST CRACK MOMENT			GLUE FIRST CRACK MOMENT			FAILURE MOMENTS						
											RATIOS		
	THEORY[a] kNm	TEST kNm	RATIO TEST/THEORY	THEORY[b] kNm	TEST kNm	RATIO TEST/THEORY	THEORY[c] kNm	THEORY[d] kNm	THEORY[e] kNm	TEST kNm	TEST/ THEORY	TEST/ THEORY	TEST/ THEORY
A1	3·06	4·45	1·45	5·59	5·15	0·92	5·54	5·64	2·05	5·71	1·03	1·01	2·79
A2	3·06	4·81	1·57	5·59	5·32	0·95	5·99	6·10	2·05	6·43	1·08	1·06	3·14
A3	3·06	4·00	1·29	5·59	4·24	0·76	5·08	5·19	2·04	5·34	1·05	1·03	2·61
A4	3·06	5·00	1·63	5·59	5·32	0·95	6·46	6·56	2·07	6·87	1·06	1·05	3·32
A5	3·06	4·90	1·58	5·59	4·81	0·86	5·36	5·46	2·05	5·60	1·05	1·03	2·73
A6	3·06	4·27	1·37	5·59	4·56	0·82	5·09	5·20	2·05	5·95	1·17	1·14	2·90
A7	–	2·02	–	–	–	–	2·56	2·56	2·56	2·02	0·79	0·79	0·79
A8	–	2·82	–	–	–	–	2·89	2·89	2·89	2·82	0·98	0·98	0·98

a – based on uncracked transformed section, E glue = 6000 N/mm^2

b – based on cracked transformed section, tensile strength of glue = 60 N/mm^2

c – based on yield stress of plate, plus tensile strength of glue.

d – based on ultimate stress of plate, plus tensile strength of glue.

e – based on ultimate stress of plate, no tensile strength of glue.

TABLE 4·4 TEST RESULTS FOR PLAIN CONCRETE BEAMS : SERIES B

BEAM MK No.	CONCRETE FIRST CRACK MOMENTS			GLUE FIRST CRACK MOMENTS			FAILURE MOMENTS						
	THEORY[a] kNm	TEST kNm	RATIO TEST/THEORY	THEORY[b] kNm	TEST kNm	RATIO TEST/THEORY	THEORY[c] kNm	THEORY[d] kNm	THEORY[e] kNm	TEST KNm	RATIOS TEST/THEORY	TEST/THEORY	TEST/THEORY
B1	2·20	3·58	1·63	3·98	4·18	1·07	3·81	3·89	1·53	4·74	1·24	1·22	3·09
B2	2·20	3·03	1·38	3·98	3·30	0·83	3·47	3·54	1·53	4·13	1·18	1·16	2·70
B3	2·20	4·97	2·26	3·98	4·18	1·07	4·83	4·91	1·56	5·73	1·18	1·17	3·71
B4	2·20	3·30	1·50	3·98	3·30	0·83	3·47	3·55	1·52	4·57	1·31	1·29	2·99
B5	-	1·84	-	-	-	-	1·97	1·97	1·97	1·90	0·96	0·96	0·96
B6	-	2·16	-	-	-	-	1·98	1·98	1·98	2·16	1·09	1·09	1·09
B7	-	1·61	-	-	-	-	1·91	1·91	1·97	1·66	0·84	0·84	0·84
B8	-	2·10	-	-	-	-	1·98	1·98	1·98	2·16	1·09	1·09	1·09
B9	2·20	4·30	1·96	3·98	3·56	0·89	3·82	3·90	1·54	4·70	1·23	1·21	3·06
B10	2·20	3·30	1·50	3·98	3·98	1·00	3·47	3·55	1·52	4·26	1·23	1·20	2·81

a - based on uncracked transformed section, E glue = 6000 N/mm^2
b - based on cracked transformed section, tensile strength of glue = 60 N/mm^2

c - based on yield stress of plate, plus tensile strength of glue.
d - based on ultimate stress of plate, plus tensile strength of glue.
e - based on ultimate stress of plate, no tensile strength in glue.

TABLE 4·5 TEST RESULTS FOR PLAIN CONCRETE BEAMS : SERIES A

BEAM MK. No.	GLUE FIRST CRACK MOMENTS			FAILURE MOMENTS						
	THEORY b. kNm	TEST kNm	RATIO TEST / THEORY	THEORY c. kNm	THEORY d. kNm	THEORY e. kNm	TEST kNm	RATIOS		
								TEST/ THEORY	TEST/ THEORY	TEST/ THEORY
A1	1·40	5·15	3·68	2·91	3·02	2·05	5·71	1·96	1·89	2·79
A2	1·40	5·32	3·80	3·04	3·15	2·05	6·43	2·12	2·04	3·14
A3	1·40	4·24	3·02	2·78	2·89	2·04	5·34	1·92	1·85	2·61
A4	1·40	5·32	3·80	3·17	3·28	2·07	6·87	2·17	2·09	3·32
A5	1·40	4·81	3·44	2·86	2·97	2·05	5·60	1·96	1·89	2·73
A6	1·40	4·56	3·26	2·91	3·02	2·05	5·95	2·04	1·97	2·90
A7&8	as on	table	4·3							

TABLE 4·6 TEST RESULTS FOR PLAIN CONCRETE BEAMS : SERIES B

BEAM MK. No.	GLUE FIRST CRACK MOMENTS			FAILURE MOMENTS						
	THEORY b. kNm	TEST kNm	RATIO TEST / THEORY	THEORY c. kNm	THEORY d. kNm	THEORY e. kNm	TEST kNm	RATIOS		
								TEST/ THEORY	TEST/ THEORY	TEST/ THEORY
B1	1·10	4·18	3·80	2·09	2·17	1·53	4·74	2·27	2·18	3·09
B2	1·10	3·30	3·00	1·99	2·07	1·53	4·13	2·08	2·00	2·70
B3	1·10	4·18	3·80	2·38	2·46	1·54	5·73	2·41	2·33	3·71
B4	1·10	3·30	3·00	1·99	2·07	1·52	4·57	2·30	2·21	2·99
B5 - B8	as on	table	4·4							
B9	1·10	3·56	3·24	2·09	2·17	1·54	4·70	2·25	2·17	3·06
B10	1·10	3·98	3·61	1·99	2·07	1·52	4·26	2·14	2·06	2·81

b – based on cracked transformed section, E glue 2000 N/mm^2, tensile strength glue 16 N/mm^2.
c – based on yield stress of plate, plus tensile strength of glue (16 N/mm^2).
d – based on ultimate stress of plate, = = = = =
e – = = = = = = no tensile strength in glue.

tensile strength but when assuming 16 N/mm^2 the theoretical loads are below the first crack load in the concrete which is not possible!

The theoretical ultimate failure loads shown in Tables 4.3 and 4.4 are based on a rectangular stress block for the concrete in compression with a stress value of 0.6 fcu. Three stress distributions in the tension zone are considered as detailed in Appendix 3. The results suggest that the computations based on the ultimate strength of the plate and including the force in the glue give results closest to experimental values. It appears that although the plates did not fracture, considerable straining had taken place at crack positions leading to large interface shear strains and strain hardening of the steel. This, together with the spread of yield of the plate at each side of a crack, leads to local debonding.

The theoretical first crack and failure loads given in Tables 4.5 and 4.6 show poor agreement with experimental values. It would appear that although the glue tests gave a tensile strength of 16 N/mm^2, the actual tensile properties are different when the glue is acting compositely with the steel plate and concrete beam. The experimental failure moments were all almost twice the theoretical values assuming 16 N/mm^2 for the glue tensile strength (Tables 4.5 and 4.6).

4.3 CONCLUSIONS

From the results reported in this chapter, the following conclusions can be drawn. It is emphasised that these conclusions are limited to the variables studied here.

The use of external reinforcement in the form of steel plates glued to the tension face of plain concrete beams has the following effects:

(a) it increases the range of elastic behaviour

(b) for a given load, it reduces the tensile strains in the concrete, due to the composite action of the concrete, glue and steel plate, compared to those in unplated beams

(c) it delays the appearance of the first visual cracks with a resulting increase in service loads

(d) it increases flexural stiffness throughout loading and thus reduces deflections at corresponding loads

(e) it enhances the ultimate flexural capacity

(f) it increases the ductility at failure.

For a constant plate area, the stiffness of the beams increased as glue thickness increased. Lapping plates increased stiffness compared to a corresponding beam with a continuous plate, probably due to the increase in lever arm. Strain measurements showed that plane sections remained plane throughout loading, above the neutral axis. Below the neutral axis it was linear with some beams and irregular with others. This is because once the beam has cracked, the strain gauge reading is not the true strain, but is an average strain which depends on the position of the cracks.

For the variables studied in this series it was found that in plain concrete beams, with reinforcing plates of low yield strength, the glue makes a significant contribution to the ultimate strength of the composite section. The values of first crack load in the glue and the ultimate load, based on experimentally determined glue properties, were far below those observed in the tests. This suggests that the glue exhibits properties, when acting compositely with the steel and concrete, different from those found by testing samples of glue in unrestrained tests. However, further tests would be needed to confirm this.

The results indicate that the glue cannot be cracked at failure because if it were then the theoretical failure loads would be approximately half of the values found by experiment. There was, however, some evidence of surface cracking in the glue approaching failure.

It was interesting to find that even when large voids were present in the glue line, up to 50% of the width at the critical section in beam A3, the beam was able to sustain 94% of the load achieved by a similar beam with no voids in the glue.

Experience with the preparation of the steel and concrete surfaces gained from these tests emphasises the need for care at all stages. With plates only

1.5 mm thick it was essential to grit blast both sides of the plates to prevent warping. Applying the glue to both concrete and plate minimises voids at the interfaces and confines them to the body of the glue where they are less critical.

CHAPTER 5

STRENGTH PROPERTIES

5.1 INTRODUCTION

The performance of a structure is determined by the behaviour of its component members which in turn depend on the properties of the materials and the methods adopted for their design.

Plain concrete has low tensile strength and little resistance to crack propagation. Flaws or microcracks develop in the material during manufacture, even before any external load is applied, due to inherent volumetric and micro-structural changes. The poor tensile strength is due to the enlargement and propagation of the internal flaws which lead to brittle fracture on loading.

In order to use concrete in a load-bearing element, it is necessary to impart tensile resistance properties to it. The use of reinforcing bars provides tensile strength in a structural member but does not increase the tensile strength of the concrete itself. For this reason it has become practice, since the establishment of reinforced concrete design techniques, to ignore the tensile strength of the concrete when estimating the flexural strength of a member.

The present trend towards using high strength materials, refined design techniques and slender members produces structures in which the serviceability conditions may be more critical than strength considerations. Codes of practice recommend that the width of surface cracks, and magnitude of deflections at service loads should not exceed certain limits, which are based on criteria such as corrosion, aesthetics or damage to non-structural elements.

The preliminary test series showed the effects of external reinforcement on plain concrete beams. It should therefore follow, that the addition of a bonded steel plate to the tensile face of a reinforced concrete member should result in:

(a) producing higher cracking loads

(b) a more even distribution of cracking

(c) a reduced crack propagation

(d) reduced deformations, i.e. rotation, deflection, strains etc.

throughout the loading, up to failure.

This part of the investigation compares the experimental first crack, service and ultimate loads with those calculated by accepted methods. The increase in service load of the plated beams, above that of the unplated beam, is studied, using as a basis the different criteria of deflections, rotations, crack width and steel bar strains.

5.2 EXPERIMENTAL PROGRAMME

Previous work (54-73) has shown external bonding of steel plates onto reinforced concrete beams to be effective in controlling deformations and increasing post cracking stiffness of flexural members.

Twenty four beams were tested in this series. The main variables were glue thickness; plate thickness and lapping techniques. Details of the beams are given in Table 5.1 and the properties of the materials used were described in Chapter 4.

Three glue thicknesses were used, beams 203 to 206 had a 1.5 mm thick adhesive layer; beams 207 to 215 had a 3 mm thick adhesive layer and beams 216 to 219 had a 6 mm thick layer. For each thickness of glue three thicknesses of plate were used; beams 203, 207, 211, 212 and 216 had 1.5 mm thick plate; beams 204, 208, 215 and 217 had 3 mm thick plate; and beams 205, 209, 210, 218 and 219 had 6 mm thick plate.

Beams 206, 213 and 214 had two layers of 1.5 mm thick plate for comparison with beams with a single layer of 3 mm plate.

Beams 211, 212, 213, 214 and 215 had laps in their plates for comparison with beams having continuous layers of plate.

Beams 222 to 224 were preloaded and cracked before their plates were bonded on.

Beam 220 had an adhesive layer of variable thickness, 3 mm to 8 mm, along its length.

Beam 221 had 'V' notches cut in its tension face, at the loading points, to produce points of stress concentration.

Beam 202 had an adhesive layer 3 mm thick, but without a plate, to investigate cracking of the glue.

Beam 201 was unreinforced externally, having neither glue nor plate and was used for comparison.

The beams were all identical in size: 155 mm wide, 255 mm deep and 2.5 m long. All beams were tested under four point bending on a span of 2.3 m. Stirrups, 6 mm diameter at 75 mm centres, were provided in the shear spans to prevent shear failure. The beam details and instrumentation are shown in Figs. 5.1 and 5.2.

5.3 TEST PROCEDURE

The beams were manufactured from the same materials and in the same manner as in the preliminary test series described in Chapter 4, with three control cubes for compressive strength and three 100 x 100 x 500 mm prisms for modulus of rupture testing, with each beam.

The beams and control specimens were stripped after 24 hours and cured in uncontrolled laboratory conditions.

After approximately fourteen days the beams were prepared for bonding as described in Chapter 4. The plates were degreased with trichlorethylene 24 hours prior to shotblasting. Because of the large size of the plates they had to be taken to a commercial shotblasting company where they were abraded with steel grit of 340 micron mean size, and then returned to the laboratory immediately for bonding to prevent surface corrosion and contamination. The mixing and bonding were carried out as described in Chapter 4. A minimum of 14 days was required between plating and testing.

Electrical resistance strain gauges of 7 mm gauge length were glued to the longitudinal bar reinforcement at three locations as shown in Fig. 5.2, one day prior to casting. Electrical resistance strain gauges of 6 mm gauge length were glued to the external reinforcing plates, after being bonded onto the beam, at locations as shown in Fig. 5.2.

The day prior to testing the beam was whitewashed to facilitate crack viewing. Demec discs were used to locate a mechanical extensometer on a base of 200 mm along the side of the beam at the centre section. The concrete surface was roughened and cleaned with acetone prior to gluing on the discs with 'Plastic

TABLE 5·1 DETAILS OF TEST BEAMS

BEAM NUMBER	201	202	203	204	205	206	207	208	209	210	211	212	213	214	215	216	217	218	219	220	221	222	223	224
Glue thickness mm.	–	3	1·5	1·5	1·5	1·5	3	3	3	3	3	3	3	3	3	6	6	6	6	2–8	3[1]	3	3	3
Plate thickness mm.	–	–	1·5	3	6	1·5	1·5	3	6	6	1·5	1·5	1·5	1·5	3	1·5	3	6	6	1·5	1·5	1·5	1·5	3
Number of plate layers	–	–	1	1	1	2[2]	1	1	1	1	1	1	2	2	1	1	1	1	1	1	1	1	1	1
Position of plate laps[3]	–	–	–	–	–	–	–	–	–	–	c	lp	c	lp	c	–	–	–	–	–	–	–	–	–
% load before plating	–	–	–	–	–	–	–	–	–	–	–	–	–	–	–	–	–	–	–	–	–	50	90	50
Cube strength N/mm^2	63·9	70·9	63·3	66·4	70·2	68·8	70·2	68·0	72·2	70·3	72·0	63·9	67·2	69·2	71·5	68·4	68·6	71·5	73·0	68·2	65·9	65·2	72·0	71·1
Modulus of rupture N/mm^2	5·47	5·61	5·48	5·50	5·52	5·50	5·56	5·50	5·51	5·51	5·61	5·45	5·48	5·51	5·60	5·52	5·50	5·60	5·68	5·50	5·49	5·46	5·65	5·60
Effective depth to bars. mm	220	220	220	220	220	220	220	220	220	220	220	220	220	220	220	220	220	220	220	220	220	220	220	220
Area of bars[4] mm^2	943	943	943	943	943	943	943	943	943	943	943	943	943	943	943	943	943	943	943	943	943	943	943	943
Area of plate[5] mm^2	–	–	187	375	750	375	187	375	750	750	187	187	375	375	375	187	375	750	750	187	187	187	187	375

(1) V Notches cut in the tension face of the beam to form stress concentrations above the load points.

(2) The second layer of plate was stopped 380 mm from the ends of the first layer.

(3) c – denotes central plate lap, lp – denotes laps above the load points.

(4) TORBAR characteristic strength 425 N/mm^2

(5) Plate = = = 250 N/mm^2

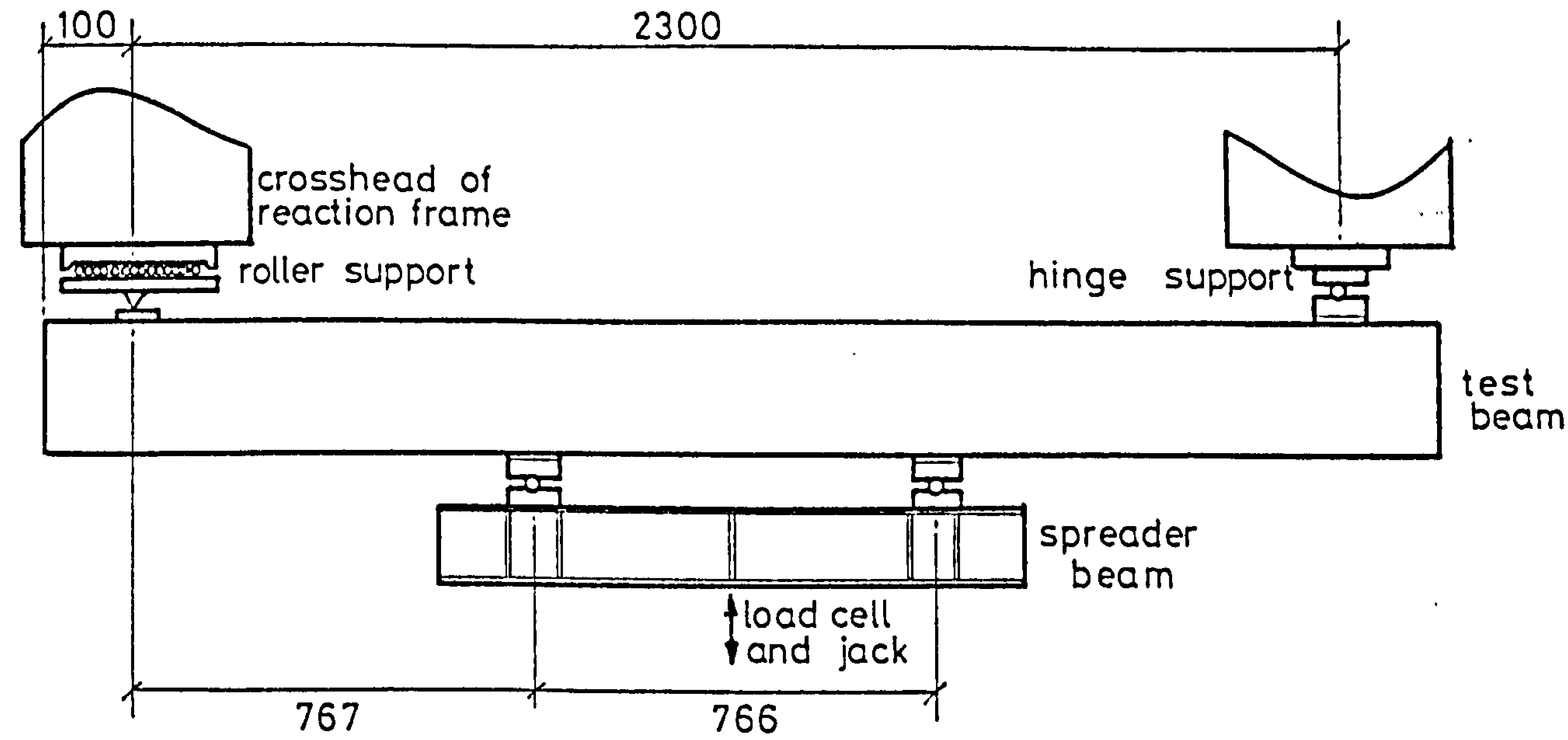

(a) LOADING RIG AND SUPPORT SYSTEM

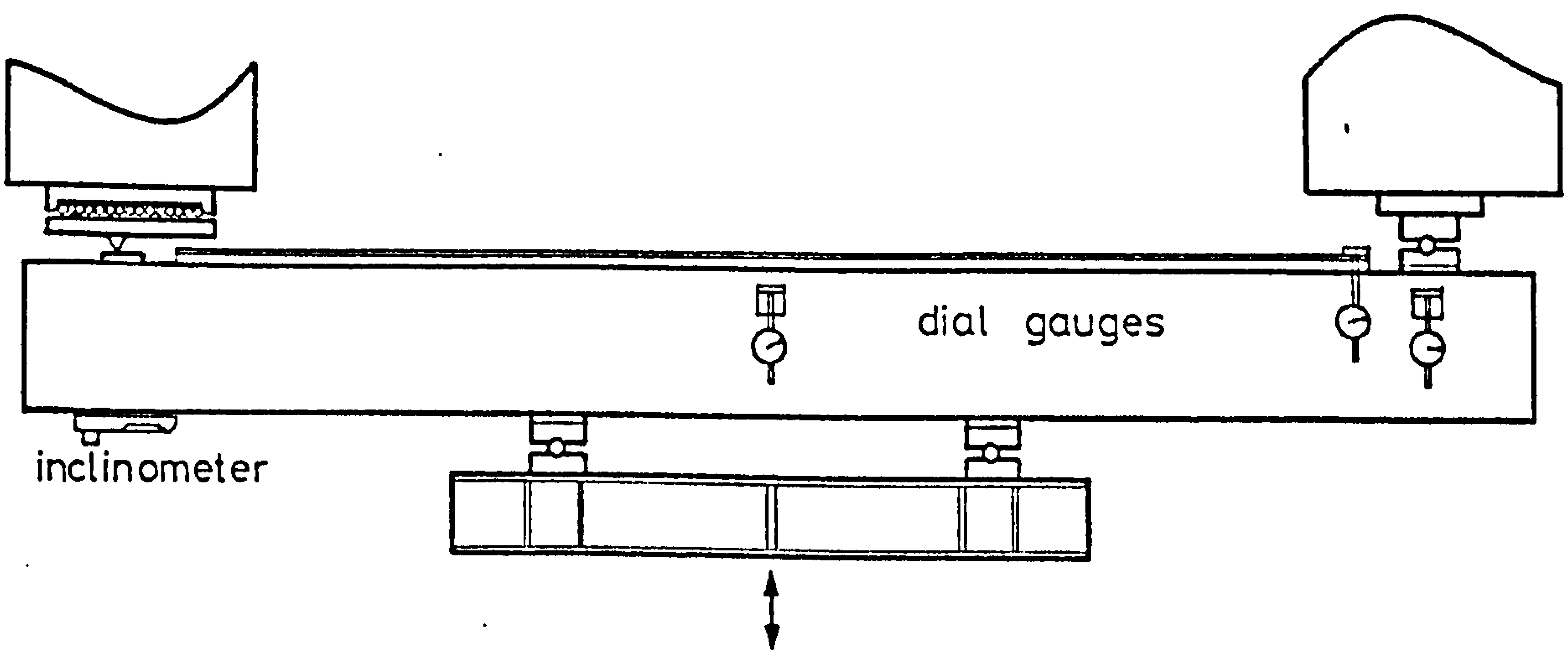

(b) MECHANICAL INSTRUMENTATION

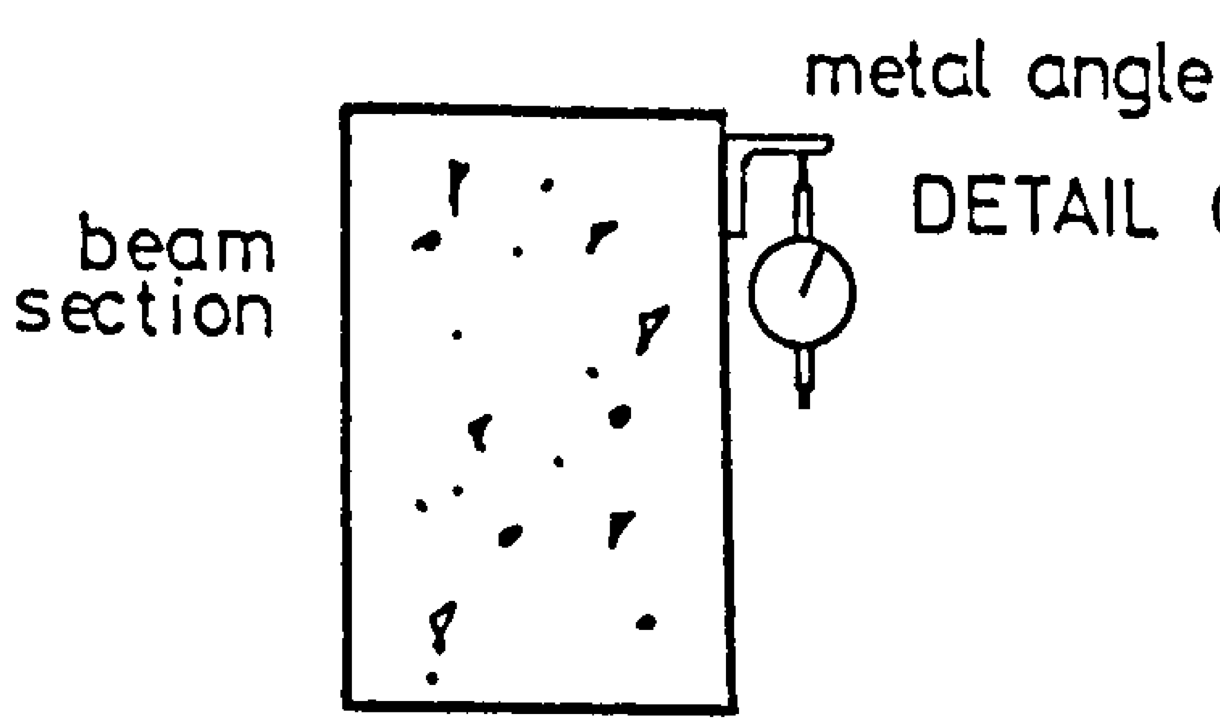

DETAIL ON DIAL GAUGE

FIGURE 5·1 LOADING RIG AND MECHANICAL INSTRUMENTATION

FIGURE 5·2 DETAILS OF REINFORCEMENT AND STRAIN GAUGE LOCATIONS

Padding'. In the first beam demec discs were stuck to both sides of the beam at midspan, but as the results showed the readings on each face to be consistent, in subsequent beams the discs were glued on one side only.

For measuring rotations, ball bearings resting on steel nuts were glued, 150 mm apart at the support and loading points. An inclinometer with one second divisions was used.

Deflections were measured at midspan and support with dial gauges having 0.01 mm divisions. On the plated beams the relative vertical movement of the plate to the beam was also measured. The location of dial gauges is shown in Fig. 5.1.

The beams were tested with their tension face uppermost to facilitate crack observation and measurements. Load was applied upwards at positions 383 mm on either side of midspan by means of a stiffened, 150 mm deep, wide flange spreader beam resting on a 50 ton capacity hand operated hydraulic jack at its mid point. The load was measured by a linear differential voltmeter and a calibrated load cell placed between the jack and the spreader beam. The ends of the beam were positioned between pairs of 35 mm diameter Macalloy bars up to crossheads that were secured at the top. One end was a fixed support and the other moving on rollers longitudinally. Both supports allowed rotation. The test rig is shown in Plate 5.1.

Load was applied gradually until the first crack appeared, which was detected visually using a magnifying glass. Load was then applied in increments up to failure. Each increment was approximately 12½% of the loading range. At each load stage the deflection; rotations; steel reinforcing bar and plate strains; concrete strains; crack width, spacing and height were measured and recorded.

The beams were loaded to failure in order to observe the mode of rupture of the plate/glue/concrete composite system. After failure the cracks were outlined by thick black marking pen and the beams were then photographed as shown in Plates 5.2 to 5.8.

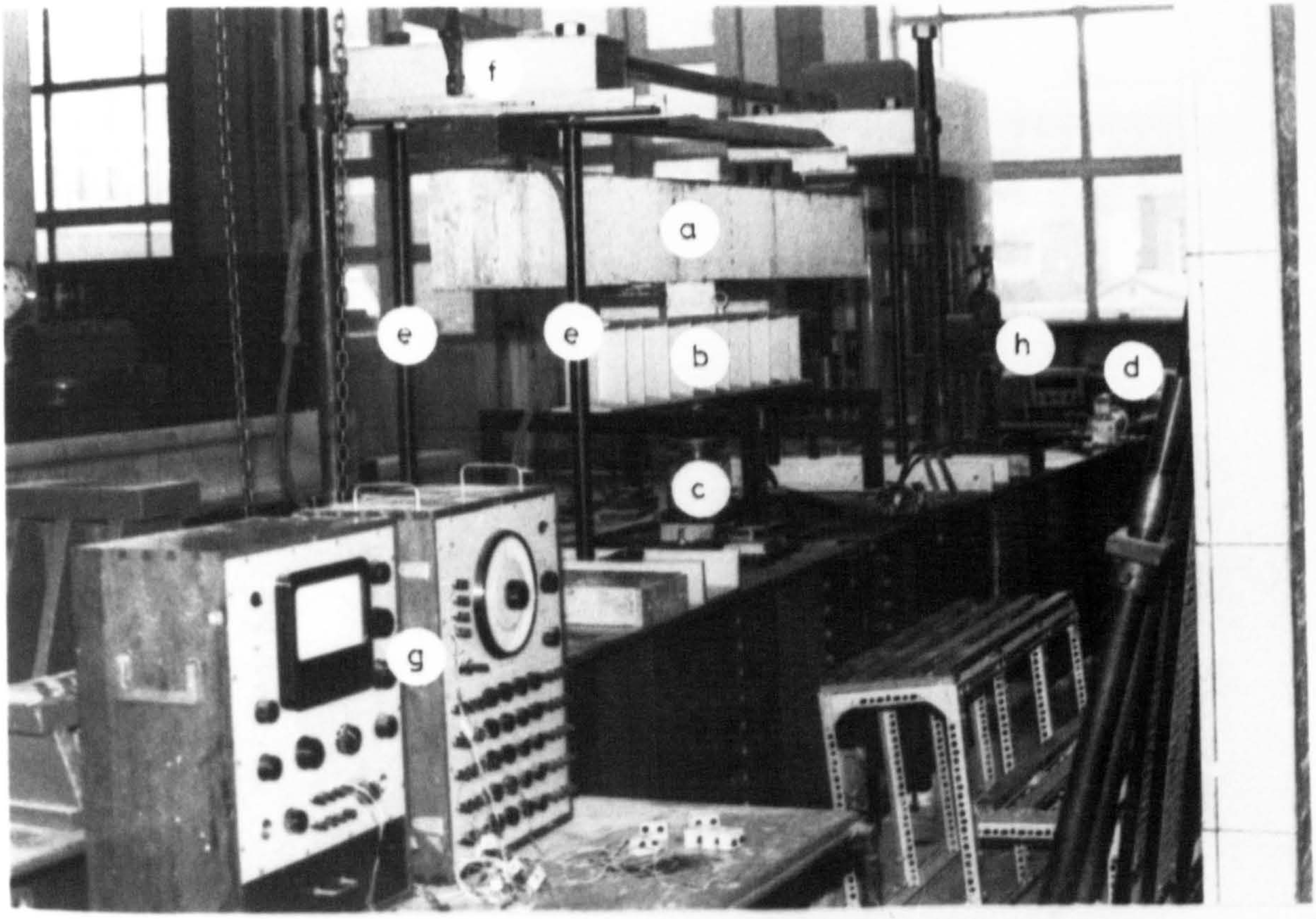

a - test beam
b - spreader beam
c - loading jack
d - hand pump
e - tie rods
f - crosshead
g - strain gauge apparatus
h - digital voltmeter

PLATE 5·1 LOADING ARRANGEMENT

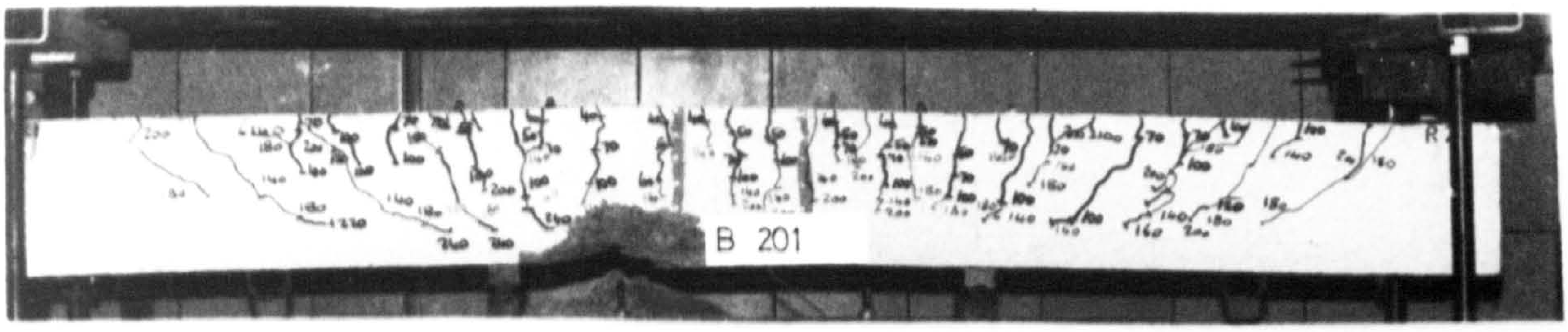

UNPLATED BEAM – noglue or plate.

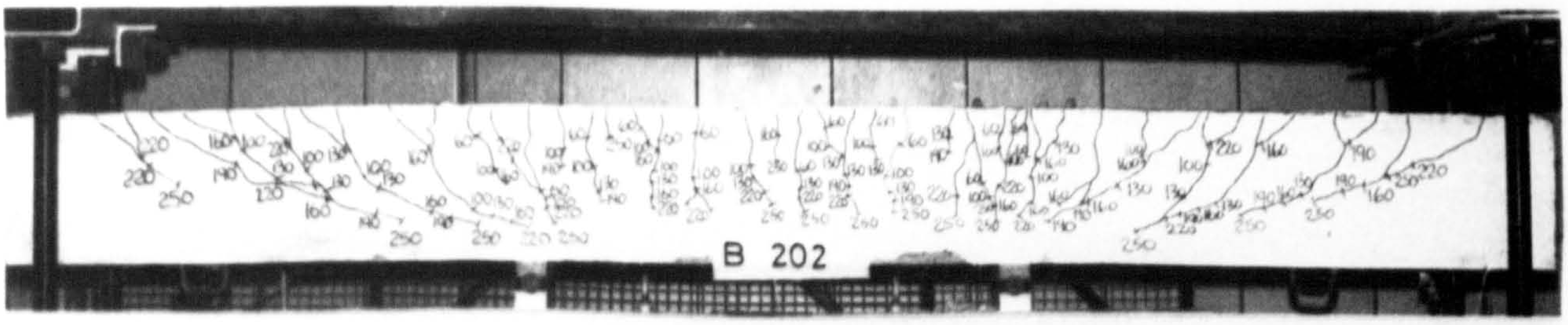

3mm glue thickness, no plate.

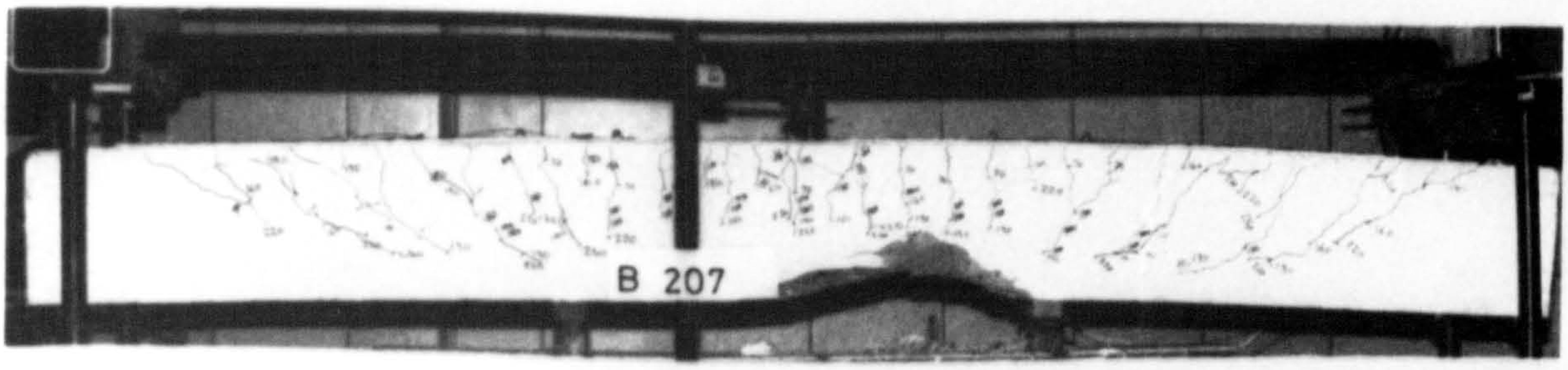

3mm glue thickness, 1·5mm plate thickness.

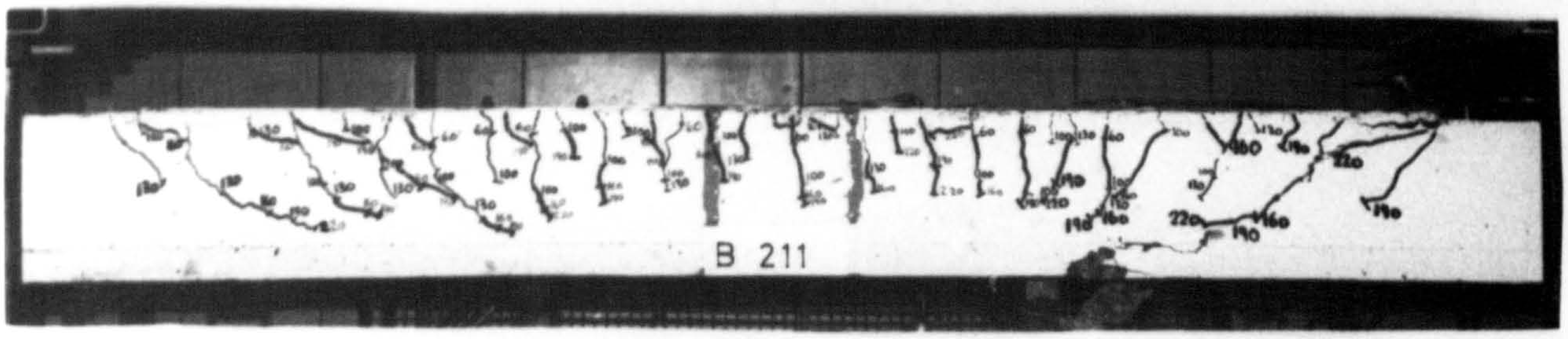

3mm glue thickness, 1·5 mm plate thickness, centre plate lap.

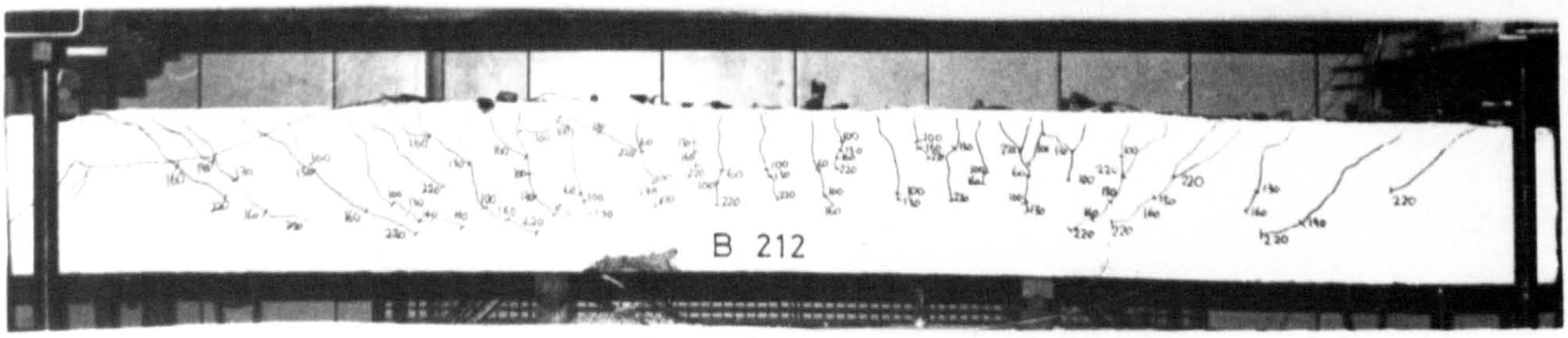

3mm glue thickness, 1·5 mm plate thickness, lapped plates above the load points.

PLATE 5·2 CRACK PATTERNS - PLATED AND UNPLATED BEAMS

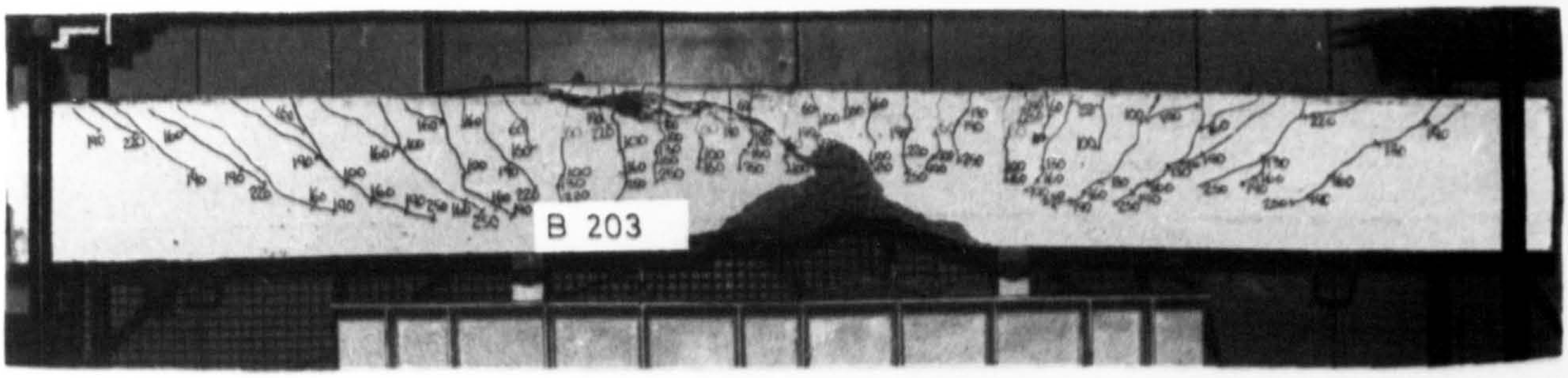

1.5mm plate thickness.

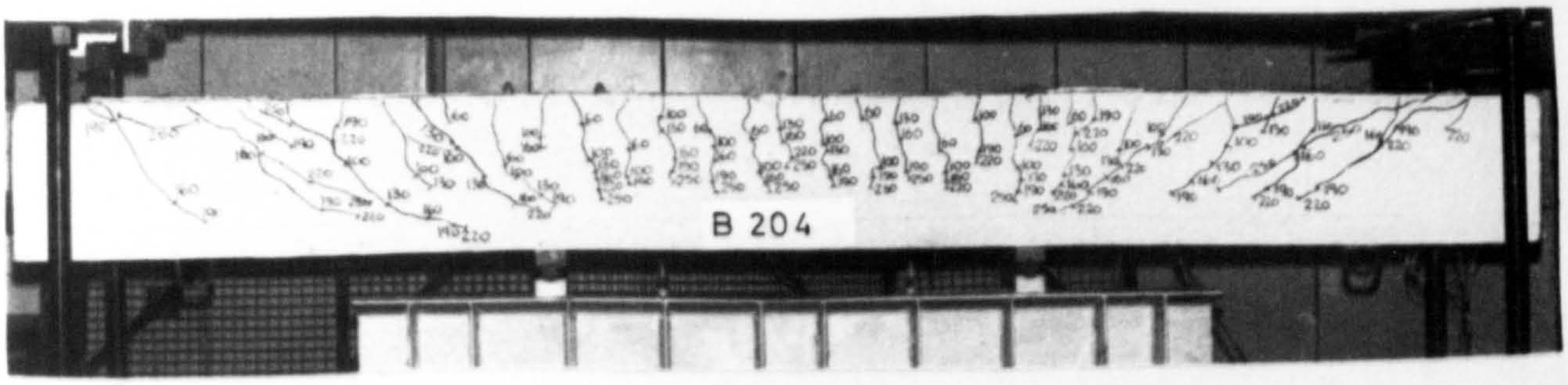

3mm plate thickness.

6mm plate thickness.

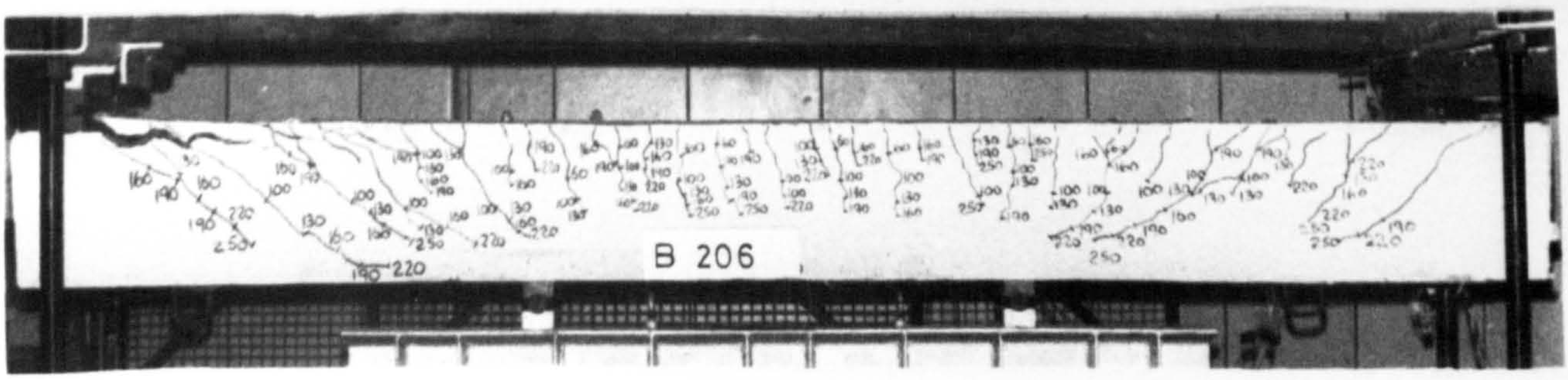

2 layers of 1.5mm plate.

PLATE 5.3 CRACK PATTERNS - BEAMS WITH 1.5mm GLUE THICKNESS.

1.5 mm plate thickness.

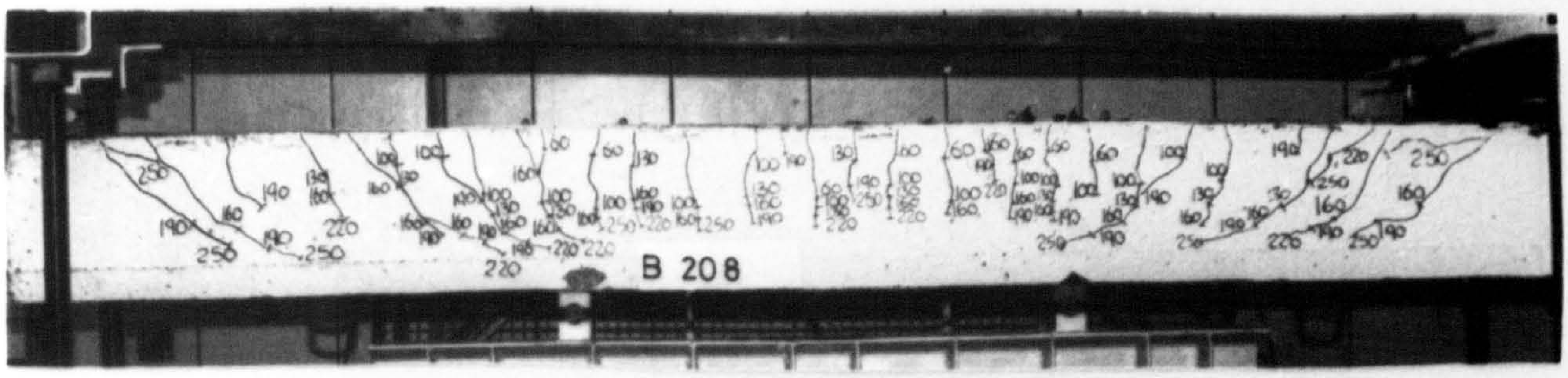

3mm plate thickness.

6mm plate thickness.

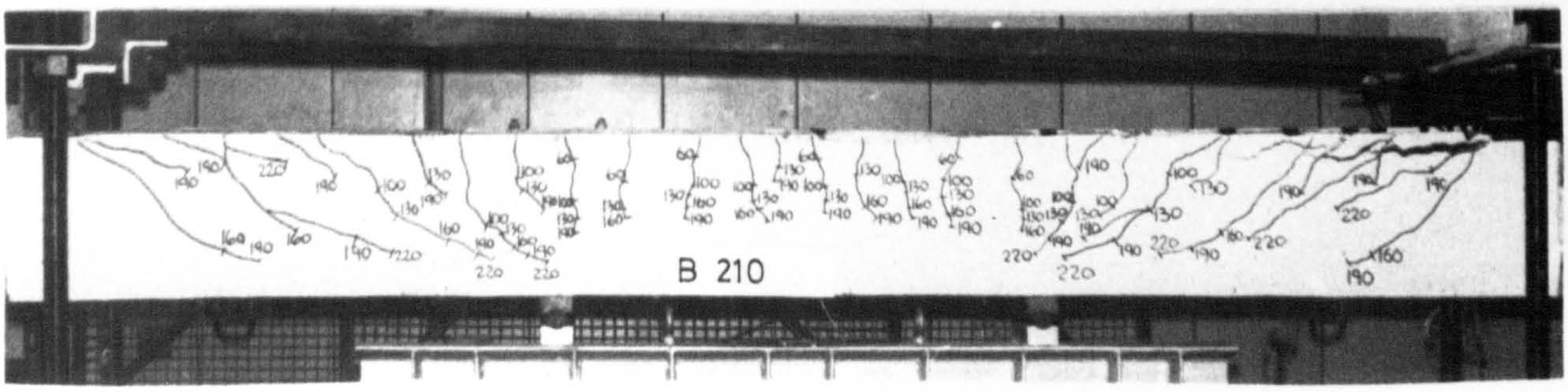

6mm plate thickness.

PLATE 5·4 CRACK PATTERNS - BEAMS WITH 3mm GLUE THICKNESS.

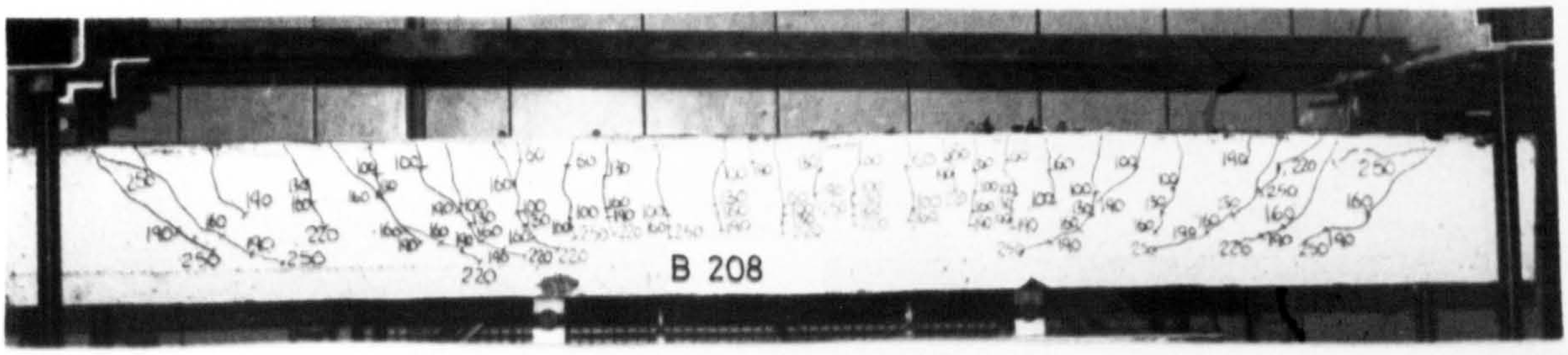

3mm plate thickness.

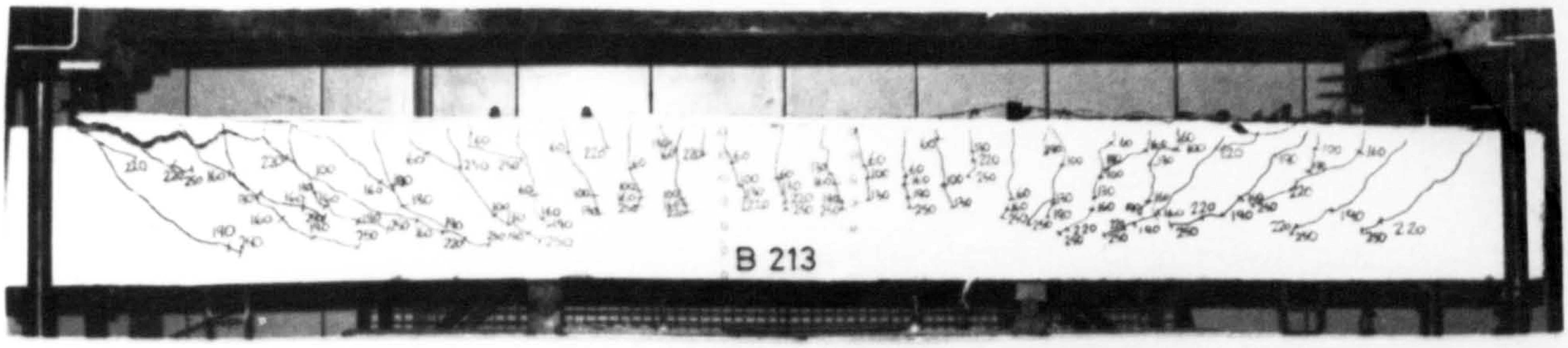

2 layers of 1·5mm plate, centre plate lap.

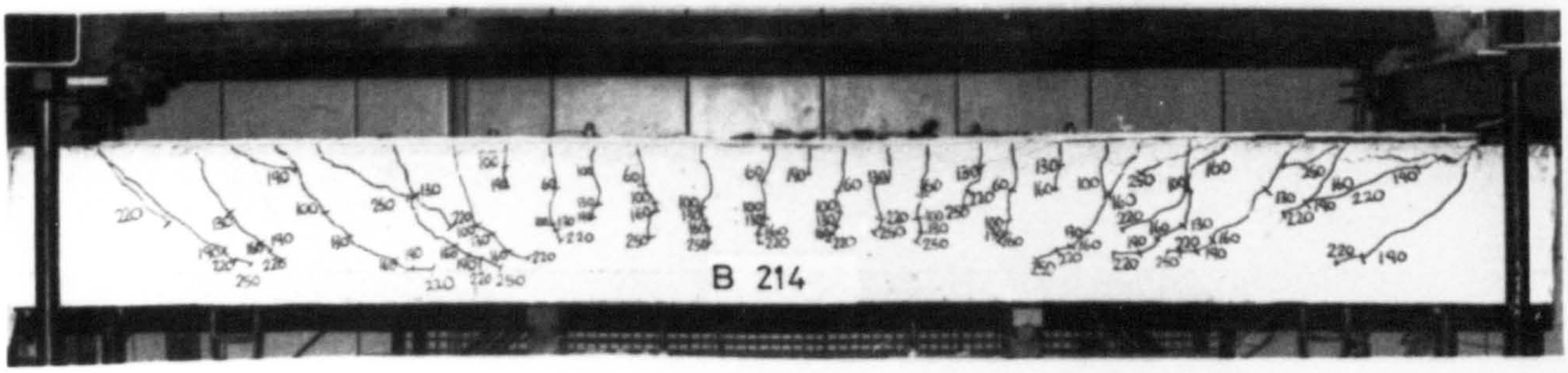

2 layers of 1·5mm plate, lapped plates above the load points.

PLATE 5·5 CRACK PATTERNS – 3mm GLUE THICKNESS

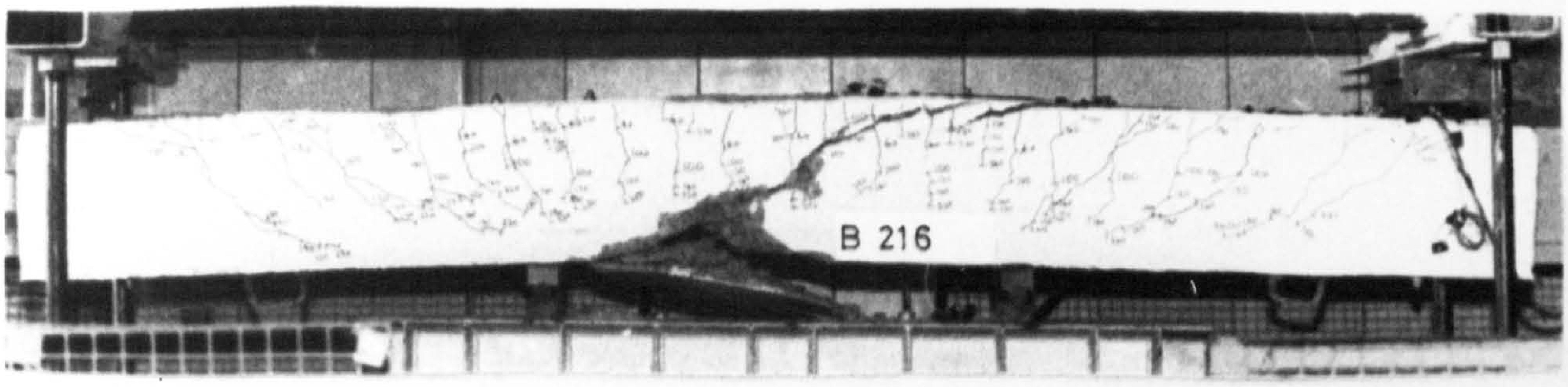

1·5 mm plate thickness

3 mm plate thickness.

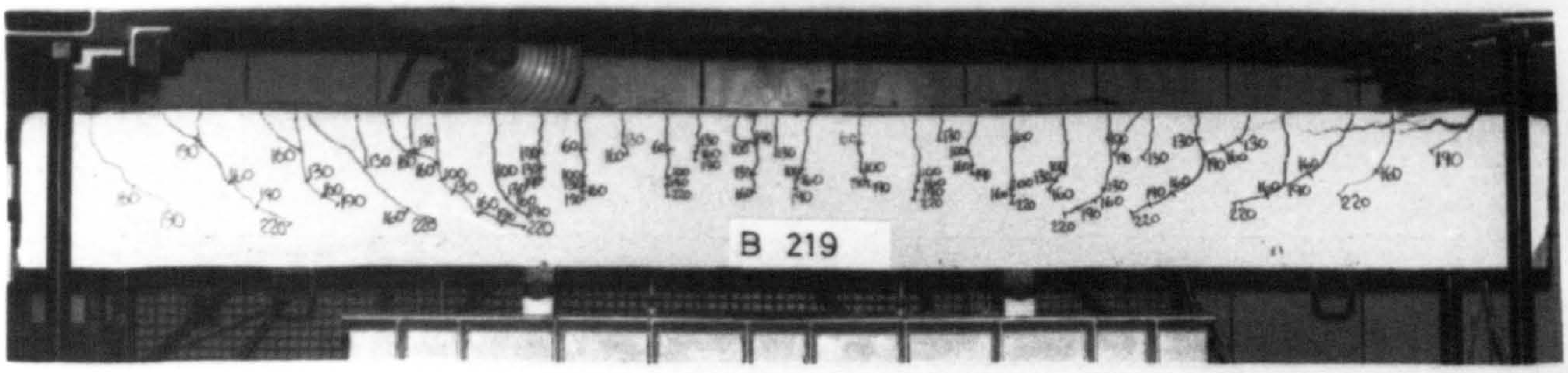

6 mm plate thickness.

PLATE 5·6 CRACK PATTERNS - BEAMS WITH 6mm GLUE THICKNESS.

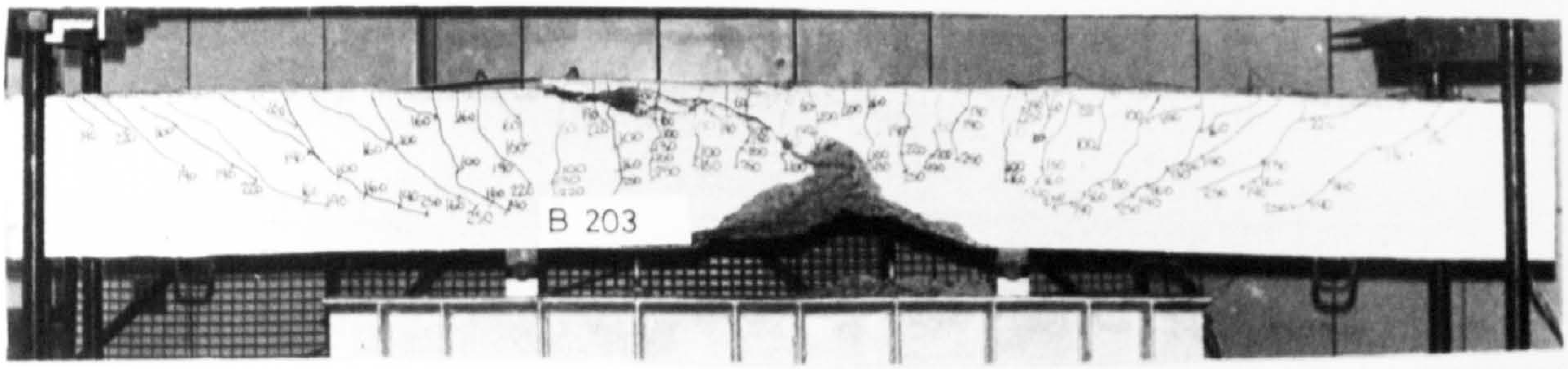

1.5 mm glue thickness.

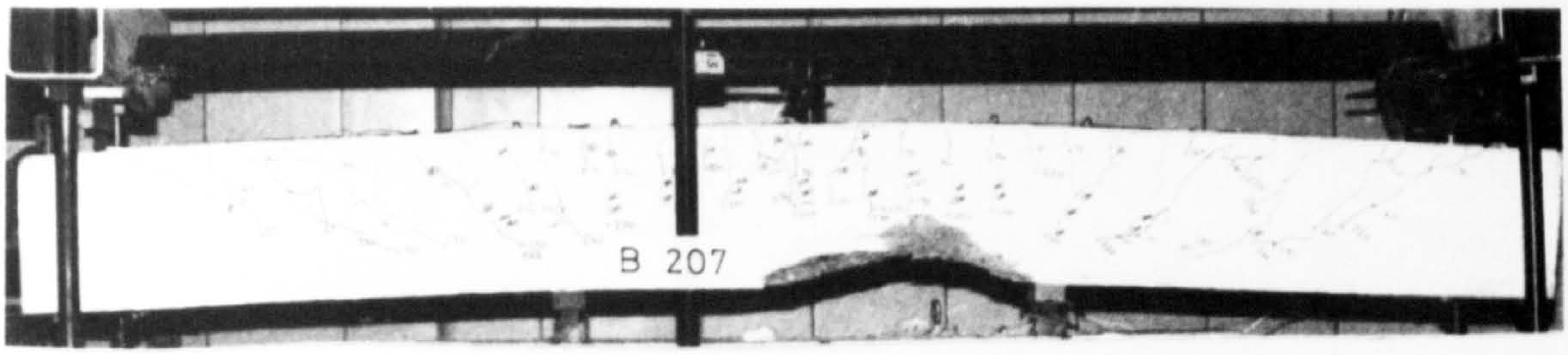

3 mm glue thickness.

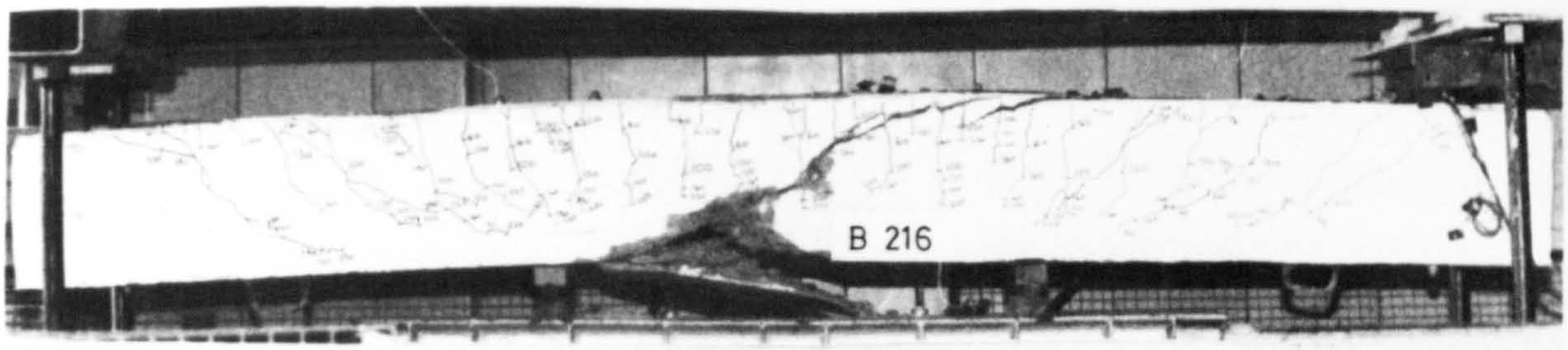

6 mm glue thickness.

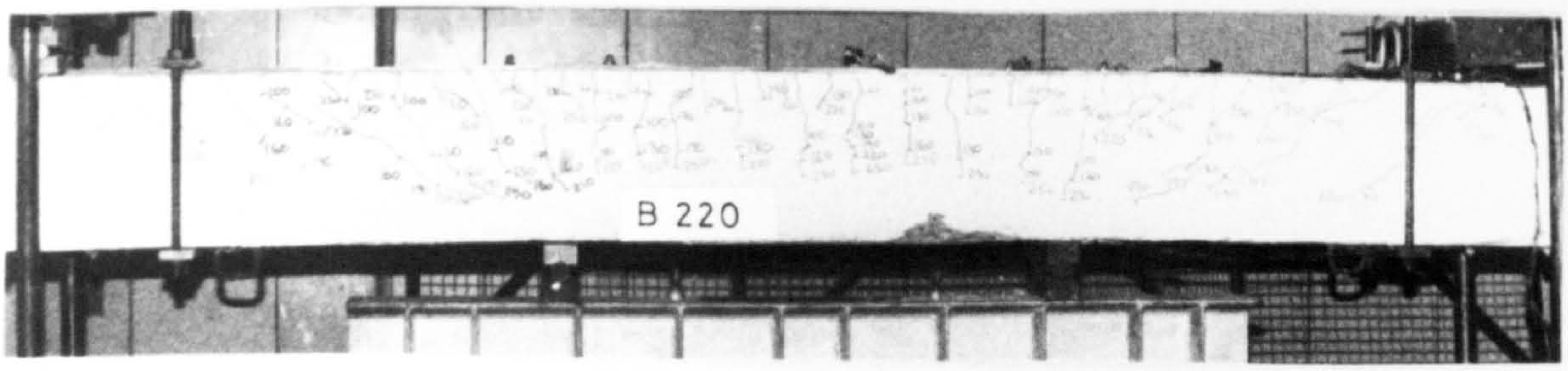

2mm - 8mm variable glue thickness along the beam.

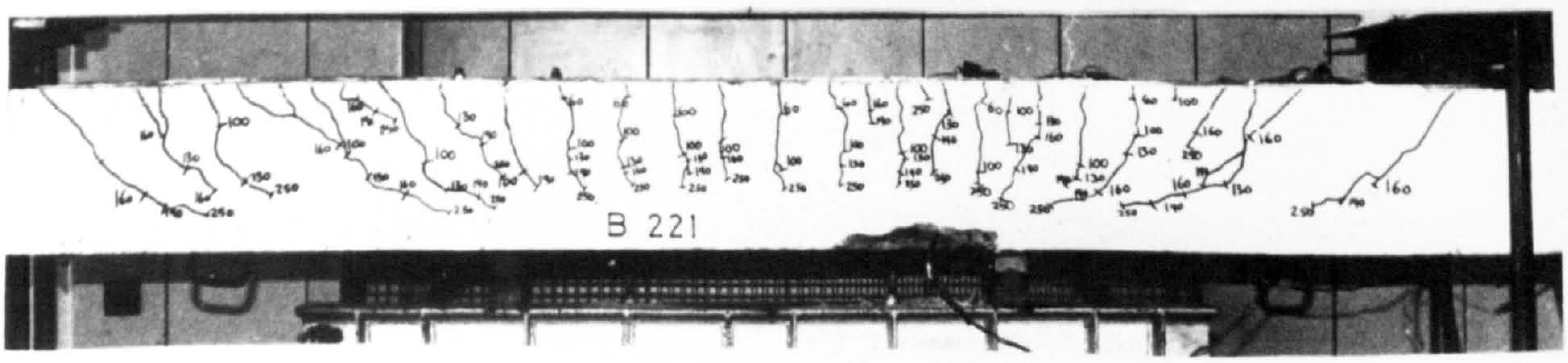

3mm glue thickness with nothes cut in the beam, to form stress concentrations above the load points.

PLATE 5.7 CRACK PATTERNS - 1.5mm PLATE THICKNESS.

3mm glue thickness, 1·5mm plate thickness

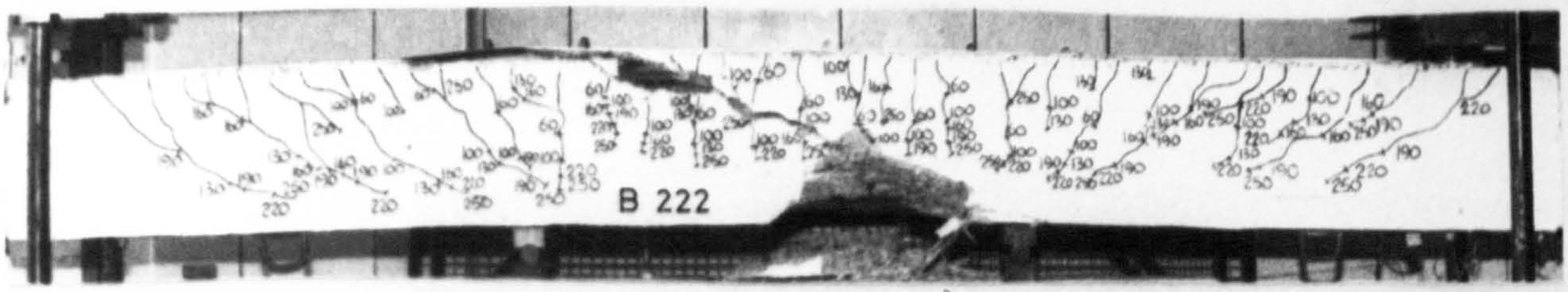

3mm glue thickness, 1·5mm plate thickness, beam loaded to 50% ultimate load before bonding the plate on.

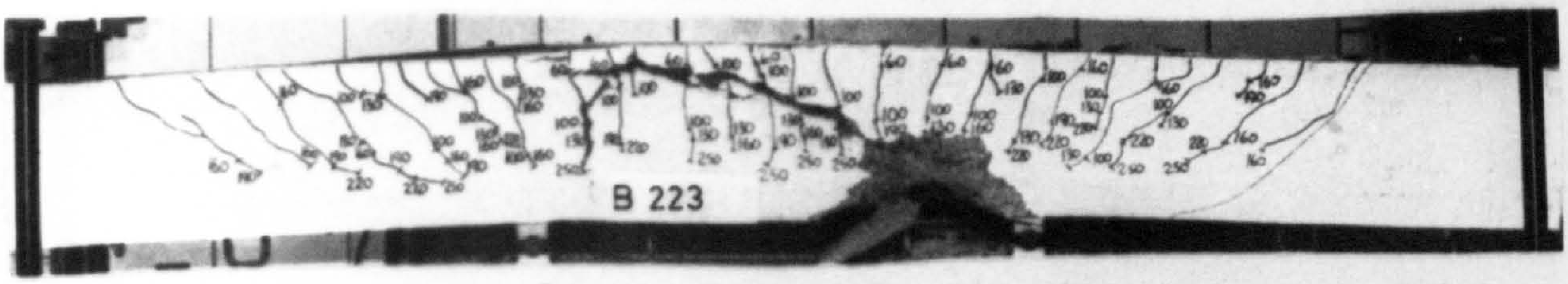

3mm glue thickness, 1·5mm plate thickness, beam loaded to 90% ultimate load before bonding the plate on.

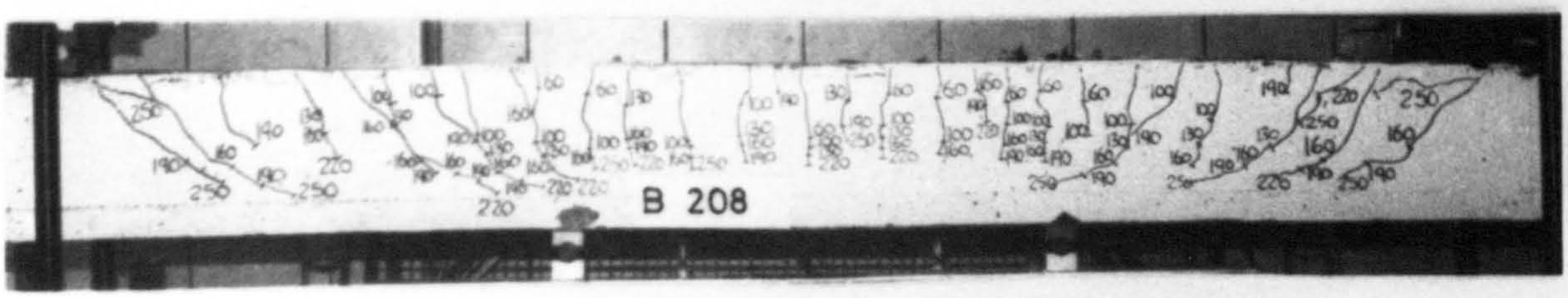

3mm glue thickness, 3mm plate thickness.

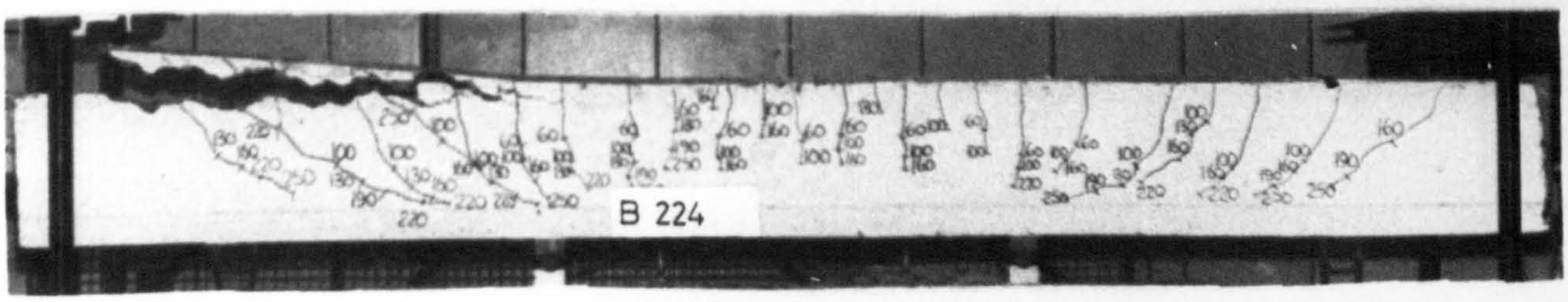

3mm glue thickness, 3mm plate thickness, beam loaded to 50% ultimate load before bonding the plate on.

PLATE 5·8 CRACK PATTERNS - PRELOADED BEAMS.

5.4 DISCUSSION OF RESULTS

5.4.1 First Crack Loads

The first crack loads for the concrete, at the tension face of the beam, were calculated based on the uncracked, transformed moment of inertia and using the value of modulus of rupture of the concrete from the test prisms. The experimental values, given in Table 5.2, were observed with a magnifying glass. For the plated beams the experimental load was, on average, 1.38 times the theoretical value. The same ratio for the unplated beam was 1.12. The experimental values being obtained visually are not accurate and the load would be recorded after cracking had initiated. However, the restraining effect of the glue and plate on the increase of crack width is apparent from the two ratios given above. Fig. 5.3 shows the variation of first crack load with the plate and glue thickness. It can be seen that there was little effect on the cracking load for the range of glue and plate thicknesses used. However it is clear that the cracking load is well above the value for the unplated beam. The CP110 service load was calculated from the CP110 failure load, with $\gamma_m = 1.15$ for steel and 1.5 for concrete. The ratio of experimental first crack load to CP110 service load was 0.35 for the unplated beam. The mean values for beams with 1.5 mm, 3 mm and 6 mm thick plates were 0.45, 0.37 and 0.32 respectively. (Table 5.2)

5.4.2 Increase of Service Loads

The deflection, rotation, maximum crack width and strain in the reinforcing bars at the centre section were found for the unplated beam at its CP110 service load; 100 kN. This being defined as the ultimate load, as found by CP110 recommendations, divided by 1.6. The properties described above were as follows:

(a) deflection 4.6 mm

(b) rotation 113×10^{-4} radians

(c) maximum crack width 0.09 mm

(d) steel bar strain 1020×10^{-6} m/m.

For each plated beam the corresponding loads which produced the same respective deflection, rotation, crack width and strain were found from the experimental results. All these values are given in Table 5.3.

TABLE 5.2 STRENGTH CHARACTERISTICS

BEAM NUMBER	EXPERIMENT FIRST CRACK LOAD (1) kN	CP 110 SERVICE LOAD (2) kN	(1)/(2)	EXPERIMENT SERVICE LOAD (3) kN	EXPERIMENT ULTIMATE LOAD (4) kN	(3)/(2)	(4)/(2)	GLUE mm THICKNESS	PLATE mm THICKNESS
201	35.0	100	0.35	145	232	1.45	2.32	0	0
202	39.9	102	0.39	153	245	1.50	2.40	3.0	0
203	50.1	116	0.43	169	270	1.46	2.33	1.5	1.5
204	50.1	134	0.37	169	270	1.26	2.01	1.5	3.0
205	54.8	166	0.33	133	213	0.80	1.28	1.5	6.0
206	55.0	135	0.41	138	220	1.02	1.63	1.5	2x1.5
207	55.0	119	0.46	164	262	1.38	2.20	3.0	1.5
208	49.0	135	0.36	165	264	1.22	1.96	3.0	3.0
209	52.4	167	0.31	138	220	0.83	1.31	3.0	6.0
210	50.1	166	0.30	134	215	0.81	1.30	3.0	6.0
211	54.8	119	0.46	158	253	1.33	2.13	3.0	1.5L
212	47.0	117	0.40	155	248	1.32	2.12	3.0	1.5L
213	50.1	135	0.37	158	253	1.17	1.87	3.0	2x1.5L
214	50.1	135	0.37	158	253	1.17	1.87	3.0	2x1.5L
215	49.8	134	0.37	156	250	1.16	1.87	3.0	3.0L
216	54.0	118	0.46	164	262	1.39	2.22	6.0	1.5
217	48.0	135	0.36	161	257	1.19	1.90	6.0	3.0
218	51.4	168	0.31	121	194	0.72	1.15	6.0	6.0
219	55.0	168	0.33	138	220	0.82	1.31	6.0	6.0
220	54.8	118	0.46	164	263	1.39	2.23	3-8	1.5
221	54.8	117	0.47	161	268	1.38	2.21	3.0	1.5
222	51.1	117	0.44	168	268	1.44	2.29	3.0	1.5P
223	53.0	118	0.45	165	264	1.40	2.24	3.0	1.5P
224	47.2	136	0.35	156	250	1.15	1.83	3.0	3.0P

L - lapped plates. P - precracked beams.

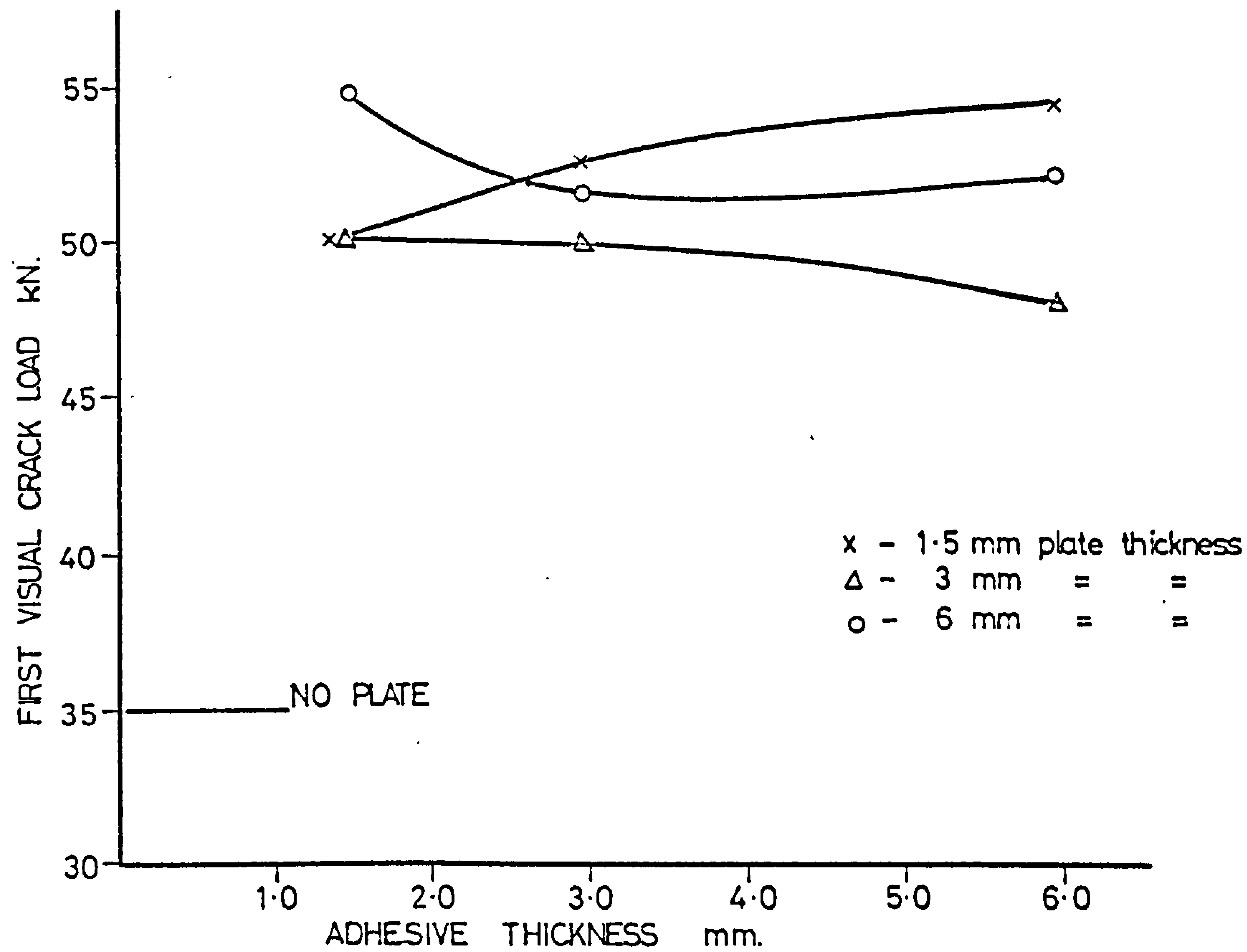

FIGURE 5·3 VARIATION OF FIRST CRACK LOAD

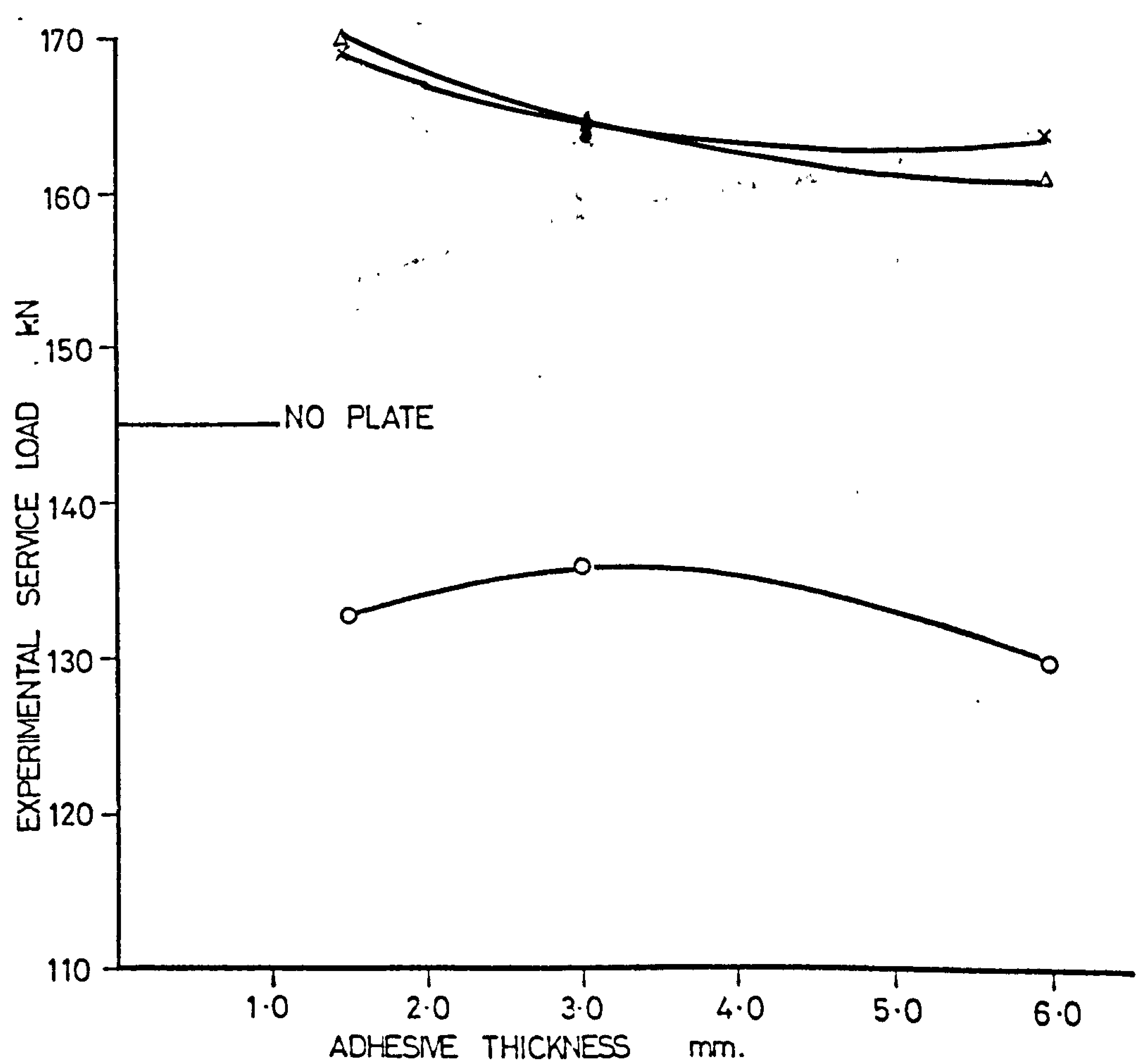

FIGURE 5·4 VARIATION OF EXPERMENTAL SERVICE LOAD

TABLE 5·3 INCREASE OF SERVICE LOADS

BEAM NUMBER	(1) LOAD 1 kN	(2) LOAD 2 kN	(3) LOAD 3 kN	(4) LOAD 4 kN	(1)/100*	(2)/100	(3)/100	(4)/100	GLUE mm. THICKNESS	PLATE mm THICKNESS
202	101	102	106	102	1·01	1·02	1·06	1·02	3·0	0
203	104	106	144	120	1·04	1·06	1·44	1·20	1·5	1·5
204	110	124	153	151	1·10	1·24	1·53	1·51	1·5	3·0
205	131	138	170	171	1·31	1·38	1·70	1·71	1·5	6·0
206	113	123	158	155	1·13	1·23	1·58	1·55	1·5	2x1·5
207	111	106	153	116	1·11	1·06	1·53	1·16	3·0	1·5
208	126	134	160	150	1·26	1·34	1·60	1·50	3·0	3·0
209	130	144	184	210	1·30	1·44	1·84	2·10	3·0	6·0
210	133	146	199	170	1·33	1·46	1·99	1·70	3·0	6·0
211	111	117	145	130	1·11	1·17	1·45	1·30	3·0	1·5L
212	111	114	137	130	1·11	1·14	1·37	1·30	3·0	1·5L
213	110	130	138	154	1·10	1·30	1·38	1·54	3·0	2x1·5L
214	119	137	142	153	1·19	1·37	1·42	1·53	3·0	2x1·5L
215	120	133	158	168	1·20	1·33	1·58	1·68	3·0	3·0L
216	111	113	145	143	1·11	1·13	1·45	1·43	6·0	1·5
217	123	133	145	165	1·23	1·33	1·45	1·65	6·0	3·0
218	134	156	-	190	1·34	1·56	-	1·90	6·0	6·0
219	136	160	180	200	1·36	1·60	1·80	2·00	6·0	6·0
220	104	106	146	130	1·04	1·06	1·46	1·30	3–8	1·5
221	111	111	148	128	1·11	1·11	1·48	1·28	3·0	1·5
222	100	120	123	143	1·00	1·20	1·23	1·43	3·0	1·5P
223	85	108	123	140	0·85	1·08	1·23	1·40	3·0	1·5P
224	120	133	160	172	1·20	1·33	1·60	1·72	3·0	3·0P

L- lapped plates . P- precracked beams. *-CP110 service load - unplated beam.

LOAD 1- load in plated beam corresponding to 4·6mm deflection (unplated beam at 100 kN)

LOAD 2- " " " " 113×10^{-4} rad. rotation (" " " ")

LOAD 3- " " " " 0·09 mm crack width (" " " ")

LOAD 4- " " " " 1020 microstrain (" " " ")

5.4.2.1 Deflection

The plated beams were able to sustain higher loads than the unplated beam before reaching a deflection of 4.6 mm. The increase varied as follows: 7 to 11% for beams strengthened with 1.5 mm thick plate; 10 to 23% for beams strengthened with 3 mm thick plate and 30 to 37% for beams strengthened with 6 mm thick plate.

5.4.2.2 Rotation

The plated beams again were able to sustain higher loads before reaching a rotation of 113.10^{-4} radians. The corresponding beams as for deflections gave the following increases: 10 to 17% for 1.5 mm thick plates; 25 to 36% for 3 mm thick plates and 38 to 42% for 6 mm thick plates.

5.4.2.3 Maximum Crack Width

When considering crack width the increases for the corresponding beams were as follows: 37 to 50% for 1.5 mm thick plates; 38 to 60% for 3 mm thick plates and 70 to 99% for 6 mm thick plates.

5.4.2.4 Steel Bar Strain

When considering the steel bar strains the corresponding increases were 16 to 43% for 1.5 mm thick plates; 50 to 68% for 3 mm thick plates and 70 to 110% for 6 mm thick plates.

In general it can be seen that the addition of the external reinforcing plates had the effect of increasing the limit states for serviceability.

Table 5.2 shows the ratio of experimental service load, (experimental ultimate load ÷ 1.6), to CP110 service load. All these ratios are greater than 1.0, except for the beams with 6 mm thick plates, which did not reach their flexural capacity due to their mode of failure. The ratios for the beams with 1.5 mm and 3 mm thick plates varied from 1.02 to 1.46, with a mean value of 1.28. This value would be expected to be greater than 1.0 as CP110 includes material safety factors.

Fig. 5.4 shows the variation of experimental service load with glue and plate thickness. The beams with 1.5 and 3 mm thick plates show an increase in service load whereas those with 6 mm plate thickness show a decrease.

5.4.3 Ultimate Loads

Three methods were used for calculating the theoretical ultimate loads of the test beams.

(a) Ultimate Limit State to CP110.

(b) Strain Compatibility - glue cracked.

(c) Strain Compatibility - glue uncracked.

The general assumptions and examples of calculations are given in Appendix 4.

The increase in the ultimate flexural moment capacity over that of an unplated beam varied from 8 to 17% for beams with 1.5 mm and 3 mm thick plates. The beams with 6 mm thick reinforcing plates showed a decrease in ultimate moment capacity compared with the unplated beam varying from 5 to 16%. Plates 5.2 to 5.8 show the beams after failure.

5.4.3.1 Beams with 1.5 mm Plate Thickness

From Table 5.4 it can be seen that there was good agreement between the theoretical and experimental failure moments. The mean ratio of experimental to theoretical moments for the three methods of calculation, i.e. CP110, strain compatibility with no tensile contribution from the glue and strain compatibility including the tensile force in the glue, were 1.09, 1.06 and 1.05 respectively, with a coefficient of variation of 3% in each case. This ratio varies only marginally when the tensile force in the glue is included. In the preliminary test series the variation was very large due to the fact that the plate used had a low yield strength and was only 1 mm thick. The glue, therefore, was providing a large proportion of the tensile force in the beam, as there was no internal reinforcement. As shown in Appendix 4, the experimental stress strain curve for the glue was used when calculating the moments by strain compatibility. More testing needs to be done to determine the actual stress condition in the glue in the composite condition. The test on beam 202, with a 3 mm thick adhesive layer and no plate, showed that the glue was not cracked at failure. Beam 221, with V notches cut in the tension face to form stress concentrations had no significant differences from similar beams without these notches.

TABLE 5·4 ULTIMATE LOADS

BEAM NUMBER	CP 110 ULTIMATE MOMENT kNm (1)	STRAIN COMPATIBILITY ULTIMATE MOMENT (NO GLUE) kNm (2)	STRAIN COMPATIBILITY ULTIMATE MOMENT (+ GLUE) kNm (3)	EXPERIMENT ULTIMATE MOMENT kNm (4)	$\frac{(4)}{(1)}$	$\frac{(4)}{(2)}$	$\frac{(4)}{(3)}$	FAILURE MODE	GLUE THICKNESS mm	PLATE THICKNESS mm
201	81·2	83·7	83·7	88·9	1·09	1·06	1·06	FLEXURE	0	0
202	82·8	85·9	87·0	93·9	1·13	1·09	1·08	FLEXURE	3·0	0
203	90·1	92·4	92·8	103·5	1·15	1·12	1·12	FLEXURE	1·5	1·5
204	100·1	102·5	102·9	103·5	1·03	1·01	1·01	FLEXURE/ SHEARBOND	1·5	3·0
205	118·7	120·3	120·6	81·7	0·69*	0·68*	0·68*	SHEARBOND	1·5	6·0
206	100·9	104·3	104·9	104·3	1·03	1·00	0·99	FLEXURE/ SHEAR BOND	1·5	2x1·5
207	92·2	95·5	96·6	100·6	1·09	1·05	1·04	FLEXURE	3·0	1·5
208	100·9	103·6	104·2	101·2	1·00	0·98	0·97	FLEXURE/ SHEAR BOND	3·0	3·0
209	119·9	122·1	122·4	84·3	0·70*	0·69*	0·69*	SHEAR BOND	3·0	6·0
210	118·9	120·8	121·2	82·4	0·69*	0·68*	0·68*	SHEARBOND	3·0	6·0
211	92·7	96·3	97·2	97·3	1·05	1·01	1·00	FLEXURE	3·0	1·5 L
212	90·4	92·9	93·5	95·8	1·06	1·03	1·02	FLEXURE	3·0	1·5 L
213	101·0	103·4	104·0	96·9	0·96	0·94	0·93	FLEXURE/ SHEARBOND	3·0	2x1·5L
214	101·3	104·2	104·9	97·0	0·96	0·93	0·92	FLEXURE/ SHEARBOND	3·0	2x1·5L
215	102·0	105·2	106·0	95·8	0·94	0·91	0·90	FLEXURE/ SHEARBOND	3·0	3·0L
216	91·9	95·1	96·7	100·6	1·09	1·06	1·04	FLEXURE	6·0	1·5
217	101·3	104·2	105·5	98·6	0·97	0·95	0·93	FLEXURE/ SHEARBOND	6·0	3·0
218	120·2	122·3	122·7	74·5	0·62*	0·61*	0·60*	SHEARBOND	6·0	6·0
219	120·8	123·1	124·3	84·3	0·70*	0·68*	0·68*	SHEARBOND	6·0	6·0
220	91·7	95·0	96·3	100·8	1·10	1·06	1·05	FLEXURE	2–8	1·5
221	91·3	93·9	94·6	98·9	1·08	1·05	1·04	FLEXURE	3·0	1·5
222	91·4	93·9	96·3	102·7	1·12	1·09	1·07	FLEXURE	3·0	1·5P
223	92·8	96·3	96·9	101·2	1·09	1·05	1·04	FLEXURE	3·0	1·5P
224	102·0	105·1	105·8	95·8	0·94	0·91	0·91	FLEXURE/ SHEARBOND	3·0	3·0P
				MEAN VALUES	1·05	1·01	1·00 (* not included)			

5.4.3.2 Beams with Two Layers of 1.5 mm Thick Plate or One Layer of 3 mm Thick Plate

From Table 5.4 it can be seen that there was good agreement between the theoretical and experimental failure moments. The mean ratio's, as before, were 0.98, 0.95 and 0.95 respectively, with a coefficient of variation of 4% in each case. There was no difference between the mean ratios of failure moments, as given above, for the beams with one layer of 3 mm plate or two layers of 1.5 mm plate.

5.4.3.3 Beams with 6 mm Thick Plate

From Table 5.4 the mean ratios of experimental to theoretical failure moments, as before, were 0.68, 0.67 and 0.67 with a coefficient of variation of 5% in each case. It is apparent, therefore, that it is not possible to increase the ultimate capacity of a beam beyond a certain point by simply adding thicker and thicker plates. Nevertheless, it should be noted that the thicker plates greatly enhance the deformational properties at service loads. In general the mean ratio found from CP110 calculations were higher than those from strain compatibility. This is due to the fact that the CP110 calculation uses the proof stress of the steel and takes no account of strain hardening beyond this point.

The ratios of experimental ultimate load to CP110 service load are given in Table 5.2. Except for the beams with 6 mm thick plates, the values ranged from 1.83 to 2.33 with a mean value of 2.08. This compares with 1.60 as recommended by CP110. This difference is largely due to the material safety factors included in the CP110 design method.

5.4.4 Modes of Failure

5.4.4.1 Beams with 1.5 mm Thick Plates

All beams with 1.5 mm thick reinforcing plates failed in a flexural mode by combined yielding of the tensile bar and plate reinforcement followed by crushing of the concrete in the compression zone. As the tensile reinforcement started to yield, the width of one or two cracks at or near the critical section, increased at a faster rate. With increase in load the adjacent cracks grew wider indicating a spread of yield in the steel bars and plate along the beam. The increase in crack width was accompanied by a slow propagation of crack height towards the compression face. Finally the concrete crushed at a point between the loads. None of these beams showed any signs of the plate debonding from the glue and/or concrete, except after failure of the compression zone. The debonding then occurred in the constant moment region and was only apparent after unloading. This debonding was probably due to the large post-failure deflections, which would have caused very high strains in the plates.

5.4.4.2 Beams with Two Layers of 1.5 mm Plate or One Layer of 3 mm Thick Plate

These beams failed in a mode which was a combination of flexure and shear/bond. Flexure, however, must have been predominant as they achieve between 94 and 103% of their theoretical CP110 ultimate moment capacity. There was no sign of debonding between the glue and concrete or plate. The strain readings in the steel bars and plates indicated that yielding had occurred prior to failure.

A shear crack initiated at the end of the plate and propagated diagonally towards the concrete compression zone widening the crack at its root and eventually causing partial separation of the plate. No debonding occurred but the concrete cover to the internal bars was ripped away.

It was thought that this shear/bond type of failure could be prevented by reducing the area of plate at the ends. The method used to accomplish this was to use two layers of 1.5 mm thick plate, the first layer being glued along the full length as usual but the second layer was stopped halfway between the loading and support points. This beam, 206, therefore had 3 mm plate thickness across the constant bending moment region and 1.5 mm plate thickness at the ends. Its behaviour was compared with beams 213 and 214 which had two full length layers of plate 1.5 mm thick. Beam 206 reached 103% of its theoretical CP110 ultimate capacity compared with only 96% for beams 213 and 214, as given in Table 5.4. The mode of failure was still by shear/bond, however, the load-deflection and moment-rotation characteristics of beams 206 and 213 were almost identical. Further tests need to be done to investigate this technique.

5.4.4.3 Beams with 6 mm Plate Thickness

All these beams failed by shearing off the concrete along the level of the internal reinforcement, effectively ripping off the concrete cover. There was no sign of debonding of the glue and concrete or plate prior to failure, nor was there any sign of cracking in the glue. The strain readings in the steel bars and plate indicated that yielding had not occurred prior to failure.

Fig. 5.5 shows the variation of the failure load with the plate and glue thickness, and their modes of failure. It is apparent that the beams strengthened with 6 mm plates were not satisfactory from the ultimate load point of view. However, their behaviour when considering deflections, rotations and cracking characteristics at service loads are discussed in Chapter 6. Fig. 5.5 is replotted in Fig. 5.6 with ordinates changed to experimental/theoretical failure load. Values obtained by Cusens and Smith (28) are included for comparison.

5.5 CONCLUSIONS

Based on the results presented in this section the following conclusions can be made.

1. The use of external reinforcement delays the appearance of the first visual cracks with a resulting increase in service loads.

2. No debonding of the glue from the concrete or steel occurred prior to failure, thus full composite action was achieved throughout loading.

3. No cracking was observed in the glue prior to failure, including the beam which had a layer of adhesive without a plate. Further tests need to be performed to determine the stress conditions in the glue layer when acting compositely with steel and concrete.

4. The maximum increase in the ultimate strength of an unplated beam by the addition of externally bonded steel plates was found to be only 17%.

5. The ultimate flexural capacity of the concrete beams with external plate reinforcement could be satisfactorily predicted using all three methods detailed in Appendix 4.

6. More research is needed to investigate methods of preventing shear/bond failures. This could possibly be achieved by:

(a) variation of plate end geometry, either by reducing the width or thickness

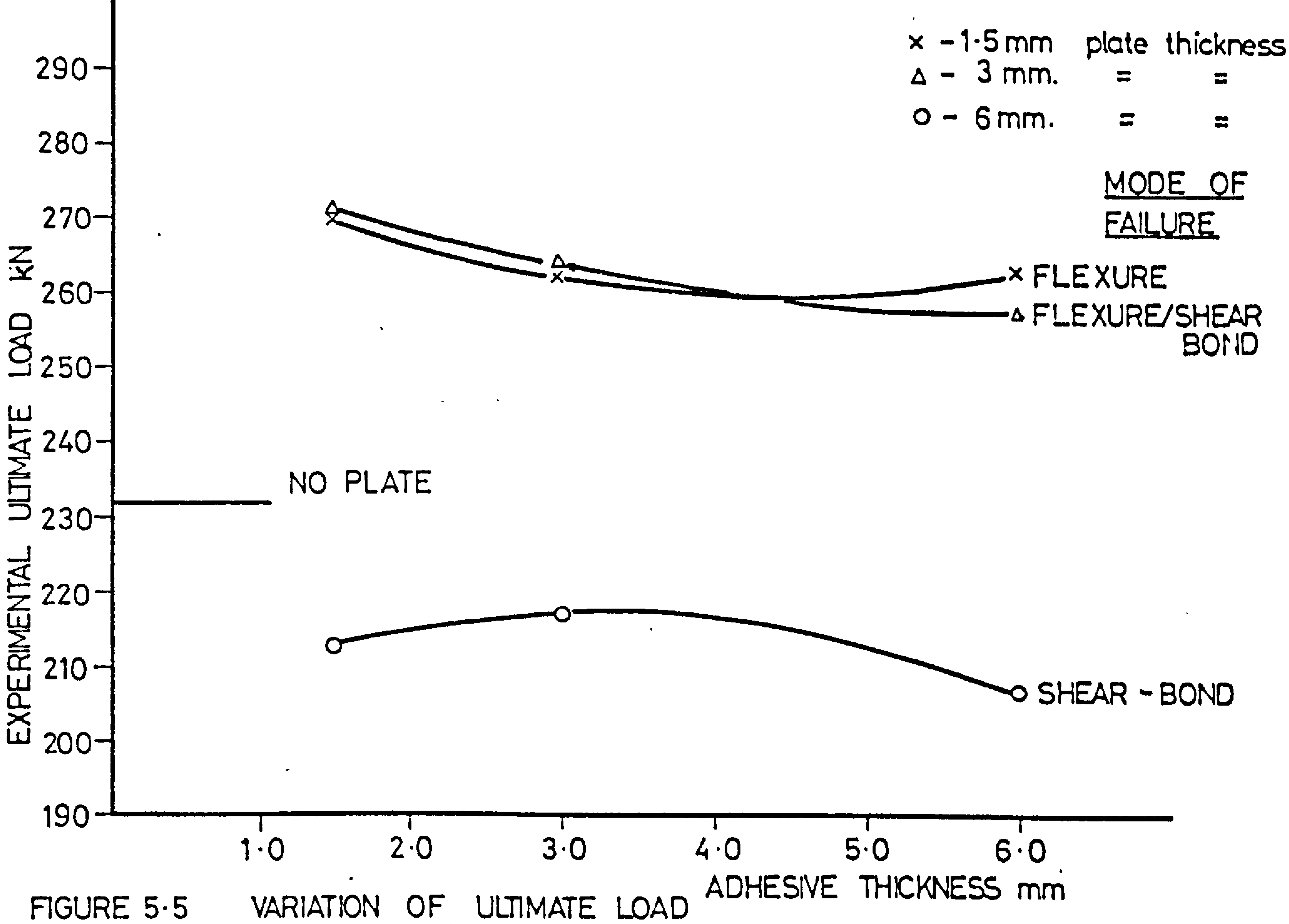

FIGURE 5·5 VARIATION OF ULTIMATE LOAD

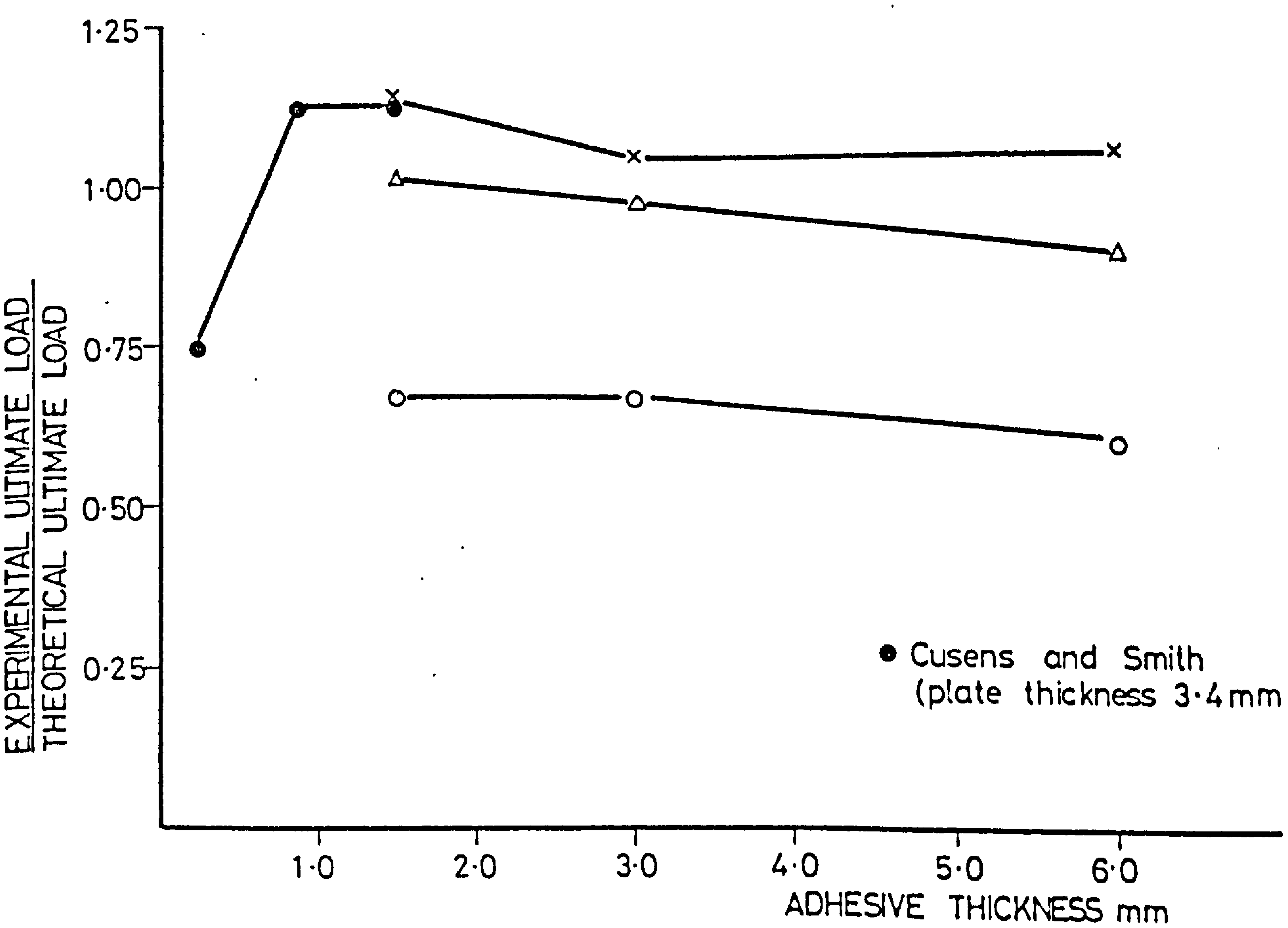

FIGURE 5·6 EFFECT OF ADHESIVE THICKNESS

(b) variation of the glue's elastic modulus at the plate ends. A lower elastic modulus near the plate ends would reduce the shear stresses and should therefore delay the onset of the propagation of large shear cracks

(c) provision of anchor bolts or straps at the plate ends.

CHAPTER 6

DEFORMATION PROPERTIES

6.1 INTRODUCTION

In the past, the allowable stresses for both steel and concrete were low and as a result reinforced concrete members were not severely cracked under service load conditions. Therefore, small deflections and rotations resulted due to their high stiffness.

The present trend towards the use of high strength steels and concrete, and the development of more accurate and sophisticated ultimate strength design procedures have made it possible to use slender members. However, there has been no corresponding increase in the elastic moduli of the construction materials. Although correctly maintaining an adequate factor of safety against collapse, this gives rise to a greater possibility of local damage due to increased deformations.

Limit design theories for statically indeterminate structures require a knowledge of the deformational capacity of hinging regions in members. The major advantage of including inelastic behaviour in a design method is that moment redistribution can be used. This means transferring some calculated moment at one position to another position in a member. If the calculated moment at a support is reduced then this means that the resistance moment at that section will be incapable of resisting the total moment it can get. So at this position the member will become plastic and yield. The amount of redistribution depends on the deformational capacity of the structure. Several theories of limit design have been proposed which are based either on a knowledge of the moment-curvature relationship, such as that proposed by Sawyer (87), or on a knowledge of the moment-rotation relationship, such as that proposed by Baker (88).

It is obvious that excessive deflection can cause structural problems and can also give rise to public concern. The prediction and control of deformation is of great importance but it is complicated by the many factors which influence the behaviour of a member such as: the magnitude and distribution of loading; span and support conditions, materials and section properties; and the extent of cracking. Additional variables controlling long term deflections which are of primary importance are the effects of creep and shrinkage.

The object of this part of the investigation was to assess the effects of varying glue and plate thickness, lapping techniques, multiple plate layers and degree of precracking on the load-strain, load-deflection and moment-rotation characteristics.

The load-strain behaviour was observed for both the internal steel reinforcing bars and the externally bonded steel plates. In addition the concrete surface strain distribution was measured.

The use of accepted methods for predicting the deflections and rotation of normally reinforced concrete beams were assessed for the plated beams.

6.2 EXPERIMENTAL PROGRAMME/PROCEDURE

The twenty four beams described in Section 5.2 were used in this part of the investigation. The instrumentation, test apparatus and procedure are described in Section 5.3. The strains in the steel bars and plate were measured by electrical resistance strain gauges at various locations, and the concrete strains were measured by a demountable extensometer of 200 mm gauge length at the centre section only. The central deflection was measured by dial gauge and the rotations by inclinometer. The load was applied incrementally, the readings described above being taken at each stage.

6.3 DISCUSSION OF RESULTS

6.3.1 Introduction

Tables 6.1 to 6.3 summarise the main results obtained from the tests. The deflections, rotations and strains are taken directly from the measurements. The neutral axis depth is obtained from the strain distribution in the concrete. The curvature is then found by dividing the measured concrete compressive strain by the neutral axis depth. The experimental flexural rigidity was calculated by dividing the applied bending moment by the curvature.

TABLE 6·1 A DEFORMATION CHARACTERISTICS AT FIRST VISIBLE CRACK LOAD.

BEAM NUMBER	201	202	203	204	205	206	207	208	209	210	211	212	213	214	215	216	217	218	219	220	221	222	223	224
Deflection mm.	1·0	1·2	1·7	1·65	1·2	1·4	1·8	1·4	1·3	1·2	1·65	1·35	1·45	1·35	1·35	1·6	1·0	0·9	1·2	1·7	1·7	2·0	2·6	1·65
Span/deflection	2300	1916	1353	1394	1916	1642	1278	1645	1769	1916	1393	1704	1586	1704	1704	1437	2300	2556	1917	1353	1353	1150	885	1394
Total rotation – radians 10^{-3}	3·5	375	4·5	3·75	3·0	3·5	5·25	3·5	3·2	3·0	4·25	4·0	3·75	3·5	3·5	4·25	3·25	2·95	2·5	4·75	4·75	4·5	5·25	3·25
Bar strain 10^{-6}	300	360	350	220	210	220	460	230	160	150	360	330	200	200	220	280	160	100	120	330	330	250	280	170
Compressive concrete strain 10^{-6}	290	280	300	280	280	270	390	270	300	300	350	330	340	300	260	360	310	280	300	350	400	300	390	290
Neutral axis depth mm.	110	110	110	120	125	125	115	120	120	125	120	115	135	120	125	125	115	125	130	100	110	110	100	125
Curvature – radians/m 10^{-3}	2·63	2·55	2·72	2·33	2·24	2·16	3·39	2·25	2·50	2·40	2·81	2·87	2·51	2·50	2·08	2·88	2·69	2·24	2·30	3·50	3·64	2·73	3·90	2·32
Stiffness EI kNm^2	5080	6013	7046	8226	9375	8888	6220	8358	8042	8000	7245	6271	7644	7679	9188	7190	6850	8527	9174	6024	5792	6931	5205	7801
Calculated EI'_u kNm^2	9135	9150	9673	10174	11160	10174	9688	10220	11232	11232	9695	9695	10220	10220	10303	9695	10303	11628	11628	9695	8615	9688	9688	10220
EI/EI'_u	0·56	0·66	0·73	0·81	0·84	0·87	0·64	0·80	0·72	0·71	0·73	0·64	0·75	0·75	0·89	0·73	0·66	0·73	0·79	0·62	0·60	0·71	0·54	0·76
Experimental first crack load. kN.	35·0	40·0	50·0	50·0	55·0	50·0	55·0	49·0	52·5	50·0	55·0	47·0	50·0	50·0	49·8	54·0	48·0	51·4	55·0	55·0	55·0	51·1	53·0	47·2
Experimental first crack moment. kNm	13·4	15·3	19·2	19·2	21·0	19·2	21·0	18·8	20·1	19·2	21·0	18·0	19·2	19·2	19·1	20·7	18·4	19·7	21·0	21·0	21·0	19·6	20·3	18·1
Theoretical first crack moment. kNm	11·9	12·2	12·9	14·0	16·0	14·0	13·2	14·1	16·5	16·5	13·3	12·9	14·0	14·1	14·5	13·1	14·2	17·1	17·1	13·1	13·1	-	-	-
$\frac{\text{Experimental}}{\text{Theoretical}}$ moment.	1·12	1·25	1·48	1·37	1·31	1·37	1·60	1·33	1·21	1·16	1·58	1·40	1·37	1·36	1·31	1·58	1·30	1·15	1·23	1·60	1·60	-	-	-

I'_u = uncracked, transformed moment of inertia.

TABLE 6·1 B DEFORMATION CHARACTERISTICS AT 60kN LOAD

BEAM NUMBER	201	202	203	204	205	206	207	208	209	210	211	212	213	214	215	216	217	218	219	220	221	222	223	224
Deflection mm.	2·0	2·0	1·92	1·90	1·88	1·60	1·80	1·65	1·55	1·60	1·80	1·80	1·80	1·65	1·65	1·70	1·40	1·20	1·20	1·80	2·00	2·50	2·80	2·00
Span/deflection	1150	1150	1211	1211	1211	1438	1278	1394	1484	1438	1278	1278	1278	1394	1394	1353	1643	1917	1917	1278	1150	920	871	1150
Total rotation - radians 10^{-3}	6·50	6·50	6·00	4·50	3·75	4·25	5·50	4·50	3·75	3·50	5·00	5·25	4·25	4·60	4·25	5·20	4·50	3·80	3·25	5·50	5·50	5·25	6·00	4·25
Bar strain 10^{-6}	550	550	440	260	180	260	440	320	180	180	430	430	280	280	280	350	280	150	150	380	380	350	350	230
Compression concrete strain 10^{-6}	455	440	350	360	300	330	410	340	350	350	390	430	490	310	320	430	390	300	330	420	450	350	440	380
Neutral axis depth mm	100	108	108	118	123	123	112	118	118	123	118	114	130	118	123	123	114	123	128	99	108	108	100	123
Curvature - radians/m 10^{-3}	4·55	4·07	3·24	3·05	2·44	2·68	3·66	2·88	2·97	2·85	3·31	3·77	3·77	2·63	2·60	3·50	3·42	2·44	2·58	4·24	4·17	3·24	4·40	3·09
Stiffness EI kNm^2	5055	5651	7099	7541	9426	8582	6289	7986	7744	8070	6949	6101	6101	8745	8846	6571	6725	9426	8915	5425	5516	7099	5227	7443
Calculated EI'_u kNm^2	9135	9150	9673	10174	11160	10174	9688	10220	11232	11232	9695	9695	10220	10220	10303	9695	10303	11628	11628	9695	8615	9688	9688	10220
EI / EI'_u	0·55	0·62	0·73	0·74	0·84	0·84	0·65	0·78	0·69	0·72	0·72	0·63	0·60	0·86	0·86	0·68	0·65	0·81	0·77	0·56	0·64	0·73	0·54	0·73

I'_u = uncracked, transformed moment of inertia.

TABLE 6·2 A DEFORMATION CHARACTERISTICS AT DESIGN SERVICE LOAD (A)[1]

BEAM NUMBER	201	202	203	204	205	206	207	208	209	210	211	212	213	214	215	216	217	218	219	220	221	222	223	224
Service load (A) kN	100	102	116	134	166	135	119	135	167	166	119	117	135	135	136	118	135	168	168	118	117	117	135	136
Deflection mm	4·6	4·6	5·7	6·4	6·7	6·1	5·2	5·2	6·9	6·6	5·0	5·0	5·7	5·0	5·0	4·8	5·1	6·5	6·4	4·6	5·8	5·4	6·3	6·0
Span / deflection	500	500	404	359	343	377	442	442	333	348	460	460	404	460	460	479	442	354	359	500	397	426	365	460
Total rotation-radians 10^{-3}	11·3	11·5	12·5	12·0	15·0	12·2	13·5	11·8	14·5	13·7	11·3	12·0	11·5	11·0	11·0	11·0	11·3	12·8	12·3	12·3	12·2	11·0	12·5	11·7
Bar strain 10^{-6}	1020	1000	930	850	960	820	1000	860	700	940	900	880	860	860	700	750	750.	800	700	870	860	750	830	700
Compressive concrete strain 10^{-6}	1050	780	800	840	960	950	950	790	1010	1000	1000	875	1030	920	1080	975	975	995	960	900	910	765	880	890
Neutral axis depth mm	96	95	100	109	114	114	106	109	109	114	112	108	113	109	118	118	105	119	119	97	104	105	100	109
Curvature-radians/m 10^{-3}	10·8	8·2	8·0	7·7	8·4	8·3	9·0	7·2	9·3	8·8	8·9	8·1	9·1	8·4	9·2	8·3	9·3	8·4	8·1	9·3	8·7	7·3	8·8	8·2
Stiffness EI kNm^2	3537	4780	5575	6662	7571	6212	5066	7167	6892	7250	5146	5519	5670	6167	7021	5490	5570	7690	7960	4882	5172	6160	5205	6340
Calculated EI'_{cr} kNm^2	4522	4557	5519	6384	7992	6384	5568	6475	8124	8124	5665	5665	6475	6475	6599	5665	6599	8300	8300	5665	5900	5568	5568	6475
EI / EI'_{cr}				1·04	0·95	0·97	0·91	1·11	0·85	0·89	0·91	0·97	0·88	0·95	1·06	0·97	0·84	0·93	0·96	0·86	0·88	1·11	0·93	0·98

I'_{cr} = cracked, transformed moment of inertia.

(1) Design service load (A) - calculated from CP 110 including material safety factors:

$$1{\cdot}6\,[\text{service load (A)}] + 1{\cdot}4\,[\text{dead load}] = 0{\cdot}87\, f_y \rho \left(1 - \frac{1{\cdot}1\, f_y \rho}{f_{cu}}\right) bd^2$$

TABLE 6·2 B DEFORMATION CHARACTERISTICS AT DESIGN SERVICE LOAD (B)[1]

BEAM NUMBER	201	202	203	204	205	206	207	208	209	210	211	212	213	214	215	216	217	218[2]	219	220	221	222	223	224
Service load (B) kN	137	144	153	168	197	170	157	170	200	198	159	153	170	171	172	157	171	201	202	157	154	154	159	173
Deflection mm	8·0	8·4	8·8	9·0	8·8	8·5	8·2	7·6	9·5	9·5	8·0	7·6	84	7·8	7·4	7·8	7·5	–	9·0	7·4	8·5	8·0	9·2	7·2
Span / deflection	288	280	261	256	261	271	280	303	242	261	288	303	274	295	311	295	307	–	256	311	271	288	250	319
Total rotation – radians 10^{-3}	17·1	18·0	18·5	16·5	19·5	17·3	18·8	16·3	20·0	19·0	17·0	17·0	17·0	16·0	16·5	17·5	15·8	–	15·8	18·1	17·6	15·0	17·5	16·0
Bar strain 10^{-6}	1200	1480	1430	1200	1330	1180	1470	1170	930	1330	1400	1250	1200	1200	1330	1100	1020	–	1000	1280	1250	1080	1180	1000
Compressive concrete strain 10^{-6}	1350	1110	1070	1150	1260	1200	1400	1050	1200	1280	1260	1300	1500	1140	1350	1320	1300	–	1170	1400	1300	1050	1270	1180
Neutral axis depth mm	80	83	93	109	115	112	95	106	109	114	100	100	110	106	116	110	103	–	119	95	94	98	98	108
Curvature – radians/m 10^{-3}	16·9	13·4	11·5	10·6	11·0	10·7	14·7	9·9	11·0	11·2	12·6	13·0	13·6	10·8	11·6	11·9	12·6	–	9·8	14·7	13·8	10·7	10·9	11·6
Stiffness EI kNm^2	3112	4112	5096	6075	6882	6090	4088	6576	6982	6777	4722	4523	4786	6050	6672	5050	5190	–	7898	4088	4283	5523	4700	6100
Calculated EI'_{cr} kNm^2	4522	4567	5519	6384	7992	6384	5568	6475	8124	8124	5665	5665	6475	6475	6599	5665	6559	8300	8300	5665	5900	5568	5568	6475
EI / EI'_{cr}	0·68	0·90	0·92	0·95	0·86	0·95	0·73	1·02	0·86	0·83	0·84	0·80	0·74	0·93	1·01	0·89	1·79	–	0·95	0·72	0·73	0·99	0·84	0·94

I'_{cr} = cracked, transformed moment of inertia.

(1) Design service load (B) – calculated from strain compatibility without material safety factors.

$$1{\cdot}6\,[\text{service load}] + 1{\cdot}4\,[\text{dead load}] = M_u$$

(2) Beam 218 failed before reaching this load.

TABLE 6·2 C DEFORMATION CHARACTERISTICS AT 130 kN LOAD

BEAM NUMBER	201	202	203	204	205	206	207	208	209	210	211	212	213	214	215	216	217	218	219	220	221	222	223	224
Deflection mm	7·3	6·9	6·6	6·0	4·6	5·7	6·0	5·0	4·5	4·3	5·8	5·8	5·4	4·8	4·7	5·7	4·8	4·2	4·2	5·4	6·6	6·4	7·0	4·8
Span/deflection	315	333	348	383	500	404	383	460	511	535	397	397	426	479	489	404	479	548	548	426	348	360	329	479
Total rotation-radians 10^{-3}	16·0	15·7	15·0	11·6	10·2	11·6	14·5	11·0	11·0	9·5	13·0	13·8	11·3	11·1	11·0	13·3	11·0	8·8	8·2	14·3	14·3	12·7	15·0	11·0
Bar strain 10^{-6}	1350	1320	1100	770	530	740	1100	740	500	550	1000	1020	750	760	750	900	670	500	460	1000	1000	830	950	650
Compressive concrete strain 10^{-6}	1260	950	900	800	760	950	1000	750	770	800	1100	920	950	900	750	1070	920	750	720	1000	1000	860	1000	850
Neutral axis depth mm	88	85	95	110	115	115	100	110	110	115	105	102	115	110	120	115	106	120	120	95	98	100	100	110
Curvature-radians/m 10^{-3}	14·3	11·1	9·5	7·3	6·6	8·3	10·0	6·8	7·0	7·0	10·5	9·0	8·3	8·2	6·3	9·4	8·7	6·3	6·0	10·5	10·2	8·6	10·0	7·7
Stiffness EI kNm^2	3496	4489	5262	6855	7474	6033	4980	7318	7119	7160	4690	5537	6033	6093	7840	5373	5740	7840	8300	4737	4885	5794	4983	6446
Calculated EI'_{cr} kNm^2	4522	4557	5519	6384	7992	6384	5568	6475	8124	8124	5665	5665	6475	6475	6599	5665	6599	8300	8300	5665	5900	5568	5568	6475
EI/EI'_{cr}	0·74	0·99	0·95	1·07	0·94	0·96	0·79	1·13	0·88	0·88	0·84	0·84	0·93	0·94	1·19	0·95	0·87	0·94	1·00	0·84	0·78	1·04	0·89	0·99

I'_{cr} = cracked, transformed moment of inertia.

TABLE 6·3 DEFORMATION CHARACTERISTICS NEAR FAILURE LOAD.

BEAM NUMBER	201 (1)	202 (1)	203	204	205 (2)	206	207	208	209 (1)	210 (2)	211	212 (1)	213	214	215	216	217	218 (2)	219 (1)	220	221	222	223	224
Deflection mm	20·0	17·6	21·6	16·8	8·4	15·8	20·8	15·8	11·6	8·0	18·4	14·8	17·3	15·3	15·1	19·0	15·0	8·2	8·0	18·4	19·8	18·0	18·5	14·2
Span/deflection	115	130	106	137	274	145	111	146	198	280	125	155	133	150	152	121	153	280	288	125	116	128	124	162
Total rotation-radians 10^{-3}	36·2	35·5	44·3	38·0	18·8	36·0	42·5	36·0	25·5	17·5	38·0	30·2	35·5	36·0	33·7	43·0	35·2	17·5	14·5	40·0	41·0	35·5	36·0	31·5
Bar strain 10^{-6}	4400	3100	3560	2500	1250	2400	3600	2430	1065	1250	3800	2720	2600	2520	2330	2950	2200	960	850	3250	3400	2700	2150	2350
Compressive concrete strain 10^{-6}	3350	2400	2300	2050	1200	1810	2500	1980	1400	1200	2450	2150	2520	1860	1970	2600	2370	1200	1150	2500	2350	2210	2200	1920
Neutral axis depth mm	62	75	85	106	113	106	80	100	105	110	95	95	105	100	110	100	97	118	116	90	85	90	100	100
Curvature-radians/m 10^{-3}	54·0	32·0	27·0	19·3	10·6	17·1	31·3	19·8	13·3	10·9	25·8	22·6	24·0	18·6	17·9	26·0	24·4	10·2	9·9	27·8	27·6	24·6	22·0	19·2
Stiffness EI kNm^2	1562	2635	3549	4965	6871	5604	3282	4840	6340	6681	3717	4233	4008	5210	5354	3689	3927	7140	7349	3447	3630	3895	4356	4991
Calculated EI'_{cr} kNm^2	4521	4557	5519	6384	7992	6384	5568	6475	8124	8124	5665	5665	6475	6475	6599	5665	6599	8300	8300	5665	5900	5568	5568	6475
EI/EI'_{cr}	0·35	0·58	0·64	0·78	0·84	0·88	0·59	0·75	0·78	0·82	0·66	0·75	0·62	0·80	0·81	0·65	0·60	0·86	0·89	0·61	0·62	0·62	0·69	0·77
Experimental failure moment kNm	88·9	93·9	103·5	103·5	81·7	104·3	100·6	101·2	84·3	82·4	97·3	95·8	96·9	97·0	95·8	100·6	98·6	74·5	84·3	100·8	98·9	102·7	101·2	95·8
Theoretical failure moment (3) kNm	83·7	87·0	92·8	102·9	120·6	104·9	96·6	104·2	122·4	121·2	97·2	93·5	104·0	104·9	106·0	96·7	105·5	122·7	124·3	96·3	94·6	96·3	96·9	105·8
$\frac{\text{Experimental}}{\text{Theoretical}}$ moment	1·06	1·08	1·12	1·01	0·68	0·99	1·04	0·97	0·69	0·68	1·00	1·02	0·93	0·92	0·90	1·04	0·93	0·60	0·68	1·05	1·04	1·07	1·04	0·91

(1) Readings at 220 kN load } all other readings at 250 kN load.
(2) Readings at 190 kN load }
(3) Calculated by strain compatibility, including the tensile force in the glue.

Tables 6.1A and 6.1B show the deformation characteristics at first visible crack load and at 60 kN, which is just above the first crack loads. The latter being used for comparisons.

Tables 6.2A, 6.2B and 6.2C show the deformation characteristics at design service loads. Table 6.2A is for design service load A, which was calculated by CP 110 methods including the material safety factors - 1.5 for concrete and 1.15 for steel. Table 6.2B is for design service load B, which was calculated by taking the ultimate load found by strain compatibility methods and dividing by 1.6. Design service load C was taken as 130 KN for comparative purposes, as given in Table 6.2C.

Table 6.3 shows the deformation characteristics near ultimate load.

The flexural rigidities found from the experimental readings were compared with the theoretical values both before and after cracking (Tables 6.1 to 6.3).

At 60 kN load, the flexural rigidities of the plated beams were between 3% and 86% higher than the unplated beam. When compared with the calculated rigidity for the uncracked sections the unplated beam gave a ratio of experimental to theoretical of 0.56 while the plated beams gave values ranging from 0.56 to 0.86, except the precracked beam 223 which gave 0.54. For beams with 1.5 mm thick plates the mean value was 0.66, for 3 mm thick plates it was 0.76 and for 6 mm plates 0.77. Thus it can be seen at this load, just above the first crack load, the plates have reduced the extent of cracking and therefore increased the stiffness of the beams.

At 130 kN the flexural rigidities of the plated beams were between 40 and 140% higher than the unplated beam. However, these figures represent the behaviour only in the constant moment region and a better representation of the flexural rigidity of the beams as a whole is found through the deflections and rotations. The ratio of experimental to theoretical flexural rigidity for the unplated beam was 0.74. For beams reinforced with 1.5 mm thick plates the mean ratio was 0.86; for beams with 3 mm plates it was 1.0 and for 6 mm plates 0.93. At service loads, therefore, the plates are effectively increasing the flexural rigidity above that of the unplated beam.

At 190 kN load, the flexural rigidities of the plated beams were between 100 and 300% higher than the unplated beam. However, again a better representation of the total beam behaviour is obtained from the rotation and deflection characteristic as reported below.

6.3.2 Load-Strain Characteristics

6.3.2.1 Literature Review

It has been shown by many authors (94, 96, 97) that the tensile strain on the concrete surface between cracks is a very small amount that may be neglected. Since the crack width at the surface is given by the extension of the bars between two cracks, it can be concluded that the strain in the reinforcing bar, and therefore the strain in the concrete surface across cracks, at the same level are identical. The demec gauge had a gauge length of 200 mm so that it crossed at least one crack each time it was read. The load-strain curves given in Fig. 6.1 confirmed that the bar and concrete surface strains are almost identical.

6.3.2.2 Reinforcing Bar Strains

Fig. 6.2 shows that for a glue thickness of 1.5 mm, the bar strains are decreased as the plate thickness increases. Beam 204, with 3 mm thick plat e, behaved identically to Beam 206, with two layers of 1.5 mm plate up to service load, and very closely thereafter.

Figs. 6.3 and 6.4 show similar behaviour for beams with 3 mm and 6 mm thick glue layers respectively. Beams 209 and 210 both had 6 mm thick plates and 3 mm thick glue layer, but Beam 210 was considerably more flexible above service loads, in fact its behaviour was almost identical to Beam 205 (Fig. 6.9) which had a 1.5 mm thick glue layer. It is thought, therefore, that some of the spacers placed in the glue line to control its thickness must have been squeezed out with the excess glue.

Fig. 6.4 shows that a beam with a glue layer only was slightly stiffer than the unplated beam. Beams 211 and 212, which had lapped plates, behaved almost identically with Beam 207 which had a continuous layer of plate. Up to

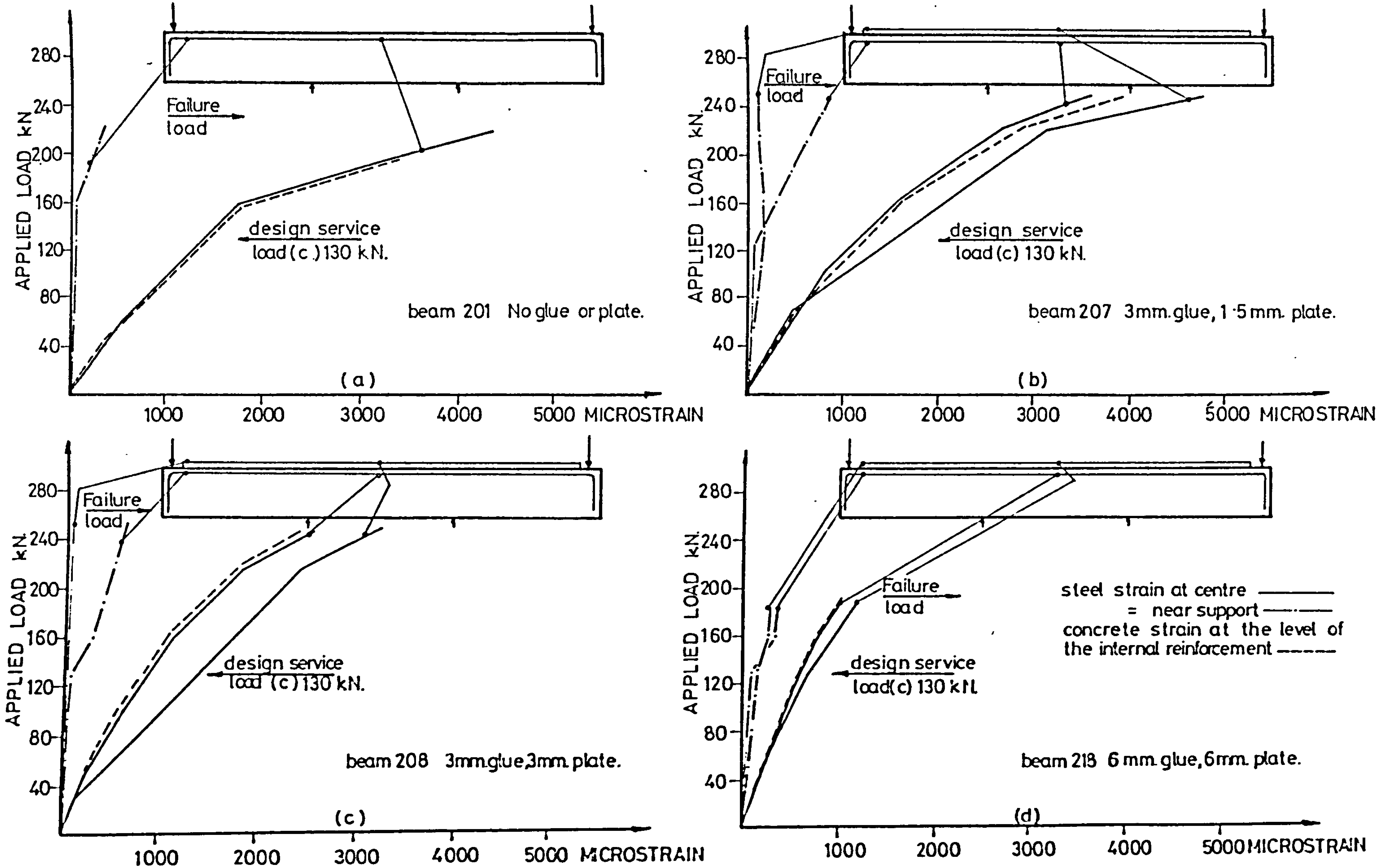

FIGURE 6:1 TYPICAL LOAD-STRAIN CURVES

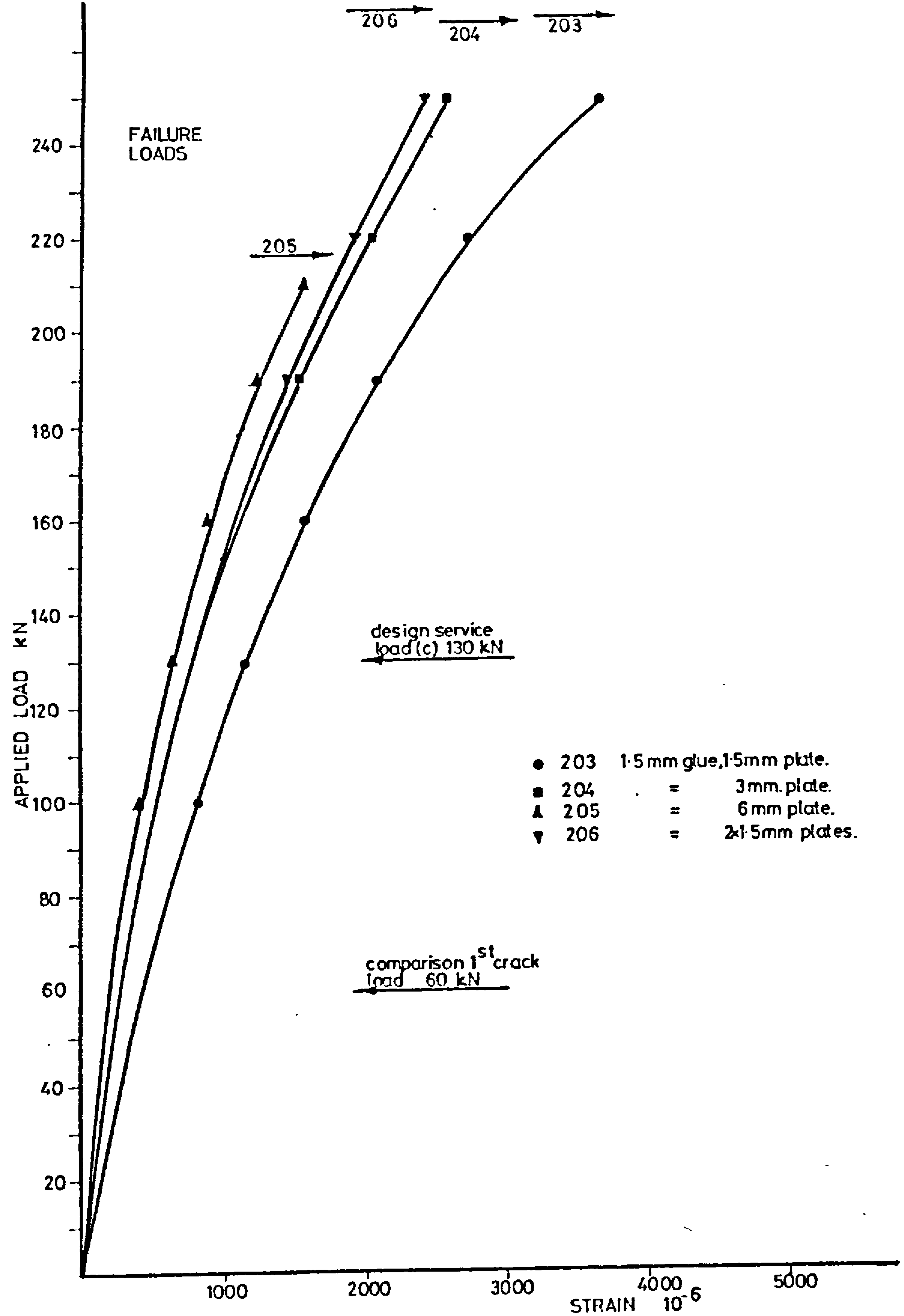

FIGURE 6·2 LOAD-STRAIN CURVES INTERNAL STEEL BARS - CENTRE SECTION

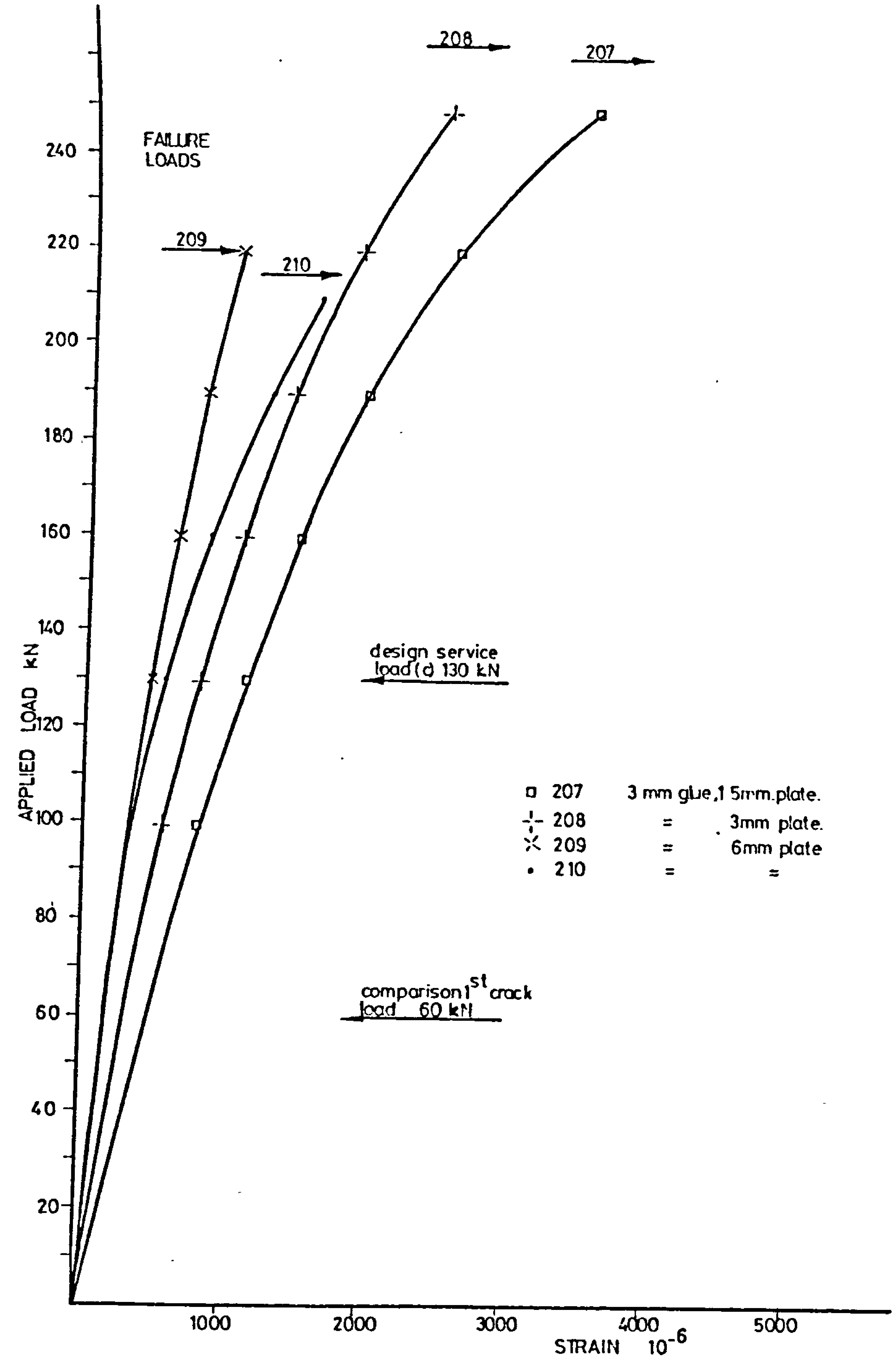

FIGURE 6·3 LOAD-STRAIN CURVES INTERNAL STEEL BARS - CENTRE SECTION

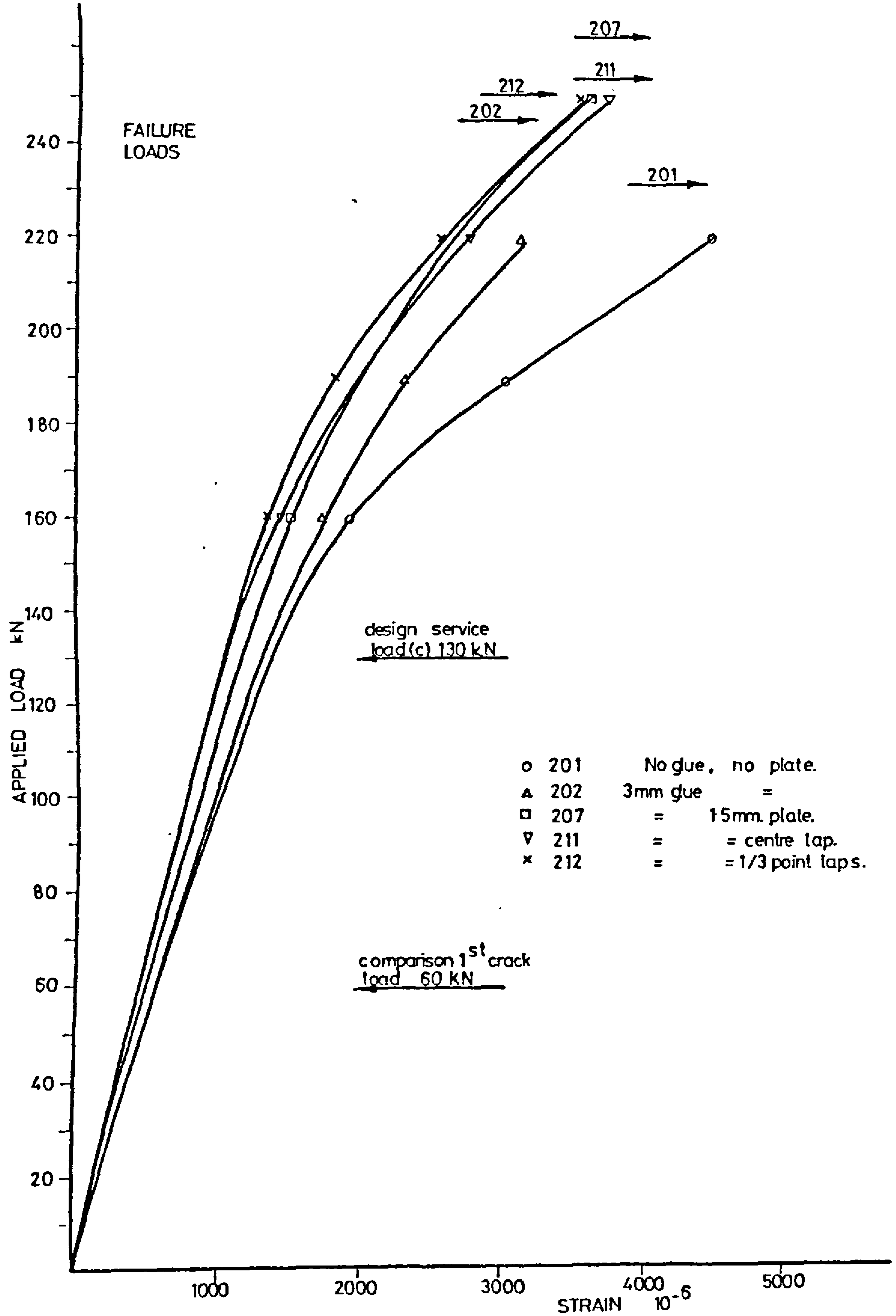

FIGURE 6·4 LOAD-STRAIN CURVES INTERNAL STEEL BARS - CENTRE SECTION

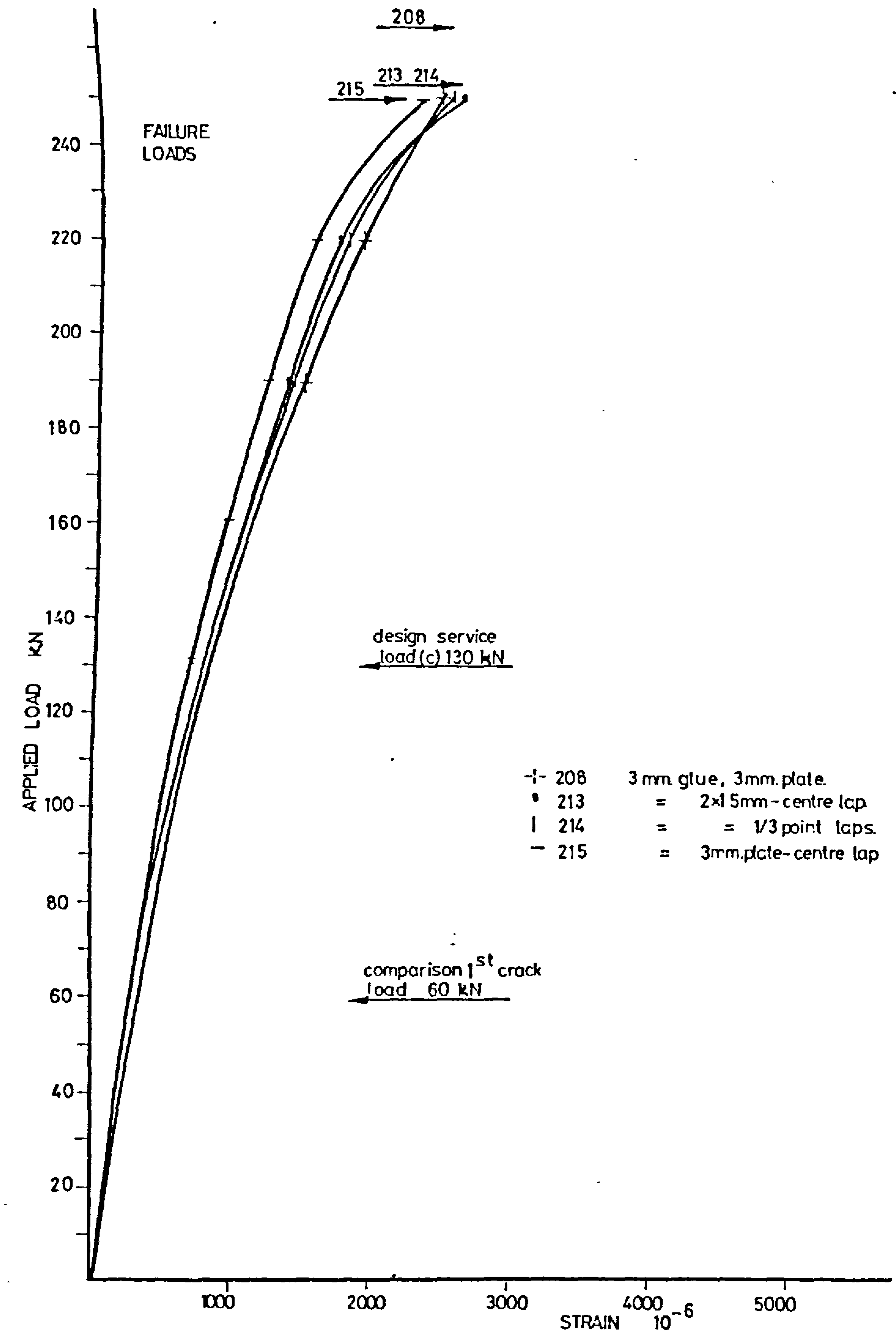

FIGURE 6·5 LOAD-STRAIN CURVES INTERNAL STEEL BARS - CENTRE SECTION

service load the beams with lapped plates were slightly stiffer. This would be expected as the lever arm is slightly increased.

Fig. 6.5 compares Beam 208 with an unlapped 3 mm thick plate, to Beam 215 which had a 3 mm thick lapping plate at the centre section. Beams 213 and 214 had two layers of 1.5 mm plate, the upper layers were lapped. These four beams behaved in a similar manner; the beams having lapped plates being slightly stiffer and the beam with a single 3 mm lapped plate showed lower strains than the beams with two layers of 1.5 mm plate. This could be explained by the fact that there must be a certain amount of movement between the two layers of 1.5 mm plate.

Figs. 6.7, 6.8 and 6.9 show the behaviour of beams with constant plate thicknesses of 1.5 mm, 3 mm and 6 mm respectively, when the glue thickness is varied. There is a general reduction in bar strains for an increase in glue thickness, although the effect was not as large as the reduction found when increasing the plate thickness for constant glue thickness. The behaviour of the beams with variable and notched glue layers, 220 and 221, was between that of the beams with 3 mm and 6 mm glue thickness.

Figs. 6.10 and 6.11 show that for the beams which were precracked, before bonding on the plates, the reinforcing bar strains were reduced in comparison to those found in a similar beam which was not precracked. This behaviour seems somewhat anomalous. It could be expected that the precracked beams would be relatively less stiff than the beams that were not cracked prior to bonding on their plates. However, this behaviour could perhaps be explained by assuming that the glue has penetrated into the existing cracks at the tensile face and is resisting their propagation. This should result in an increased number of cracks with a reduced mean height and spacing. If the cracking results for beams 207 (no precracking) and 223 (90% ultimate load before bending) are compared the above hypothesis is not confirmed.

Alternatively the reduced bar strains could be explained by assuming that bond failure had occurred adjacent to cracks when loading to 90% ultimate before bonding. The bar extension, after bonding on the plate, would then give

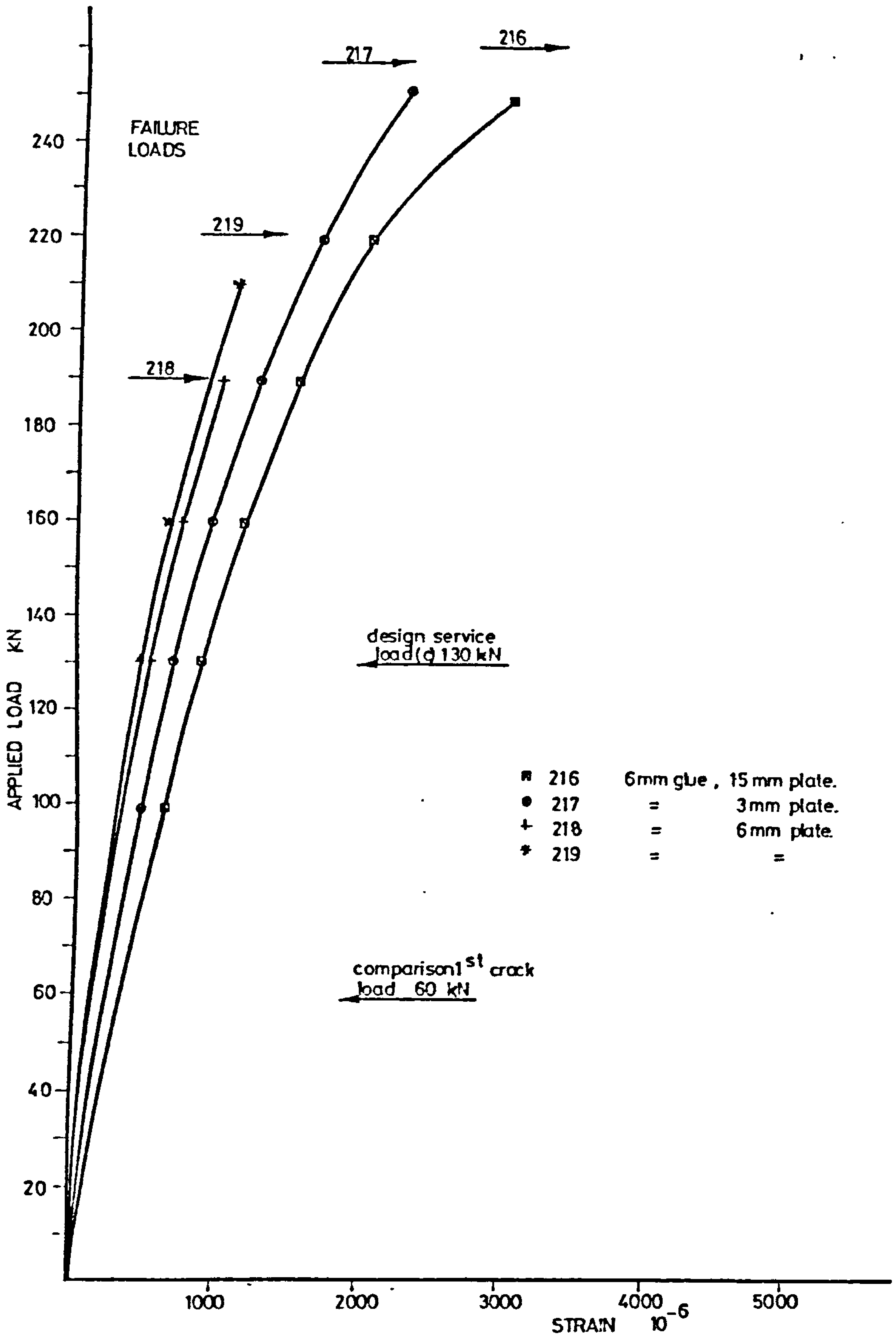

FIGURE 6·6 LOAD-STRAIN CURVES INTERNAL STEEL BARS - CENTRE SECTION

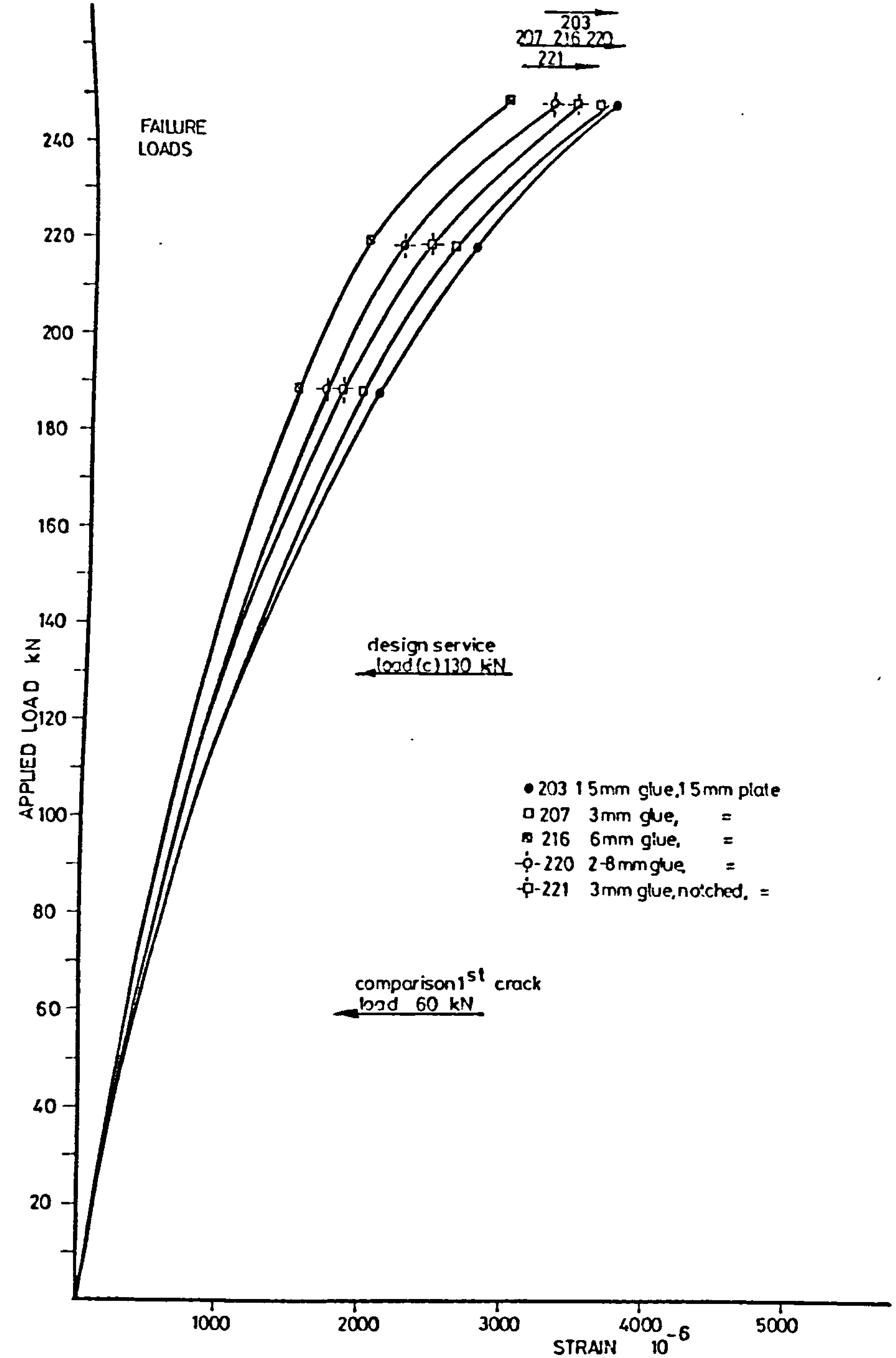

FIGURE 6·7 LOAD-STRAIN CURVES INTERNAL STEEL BARS - CENTRE SECTION

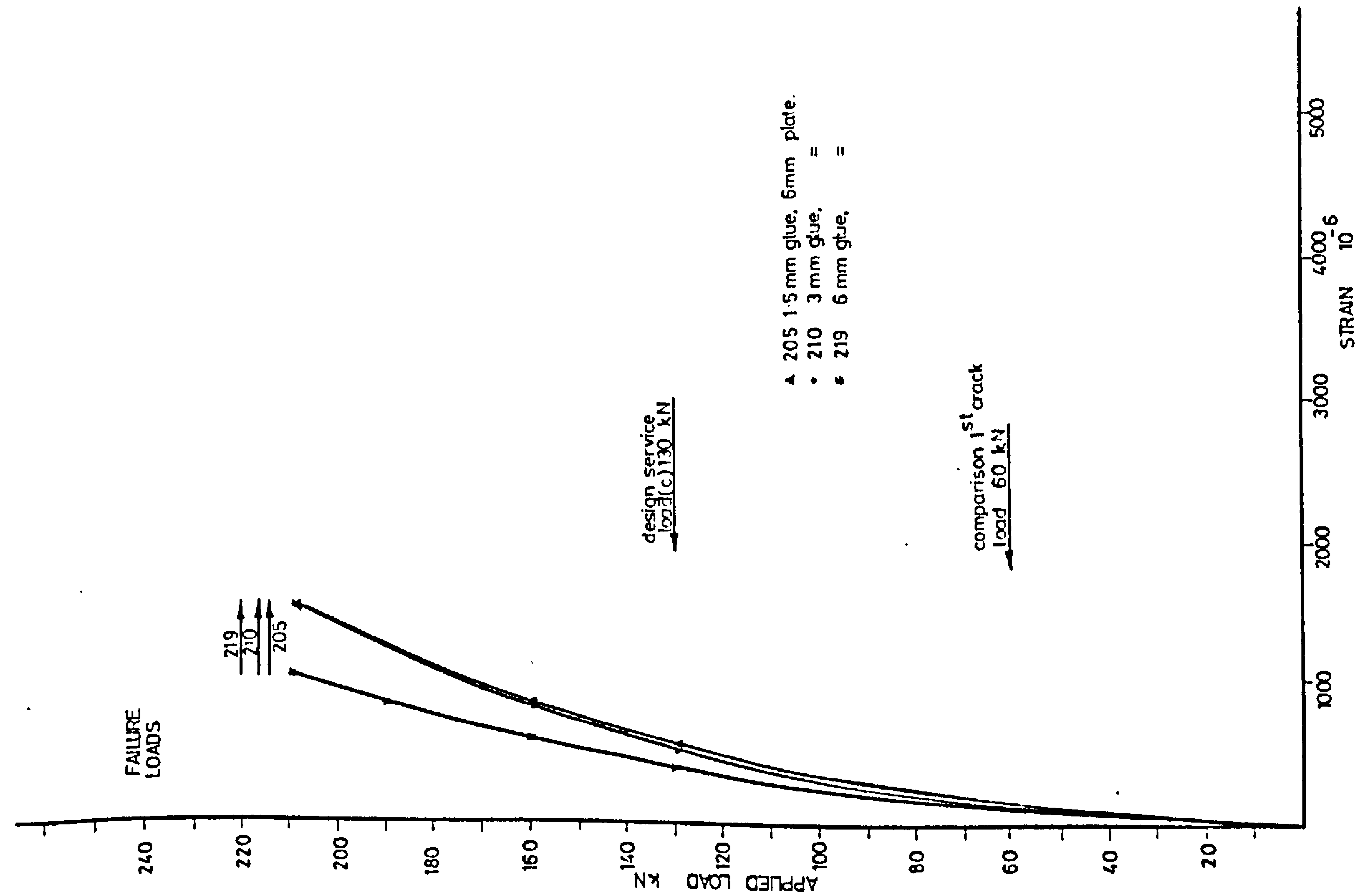

FIGURE 6·9 LOAD-STRAIN CURVES

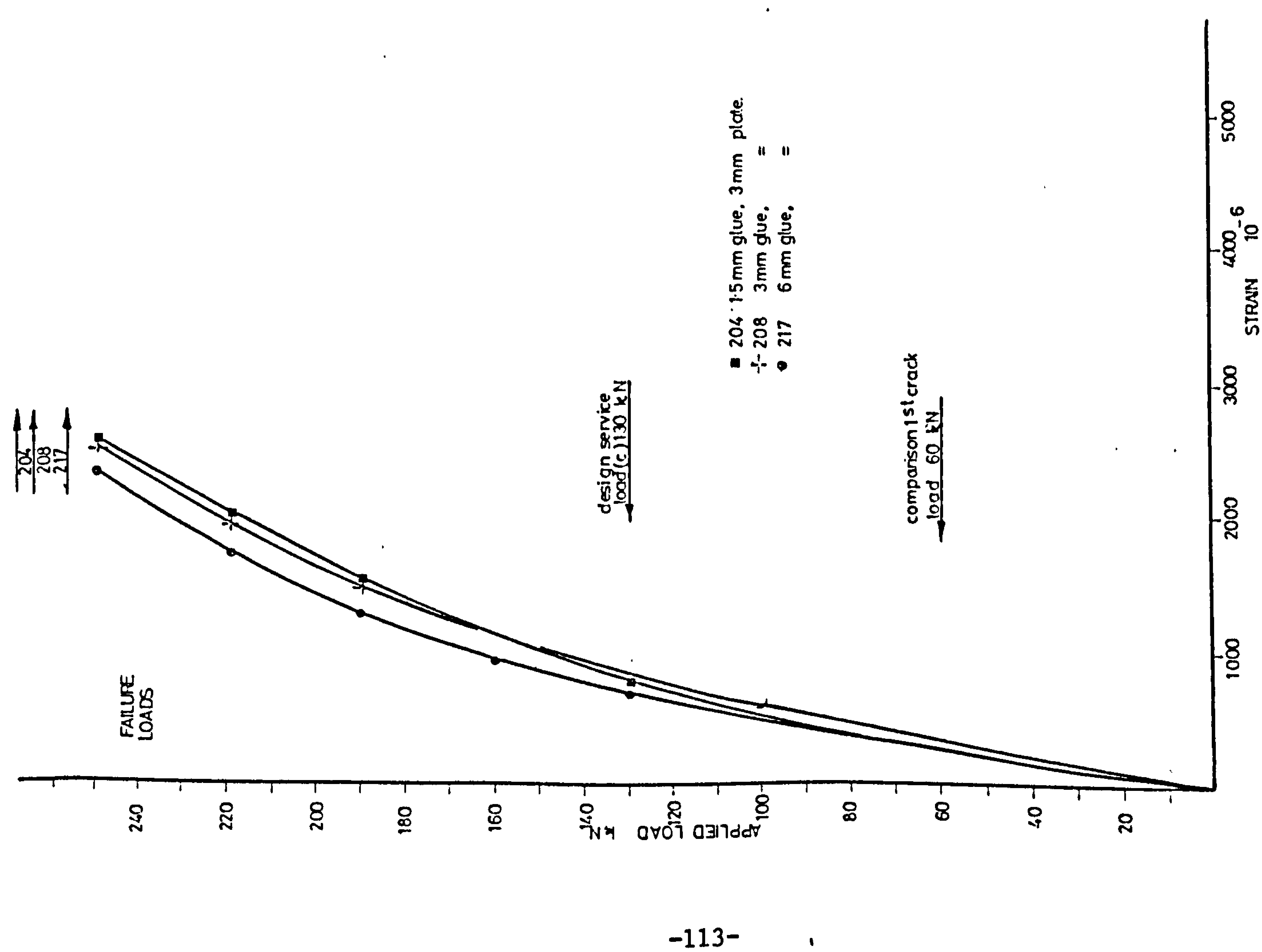

FIGURE 6·8 LOAD-STRAIN CURVES

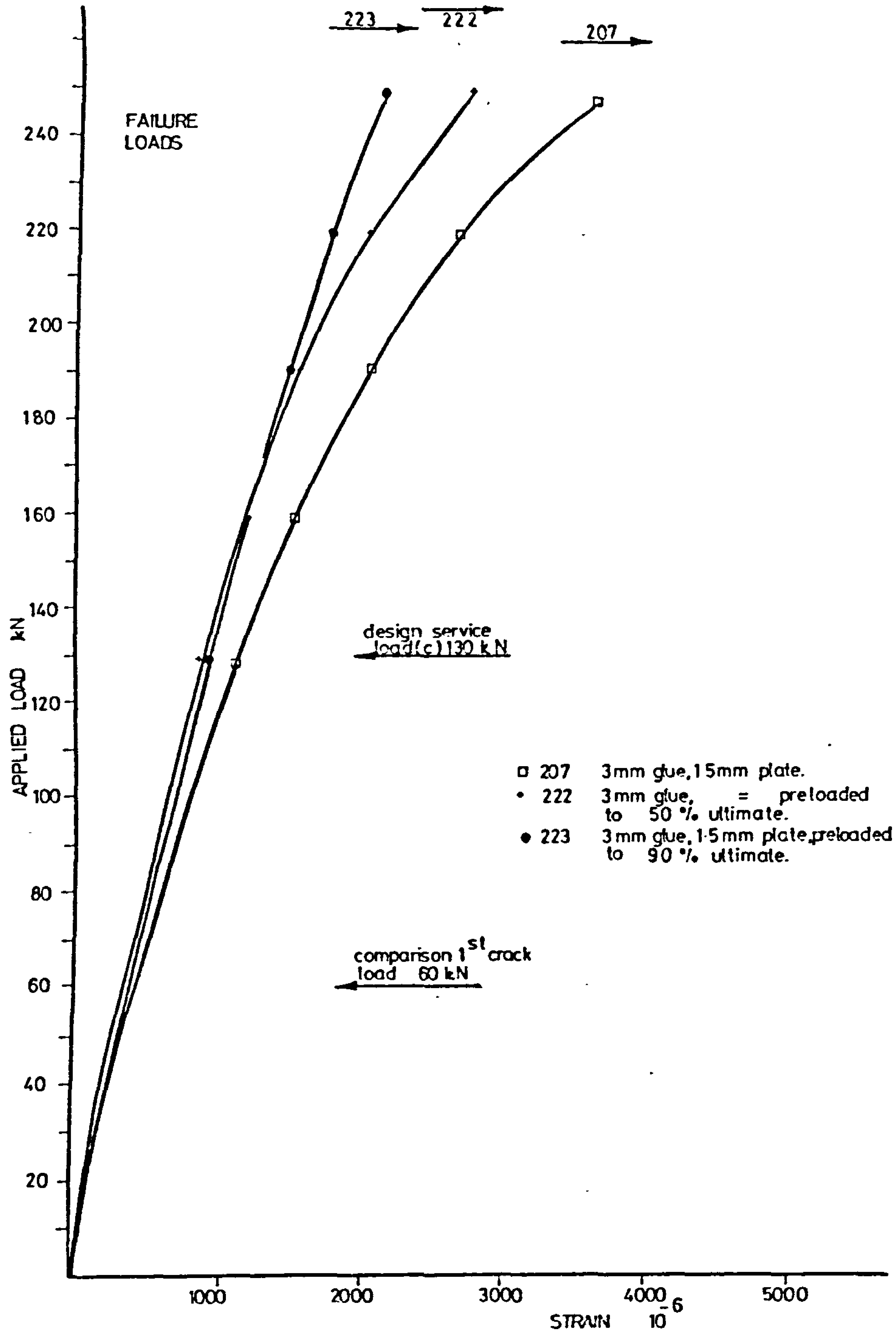

FIGURE 6.10 LOAD-STRAIN CURVES INTERNAL STEEL BARS - CENTRE SECTION

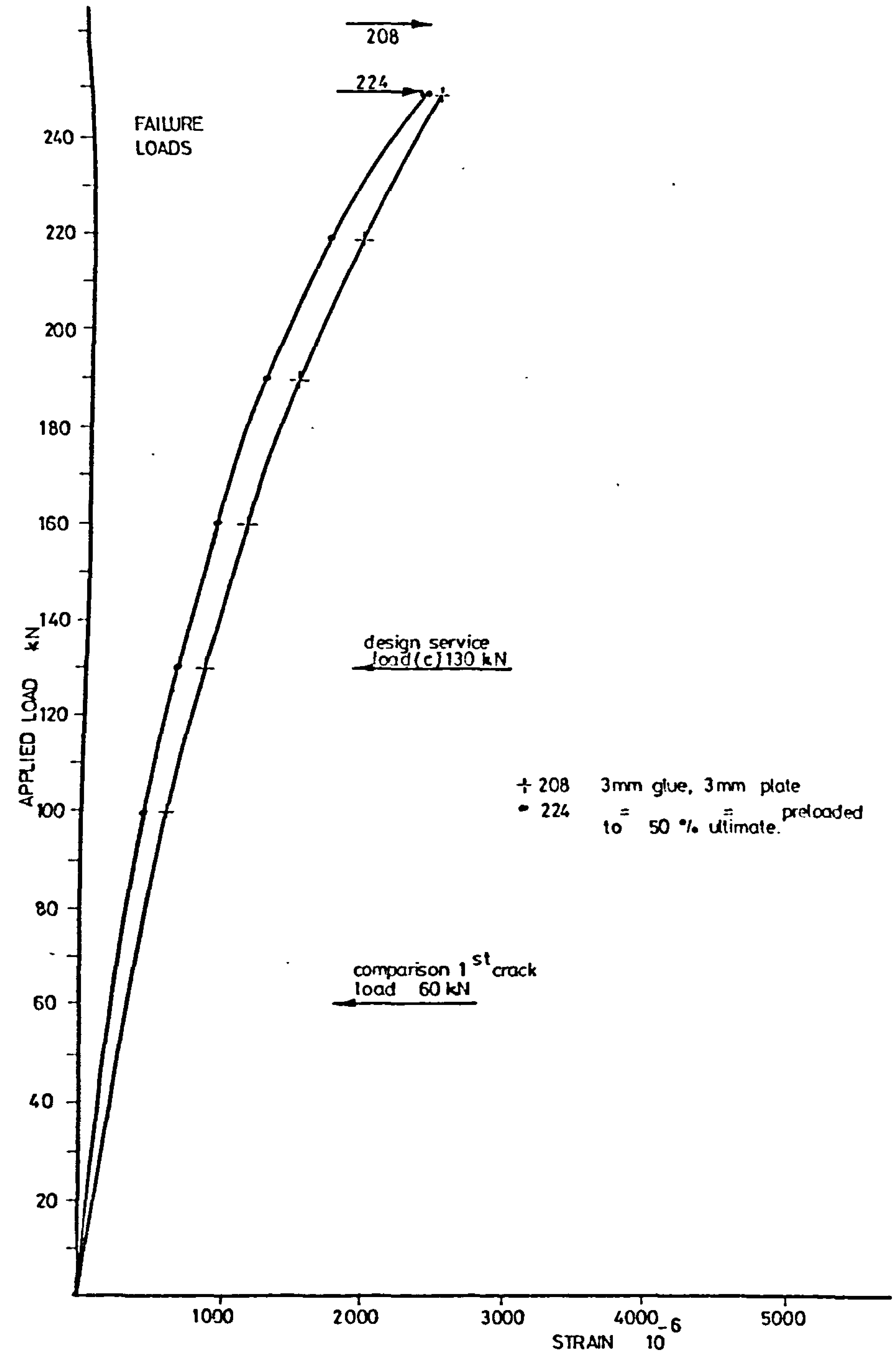

FIGURE 6.11 LOAD-STRAIN CURVES INTERNAL STEEL BARS - CENTRE SECTION

smaller strain. However, the same behaviour is also apparent in the beams preloaded to only 50% ultimate load and it is unlikely that bond failure would have occurred at this stage. This area of research must be studied further.

As shown in Table 6.1B at 60 kN load the internal bar strains were reduced to 64-80%, of the values for the unplated beam for beams strengthened with 1.5 mm thick plates; 47-58% for beams strengthened with 3 mm thick plates; and 27-33% for beams with 6 mm plates. At 130 kN load these same strains were reduced to 70-81% (1.5 mm); 50-58% (3 mm); and 34-41% (6 mm). Similarly at 190 kN load the strains were reduced to 46-62% (1.5 mm); 38-46% (3 mm); and 24-43% (6 mm). This information is given in Fig. 6.23. If, instead of adding external reinforcement, the bar area had been increased by the same area as the plates, the calculated stresses in the bars would be reduced to 84%, 72% and 55% of the original beam stresses, for 1.5 mm, 3 mm and 6 mm plates respectively. The decrease in strains obtained with the plated reinforcement is greater than would have been found for the same increase in bar area. This would be expected to some extent due to the increased lever arm of the plates. However, it shows that there is good composite action between the glue, plate and concrete.

The bar strains for the beams strengthened with 1.5 mm thick plates varied from 2520 to 3600 microstrain at the load stage prior to failure. This indicates that the bars were yielding as the elastic limit of the steel is approximately 2000 microstrain, see Fig. 3.8.

The beams strengthened with 3 mm thick plates had bar strains varying from 2200 to 2600 at the same load stage, again indicating yielding of the bars.

The beams with 6 mm thick plates had bar strains varying from 850 to 1250 microstrain indicating that the steel was well below its elastic limit.

6.3.2.3 External Plate Reinforcement Strains

Figs. 6.12 to 6.21 show similar behaviour for the plate strains as for the internal bar strains. The behaviour of the precracked beams was again not as expected.

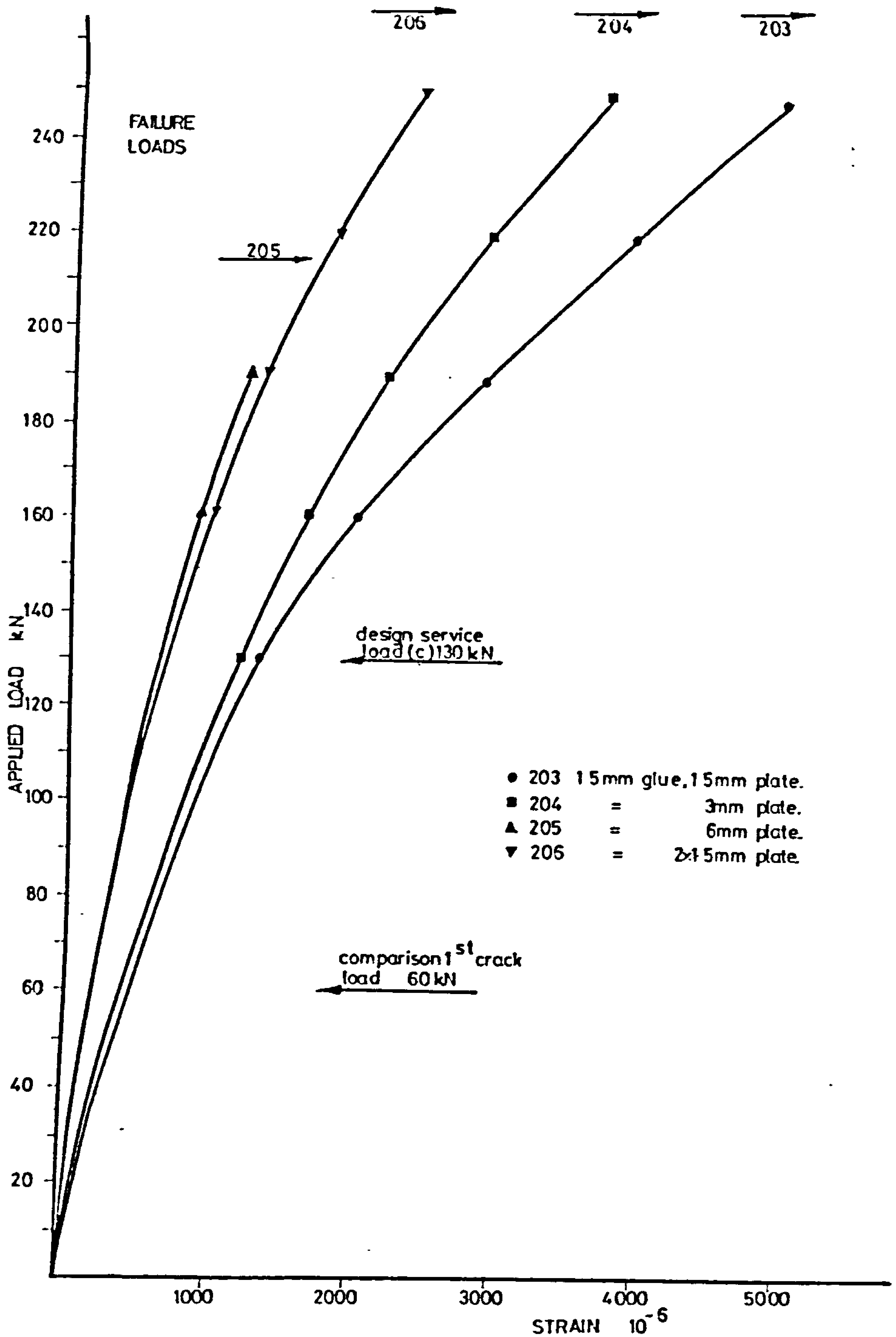

FIGURE 6.12 LOAD-STRAIN CURVES EXTERNAL STEEL PLATE - CENTRE SECTION

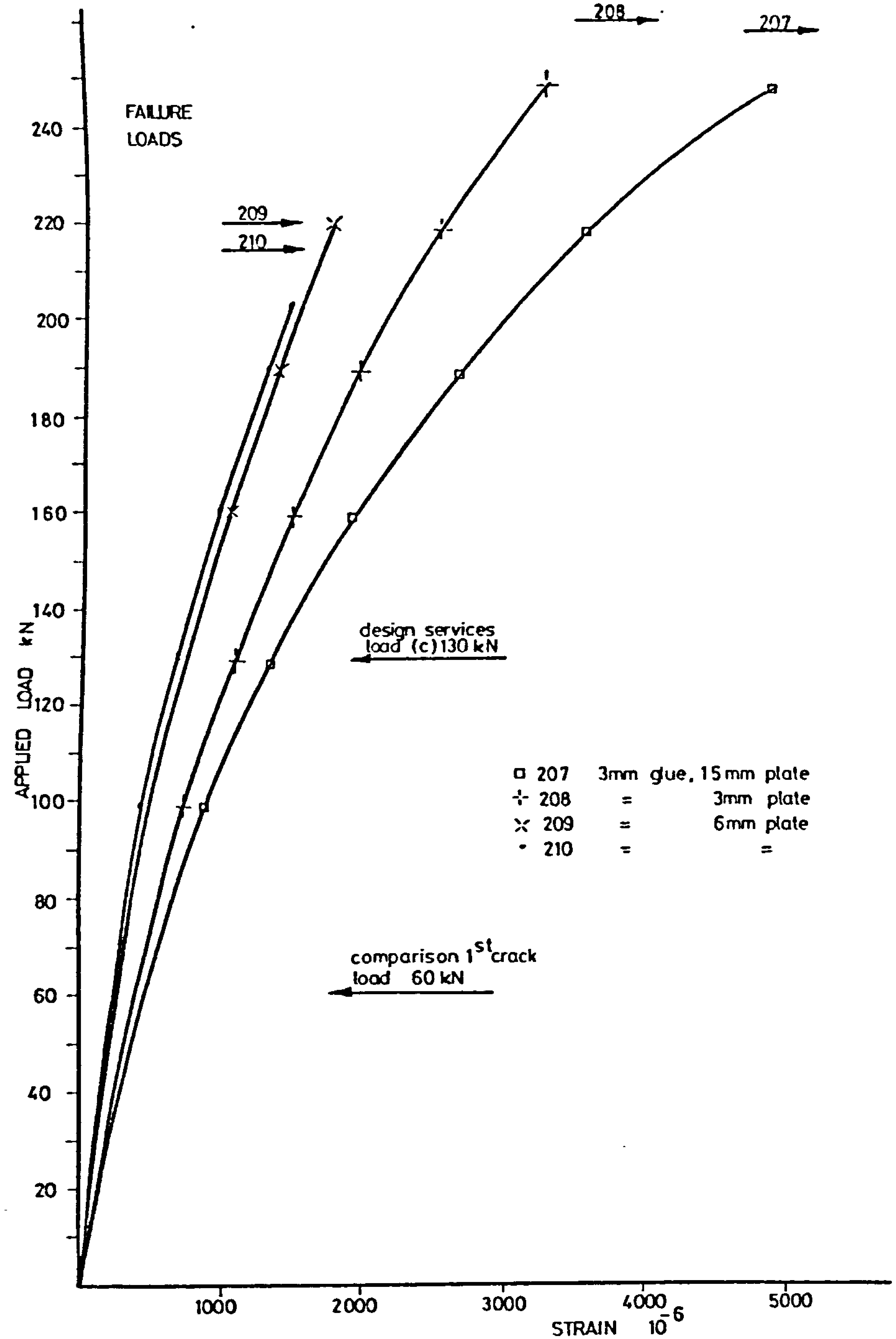

FIGURE 6.13 LOAD-STRAIN CURVES EXTERNAL STEEL PLATE - CENTRE SECTION

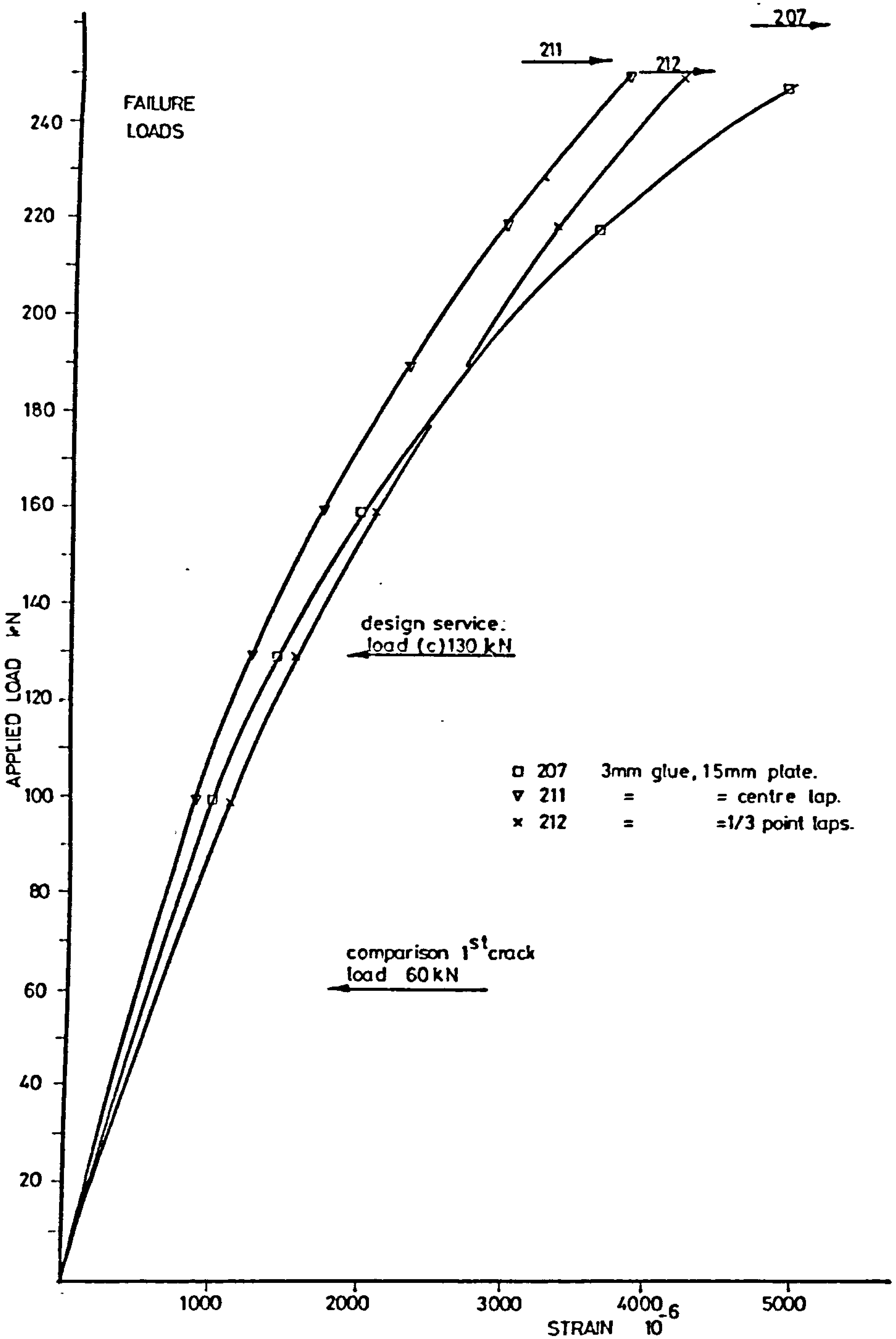

FIGURE 6·14 LOAD-STRAIN CURVES EXTERNAL STEEL PLATE - CENTRE SECTION

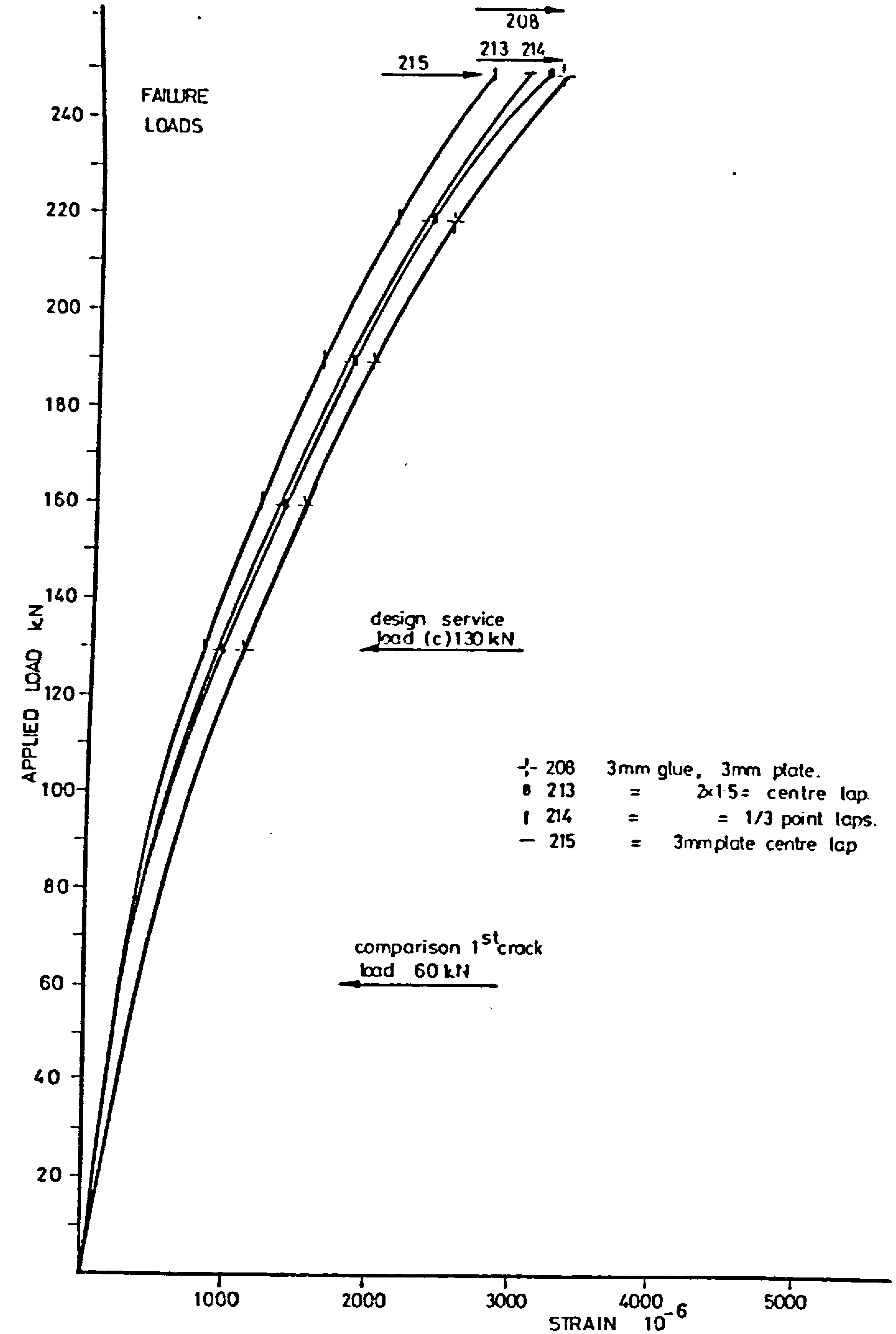

FIGURE 6·15 LOAD-STRAIN CURVES EXTERNAL STEEL PLATE - CENTRE SECTION

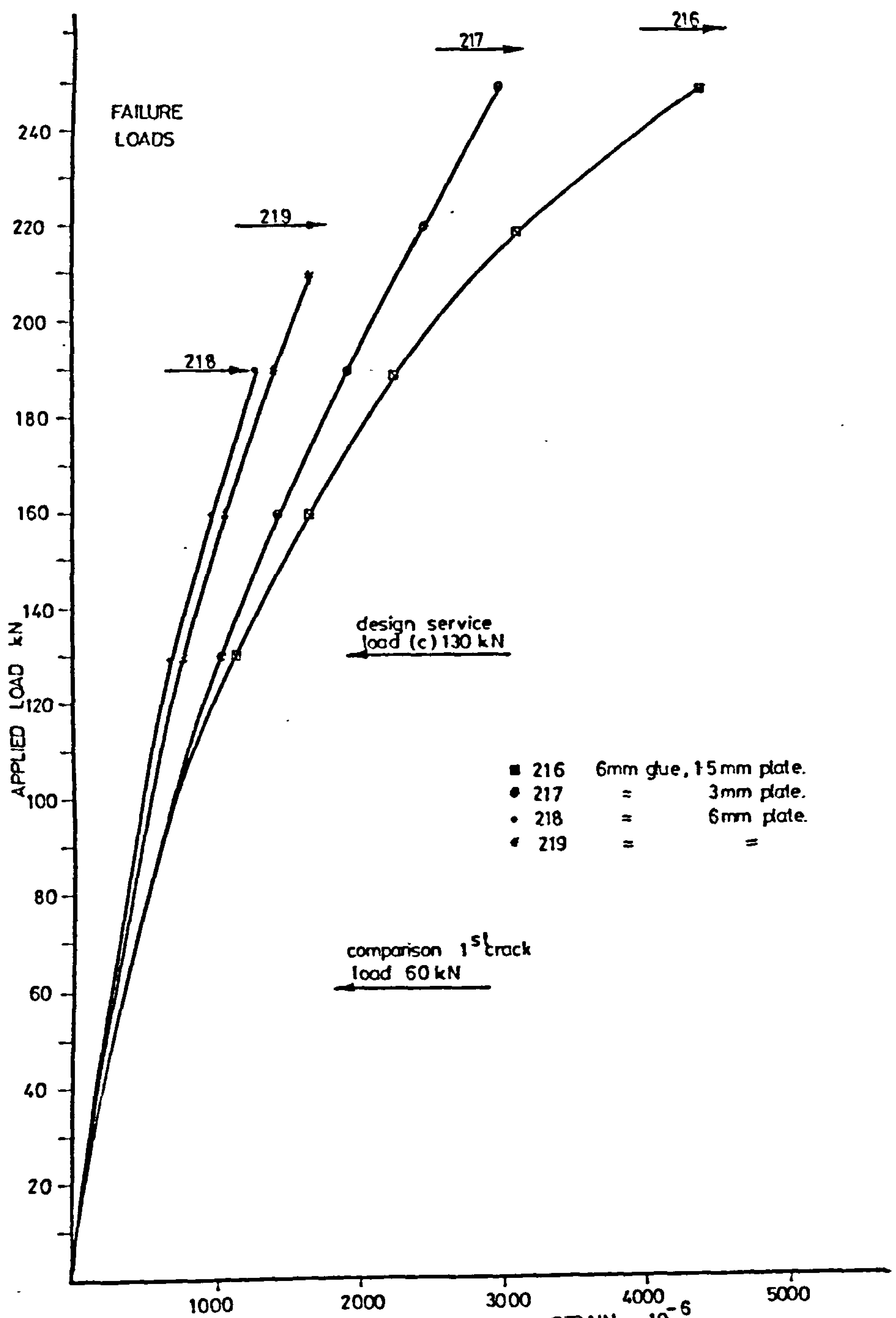

FIGURE 6·16 LOAD-STRAIN CURVES EXTERNAL STEEL PLATE - CENTRE SECTION

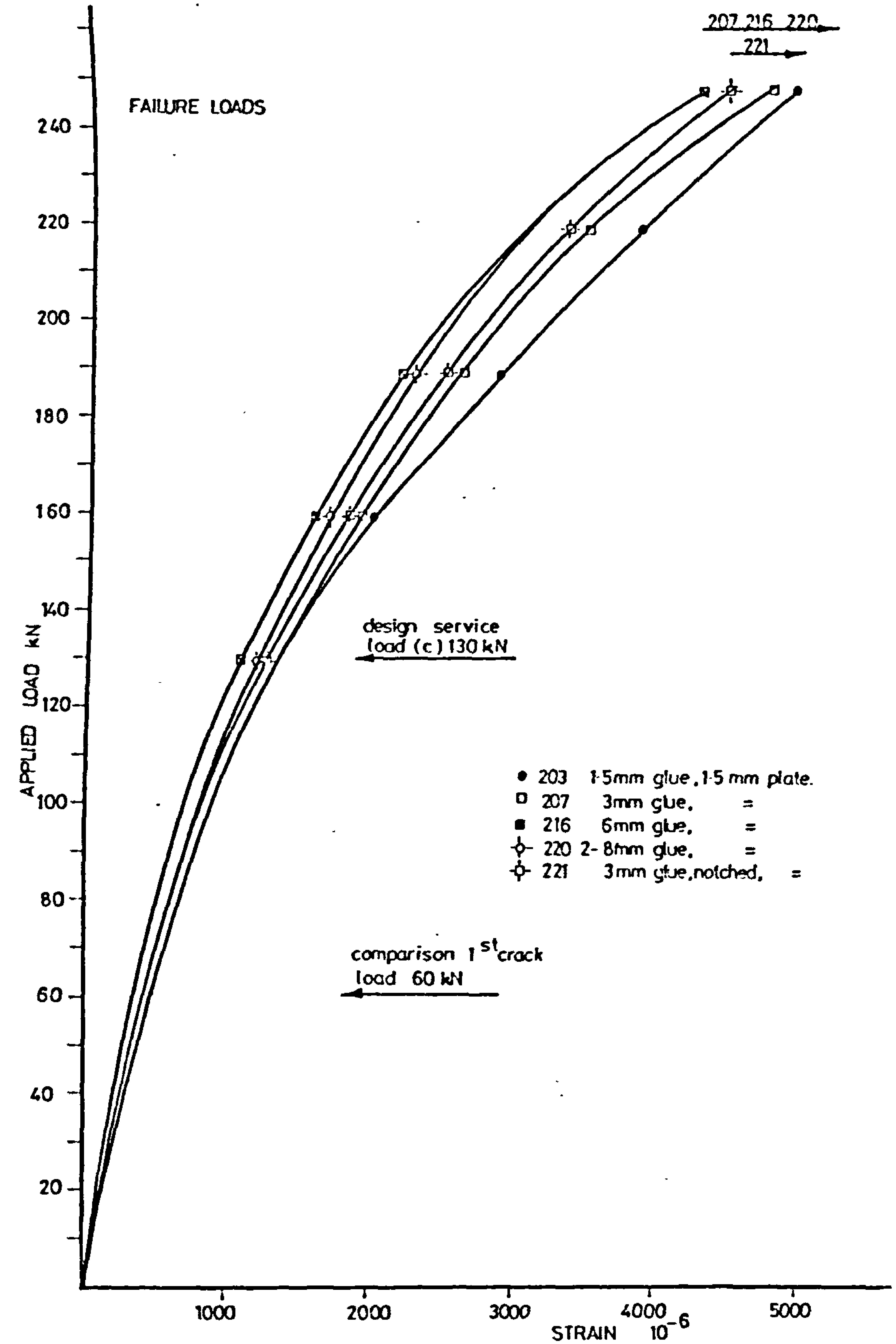

FIGURE 6·17 LOAD-STRAIN CURVES EXTERNAL STEEL PLATE - CENTRE SECTION

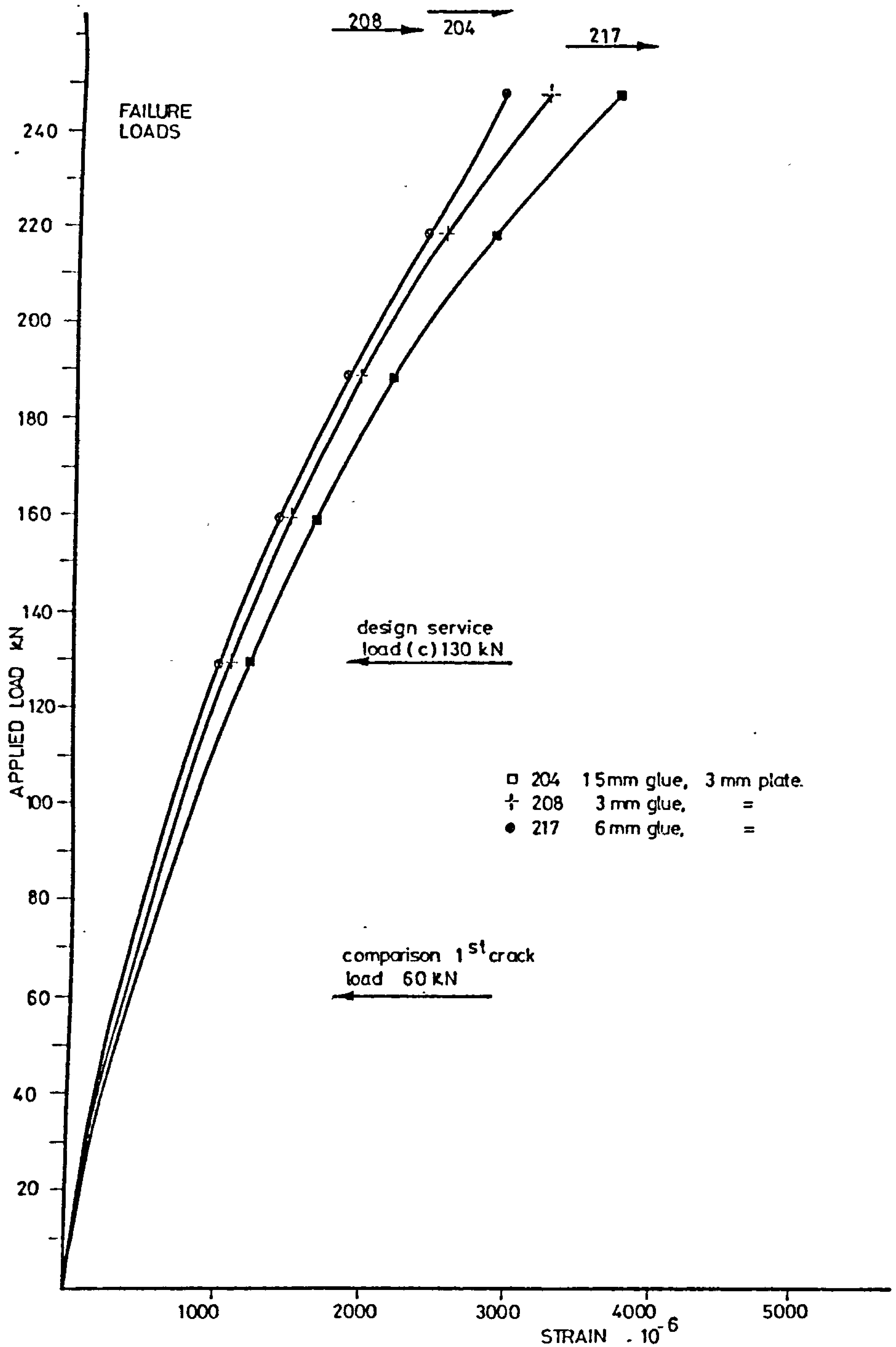

FIGURE 6.18 LOAD-STRAIN CURVES EXTERNAL STEEL PLATE - CENTRE SECTION

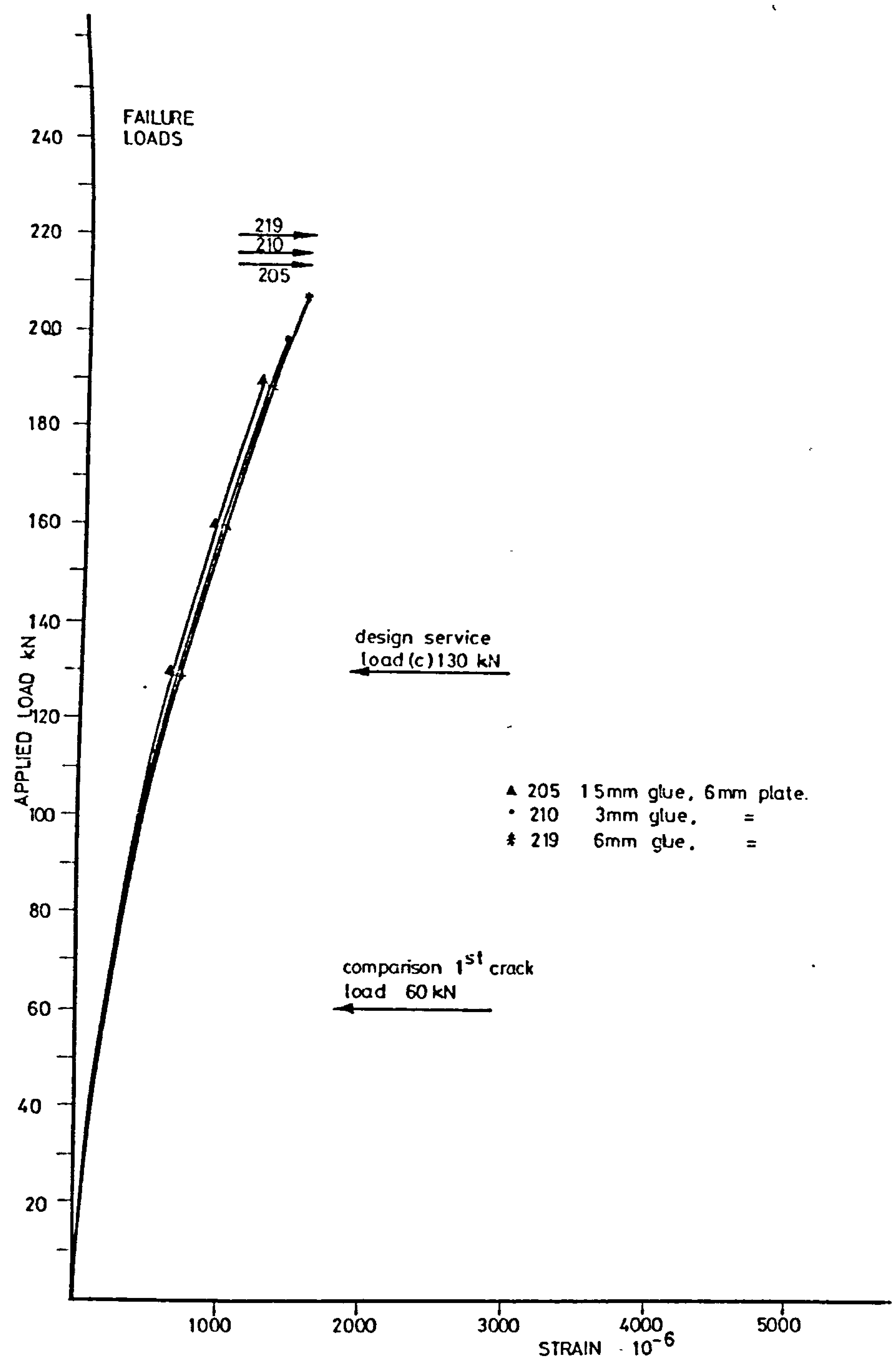

FIGURE 6.19 LOAD-STRAIN CURVES EXTERNAL STEEL PLATE - CENTRE SECTION

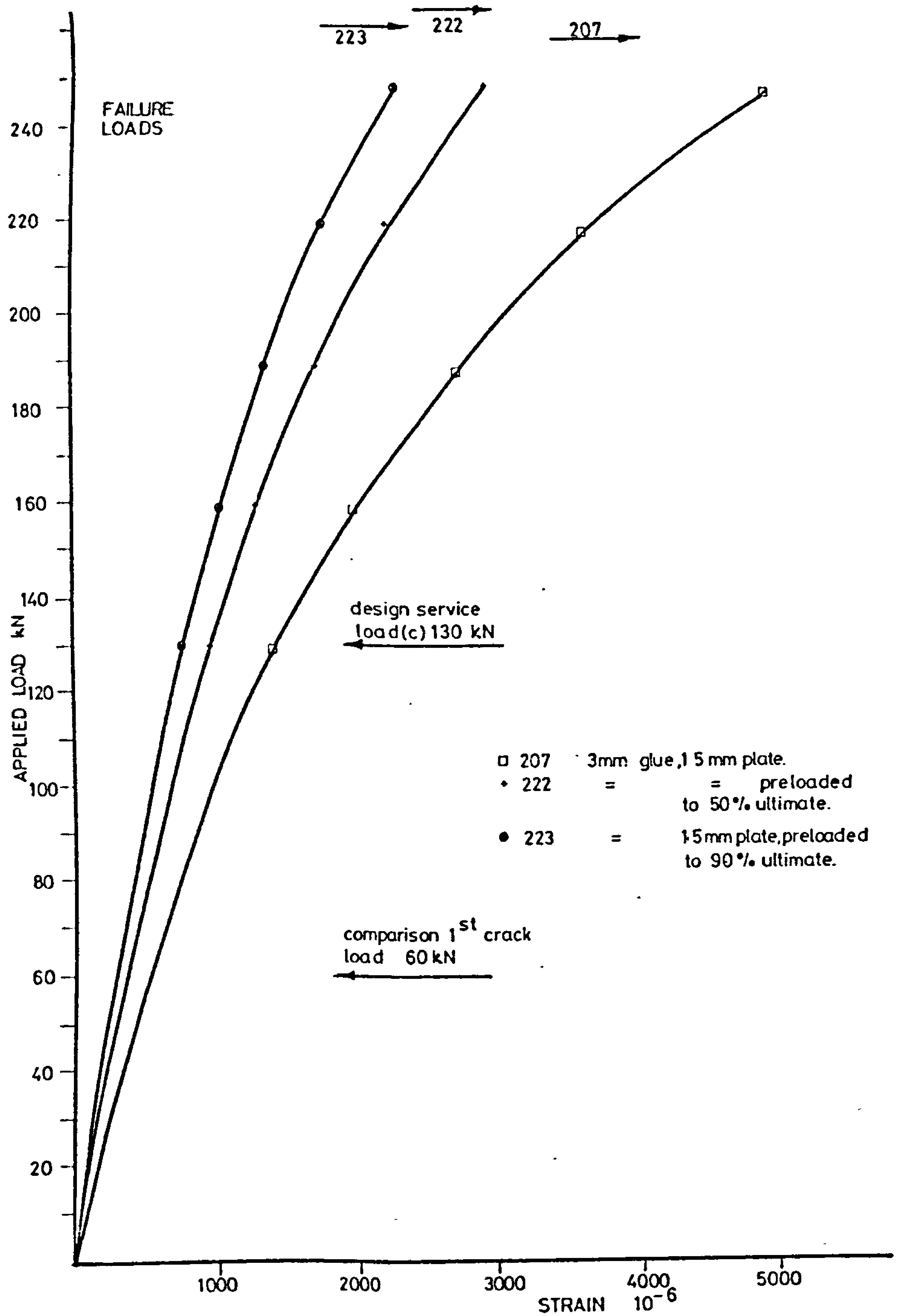

FIGURE 6·20 LOAD-STRAIN CURVES EXTERNAL STEEL PLATE-CENTRE SECTION

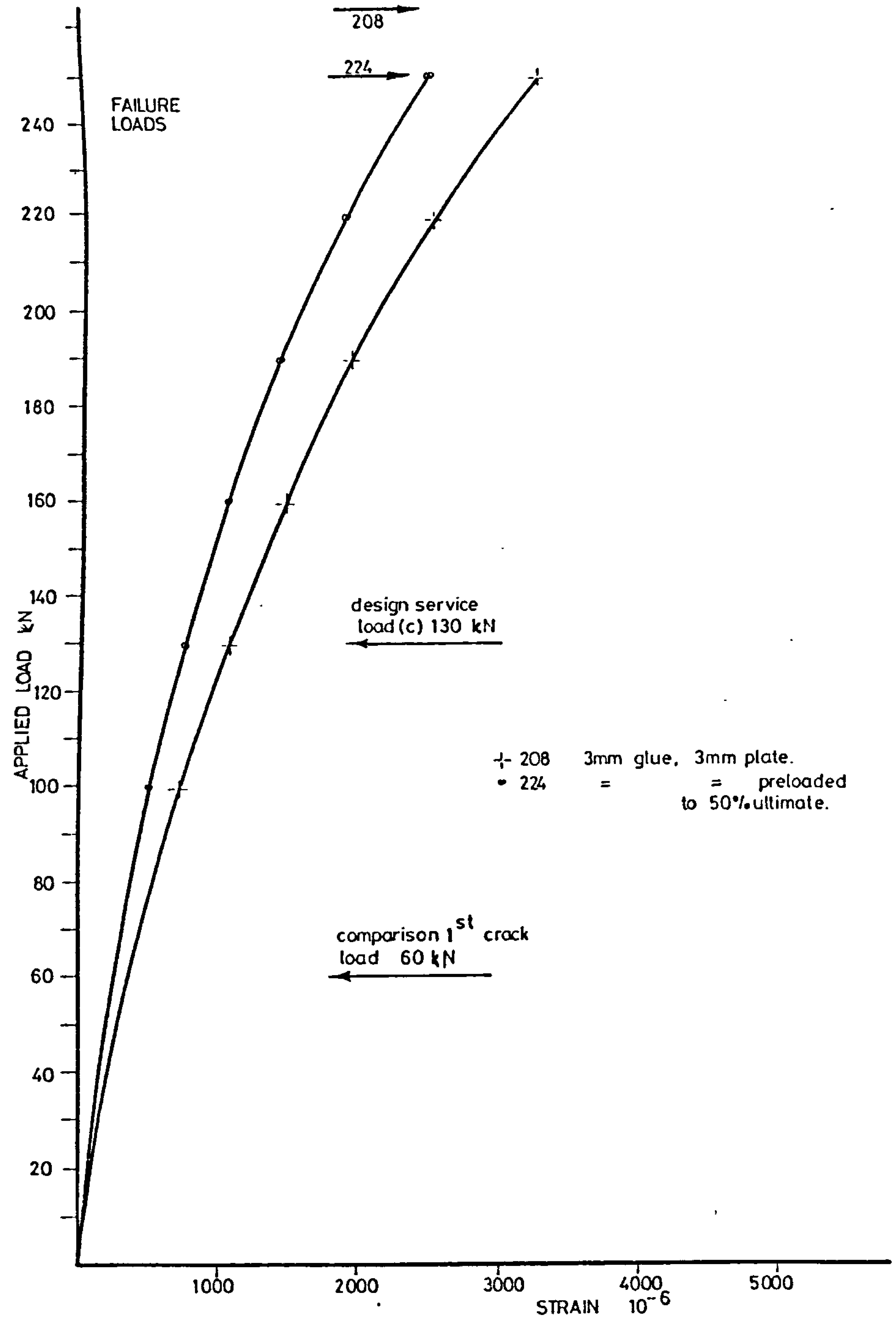

FIGURE 6·21 LOAD-STRAIN CURVES EXTERNAL STEEL PLATE-CENTRE SECTION

Fig. 6.22 shows the longitudinal distribution of plate strains. For a constant glue thickness, increasing the plate thickness reduces the general level of straining. Increasing the glue thickness for a constant plate thickness has a similar but much reduced effect. It can be seen that the strain increases along the beam, as the bending moment, until it reaches the load points. The strain varies only slightly in the constant moment region. The strain gradient is largest at the end of the plate, but the 6 mm gauge length was not suitable for obtaining an accurate measurement of this gradient. A more accurate measurement of the rapidly changing stress fields around the end of the plate, at joints and around cracks, must be developed.

The measured values of strain can only be an approximation to the local strains as they are based on average values over a finite gauge length. Therefore, it follows that the smaller the gauge length the more accurate a representation of the strain distribution is obtained. It should be noted that the strain in the plate at any particular distance from the end of the plate is not constant across the width. To obtain the stress contours in such areas, or around joints and cracks in the concrete, many strain gauges of small gauge length would be needed in a grid pattern over the entire area. Such an array of gauges would best be monitored by a data logger. Alternatively it may be possible to use photoelastic techniques. It would also be useful to have strain gauges embedded within the glue layer to obtain similar distributions of adhesive stresses.

The variations of external plate strains with plate and glue thickness are shown diagrammatically in Fig. 6.24. The effect of plate thickness can be seen to be greater than that of glue thickness.

At the load stage prior to failure, the strain gauges at the centre section of the beams with 1.5 mm thick plate reinforcement indicated that the strains in the plates varied from 3000 to 3900 microstrain. The yield strain of the 1.5 mm thick plate is 1300 microstrain, as shown in Fig. 3.9. This indicates that extensive yielding has occurred prior to failure. Although this was not visually evident while the beam was under load, it became obvious when

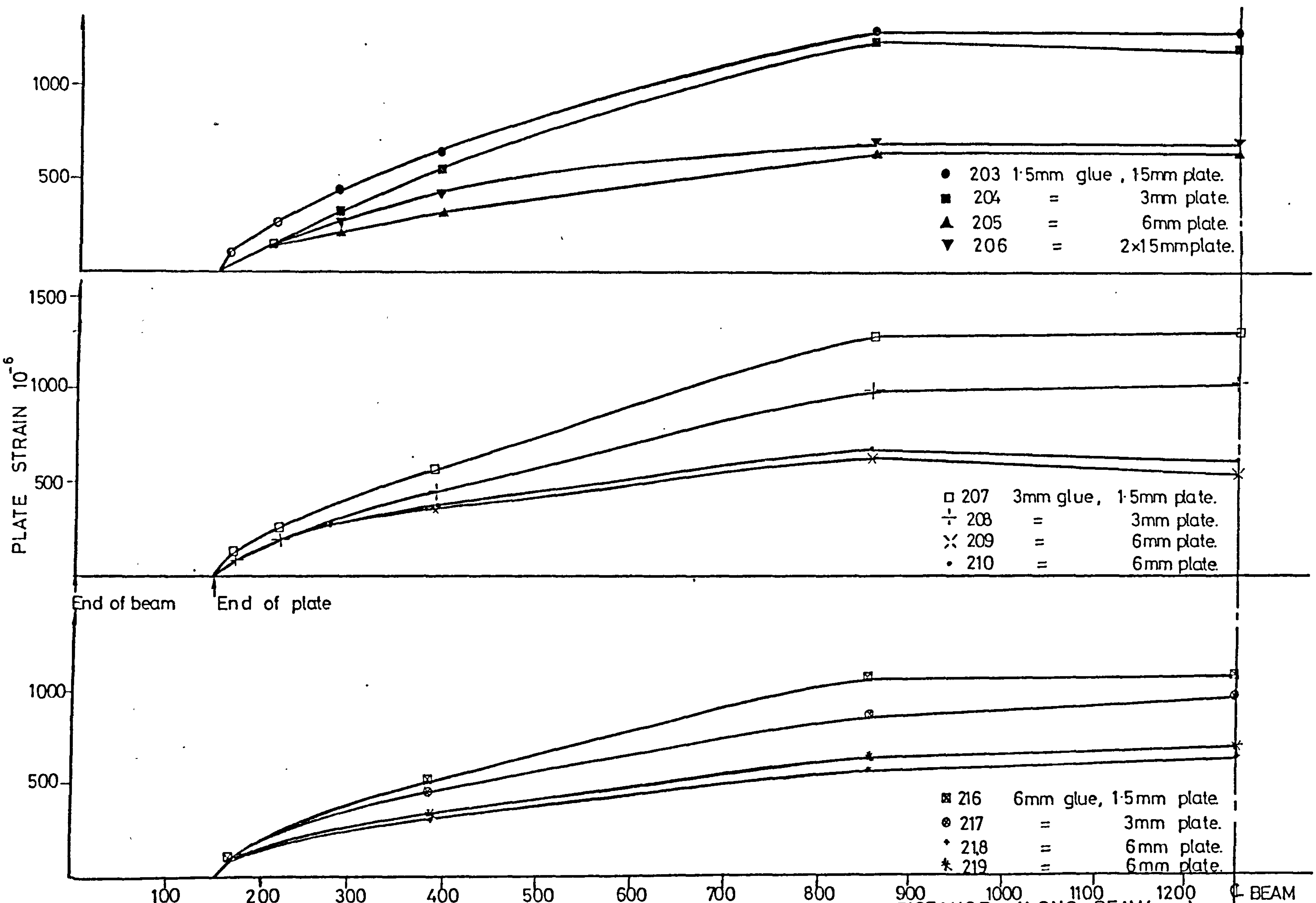

FIGURE 6·22 TYPICAL LONGITUDINAL STRAIN DISTRIBUTIONS

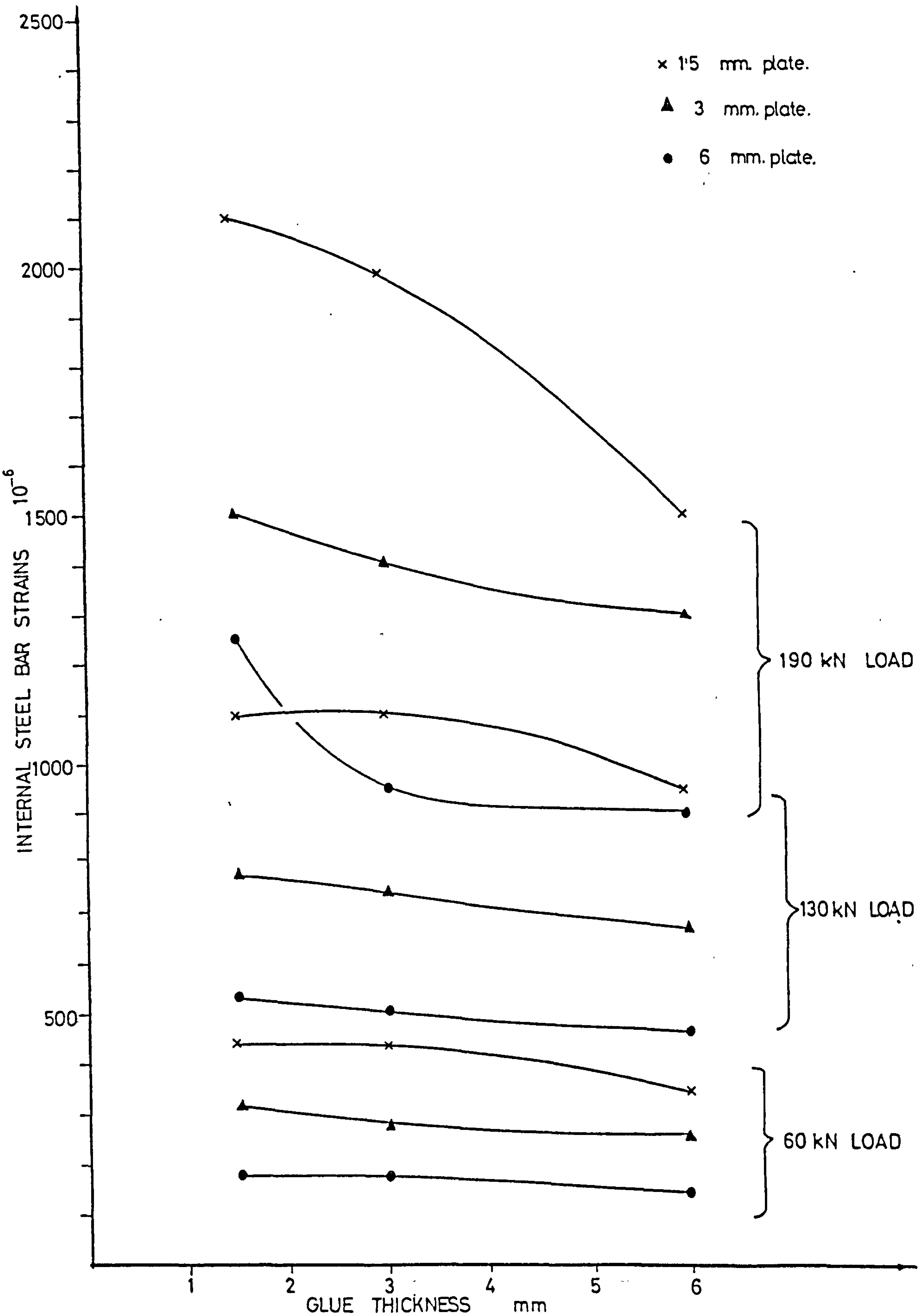

FIGURE 6·23 INTERNAL STEEL BAR STRAIN v PLATE & GLUE THICKNESS

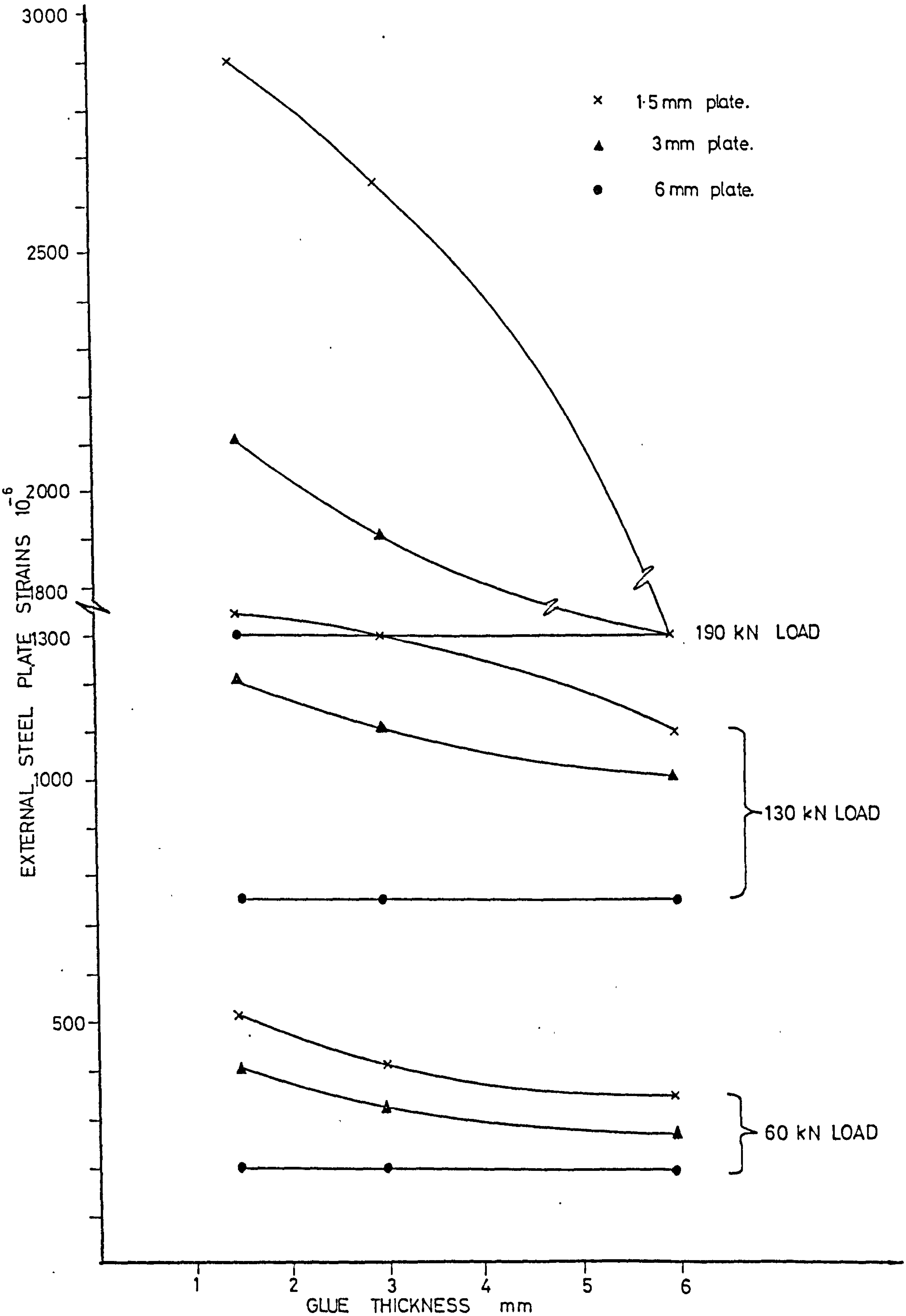

FIGURE 6·24 EXTERNAL STEEL PLATE STRAIN v PLATE & GLUE THICKNESS releasing the load after failure. At this stage the plastically deformed plate warped away from the concrete beam.

At the load stage prior to failure for the beams with 3 mm thick plates, the plate strains varied from 2300 to 2900 microstrain, again indicating yielding of the plates.

For the beams with 6 mm thick plates the strains varied from 1200 to 1300 microstrain. The yield strain, Fig. 3.9, was 1500 microstrain. This indicates that the plates are approaching their yield point at failure.

In Appendix 7 some assessments of interfacial stresses are made. The shear stress and the anchorage bond stress are calculated from the measured plate strains. Local bond stresses are also given. It should be emphasised that these evaluations of interfacial stresses should be treated qualitatively. The tests were not designed to study such properties and the values found are not limiting nor ultimate stresses.

6.3.2.4 Concrete Strains

At 60 kN load, the compressive concrete strain in the unplated beam was 455 microstrain. For the plated beams the mean values were as follows: for beams with 1.5 mm thick plates - 410 microstrain; for beams with 3 mm thick plates - 356 microstrain and for beams with 6 mm thick plates - 226 microstrain.

At the load stage prior to failure the values were: unplated beam 3350 microstrain; 1.5 mm plate - 2407 microstrain; 3 mm plate - 2080 microstrain; 6 mm plate - 1230 microstrain.

The determination of the ultimate strains involves having the gauge length of the demec extensometer straddling the section at which the beam would fail. Furthermore, the strains recorded are those measured prior to, and not at failure.

Values of 1200 to 5000 microstrain for the ultimate limiting strain of normal strength concrete have been reported (98). For beams with 1.5 mm thick plates and some beams with 3 mm thick plates it would appear that the full strain capacity had been achieved, as was exhibited by crushing of the concrete at failure. The beams with 6 mm plate did not reach their full strain capacity.

Typical concrete strain distributions are given in Fig . 6.25. Before the beams cracked the difference between the strains at the outer tension and compression faces was a small amount arising from the fact that the neutral axis of the composite section is slightly removed from the half depth. This indicates that the modulus of elasticity of the concrete is of the same order in both tension and compression. Above the first crack load, the strain distributions were approximately linear above the neutral axis but non-linear below it. This is because once the concrete has cracked the demec reading is not the true strain, but is an average 'strain' which depends on the positions of cracks. In all the beams the neutral axis position moved closer to the compression face prior to failure, as the steel started to yield. The rise of neutral axis position was greater in the beams with 1.5 mm plate than for beams with 3 mm and 6 mm plates. This showed that the beams were changing from being well under reinforced (1.5 mm plate) to an almost balanced section (6 mm plate).

The mean ratios of neutral axis to effective depths, at the load stage prior to failure were: 0.31 for the unplated beam; 0.40 for beams with 1.5 mm plate; 0.44 for beams with 3 mm plates; and 0.47 for beams with 6 mm plates.

In normally reinforced concrete beams some limitation is placed on the percentage of tension steel in a beam, during the design process. The purpose of this is to ensure that the steel will reach its yield stress before the concrete fails in compression, and thus avoid brittle failure. As tension steel is added to a beam the ratio x/d increases. It has been found by experiment that the steel does not yield when x/d is approximately 0.6, therefore for design it is generally limited to 0.5. For the plated beams in the present series the transition from purely flexural to a more brittle shear/bond failure appears to come between the beams with 1.5 mm and 3 mm plates. Their values of x/d being 0.4 and 0.44 respectively. It would seem, therefore, that a limiting value of x/d of 0.4 would be better for plated beams.

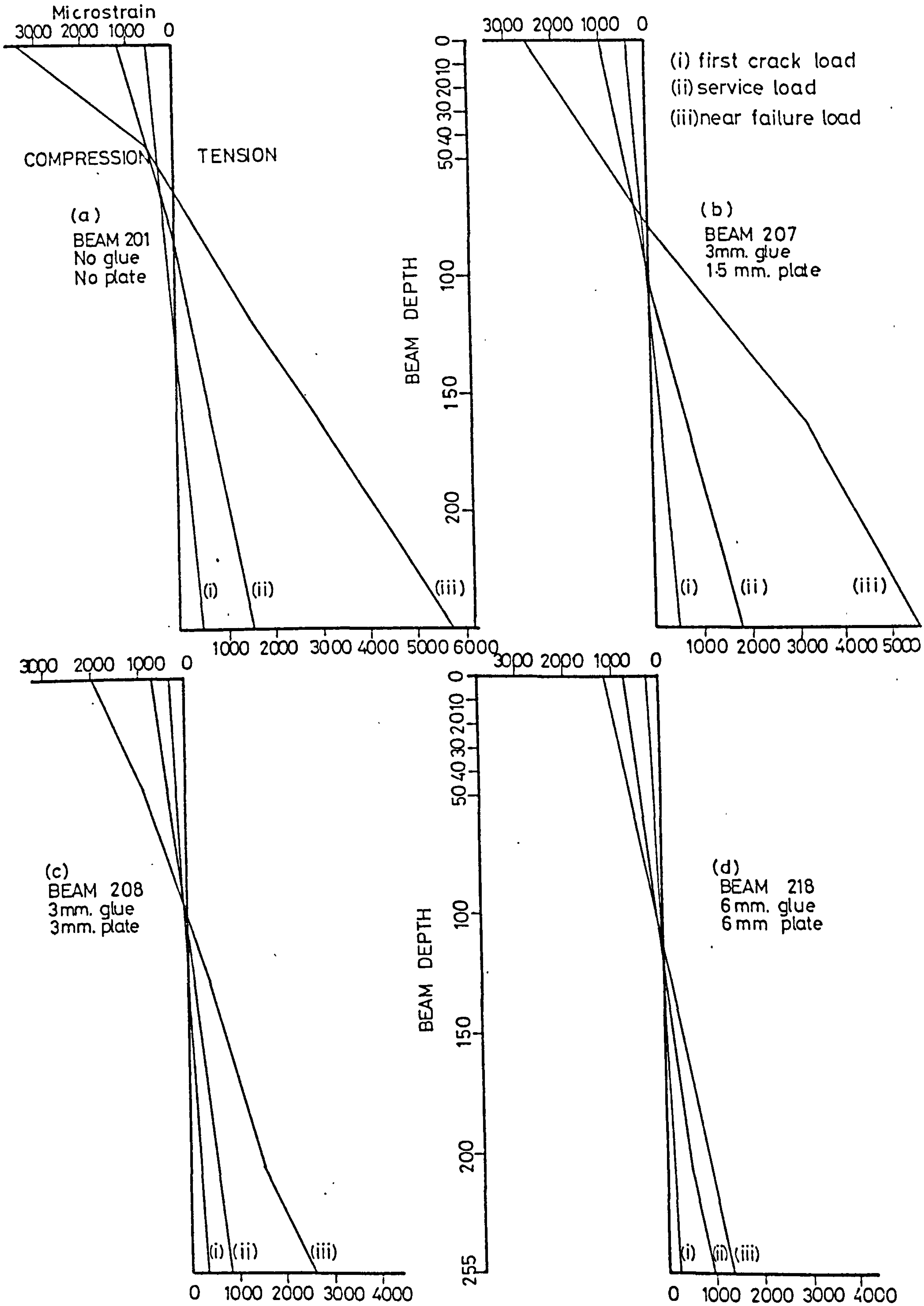

FIGURE 6·25 TYPICAL STRAIN DISTRIBUTIONS IN THE CONCRETE AT THE CENTRE SECTION

The beams tested by Ang (72) showed a transition from flexural to shear/bond also. This occurred between beams with 3 mm and 5 mm plate, their values of x/d being 0.39 and 0.47 respectively.

However, it is thought that the type of shear bond failure found in the beams with thicker plates could be alleviated, as discussed in Chapter 5 under ultimate loads. By modifying the plate ends such failures could be changed back to a flexural mode. Further testing is needed to verify this, and then the limiting value of x/d suggested by the present series may be increased.

6.3.3 Load Deflection Characteristics

6.3.3.1 Review of Literature

The actual deflection behaviour in beams is probabilistic in nature and requires statistical methods for a rational analysis. Even with the most sophisticated methods of analysis using experimentally determined material properties, the range of variation between measured and computed results is surprisingly high. Studies (82) have shown that the coefficient of variation for such deflections is of the order of 15 to 20%. In addition this difficulty is compounded when applied to actual structures, since the only property of the concrete known to the designer is the specified characteristic strength.

Because of the variability of deflection, it would appear to be not only feasible but also essential that relatively simple procedures be used so that engineers will not place undue reliance on predicted results.

When subjected to a load, a section of a beam undergoes compression on one side and tension on the other, which gives rise to a local curvature at that section. This curvature $\emptyset$ may be expressed by

$$\emptyset = \frac{\varepsilon_c + \varepsilon_t}{h}$$

where ε_c is the maximum compressive strain at the section,

ε_t is the maximum tensile strain at the section, and

h is the depth of the section.

For a beam consisting of an elastic material, the local curvature ϕ is given by

$$\phi = \frac{M}{EI}$$

where M is the applied moment at the section,

E is the elastic modulus of the beam material, and

I is the second moment of area of the section.

The rotation or deflection of the beam may be found by computing the single or double integral of the local curvatures respectively. In general the deflection, a, is given by

$$a = k \phi \ell^2$$

where k is a constant depending on the variation of curvature along the beam and ℓ is the span of the beam.

The most important methods of predicting short term deflections of reinforced concrete members, proposed over the last 20 years are given below:

(a) <u>1960 - Yu and Winter (76)</u> presented two simple methods for the calculation of instantaneous deflections under service load.

Method A. The deflections are calculated using elastic methods. The cracked, transformed moments of inertia at the midspan is used as a constant value throughout the length of the beam for simple spans.

Method B. To account for the contribution of the concrete between tension cracks to the rigidity of the beam the deflections from method A were multiplied by a correction factor F

$$F = 1 - \frac{M_1}{M}$$

where $M_1 = 0.1\ f_{cu}{}^{2/3}\ h(h - x)$ and M = service moment. The derivation of the correction factor followed an elastic theory approach with the factor 0.1 having been determined empirically. Comparison with test data for 90 beams indicated that method B gave somewhat better results.

(b) 1961 - Comité European du Beton (78) (CEB) gave a simplified method for determining deflections under short term loads, in which the value of instantaneous deflection was considered equal to the sum of the deflection of the uncracked section under the moment at which cracking is produced, and the deflection of the cracked section under a moment equal to the working moment less the moment at which cracking is produced. This latter moment being calculated from the tensile strength of the concrete in bending. This can be expressed by:

$$a = k\,\ell^2 \left[\frac{M_{cr}}{E_c\, I'_u} + \frac{4}{3}\, \frac{(M - M_{cr})}{E_s\, A_s\, d^2 (1 - 2q)\, (1 - 2q/3)} \right]$$

where M_{cr} is the moment at which cracking is produced,

M is the moment under consideration,

E_c, E_s are the elastic moduli of concrete and steel,

I'_u is the uncracked transformed moment of inertia,

A_s is the area of reinforcement,

d is the effective depth, and

$$q = \left(\frac{A_s}{bd}\right) \left(\frac{f_y}{f_{cu}}\right)$$

This is a sound and logical method which can allow for the application of a load lower than the working load. In practice, however, there is some uncertainty in assessing the tensile strength of the concrete as this can be reduced considerably by shrinkage.

(c) 1963 - D. E. Branson (77) gave a form of expression for the effective moment of inertia of a beam in which the effect of bending moment, section properties, concrete strength and extent of cracking is included. The expression satisfies the limiting conditions $I_{eff} = I'_u$ when the moment at that section $M = M_{cr}$ the cracking moment, and I_{eff} = approaches I'_{cr} when M is very large in relation to M_{cr}.

$$I_{eff} = I'_u - (I'_u - I'_{cr}) \left[1 - \left(\frac{M_{cr}}{M}\right)^n\right]$$

where n is an unknown power. A precedent for a power function relation relative to the distribution of cracking effects was established by Murashev (83). Branson used the results from some 58 laboratory beams, (simple and two span rectangular beams and simply supported T beams), to empirically determine the value for n. For the effective moment of inertia at an individual section n = 4 was found to give good agreement. It was further determined that the same type of equation but with n = 3 could be used for an average I_{eff} for simply supported beams with uniform loading. The equation given above was rewritten as:

$$I_{eff} = \left(\frac{M_{cr}}{M}\right)^3 I'_u + \left[1 - \left(\frac{M_{cr}}{M}\right)^3\right] I'_{cr}$$

The deflection, a, is then given by

$$a = \frac{k\ M\ L^2}{E_c\ I_{eff}}$$

where k is a coefficient which depends on the type of loading and support conditions.

(d) 1968 - Beeby (84) proposed an idealised form of the moment curvature relationship where $\emptyset$, the curvature was given by:

$$\emptyset = \frac{M_{cr}}{E_c\ I'_u} + \frac{M - M_{cr}}{X}$$

Firstly, it was assumed that $X = E_c\ I'_{cr}$ but this overestimated the values when compared with the results from 133 test beams. Alternative values for X were given as:

$$X = E_c\ (0.825\ I'_{cr})$$

and

$$X = (0.57\ E_c)\ I'_{cr}$$

(e) 1970 - CEB (85) for beams of constant section, loaded in simple bending and subjected to symmetrical loading the midspan deflection is given by:

$$a = k\ \ell^2 \left(\frac{M_{cr}}{E_c\ I'_u} + \frac{4}{3}\frac{M - M_{cr}}{E_s\ A_s\ z(d - x)}\right)$$

where M_{cr}, M, E_c, E_s, I'_u have the same meaning as before

z = lever arm,

d = effective depth, and

x = neutral axis depth.

This is similar to their earlier recommendations (1961) with the part relating to post cracking stiffness being modified.

(f) 1972 - Stevens (80) describes two methods for determining deflections from curvatures determined using the maximum tensile and compressive strain in the steel and concrete respectively. In the first method it was assumed that the concrete in the tension zone has no contribution to the rigidity of the beam. In the second method the concrete resists tension between the cracks with as much as 75% of its flexural strength. The second method was found to give better results.

(g) 1972 - CP 110 (86) suggests an approach which involves finding the curvatures of sections initially, and then calculating the deflection by numerical integration along the beam. The code does, however, suggest a simplified approach.

6.3.3.2 Load-Deflection Curves

Figs. 6.26 to 6.35 show the load-deflection curves for the test beams. Fig. 6.26 shows that for a constant 1.5 mm glue thickness the deflections are reduced with increasing plate thickness. The beam with two layers of 1.5 mm plate gave almost identical results to the beams with a single layer of 3 mm plate. Figs. 6.27 and 6.30 show similar behaviour for beams with 3 mm and 6 mm plates respectively.

Fig. 6.28 shows that the beam with a glue layer, but no plate, is slightly stiffer than the unplated beam. The beams with lapped plates showed the same behaviour as for strains, i.e. slightly reduced deflections compared with those of the beam with a continuous plate layer. Fig. 6.29 also compares a beam with an unlapped 3 mm thick plate to another beam having 3 mm plate and a central lap joint. Two other beams are shown which had two layers

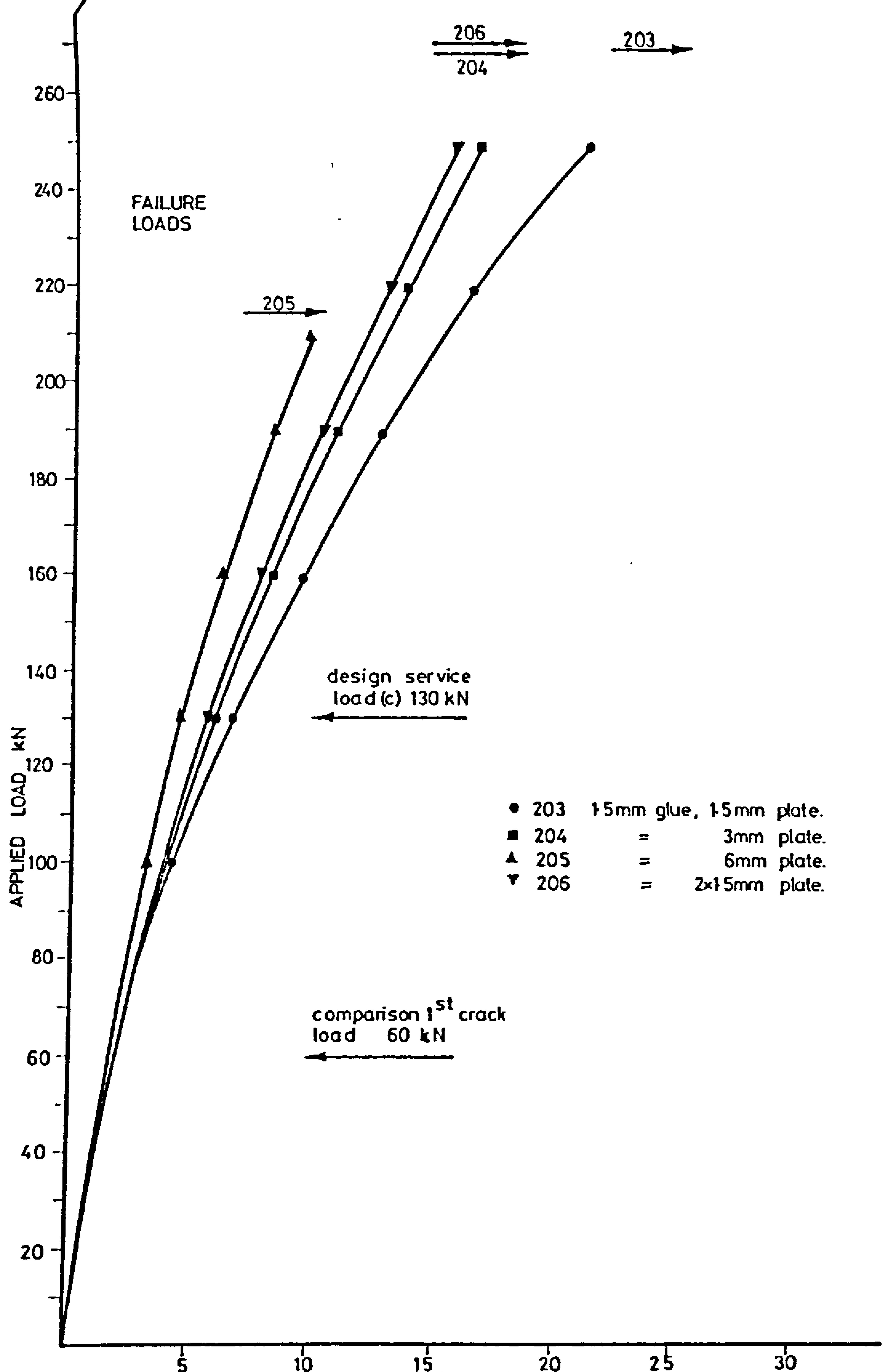

FIGURE 6 26 LOAD-DEFLECTION CHARACTERISTICS

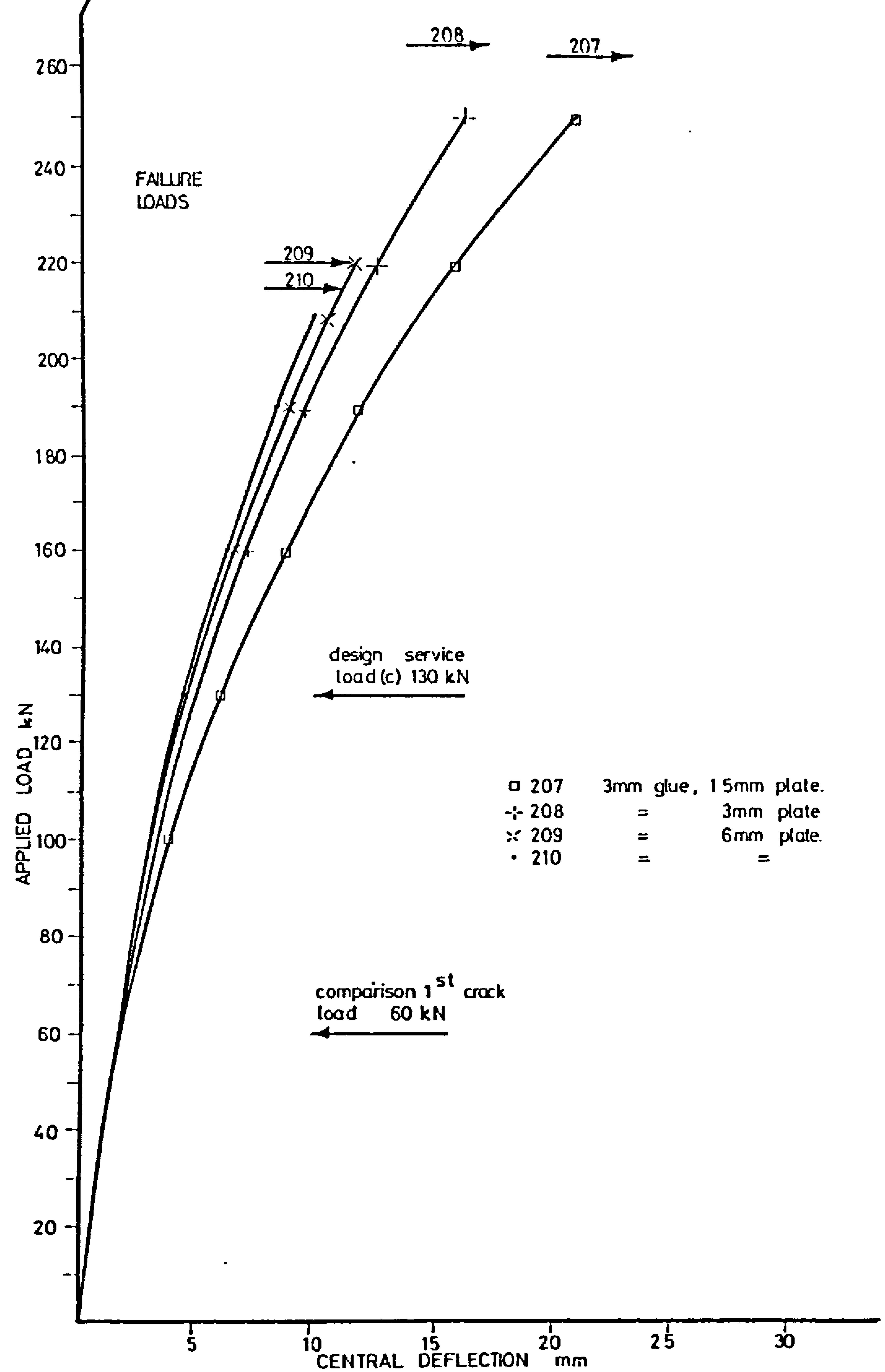

FIGURE 6·27 LOAD-DEFLECTION CHARACTERISTICS

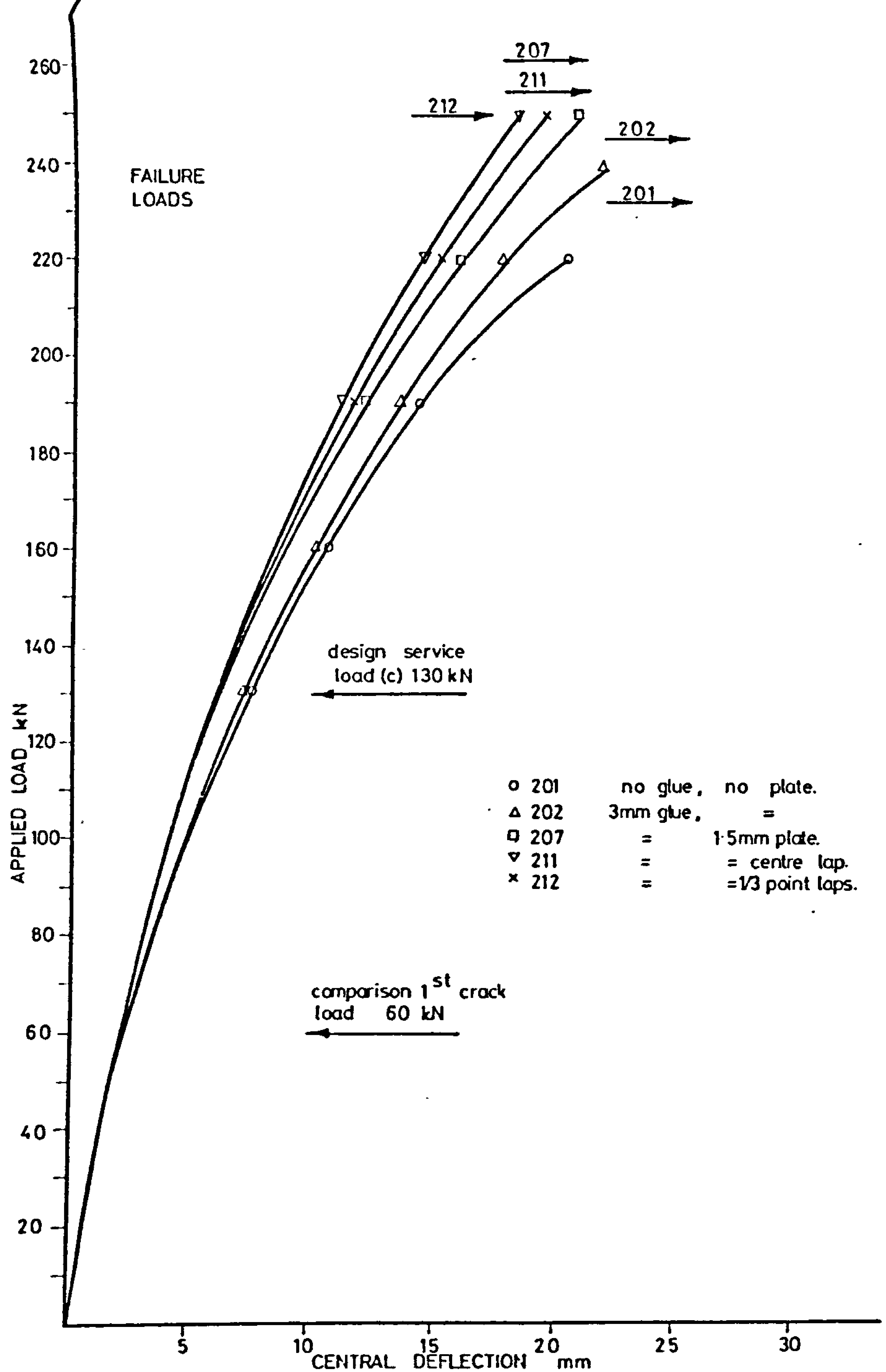

FIGURE 6·28 LOAD-DEFLECTION CHARACTERISTICS

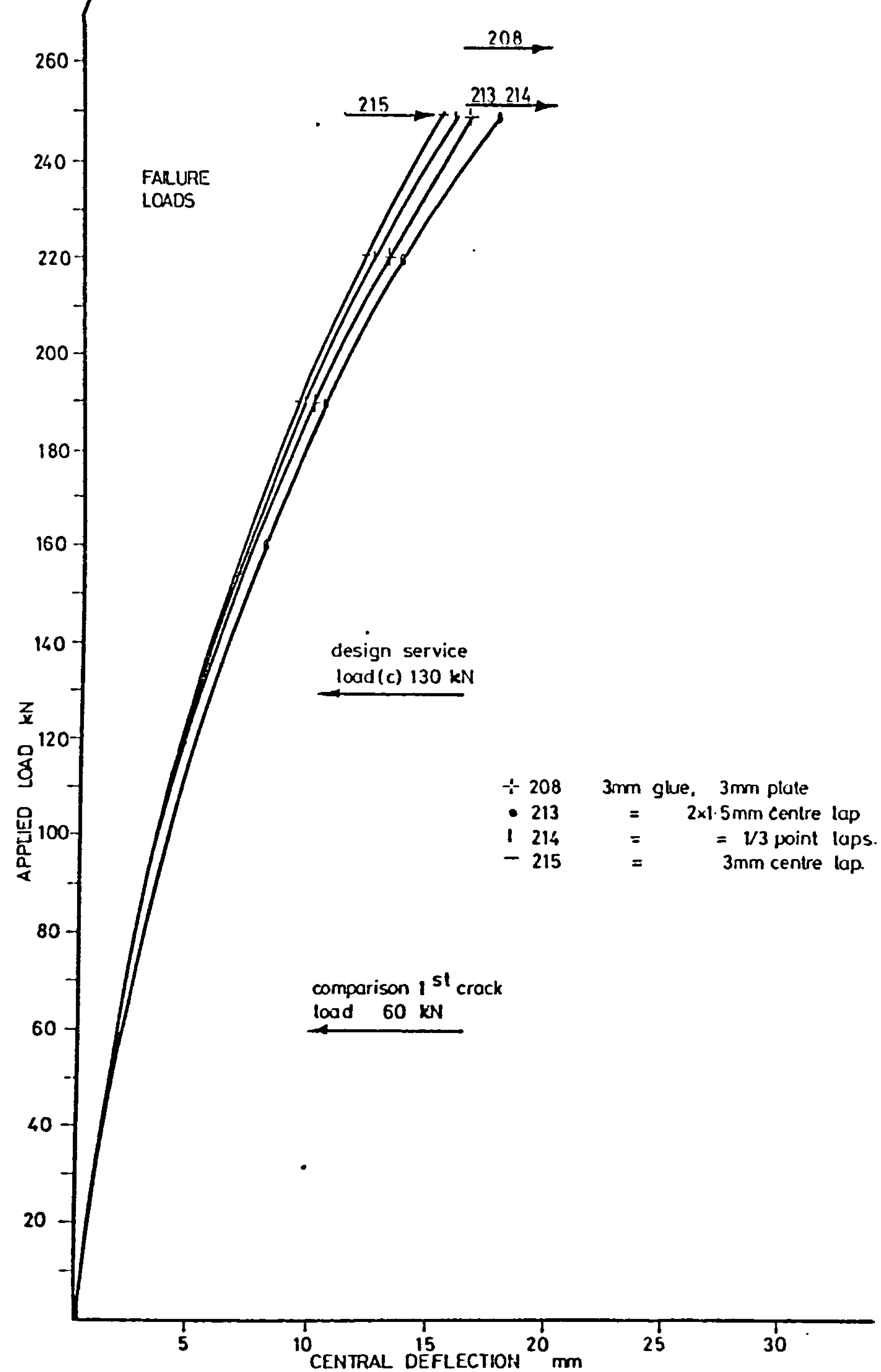

FIGURE 6·29 LOAD-DEFLECTION CHARACTERISTICS

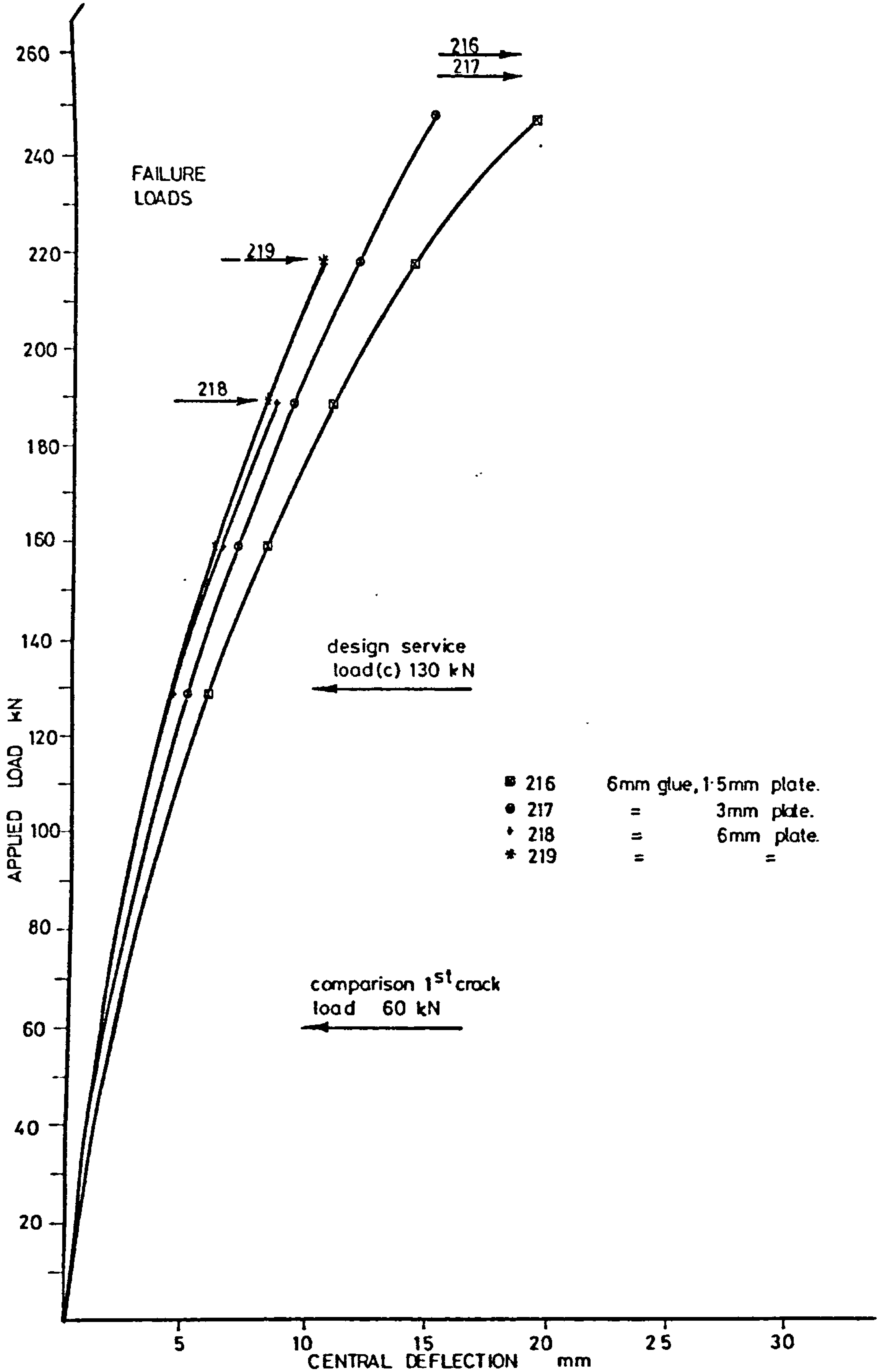

FIGURE 6·30 LOAD- DEFLECTION CHARACTERISTICS

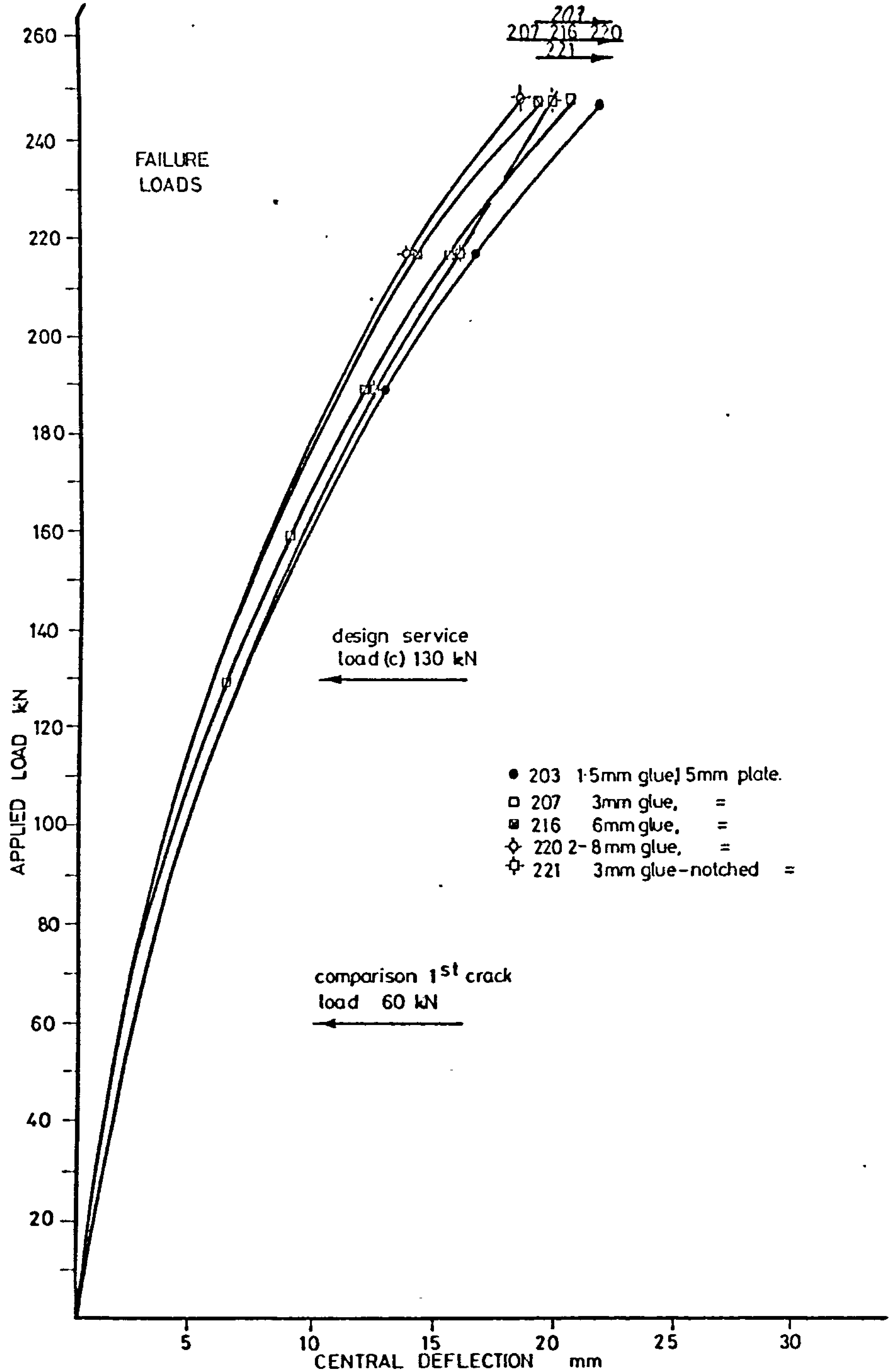

FIGURE 6·31 LOAD- DEFLECTION CHARACTERISTICS of 1.5 mm plate, the outer layer being lapped. The behaviour of all four beams fell within ±6% of the beam with the unlapped 3 mm thick plate.

Fig. 6.31 compares beams with a 1.5 mm plate thickness for varying glue thickness. The deflections are reduced as the glue thickness increases, but not so much as when the plate thickness is increased for constant glue thickness. The beams with variable and notched glue lines follow very closely to similar beams with constant glue thickness. Figs. 6.32 and 6.33 show similar behaviour for beams with 3 mm and 6 mm thick plates. The stiffening produced by increasing the glue thickness is reduced as the plate thickness increases.

Figs. 6.34 and 6.35 indicate that the beams loaded prior to bonding on the plates have deflections greater than their control beams up to working load, but less than the control beams above this. The control beams were not precracked. This behaviour, as for load-strains needs further examination.

From Table 6.18 it can be seen that at 60 kN load the deflections, except for the precracked beams, were decreased to 85 to 100% (1.5 mm plate), 70 to 95% (3 mm plate) and 60 to 94% (6 mm plate) of the values of the unplated beam. At 130 kN the deflections were similarly reduced to 78 to 96% (1.5 mm plate), 68 to 87% (3 mm plate), and 61 to 67% (6 mm plate) of the unplated beam's deflection. At 190 kN the deflections were reduced to 69 to 83% (1.5 mm plate), 59 to 69% (3 mm plate) and 51 to 54% (6 mm plate). These results are shown diagrammatically in Fig. 6.36.

6.3.3.3 <u>Theoretical Predictions of Deflections</u>

Table 6.4 shows experimental deflections at 220 kN, 130 kN and 60 kN loads. A measure of the ductility of the beams was found by comparing the deflections at 220 kN and 130 kN loads for each of the test beams. There is a small reduction in ductility in the plated beams, however, only one value was obtained for an unplated beam. The reductions were as follows: 10% for beams with 1.5 mm thick plates; 13% (3 mm plates) and 11% (6 mm plates). It should be noted that two beams, 210 and 218 failed before reaching 220 kN load and their values were extrapolated.

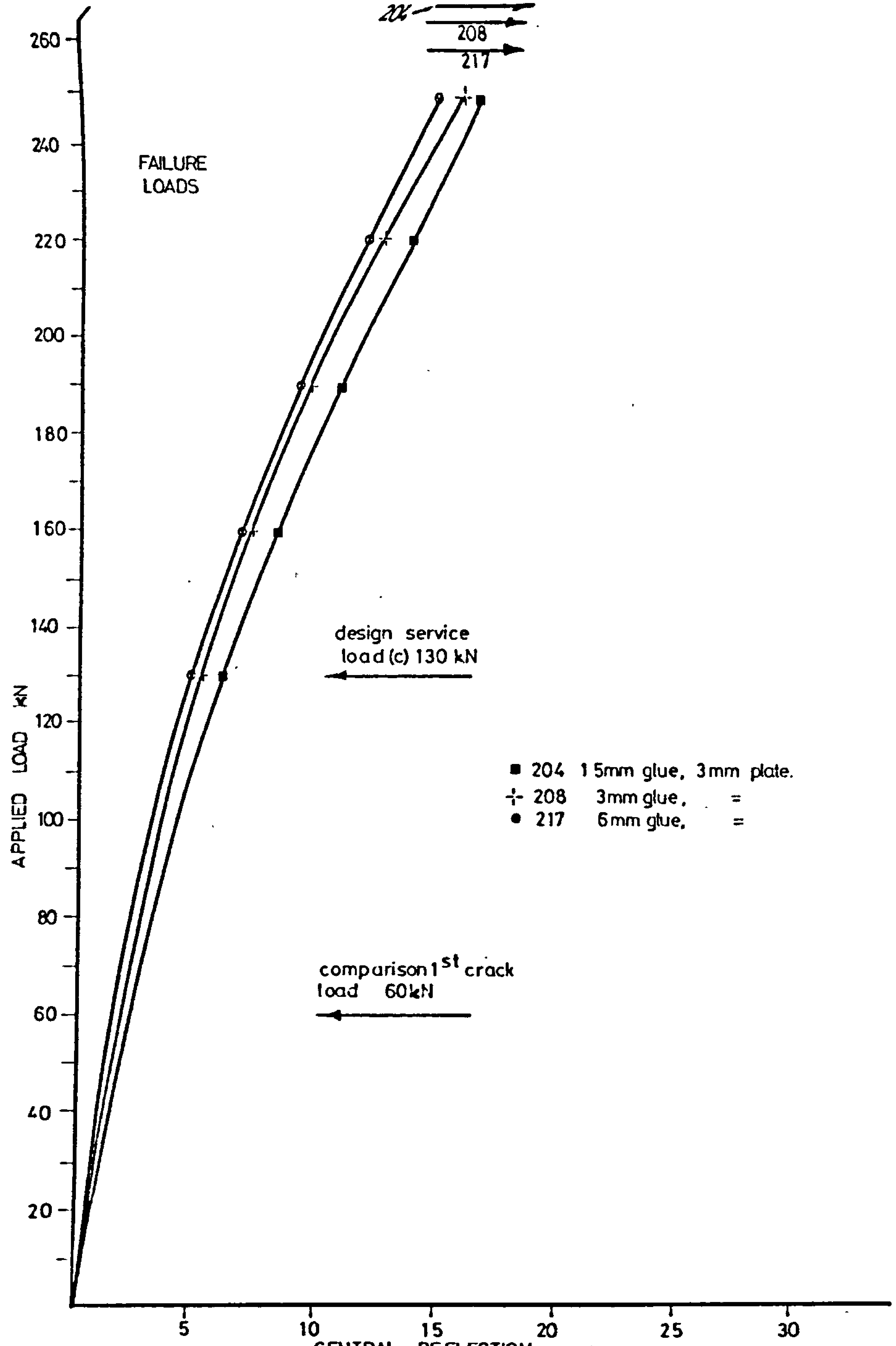

FIGURE 6·32 LOAD-DEFLECTION CHARACTERISTICS

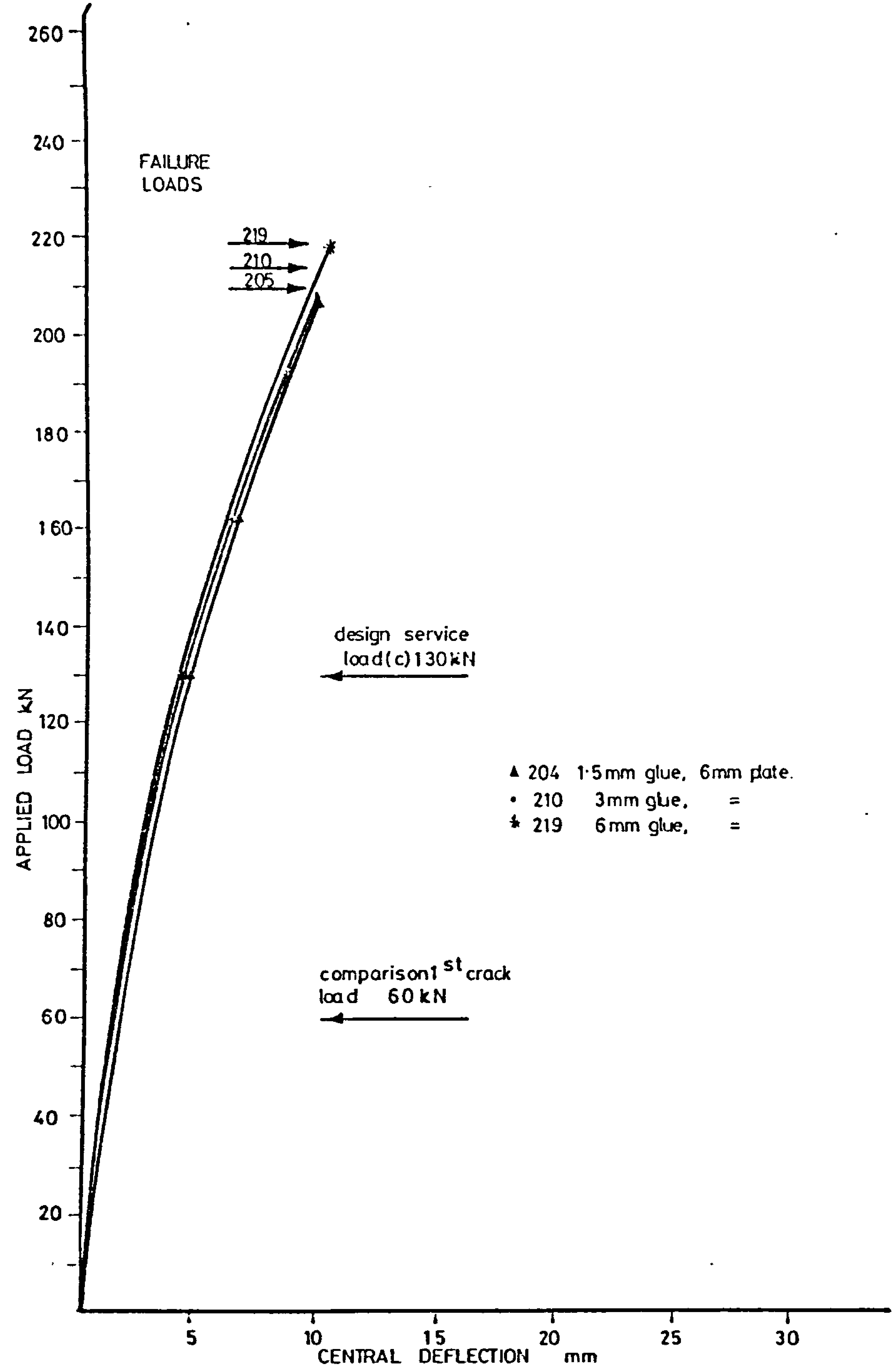

FIGURE 6·33 LOAD-DEFLECTION CHARACTERISTICS

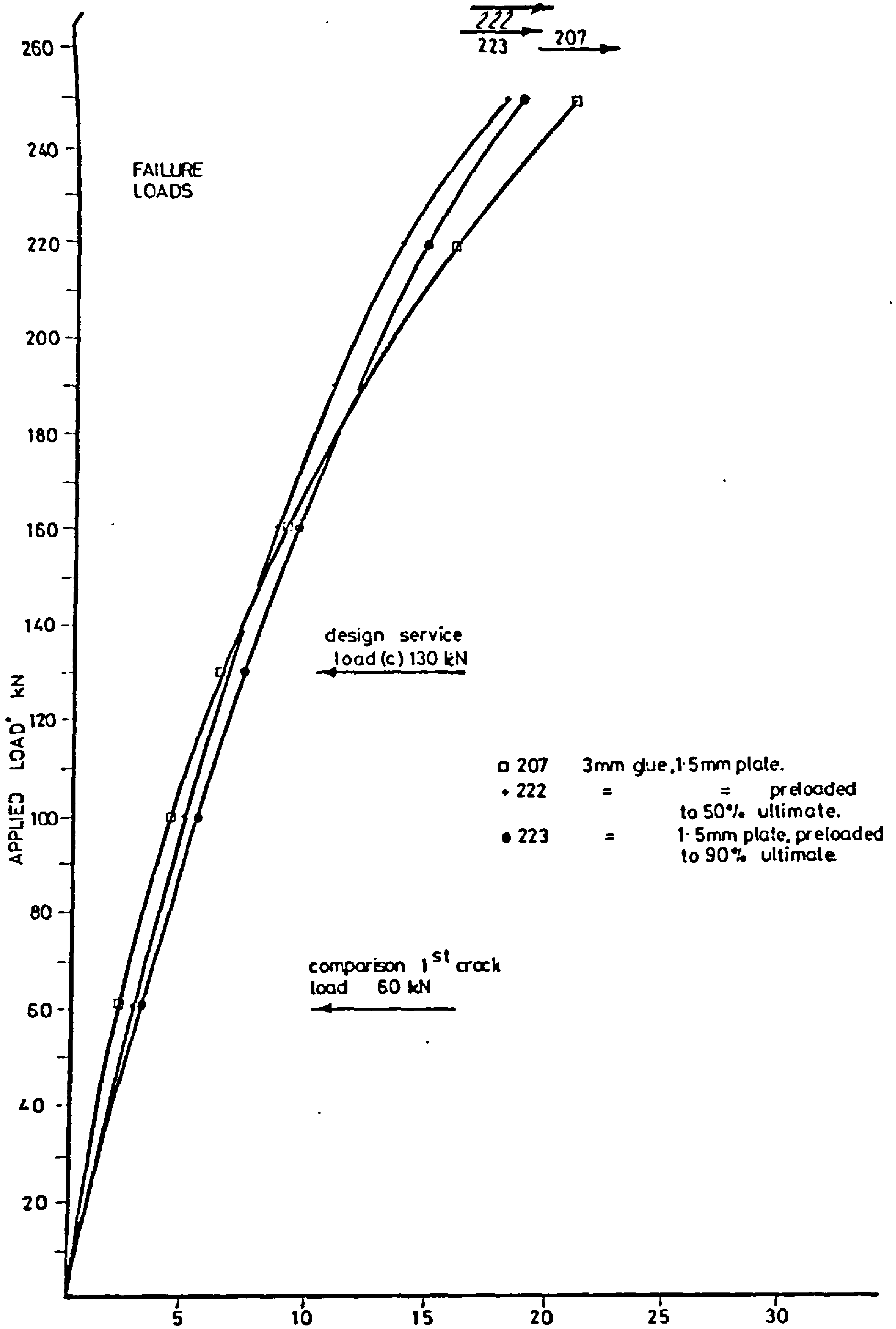

FIGURE 6·34 LOAD-DEFLECTION CHARACTERISTICS

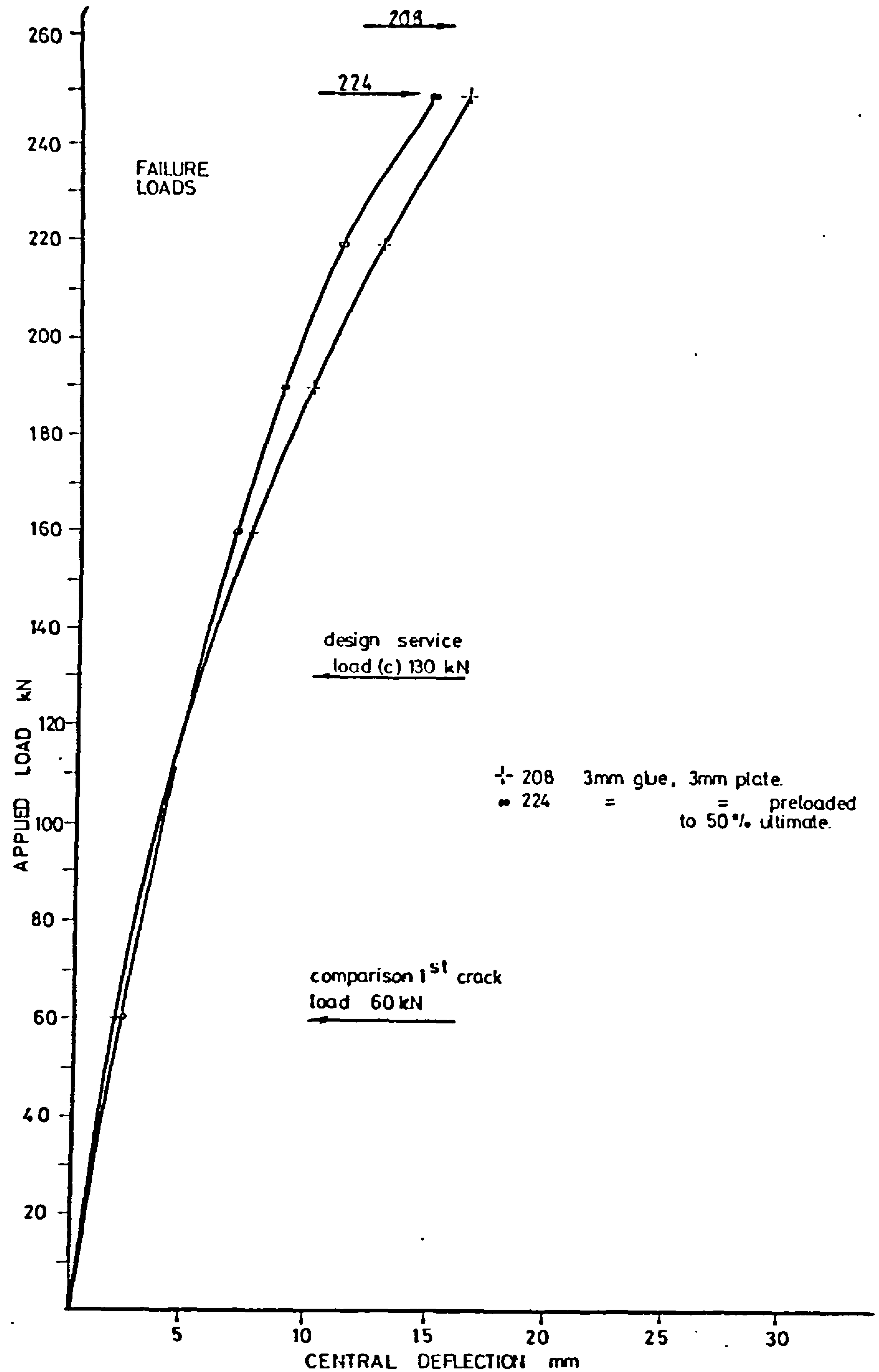

FIGURE 6·35 LOAD-DEFLECTION CHARACTERISTICS

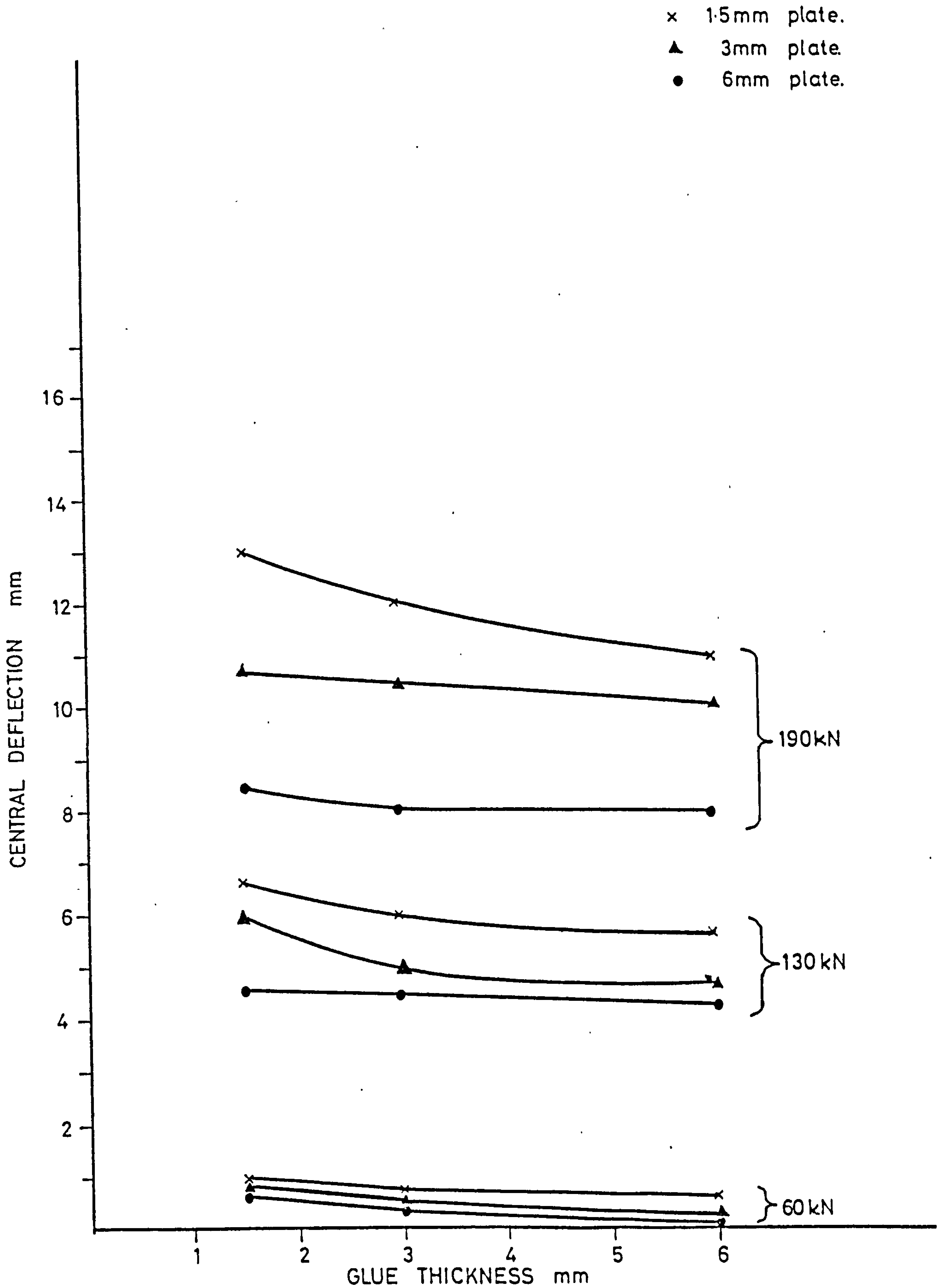

FIGURE 6·36 CENTRAL DEFLECTION v. PLATE & GLUE THICKNESS

TABLE 6·4 DEFLECTION CHARACTERISTICS

BEAM NUMBER	GLUE THICKNESS	PLATE THICKNESS	EXPERIMENTAL DEFLECTIONS mm.			THEORETICAL DEFLECTIONS – (130 kN)			EXPERIMENTAL / THEORETICAL			DUCTILITY defln 220 / defln 130
			FIRST CRACK	130 kN	220 kN	CP110. mm	ACI. mm	CEB. mm	CP110. mm	ACI. mm	CEB. mm	
201	-	-	1·00	7·30	20·40	6·12	6·10	7·10	1·19	1·20	1·03	2·79
202	3	-	1·20	6·90	17·70	6·12	6·10	7·10	1·13	1·13	0·97	2·56
203	1·5	1·5	1·70	6·60	16·20	5·00	5·00	5·81	1·32	1·33	1·14	2·45
204	1·5	3	1·65	6·00	13·80	4·20	4·30	4·99	1·43	1·40	1·20	2·30
205	1·5	6	1·20	4·60	11·00	3·50	3·43	3·97	1·31	1·34	1·16	2·39
206	1·5	2x1·5	1·40	5·70	13·00	4·20	4·30	4·99	1·36	1·33	1·14	2·28
207	3	1·5	1·80	6·00	16·00	5·00	5·00	5·81	1·20	1·21	1·03	2·67
208	3	3	1·40	5·00	12·60	4·20	4·30	4·99	1·19	1·16	1·00	2·52
209	3	6	1·30	4·50	11·50	3·50	3·43	3·97	1·29	1·31	1·13	2·56
210	3	6	1·20	4·30	11·00	3·50	3·43	3·97	1·23	1·25	1·08	2·56
211	3	1·5L	1·65	5·80	14·00	5·00	4·89	5·83	1·16	1·19	0·99	2·41
212	3	1·5L	1·35	5·80	14·80	5·00	4·89	5·83	1·16	1·19	0·99	2·55
213	3	2x1·5L	1·45	5·40	13·00	4·20	4·30	4·99	1·29	1·26	1·08	2·41
214	3	2x1·5L	1·35	4·80	12·00	4·20	4·30	4·99	1·14	1·12	0·96	2·50
215	3	3L	1·35	4·70	11·60	4·20	4·30	4·99	1·12	1·09	0·94	2·47
216	6	1·5	1·60	5·70	14·00	5·00	4·89	5·83	1·14	1·17	0·98	2·46
217	6	3	1·00	4·80	11·60	4·20	4·22	4·99	1·14	1·12	0·96	2·42
218	6	6	0·90	4·20	10·80	3·50	3·43	3·97	1·20	1·22	0·96	2·57
219	6	6	1·20	4·20	10·40	3·50	3·43	3·97	1·20	1·22	1·06	2·48
220	2 8	1·5	1·70	5·40	13·80	5·00	4·89	5·83	1·08	1·10	0·93	2·56
221	3	1·5	1·70	6·60	16·00	5·00	4·89	5·83	1·32	1·39	1·13	2·42
222	3	1·5P	2·00	6·40	13·50	5·00	5·00	5·81	1·28	1·29	1·10	2·11
223	3	1·5P	2·60	7·00	14·60	5·00	5·00	5·81	1·40	1·41	1·20	2·01
224	3	3.P	1·65	4·80	11·00	4·20	4·30	4·99	1·14	1·12	0·96	2·29
							mean ratios		1·23	1·23	1·05	

L – lapped plates.
P – precracked.

The deflections of all the beams, as calculated by the three methods described in Appendix 5, are given in Table 6.4 for comparison with experimental values at 130 kN load. The mean ratio of measured to predicted deflection for all the beams were as follows: 1.23 (CP110); 1.23 (A.C.I.); 1.05 (CEB).

Within the present tests the CEB method for predicting deflections gives the best results. The test results by Ang (72) were studied and the three methods of calculation were found to give mean ratios of measured to theoretical deflections of 1.15 (CP110), 1.21 (A.C.I.) and 1.01 (CEB), confirming the latter as the most appropriate method.

6.3.4 Moment-Rotation Characteristics

6.3.4.1 Literature Review

Figure 6.37(a) shows the moment-curvature diagram of a typical reinforced concrete beam. The total rotation can be found by integrating the local curvatures along the beam. The shape of the curve is a reflection of the behaviour of the materials making up the cross section. The curve can be divided into three parts corresponding to the different stages of behaviour. The first part, OX, is characterised by a linear relationship between the moment and curvature, since the section is uncracked and both concrete and steel behave elastically. The second part, XY, is characterised by a changing slope of the curve. In this region the area of concrete in compression is decreasing as the cracks spread towards the compression face. The concrete compression fibres and the steel are approaching their inelastic strain range. At point Y, either the steel or concrete begins to behave inelastically. The third part, YZ, is characterised by a rapidly changing slope of the curve. Between Y and Z the section reaches its ultimate capacity, the concrete under compression starts cracking and the tension steel reaches its strain hardening stage, at least in under-reinforced beams. The curvatures at these stages are shown in Fig. 6.37(b). Distribution 1 is typical when the beam is in the uncracked state and the characteristics of the beam along its length are the

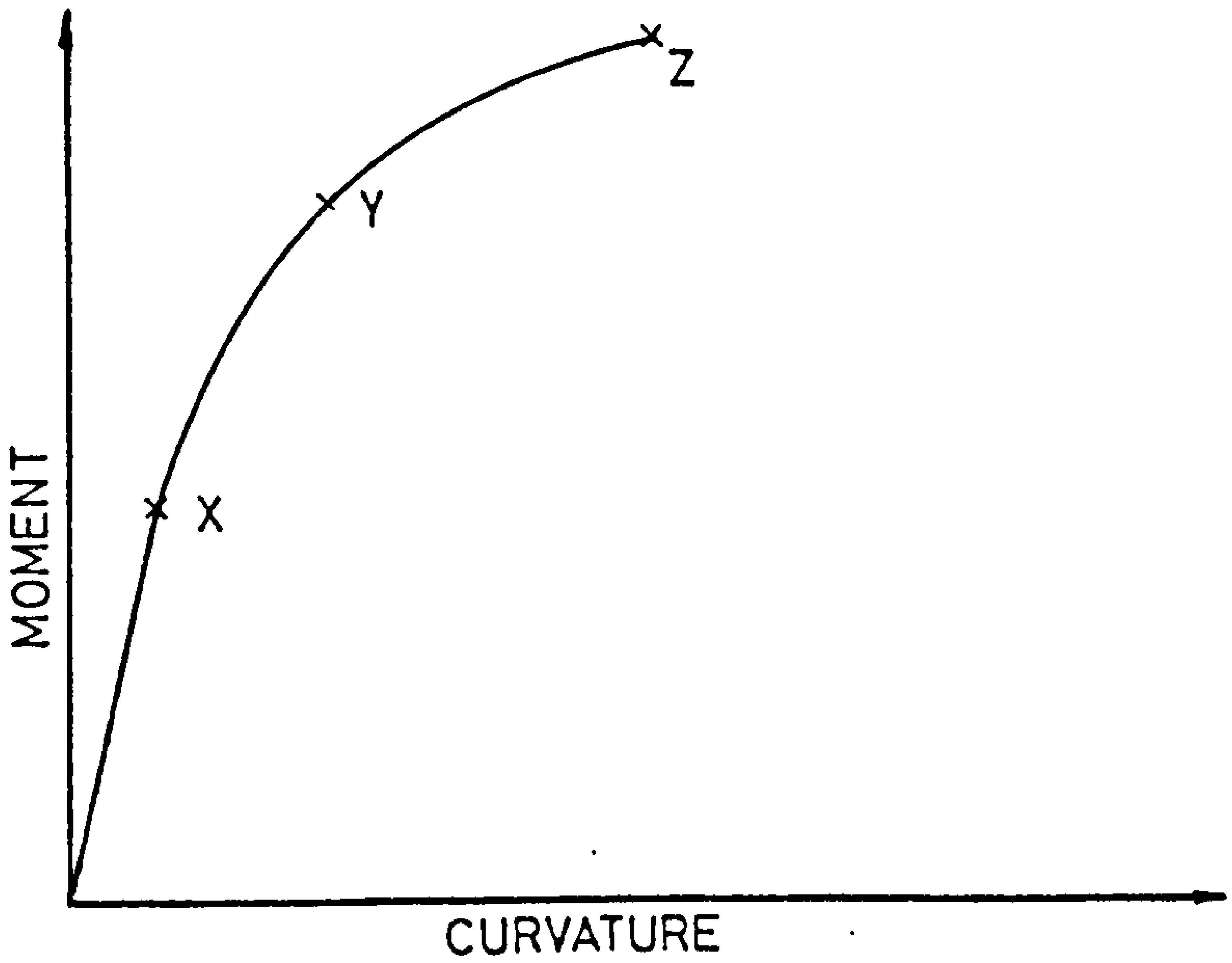

(a) MOMENT CURVATURE RELATIONSHIP

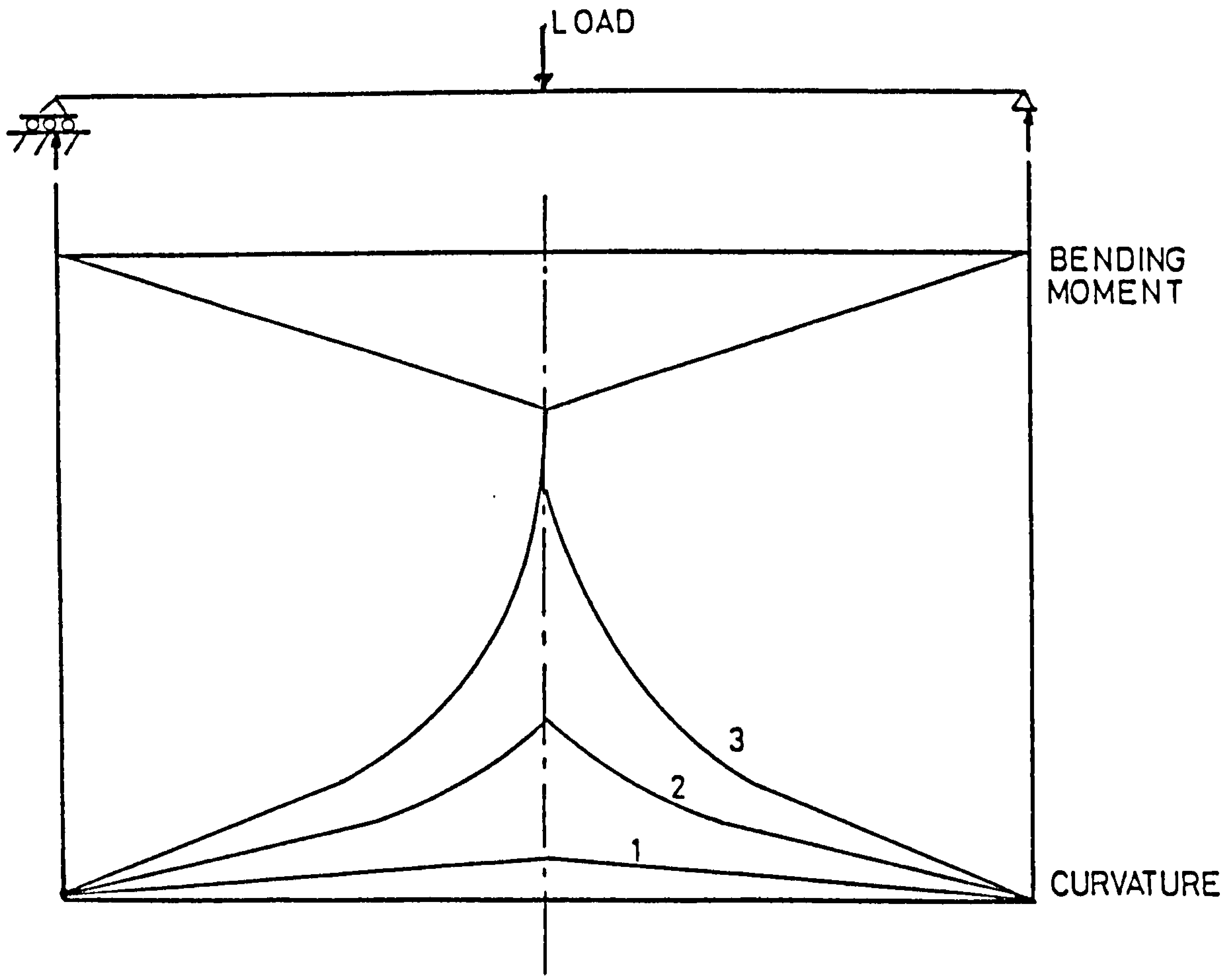

(b) MOMENT AND CURVATURE DISTRIBUTION

FIGURE 6·37 MOMENT CURVATURE RELATIONSHIP same, thus the curvature distribution follows the bending moment distribution. As a result of the spread of cracks along the tension side, the characteristics of the cross-section vary along the beam. This corresponds to Distribution 2 and point Y. The distribution is non-linear, especially near the loading point. Distribution 3 corresponds to point Z on the moment curvature curve. The curvature increases very rapidly over the region near the critical section, while it remains nearly linear over the rest of the beam. The total rotation over the length of the beam at any particular stage of loading can be obtained either by integrating the curvature along the length of the beam or by measuring the support rotations and adding them together.

6.3.4.2 Moment Rotation Curves

Figs. 6.38 and 6.47 shows the moment-rotation curves of the twenty four test beams. The same general behaviour, discussed under load-strain and load-deflection, was observed for the moment-rotation curves.

In Tables 6.1 and 6.3 the experimental rotations are given. At 60 kN load, which is slightly above their first crack load, the total rotations of the plated beams were decreased to between 50 and 92% of the value for the unplated beam. For beams strengthened with 1.5 mm plate the rotations were reduced to 80-92% of the unplated beams value. Similarly for 3 mm and 6 mm plates the reductions were to 65-70% and 50-58% respectively. At 130 kN load the rotations were reduced in a similar manner to 81-94% (1.5 mm plate); 69-73% (3 mm plate) and 51-69% (6 mm plate). At 190 kN the rotations were reduced to 83-94% (1.5 mm plate); 69-75% (3 mm plate) and 51-70% (6 mm plate). These results are shown diagramatically in Fig. 6.48.

6.3.4.3 Theoretical Prediction of Rotations

Table 6.5 shows the comparison between the measured rotations and those calculated in Appendix 6. It can be seen that as the load increases, the difference between experiment and theory increases. The rotations are greatly under estimated above service load. The calculated values assuming the tensile strength of concrete was 1 N/mm^2 gave slightly better values than for 3 N/mm^2.

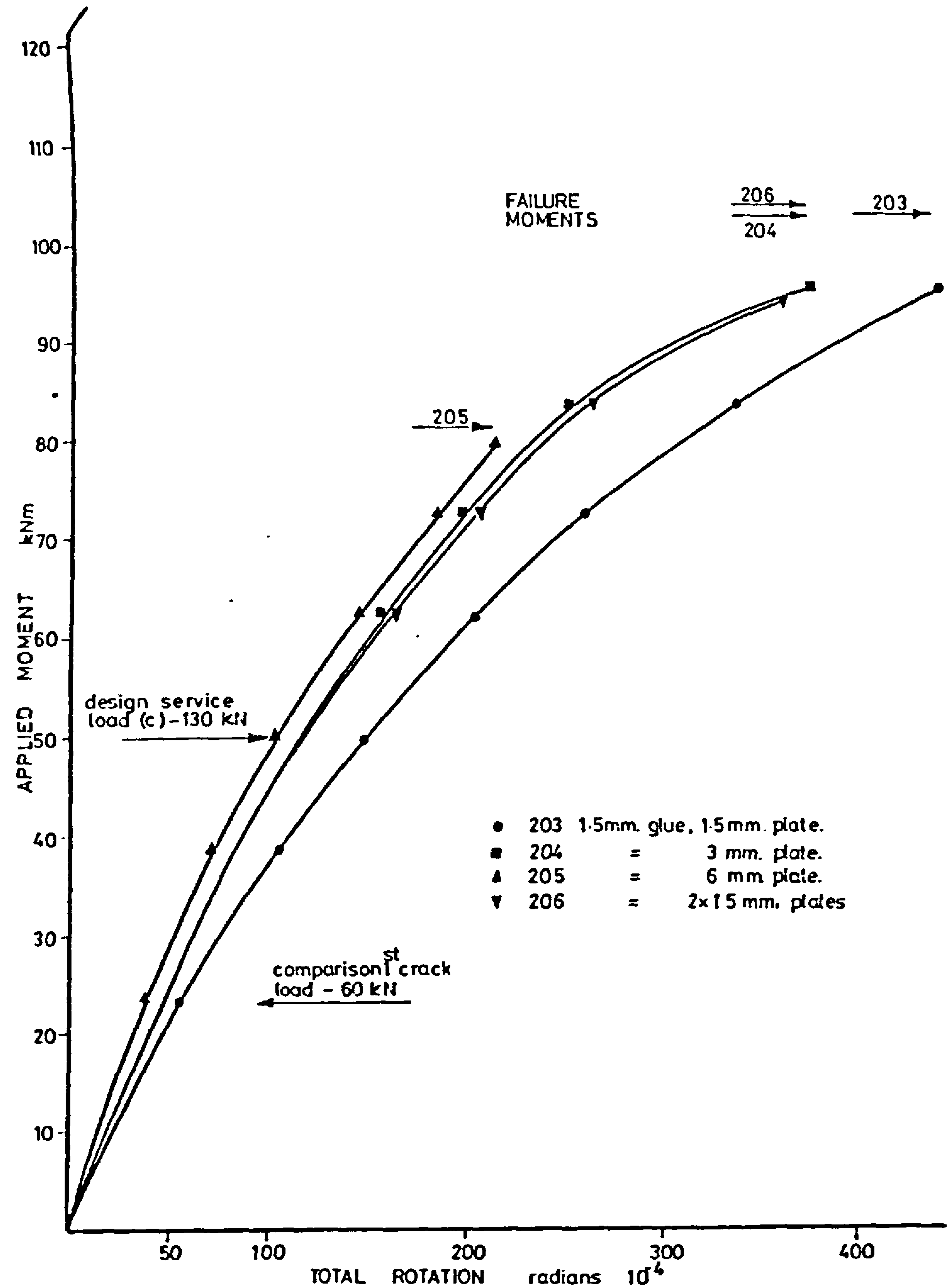

FIGURE 6·38 MOMENT - ROTATION CHARACTERISTICS

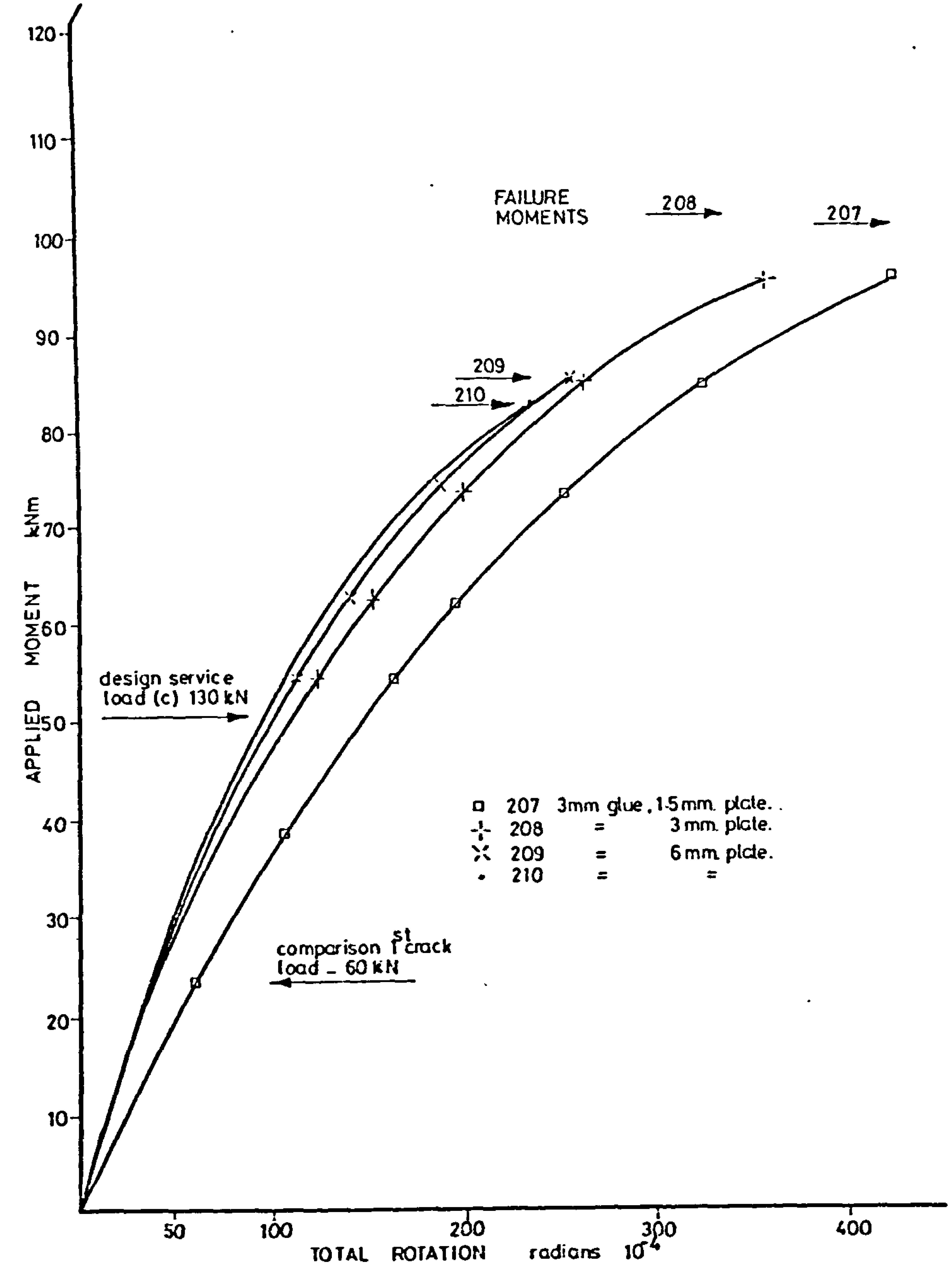

FIGURE 6·39 MOMENT - ROTATION CHARACTERISTICS

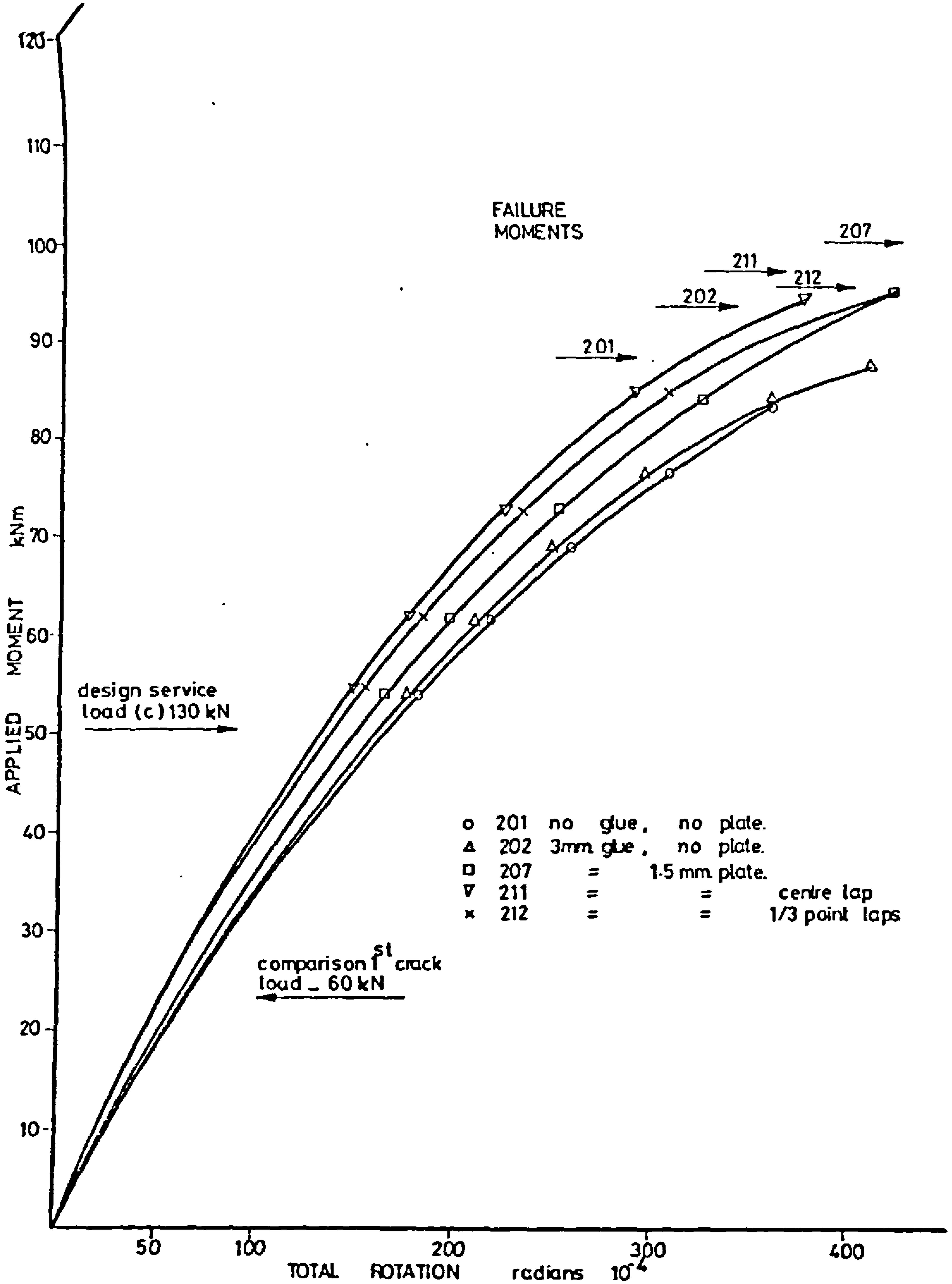

FIGURE 6·40 MOMENT - ROTATION CHARACTERISTICS

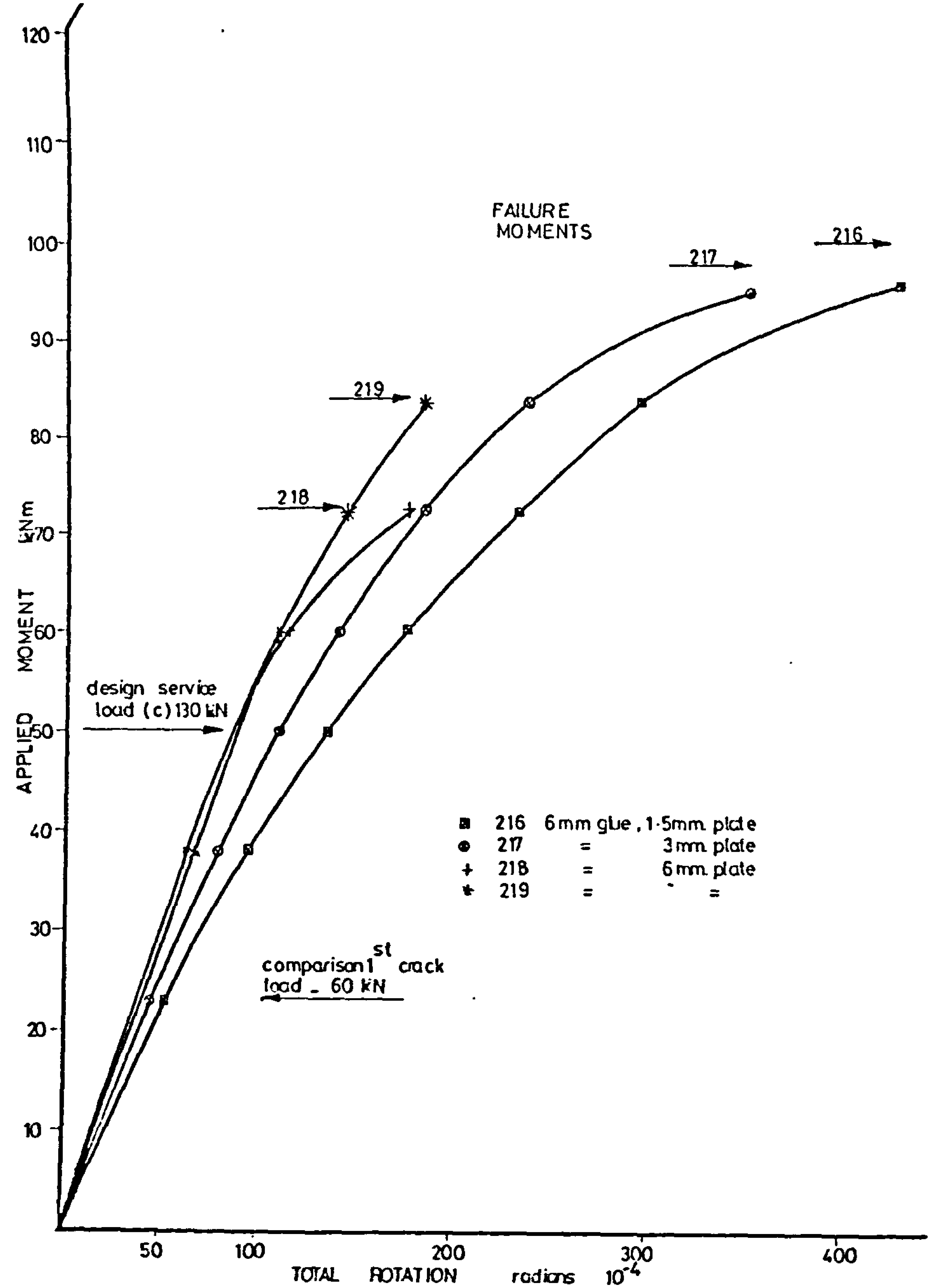

FIGURE 6·41 MOMENT - ROTATION CHARACTERISTICS

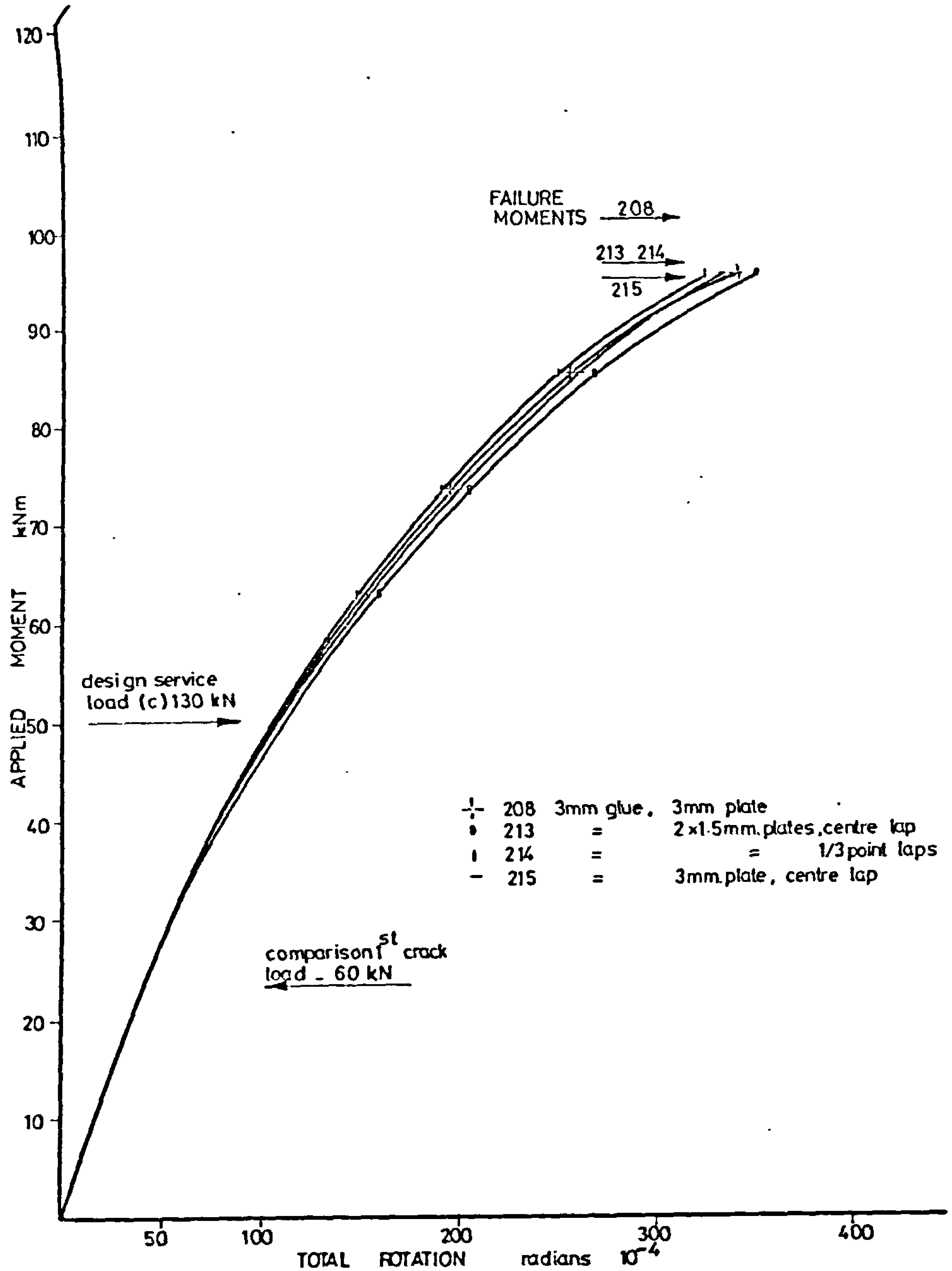

FIGURE 6·42 MOMENT - ROTATION CHARACTERISTICS

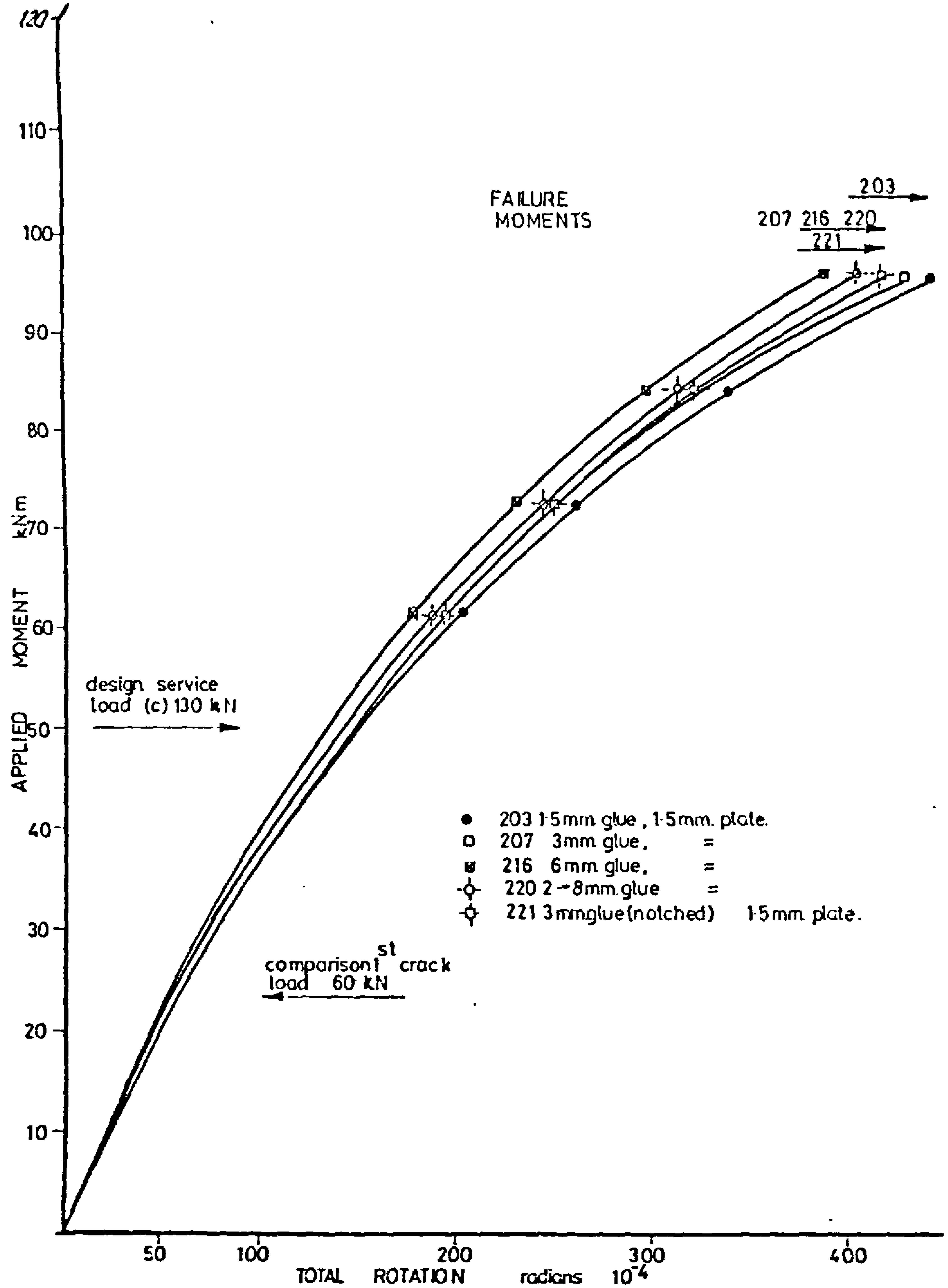

FIGURE 6·43 MOMENT - ROTATION CHARACTERISTICS

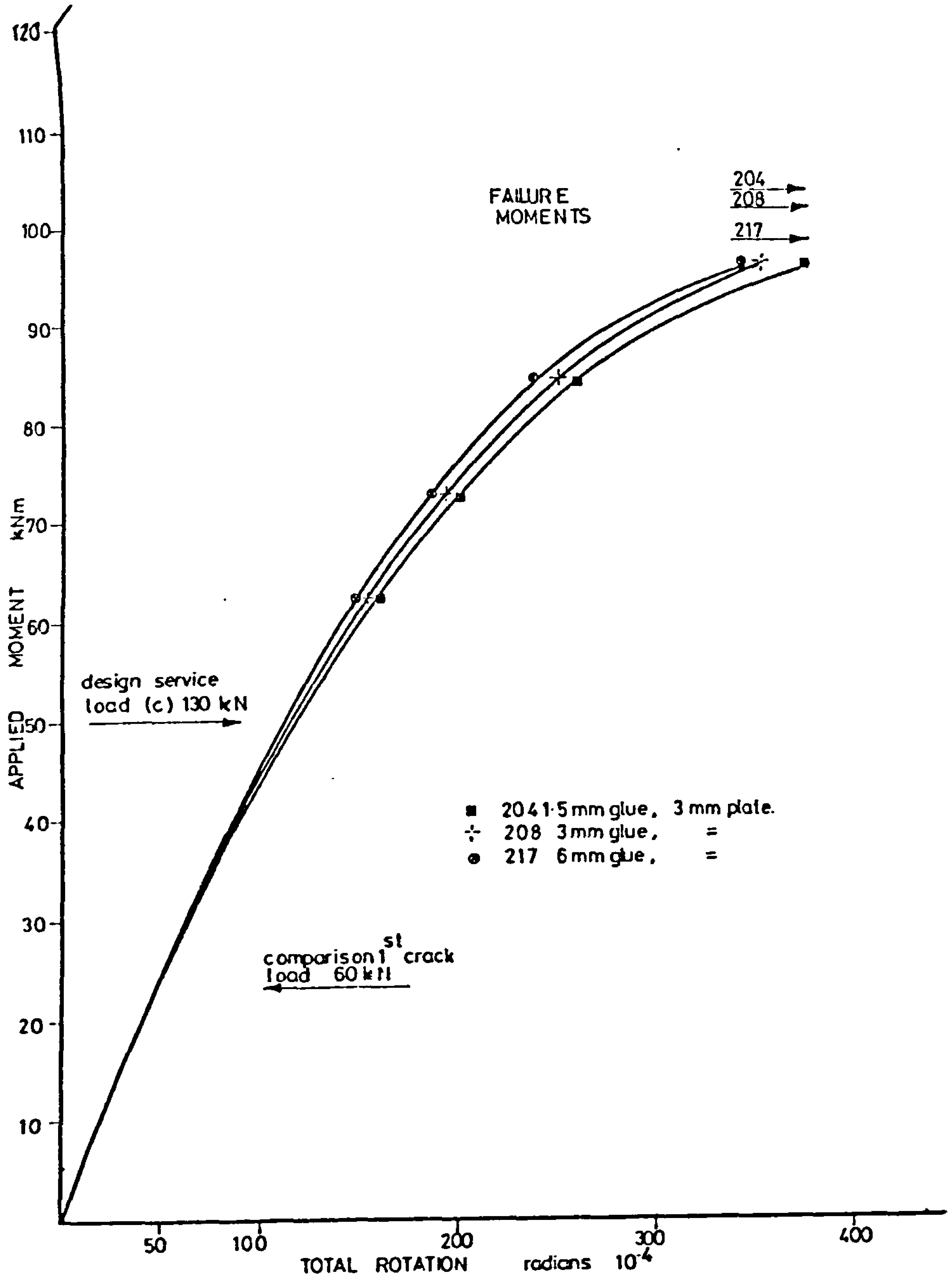

FIGURE 6·44 MOMENT–ROTATION CHARACTERISTICS

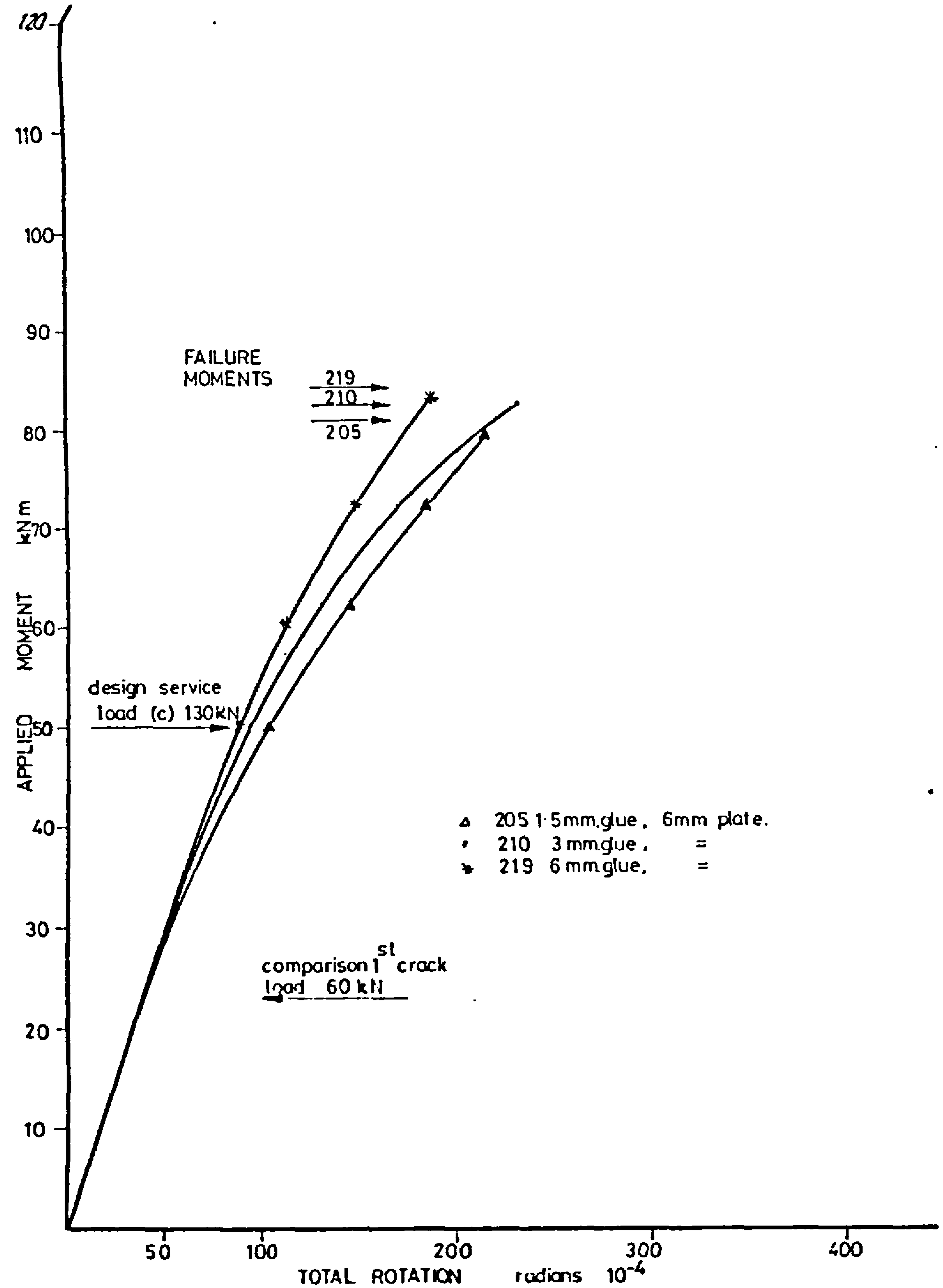

FIGURE 6·45 MOMENT–ROTATION CHARACTERISTICS

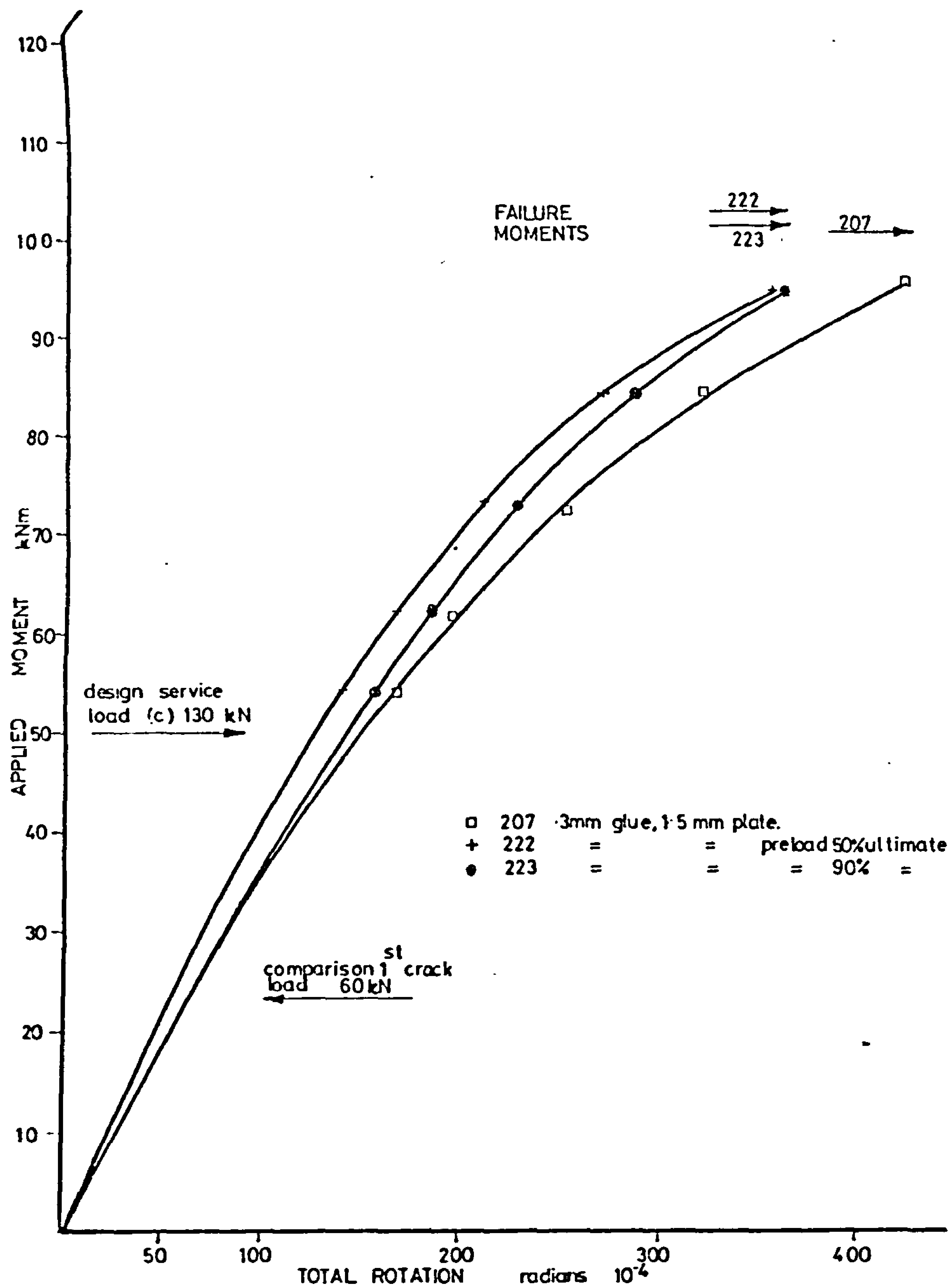

FIGURE 6·46 MOMENT ROTATION CHARACTERISTICS

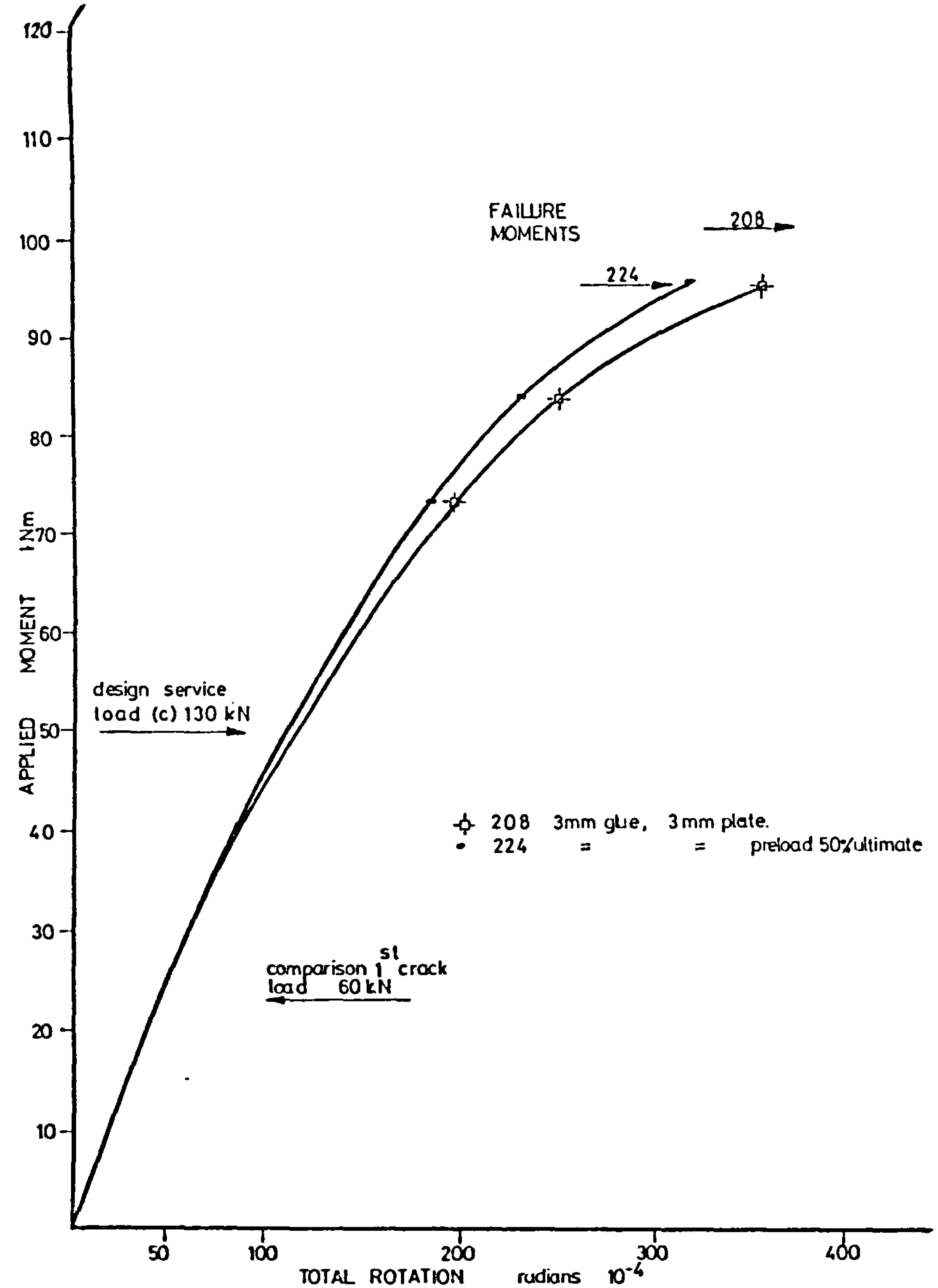

FIGURE 6·47 MOMENT ROTATION CHARACTERISTICS

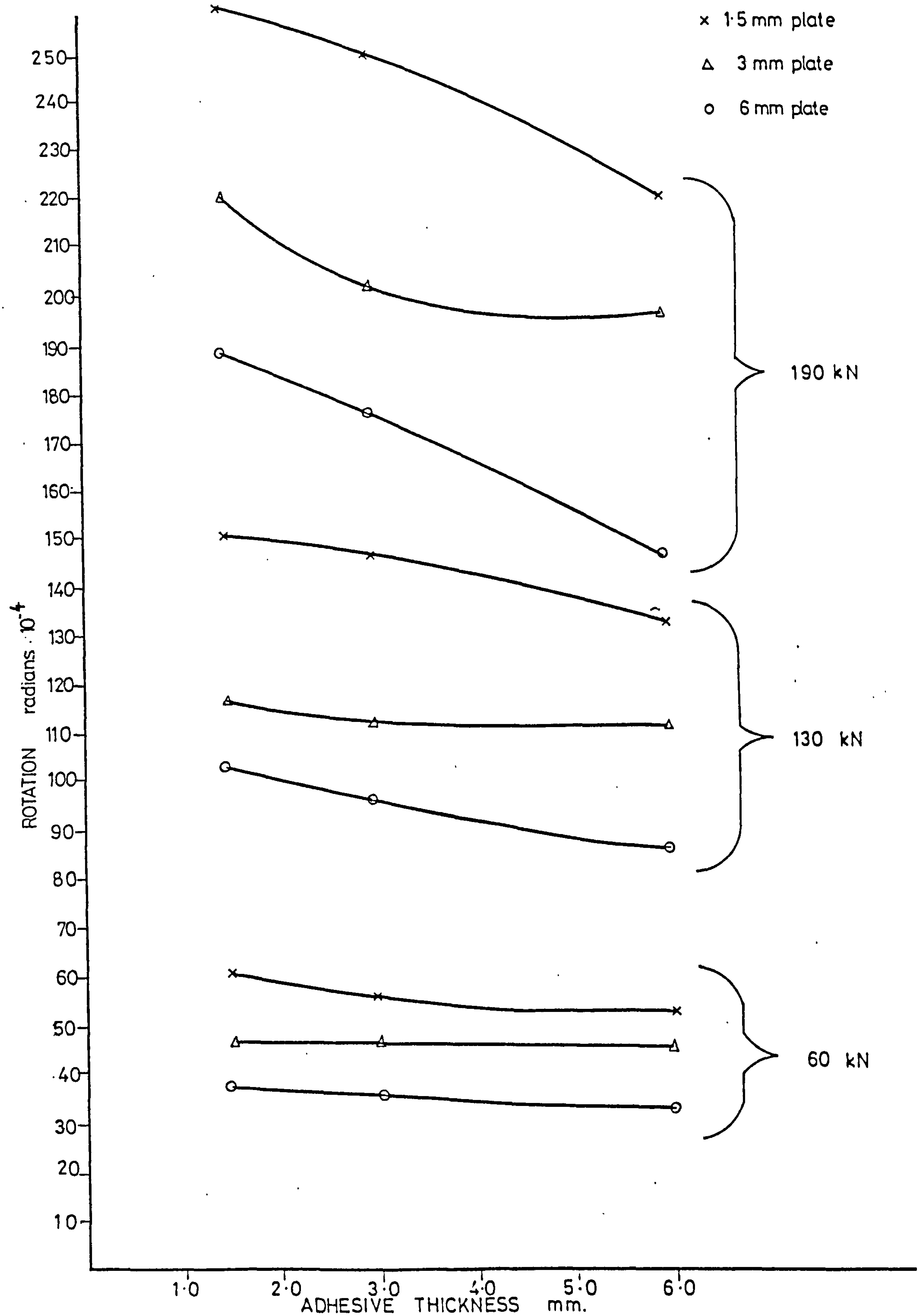

FIGURE 6·48 ROTATION CHARACTERISTICS

TABLE 6·5 COMPARISON OF EXPERIMENTAL AND THEORETICAL ROTATIONS

BEAM NUMBER	PLATE THICKNESS mm	GLUE THICKNESS mm	EXPERIMENTAL ROTATIONS radians 10^{-4}				ROTATION FROM THEORY IN APP. 6 radians 10^{-4}				ROTATION FROM EMPIRICAL FORMULA radians 10^{-4}				% DIFFERENCE BETWEEN MEASURED & EMPIRICAL FORMULA.			
			60 kN	130 kN	190 kN	250 kN	60 kN	130 kN	190 kN	250 kN	60 kN	130 kN	190 kN	250 kN	60 kN	130 kN	190 kN	250 kN
203	1·5	1·5	60	150	260	443	60 52	134 125	195 187	253 247	61	152	258	426	+2	+1	−1	−4
207	1·5	3·0	55	145	250	430	61 53	135 126	195 186	247 237	61	150	255	413	+11	+3	+2	−4
216	1·5	6·0	52	133	235	430	56 50	131 124	199 190	263 257	56	146	253	418	+8	+9	+8	−3
			60 kN	130 kN	190 kN	250 kN	60 kN	130 kN	190 kN	250 kN	60 kN	130 kN	190 kN	250 kN	60 kN	130 kN	190 kN	250 kN
204	3·0	1·5	45	116	200	380	50 45	116 110	172 168	227 224	50	128	215	341	+11	+12	+8	−10
208	3·0	3·0	45	110	195	360	50 44	115 110	169 165	212 209	50	121	209	330	+11	+10	+7	−12
217	3·0	6·0	45	110	185	352	50 45	115 109	168 164	224 220	50	122	209	323	+11	+11	+11	−9
			60 kN	130 kN	160 kN	190 kN	60 kN	130 kN	160 kN	190 kN	60 kN	130 kN	160 kN	190 kN	60 kN	130 kN	190 kN	250 kN
205	6·0	1·5	37	102	145	188	42 37	93 89	115 113	137 136	42	100	128	160	+8	−2	−12	−10
209	6·0	3·0	37	110	140	185	41 36	92 87	133 130	153 152	41	98	148	179	+8	−11	+6	−3
218	6·0	6·0	38	88	120	175	41 36	91 87	112 110	134 133	41	98	125	155	+8	+11	+4	−11

upper value $f_{ct} = 1N/mm^2$ $f_{d} = 1N/mm^2$
lower value $f_{ct} = 3N/mm^2$

To produce a more accurate prediction of rotational behaviour, some allowance must be made for the change in Young's Modulus which occurs as the strain in the compressive concrete increases. In order to check the validity of the present test results the 'correction' to E_c should include a factor which can be applied to other test beams. The compressive strain in the concrete at any particular load is dependant upon the degree of loading in relation to its theoretical capacity. Then we have

$$E_{corrected} = E_c - k \left(\frac{W}{W_{ultimate}}\right)^c$$

where k and c are constants,

W = load stage under consideration,

$W_{ultimate}$ = theoretical ultimate load.

Then $\log (E_c - E_{corrected}) = \log k + c \log \left(\frac{W}{W_{ultimate}}\right)$.

The experimental rotations are used to find the $E_{corrected}$ required at each load stage, using 1 N/mm^2 for the tensile strength of concrete. The value of $E_c - E_{corrected}$ is then found and the log values were plotted against $\log \left(\frac{W}{W_{ultimate}}\right)$ in Fig. 6.49. The values of k and c were found by plotting the best fit line by linear regression.

The resulting formula is: $E_{corrected} = E_c - 1{\cdot}37.10^4 \left(\frac{W}{W_{ultimate}}\right)^{1{\cdot}88}$.

Table 6.5 gives the results from this formula and also the percentage difference between these values and experiment. In Fig. 6.50 the calculated values are plotted against experimental values and for the range of glue and plate thicknesses used, all points fell within ±12% of the experimental = theoretical line.

6.4 CONCLUSIONS

Based on the results presented in this Chapter the following conclusions can be drawn.

1. As the thickness of the reinforcing plate was increased, for a constant glue line thickness, there was a corresponding reduction in: plate, bar and concrete strains, central deflection and total rotation

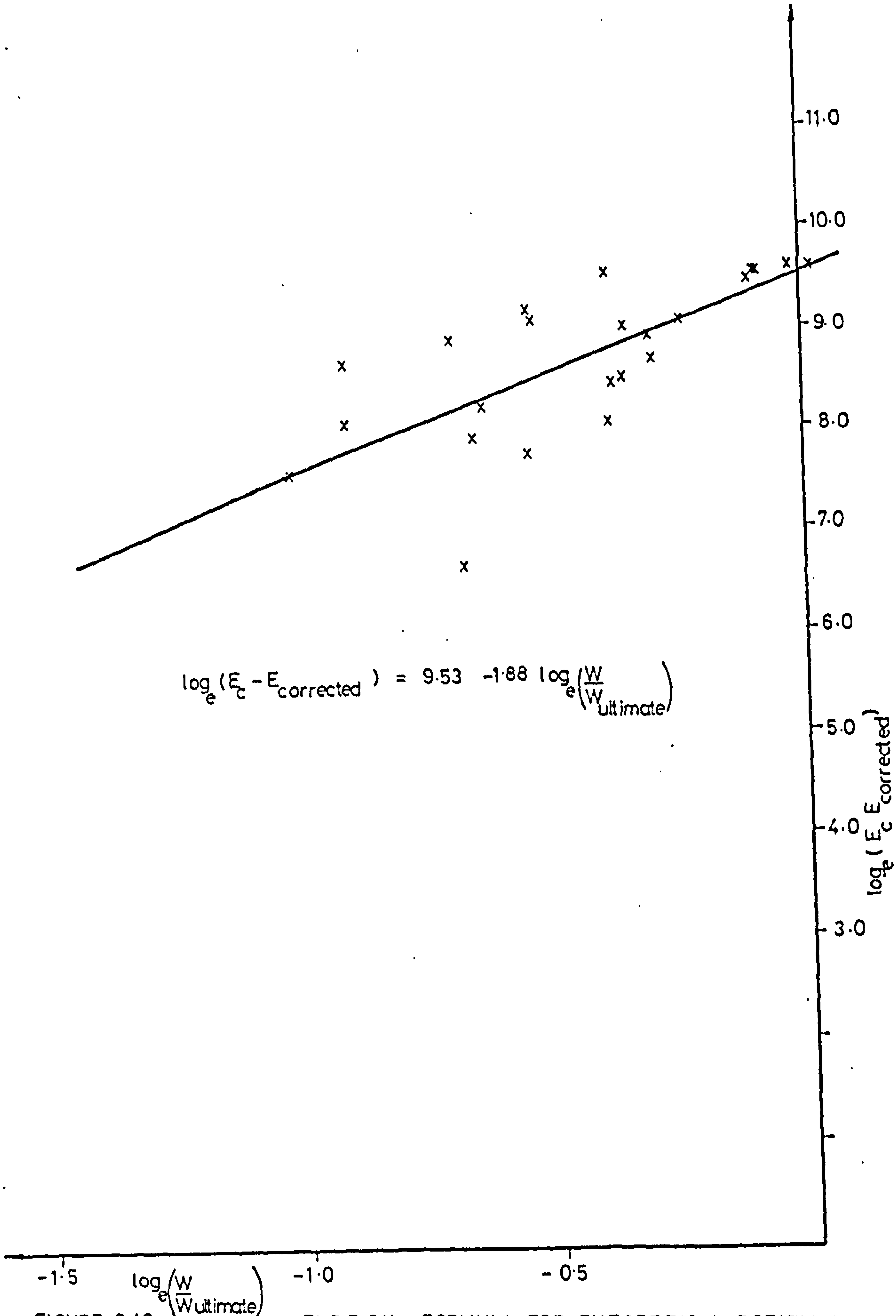

FIGURE 6.49 EMPIRICAL FORMULA FOR THEORETICAL ROTATIONS

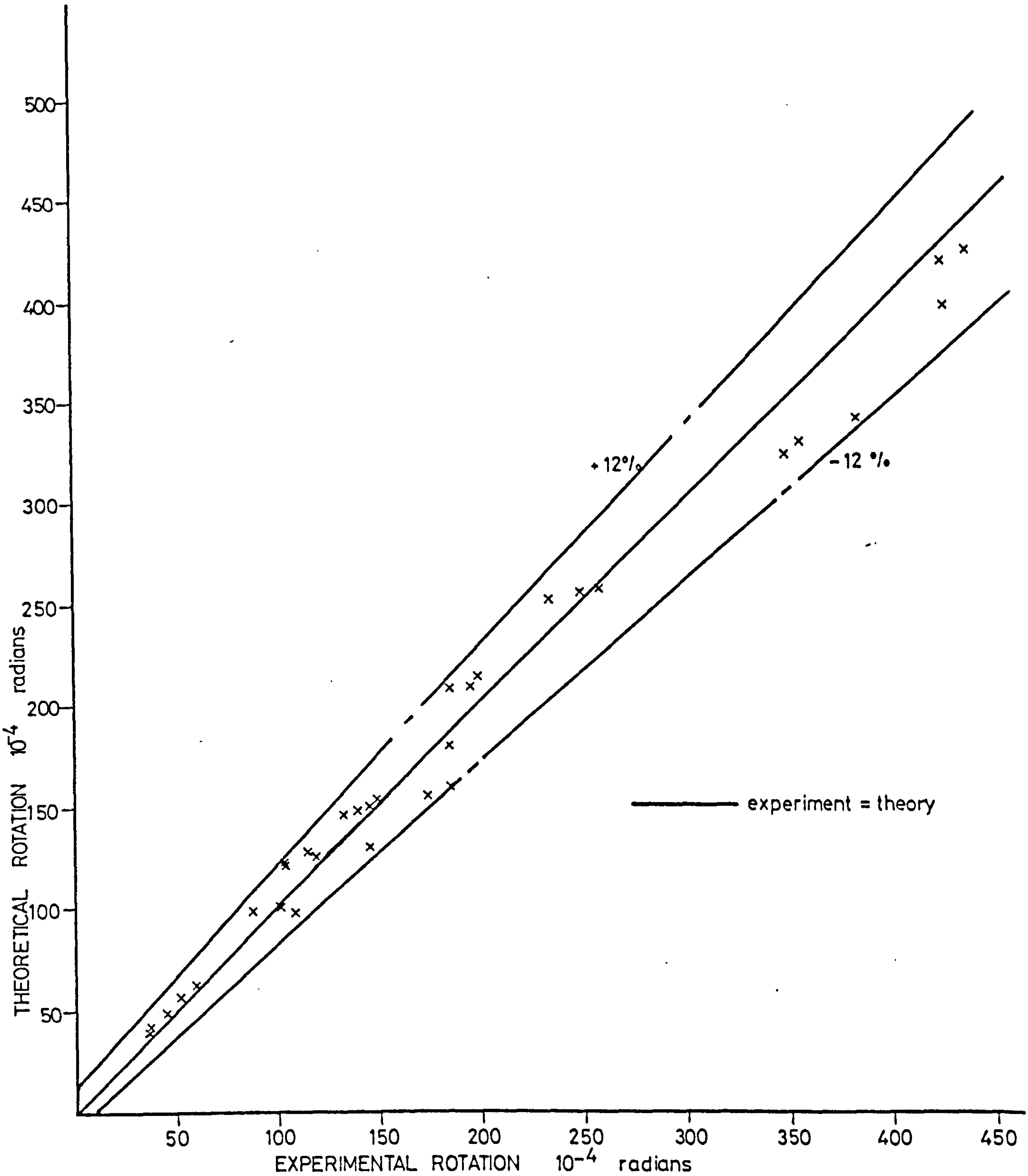

FIGURE 6·50 EXPERIMENTAL V. THEORETICAL ROTATIONS

2. As the thickness of the glue line was increased, for a constant plate thickness, there was a reduction in these same properties but to a lesser degree.

3. Beams with multiple layers of plate behaved almost identically to beams with a single plate of the same total thickness.

4. Beams with lapped plates were slightly stiffer than beams with continuous plates of the same thickness. This was probably due to the slightly increased lever arm of the lapping plate at the critical section.

5. The beams with notched and variable glue line thickness behaved almost identically to the corresponding beam with a constant glue thickness.

6. The preloaded beams had smaller strains, deflections and rotations, in general, than corresponding beams which had not been cracked prior to bonding on the plates. This behaviour does not seem logical and further testing should be performed to investigate these findings more fully.

7. The deflections at service loads were slightly underestimated using CP110 and A.C.I. recommended calculations. The method given by CEB gave the best results having a mean ratio of experimental to theoretical values of 1.05.

8. The ductility of the plated beams was approximately 12% less than the unplated beam. However, as there was only one result for an unplated beam this figure can only be approximate.

9. The rotations could be predicted to within ±12% of the experiment using the following formula for the Young's Modulus of the concrete.

$$E_{corrected} = E_c - 1\cdot 37.10 \left(\frac{W}{W_{ultimate}}\right)^{1\cdot 88}.$$

CHAPTER 7

CRACKING PROPERTIES

7.1 INTRODUCTION

The tensile strength of concrete is of the order of one tenth of its compressive strength, and the tensile strain at which it cracks is of the order of 100 microstrain. This is only a fraction of the ultimate strain of the steel which it surrounds. Obviously, therefore, the formation of cracks, even in well designed reinforced concrete structures, is unavoidable. Since cracking is one of the criteria which a design has to satisfy in the limit state design of reinforced concrete structures, it is necessary that the cracks should be kept as small as possible for two main reasons. Firstly, wide cracks are aesthetically unpleasant, and can cause public concern. Secondly, corrosive elements can penetrate to the main steel which can lead to weakening of the structure. In addition, in plated structures, such penetration could cause degradation of the adhesive bonding mechanism. In the past, flexural cracks cause little concern since the relatively low permissible steel stresses used in design ensured that cracks would not be large. Recently there has been a considerable increase in permissible stresses in steel, and since crack widths are proportional to steel stress the crack widths are increased. It has therefore become necessary to know, with greater certainty the factors which govern cracking and to be able to predict and control crack widths and spacings.

7.2 REVIEW OF LITERATURE

Gergely and Lutz (89) analysed, statistically, information from six experimental investigations. The major conclusions which were drawn, regarding factors affecting crack widths were:

1. The steel stress is the most important variable.
2. The cover thickness is an important variable.
3. The bar diameter is not a major variable.
4. The size of the side crack width is reduced by the proximity of the compression zone in flexural members.
5. The bottom crack width increases with concrete strain gradient across the section in flexural members.

Illston and Stevens (90) investigated surface and internal cracking in reinforced concrete beams through a resin injection technique. At working loads, the spacings of flexural cracks were found to be a function of concrete cover and the surface crack width was a function of spacing and steel stresses.

The Cement and Concrete Association conducted an extensive investigation by Base et al (91). Their report gave factors which influenced the width and distribution of cracks in zones of uniform bending moment in reinforced concrete beams. The most important factors affecting crack widths were:

1. The magnitude of the steel stress.
2. The cover thickness.
3. No evidence was found that there was any effect on the crack width when varying the type of reinforcement, and the percentage within the range 0.85 to 2.29%.
4. No evidence was produced that variation of concrete strength or curing conditions had a significant effect on cracking.

The British Code of Practice CP110, (86) recommends that the surface crack width shall not exceed certain limits depending on the environment, exposure and service requirements of a member. When exposed to aggressive environments, the assessed surface crack widths at points nearest to the main reinforcement should not exceed 0.004 times the nominal cover. The formula in Appendix A of the code was proposed by Beeby (92). ε_m the concrete surface strain is given by:

$$\varepsilon_m = \varepsilon_1 - \frac{1{\cdot}2.b.h.(\bar{a} - x).10^{-3}}{A_s.f_y.\ (h - x)}$$

The formula for determining the design crack width, W_{cr}, is then given by:

$$W_{cr} = \frac{3.\ a_{cr}.\ \varepsilon_m}{1 + 2\left(\frac{a_{cr} - C_{min}}{h-x}\right)}$$

All symbols as defined earlier.

The American Concrete Institute Code (89) recommends that the maximum crack width at the level of the reinforcement is given by:

$$W_{max} = \frac{0{\cdot}091\sqrt[3]{ts.A}\ (fs - 5).\ 10^{-3}}{1 + t_s/h_1} \qquad \text{(IMPERIAL UNITS)}$$

and that the maximum crack width at the tension face is given by:

$$W_{max} = 0{\cdot}091\sqrt[3]{t_b.A}\ .\ R(fs - 5).\ 10^{-3} \qquad \text{(IMPERIAL UNITS)}$$

where:

t_s = side cover to centre of longitudinal reinforcing bar, (inches)

t_b = bottom cover to centre of longitudinal reinforcing bar, (inches)

fs = steel stress based on an elastic cracked section, (kips/in^2)

R = h_2/h_1

h_1 = distance from neutral axis to the tension steel (inches)

h_2 = distance from neutral axis to the tension face, (inches)

A = $\frac{2b\ (h - d)}{\text{number of bars}}$

b = width of beam, (inches)

h = overall depth of beam, (inches)

d = effective depth, (inches)

It is also stated that the cross section at the maximum bending moment should be proportioned so that $fs.\sqrt[3]{tb.A}$ does not exceed 170 kips/inch for interior exposure and 145 kips/inch for exterior exposure. These values correspond to crack widths of 0.4 and 0.3 mm, respectively.

The Comité Euro-International du Beton (85) recommend that the characteristic value of the crack width, W_k, at the reinforcement level should not exceed 1.7 times the mean crack width, W_m.

$$W_m = Srm\ .\ \varepsilon sm$$

where:

Srm = the final mean crack spacing at the reinforcement level

εsm = the mean elongation of the reinforcement allowing for the contribution of the concrete in tension.

and:

$$Srm = 2c + \frac{k\phi}{\rho}$$

where,

c = cover to reinforcement

ϕ = diameter of largest bars.

$\rho = \frac{A_s}{2b(h-d)}$, A_s = area of steel bars.

k is a coefficient which depends on the type of steel and the mode of loading.

also:

$$\varepsilon_{sm} = \frac{\sigma_s}{E_s}\left[1 - \beta\left(\frac{\sigma_{sr}}{\sigma_s}\right)^2\right]$$

where,

σ_s = steel stress based on an elastic cracked section.

σ_{sr} = steel stress calculated on the assumption that the concrete in tension reaches its maximum tensile strength.

β is a coefficient which depends on bond characteristics; 0.7 for high bond bars and zero for smooth bars.

7.3 EXPERIMENTAL PROGRAMME

Previous research (89-93) has revealed that certain variables have a strong influence on cracking. The most important of these being

1. The stress in the steel
2. The cover to reinforcement
3. The proximity of the concrete compression zone.

The addition of an externally bonded steel plate should effectively satisfy all three of these requirements. As has been shown in the section on strains; for the plated beams the internal bar strains are reduced considerably, and also the neutral axis is brought closer to the level of reinforcement.

The test beams 201 to 224, already described, were used to investigate the cracking behaviour. The side and bottom cover to the reinforcement were kept constant and the effect on crack width at the level of reinforcement would then be related to the glue and plate parameters.

At each load stage the widths, heights and spacings of all the cracks in the constant moment region were noted. The crack widths and spacings were read at the level of the internal reinforcement.

7.4 DISCUSSION OF RESULTS

7.4.1 General-statistical analysis

The assessment of crack widths was made on a statistical basis. The widths of all the cracks that appeared within the constant moment region were read at the level of reinforcement, and the values of crack width which have a 1% chance of being exceeded were determined. Crack widths determined in this manner are subject to less experimental error than the measured values of maximum crack width, since the former are determined from measurements on the entire population of cracks. Normal distribution of crack widths is a generally accepted phenomenon, and has been proved by Base et al (91) in their investigations.

Instead of plotting the width of a single crack, the mean width of all cracks in the constant moment region, at the reinforcement level, was plotted against the average strain in the concrete at the same level, the latter being determined from Demec gauge readings on a 200 mm gauge length at the centre section. As was stated earlier, the strain in the reinforcing bar and the surface concrete strain are approximately equal. Figure 6.1 confirms this. The Demec readings were used, instead of electrical strain gauge readings, as they gave average strain rather than local strains. At each load stage the following values were measured and are given in Tables 7.1 - 7.6.

(i) maximum crack width

(ii) mean crack width, height, spacing and standard deviations

(iii) number of cracks in the constant moment region.

Figs. 7.1 - 7.3 show the graphs of mean crack width versus the concrete strain at the reinforcement levels. A roughly linear relationship can be obtained. Although the stress in the reinforcement is not used directly it may be calculated by reading off the strain in the concrete surface at the reinforcement level and multiplying by the elastic modulus of steel. For stresses within the linear range of the steel behaviour, the graphs indicated that the mean crack width was proportional to the stress in the reinforcement, as confirmed by many other authors. (89-93).

TABLE 7·1 CRACKING CHARACTERISTICS

LOAD kN	NUMBER OF CRACKS	MEAN CONCRETE STRAIN 10^{-6}	MEAN CRACK WIDTH 10^{-2} mm	STANDARD DEVIATION $.10^{-2}$ mm	COEFF. OF VARIATION $.10^{-2}$	MAXIMUM CRACK WIDTH 10^{-2} mm	MEAN CRACK SPACING mm	STANDARD DEVIATION mm	MEAN CRACK HEIGHT mm	STANDARD DEVIATION mm
60	9	550	2·67	1·33	50	5·0	83	19	82	24
100	12	1110	4·29	2·30	53	9·0	62	22	95	38
130	12	1460	6·67	2·51	38	12·0	62	22	113	33
160	13	1750	8·54	3·34	39	14·0	57	21	119	34
220	14	3400	16·70	6·02	36	25·0	52	24	146	28
250	-	-	-	-	-	-	-	-	-	-

(a) beam 201 $W_{max} / W_{mean} = 1{\cdot}78$

LOAD kN	NUMBER OF CRACKS	MEAN CONCRETE STRAIN 10^{-6}	MEAN CRACK WIDTH 10^{-2} mm	STANDARD DEVIATION $.10^{-2}$ mm	COEFF. OF VARIATION $.10^{-2}$	MAXIMUM CRACK WIDTH 10^{-2} mm	MEAN CRACK SPACING mm	STANDARD DEVIATION mm	MEAN CRACK HEIGHT mm	STANDARD DEVIATION mm
60	10	580	2·65	1·43	59	5·0	83	27	92	35
100	12	1080	4·20	1·90	56	8·0	67	20	109	40
130	12	1450	6·75	3·00	52	12·0	67	20	113	47
160	14	1800	8·21	3·94	49	13·0	60	14	115	44
220	14	3100	14·60	5·70	39	24·0	60	14	132	49
250	-	-	-	-	-	-	-	-	-	-

(b) beam 202 $W_{max} / W_{mean} = 1{\cdot}76$

LOAD kN	NUMBER OF CRACKS	MEAN CONCRETE STRAIN 10^{-6}	MEAN CRACK WIDTH 10^{-2} mm	STANDARD DEVIATION $.10^{-2}$ mm	COEFF. OF VARIATION $.10^{-2}$	MAXIMUM CRACK WIDTH 10^{-2} mm	MEAN CRACK SPACING mm	STANDARD DEVIATION mm	MEAN CRACK HEIGHT mm	STANDARD DEVIATION mm
60	8	520	1·88	0·64	34	3·0	96	29	74	36
100	11	1060	2·60	1·02	39	4·0	68	12	105	39
130	12	1200	3·90	1·62	42	6·5	64	15	112	44
160	13	1850	5·10	2·50	49	11·0	60	15	118	35
220	14	2850	8·54	3·14	36	14·0	55	18	123	39
250	14	3900	12·50	8·13	65	20·0	55	18	131	41

(c) beam 203 $W_{max} / W_{mean} = 1{\cdot}70$

LOAD kN	NUMBER OF CRACKS	MEAN CONCRETE STRAIN 10^{-6}	MEAN CRACK WIDTH 10^{-2} mm	STANDARD DEVIATION $.10^{-2}$ mm	COEFF. OF VARIATION $.10^{-2}$	MAXIMUM CRACK WIDTH 10^{-2} mm	MEAN CRACK SPACING mm	STANDARD DEVIATION mm	MEAN CRACK HEIGHT mm	STANDARD DEVIATION mm
60	7	260	1·71	0·27	16	3·0	108	27	65	26
100	9	700	2·89	1·11	38	4·0	80	23	76	31
130	12	940	3·08	1·95	63	6·0	63	22	88	39
160	13	1200	4·46	2·00	44	10·0	53	16	96	34
220	14	1940	7·64	2·53	33	13·0	53	16	116	22
250	14	2400	9·86	5·74	38	18·0	53	15	125	20

(d) beam 204 $W_{max} / W_{mean} = 1{\cdot}81$

TABLE 7·2 CRACKING CHARACTERISTICS

LOAD kN	NUMBER OF CRACKS	MEAN CONCRETE STRAIN 10^{-6}	MEAN CRACK WIDTH 10^{-2} mm	STANDARD DEVIATION 10^{-2} mm	COEFF. OF VARIATION 10^{-2}	MAXIMUM CRACK WIDTH 10^{-2} mm	MEAN CRACK SPACING mm	STANDARD DEVIATION mm	MEAN CRACK HEIGHT mm	STANDARD DEVIATION mm
60	6	200	1·50	0·45	30	2·0	132	60	51	19
100	9	450	2·28	0·78	34	3·0	82	30	88	26
130	11	680	2·80	1·52	54	5·0	68	19	93	33
160	12	800	4·64	1·91	47	8·0	58	23	98	37
190	13	1000	5·86	2·15	42	10·0	55	19	100	38
220	-	-	-	-	-	-	-	-	-	-

(a) beam 205 $W_{max} / W_{mean} = 1{\cdot}57$

LOAD kN	NUMBER OF CRACKS	MEAN CONCRETE STRAIN 10^{-6}	MEAN CRACK WIDTH 10^{-2} mm	STANDARD DEVIATION 10^{-2} mm	COEFF. OF VARIATION 10^{-2}	MAXIMUM CRACK WIDTH 10^{-2} mm	MEAN CRACK SPACING mm	STANDARD DEVIATION mm	MEAN CRACK HEIGHT mm	STANDARD DEVIATION mm
60	9	260	1·67	0·56	34	2·5	89	20	50	25
100	10	530	2·90	0·99	34	4·5	78	22	92	25
130	11	740	3·63	1·34	37	6·0	64	22	104	30
160	14	1050	4·13	2·15	52	9·0	55	18	105	41
190	15	1370	5·17	2·40	46	9·0	51	17	106	38
220	16	1750	6·63	2·66	40	12·0	47	14	109	37

(b) beam 206 $W_{max} / W_{mean} = 1{\cdot}67$

LOAD kN	NUMBER OF CRACKS	MEAN CONCRETE STRAIN 10^{-6}	MEAN CRACK WIDTH 10^{-2} mm	STANDARD DEVIATION 10^{-2} mm	COEFF. OF VARIATION 10^{-2}	MAXIMUM CRACK WIDTH 10^{-2} mm	MEAN CRACK SPACING mm	STANDARD DEVIATION mm	MEAN CRACK HEIGHT mm	STANDARD DEVIATION mm
60	6	467	2·42	0·93	38	4·0	92	62	54	18
100	8	820	2·72	0·87	32	5·0	79	32	82	24
130	11	1180	2·95	0·83	28	6·0	68	25	92	33
160	14	1565	4·39	2·33	53	10·0	54	25	94	40
220	15	2800	7·53	3·22	43	12·0	53	25	97	48
250	16	3700	14·18	8·17	58	30·0	48	21	108	54

(c) beam 207 $W_{max} / W_{mean} = 1{\cdot}98$

LOAD kN	NUMBER OF CRACKS	MEAN CONCRETE STRAIN 10^{-6}	MEAN CRACK WIDTH 10^{-2} mm	STANDARD DEVIATION 10^{-2} mm	COEFF. OF VARIATION 10^{-2}	MAXIMUM CRACK WIDTH 10^{-2} mm	MEAN CRACK SPACING mm	STANDARD DEVIATION mm	MEAN CRACK HEIGHT mm	STANDARD DEVIATION mm
60	6	300	1·75	0·82	47	3·0	143	53	57	12
100	10	600	2·85	1·08	38	4·0	88	17	92	17
130	12	800	3·67	1·23	34	6·0	74	20	97	33
160	12	1060	4·75	1·54	33	9·0	64	20	109	34
220	14	1800	7·71	2·97	38	14·0	54	15	117	37
250	15	2600	10·50	4·90	46	20·0	52	18	120	36

(d) beam 208 $W_{max} / W_{mean} = 1{\cdot}73$

TABLE 7·3 CRACKING CHARACTERISTICS

LOAD kN	NUMBER OF CRACKS	MEAN CONCRETE STRAIN 10^{-6}	MEAN CRACK WIDTH 10^{-2} mm	STANDARD DEVIATION 10^{-2} mm	COEFF. OF VARIATION 10^{-2}	MAXIMUM CRACK WIDTH 10^{-2} mm	MEAN CRACK SPACING mm	STANDARD DEVIATION mm	MEAN CRACK HEIGHT mm	STANDARD DEVIATION mm
60	3	200	117	0·29	25	2·0	125	64	47	7
100	8	350	1·80	0·60	33	3·0	101	32	83	21
130	10	580	2·80	1·20	43	4·5	79	23	93	30
160	12	830	3·90	2·20	56	7·0	60	21	98	35
220	14	1030	6·10	3·40	56	10·0	53	20	109	31
250	-	-	-	-	-	-	-	-	-	-

(a) beam 209 $W_{max}/W_{mean} = 1·63$

LOAD kN	NUMBER OF CRACKS	MEAN CONCRETE STRAIN 10^{-6}	MEAN CRACK WIDTH 10^{-2} mm	STANDARD DEVIATION 10^{-2} mm	COEFF. OF VARIATION 10^{-2}	MAXIMUM CRACK WIDTH 10^{-2} mm	MEAN CRACK SPACING mm	STANDARD DEVIATION mm	MEAN CRACK HEIGHT mm	STANDARD DEVIATION mm
60	6	280	1·41	0·66	47	2·0	145	46	58	18
100	9	560	2·33	1·03	44	4·0	87	25	84	29
130	11	780	2·80	1·31	46	5·0	70	16	88	37
160	11	1000	4·22	1·60	38	7·0	70	16	110	32
190	13	1300	7·05	3·85	56	12·0	56	16	118	33
220	-	-	-	-	-	-	-	-	-	-

(b) beam 210 $W_{max}/W_{mean} = 1·66$

LOAD kN	NUMBER OF CRACKS	MEAN CONCRETE STRAIN 10^{-6}	MEAN CRACK WIDTH 10^{-2} mm	STANDARD DEVIATION 10^{-2} mm	COEFF. OF VARIATION 10^{-2}	MAXIMUM CRACK WIDTH 10^{-2} mm	MEAN CRACK SPACING mm	STANDARD DEVIATION mm	MEAN CRACK HEIGHT mm	STANDARD DEVIATION mm
60	4	430	2·75	0·87	32	4·0	138	42	27	5
100	11	850	2·91	1·11	38	5·0	87	23	67	35
135	13	1150	3·84	1·78	46	8·0	67	24	88	37
160	15	1760	4·63	2·23	48	10·0	49	26	91	42
220	17	2790	8·67	5·94	69	19·0	43	16	93	51
250	17	3990	13·82	8·22	59	30·0	43	16	100	52

(c) beam 211 $W_{max}/W_{mean} = 2·20$

LOAD kN	NUMBER OF CRACKS	MEAN CONCRETE STRAIN 10^{-6}	MEAN CRACK WIDTH 10^{-2} mm	STANDARD DEVIATION 10^{-2} mm	COEFF. OF VARIATION 10^{-2}	MAXIMUM CRACK WIDTH 10^{-2} mm	MEAN CRACK SPACING mm	STANDARD DEVIATION mm	MEAN CRACK HEIGHT mm	STANDARD DEVIATION mm
60	7	400	2·14	1·06	49	4·0	122	30	56	24
100	10	775	3·15	1·73	55	7·0	82	30	86	30
130	11	1050	4·36	1·95	45	8·0	73	19	106	38
160	13	1400	6·50	2·80	43	12·0	60	21	105	46
220	15	2330	9·20	4·70	51	21·0	55	16	108	43
250	17	3300	12·94	7·20	55	30·0	48	15	111	44

(d) beam 212 $W_{max}/W_{mean} = 2·0$

TABLE 7·4 CRACKING CHARACTERISTICS

LOAD kN	NUMBER OF CRACKS	MEAN CONCRETE STRAIN 10^{-6}	MEAN CRACK WIDTH 10^{-2} mm	STANDARD DEVIATION 10^{-2} mm	COEFF. OF VARIATION 10^{-2}	MAXIMUM CRACK WIDTH 10^{-2} mm	MEAN CRACK SPACING mm	STANDARD DEVIATION mm	MEAN CRACK HEIGHT mm	STANDARD DEVIATION mm
60	8	250	2·50	0·75	30	4·0	101	16	85	14
100	9	585	3·80	1·70	45	7·0	87	22	104	25
130	10	870	5·01	2·83	57	8·0	77	23	108	31
160	13	1200	5·92	3·20	54	11·0	65	28	108	38
220	13	1930	10·53	3·24	31	20·0	65	28	117	27
250	15	2560	14·26	8·10	57	29·0	59	30	132	41

(a) beam 213 $W_{max}/W_{mean} = 2·0$

LOAD kN	NUMBER OF CRACKS	MEAN CONCRETE STRAIN 10^{-6}	MEAN CRACK WIDTH 10^{-2} mm	STANDARD DEVIATION 10^{-2} mm	COEFF. OF VARIATION 10^{-2}	MAXIMUM CRACK WIDTH 10^{-2} mm	MEAN CRACK SPACING mm	STANDARD DEVIATION mm	MEAN CRACK HEIGHT mm	STANDARD DEVIATION mm
60	6	350	2·20	0·82	37	3·0	129	48	71	12
100	10	660	3·10	1·30	42	6·0	79	24	83	29
130	12	1000	4·50	2·30	50	8·0	63	13	101	30
160	12	1240	6·00	2·50	41	10·0	63	13	108	32
220	14	1850	7·85	4·80	61	17·0	58	10	111	39
250	15	2500	14·1	7·80	55	28·0	55	12	121	41

(b) beam 214 $W_{max}/W_{mean} = 1·82$

LOAD kN	NUMBER OF CRACKS	MEAN CONCRETE STRAIN 10^{-6}	MEAN CRACK WIDTH 10^{-2} mm	STANDARD DEVIATION 10^{-2} mm	COEFF. OF VARIATION 10^{-2}	MAXIMUM CRACK WIDTH 10^{-2} mm	MEAN CRACK SPACING mm	STANDARD DEVIATION mm	MEAN CRACK HEIGHT mm	STANDARD DEVIATION mm
60	6	220	1·33	0·41	31	3·0	144	36	59	24
100	9	480	2·56	1·10	43	4·0	90	40	89	25
130	11	670	3·78	2·17	57	6·0	71	27	93	37
160	12	900	4·71	2·68	56	9·0	65	25	98	38
220	15	1520	7·73	5·54	72	19·0	51	12	111	37
250	15	2200	10·60	7·10	67	20·0	51	12	119	36

(c) beam 215 $W_{max}/W_{mean} = 1·94$

LOAD kN	NUMBER OF CRACKS	MEAN CONCRETE STRAIN 10^{-6}	MEAN CRACK WIDTH 10^{-2} mm	STANDARD DEVIATION 10^{-2} mm	COEFF. OF VARIATION 10^{-2}	MAXIMUM CRACK WIDTH 10^{-2} mm	MEAN CRACK SPACING mm	STANDARD DEVIATION mm	MEAN CRACK HEIGHT mm	STANDARD DEVIATION mm
50	5	390	2·58	0·90	35	4·0	109	72	48	21
100	9	700	3·00	1·35	45	5·0	88	24	87	26
130	10	960	4·30	2·07	48	7·0	71	29	97	28
160	12	1280	6·58	3·04	46	11·0	60	22	103	37
220	14	2120	9·93	4·07	41	16·0	53	22	105	44
250	15	3310	14·86	9·07	61	30·0	47	21	112	50

(d) beam 216 $W_{max}/W_{mean} = 1·70$

TABLE 7·5 CRACKING CHARACTERISTICS

LOAD kN	NUMBER OF CRACKS	MEAN CONCRETE STRAIN 10^{-6}	MEAN CRACK WIDTH 10^{-2} mm	STANDARD DEVIATION 10^{-2} mm	COEFF. OF VARIATION 10^{-2}	MAXIMUM CRACK WIDTH 10^{-2} mm	MEAN CRACK SPACING mm	STANDARD DEVIATION mm	MEAN CRACK HEIGHT mm	STANDARD DEVIATION mm
60	6	400	1·80	0.45	22	3.0	138	48	59	23
100	9	700	3.33	1·60	48	5.0	93	37	76	31
130	10	870	4.00	1.80	45	6.0	82	22	101	22
160	13	1060	5.90	3.00	44	12.0	62	21	101	25
220	15	1800	9.50	4.10	43	17.0	53	20	111	31
250	15	2240	12.10	5.40	45	24.0	53	20	124	29

(a) beam 217 W_{max}/W_{mean} = 1·75

LOAD kN	NUMBER OF CRACKS	MEAN CONCRETE STRAIN 10^{-6}	MEAN CRACK WIDTH 10^{-2} mm	STANDARD DEVIATION 10^{-2} mm	COEFF. OF VARIATION 10^{-2}	MAXIMUM CRACK WIDTH 10^{-2} mm	MEAN CRACK SPACING mm	STANDARD DEVIATION mm	MEAN CRACK HEIGHT mm	STANDARD DEVIATION mm
60	6	220	1·33	0·41	31	3.0	144	36	59	24
100	9	480	2.56	1·10	43	4.0	90	40	89	25
130	11	670	3.78	2.17	57	6.0	71	27	93	37
160	12	900	4.71	2.68	56	9.0	65	25	98	38
220	15	1520	7.73	5·54	72	19.0	51	12	111	37
250	15	2200	10.6	7·10	67	20.0	51	12	119	36

(b) beam 218 W_{max}/W_{mean} = 1·94

LOAD kN	NUMBER OF CRACKS	MEAN CONCRETE STRAIN 10^{-6}	MEAN CRACK WIDTH 10^{-2} mm	STANDARD DEVIATION 10^{-2} mm	COEFF. OF VARIATION 10^{-2}	MAXIMUM CRACK WIDTH 10^{-2} mm	MEAN CRACK SPACING mm	STANDARD DEVIATION mm	MEAN CRACK HEIGHT mm	STANDARD DEVIATION mm
60	6	250	1.28	0.30	23	2.0	138	42	57	10
100	7	380	2.92	0.89	31	4.0	113	57	87	20
130	12	590	3.58	1·24	35	5.0	88	29	96	26
160	12	720	4.68	1·40	34	7.0	68	19	98	26
190	14	900	5.99	3.05	48	10.0	57	19	105	31
220	-	-	-	-	-	-	-	-	-	-

(c) beam 219 W_{max}/W_{mean} = 1·55

LOAD kN	NUMBER OF CRACKS	MEAN CONCRETE STRAIN 10^{-6}	MEAN CRACK WIDTH 10^{-2} mm	STANDARD DEVIATION 10^{-2} mm	COEFF. OF VARIATION 10^{-2}	MAXIMUM CRACK WIDTH 10^{-2} mm	MEAN CRACK SPACING mm	STANDARD DEVIATION mm	MEAN CRACK HEIGHT mm	STANDARD DEVIATION mm
60	6	400	2.25	0.82	36	3.0	107	24	48	25
100	9	800	3.05	1.01	33	4.0	80	23	85	32
130	12	1120	4·25	1·62	38	6.0	62	27	94	41
160	13	1460	6.04	2·83	47	12·0	58	27	97	46
220	16	2480	8.16	4·77	58	17.0	47	18	108	46
250	17	3440	14·18	7.80	55	30.0	45	17	115	50

(d) beam 220 W_{max}/W_{mean} = 1·71

TABLE 7·6 CRACKING CHARACTERISTICS

LOAD kN	NUMBER OF CRACKS	MEAN CONCRETE STRAIN 10^{-6}	MEAN CRACK WIDTH 10^{-2} mm	STANDARD DEVIATION 10^{-2} mm	COEFF OF VARIATION 10^{-2}	MAXIMUM CRACK WIDTH 10^{-2} mm	MEAN CRACK SPACING mm	STANDARD DEVIATION mm	MEAN CRACK HEIGHT mm	STANDARD DEVIATION mm
60	5	450	2.50	0.94	38	3.5	107	26	32	23
100	10	910	3.15	1.67	53	6.0	78	30	82	27
130	13	1130	3.88	1.10	28	6.0	68	15	90	38
160	14	1550	5.28	1.68	32	11·0	55	16	111	40
220	17	2710	10.24	3.85	38	17.0	45	15	111	52
250	17	4660	16.00	8.47	34	27.0	45	15	126	56

(a) beam 221 W_{max}/W_{mean} = 1·71

LOAD kN	NUMBER OF CRACKS	MEAN CONCRETE STRAIN 10^{-6}	MEAN CRACK WIDTH 10^{-2} mm	STANDARD DEVIATION 10^{-2} mm	COEFF OF VARIATION 10^{-2}	MAXIMUM CRACK WIDTH 10^{-2} mm	MEAN CRACK SPACING mm	STANDARD DEVIATION mm	MEAN CRACK HEIGHT mm	STANDARD DEVIATION mm
60	9	380	1.83	0.80	44	3.5	82	34	76	26
100	12	720	3.13	1·38	42	5.5	60	17	107	28
130	12	930	5.56	2.10	38	10.0	60	17	118	30
160	13	1250	6.68	2.36	35	12.0	59	16	120	37
220	15	1900	9.51	3.31	35	14.0	54	12	127	42
250	15	2870	15.72	4.91	31	24.0	54	12	130	39

(b) beam 222 W_{max}/W_{mean} = 1·72

LOAD kN	NUMBER OF CRACKS	MEAN CONCRETE STRAIN 10^{-6}	MEAN CRACK WIDTH 10^{-2} mm	STANDARD DEVIATION 10^{-2} mm	COEFF OF VARIATION 10^{-2}	MAXIMUM CRACK WIDTH 10^{-2} mm	MEAN CRACK SPACING mm	STANDARD DEVIATION mm	MEAN CRACK HEIGHT mm	STANDARD DEVIATION mm
60	6	400	1.80	0.98	54	3.0	131	59	51	23
100	9	680	3.44	2.10	60	6.0	83	27	83	42
130	11	930	5.36	2.57	48	10.0	67	15	99	43
160	14	1200	6.35	3.30	51	12.0	50	20	114	34
220	14	1700	9.10	3.20	36	16.0	50	20	124	31
250	14	2200	14.00	4.30	30	20.0	50	20	130	34

(c) beam 223 W_{max}/W_{mean} = 1·73

LOAD kN	NUMBER OF CRACKS	MEAN CONCRETE STRAIN 10^{-6}	MEAN CRACK WIDTH 10^{-2} mm	STANDARD DEVIATION 10^{-2} mm	COEFF OF VARIATION 10^{-2}	MAXIMUM CRACK WIDTH 10^{-2} mm	MEAN CRACK SPACING mm	STANDARD DEVIATION mm	MEAN CRACK HEIGHT mm	STANDARD DEVIATION mm
60	10	270	1.45	0.44	30	3.0	79	18	77	26
100	12	590	2.54	1.16	46	4.5	65	17	99	29
130	12	700	3.67	1.43	39	7.0	65	17	108	31
160	12	900	5.50	1.78	32	9.0	65	17	114	29
220	13	1480	8.00	3.40	42	14.0	59	21	118	31
250	13	1850	10.76	5.10	48	19.0	59	21	122	32

(d) beam 224 W_{max}/W_{mean} = 1·72

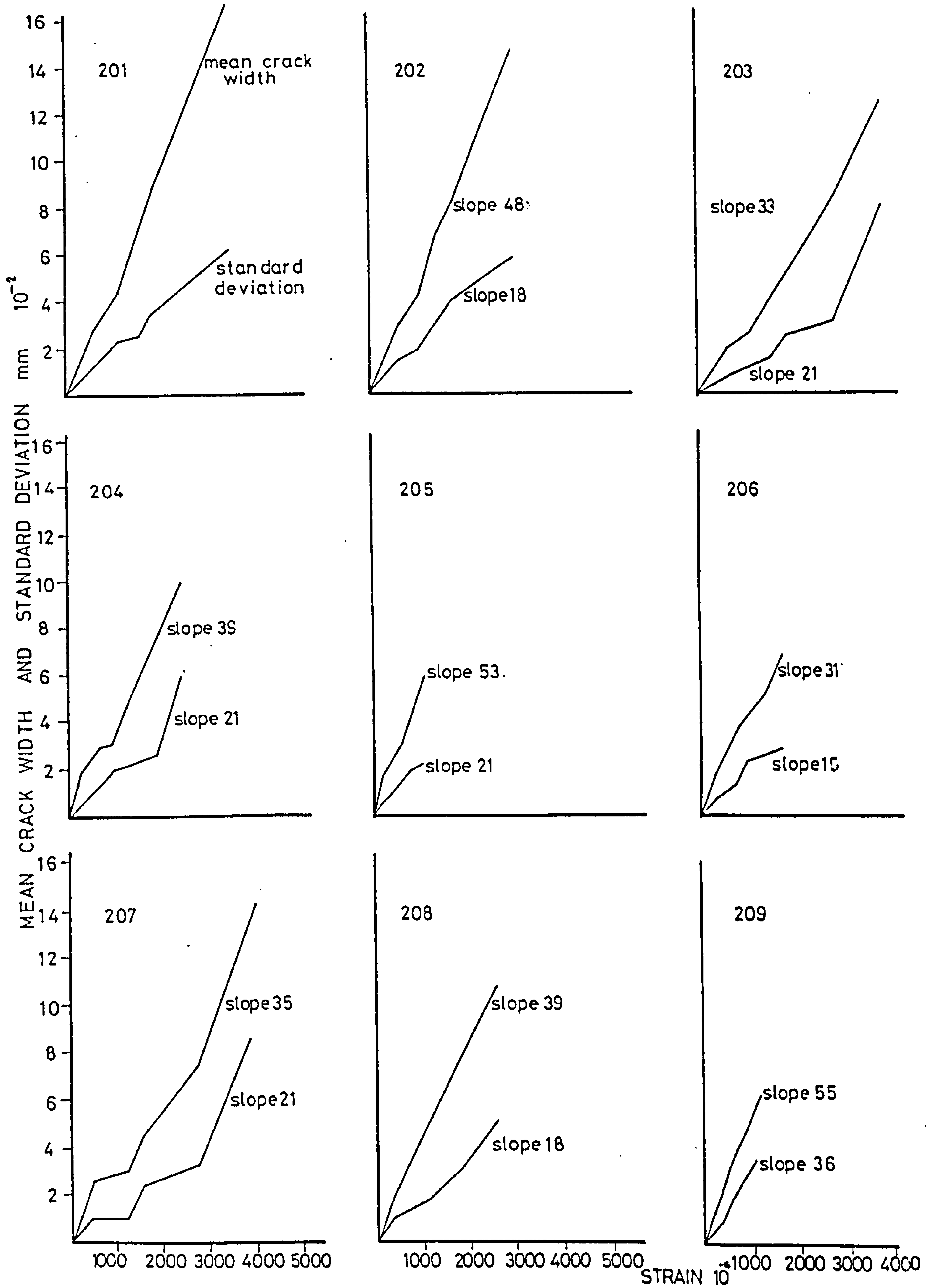

FIGURE 7·1 MEAN CRACK WIDTH & STANDARD DEVIATION V. CONCRETE STRAIN AT THE LEVEL OF INTERNAL REINFORCEMENT

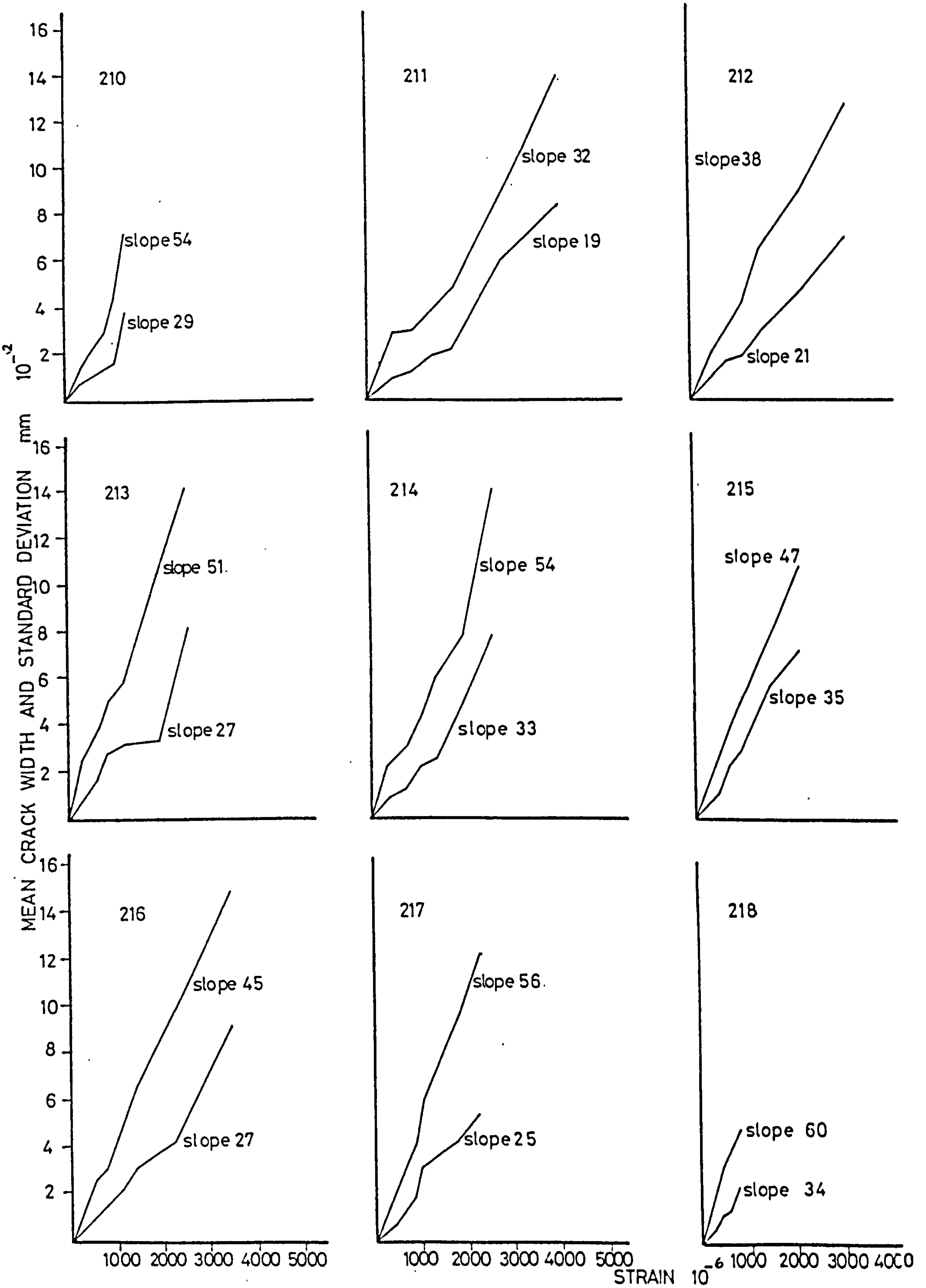

FIGURE 7·2 MEAN CRACK WIDTH & STANDARD DEVIATION V. CONCRETE STRAIN AT THE LEVEL OF INTERNAL REINFORCEMENT

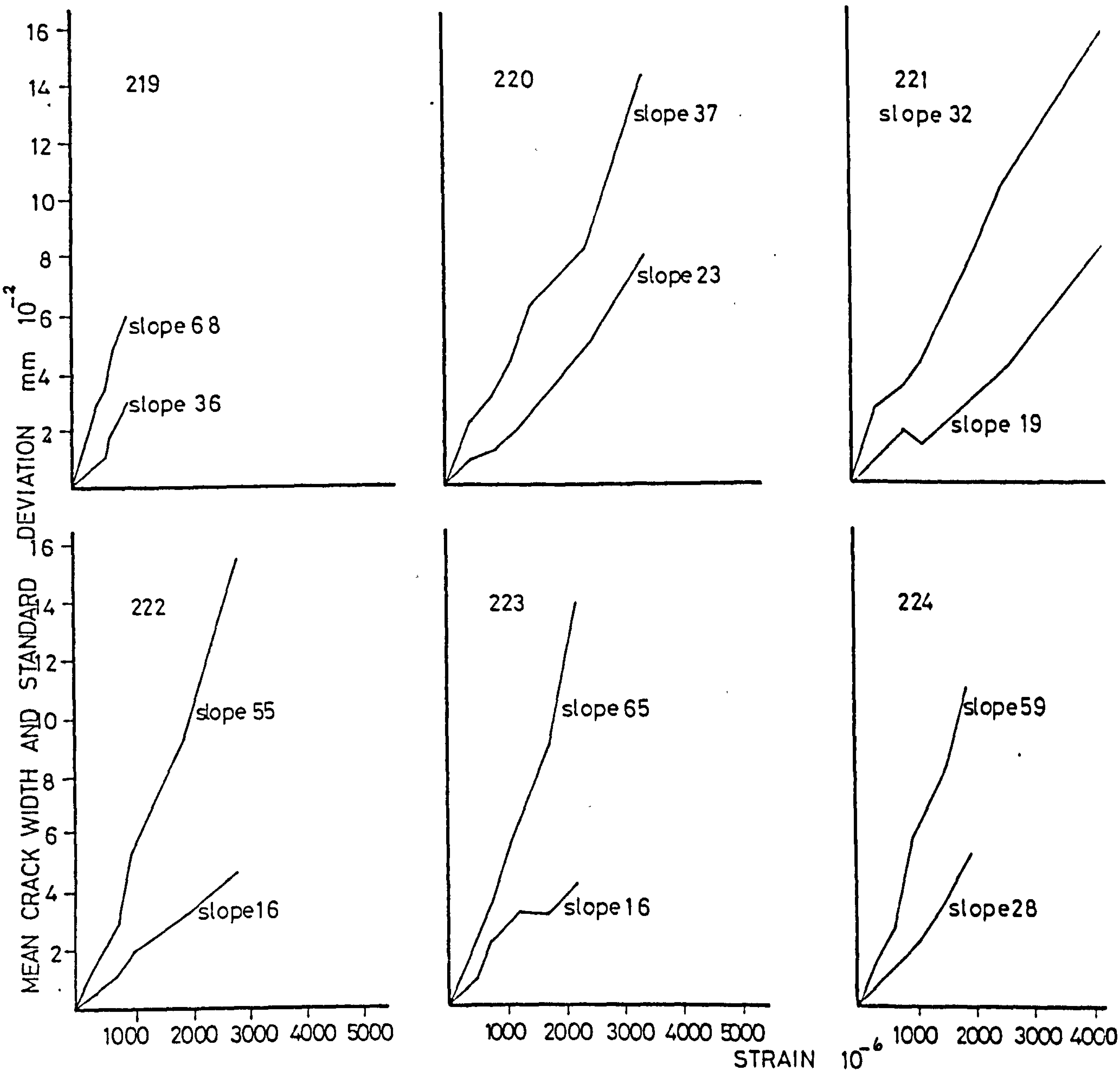

FIGURE 7·3 MEAN CRACK WIDTH & STANDARD DEVIATION V. CONCRETE STRAIN AT THE LEVEL OF INTERNAL REINFORCEMENT

The method of analysis of the results was based upon the slopes of the graphs of mean crack width and standard deviation against the average concrete surface strain, at the level of reinforcement. The slopes in all cases were found from computed "best fit" lines based on a linear regression analysis. (See also Appendix 9). The values, as shown on Figs. 7.1 to 7.3, were then plotted against the thickness of reinforcing plate for each glue line thickness as shown in Fig. 7.4.

It can be seen from Fig. 7.4 that the results are relatively scattered. However, this is not unexpected as it has been shown that cracking is a random phenomenon (89,93), and a scatter of ±50% could be expected. For each glue thickness a best fit line was plotted resulting in an experimental expression for the relationship between the slope of the mean crack width v. concrete strain, S, and the plate thickness, t_p. To combine the three equations shown on Fig. 7.4 it is assumed that there is a linear variation of S with change of glue thickness, t_g. The combined equation is then in the form:

$$S = (K_1 + K_2 t_g) t_p + K_3 t_g + K_4$$

To find the values of K_1 to K_4, the slopes and intercepts of each of the three relationships given on Fig. 7.4 are plotted against glue thickness in Fig. 7.5, and the best fit lines were then drawn. The resulting relationship for all three glue and plate thicknesses is:

$$S = \left[(47.2 - 1.55\, t_g) t_p + 34.3\, t_g + 210\right] . 10^{-1}$$

The slopes found from this expression, over the range of experimental glue and plate thicknesses, were plotted against the experimental values as shown in Fig. 7.6. All values fell within +13% and -5%.

The results found by Ang (72) were also plotted for comparison. These values are consistently greater than those found in the present investigation. More beam test results need to be added to refine the proposed formula.

In Fig. 7.7 the mean ultimate crack spacings, S_u, were plotted against the mean initial crack heights, for all the beams except those which had been precracked and beams 210 and 218, with 6 mm thick reinforcing plates, which failed

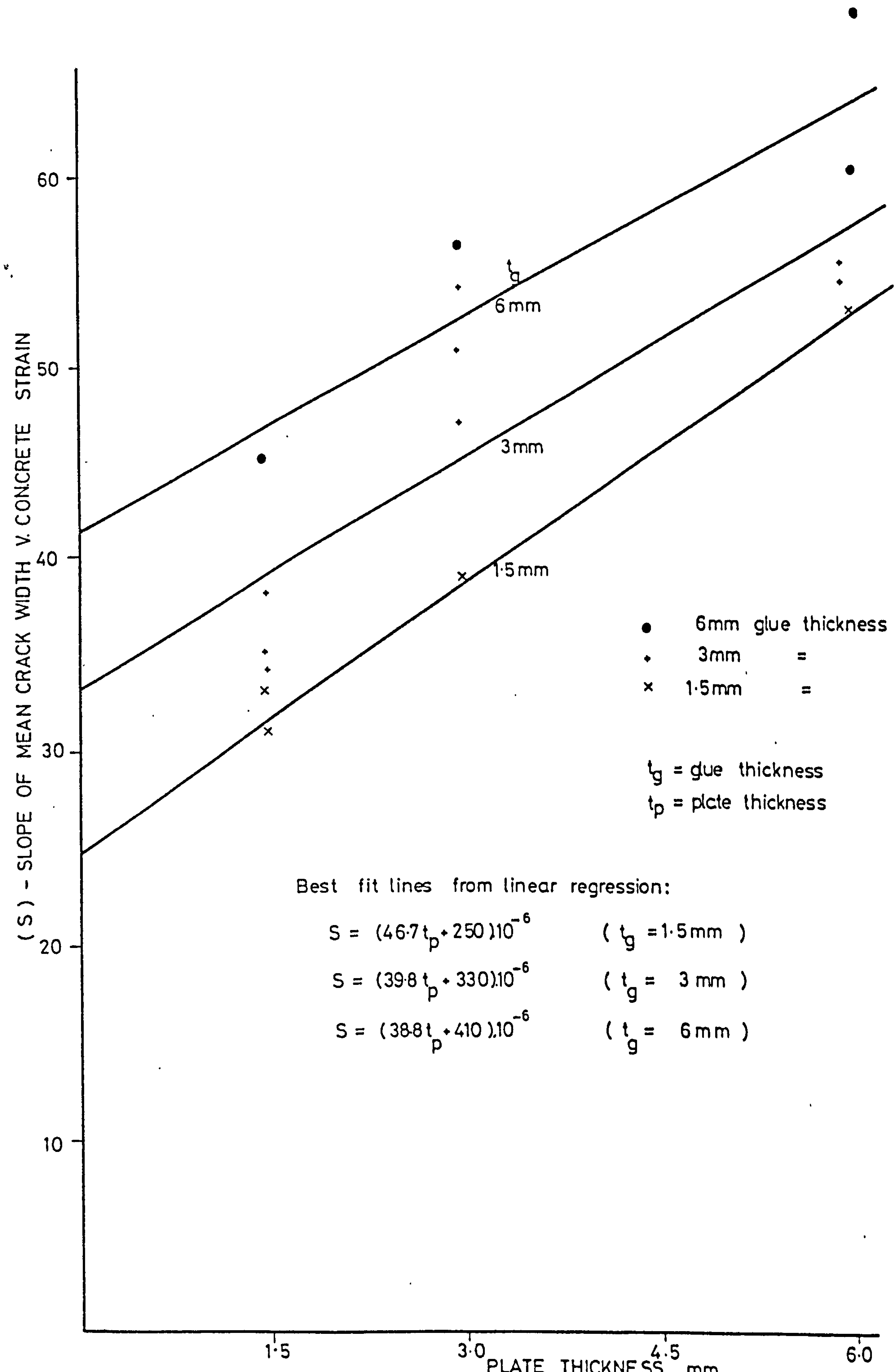

FIGURE 7·4 SLOPE OF MEAN CRACK WIDTH v. CONCRETE STRAIN v. PLATE THICKNESS, FOR EACH GLUE THICKNESS

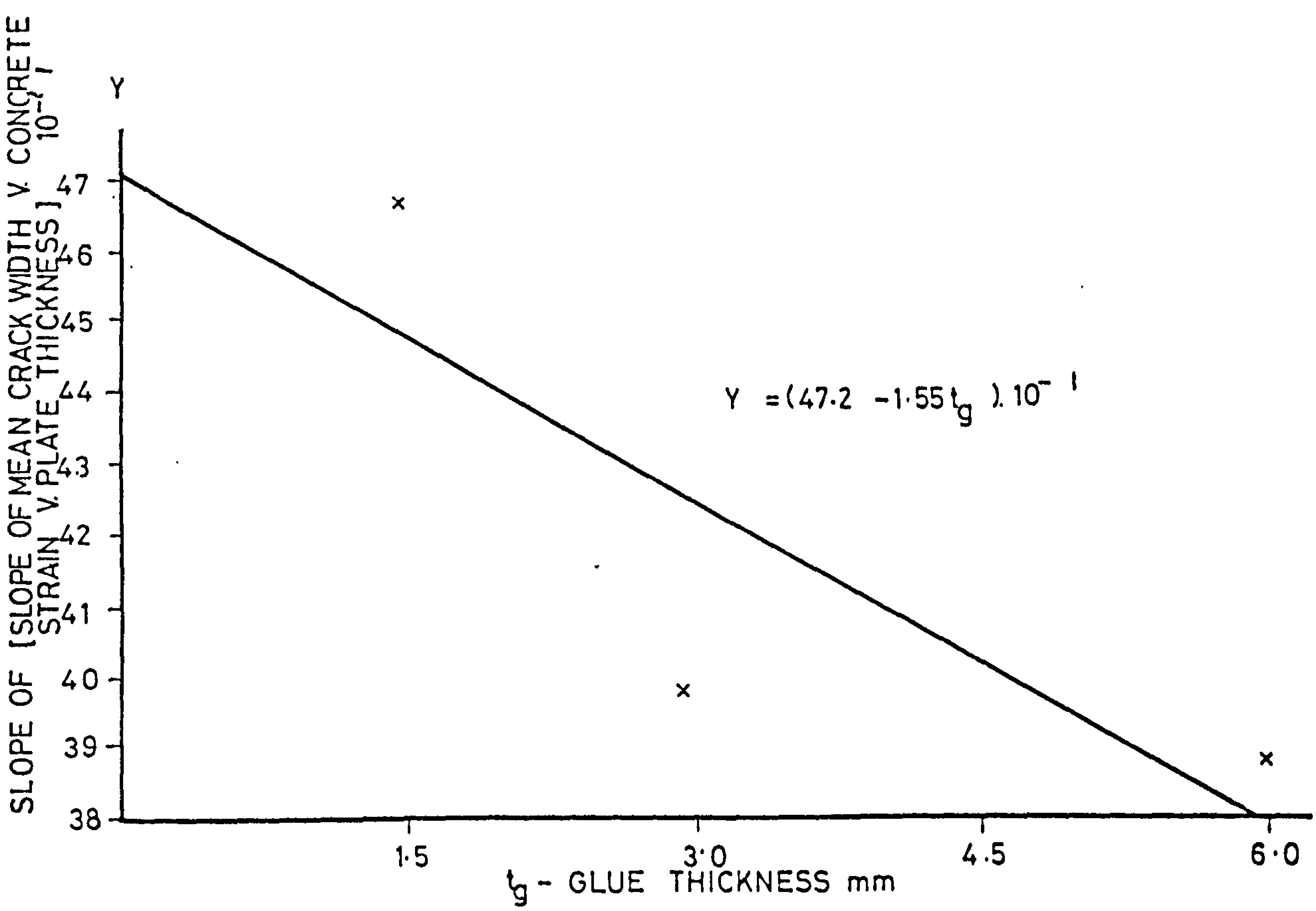

LINEAR REGRESSION ANALYSIS FOR COEFFICIENTS K1 AND K2

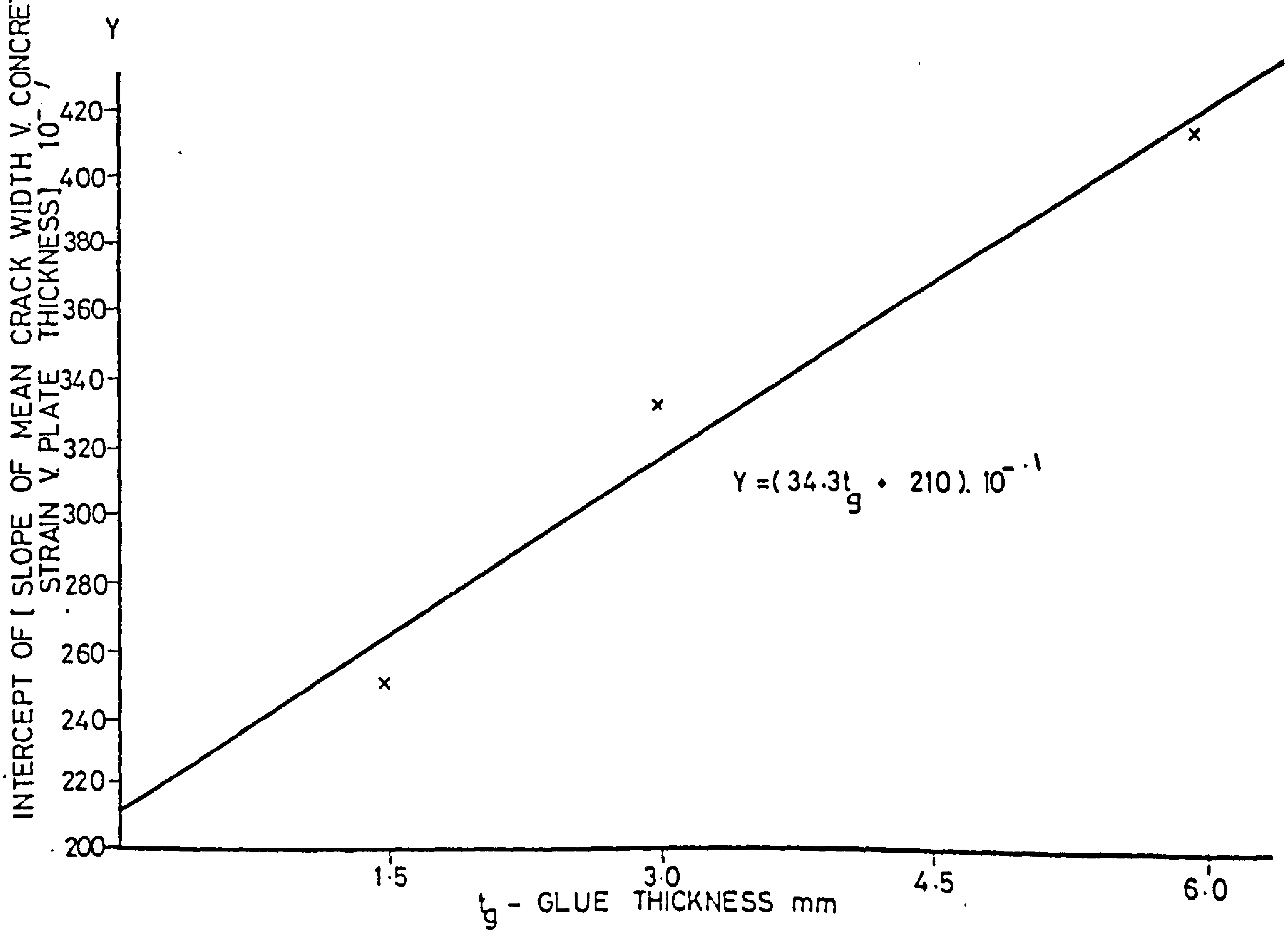

FIGURE 7·5 LINEAR REGRESSION ANALYSIS FOR COEFFICENTS K3 AND K4

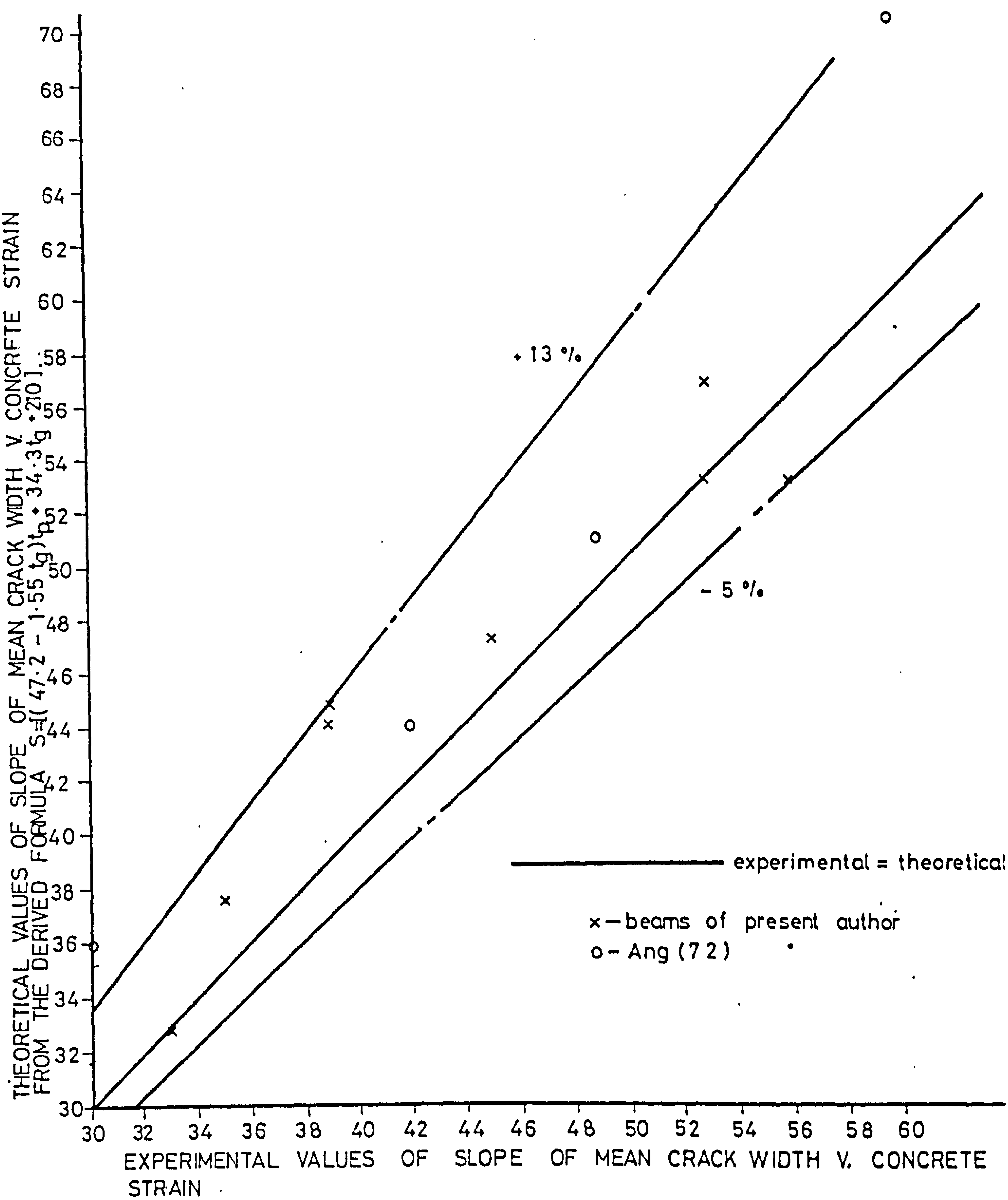

FIGURE 7·6 EXPERIMENTAL V. THEORETICAL VALUES OF THE SLOPE OF MEAN CRACK WIDTH V. CONCRETE STRAIN

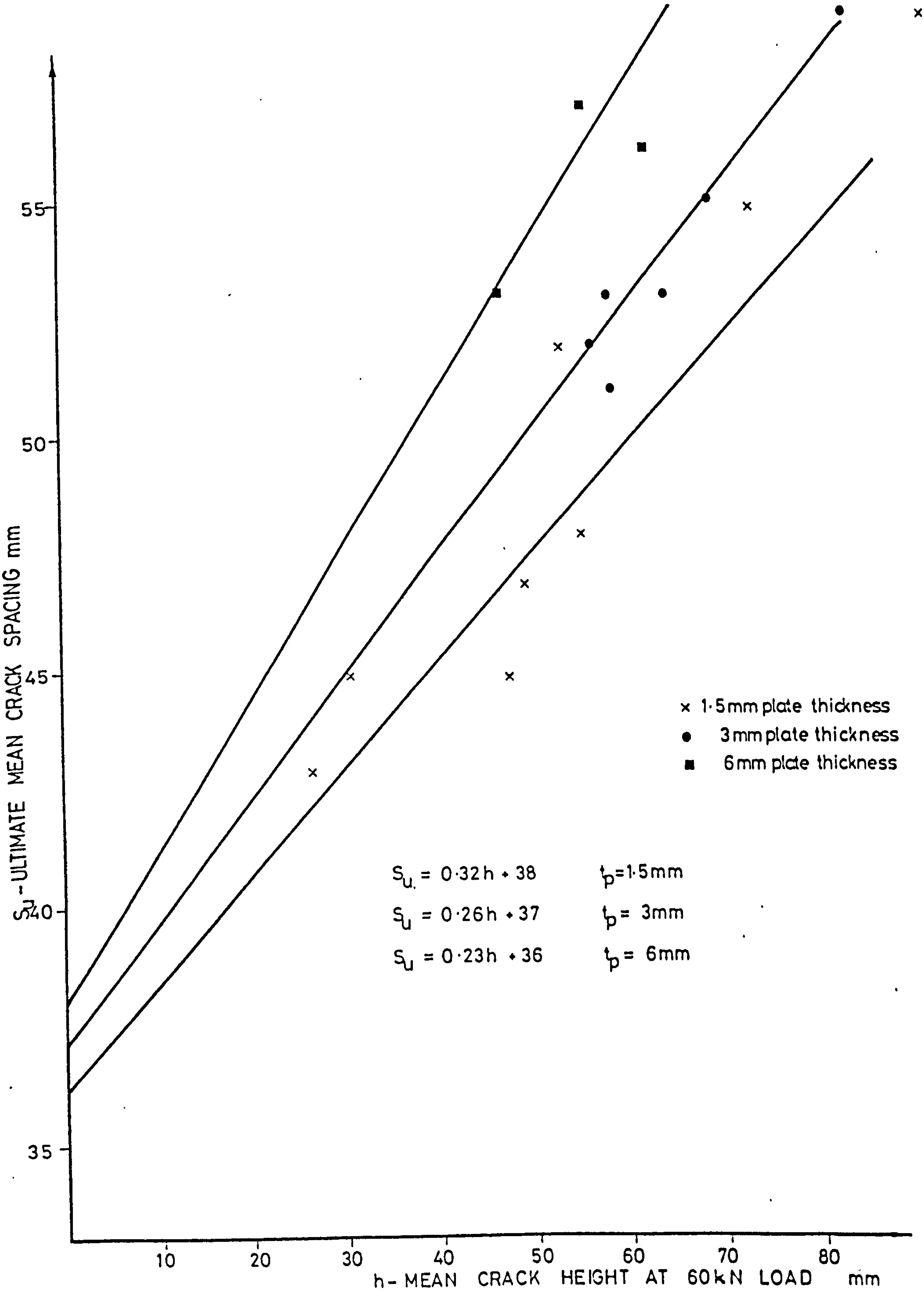

FIGURE 7·7 ULTIMATE MEAN CRACK SPACING V. MEAN CRACK HEIGHT AT 60 kN before their ultimate spacings had been reached. The initial crack height is that at 60 KN, just above the first crack load. Best fit lines were drawn for each plate thickness and the following relationship was found when combining the three plate thicknesses:

$$S_u = (0{\cdot}02\ t_p + 0{\cdot}2)h_{60} + 0{\cdot}43\ t_p + 35{\cdot}5$$

The values found from this formula were plotted against the results from experiments in Fig. 7.8. Al values fell within ±5% of the experimental = theoretical line. However, the above formula does not contain a term relating to concrete cover, which is a major factor in crack formation. Further tests need to be done with different covers to produce a formula for crack spacings which could be applied to any plated beam.

Plates 5.2 to 5.8 show the number of cracks that reach almost to the neutral axis is less than at the reinforcement level. Broms (93) pointed out that in a reinforced concrete member primary cracks formed first which nearly extend to the neutral axis; with a further increase in load secondary cracks of shorter length are formed between these. Base et al (91) explained this in a different way. In the zone just below the neutral axis there would be no cracking since the tensile strain in the concrete is very small. In the zone near the tension face the crack spacing would be a certain value, while in between there would be a transition from this certain spacing to an infinite spacing.

7.4.2 Maximum Crack Widths

Figs. 7.9 to 7.18 show the relationship between the maximum crack width, in the constant bending moment region, and the applied load. The unplated beam had a crack width of 0·12 mm at 130 kN load, approximately the service load condition. For beams with 1·5 mm and 3 mm thick reinforcing plates this width was reduced by 33 to 50%. For beams with 6 mm thick plates the reduction was 58 to 63%. The beams with 1·5 mm lapped plates had between 1·0 and 1·33 times the crack width of similar beams with a continuous layer of plate. Similarly, the beams with two layers of 1·5 mm plate, or one layer of 3 mm plate with lapped joints had between 1·0 and 1·33 times the crack width of similar beams with a continuous layer of 3 mm thick plate. The precracked beams with 1·5 mm thick

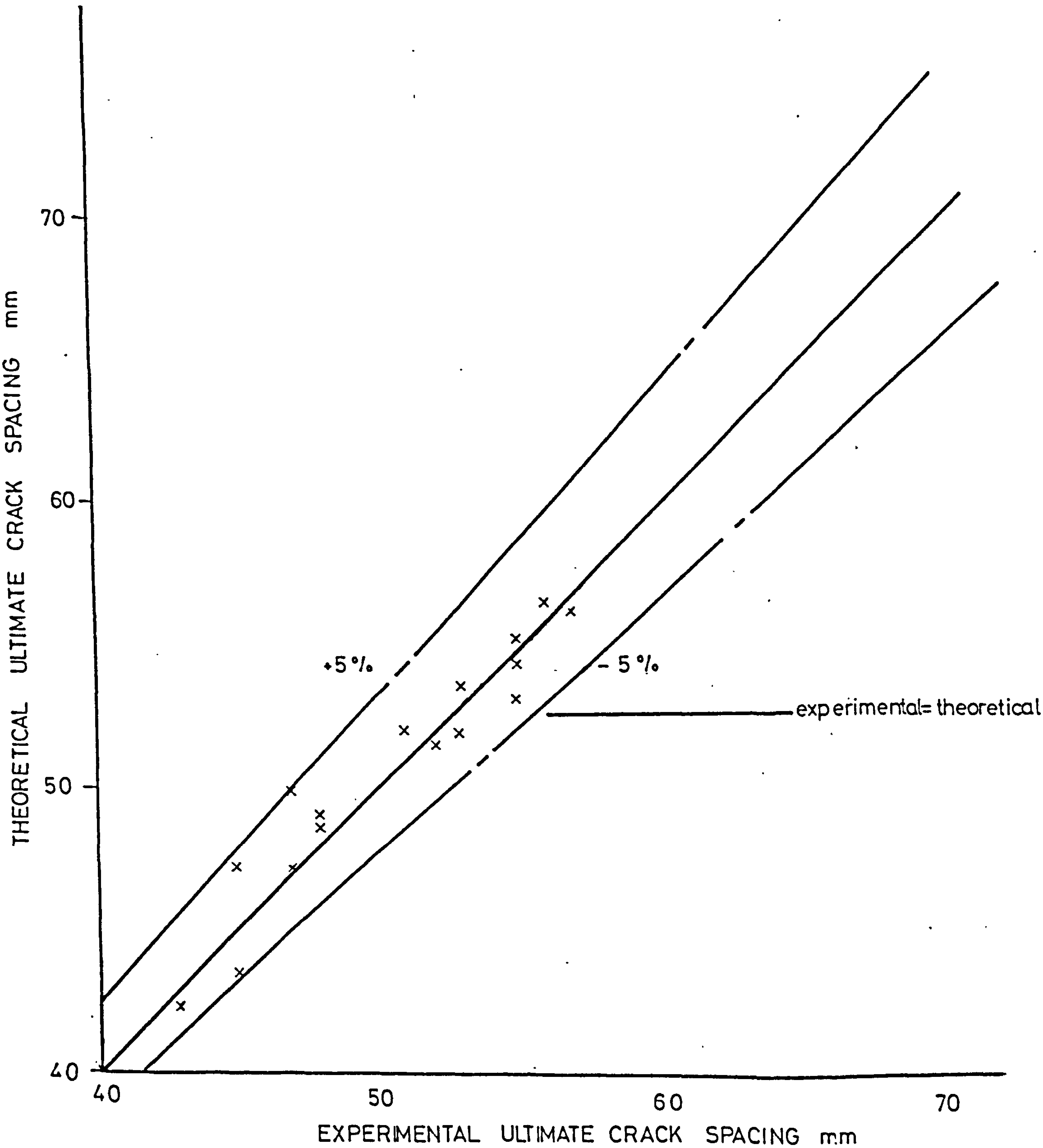

FIGURE 7·8 THEORETICAL V. EXPERIMENTAL ULTIMATE CRACK SPACINGS

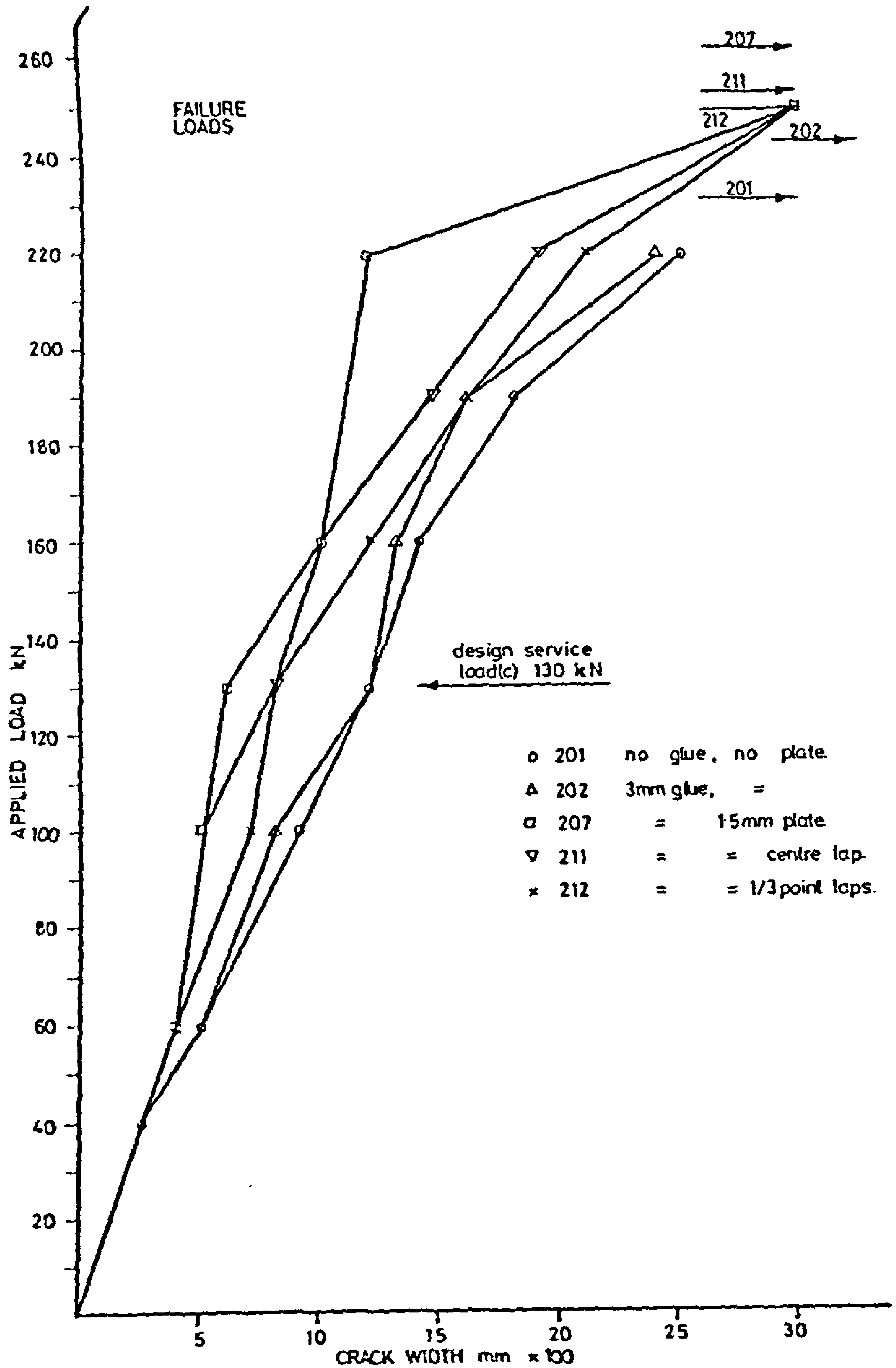

FIGURE 7·9 MAXIMUM CRACK WIDTH V. APPLIED LOAD

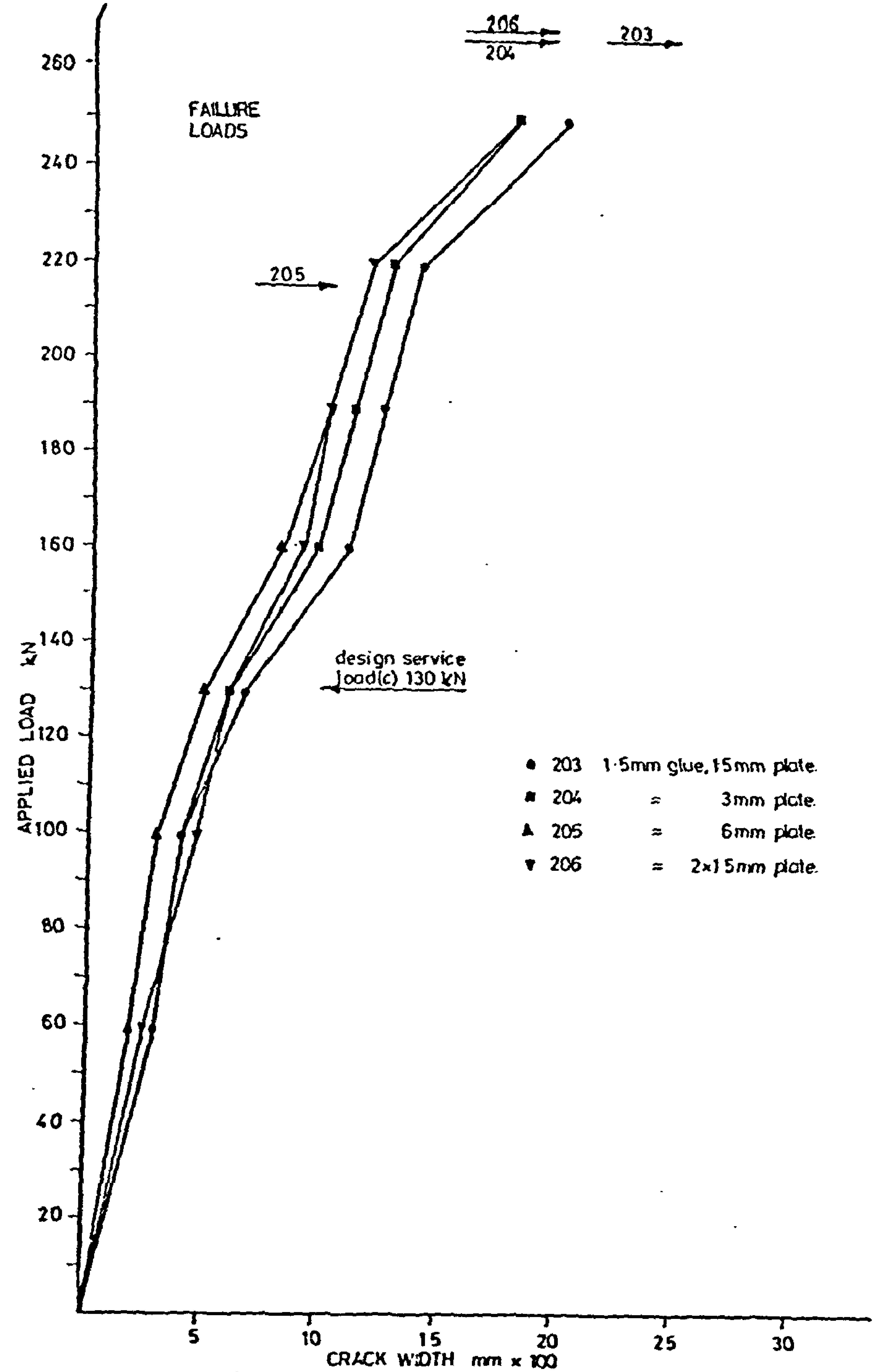

FIGURE 7·10 MAXIMUM CRACK WIDTH V. APPLIED LOAD

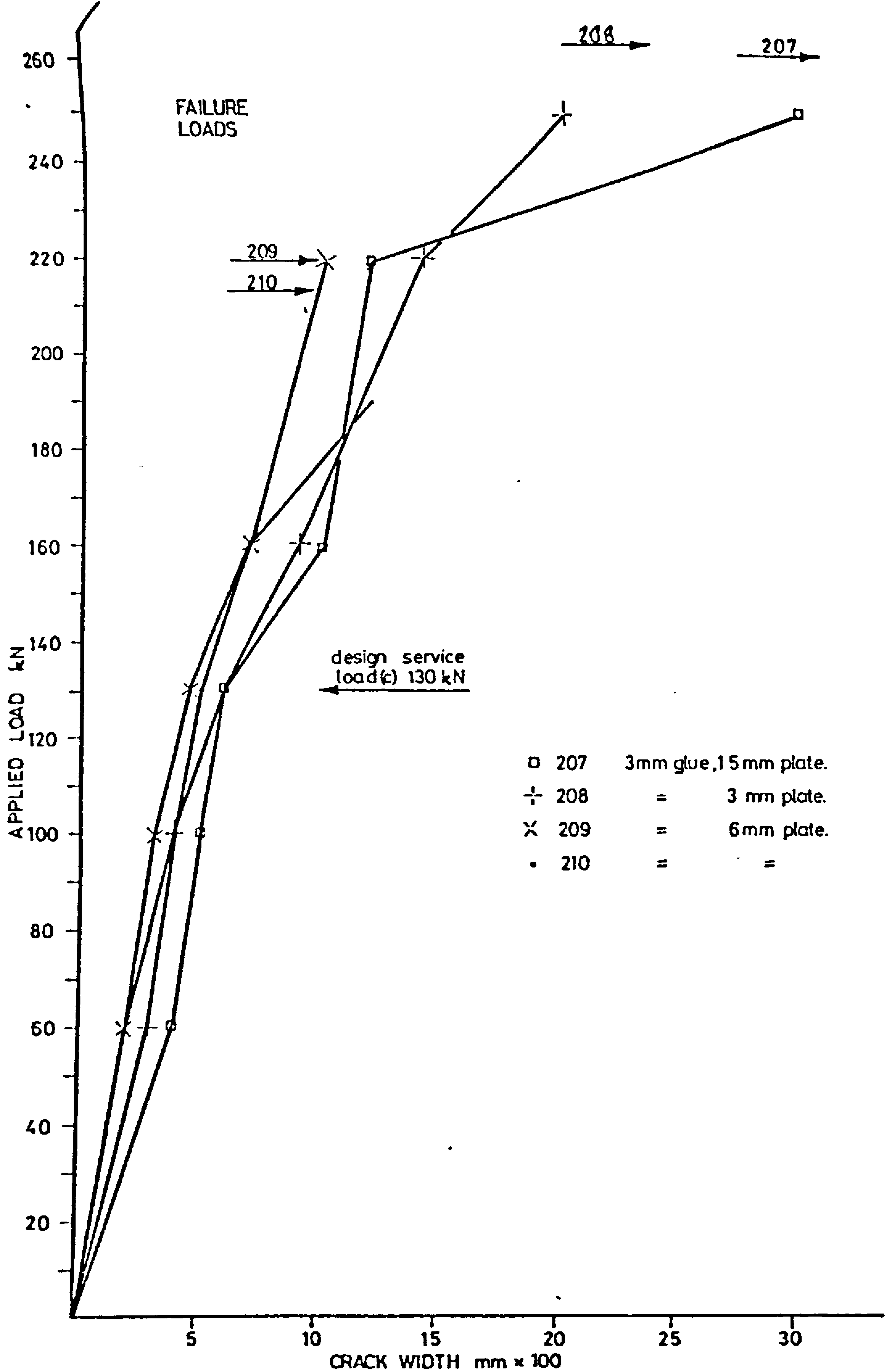

FIGURE 7·11 MAXIMUM CRACK WIDTH V. APPLIED LOAD

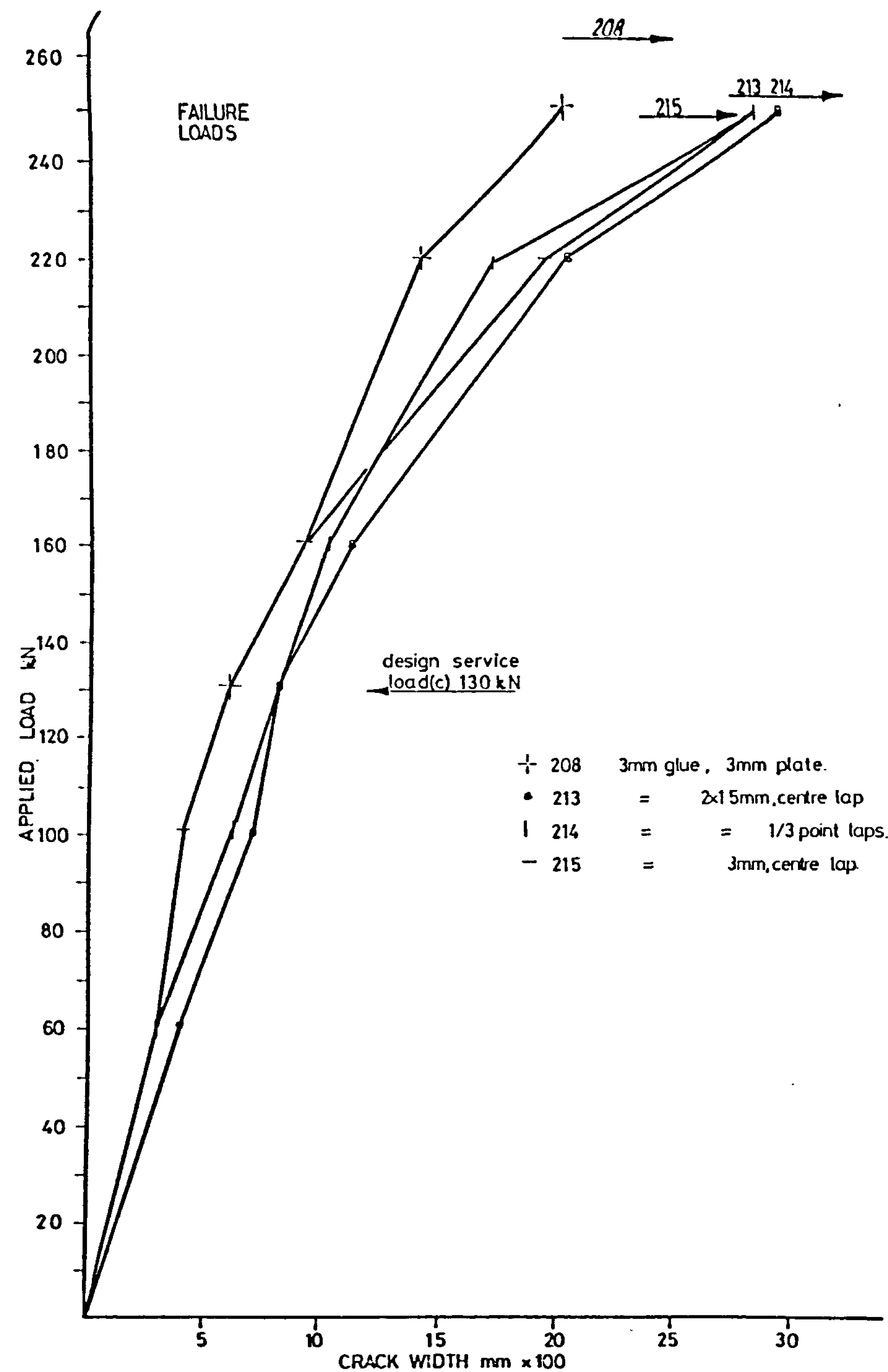

FIGURE 7·12 MAXIMUM CRACK WIDTH V. APPLIED LOAD

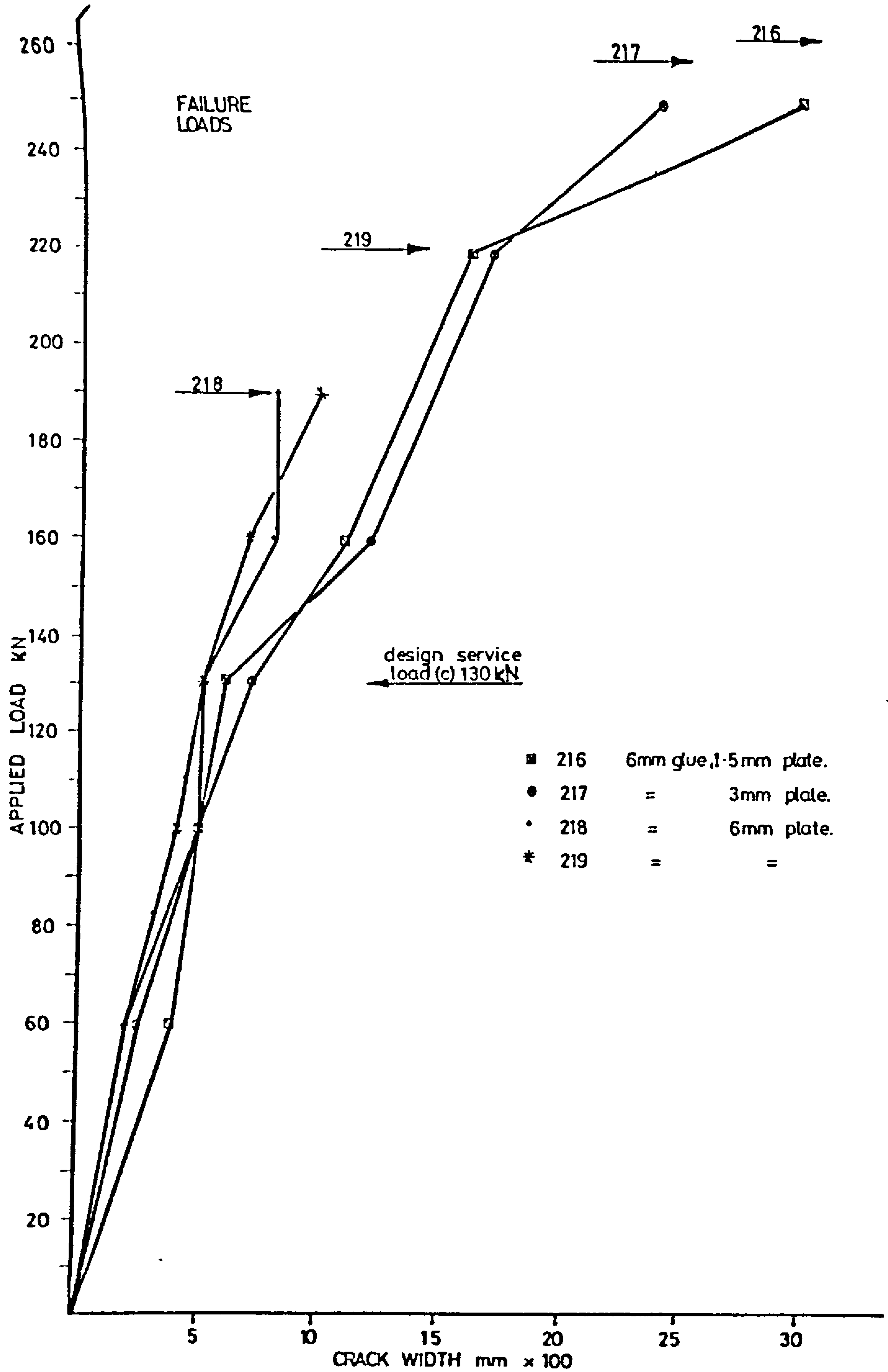

FIGURE 7·13 MAXIMUM CRACK WIDTH V APPLIED LOAD

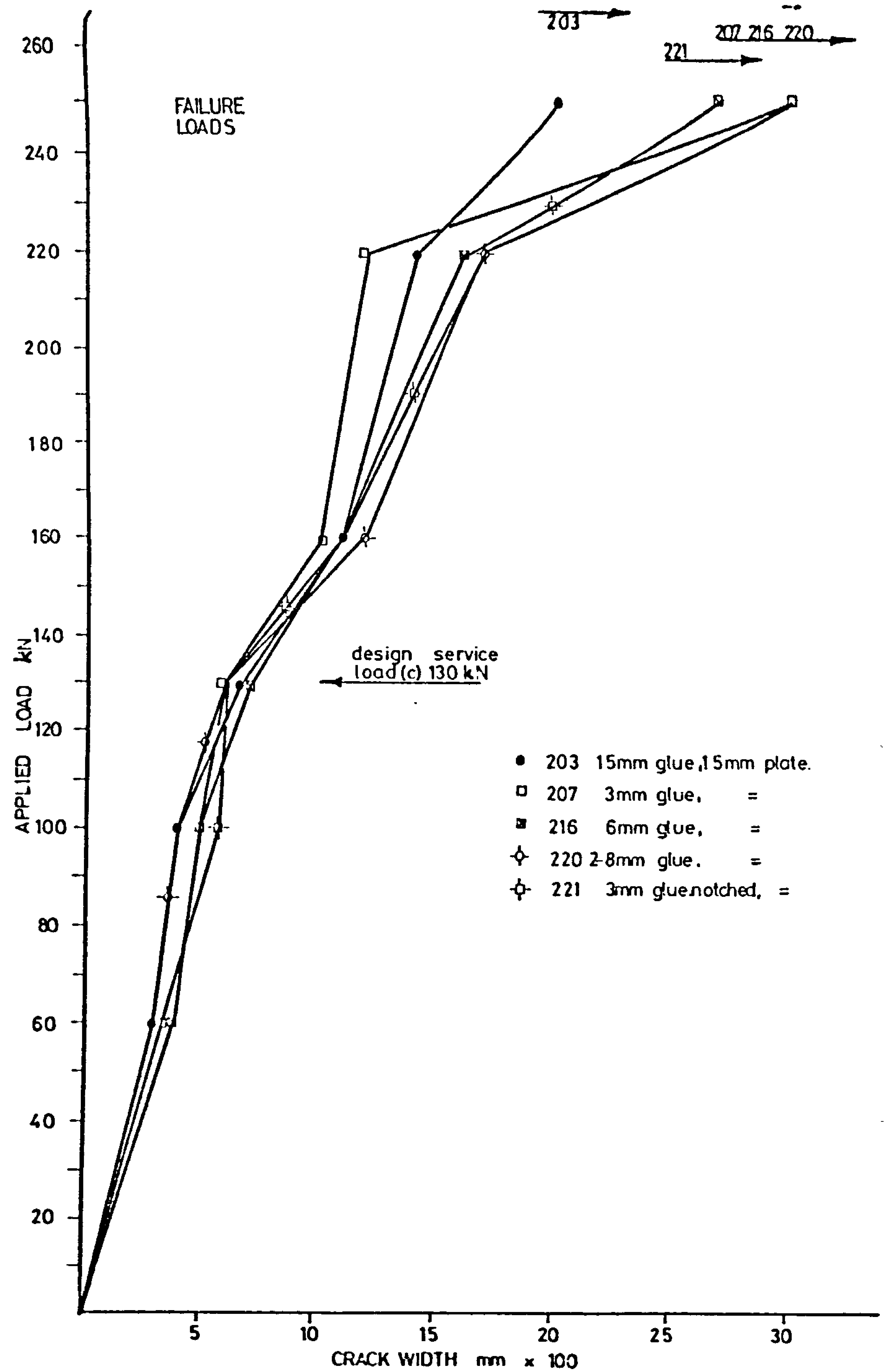

FIGURE 7·14 MAXIMUM CRACK WIDTH V APPLIED LOAD

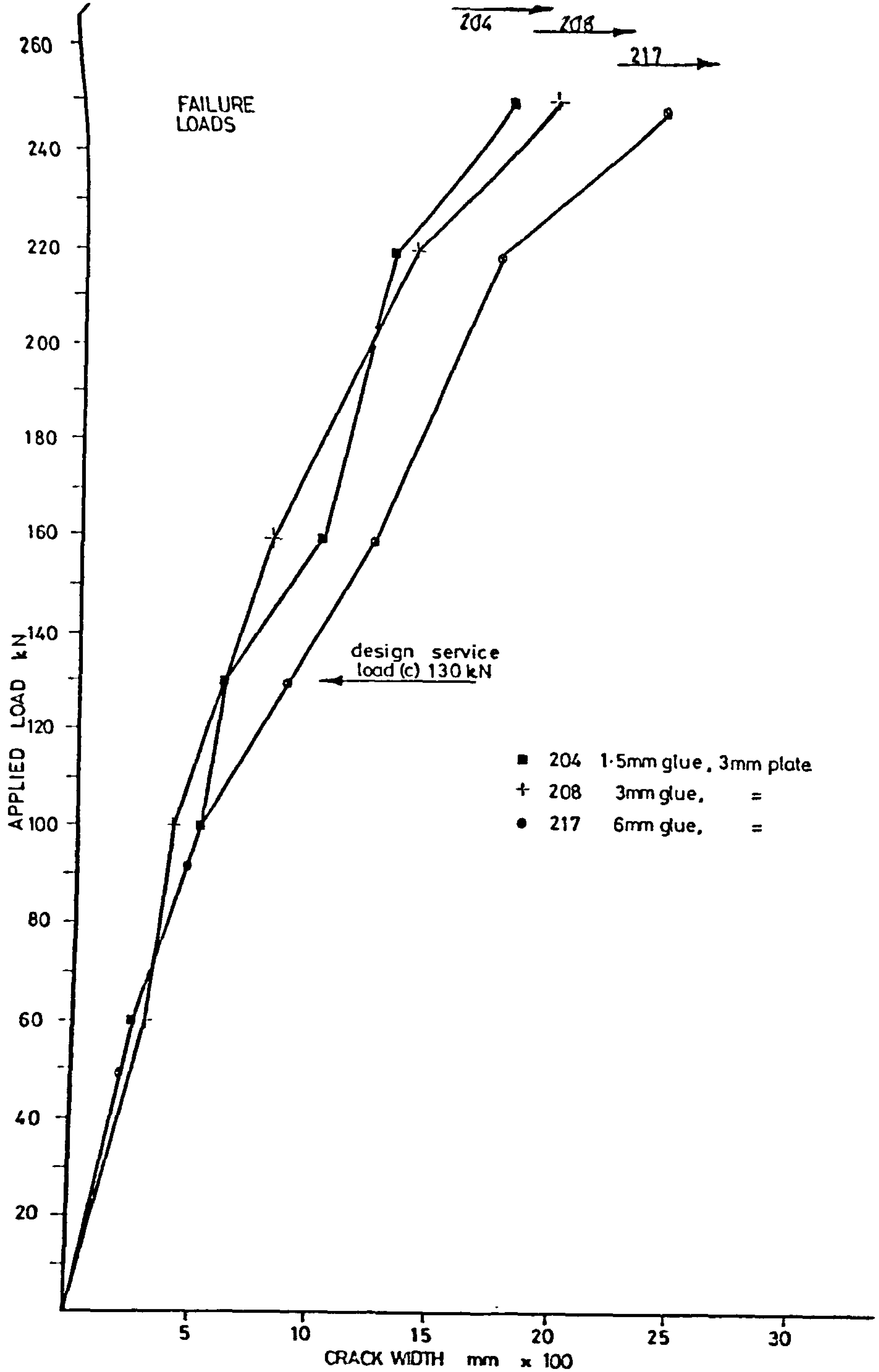

FIGURE 7·15 MAXIMUM CRACK WIDTH V. APPLIED LOAD

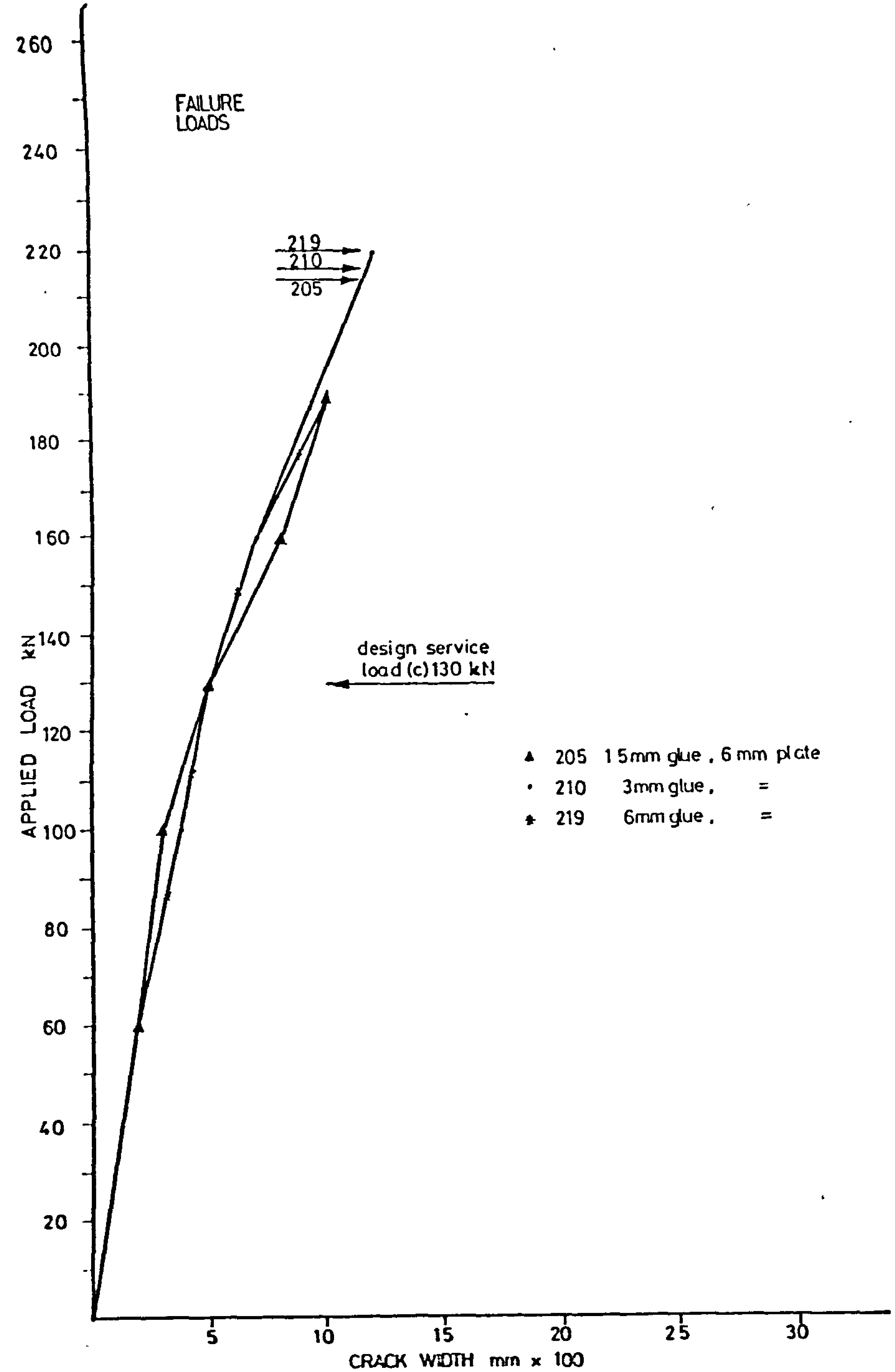

FIGURE 7·16 MAXIMUM CRACK WIDTH V. APPLIED LOAD

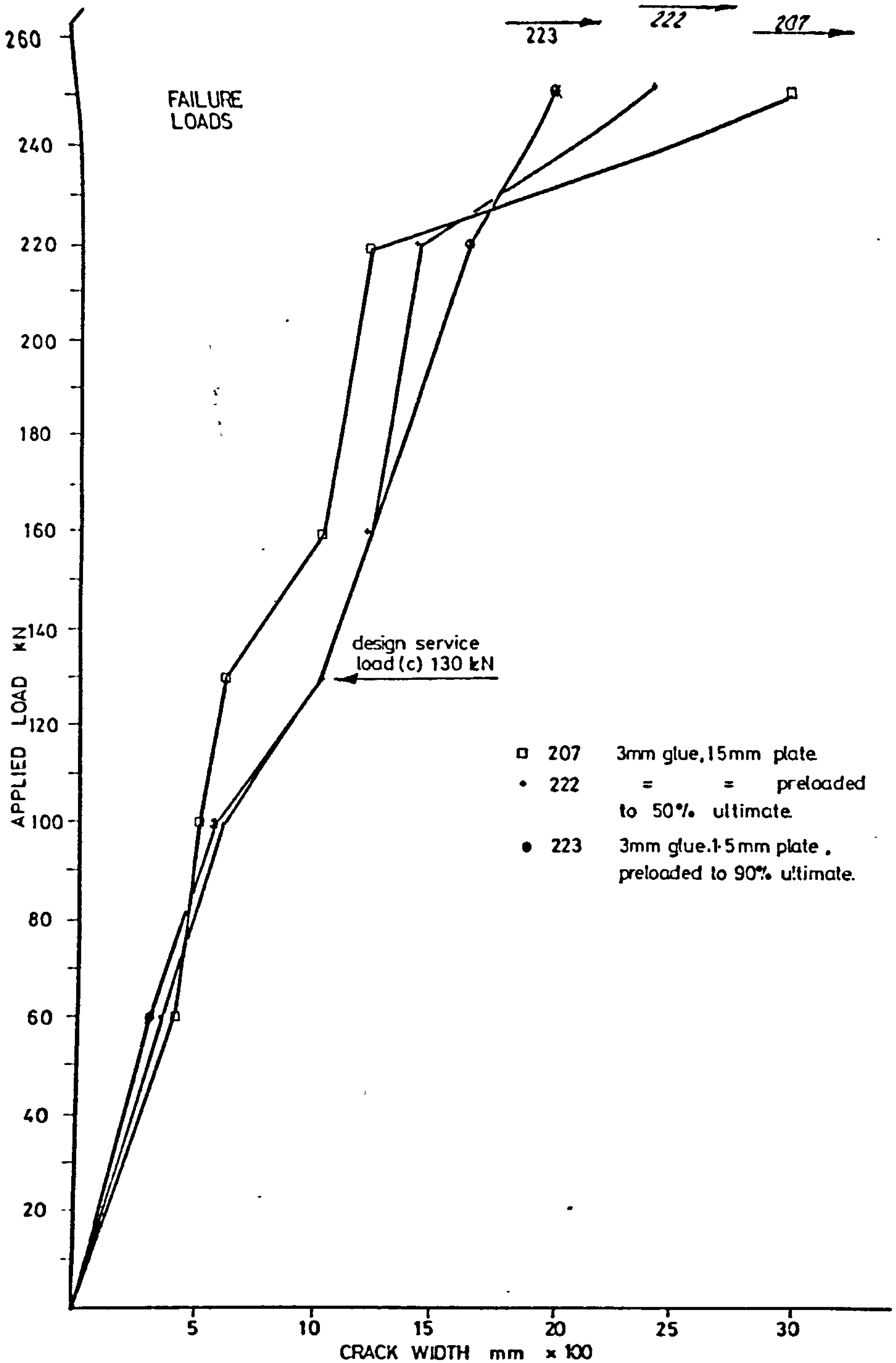

FIGURE 7·17 MAXIMUM CRACK WIDTH V. APPLIED LOAD

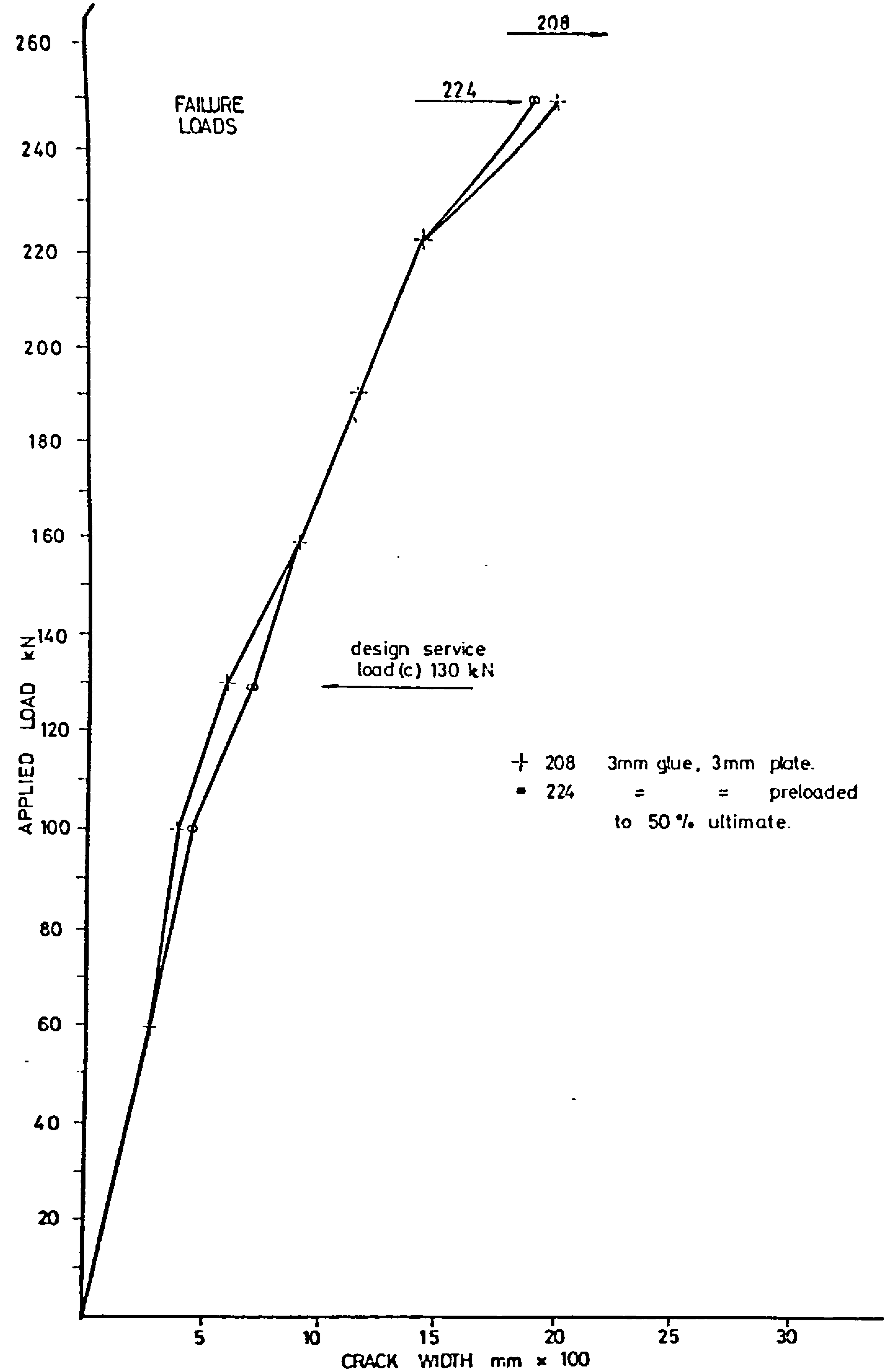

FIGURE 7·18 MAXIMUM CRACK WIDTH V APPLIED LOAD plates had maximum crack widths 83-100% of the unplated beam while the precracked beam with 3 mm plate had 58% of the crack width of the unplated beam. In general, the maximum crack width of the precracked beams was greater than for similar beams which had not been precracked.

The variation of mean crack width with glue and plate thickness is shown diagrammatically in Fig. 7.19. In general, there is an increase in crack width for a decrease in plate thickness and for an increase in glue thickness, the latter having the lesser effect.

7.4.3 Crack Width Prediction Formulae

The crack widths were calculated, as outlined in Appendix 8, for all beams with a single layer of plate which had not been precracked. The experimental and theoretical crack widths are shown in Table 7.7. The CP 110 and ACI methods greatly overestimated the crack widths for the plated beams. This is further evidence that the bonded plates reduce crack widths considerably. It is apparent that good composite action is being achieved and that the presence of the bonded plate at the concrete tensile surface is having a restraining effect on the increase of crack width.

Modifications were made to the two methods by factoring the equations to produce the best agreement with experimental results. This produces equations in which the crack width is dependent on the plate thickness, in addition to the other variables applicable to normally reinforced concrete beams.

In Fig. 7.20, the coefficient, C_1, by which $a_{cr} \cdot \varepsilon_m$ must be multiplied for each test beam, in order to produce the experimental crack width, was plotted against the plate thickness. The best fit line produces the modified CP 110 formula:

$$W_{cr} = (2 \cdot 0 + 0 \cdot 1\ t_p)\ a_{cr} \cdot \varepsilon_m$$

As shown in Table 7.7 this formula, which is derived from experimental results, gave ratios of theoretical to experimental crack widths varying from 0·90 to 1·09.

The ACI formula was treated in a similar manner. The coefficient C_2, required to produce the experimental crack width is plotted against plate thickness

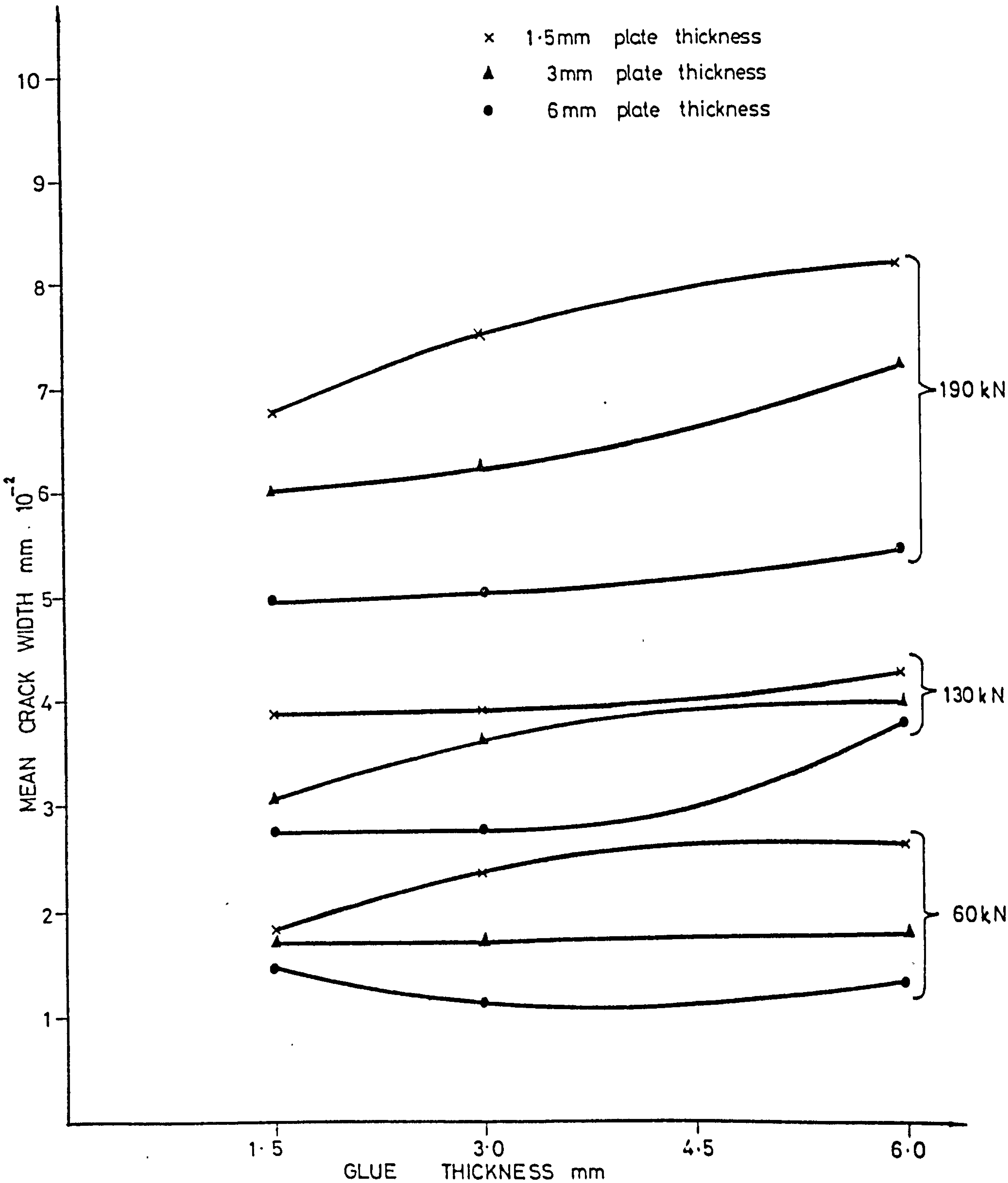

FIGURE 7·19 MEAN CRACK WIDTH V PLATE & GLUE THICKNESS

TABLE 7·7 CRACK WIDTHS AT 130kN LOAD

BEAM NUMBER	1 EXPERIMENT WIDTH mm 10^{-2}	C.P 110 THEORY mm 10^{-2}	A.C.I. THEORY mm 10^{-2}	2 C.P 110 CORRECTED mm 10^{-2}	3 A.C.I. CORRECTED mm 10^{-2}	$\frac{2}{1}$	$\frac{3}{1}$	GLUE THICKNESS mm	PLATE THICKNESS mm
201	12·0	10·0	10·5	–	–	–	–	–	–
203	6·5	8·8	9·3	6·3	6·4	0·97	0·98	1·5	1·5
204	6·0	7·4	7·6	5·7	5·9	0·95	0·98	1·5	3·0
205	5·0	5·6	5·4	4·9	5·0	0·98	1·00	1·5	6·0
207	6·0	8·8	9·3	6·3	6·4	1·05	1·07	3·0	1·5
208	6·0	7·4	7·6	5·7	5·9	0·95	0·98	3·0	3·0
209	4·5	5·6	5·4	4·9	5·0	1·09	1·11	3·0	6·0
210	5·0	5·6	5·4	4·9	5·0	0·98	1·00	3·0	6·0
216	7·0	8·8	9·3	6·3	6·4	0·90	0·91	6·0	1·5
217	6·0	7·4	7·6	5·7	5·9	0·95	0·98	6·0	3·0
218	5·0	5·6	5·4	4·9	5·0	0·98	1·00	6·0	6·0
219	5·0	5·6	5·4	4·9	5·0	0·98	1·00	6·0	6·0
220	6·0	8·8	9·3	6·3	6·4	1·05	1·07	3·0 – 8·0	1·5
221	6·0	8·8	9·3	6·3	6·4	1·05	1·07	3·0	1·5

TABLE 7·8 RATIO OF MAXIMUM TO MEAN CRACK WIDTH

	Hognestad. (94)	Broms. (93)	Base et al. (91)	Borges. (95)	Illston. (90)	Clark (96)	Present investigations
RATIO	1·50	1·66	2·00	1·72 or 1·66*	2·00	1·64	1·78 or 2·25*
RANGE	1·03 – 210	1·20 – 2·40	–	–	1·50 – 2·88	1·18 – 2·77	1·50 – 2·20

* PROBABILISTIC VALUES

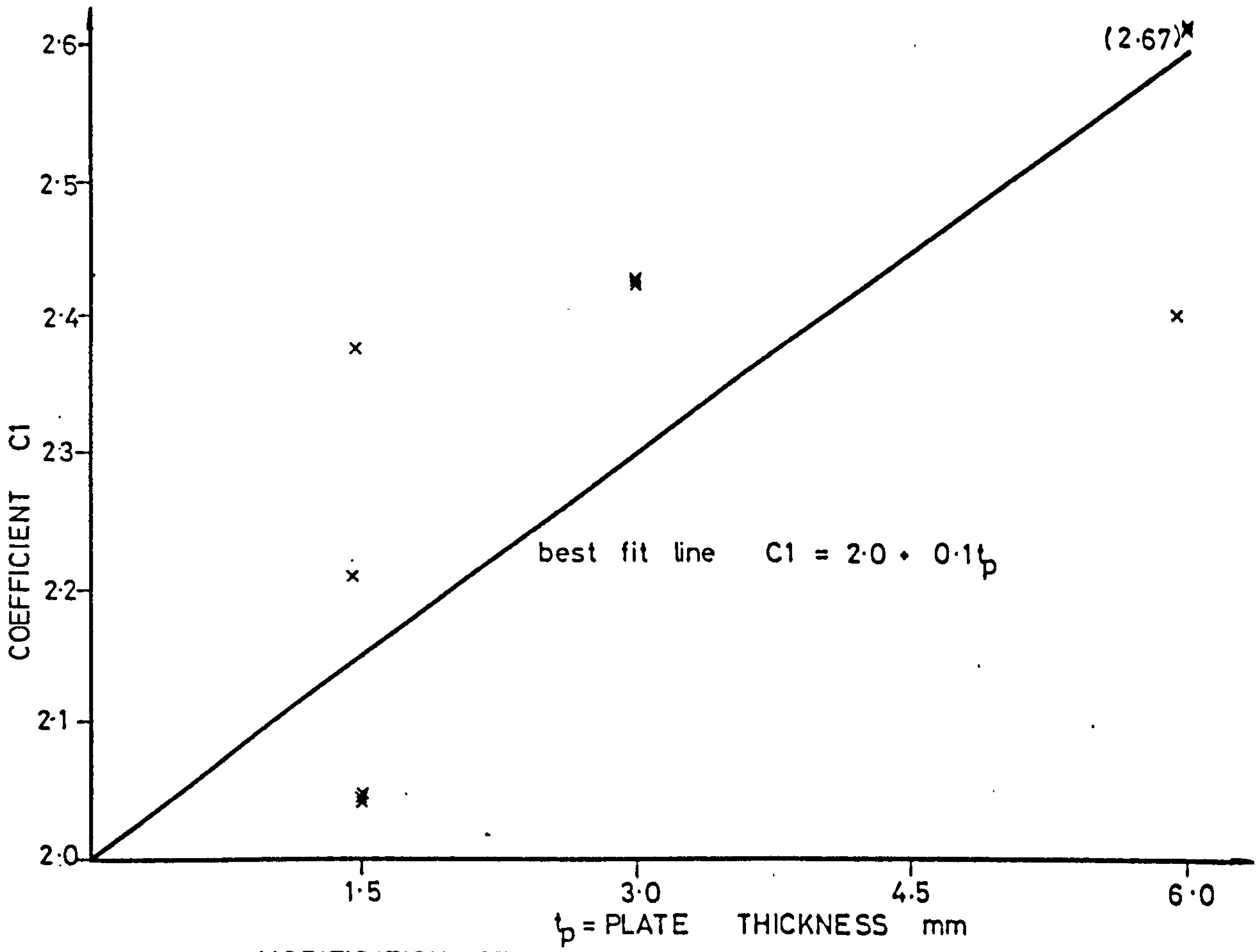

FIGURE 7·20 MODIFICATION OF CP 110 CRACK WIDTH FORMULA

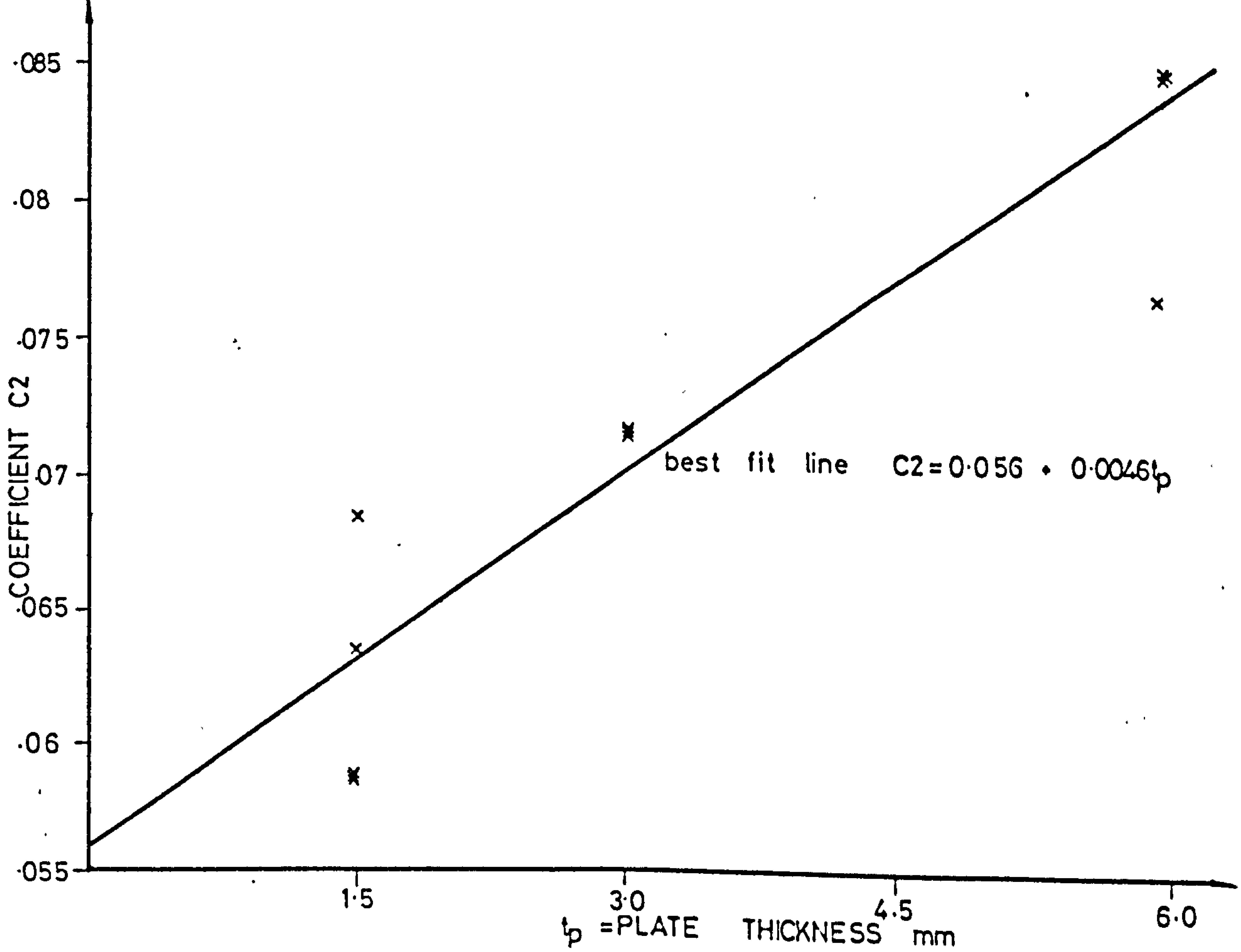

FIGURE 7·21 MODIFICATION OF ACI CRACK WIDTH FORMULA as shown in Fig. 7.23. The best fit line produces the modified ACI formula:

$$W_{max} = \frac{(0{\cdot}056 + 0{\cdot}0046\ t_p)\sqrt[3]{ts.A}\ (fs - 5).\ 10^{-3}}{1 + ts/h_1}$$

As shown in Table 7.7 this formula, derived from experimental results, gives ratios of theoretical to experimental crack widths varying from 0·91 to 1·11.

7.4.4 Relationship between Maximum and Average Crack Width

Different values of the ratio of maximum to average crack width have been suggested by many authors, as shown in Table 7.8. In Fig. 7.22 the slopes of the mean crack width against concrete strain are plotted against the slopes of their standard deviations against concrete strain (Figs. 7.1 to 7.3). The best fit line, forced through the origin is given by:

$$\frac{\sigma}{\varepsilon} = 0{\cdot}5\,\frac{W}{\varepsilon}$$

If a one percent chance of a certain crack width being exceeded is chosen, the maximum crack width is given by:

$$W_{max} = W_{mean} + 2{\cdot}5.(\text{Standard Deviation}) \qquad (\text{Appendix 9})$$

It should be mentioned here that the average coefficient of variation $\left(\frac{\sigma}{W_{mean}}\right)$, calculated at the reinforcement level at each load stage from Tables 7.1 to 7.6 (108 results) was 0·46 which is in good agreement with the value from Fig. 7.22. These values are a little higher than those found by Base et al (91) 42% and by Borges (95) 40%. It is thought that the random nature of cracking and the effects of experimental error in the techniques of crack measurement may account for this. The resulting relationship between maximum and average crack widths is given by:

$$W_{max} = W_{mean} + 2{\cdot}5\ (0{\cdot}5.W_{mean})$$

or $$\underline{W_{max} = 2.25\ W_{mean}}$$

The average ratio of maximum crack width to average crack width found in the tests was 1·78, ranging from 1·5 to 2·2. These are from 108 sets of readings as given in Tables 7·1 to 7·6. Both the range and the mean are in good agreement with the values found by others as shown in Table 7.8.

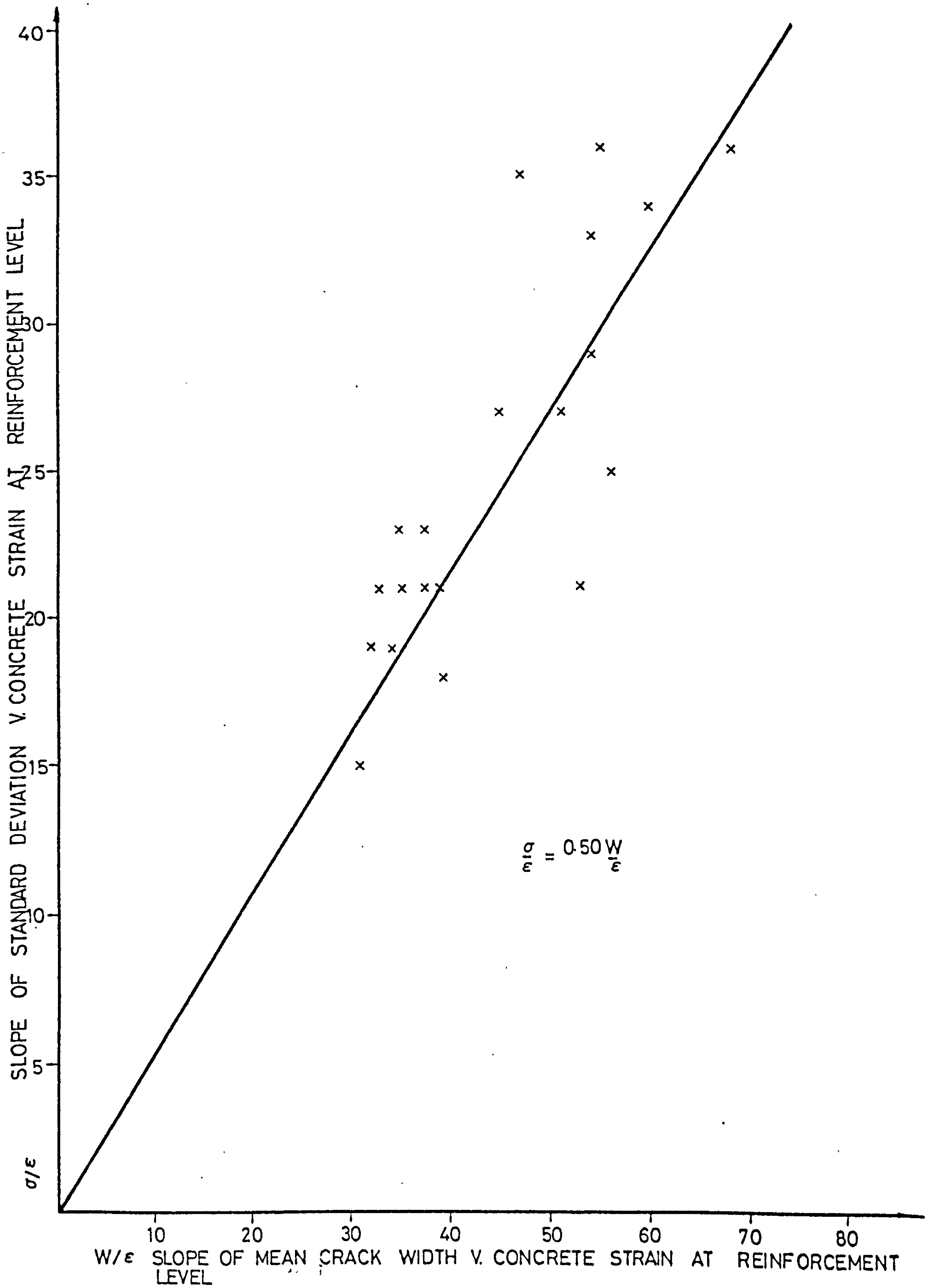

FIGURE 7·22 SLOPE OF STANDARD DEVIATION V. CONCRETE STRAIN
V.
SLOPE OF MEAN CRACK WIDTH V. CONCRETE STRAIN

From Figs. 7.4 and 7.5 the following relationship was found:

$$W_{mean} = [(47{\cdot}2 - 1{\cdot}55\ t_g)t_p + 34{\cdot}3\ t_g + 210].\varepsilon_m.10^{-1}$$

Using the probabilistic value of $W_{max} = 2{\cdot}25\ W_{mean}$ the maximum crack width which has only a 1% chance of being exceeded can be computed from:

$$W_{max} = 2{\cdot}25.\varepsilon_m\ [(47{\cdot}2 - 1{\cdot}55\ t_g)t_p + 34{\cdot}3\ t_g + 210].10^{-1}$$

Using the calculated values of ε_m, (CP 110 assumptions, Appendix 8) for the plated beams, the values of W_{max} were calculated from the above formula. In Fig. 7.23 these are plotted against the measured maximum crack widths. In no case did the experimental value exceed the predicted value, which in theory has only a 1% chance of being exceeded.

It should be emphasised that this formula is only valid within the limitations of the present test series and further tests would be required to check its validity for other plated beams.

7.4.5 Concrete Surface Strain

The concrete in the tension zone of a flexural member contributes to its stiffness. Therefore, the concrete strain is less than the value calculated on the basis of zero tensile strength in the concrete. Various expressions have been proposed, by many authors, to account for the reduction of the calculated value of strain, by allowing for the tension stiffening effect of the tensile concrete. Two are given below:

$$\varepsilon_m = \varepsilon_1 - \frac{1{\cdot}2\ b_t\ h\ (a^1 - x)\ .10^{-3}}{A_s\ (h - x)\ f_y} \qquad \text{CP 110 (86)}$$

$$\varepsilon_m = \varepsilon_1 - \frac{4{\cdot}5.\ b\ (h - x)}{A_s}\ 10^{-6} \qquad \text{Beeby (92)}$$

ε_m - concrete surface strain

ε_1 - value calculated on basis of zero tensile strength in concrete.

When calculating these values of ε_m the combined centroid position for bars and plate must be used. The values of steel area are for both steel and plate. Table 7.9 shows the average strain, at the level of intonal reinforcement for the beams, from three sources:

(a) experimental values

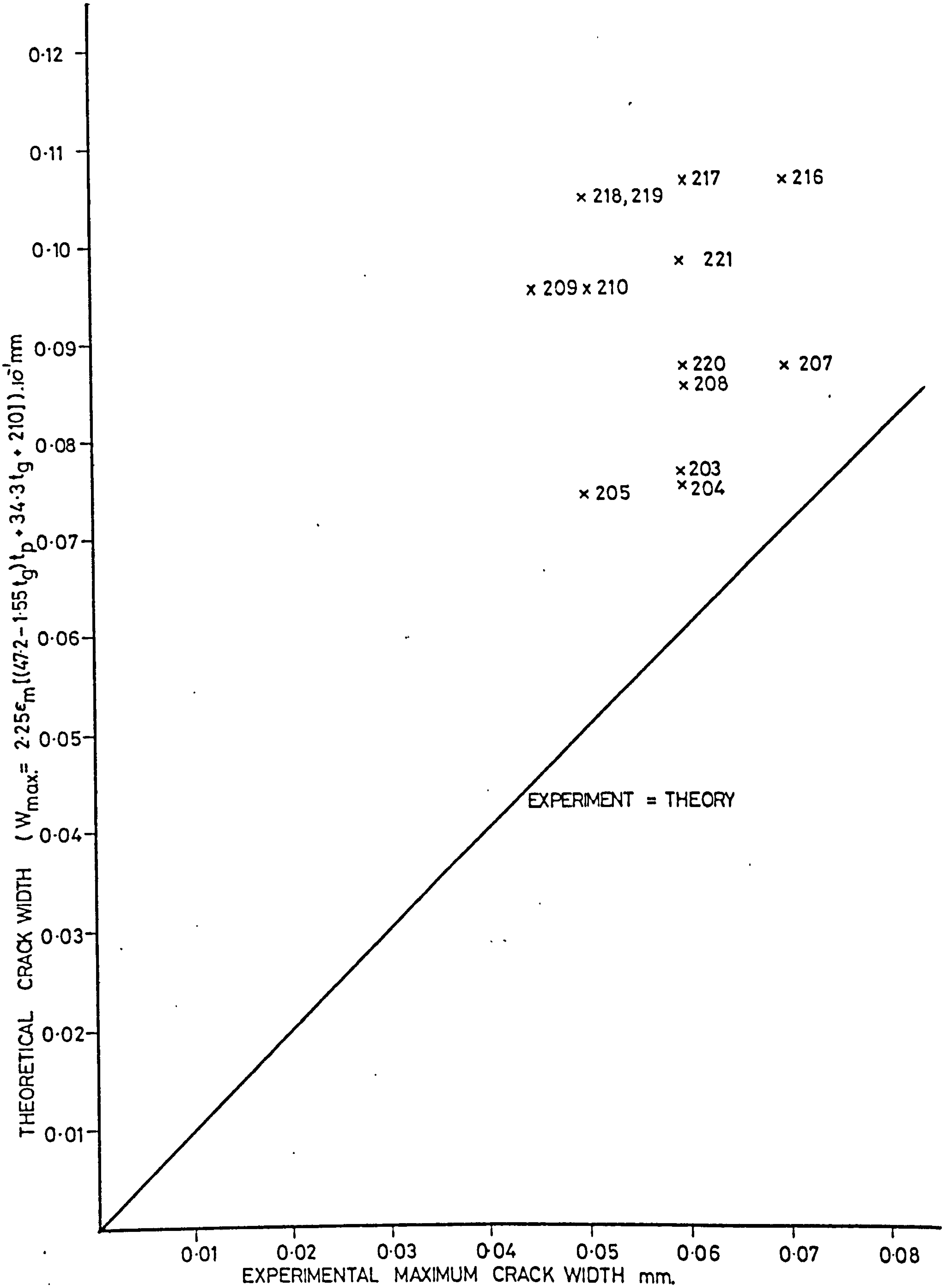

FIGURE 7·23 THEORETICAL V. EXPERIMENTAL MAXIMUM CRACK WIDTH

TABLE 7·9 COMPARISON OF MEASURED AND CALCULATED VALUES OF CONCRETE SURFACE STRAIN AT THE LEVEL OF THE INTERAL REINFORCING BARS.

BEAM NUMBERS		203, 207, 211, 212, 216, 220, 221.	204, 206, 213, 214, 215, 217	205, 209, 210, 218, 219
PLATE THICKNESS		1·5	3·0	6·0
MEASURED STRAINS 10^{-6}	MEAN	1170	841	624
	RANGE	960 - 1260	670 - 1000	580 - 780
VALUES FROM CP110 EQUATION 10^{-6}		1130	946	725
VALUES FROM BEEBY EQUATION 10^{-6}		1130	960	751
RATIO $\frac{\text{EXPERIMENTAL}}{\text{THEORETICAL}}$	CP110	1·04	0·89	0·86
	BEEBY	1·04	0·87	0·83

TABLE 7·10 MEASURED AND CALCULATED VALUES OF THE DIFFERENCE BETWEEN THE INTERNAL BAR STRAIN AND THE CONCRETE SURFACE STRAIN AT THE SAME LEVEL.

BEAM NUMBERS	203, 207, 211, 212, 216, 220, 221	204, 206, 213, 214, 215, 217	205, 209, 210, 218, 219
PLATE THICKNESS	1·5	3·0	6·0
MEAN MEASURED DIFFERENCE 10^{-6}	96	134	148
MEAN DIFFERENCE FROM FIGURES 10^{-6}	85	120	140
CP110 - $\frac{1{\cdot}2\, bh\,(d'-x).10^{-3}}{A_s f_y\ (h-x)}$	86	80	69
BEEBY - $\frac{4{\cdot}5\, b\,(h-x).10^{-6}}{A_s}$	80	65	43
PRESENT INVESTIGATION $(2{\cdot}3+2{\cdot}22\, t_p)\ \frac{b\,(h-x)}{A_s}\, 10^{-6}$	100	129	149

(b) CP 110 equation

(c) Beeby's equation.

For plate thicknesses of 1·5 mm, 3 mm and 6 mm the number of beams used to find the mean experimental readings were 7, 6 and 5 respectively. These values and the range for each plate thickness are given in Table 7.9. The ratio of experimental to theoretical values was 1·04 (1·5 mm plate) for both CP 110 and Beeby's equation. For 3 mm and 6 mm plate thicknesses the agreement between experiment and theory was not so good. In order to improve the prediction equations Figs. 7.24 7.25 and 7.26 were plotted. These show the calculated steel stress, on the basis of zero tensile strength in the concrete, plotted against the measured value of concrete strain at the reinforcement level.

As shown in Appendix 8, at service load beams with 1·5 mm plate have a steel stress of 230 N/mm^2. Similarly, beams with 3 mm and 6 mm plates, at service load, have steel stresses of 195 and 150 N/mm^2 respectively. Calculations for steel stresses were also made at 60 kN and 190 kN loads. These values are then plotted against the experimental value of concrete strain, for each beam, at the level of the internal reinforcement.

Best fit lines were plotted by linear regression and all the experimental points fell within ±15% for beams strengthened with 1·5 mm thick plate, +28 and -30% for beams with 3 mm thick plate and +35 and -19% for beams with 6 mm thick plates.

Since crack widths are usually checked at working load conditions the difference between the actual measured strain and the strain in the steel at the same stress, calculated from the steel's elastic stress/strain relationship was found. A comparison similar to that in Table 7.9 is shown in Table 7.10. The differences from Figs. 7.24 to 7.26 are compared with the values from measured readings and the two theoretical methods given below.

(a) $$\frac{1{\cdot}2\ 6{+}h\ (a^1 - x).\ 10^{-3}}{A_s\ (h - x)\ f_y}$$

(b) $$4{\cdot}5\ \frac{b\ (h - x)}{A_s}.\ 10^{-6}$$

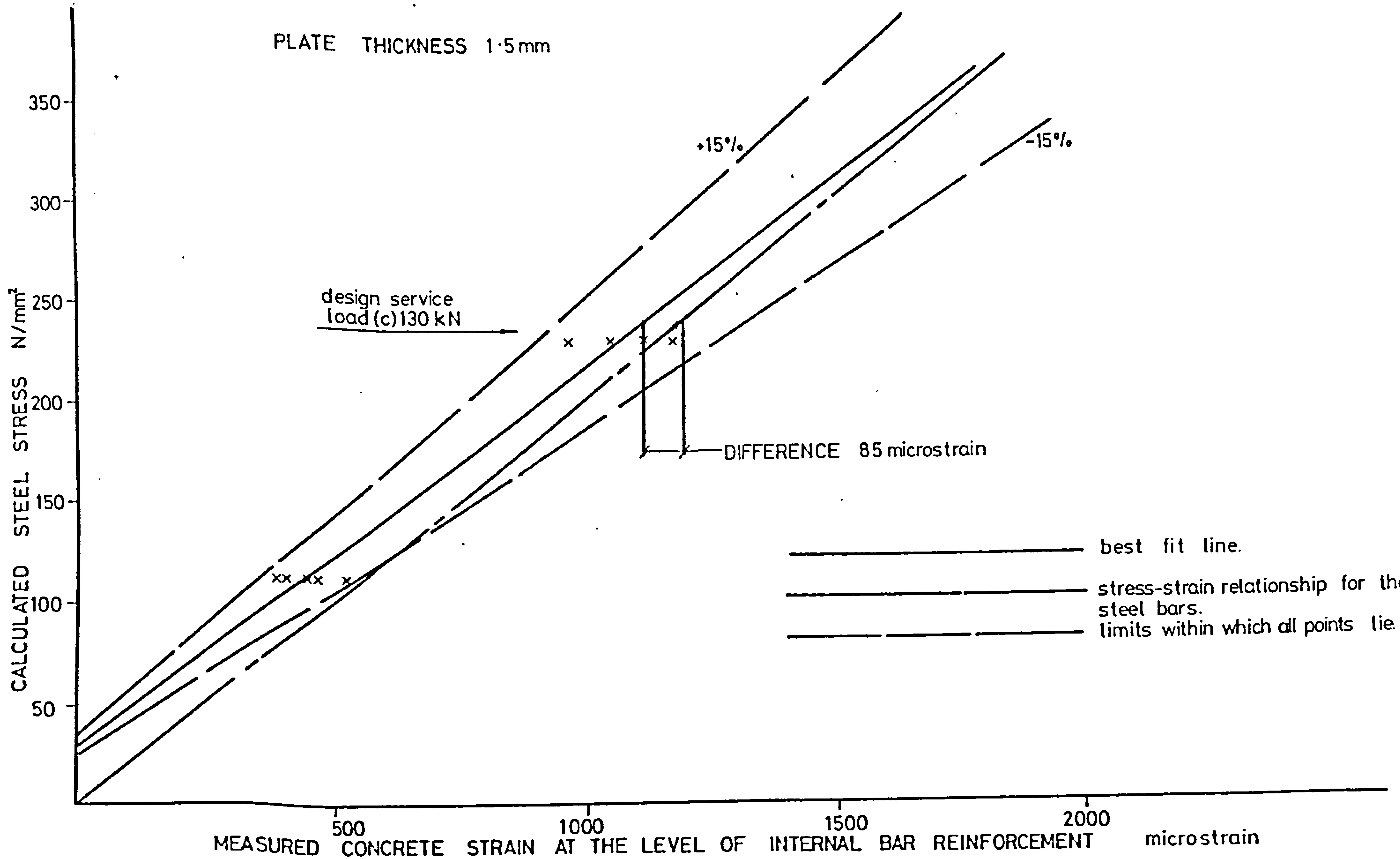

FIGURE 7·24 CALCULATED STEEL STRESS V MEASURED CONCRETE STRAIN

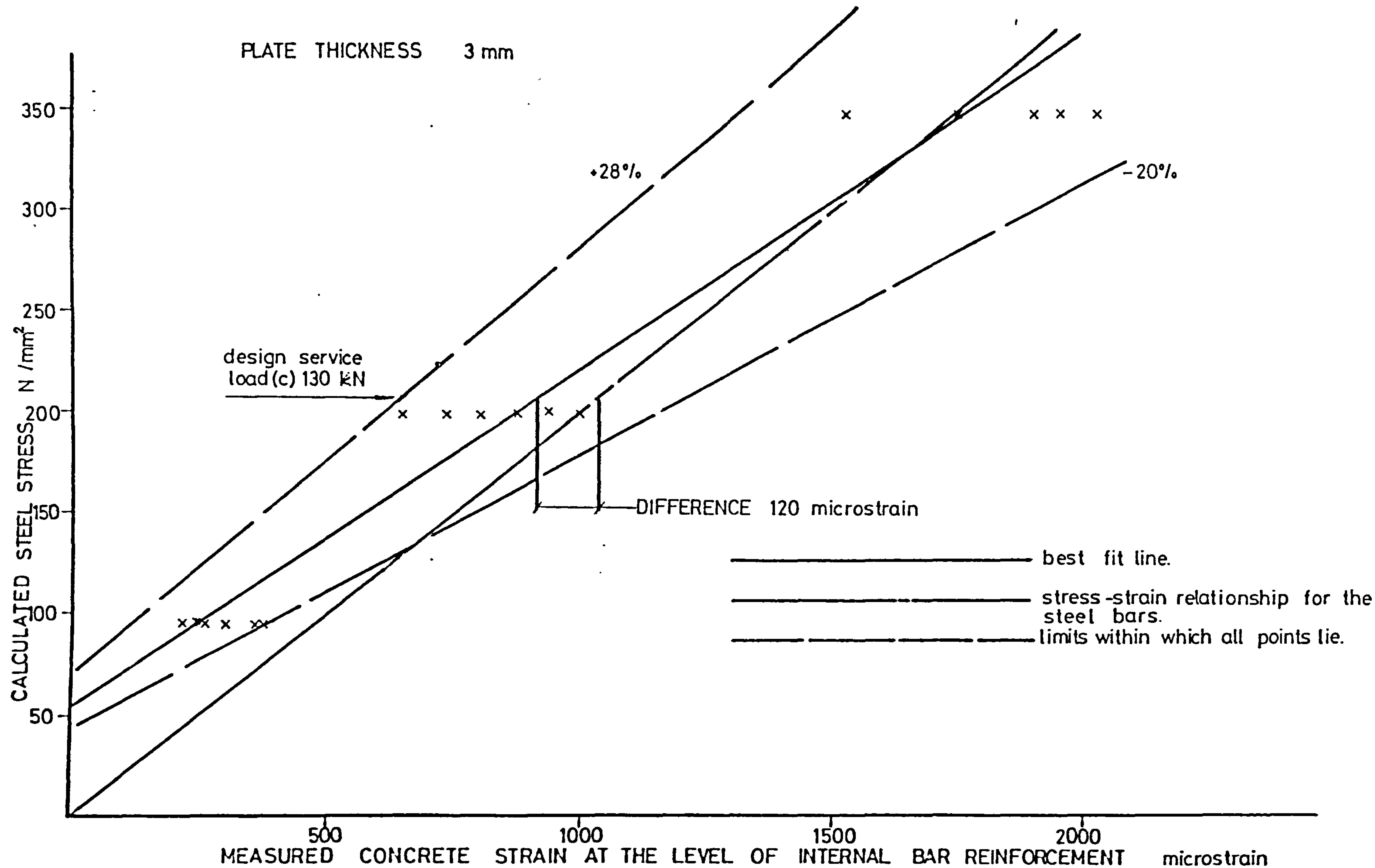

FIGURE 7·25 CALCULATED STEEL STRESS V. MEASURED CONCRETE STRAIN

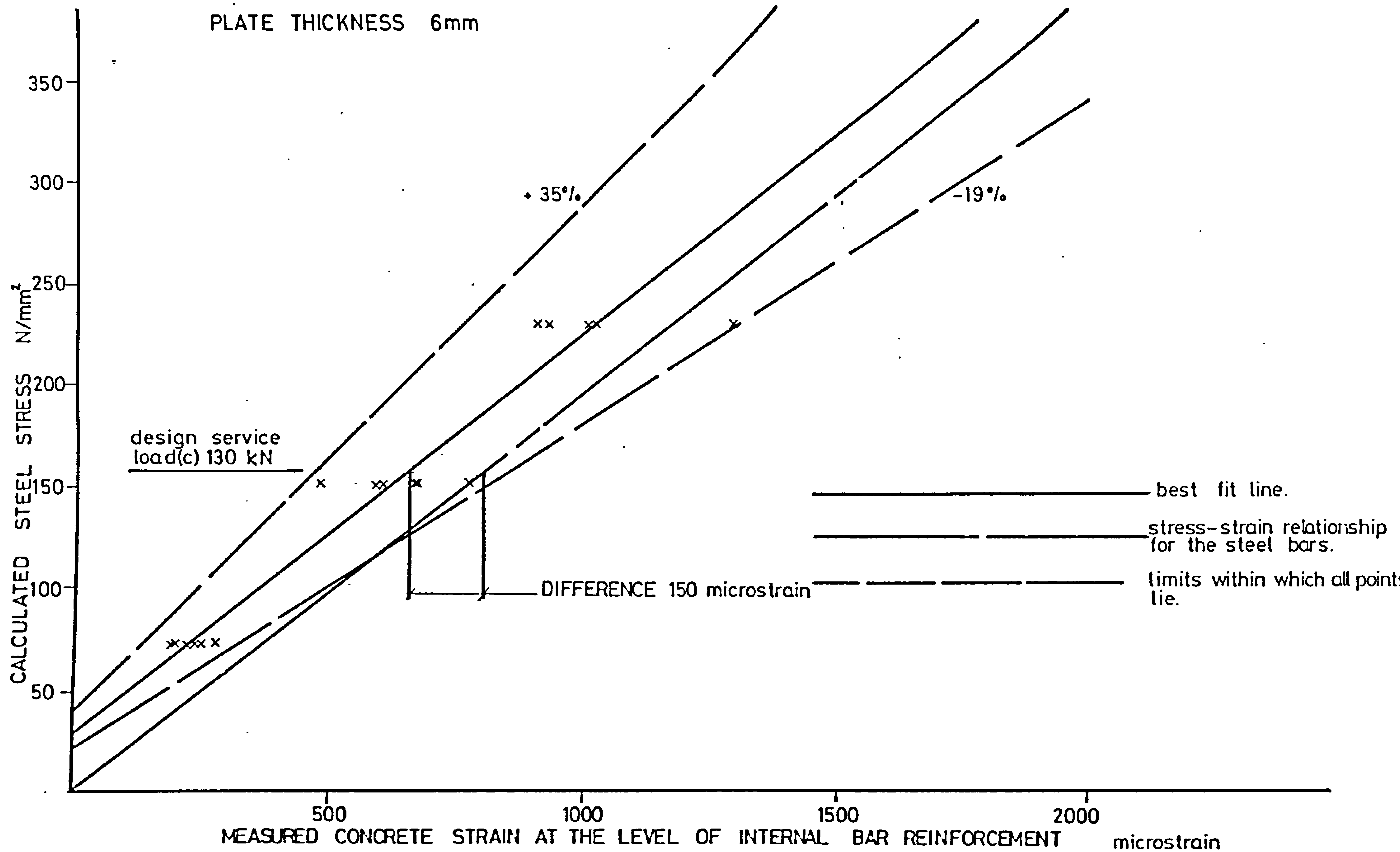

FIGURE 7·26 CALCULATED STEEL STRESS V. MEASURED CONCRETE STRAIN

The measured values are the difference between the mean steel strain, from Table 6.2 (c) and the mean concrete strain at the reinforcement level from Tables 7.1 to 7.6. The values for 1·5 mm plate gave good agreement but 3 mm and 6 mm plates gave progressively worse agreement.

The modified formula: $\varepsilon_m = \varepsilon_1 - (2{\cdot}22\ t_p + 2{\cdot}30)\ \frac{b(h - x).10^{-6}}{As}$ was found to give good agreement as shown in Table 7.10.

It should be noted that in calculations for ε_m, the centroid of both plate and bars was found and then the neutral axis position. The value of h is taken as the depth of the beam i.e. 255 mm. In Fig. 7.27 the method of derivation of the above formula is shown. The coefficient, C_3, required to multiply Beeby's expression $\frac{b(h - x).10^{-6}}{As}$ to produce the measured value was plotted against plate thickness. The best fit line was then plotted by linear regression.

7.4.6 Stresses Carried by Concrete in the Tension Zone

It is generally accepted that concrete in a tension or flexural member adds considerably to its stiffness through the tension zone. Yu and Winter (76) were the first researchers who took into account the contribution of the concrete in tension to the stiffness of a member. However, they did not give any numerical value for the effective tensile stress of the concrete to be used for this contribution. In 1972 Beeby (97) found that stresses in the concrete, for members subjected to pure tension and reinforced with deformed bars, remain approximately constant at about 1·0 N/mm^2. The results for specimens reinforced with plain bars were considerably lower.

A series of sustained loading tests on reinforced concrete beams was described by Stevens (80), in which the major factors affecting the development of deflection were varied. He found that there was no consistent difference between beams reinforced with round or deformed bars; and that varying the cover from 25 mm to 50 mm gave no consistent difference either. An expression was proposed for the average tensile force, T, in the concrete after cracking.

$T = 3/16\ b.\ h.\ f_{rm}$ $\quad f_{rm}$ = strength in bending.

CP 110 recommends that the curvature of any section may be calculated by assuming that the stress distribution in the concrete is triangular, having a value of

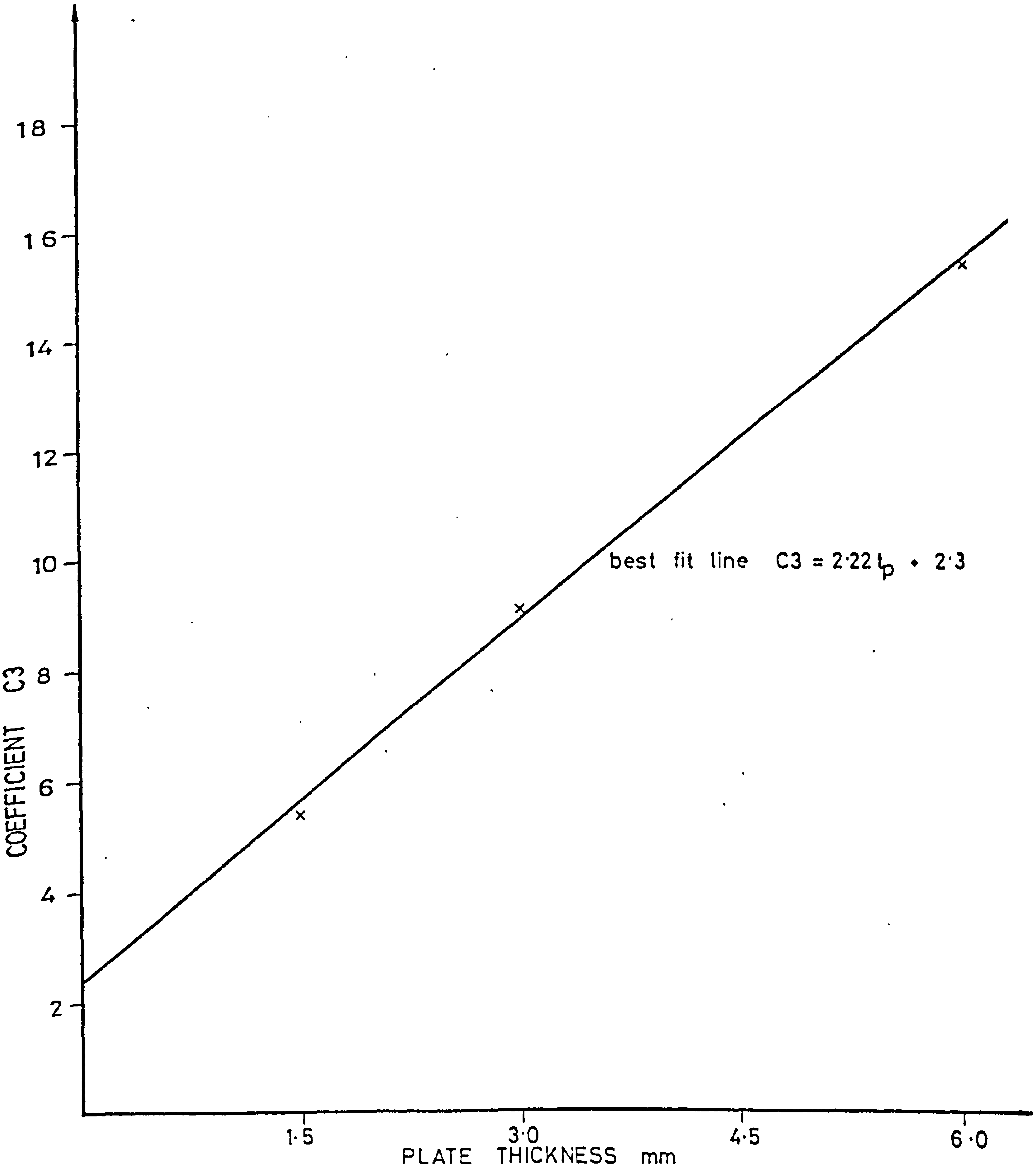

FIGURE 7·27 MODIFICATION TO BEEBY'S FORMULA zero at the neutral axis and $1{\cdot}0\ N/mm^2$ at the reinforcement level.

Fig. 7.28 shows the stress distribution in the plated beams at service load. The concrete is assumed to be elastic up to a compression of 1000 micro-strain.

Taking moments of the tension steel about the centroid of the compression block: $M_{TS} = f_s . A_s . (d - \frac{x}{3})$, but, as shown in Fig. 7.28, the steel is composed of bars and plates and d is the distance from the compression face to their combined centroid.

Hence $\quad M_{TS} = (f_b . A_b + f_p A_p)\ (d - \frac{x}{3})$

The difference between the applied moment M_a and M_{TS} is thefefore the contribution of the concrete in the tension zone, M_c.

But $\quad M_c = \sigma_f\ (\frac{h - x}{3}) .\ b.\ h.$

$$\text{or} \quad \sigma f = \frac{3M_c}{b.h.\ (h - x)}$$

where σ_f = the tensile stress in the concrete at the tension face. The calculated values are given in Table 7.11. Since the beams were loaded incrementally, three values for each beam in the elastic range of both steel and concrete are given. These values did not show any significant change with increasing load and the average values were found for each beam. In Table 7.11, the strains given for the bars and plates are obtained from Figs. 6.2 to 6.21 and the neutral axis positions are from demec readings at 100 KN, plus the values given in Tables 6.1 (b) (60 kN) and 6.2 (c) (130 kN). The average values of tensile stress for each glue and plate thickness are shown in Table 7.12. The mean tensile stress in the concrete was then plotted against the plate thickness for each glue thickness, as shown in Fig. 7.29. Best fit lines were plotted and the combined equation, allowing for a linear change in tensile concrete stress with glue thickness was given by:

$$\sigma_f = (0.81 - 0{\cdot}058\ t_g)\ tp + 0{\cdot}59\ t_g + 0{\cdot}36.$$

The values found from this expression are given in Table 7.13 for comparison with Table 7.12.

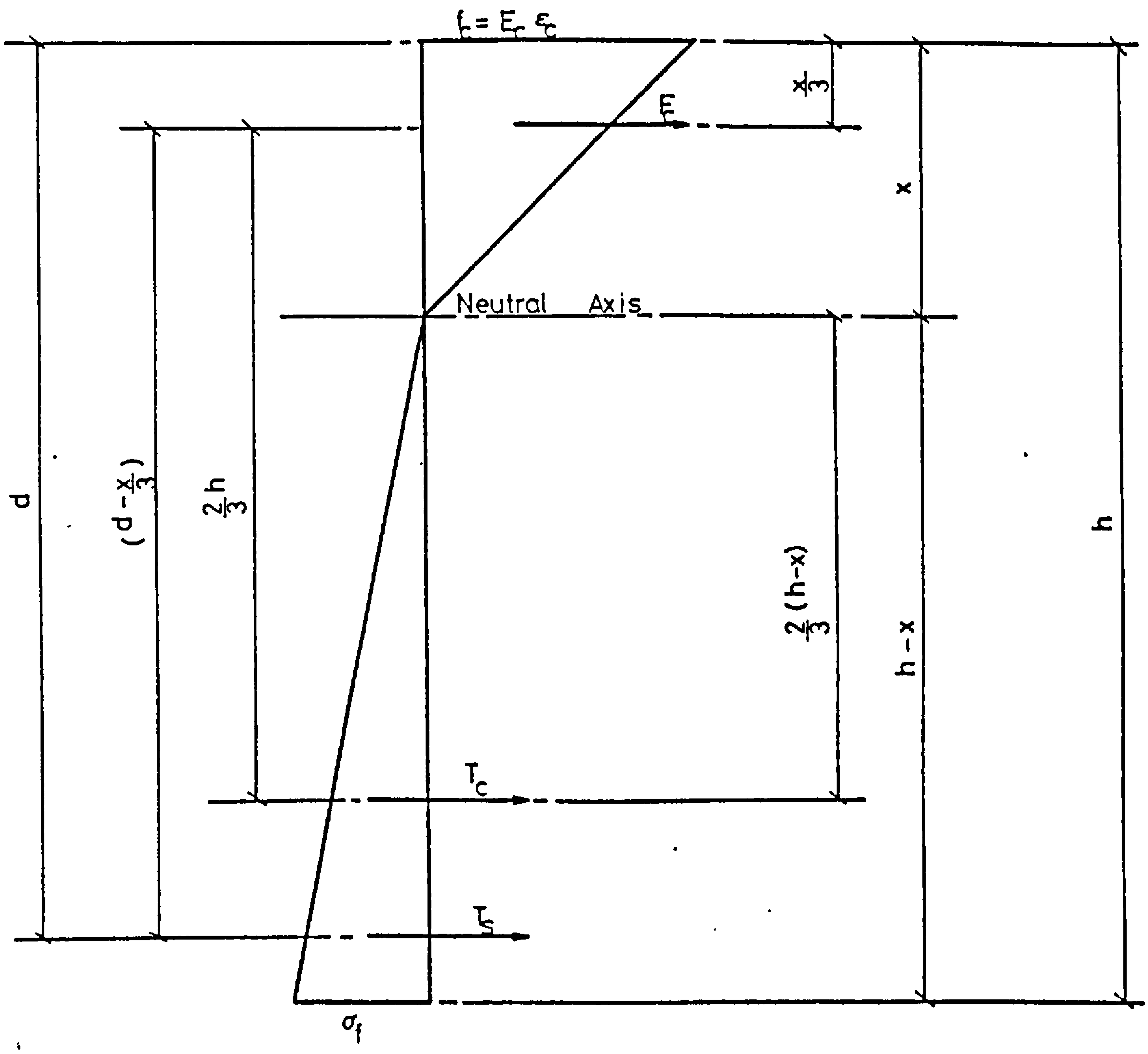

FORCES

$F_c = b.f_c\frac{x}{2}$ compressive force in the concrete above the neutral axis.

$T_c = \sigma_f.b(\frac{h-x}{2})$ tensile = = = = below = = =

$T_s = (f_p A_p + f_r A_r)$ tensile = = = steel plate and bars.

SYMBOLS

d combined centroid of steel bars and plate.

subscript p denotes plate
= r = bars

x neutral axis depth found from the measured strain distribution in the concrete.

h overall beam depth.

FIGURE 7·28 STRESS DISTRIBUTION IN PLATED BEAMS AT SERVICE LOAD.

TABLE 7·11 TENSILE STRESS IN THE CONCRETE

BEAM NUMBER	60kN BAR STRAIN 10^{-6}	60kN PLATE STRAIN 10^{-6}	100 kN BAR STRAIN 10^{-6}	100 kN PLATE STRAIN 10^{-6}	130 kN BAR STRAIN 10^{-6}	130 kN PLATE STRAIN 10^{-6}	DEPTH TO CENTROID OF BARS + PLATES mm	60 NEUTRAL AXIS DEPTH mm	100 NEUTRAL AXIS DEPTH mm	130 NEUTRAL AXIS DEPTH mm	AREA OF STEEL BARS mm^2	AREA OF STEEL PLATE mm^2	MOMENT OF THE TENSION STEEL ABOUT THE CENTROID OF COMPRESSION 60 KNm	100 KNm	130 KNm	TENSILE STRESS IN THE CONCRETE AT THE EXTREME FIBRE 60 N/mm^2	100 N/mm^2	130 N/mm^2
201	550	0	1030	0	1350	0	220	100	96	88	943	0	19·4	36·5	48·5	1·8	0·9	0·8
202	550	0	960	0	1320	0	220	108	96	85	943	0	19·1	34·0	44·7	2·0	2·1	1·0
203	440	500	780	900	1100	1280	226	108	102	95	943	187	19·3	34·7	49·0	2·0	1·7	0·6
204	260	400	500	830	770	1200	231	118	114	110	943	375	15·1	302	45·7	4·4	4·4	2·3
205	180	185	500	450	530	650	238	123	119	115	943	750	122	321	39·4	6·2	3·5	5·7
206	260	185	400	450	740	700	231	123	119	115	943	375	12·0	28·3	37·0	6·3	5·6	7·1
207	440	500	800	900	1100	1280	226	112	106	100	943	187	19·2	35·2	49·0	2·0	1·6	0·6
208	320	370	560	750	740	1080	231	118	114	110	943	375	16·8	31·2	42·9	4·2	3·8	3·7
209	180	220	330	480	500	700	238	118	114	110	943	750	13·3	26·9	40·1	6·1	6·1	5·2
210	180	200	370	480	490	680	238	123	119	115	943	750	12·6	28·1	38·8	6·0	5·7	6·1
211	430	465	750	850	1000	1250	226	118	111	105	943	187	18·4	32·7	45·0	3·3	3·0	2·5
212	430	600	750	1050	1020	1550	226	114	108	102	943	187	19·5	34·3	48·1	2·4	2·1	1·0
213	280	300	520	600	750	930	231	130	120	115	943	375	14·1	26·6	40·7	6·7	6·6	5·0
214	280	250	520	530	760	800	231	118	114	110	943	375	13·7	26·6	39·5	6·2	6·3	5·5
215	230	250	460	550	700	900	231	123	121	120	943	375	13·6	24·4	38·1	5·4	7·9	6·7
216	350	350	600	700	950	1100	226	123	119	115	943	187	14·6	26·0	41·3	4·8	6·9	4·7
217	280	350	470	650	670	1000	231	114	110	106	943	375	15·3	26·7	39·4	5·0	6·1	5·4
218	150	230	330	460	500	660	238	123	121	120	943	750	12·4	259	38·3	6·1	7·0	6·6
219	150	265	300	520	460	750	238	128	124	120	943	750	13·3	26·5	39·4	5·8	6·8	6·0
220	380	400	700	780	1000	1180	226	99	97	95	943	187	16·7	31·2	45·2	3·1	3·4	2·3
221	380	400	700	780	1000	1250	226	108	103	98	943	187	16·5	30·9	45·5	4·2	3·7	2·2
222	350	350	600	660	830	950	226	108	104	100	943	187	15·0	26·4	37·0	4·1	6·0	7·4
223	350	270	650	560	950	750	226	100	100	100	943	187	14·7	27·7	40·0	4·1	5·2	4·9
224	230	270	430	500	650	750	231	123	116	110	943	375	12·1	22·8	34·8	6·3	8·5	8·0

TABLE 7·12 MEAN VALUES OF TENSILE STRESS IN THE CONCRETE FROM TABLE 7·11

glue thickness \ plate thickness	1·5	3·0	6·0
1·5	1·4	3·7	5·1
3·0	2·4	5·7	5·9
6·0	4·2	5·5	6·4

TABLE 7·13 TENSILE STRESS IN THE CONCRETE FROM THE DERIVED EQUATION $\sigma_f = (0{\cdot}81 - 0{\cdot}058\,t_g)t_p + 0{\cdot}59\,t_g + 0{\cdot}36$

glue thickness \ plate thickness	1·5	3·0	6·0
1·5	2·3	3·4	5·6
3·0	3·1	4·4	6·0
6·0	4·6	5·3	6·7

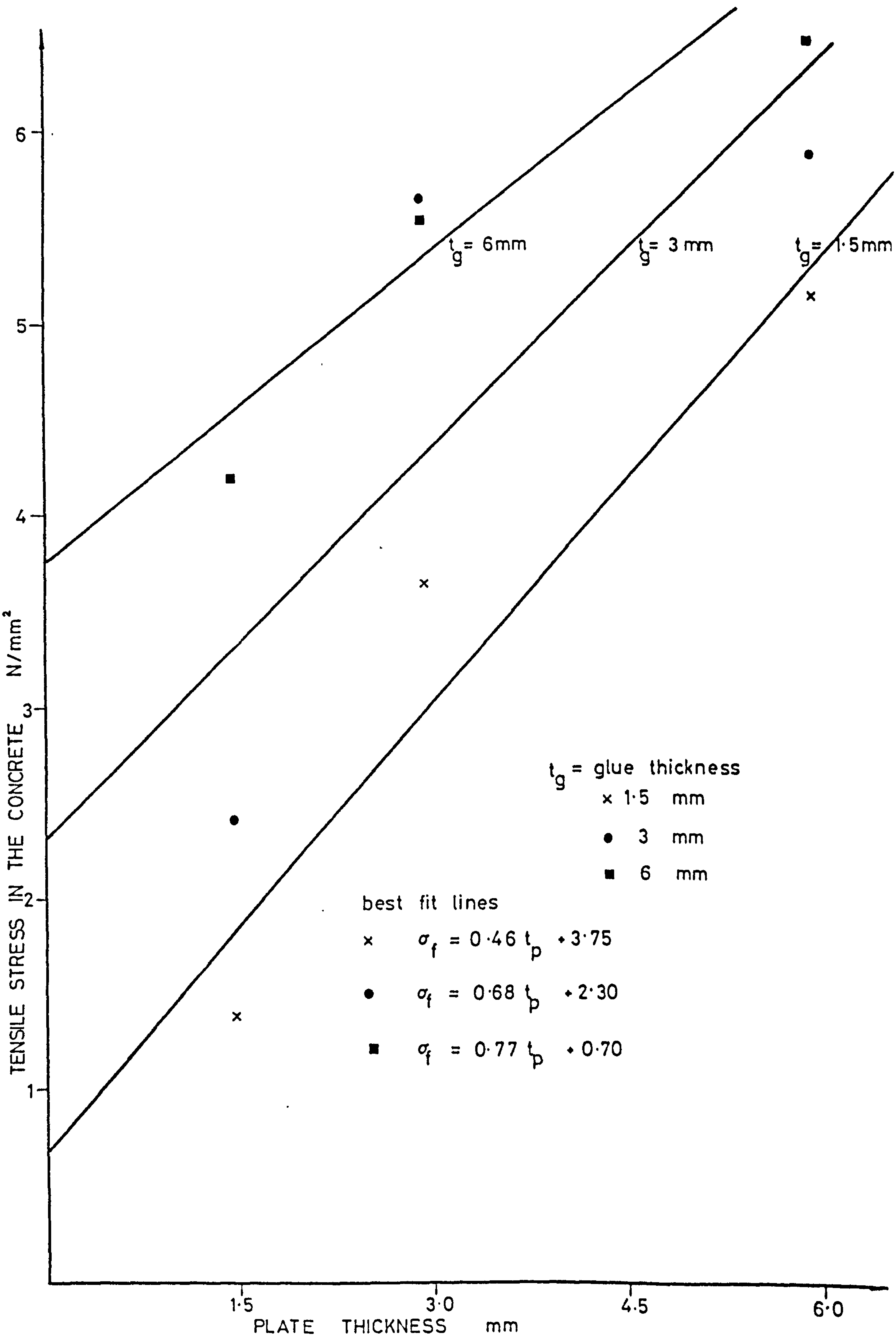

FIGURE 7·29 TENSILE STRESS IN THE CONCRETE V. PLATE THICKNESS FOR EACH GLUE THICKNESS

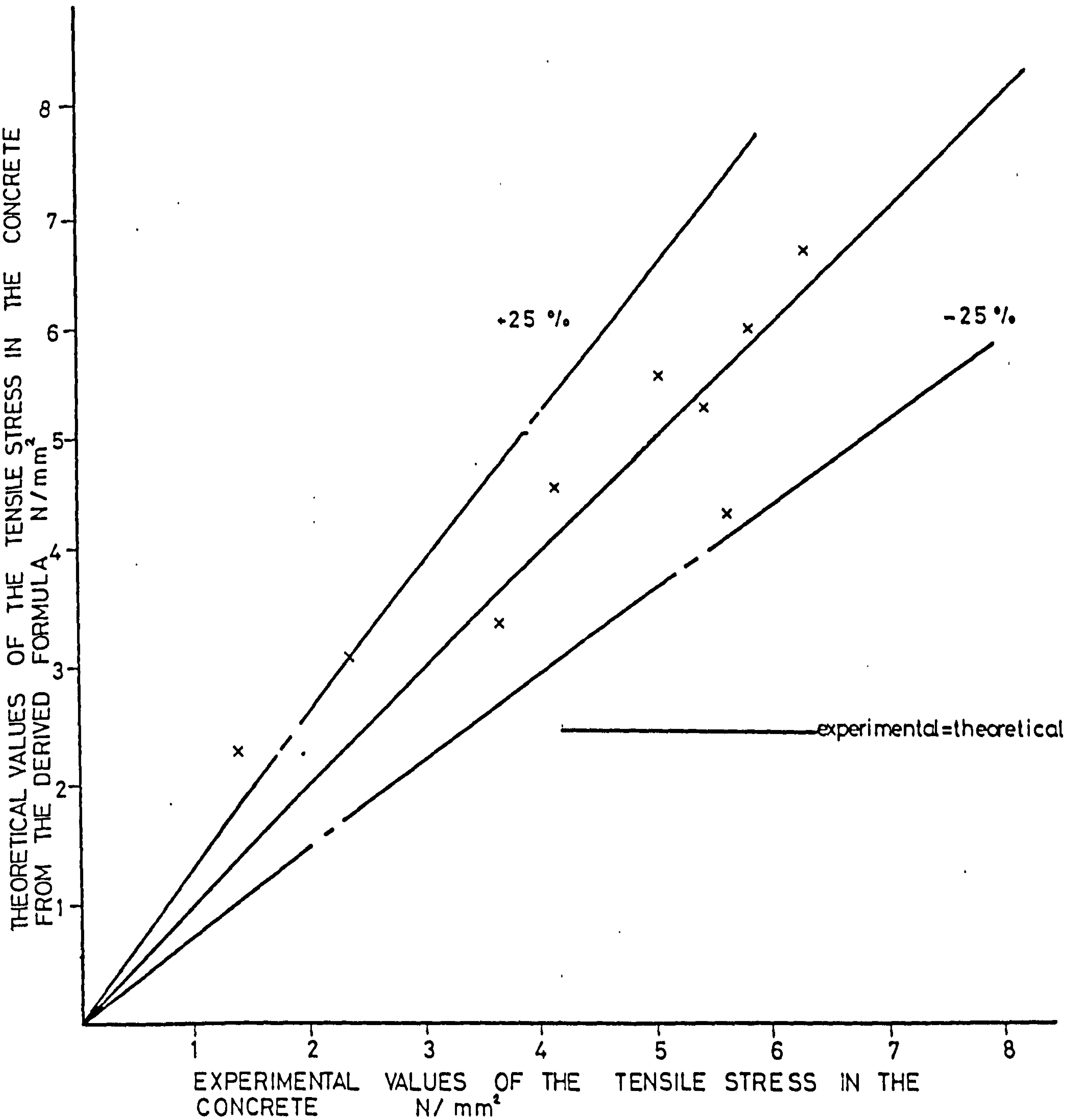

FIGURE 7·30 EXPERIMENTAL V. THEORETICAL VALUES OF THE TENSILE STRESS IN THE CONCRETE

In Fig. 7.30 the calculated values of σ_f from this formula were plotted against the experimentally determined values. All points, except one, lie within ±25%.

7.5 CONCLUSIONS

Based on the tests carried out in this investigation the following conclusions are drawn:

1. At a given steel stress and at a certain distance from a reinforcing bar, crack widths in concrete beams with externally bonded steel plates were less than those which would result in ordinary reinforced concrete beams. This allows a higher internal bar stress for a particular crack width to be developed, therefore increasing the limit state of cracking.

2. The mean crack width was found to be proportional to the steel stress and the following relationship was derived between the slope of the mean crack width v. concrete strain and the plate and glue thicknesses.

$$S = \left[(47{\cdot}2 - 1{\cdot}55\ t_g)\ t_p + 34{\cdot}3\ t_g + 210\right].\ 10^{-6}$$

3. The ultimate crack spacings were related to the plate thickness and the crack height just after first crack. The mean ultimate crack spacing was given by:

$$Su = (0{\cdot}02\ t_p + 0{\cdot}2).\ h + 0{\cdot}43\ t_p + 35{\cdot}5$$

4. The application of crack width prediction formulae recommended by Codes of Practice, for normally reinforced concrete beams, highly overestimated the crack widths for the plated beams. This shows that the presence of the bonded steel plates effectively reduces the crack widths, both by physically restraining the increase in crack width and by reducing the strain in the internal bars at any particular load, relative to an unplated beam. The CP 110 and ACI formulae were modified to satisfactorily agree with the experimental results. The resulting equations were:

$$W_{cr} = (0{\cdot}1\ t_p + 2{\cdot}0).\ a_{cr}.\ \varepsilon_m \qquad \text{(CP 110)}$$

and

$$W_{max} = \frac{(0{\cdot}056 + 0{\cdot}0046\ t_p)\sqrt[3]{ts.\ A}\ (fs - 5).\ 10^{-3}}{1 + ts/h_1} \qquad \text{(ACI)}$$

5. The relationship between maximum and average crack widths was derived statistically for the plated beams, as follows:

$$W_{max} = 2{\cdot}25\ W_{mean}$$

This compared with the experimental mean value of:

$$W_{max} = 1{\cdot}78.\ W_{mean} \qquad \text{(range 1·5 to 2·2)}$$

Both the range and mean values were in agreement with those found by other authors for normally reinforced concrete beams.

6. The application of accepted formulae for predicting concrete surface strain was found to overestimate the strains for beams strengthened with 3 mm and 6 mm thick plates. A modified formula was derived from the experimental results:

$$\varepsilon_m = \varepsilon_1 - (2{\cdot}22\ t_p + 2{\cdot}3).\ \frac{b(h - x)}{A_s}.\ 10^{-6}$$

7. The contribution of the concrete in the tension zone to the stiffness of plated beams was more than that found in the case of normally reinforced concrete beams. A formula was derived for the tensile stress in the concrete:

$$\sigma_f = (0{\cdot}81 - 0{\cdot}058\ t_g)\ t_p + 0{\cdot}59\ t_g + 0{\cdot}36$$

8. The number of cracks at the 'service load' of 130 kN is between two thirds and three quarters of those fully developed at failure. This means that the average crack spacing at service load is greater than at failure. The number of cracks at failure was generally more in the case of plated beams than for the un-plated beam.

9. It should be emphasised that the formulae derived in this section are applicable only within the limitations of the present tests. Other variables such as concrete cover and cube strength, beam size and a wider range of plate and glue thicknesses should be investigated in order to prove the validity and refine the proposed formulae.

CHAPTER 8

LONG TERM TESTING

8.1 INTRODUCTION

Concrete and epoxy resins are subject to time dependent deformations due to creep and shrinkage. Reinforced concrete elements composed of these materials are, therefore, subject to long term deformations under sustained load. These deformations may be critical to the serviceability, and sometimes to the safety of a structure. If such deformations were accompanied by a loss of cohesive and/or adhesive strength of the resin bond there could be serious results to the safety of the structure.

Highway bridges are designed for lives of 120 years, and it is necessary to have stable behaviour of the construction materials over this period. The performance of epoxy resins needs checking because experience in the aerospace industry has indicated that under unfavourable conditions the strength of bonded metal joints may be reduced drastically over periods as short as six years. Calder (62) reports some loss of bond and corrosion of the bonding surface over two years between metal/concrete bonds.

In this chapter the long term performance and durability of loaded and unloaded externally plated reinforced concrete beams, under external weathering conditions are reported.

8.2 EXPERIMENTAL PROCEDURE

The same concrete, glue and steel types which were used in the short term testing were adopted for the long term test series. The material properties were reported in Chapter 3 and the manufacture of beams was described in Chapter 5. Prisms, 100 x 100 x 500 mm, were cast for shrinkage and durability specimens. All specimens were demoulded after 24 hours and kept in the laboratory under uncontrolled conditions until they were either plated, tested or transported to their test sites.

8.3 SHRINKAGE TESTS

Three prisms were used as shrinkage specimens, these were fitted with demec points, on a 200 mm gauge length on opposite faces. Strains were read within 24 hours after demoulding and then at increasing intervals with time. At 18 months the shrinkage was 320 microstrain.

8.4 SUSTAINED LOADING/LONG TERM TESTS

8.4.1 Introduction

The details of the twenty four test beams are given in Fig. 5.2 and Table 8.1. Eight beams were subjected to sustained loading, with two unloaded beams corresponding to each loaded beam. The loaded beams were placed in rigs, as shown in Fig. 8.1, and Plate 8.1, in such a way that the maximum stress in the concrete under sustained load was approximately equal to one third of the twenty eight day cube strength. The control cubes and prisms were kept under the same conditions as the beams throughout testing. Each loading frame was designed to take two beams. The assembly and loading was performed carefully to ensure that the correct load was applied. This was checked both on a pressure gauge attached to the pump which operated the loading jack, and by checking the extensions of the Macalloy tie bars by means of a demountable mechanical extensometer of 300 mm base. All measurements of strain on the beams tension, side and compression faces were taken before and immediately after loading and thereafter at increasing intervals with time, using a demec of 200 mm gauge length. The strains in the steel plate were also measured at the centre section. Fig. 8.2 shows a typical graph of the change of maximum observed concrete compressive and steel tensile strains with time. The change in strain distribution across the beam depth is also shown. The loaded and unloaded beams were left exposed to the elements at a sewage treatment works (Plates 8.1 and 8.2).

After 18 months exposure eight of the unloaded beams were brought back for testing in the laboratory. The test rig, loading procedure, instrumentation etc. were identical to that described for the short term tests in Chapter 5, with the exception that there were no strain gauges on the internal bar reinforcement. After testing three of the eight beams it was found that there was no loss of bond due to their 18 months exposure. It was decided, therefore, to leave the remaining five beams for a longer period before testing.

TABLE 8·1 DETAILS OF LONG TERM TEST BEAMS

BEAM NUMBER	101	102	103	104	105	106	107	108	109	110	111	112
GLUE THICKNESS mm	3	6	2–8 (1)	3 (2)	3	3	3	3	3	6	2–8 (1)	3 (2)
PLATE THICKNESS mm	1·5	1·5	1·5	1·5	1·5	1·5	1·5	1·5	1·5	1·5	1·5	1·5
NUMBER OF LAYERS OF PLATE.	1	1	1	1	1	1	2	2	1	1	1	1
POSITION OF LAP JOINTS	–	–	–	–	centre	l.p.	centre	l.p.	–	–	–	–
CUBE STRENGTH AT 28 DAYS. N/mm²	66·4	63·2	68·5	65·5	76·8	76·4	65·0	77·0	70·5	69·2	78·5	73·3
CUBE STRENGTH AT PLATING N/mm²	80·0	76·6	78·3	78·3	80·3	81·7	78·3	80·6	77·8	83·0	86·0	78·4
AGE AT TESTING (3) months	18	18	30	30	30	30	30	18	60	60	60	60
CUBE STRENGTH AT TESTING N/mm²	86·3	89·0						86·6				
MODULUS OF RUPTURE AT TESTING N/mm²	5·85	5·92						5·73				
L – LOADED UL – UNLOADED	UL	UL	UL	UL	UL	UL	UL	UL	UL	UL	UL	UL

BEAM NUMBER	113	114	115	116	117	118	119	120	121	122	123	124
GLUE THICKNESS mm	3	3	3	3	3	6	2–8 (1)	3 (2)	3	3	3	3
PLATE THICKNESS mm	1·5	1·5	1·5	1·5	1·5	1·5	1·5	1·5	1·5	1·5	1·5	1·5
NUMBER OF LAYERS OF PLATE.	1	1	2	2	1	1	1	1	1	1	2	2
POSITION OF LAP JOINTS	centre	l.p.	centre	l.p.	–	–	–	–	centre	l.p.	centre	l.p.
CUBE STRENGTH AT 28 DAYS. N/mm²	73·0	74·5	72·2	80·2	80·4	71·2	81·2	80·6	69·2	79·1	79·1	81·1
CUBE STRENGTH AT PLATING N/mm²	78·4	82·2	86·4	85·3	83·2	82·2	86·8	83·4	77·7	79·4	81·5	86·9
AGE AT TESTING (3) months	60	60	60	60	60	60	60	60	60	60	60	60
CUBE STRENGTH AT TESTING N/mm²												
MODULUS OF RUPTURE AT TESTING N/mm²												
L – LOADED UL – UNLOADED	UL	UL	UL	UL	L	L	L	L	L	L	L	L

(1) glue thickness varies along the length of the beam.

(2) V notches cut in the tension face of the beam to form stress concentrations above the load load points.

(3) all beams to be tested at 30 & 60 months. by others.

All. stiffeners from 12mm thick plate.

All roller bearings 20mm diameter unless shown otherwise.

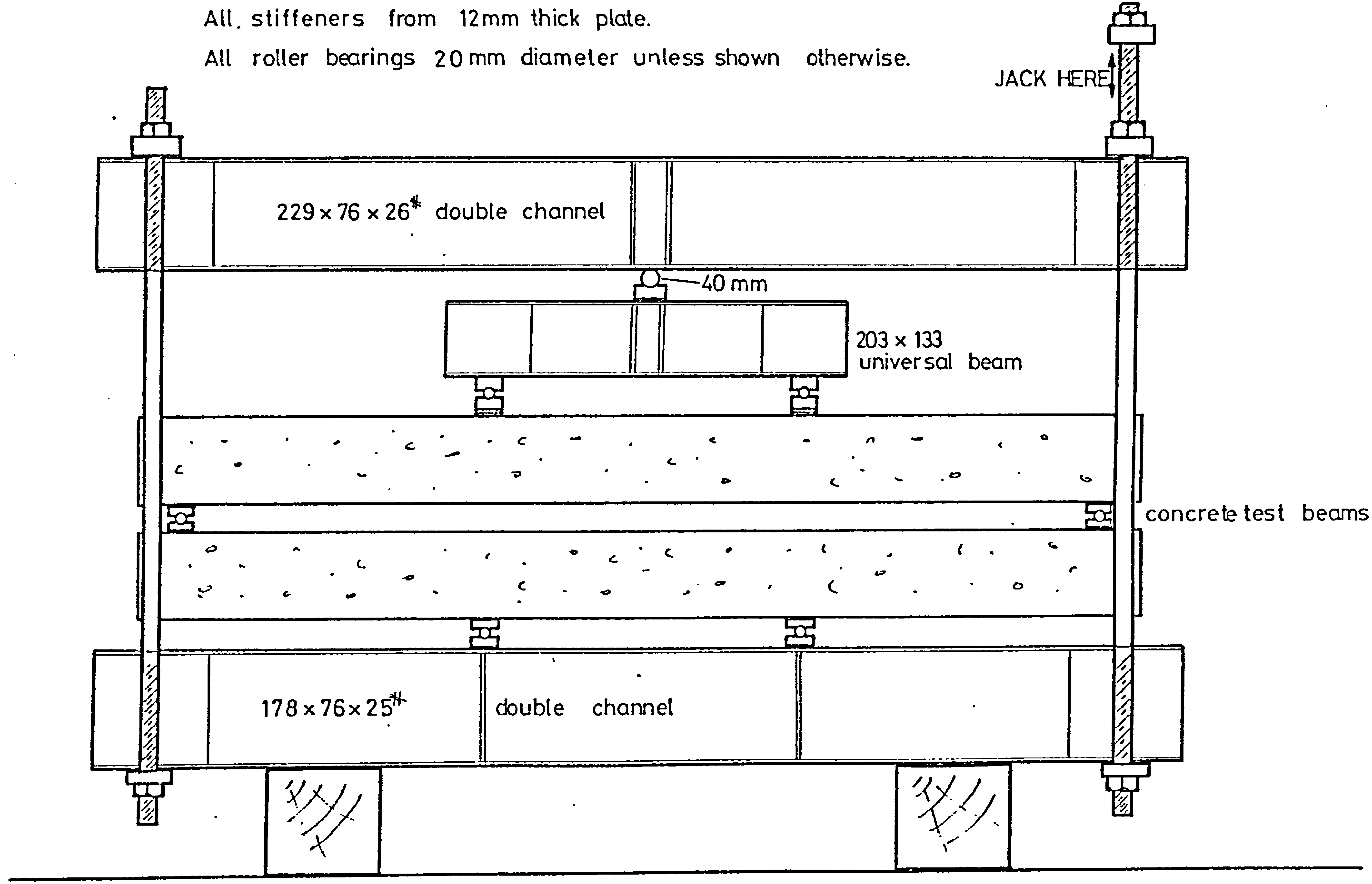

FIGURE 8·1 LONG TERM LOADING RIG

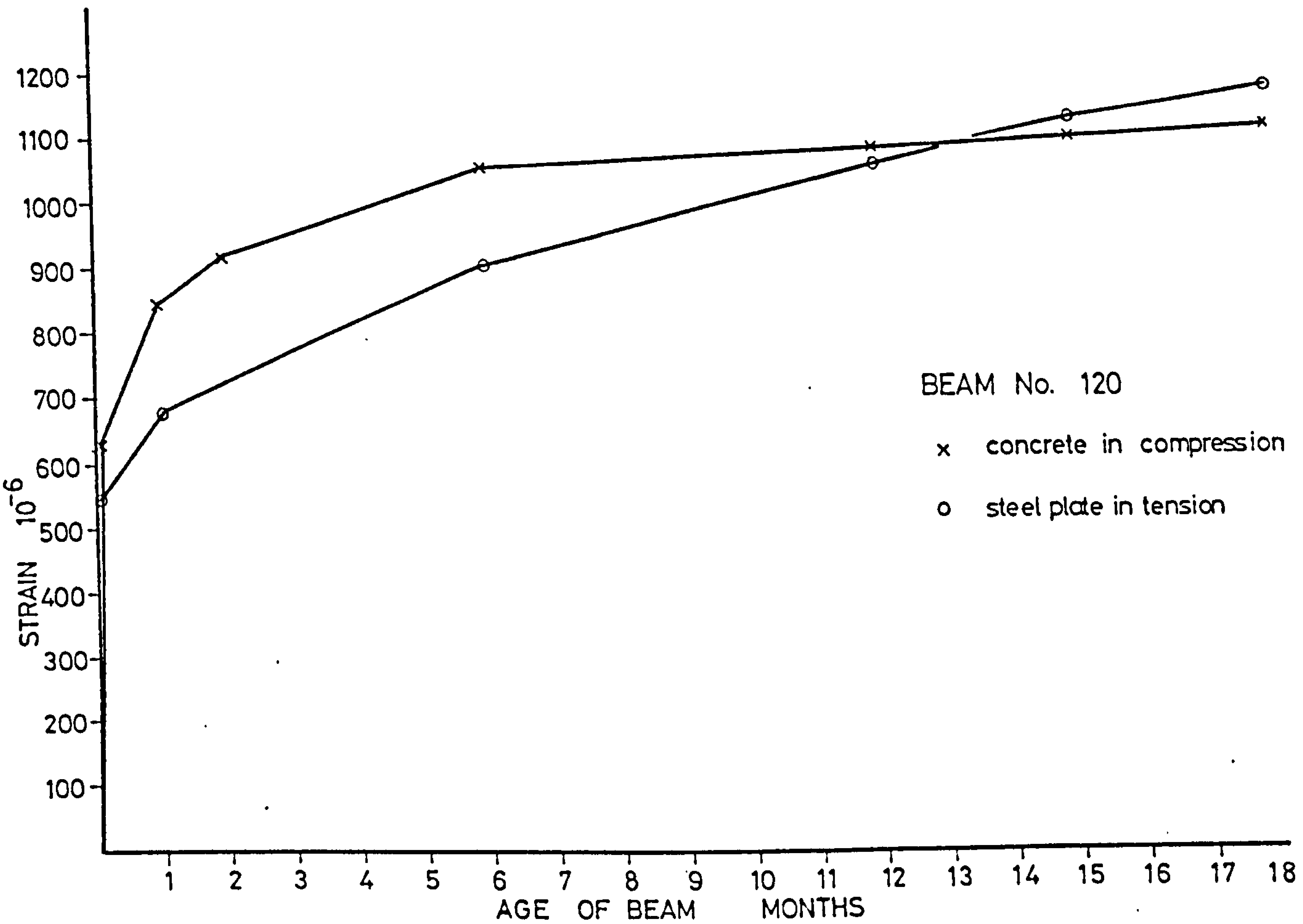

STRESS STRAIN CURVES FOR STEEL AND CONCRETE

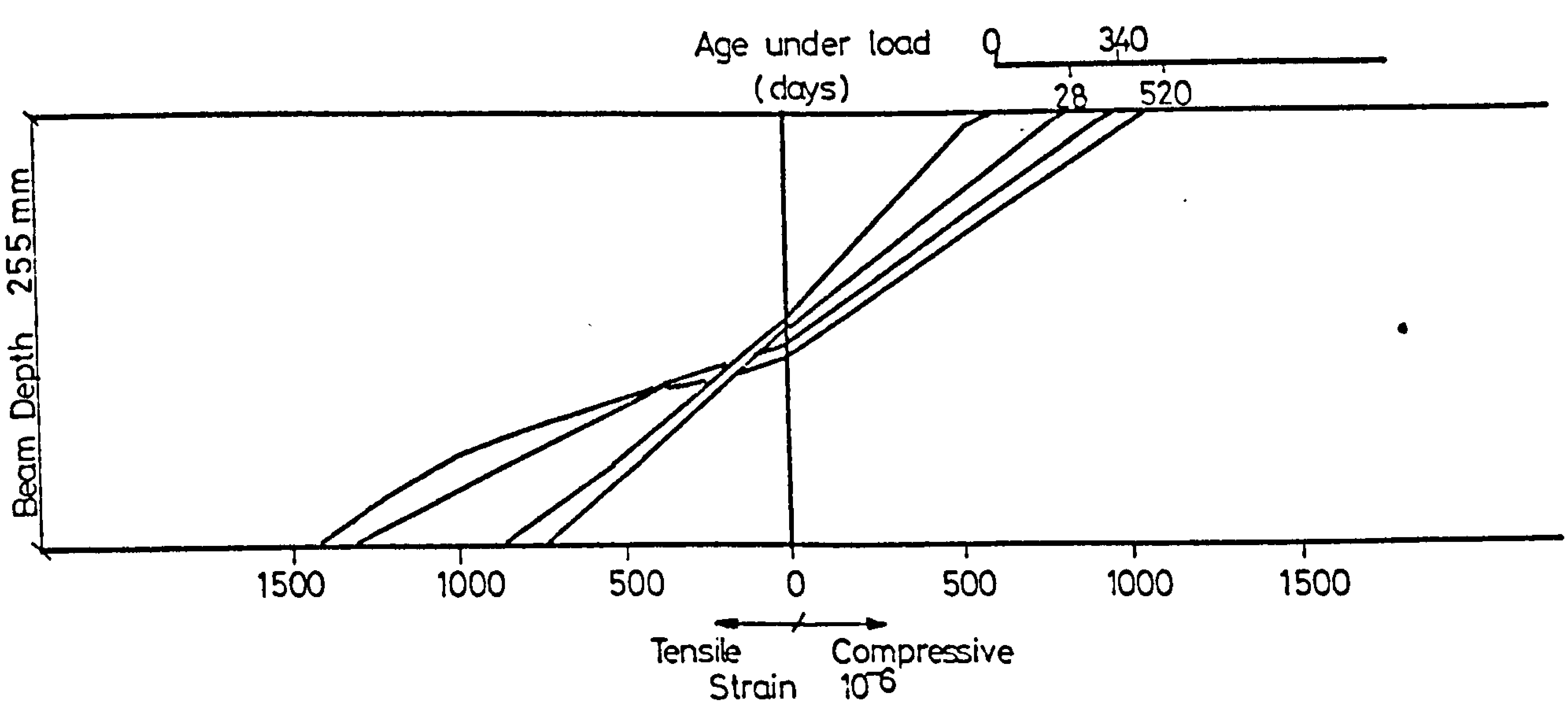

CONCRETE STRAIN DISTRIBUTION

FIGURE 8·2 VARIATION OF STRAIN WITH TIME

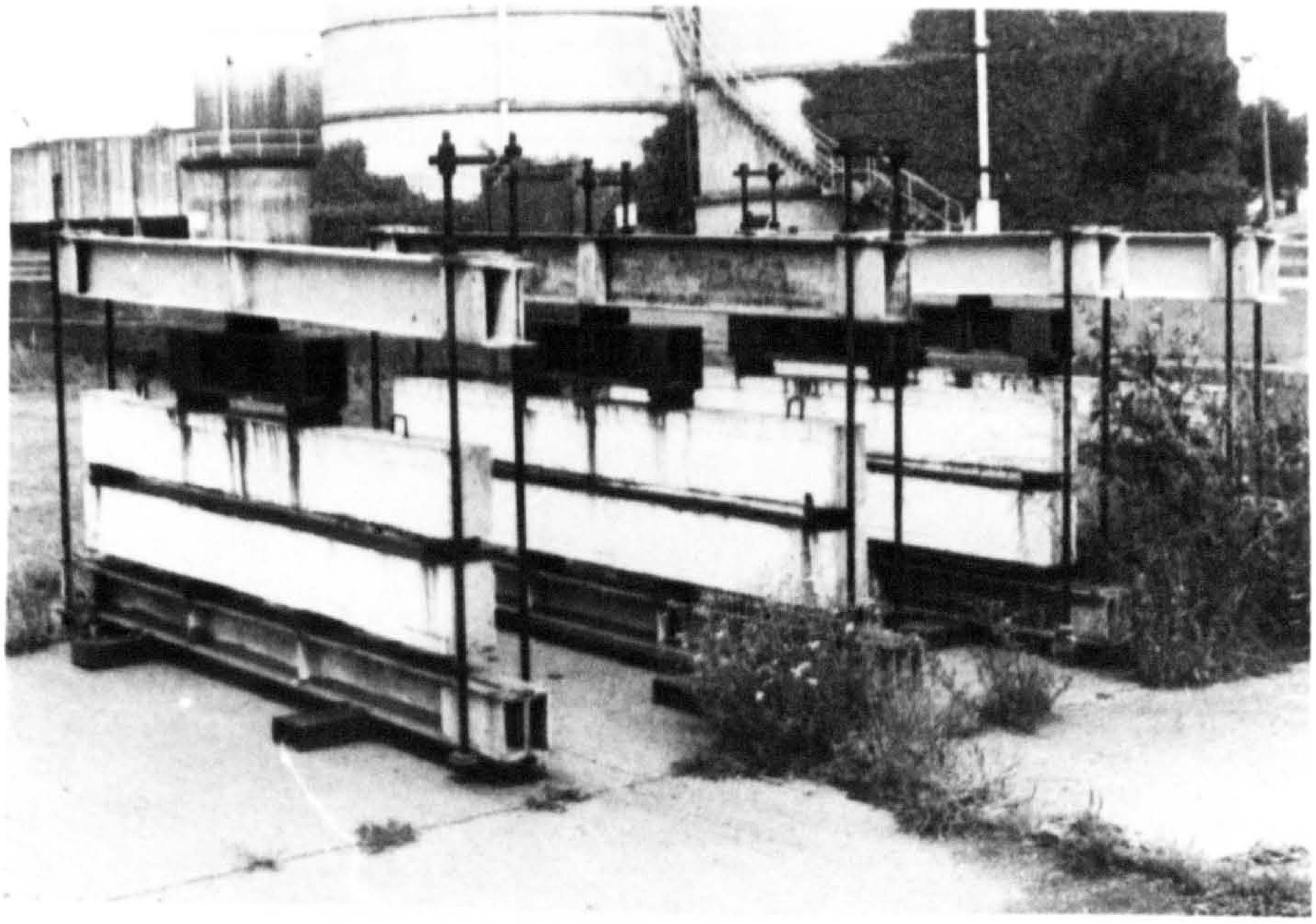

PLATE 8·1 LONG TERM TESTS : LOADED BEAMS

PLATE 8·2 LONG TERM TESTS : UNLOADED BEAMS

8.4.2 Discussion of Results

8.4.2.1 Strength Characteristics

The ultimate loads of the three beams tested at 18 months were calculated as detailed in Appendix 4 and are given in Table 8.2 together with the experimental values and the corresponding loads for similar beams tested at 28 days. For the CP110 method of calculation, the mean ratio of experimental to theoretical ultimate moment was 1.05, as compared to 1.05 at 28 days. The same ratios for the calculations by strain compatibility were 1.03 (1.01 at 28 days) assuming the glue to be cracked, and 1.02 (1.00 at 28 days) assuming the glue is not cracked.

After testing three of the beams, which had been exposed for 18 months after plating, it was thought that there was nothing to be gained, at this stage, by testing the remaining five of the set of eight beams. The beams were resisting greater moments at failure than the beams tested at 28 days as would be expected due to the ageing of the concrete, assuming that there was no degradation of the bond between the glue and plate or concrete. The plates were stripped from the beams after failure as shown in Plate 8.3. Although there was evidence of a small amount of air pockets within the glue line (less than 5% of the area) and areas of insufficiently mixed resin hardener (less than 5% of the area), there was no sign of corrosion of the steel plate, except along its edges where some of the protective paint had been chipped off during transportation. The concrete beam was cut through with a circular saw to produce a small element of the beam (Plate 8.3).

The amount of calcium hydroxide available in a hardened cement paste depends on the amount and composition of the calcium silicate phases in the cement and their degree of hydration. In time the alkalies react with the acidic constituents in the atmosphere, particularly carbon dioxide and sulphur dioxide, so that the alkalinity of the concrete is progressively reduced. Corrosion of the steel bar reinforcement occurs when moisture and oxygen gain access into the concrete and also there must be a value of pH less than 11, in other words the environment must be acidic. The diffusion of acidic vapours into the concrete converts the free lime to calcium carbonate thus reducing the pH, and consequently

TABLE 8·2 ULTIMATE MOMENTS

AGE AT TESTING	BEAM NUMBERS	1 CP 110 ULTIMATE MOMENT kNm	2 STRAIN COMPATIBILITY ULTIMATE MOMENT (NO GLUE) kNm	3 STRAIN COMPATIBILITY ULTIMATE MOMENT (+ GLUE) kNm	4 EXPERIMENT ULTIMATE MOMENT kNm	4/1	4/2	4/3	FAILURE MODE	GLUE THICKNESS mm	PLATE THICKNESS mm
28 DAYS	207	92·2	95·5	96·6	100·6	1·09	1·05	1·04	FLEXURE	3·0	1·5
	216	91·9	95·1	96·7	100·6	1·09	1·06	1·04	FLEXURE	6·0	1·5
	214	101·3	104·2	104·9	97·0	0·96	0·93	0·92	FLEXURE / SHEAR BOND	3·0	2 × 1·5
18 MONTHS	101	96·9	100·4	101·5	99·6	1·03	0·99	0·98	FLEXURE / SHEAR BOND	3·0	1·5
	102	97·7	101·1	102·8	111·9	1·15	1·11	1·09	FLEXURE	6·0	1·5
	108	107·8	110·9	111·6	109·3	1·01	0·99	0·98	FLEXURE	3·0	2 × 1·5

Section cut through a beam to test for carbonation of cement

PLATE 8·3 LONG TERM TEST BEAMS AFTER FAILURE

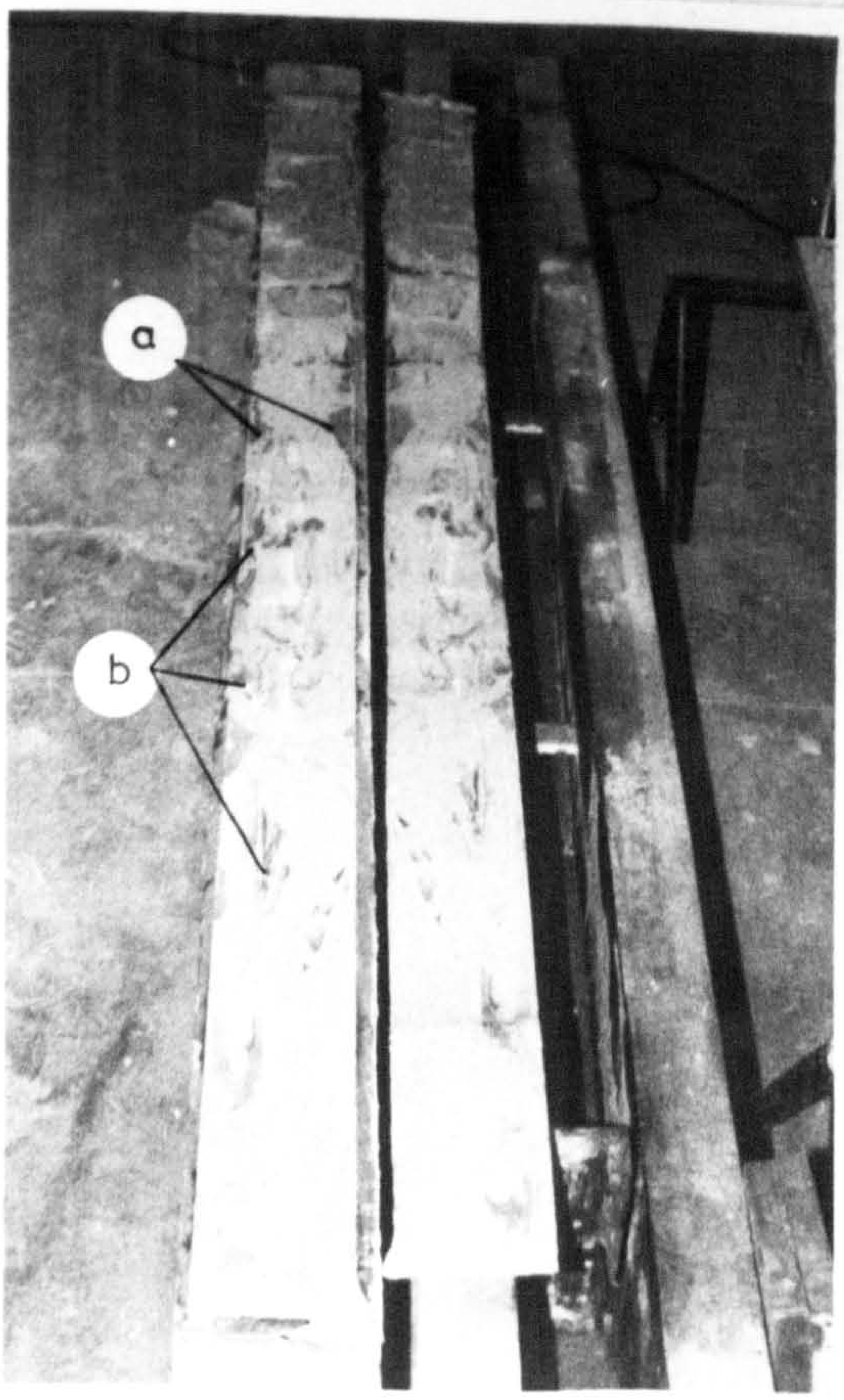

Plate peeled off the beam.

a. air pockets
b. glue not fully hardened due to insufficient mixing

the protective value of the concrete. Carbonation also tends to increase the shrinkage of the concrete and thus promotes the development of cracks. This in turn increases the penetration of moisture and chemicals which further assists corrosion. If the carbonation front reaches the steel bars then corrosion will start. Since the corrosion products occupy a greater volume than the original steel the concrete cover cracks and spalls off.

The piece of beam was treated with phenolphthalein indicator on both ends to test for carbonation. The change in colour (colourless to pink) of the phenolphthalein in the pH range between 8.2 and 9.8 indicated clearly the boundary of complete carbonation. The depth of carbonation was measured at several points and the average depth was estimated to be 2 mm at the top surface and 3 mm on the side faces. On the bottom concrete face which had the epoxy resin bonded to it there was no carbonation whatever.

It is clear from these results that the increase in ultimate strength provided by the bonded steel plate has not been adversely affected by the weathering over a period of eighteen months. The presence of the glue and plate has prevented carbonation proceeding at the bottom surface of the beam.

However, this test period is very short in comparison with the design life of a structure and the long term behaviour of plated beams must be studied for much longer periods.

It is interesting to note, nevertheless, that the plating technique not only strengthens the beams satisfactorily but also reduces the crack widths and carbonation at the beam soffit. The possibility of corrosion of the interval reinforcement should therefore be reduced.

8.4.2.2 Deformation Characteristics

Figs. 8.3, 8.4 and 8.5 show the comparison between the load-strain, load-deflection and moment rotation characteristics, respectively, of the beams tested at 28 days and 18 months. There was an increase in stiffness for both increase in glue or plate thickness and, as at 28 days, the effect of plate thickness was greater than that of glue thickness.

The load-strain curves of the beams tested at 18 months generally indicated

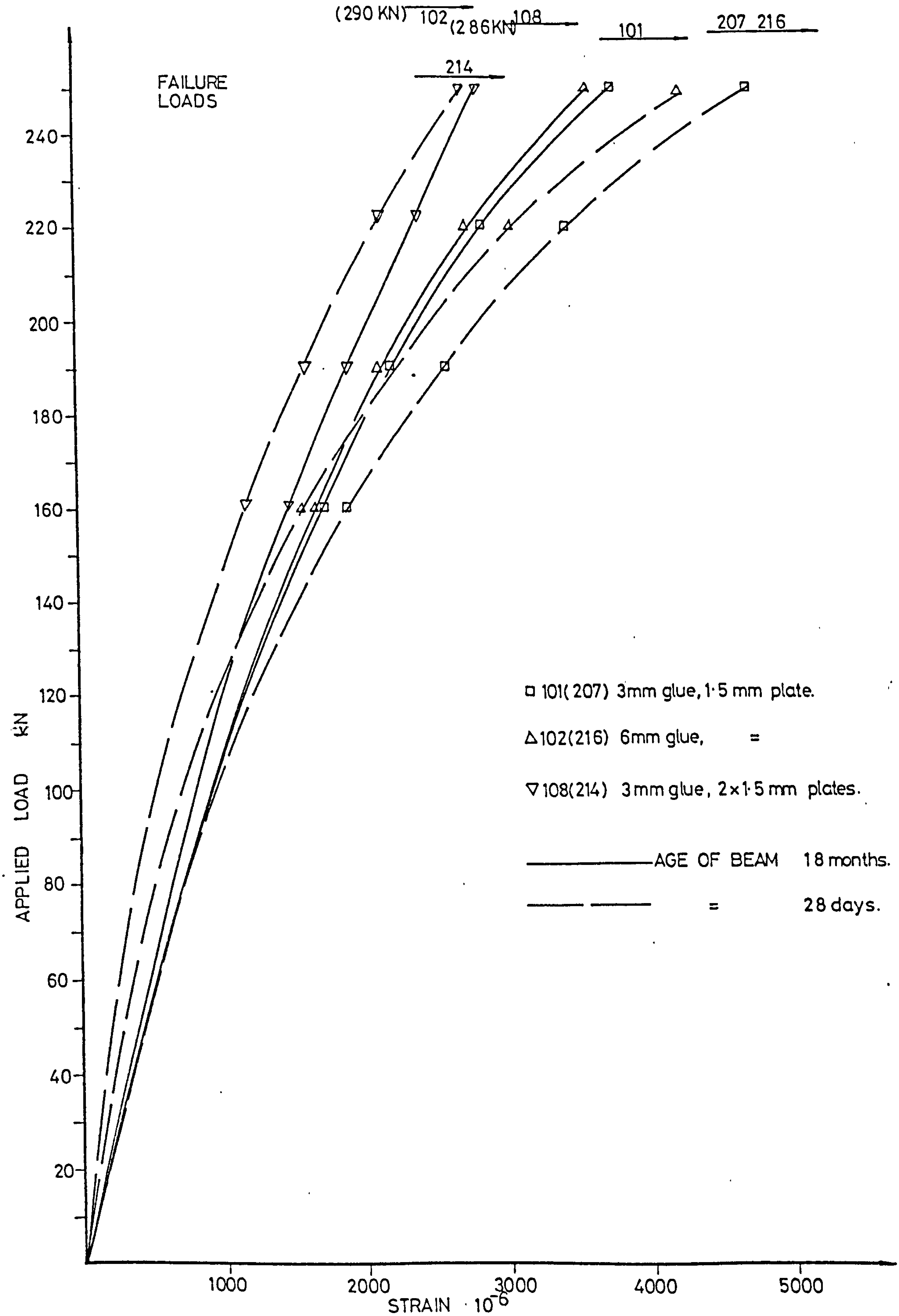

FIGURE 8·3 LOAD STRAIN CURVES - EXTERNAL STEEL PLATE - CENTRE SECTION

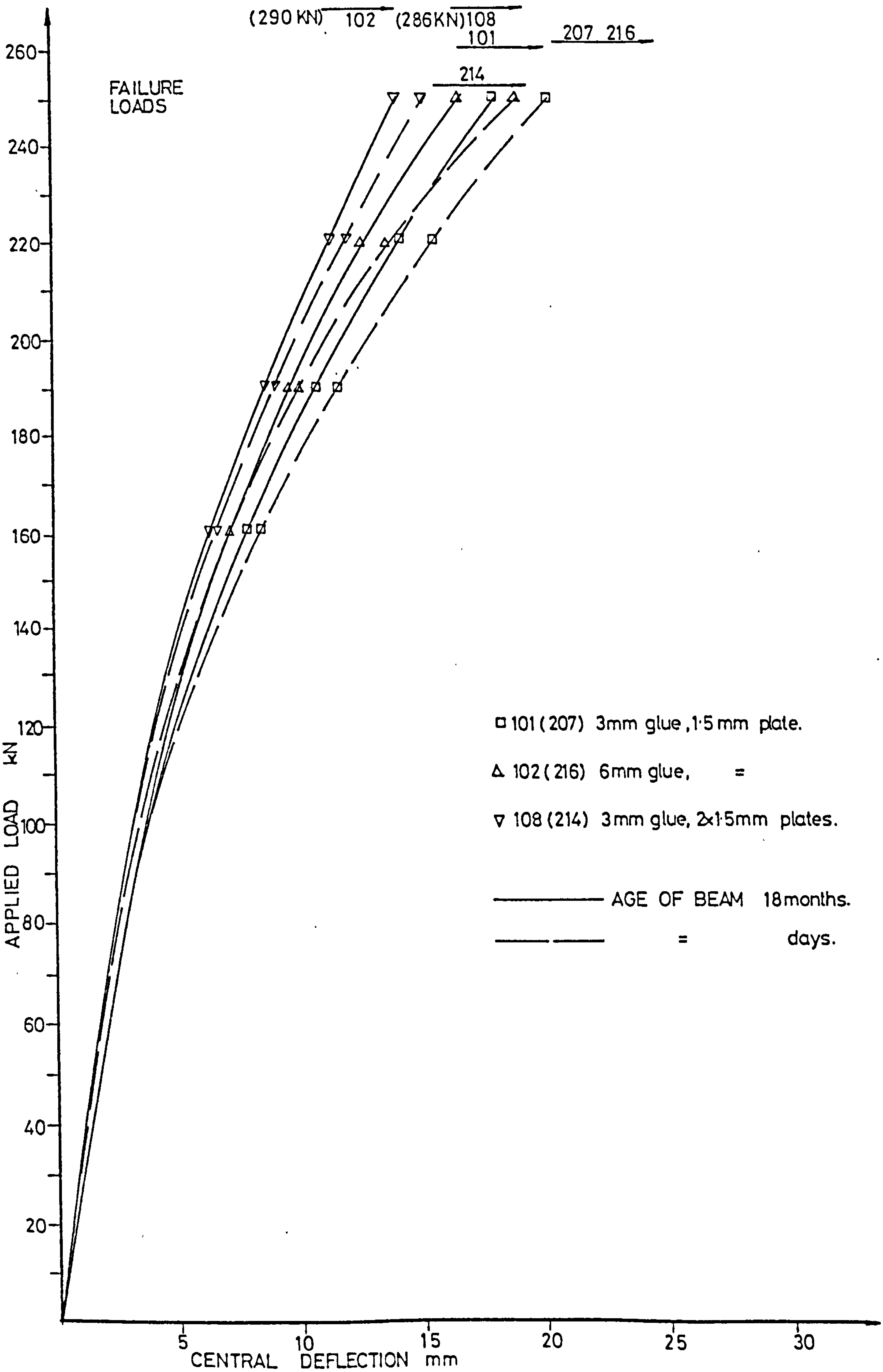

FIGURE 8·4 LOAD-DEFLECTION CHARACTERISTICS

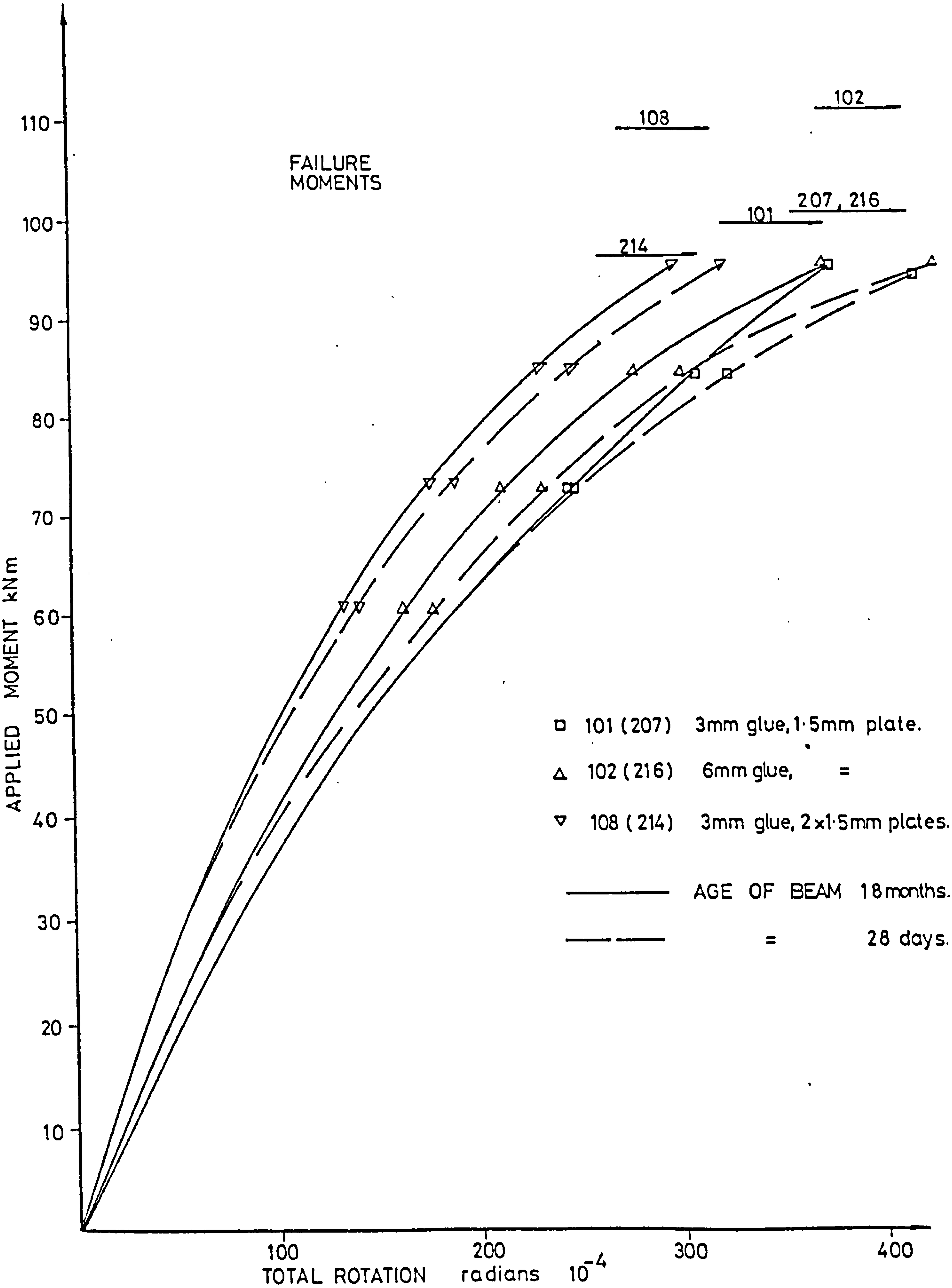

FIGURE 8·5 MOMENT - ROTATION CHARACTERISTICS

an increase of rigidity when compared with the behaviour at 28 days. The plate strains of beam 108 were greater than the comparable beam (214) at 28 days, throughout its loading. This could indicate that beam 214 had a certain amount of slipping between its plate layers. Beam 102 showed slightly higher plate strains up to service load, but above this the strains were lower than the corresponding beam tested at 28 days.

The load-deflection curves of the beams tested at 18 months all indicated an increased stiffness when compared with the behaviour at 28 days.

The values of ductility and theoretical deflections at 130 kN are given in Table 8.3 together with the experimental deflections. The ductility of the three beams tested at 18 months was slightly lower than the corresponding beams at 28 days, and the theoretical predictions gave good agreement with experiment. The calculation of deflections were as described in Appendix 5, with the Youngs Modulus of concrete = 38.9 kN/mm^2 (from experimental tests at 18 months). The mean ratios of experimental to theoretical deflections were 1.12 (CP110), 1.12 (ACI) and 0.95 (CEB), compared with 1.23 (CP110), 1.23 (ACI) and 1.05 (CEB) for all the beams tested at 28 days.

The experimental rotations were compared with theoretical values as calculated in Appendix 6. Again the Youngs Modulus of the concrete was 38.9 KN/mm^2, at 18 months. Table 8.3 shows both the experimental and theoretical rotations. As in the case of the 28 day tests, the difference between theory and experiment increases as the load increases. The empirical formula derived in Chapter 6 was also used to predict the rotations. These values, and the percentage difference between them and the measured rotations are also given in Table 8.3. For the limited series of three beams tested at 18 months the maximum difference between the predictions of the empirical formula and the measured values was ±11%, compared with ±12% at 28 days.

The moment-rotation curves closely reflect the load-deflection behaviour,all the beams being stiffer than at 28 days.

TABLE 8·3 COMPARISON OF EXPERIMENTAL AND THEORETICAL DEFLECTIONS AND ROTATIONS

AGE AT TESTING		18 MONTHS			28 DAYS		
BEAM NUMBER		101	102	108	207	216	214
GLUE THICKNESS mm		3·0	6·0	3·0	3·0	6·0	3·0
PLATE THICKNESS mm		1·5	1·5	2x1·5	1·5	1·5	2×1·5
EXPERIMENTAL DEFLECTIONS mm	FIRST CRACK LOAD	1·80	1·60	1·40	1·80	1·60	1·35
	130 kN LOAD	5·50	5·40	4·70	6·00	5·70	4·80
	220 kN LOAD	14·00	12·50	11·00	16·00	14·00	12·00
THEORETICAL DEFLECTIONS mm (130 KN LOAD)	CP 110	4·90	4·90	4·10	5·00	5·00	4·20
	ACI	4·90	4·76	4·20	5·00	4·89	4·30
	CEB	5·70	5·70	4·88	5·81	5·83	5·00
EXPERIMENT / THEORY	CP110	1·12	1·10	1·14	1·20	1·14	1·14
	ACI	1·12	1·13	1·12	1·21	1·17	1·12
	CEB	0·96	0·94	0·96	1·03	0·98	0·96
DUCTILITY DEFLN. 220 kN / DEFLN. 130 kN		2·54	2·31	2·34	2·67	2·46	2·50
EXPERIMENTAL ROTATIONS radians 10^{-4}	60 KN LOAD	55	52	46	55	52	46
	130	145	125	110	145	133	111
	190	245	210	180	250	235	193
	250	380	380	300	430	430	360
THEORETICAL ROTATIONS radians 10^{-4}	60	56 (50)	52 (46)	46 (50)	61 (53)	56 (50)	50 (44)
	130	125 (118)	121 (113)	116 (102)	135 (126)	131 (124)	115 (110)
	190	181 (175)	183 (175)	155 (152)	195 (186)	199 (190)	169 (165)
	250	235 (220)	242 (236)	194 (192)	247 (237)	263 (257)	212 (209)
ROTATIONS FROM EMPIRICAL FORMULA radians 10^{-4}	60	56	52	46	61	56	50
	130	130	125	109	150	146	123
	190	217	215	180	255	253	220
	250	355	383	308	413	418	350
% DIFFERENCE BETWEEN THE MEASURED VALUES AND EMPIRICAL FORMULA	60 KN LOAD	+2	0	0	+11	+8	+9
	130 KN LOAD	−3	0	−1	+3	+9	+11
	190 KN LOAD	−11	+2	0	+2	+8	+11
	220 KN LOAD	−9	+1	+3	−4	−3	−3

Figures in brackets assuming tensile stress in concrete = 3 N/mm^2. Otherwise 1 N/mm^2

8.4.2.3 Cracking Characteristics

The crack analysis was performed as for the beams tested at 28 days. Table 8.4 shows the test results and compared them with the 28 day tests. Plate 8.6 shows the beams after failure.

The mean crack width and standard deviation were plotted against the surface concrete strain at the level of the internal reinforcement. The slopes were computed by linear regression as shown in Fig. 8.6. If the empirical formula derived from the 28 day tests, for the slope of the mean crack width against concrete strain, is used to compute values for the 18 month old test beams the values are very close to the experimental values.

		Slope of mean crack width v. concrete strain		
Beam No.		experimental value		formula value
101		37		37
102		52		47
108		44		44

The empirical formula derived from the 28 day tests, for finding the ultimate crack spacing was then used to compute values for the 18 month old beams.

	Ultimate Crack Specing	
Beam No.	experimental spacing (mm)	formula (mm)
101	53	55
102	61	55
108	52	50

The agreement between the formula's prediction and experiment is good.

In Fig. 8.7 the slope of the mean crack width against concrete strain is plotted against the slope of the standard deviation against concrete strain. The best fit lines for the beams tested at both 28 days and 18 months are given. The limited accuracy obtained from only 3 tests at 18 months gives close agreement with the 28 day tests.

The modified CP110 and ACI crack width prediction formulae, derived from the tests at 28 days, were used to calculate the maximum crack widths for the three beams tested at 18 months, as shown in Table 8.5. The average ratio of theory to experimental values was 0.85 (ACI) or 0.84 (CP110), as compared with 0.91 at 28 days for the three comparable beams.

TABLE 8·4 CRACKING CHARACTERISTICS

LOAD kN	NUMBER OF CRACKS	MEAN CONCRETE STRAIN 10^{-6}	MEAN CRACK WIDTH 10^{-2} mm	STANDARD DEVIATION 10^{-2} mm	COEFF OF VARIATION 10^{-2}	MAXIMUM CRACK WIDTH 10^{-2} mm	MEAN CRACK SPACING mm	STANDARD DEVIATION mm	MEAN CRACK HEIGHT mm	STANDARD DEVIATION mm
60	6	467	2·42	0·93	38	4·0	92	62	54	18
	8	405	2·28	0·76	33	3·0	94	21	80	21
100	8	820	2·72	0·87	32	5·0	79	32	82	24
	9	840	3·00	1·40	47	5·0	90	22	105	24
130	11	1200	3·95	0·83	28	6·0	68	25	92	33
	10	1190	4·30	2·16	50	7·0	80	27	112	26
160	14	1565	4·39	2·33	53	10·0	54	25	94	40
	12	1590	5·20	3·46	66	10·0	66	32	118	44
220	15	2800	7·53	3·22	43	12·0	53	25	97	48
	13	2655	7·46	4·92	66	16·0	60	27	123	40
250	16	3700	14·18	8·17	58	30·0	48	21	108	54
	15	3750	15·20	9·10	66	32·0	53	25	124	41

Upper figures – 28 day test.
Lower figures – 18 month test.

(a) beams 207 $W_{max} / W_{mean} = 1·98$

101 $W_{max} / W_{mean} = 1·80$

60	5	390	2·58	0·90	35	4·0	109	72	48	21
	7	375	2·57	0·53	21	3·0	116	33	83	24
100	9	700	3·00	1·35	45	5·0	88	24	87	26
	8	790	3·75	1·16	31	6·0	100	13	107	24
130	10	980	4·30	2·07	48	7·0	71	29	97	28
	8	1080	5·87	1·55	26	8·0	100	13	110	27
160	12	1280	6·58	3·04	46	11·0	60	22	105	37
	9	1400	7·67	2·87	37	12·0	88	32	116	37
220	14	2120	9·93	4·07	41	16·0	53	21	105	44
	12	2220	11·16	5·87	53	18·0	64	31	126	41
250	14	3310	14·86	9·07	61	30·0	53	21	112	50
	13	3125	16·46	9·10	55	30·0	61	31	130	44

(b) beams 216 $W_{max} / W_{mean} = 1·70$

102 $W_{max} / W_{mean} = 1·52$

60	6	350	2·20	0·82	37	3·0	129	48	71	12
	6	250	2·81	0·50	28	3·0	124	38	51	22
100	10	660	3·10	1·30	42	6·0	79	24	83	29
	10	500	3·00	1·15	38	5·0	76	25	77	25
130	12	1000	4·50	2·30	50	8·0	68	18	101	30
	10	770	4·10	1·37	34	7·0	76	25	98	27
160	12	1240	6·00	2·50	41	10·0	63	13	108	32
	11	1030	4·90	2·20	44	9·0	68	24	101	27
220	14	1850	7·85	4·80	61	17·0	58	10	111	39
	13	1730	8·46	3·60	42	15·0	56	22	105	34
250	15	2500	14·10	7·80	55	28·0	55	12	121	41
	14	2400	10·85	5·35	49	24·0	52	16	106	38

(c) beams 214 $W_{max} / W_{mean} = 1·82$

108 $W_{max} / W_{mean} = 1·81$

TABLE 8·5 CRACK WIDTHS AT 130 kN LOAD

AGE AT TESTING	BEAM NUMBER	1 EXPERIMENT WIDTH mm 10^{-2}	CP 110 THEORY mm 10^{-2}	ACI THEORY mm 10^{-2}	2 CP 110 CORRECTED mm 10^{-2}	3 ACI CORRECTED mm 10^{-2}	$\frac{2}{1}$	$\frac{3}{1}$	GLUE THICKNESS mm	PLATE THICKNESS mm
28 DAYS	207	6·0	9·3	9·0	6·4	6·4	1·07	1·07	3·0	1·5
	216	7·0	9·3	9·0	6·4	6·4	0·91	0·91	6·0	1·5
	214	8·0	7·9	7·7	5·8	5·9	0·73	0·74	3·0	2×1·5
18 MONTHS	101	7·0	9·3	9·0	6·4	6·4	0·91	0·91	3·0	1·5
	102	8·0.	9·3	9·0	6·4	6·4	0·80	0·80	6·0	1·5
	108	7·0	7·9	7·7	5·8	5·9	0·82	0·84	3·0	2×1·5

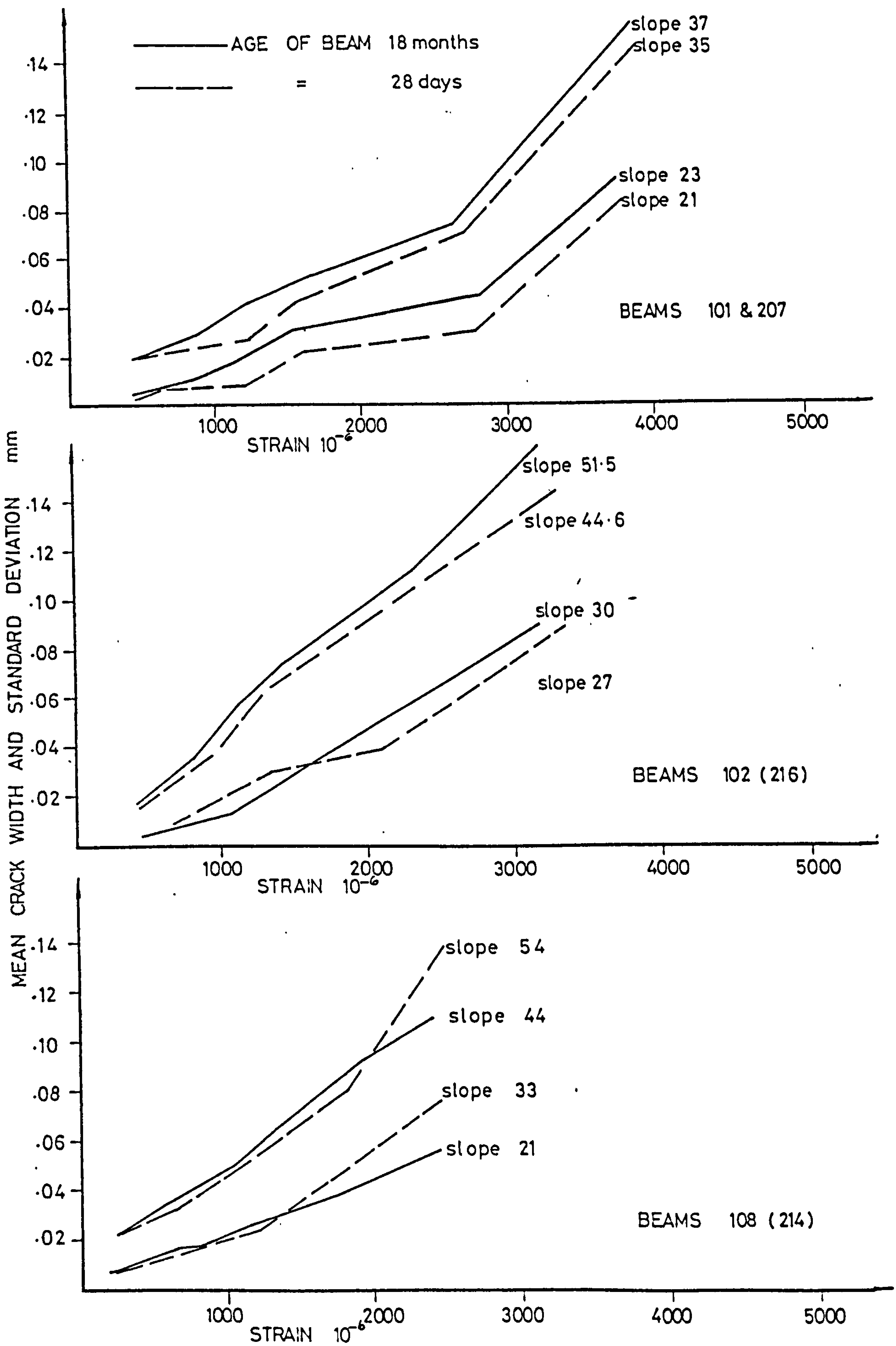

FIGURE 8·6 MEAN CRACK WIDTH AND STANDARD DEVIATION V. THE CONCRETE STRAIN AT THE LEVEL OF INTERNAL REINFORCEMENT

FIGURE 8·7 W/ε MEAN CRACK WIDTH V. CONCRETE STRAIN AT REINFORCEMENT LEVEL

The formulae derived at 28 days to predict the concrete surface strain and the tensile stress in the concrete could not be checked in the long term beams as there were no strain gauges on the reinforcing bars. Therefore the difference between the internal bar strain and the concrete surface strain was not measured.

8.5 DURABILITY TESTS

8.5.1 Introduction

This part of the test programme was designed to investigate the effects of various sealing agents on the durability of the concrete/epoxy/steel joints. Obviously, to be effective, the sealing agent must show stable behaviour under moist conditions in the long term and have good bonding to concrete, epoxy resin and steel. The following products were used:

8.5.2 Coating Details

The coatings used were easily applied using a spatula or paintbrush, as indicated.

8.5.2.1 Polyurethane Rubber (Brush)

This was a two component liquid whose shear resistance is good up to temperatures of 70°C. The product used was FLEXANE 30 manufactured by DEVCON Ltd.

8.5.2.2 Silicone Rubber (Spatula)

Generally these have the same type of resistance as the polyurethanes, but are one component systems, which cure in air at room temperature to produce a resilient rubber with heat resistance up to 260°C. The product used was SILITE 100 manufactured by DEVCON Ltd.

8.5.2.3 Acrylonitrile Phenolic (Brush)

Again these show the same sort of resistance as the polyurethanes and have heat resistance to temperatures of 150°C. They are one component systems which dry in air at room temperature. The product used was K7066 manufactured by SWIFT Ltd.

8.5.2.4 Paint (Brush)

Two coats of primer and two coats of finish coat were applied. The paint used was MANDERLAC manufactured by MANDERS Ltd.

8.5.2.5 Control Specimens

Four prisms were made with steel plates having no protective coating. Two were stored with the other test specimens described above and the other two were stored in a controlled atmosphere at 17°C, 56% relative humidity. Four unplated prisms were also cast and kept in the mist room at 20°C, 100% relative humidity.

8.5.3 Experimental procedure

The test specimens were concrete prisms 100 x 100 x 500 mm as shown in Fig. 8.8. Four prisms were cast for each of the four types of coating and the control specimens as detailed above. In all, therefore, twentyfour prisms plus three control cubes were cast. All specimens were stripped after 24 hours and placed in a mist room at 22°C, 100% relative humidity for 7 days before removal for surface preparation and plating. Ciba Giegy XD808 was used to bond on the plates, as used in the preliminary test series.

After plating, the beams were left to cure in uncontrolled laboratory conditions for seven days before application of the coatings and for a further seven days afterwards. The beams were then replaced in the mist room except two control beams with no coating which were kept at 17°C, 56% relative humidity. The beams were left in the mist room for 10 months or 20 months before testing. The loading arrangement is shown in Fig. 8.8. The beams were tested under central point loading over a span of 450 mm. The loading rate was 4 kN/minute. The first crack load in the concrete, and the ultimate load were noted. After failure the plates were stripped off the beams to investigate corrosion of the plate, and plate/glue interface.

8.5.4 Discussion of result

The results are given in Table 8.6. After 10 months in the mist room the plated control beam, with no protective coating, had a failure load of 31·6 kN. The average failure loads (2 specimens each) for the coated prisms were 34·3 kN (FLEXANE); 32·5 (SILITE); 35·3 (SWIFT) and 34·1 (PAINT). The uncoated beam which was kept at 17°C, 56% relative humidity had a failure load of 34 kN. Therefore after 10 months in the mist room there was no significant difference

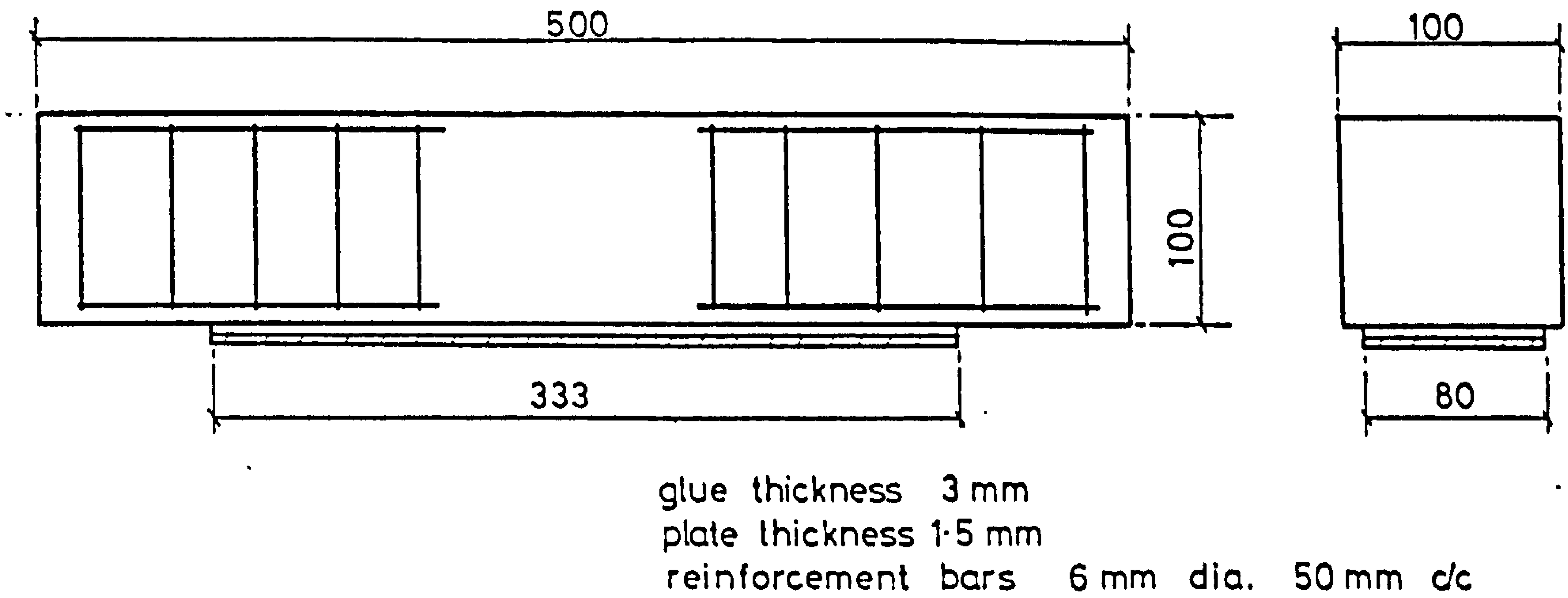

DETAILS OF DURABILITY SPECIMENS

All dimensions in mm.

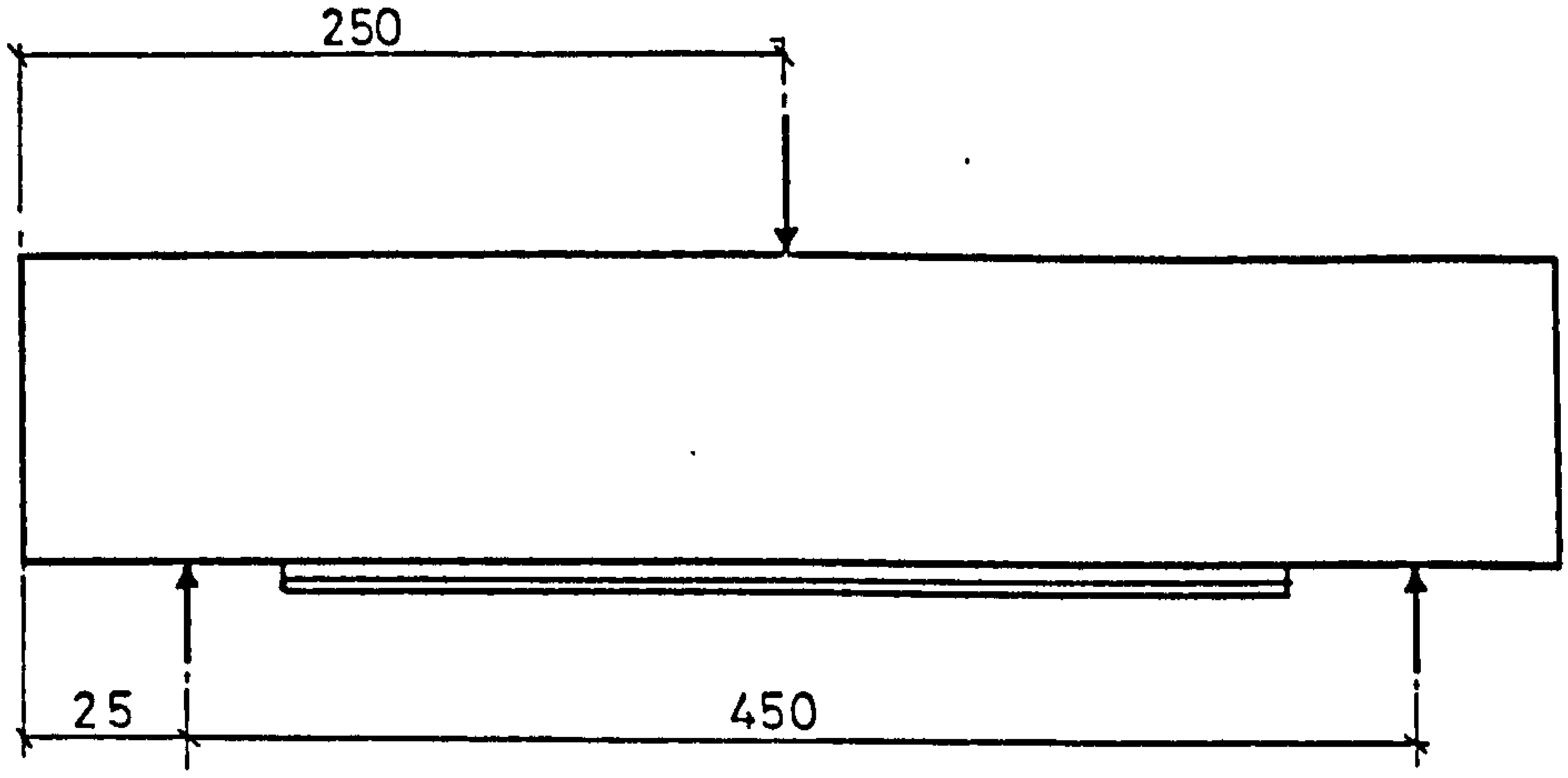

LOADING ARRANGEMENT

FIGURE 8·8 DURABILITY TEST SPECIMENS

TABLE 8·6 DURABILITY TEST RESULTS.

BEAM NUMBER	AGE AT TESTING MONTHS	TYPE OF COATING	CP 110 THEORY FIRST CRACK LOAD kN	CP 110 THEORY FAILURE LOAD kN	EXPERIMENT FIRST CRACK LOAD kN	EXPERIMENT FAILURE LOAD kN	1^{st} CRACK $\frac{EXP.}{THEORY}$	FAILURE $\frac{EXP}{THEORY}$
301	10	NONE	12·6	32·8	18·0	31·6	1·50	0·96
302 (1)	10	NONE	12·6	32·8	16·0	34·0	1·27	1·04
303	20	NONE	13·0	34·0	20·0	32·7	1·54	0·96
304 (1)	20	NONE	13·0	34·0	18·0	36·1	1·38	1·06
305	10	FLEXANE	12·6	32·8	16·0	32·3	1·27	0·98
306	10	FLEXANE	12·6	32·8	17·0	36·2	1·35	1·10
307	20	FLEXANE	13·0	34·0	16·0	37·2	1·23	1·09
308	20	FLEXANE	13·0	34·0	16·0	38·7	1·23	1·14
309	10	SILITE	12·6	32·8	18·0	31·4	1·43	0·96
310	10	SILITE.	12·6	32·8	20·0	33·6	1·59	1·02
311	20	SILITE	13·0	34·0	18·0	36·8	1·38	1·08
312	20	SILITE	13·0	34·0	20·0	38·3	1·54	1·13
313	10	SWIFT	12·6	32·8	18·0	36·2	1·35	1·10
314	10	SWIFT	12·6	32·8	17·0	34·4	1·46	1·05
315	20	SWIFT	13·0	34·0	19·0	35·4	1·46	1·04
316	20	SWIFT	13·0	34·0	16·0	37·6	1·23	1·11
317	10	PAINT	12·6	32·8	18·0	34·4	1·43	1·05
318	10	PAINT	12·6	32·8	17·0	33·8	1·35	1·03
319	20	PAINT	13·0	34·0	21·0	38·2	1·61	1·12
320	20	PAINT	13·0	34·0	17·0	36·0	1·31	1·06
321 (2)	10	NONE	9·2	9·2	9·5	9·5	-	1·03
322 (2)	10	NONE	9·2	9·2	9·2	9·2	-	1·00
323 (2)	20	NONE	9·5	9·5	9·7	9·7	-	1·02
324 (2)	20	NONE	9·5	9·5	10·0	10·0	-	1·05

(1) Uncoated, plated beams kept at 17°C, 56% RH. (2) Uncoated, unplated beams.
All beams other than those marked (1) were kept at 20°C, 100% R.H.

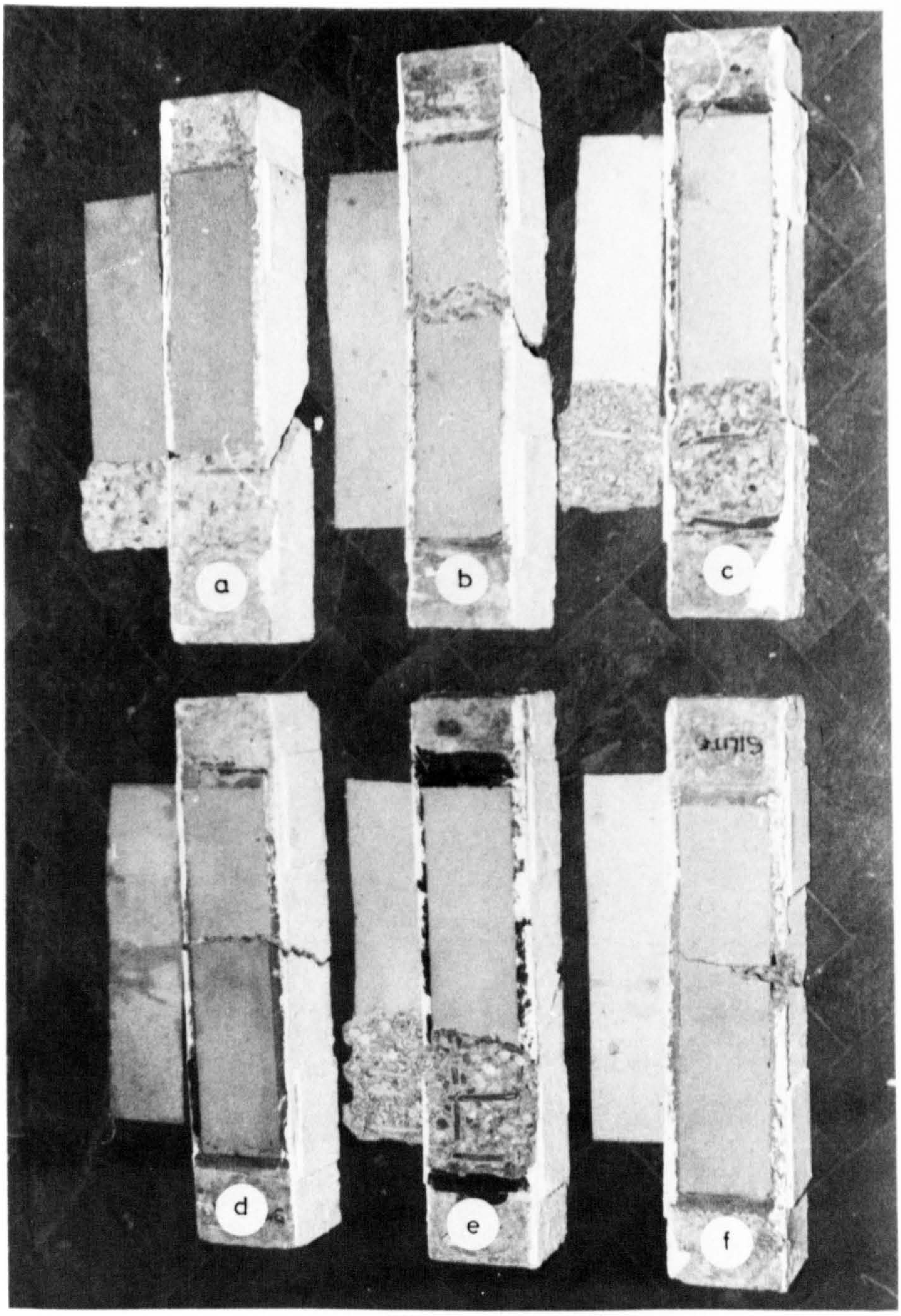

a – no coating – control specimen kept at 16 °C , 56 % Relative humidity
b – no coating – kept at 22 °C , 100 % Relative humidity.
c – SWIFT K 7066 Acrylonitrile phenolic .
d – FLEXANE 30 Polyurethane.
e – MANDERLAC Paint.
f – SILITE 100 Silicone.

PLATE 8.4 DURABILITY SPECIMENS AFTER TESTING

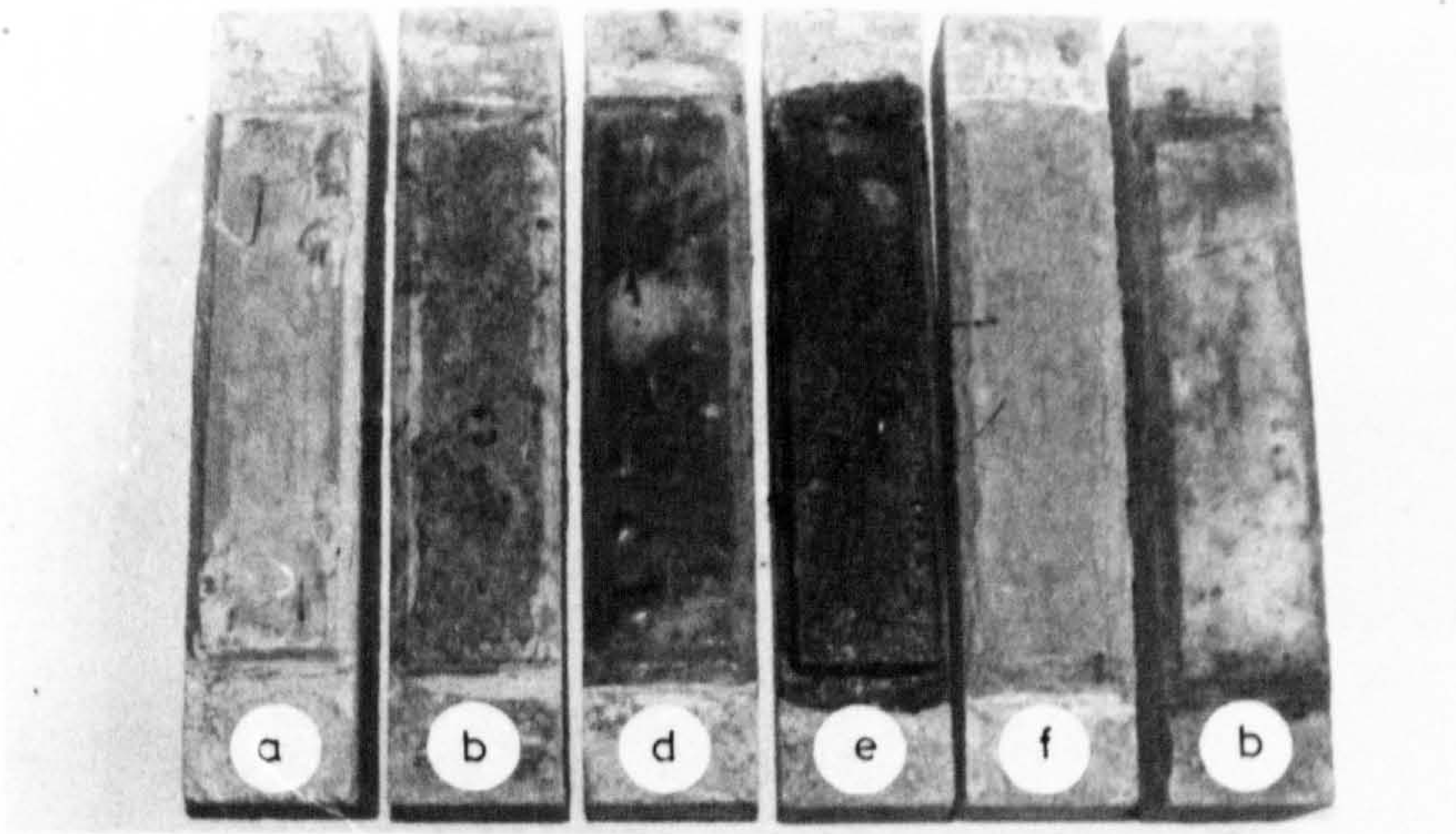

DURABILITY SPECIMENS BEFORE TESTING

a – f see Plate 8·4

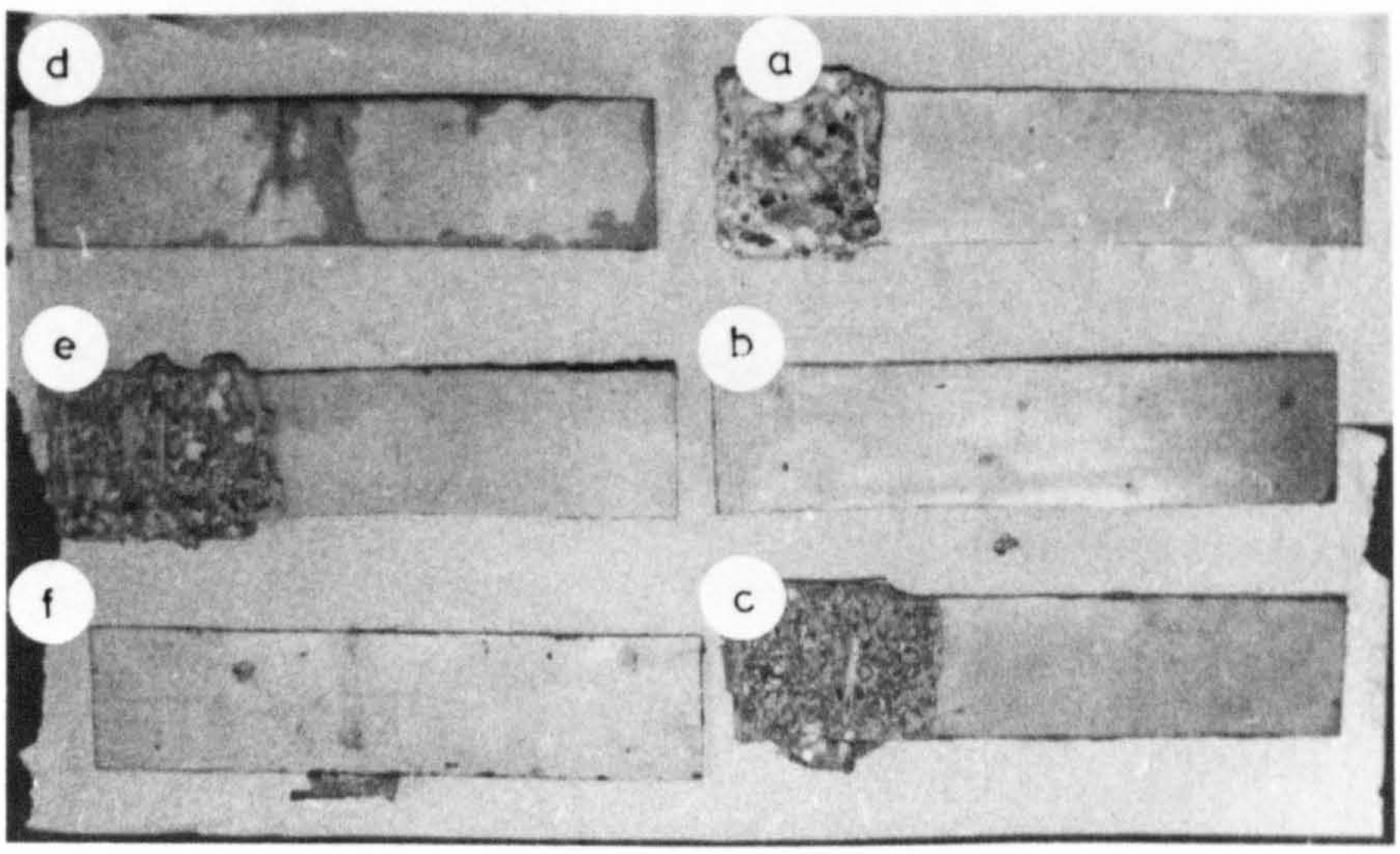

REINFORCING PLATES AFTER TESTING

PLATE 8·5 DURABILITY SPECIMEN DETAILS

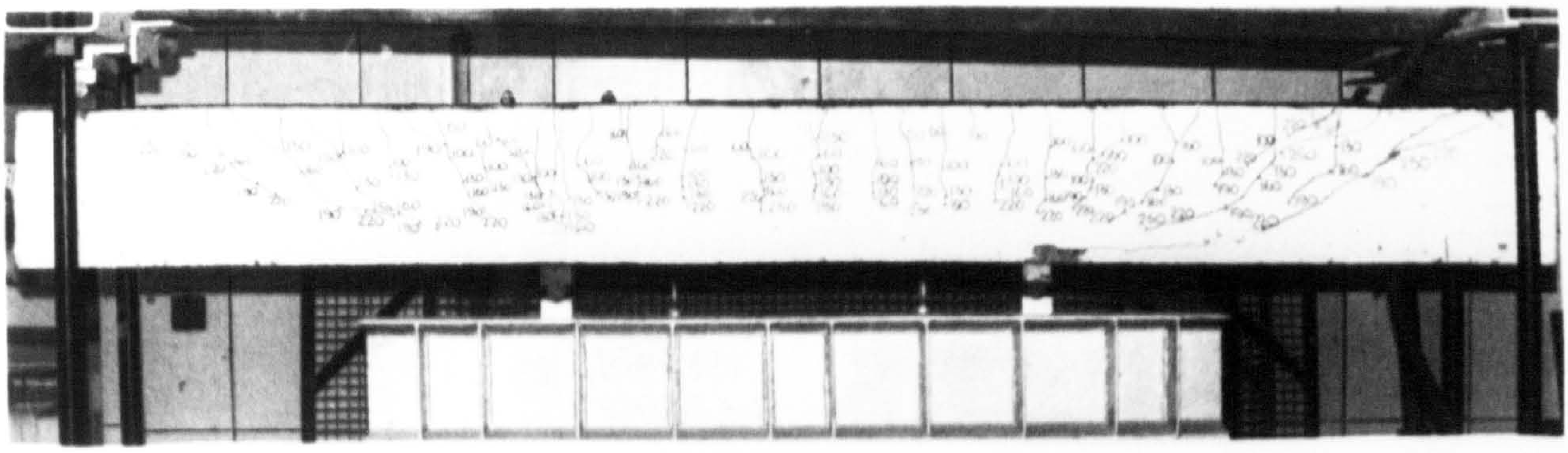

BEAM 101 3 mm glue thickness, 1·5 mm plate thickness.

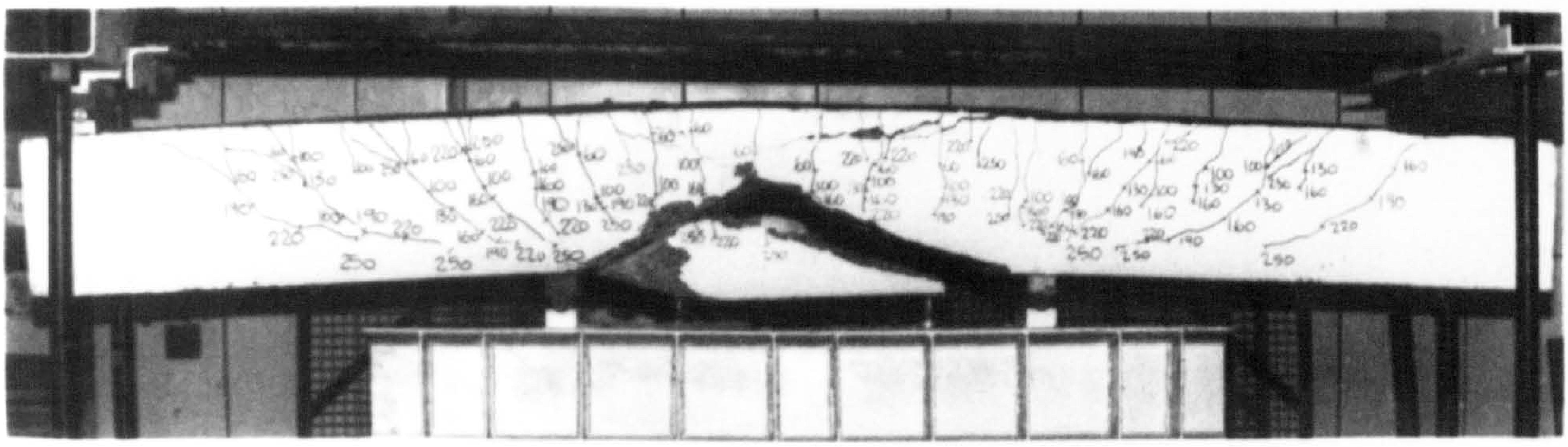

BEAM 102 6 mm glue thickness, 1·5 mm plate thickness.

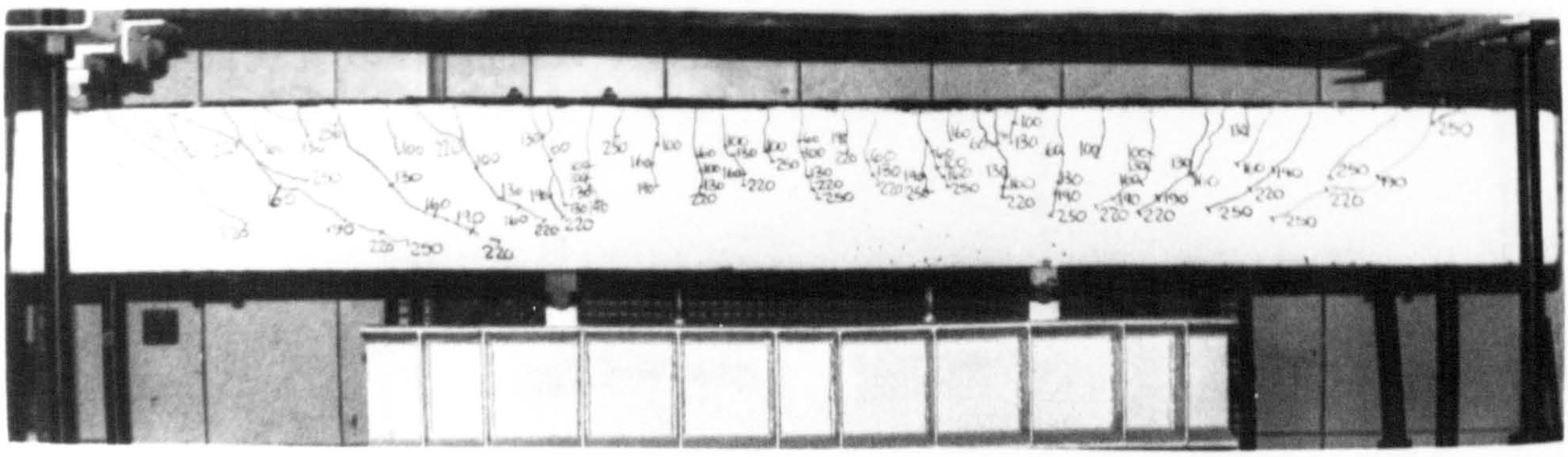

BEAM 108 3 mm glue thickness, 2 layers of 1·5 mm plate, lapped plates above the load points.

PLATE 8·6 CRACK PATTERNS - AGE OF BEAMS - 18 months.

between the protection given by the different types of coating. The control beam, without a coating, kept with the coated beams in the mist room had a slightly lower failure load than the uncoated beam which was kept under dry conditions.

After 20 months in the mist room, the control beam with no coating had a failure load of 32·7 kN. The similar beam kept at 17°C, 56% relative humidity had a failure load of 36·1 kN. There would therefore appear to be some loss in strength due to prolonged exposure to moisture when no coating is applied. The average failure loads (2 specimens each) for the coated prisms were 38·0 (FLEXANE): 37·6 (SILITE); 36·5 (SWIFT); and 37·1 (PAINT). These values all exceed the control specimen kept at 56% relative humidity showing the effectiveness of the coatings.

The failure loads were calculated by CP110 methods with material safety factors equal to unity as described in the previous Chapters. The tensile stresses in the glue and steel were taken as 16 N/mm^2 and 275 N/mm^2 respectively. The cube strengths of concrete at 10 months and 20 months were 75 and 90 N/mm^2 respectively. The average ratio of experimental to theoretical values was 1·05 at 10 months and 1·08 at 20 months.

The first crack obtained visually were all higher than the predicted loads. As explained previously, this would be expected. The composite behaviour of the steel/epoxy/concrete system was good, and in no case did failure occur by debonding. Plates 8.4 and 8.5 show the beams after failure. In no case was there any visual deterioration of the epoxy or steel plate, even in the uncoated specimens, except of course on the exposed face of the latter. The slightly lower failure loads of the uncoated, exposed prisms could be explained, not due to any loss of bond through ingress of moisture to the adhesive, but rather because of the excessive rusting and resulting loss in thickness of the steel plate. This was found to be up to 0.3 mm in places, with a mean value of approximately 0.2 mm.

8.6 CONCLUSIONS

Based on the results presented in this Chapter the following conclusions can be made.

1. The ultimate loads sustained by the beams tested after 18 months exposure were compatible with what would be expected assuming that there was no degradation of the epoxy bond and that the concrete was ageing normally. The ultimate loads could be predicted accurately by strain compatibility assuming the glue was not cracked.

2. Virtually no corrosion of the steel plates had occurred in the test beams after 18 months exposure. The only signs of rusting occurred at the edge of the plate where the paint had been chipped off during transportation. Carbonation of the cement paste was limited to 2-3 mm depth and had not occurred at all on the tension face where the concrete was protected by the epoxy bonded plate.

3. Even though there was evidence of inadequate mixing of resin and hardener, and inclusion of air pockets in the glue line (up to 10% of the area), the beams ultimate strength and deformation properties were not adversely affected.

4. The load-strain, load-deflection and moment rotation properties closely followed those for similar beams tested at 28 days. In general the older beams showed slightly stiffer behaviour.

5. The deflections calculated by the methods outlined in Appendix 5 were as accurate as those calculated at 28 days when compared with experimental values. The CEB method gave the best results.

6. The empirical formula derived for the beams tested at 28 days predicted the rotations of the beams tested at 18 months within ±11%.

7. For the limited number of tests at 18 months (3 beams only) the cracking characteristics were found to be in close agreement with the 28 day test results.

8. The durability tests showed the effectiveness of the coatings in protecting the epoxy/steel system from the penetration of moisture. However, even in the prisms which had no protective coating there was no visual evidence of corrosion of the epoxy/steel interface after 20 months. The coatings themselves showed no visual deterioration whatever.

CHAPTER 9

LIMITATIONS OF PRESENT WORK, OVERALL CONCLUSIONS AND RECOMMENDATIONS FOR FUTURE WORK

9.1 LIMITATIONS OF PRESENT WORK

The test data presented here are considered to be the first set of results systematically covering a range of glue and plate thicknesses. Limitations on the number of beams and the duration of testing has restricted this range. Nevertheless, it is hoped that this work will add to our knowledge of the flexural behaviour of reinforced concrete beams strengthened with externally bonded steel plates. The limitations within which the main series of flexural testing were conducted are:

1. The concrete strength of all the beams varied between 60-80 N/mm^2.
2. Only one type of epoxy adhesive, CXL 194, was used.
3. Only flexural tests were performed. The shear span was kept constant.
4. The amount of internal bar reinforcement was kept constant. All the beams were under reinforced prior to plating. The behaviour of actual bridge members may be different as prestressed beams often behave in an over reinforced manner.
5. Due to the duration of testing only a limited amount of replication of testing was performed.
6. The range of adhesive and plate thickness was 1·5 to 6 mm.
7. All beams had the same dimensions.
8. The long term tests were performed after a relatively short period of only 18 months.
9. The concrete cover to the internal bars was not varied.

9.2 OVERALL CONCLUSIONS

Although the conclusions derived from each chapter are summarised at the end of that chapter, the general conclusions which can be extracted from the test data presented in this thesis may be summarised as follows, (these conclusions are limited by the test conditions and procedures as outlined above):

1. The maximum increase in ultimate flexural capacity on addition of bonded

plate reinforcement was only 17%. The ultimate loads could be accurately predicted by CP 110 or strain compatibility methods when the mode of failure was flexural. The failure mode changed from purely flexural, for beams with 1·5 mm plate, to a shear/bond type failure, for beams with 6 mm plate thickness.

2. The service loads for the plated beams, assessed as the loads at which corresponding deformations in an unplated beam at its service load were attained, were up to 90% higher depending on which criterion was chosen from: deflections, rotations, steel bar strains or maximum crack widths.

3. The service load deflections in the plated beams were up to 40% less than in the unplated specimen. The measured deflections could be predicted satisfactorily by accepted methods. The CEB recommendations were found to give the best correlation.

4. The rotations were up to 48· % less in the plated beams than in the unplated beam at service loads. The measured rotations were used to produce an empirical formula for the Young's Modulus of the concrete at any stage of loading. Using this, the rotations could be predicted within ±12%.

5. The crack widths were reduced in the plated beams by up to 63%. The maximum crack widths at working loads were overestimated by the crack width prediction formulae recommended by both CP 110 and ACI. These formulae were modified to produce empirical formulae satisfying the measured values.

6. The flexural behaviour of the beams had not been adversely affected by exposure to natural weathering over a period of 18 months. No deterioration of the adhesive or adhesive/adhered interface was found over this period. Carbonation had been eliminated on the beam soffit by the presence of the bonded plate reinforcement.

7. Inspection of the plates removed from the long term specimens showed signs of inadequate mixing of the resin/hardener system and inclusions of air. In one beam these areas covered up to 10% of the bonded surface. This beam showed no loss of strength during testing.

8. The durability specimens showed that there are various sealing agents available for coating the epoxy/plat e element, which effectively prevent the ingress of moisture.

9. The preliminary test series of unreinforced concrete prisms with externally bonded plates seemed to indicate that the tensile strength of the epoxy resin when incorporated in the steel/epoxy/concrete composite system is considerably higher than the unrestrained tensile strength of the epoxy.

9.3 SUGGESTIONS FOR FUTURE WORK

The author endeavoured, within the limited time available to assess the effects of the following:

(a) glue and plate thickness, multiple layers of plate, plate jointing

(b) degree of precracking of the beams

(c) long term exposure.

The range of glue and plate thickness was from 1·5 mm to 6 mm. The thinner layers of glue behaved as well as the thicker layers from a bonding point of view although the latter did provide slightly more stiffness. It is thought that in practice the glue layer would be applied in the thinnest layer which would produce a durable high strength bond. Cusens and Smith (28) tested plated beams with glue thicknesses ranging from 0·25 to 1·5 mm and found the minimum acceptable thickness to be 1 mm. However, they were using a different technique of pouring wet concrete onto an uncured epoxy layer applied to the reinforcing plate. The range of glue thicknesses employed when bonding plates onto hardened concrete should, therefore, be extended below 1·5 mm.

The degree of precracking was investigated to a very limited extent. The tests showed that even with beams loaded up to 90% of their failure load prior to bonding on the plate, satisfactory performance was achieved with the added reinforcement. However, some of the results seemed anomalous, as the deformations of the precracked beams were generally found to be less than in the beams which were not cracked prior to plating. This aspect of behaviour needs further examination.

The mode of failure of the plated beams changed, as the plate thickness increased, from purely flexural to a shear/bond type. The latter should be avoided as there is less warning and it is more brittle. It is thought that this type of failure could be avoided by modifying the ends of the plate. The plate thickness or width near the ends of the beams could be reduced, or some means of anchoring the plate ends may be effective. In one beam of the present investigation, the thickness of the plate at the ends was reduced and this produced a slightly higher failure load. This is an area which requires further study.

The beams in the present series were all tested with an identical shear span. The effect of varying this should be investigated.

Some assessments of interfacial stresses were made from the test data of the present investigation. These were not limiting values. Tests should be designed to assess the limiting shear and bond stresses in plated beams.

The behaviour of the epoxy resin, especially its tensile contribution in the calculation of the ultimate strength of a beam, should be studied further as it is thought that its tensile strength in the composite system could be considerably higher than the unrestrained value.

Long term test beams have been set up. The tests performed after 18 months showed no loss of performance or deterioration of the epoxy resin. However, 18 months is a very short period in comparison to the life of a structure. Tests must be carried out on beams after increasing lengths of exposure to the elements.

APPENDIX 1 (12) (74)

GLOSSARY OF TERMS RELATING TO ADHESIVES TECHNOLOGY

The rapid growth in the use of adhesives has led to an extensive technical vocabulary. The following pages present a selection from various sources.

ADHERE	fasten together two surfaces by adhesion.
ADHEREND	a body which is attached to another body by an adhesive.
ADHESION	the state of being held together by means of an interlayer of adhesives between adherend interfaces; the attachment of two surfaces by interfacial forces consisting of molecular forces, chemical bonding forces, interlocking action, or combinations of these.
ADHESIVE	a material that binds other materials together by surface attachment.
BATCH	a production quantity derived from a manufacturing process or a mixture of these resulting from the same process conditions.
BOND	the union of two materials by adhesives.
CATALYST	a chemical substance which accelerates adhesive curing when added in small amounts to the larger quantities of the reactants: material which promotes cross linking in a polymer or accelerates adhesive drying.
COHESION	internal adhesion; the ability to resist rupture within the bulk material.

CORROSION	the chemical reaction between the adhesive or contamination and the adherend surfaces, due to reactive components in the adhesive leading to deterioration of the bond strength.
CREEP	the dimensional change with time of a material under sustained load.
CROSS LINKING	the union of adjacent molecules of uncured adhesives (often existing as long polymer chains) by catalytic or curing agents.
CURE	to alter the physical properties of an adhesive by chemical change, e.g. polymerisation, brought about by the agency of heat, pressure, or catalysts.
DEGREASE	to remove oil and grease from adherend surfaces.
DELAMINATION	the separation of layers due to adhesive failure.
DURABILITY	the resistance to reduction in joint strength shown by adhesives to moisture, heat, chemicals and biodeterioration etc.
EXTENDER	a non reactive liquid substance added to epoxy compounds to extend pot life, increase flexibility and lower the cost.
FAILURE, ADHESIVE	joint failure such that the separation occurs at the surface of the adherend, e.g. the failure in adhesion of a pressure sensitive tape when peeled from an adherend.
FAILURE, COHESIVE	joint failure within the adhesive.

FATIGUE	a condition of stress from repeated flexing or impact force upon the adhesive-adherend interface.
FILLER	an adhesive additive intended to improve their strength and performance.
FLEXIBILISER	a substance which will react with epoxy compounds to impart flexibility.
GEL	a semi-solid system consisting of a network of solid aggregates in which liquid is held.
HARDENER	a catalytic or cross linking material used to promote setting of adhesives.
INTERFACE	the contact area between adherend and adhesive surfaces.
JOINT	the junction of two adherends which are held together by an adhesive layer.
PASTE	a high viscosity adhesive composition.
PENETRATION	the passage of an adhesive into an adherend.
PH	a measure of acidity or alkalinity.
PHASE	a homogenous and physically distinct part of a system separated from other parts by definite bounding surfaces.
PLASTICISER	a material added to an adhesive to increase its flexibility.
POLYMER	a compound formed by the reaction of identical simple molecules containing active functional groups to produce a high molecular weight material.

POROSITY	the ability of an adherend surface to absorb an adhesive.
POT-LIFE	the effective working time for an adhesive after preparation.
PRETREATMENT	those treatments, mechanical, chemical or physical which are applied to adherends to promote adhesive properties.
PRIMER	an adherend surface coating applied before the adhesive to improve bond performance.
REACTIVE DILUTENT	a low viscosity liquid dilutent for solvent free thermosetting resins of high viscosity. The dilutent undergoes chemical reaction with the adhesive whilst curing proceeds.
RELATIVE HUMIDITY	the ratio of the weight of water in a given volume of air to the weight required to saturate it at the same temperature.
RESIN	the general term for natural and synthetic polymers which are amorphous and have no fixed melting point.
RETARDER	an additive which slows the rate of a chemical reaction.
RHEOLOGY	the study of deformation and flow behaviour of materials under stress.
SET	the conversion of an adhesive into a permanently cured state by chemical or physical means.
SHRINKAGE	the volume reduction occurring during adhesive curing.
SLIPPAGE	the movements of adherends relative to each other during bonding.
STORAGE LIFE	the time period for which an adhesive remains usable when stored under specified temperature conditions.

STRENGTH, CLEAVAGE	the tensile load expressed as force per unit width of bond required to cause cleavage separation of a test specimen of unit length.
STRENGTH, FATIGUE	the maxmimum load that a joint will sustain when subjected to repeated stress application under specified conditions, i.e. range of stress, mean value, frequency of application.
STRENGTH, IMPACT	ability of material to resist shock.
STRENGTH, PEEL	the resistance of an adhesive joint to peel stress, the force per unit width of bond at failure.
STRENGTH, SHEAR	the resistance of an adhesive joint to shearing stress. The force per unit area sheared at failure.
STRENGTH, TENSILE	the resistance of an adhesive joint to tensile stress; the force per unit area under tension at failure.
SUBSTRATE	the material surface to which an adhesive material is applied for bonding or coating or other purposes.
SURFACE PREPARATION	the physical and chemical methods employed to prepare an adherend surface for bonding.
THERMO PLASTIC	susceptible to repeated softening by heating and hardening by cooling.
THERMO SET	a material which does not soften on heating, as a result of being formed from an irreversible chemical reaction initiated by a catalyst.
VISCOSITY	a measure of resistance to flow of a liquid.

APPENDIX 2 (54)

THEORETICAL STRESS DISTRIBUTION IN A BONDED LAP JOINT UNDER COMPRESSION

Notation

u	axial deformation of adherends
γ	angular deformation
τ	shear stress in the adhesive
E	modulus of elasticity of adherends
G	modulus of rigidity of adhesive $\left[\frac{E_g}{1(2+\gamma_g)}\right]$
t_1	semi-thickness of concrete
t_2	thickness of steel plate
d'	thickness of adhesive
c	$= G/d'$
P	= applied load

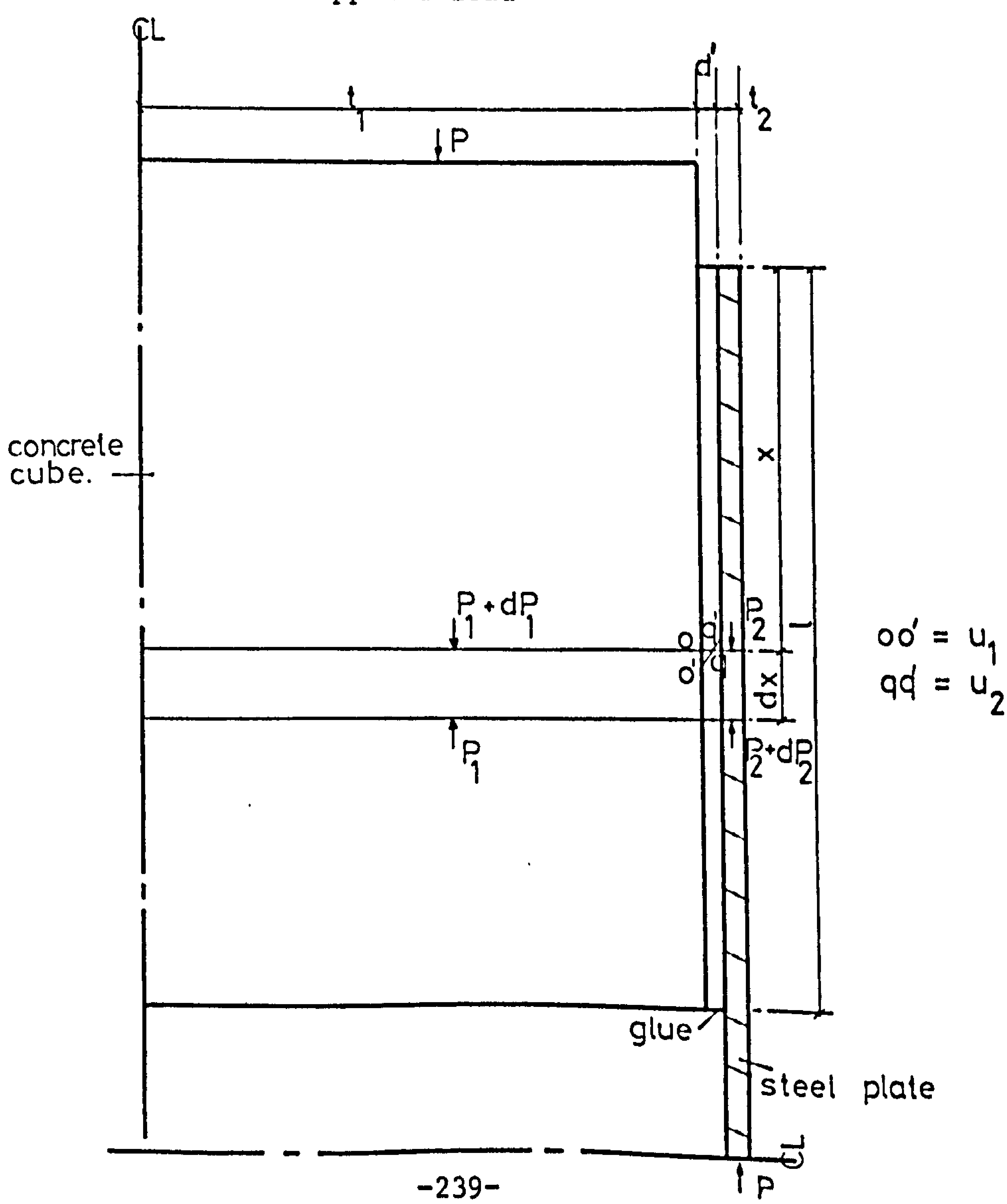

$$P_1 + P_2 = P$$

$$\gamma = \frac{u_2 - u_1}{d'} = \frac{\tau}{G}$$

or $$\tau = c\,(u_2 - u_1)$$

$$\frac{d\tau}{dx} = c\left(\frac{du_2}{dx} - \frac{du_1}{dx}\right)$$

$$\frac{du_1}{dx} = \frac{P_1}{E_1t_1} \qquad \frac{du_2}{dx} = \frac{P_2}{E_2t_2}$$

$$\frac{d\tau}{dx} = c\left(\frac{P_2}{E_2t_2} - \frac{P_1}{E_1t_1}\right) \quad \text{but } P_1 = (P - P_2)$$

$$\frac{d\tau}{dx} = c\left(\frac{P_2}{E_2t_2} + \frac{P_2}{E_1t_1}\right) - \frac{cP}{E_1t_1}$$

$$\frac{d^2\tau}{dx^2} = c\left(\frac{1}{E_1t_1} + \frac{1}{E_2t_2}\right) \quad \frac{dP_2}{dx}$$

putting $w^2 = c\left(\frac{1}{E_1t_1} + \frac{1}{E_2t_2}\right)$ and $\tau = \frac{dP_2}{dx}$

$$\frac{d^2\tau}{dx^2} - w^2\tau = 0$$

The general solution of this differential equation is:

$$= A \sinh wx + B \cosh wx$$

when $x = 0$ $\qquad P_2 = 0$

$$\frac{d\tau}{dx} = Aw = \frac{-cP}{E_1t_1} \qquad A = -\frac{c}{w}\;\frac{P}{E_1t_1}$$

when $x = 1$ $\qquad P_2 = P$

$$\frac{d\tau}{dx} = cP\left(\frac{1}{E_1t_1} - \frac{1}{E_2t_2}\right) - \frac{cP}{E_1t_1} = -\frac{c}{w}\;\frac{Pw}{E_1t_1}\cosh wl + Bw \sinh wl$$

$$\therefore \quad B = \frac{c}{w}\;\frac{P}{\sinh wl}\left(\frac{1}{E_2t_2} + \frac{\cosh wl}{E_1t_1}\right)$$

$$\therefore \qquad \tau(x) = \frac{cP}{w \sinh wl}\left(\frac{\cosh w(l-x)}{E_1t_1} + \frac{\cosh wx}{E_2t_2}\right) \qquad (1)$$

But $\tau = \dfrac{dP_2}{dx} = c(u_2 - u_1)$

$$\frac{d^2P_2}{dx^2} = c\left(\frac{du_2}{dx} - \frac{du_1}{dx}\right)$$

so
$$\frac{d^2P_2}{dx^2} = cP_2\left(\frac{1}{E_1t_1} + \frac{1}{E_2t_2}\right) - \frac{Pc}{E_1t_1}$$

then
$$\frac{d^2P_2}{dx^2} = w^2P_2 - \frac{Pc}{E_1t_1}$$

The general solution of this differential equation is:

$$P_2 = A\cosh wx + B\sinh wx + C$$

Then
$$\frac{d^2P_2}{dx^2} = w^2(A\cosh wx - B\sinh wx)$$

$$\therefore \qquad w^2(A\cosh wx + B\sinh wx) = w^2(A\cosh wx + B\sinh wx) + w^2C - \frac{Pc}{E_1t_1}$$

$$\therefore \qquad C = \frac{Pc}{w^2E_1t_1}$$

when $x = 0 \quad P_2 = 0$

$$0 = A + \frac{Pc}{w^2E_1t_1} \qquad \therefore \quad A = -\frac{Pc}{w^2E_1t_1}$$

when $x = l \quad P_2 = P$

$$P = \frac{-Pc}{w^2E_1t_1}\cosh wl + B\sinh wl + \frac{Pc}{w^2E_1t_1}$$

$$\therefore \qquad B = \left(\frac{Pc}{w^2E_1t_1}\cosh wl - \frac{Pc}{w^2E_1t_1}\right)\frac{1}{\sinh wl} + \frac{P}{\sinh wl}$$

$$\therefore \qquad P_2 = \frac{Pc}{w^2E_1t_1}\left[1 - \cosh wx + \frac{(\cosh wl - 1)}{\sinh wl}\sinh wx\right] + \frac{P\sinh wx}{\sinh wl} \qquad (2)$$

These theoretical distributions are plotted in Fig. 3.7.

APPENDIX 3

PRELIMINARY TEST SERIES

LOADING SYSTEM - Series A, Odd numbered beams.

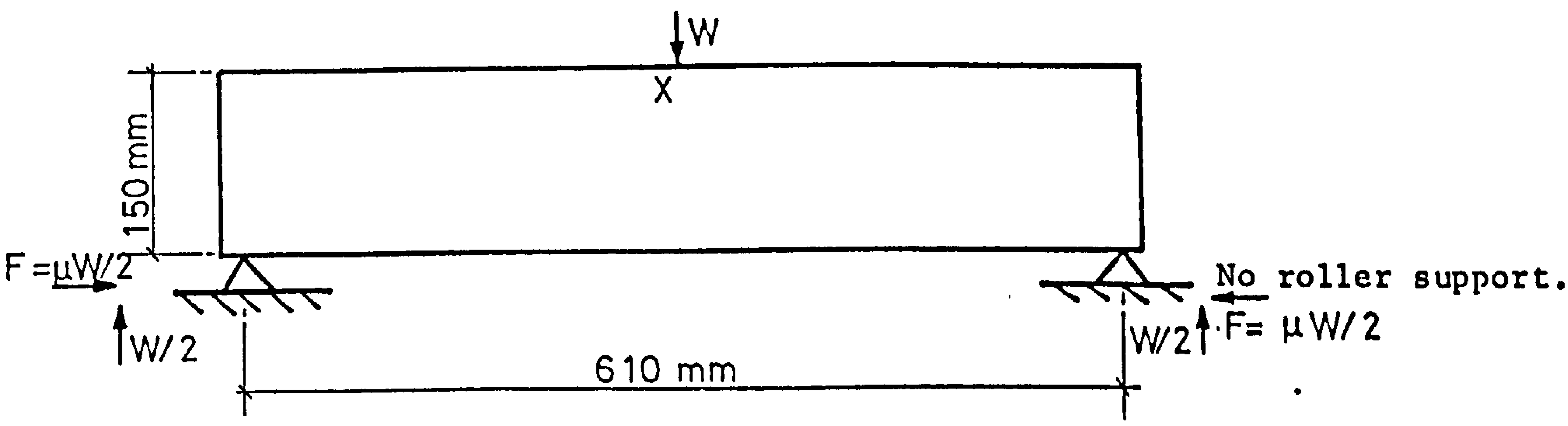

Bending moment at X:

$$\frac{W.\ 0.61}{4} - \frac{W}{2}.\ 0.15.\ \mu. \qquad \mu = \text{coeff. of friction.}$$

Assuming $\mu = 0.5$ for concrete on steel:

$$M_x = 0.152\ W - 0.0375\ W = \underline{0.1145\ W}.$$

LOADING SYSTEM - Series A, Even numbered beams.

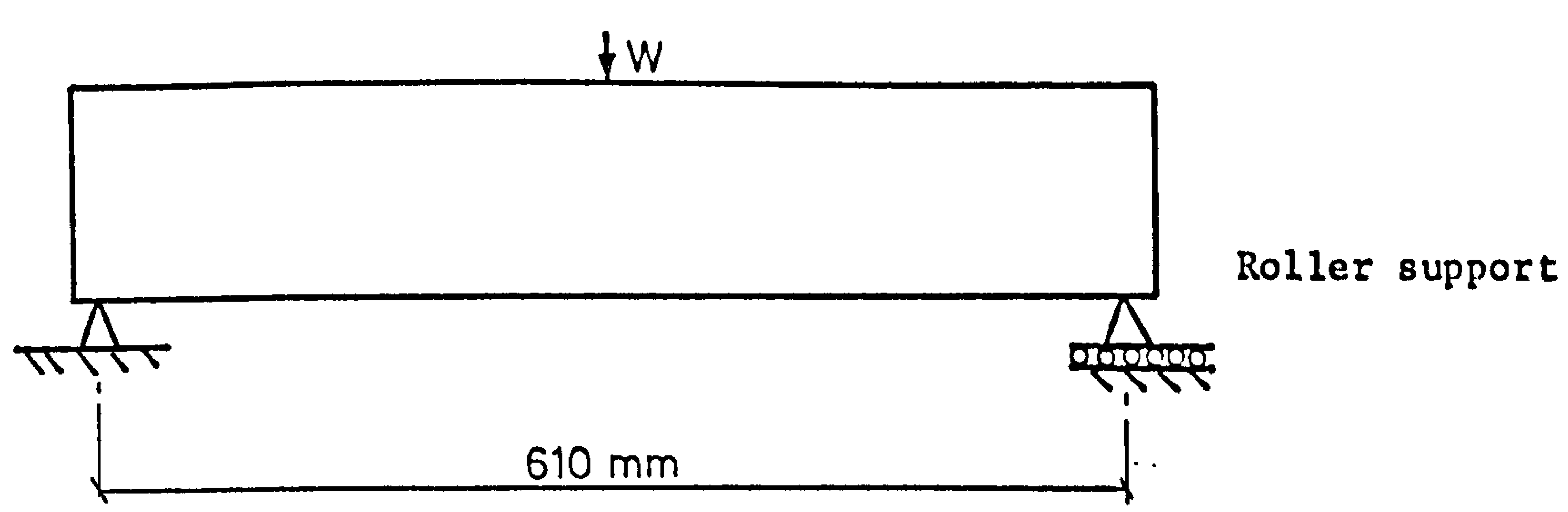

$$M = \frac{W.\ 0.61}{4} = \underline{0.152\ W}$$

CALCULATION OF FIRST CRACK LOAD IN CONCRETE - BEAM A1

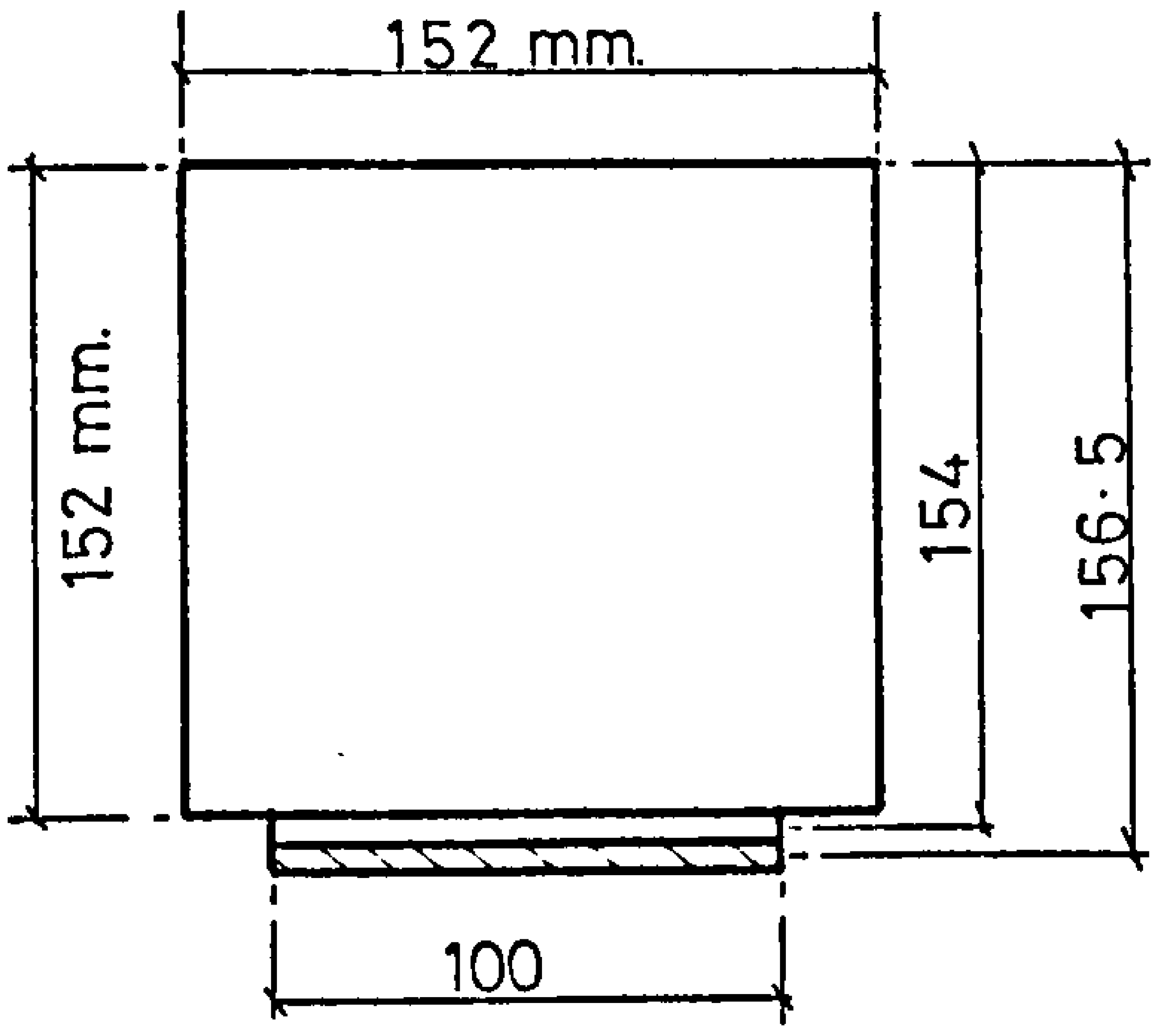

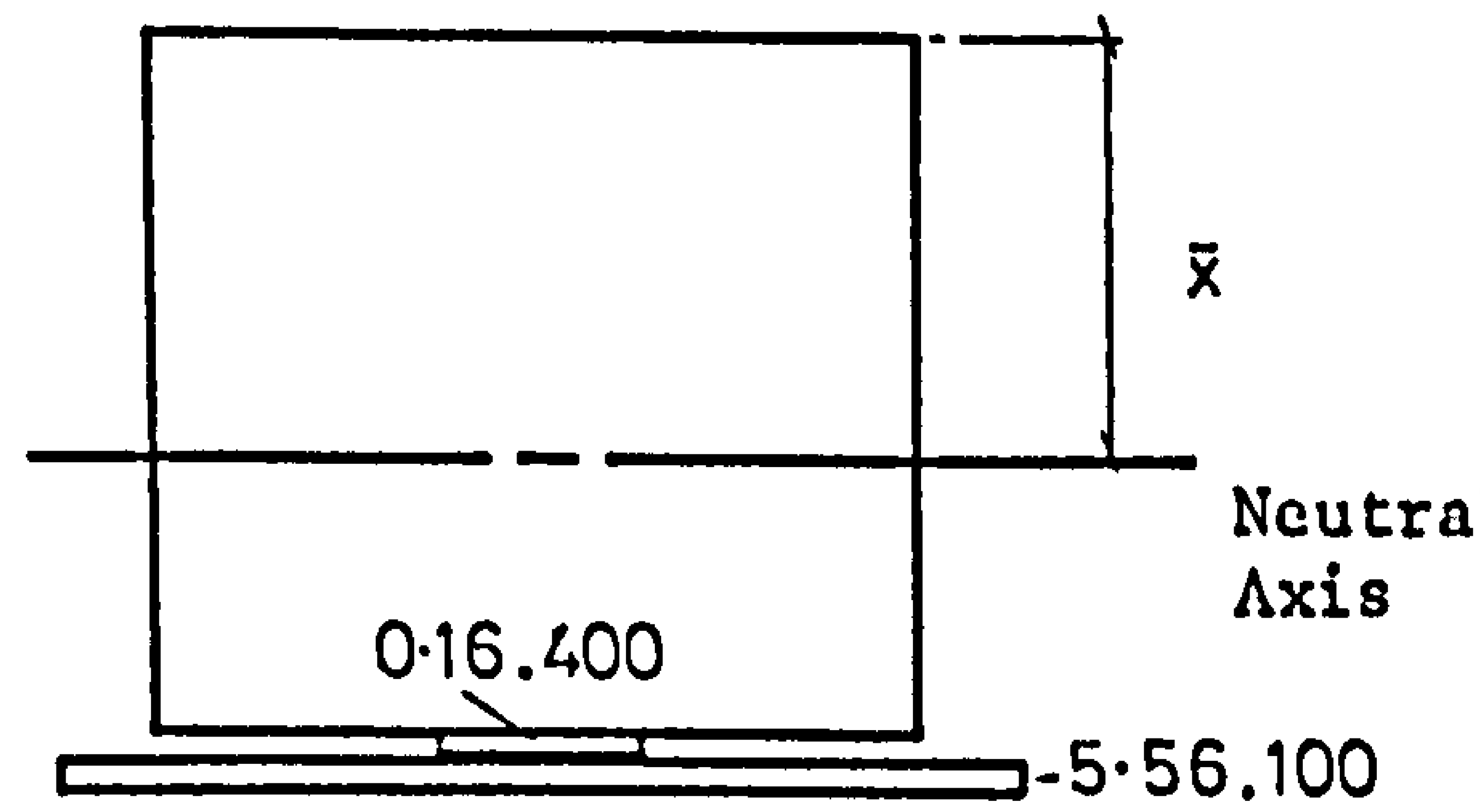

Transformed Section

Modulus of elasticity of steel plate = 200 kN/mm^2 α_s = 5·56

"   "   "   " concrete = 36 kN/mm^2

"   "   "   " glue = 6 kN/mm^2 α_g = 0·167

Location of Neutral Axis:

$$\bar{x}(152.152 + 16.4 + 556.1) = (152.\frac{152^2}{2} + 16.4.154 + 1.556.156{\cdot}5)$$

$$\underline{\bar{x} = 78{\cdot}09 \text{ mm}}$$

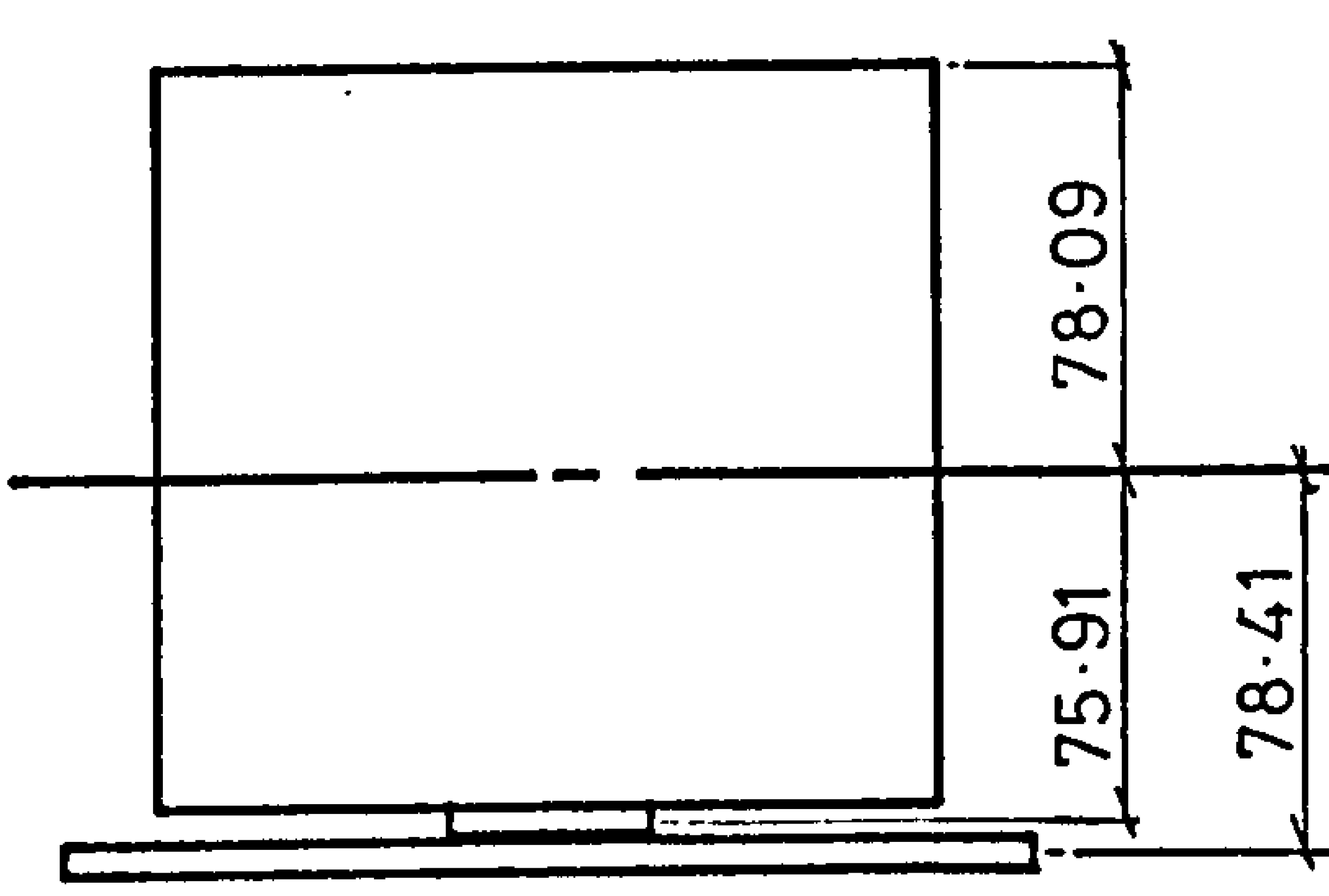

Taking moments about the Neutral Axis:

$$I = \frac{152.78{\cdot}09^3}{12} + 152.78{\cdot}09\left(\frac{78{\cdot}09}{2}\right)^2 + \frac{152.73{\cdot}91^3}{12} + 152\left(\frac{73{\cdot}91}{2}\right)^2.73{\cdot}91 \quad \text{(Concrete)}$$

$+ 16.4.75{\cdot}91^2$ (Glue, neglecting its inertia about its own axis)

$+ 555.78{\cdot}41^2$ (Steel, "   "   "   "   "   "   ")

$I_u^1 = \underline{4{\cdot}84.\ 10^7 \text{ mm}^4}.$

$M = \frac{\sigma I}{y}$ Modulus of rupture σ = 4·37 N/mm^2

y = 73·91 mm

$\therefore$ <u>First Crack Moment</u> $= \frac{4{\cdot}84.10^7.\ 4{\cdot}37}{73{\cdot}91} = \underline{3{\cdot}06 \text{ kNm}}.$

CALCULATION FOR FIRST CRACK LOAD IN THE GLUE - BEAM A1

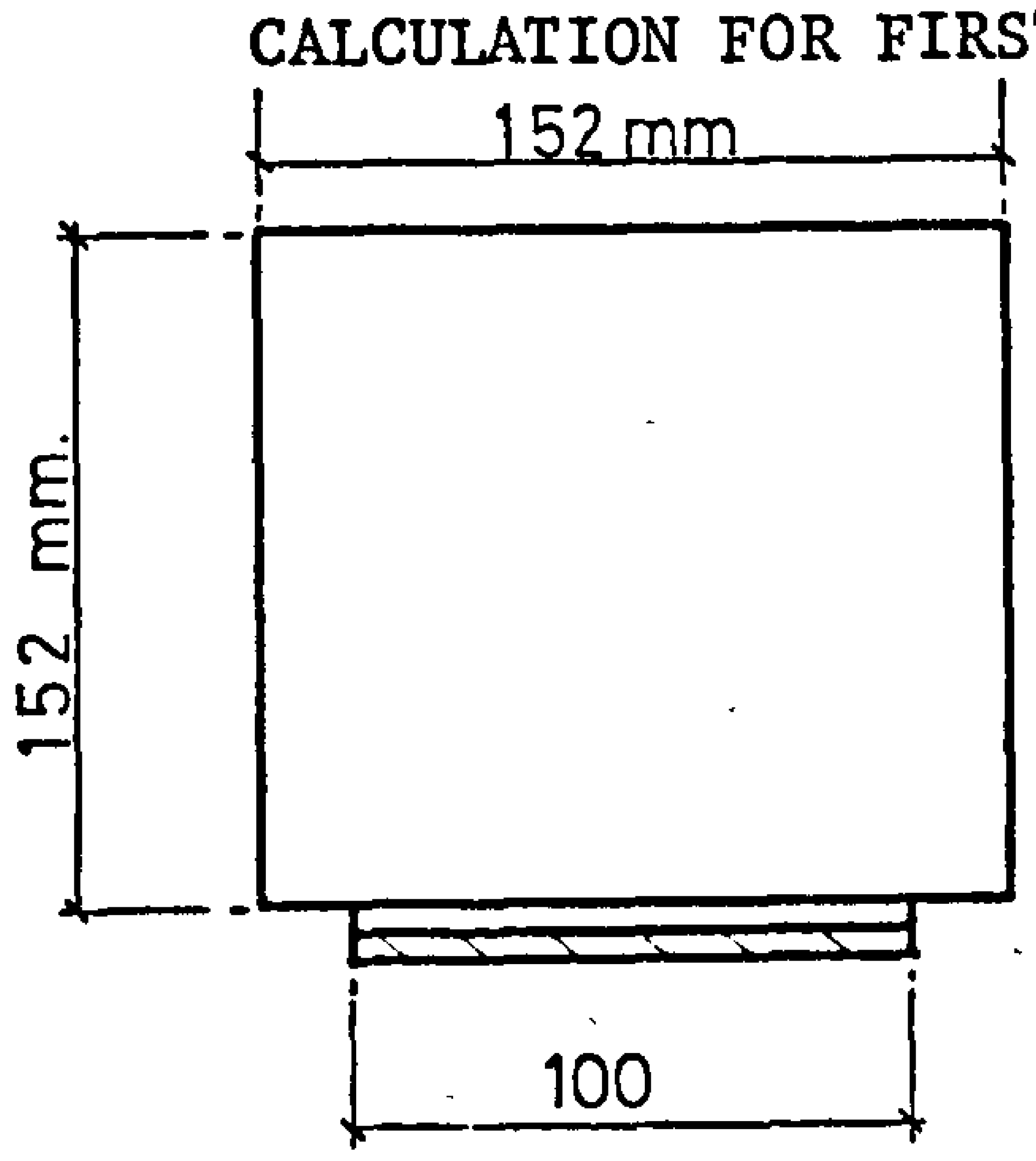

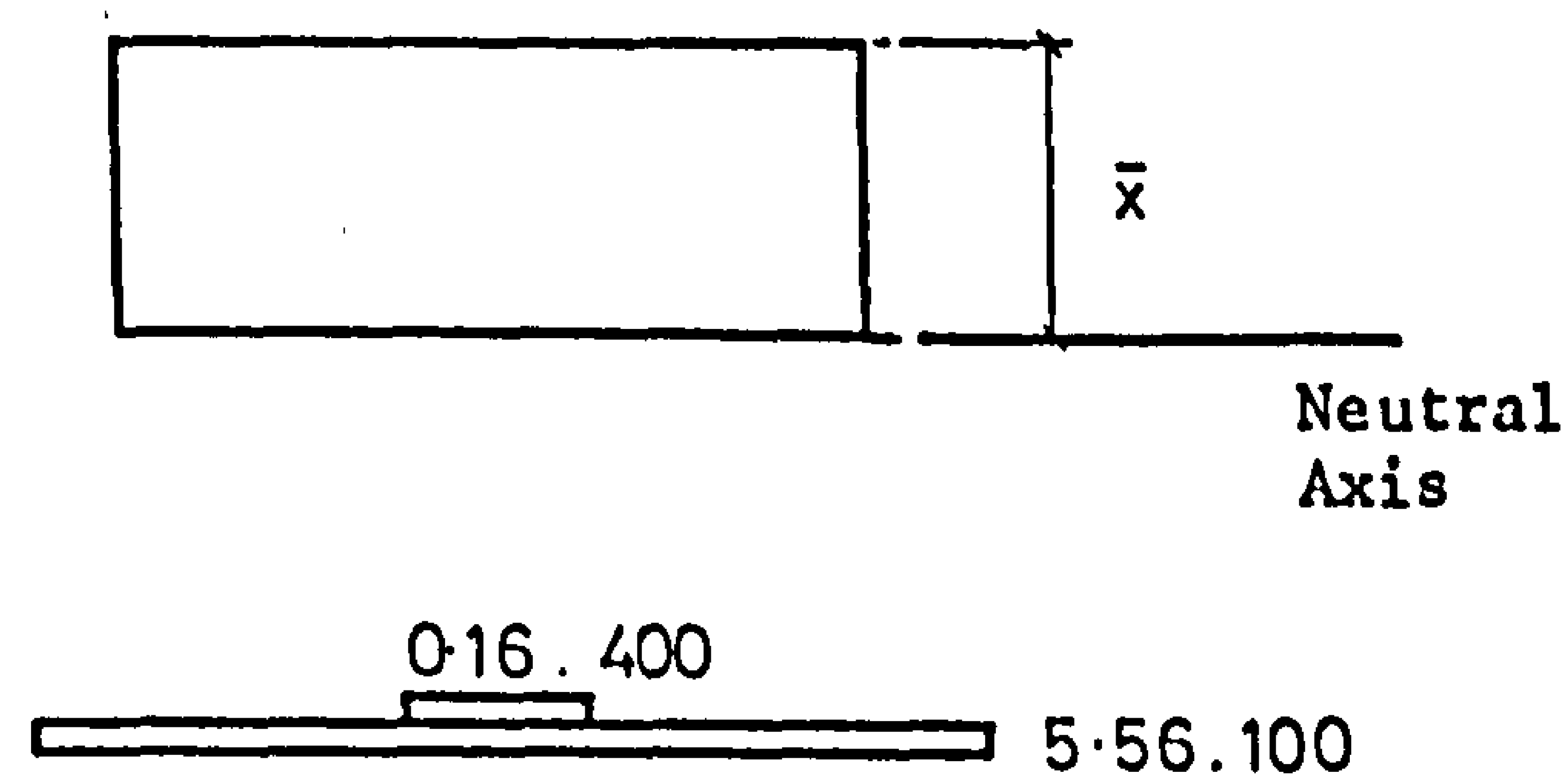

Transformed Section

Moduli as before.

Location of Netral Axis:

$$\bar{x}(152\bar{x} + 16.4 + 556.1) = \left(\frac{152\bar{x}^2}{2} + 16.4.154 + 556.1.156{\cdot}5\right)$$

$$152\bar{x}^2 + 619\bar{x} = 76\bar{x}^2 + 96714 =$$

$$\bar{x}^2 + 8{\cdot}14\bar{x} - 1273 = 0.$$

Hence $\underline{\bar{x} \;=\; 31{\cdot}8 \text{ mm}}$.

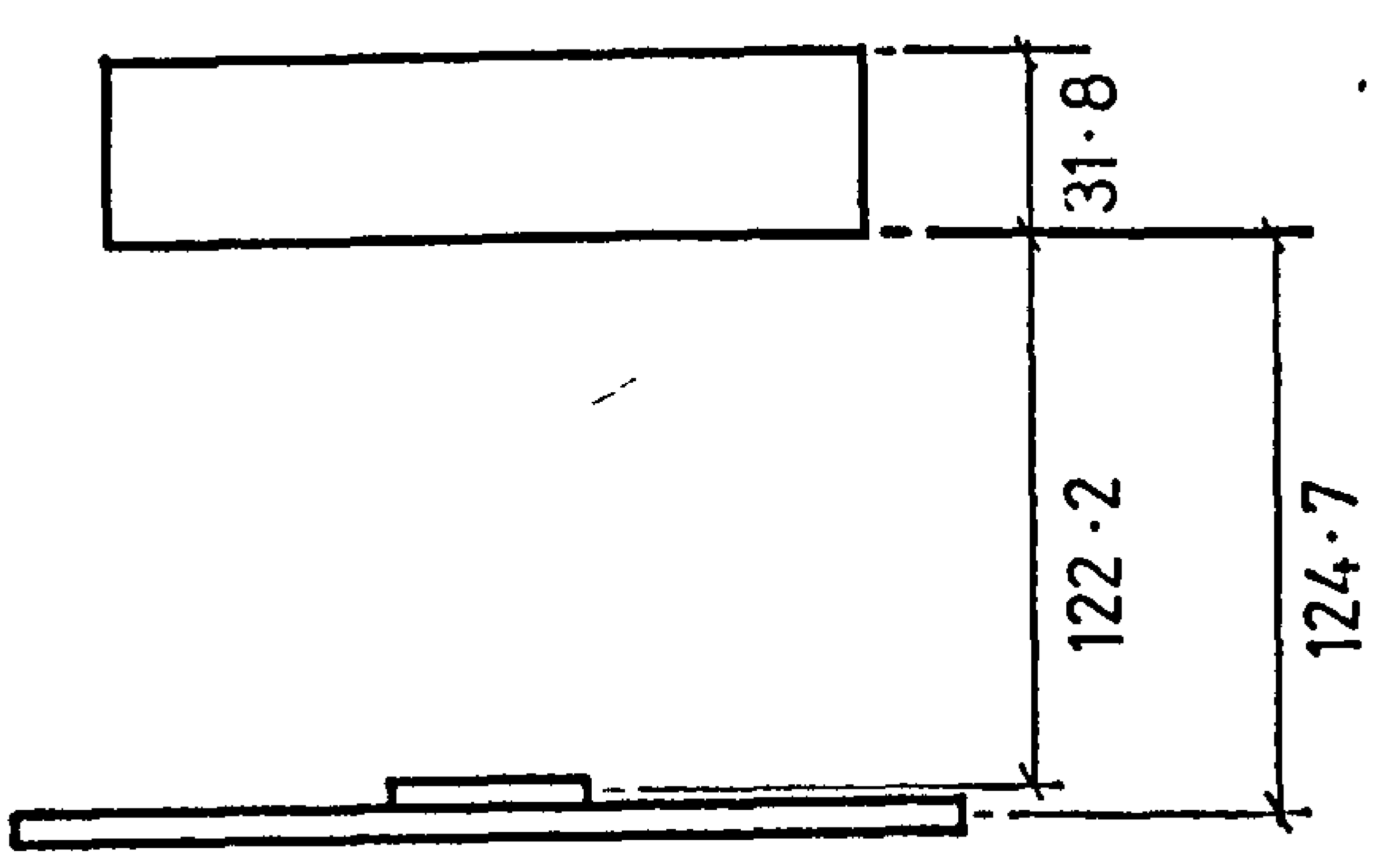

Moment of Inertia, taking moments about the Neutral Axis:

$$I = 152.\frac{31{\cdot}8^3}{12} + 152.31{\cdot}8\left(\frac{31{\cdot}8}{2}\right)^2 \text{ (Concrete)}$$

$$+\ 16.4.122{\cdot}2^2 \text{ (Glue, neglecting insertia about its own axis)}$$

$$+\ 555.1.124{\cdot}7^2 \text{ (Steel, neglecting insertia about its own axis)}$$

$$I^1_{CR} = \underline{1{\cdot}12.10^7 \text{ mm}^4}.$$

$$M = \frac{\sigma I}{y}$$

Tensile strength of glue - 60 N/mm^2

$y = 120{\cdot}2$ mm

<u>First Crack Moment</u> = <u>5·59 kNm</u>.

CALCULATIONS FOR ULTIMATE LOAD. TABLES 4.3 - 4.6.

(c) Based on yield stress of plate, plus tensile strength of glue.

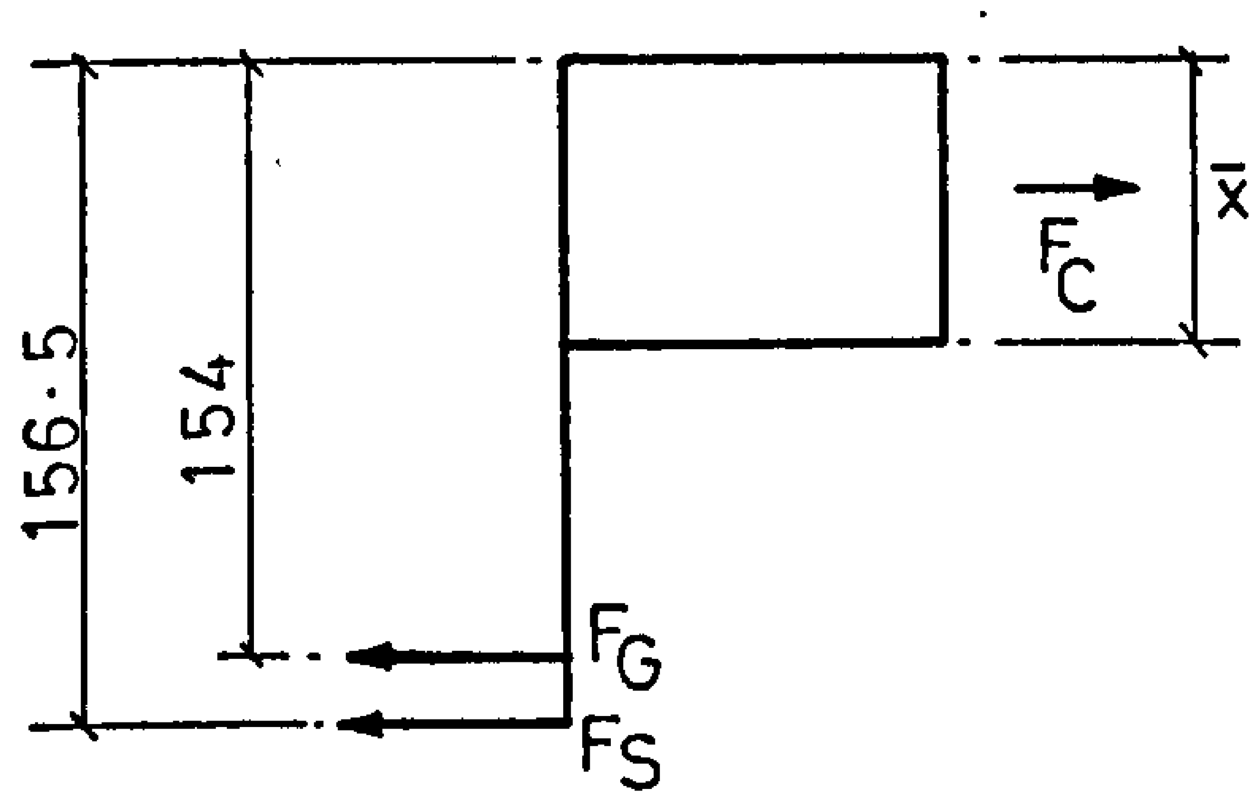

Beam A1 (glue thickness 4 mm).

Force in concrete in compression (CP110)

$0{\cdot}6.\ fcu.\ b.\ \bar{x} = 0{\cdot}6.64{\cdot}6.152\ \bar{x}.$

$F_C = 5891\ \bar{x}.$ N.

$F_G = 60.4.100 = 24000$ N.

$F_S = 125.1.100 = 12500$ N.

fcu = 64·6 N/mm^2

fg = 60 N/mm^2

fy = 125 N/mm^2.

Hence $\bar{x}$ = 6·20 mm.

Then taking moments about the centroid of the compressive force:

M = 24000 (154 - 3·1) + 12500 (156·5 - 3·1) = <u>5·539 kNm.</u>

(d) Based on ultimate stress of plate, plus tensile strength of glue.

As for (c) except F_S = 13200 N.

Hence $\bar{x}$ = 6·31 mm.

M = 24000 (154 - 3.155) + 13·2 (156·5 - 3·155) = <u>5·644 kNm.</u>

(e) Based on ultimate stress of plate, plus no tensile strength in glue.

$\bar{x}$ = 2·24 mm.

M = 13·2 (156·5 - 1·12) = <u>2·051 kNm.</u>

APPENDIX 4

CALCULATION OF ULTIMATE LOADS. BEAMS 201 - 224

Three methods are used for calculating the theoretical ultimate capacities of the test beams.

(a) Ultimate Limit State to CP110

The following assumptions are made:

1. The strain distribution in the concrete in compression is derived from the assumption that plane sections before loading remain plane up to failure.

2. The resistance of concrete in tension is ignored.

3. The relationships between stress and strain in the reinforcing bar, plate and glue are as shown in Figs. 3.8, 3.9 and 3.4 respectively.

4. The distribution of stress in the concrete at failure may be assumed to be equal to a uniform stress of 0.6 fcu over the entire compression zone. The maximum strain at the compression face is taken as 0.35% and the centroid of the stress block is at half the depth of the compression zone.

5. For the purpose of calculating the ultimate capacity of the test beams the material safety factors are equal to 1.0 and the stresses in the bar and plate are their respective 0.2% proof stresses, as taken from Figs. 3.8 and 3.9.

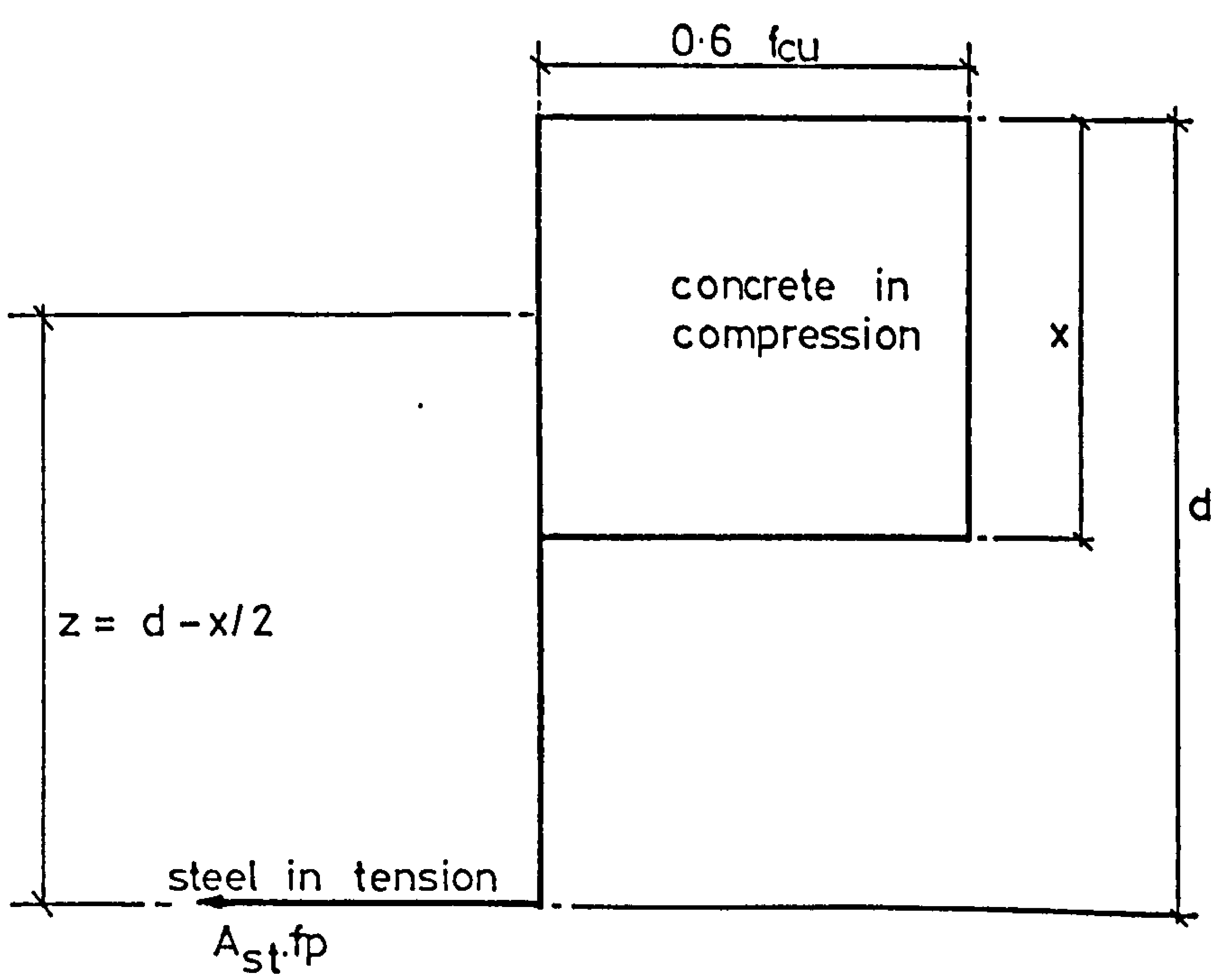

Tensile force = Ast. fp where fp = 0·2% proof stress

Compressive force = 0·6 fcu.x.b where b = width of beam

Hence $x = \dfrac{Ast.\ fp}{0{\cdot}6.b.fcu}$

Also $z = d - x/2 = d\left(1 - 0{\cdot}83\,\dfrac{Ast.\ fp}{b.d.fcu}\right)$

Therefore the ultimate moment capacity Mu is equal to:

$$Mu = Ast.\ fp\ d\left(1 - \frac{0{\cdot}83\ Ast.\ fp}{b.d.fcu}\right)$$

But also $\dfrac{Ast.}{bd} = \rho$

$$Mu = fp.\ \rho.\ bd^2\ \left(1 - \frac{0{\cdot}83\ \rho.\ fp}{fcu}\right)$$

EXAMPLE BEAM 207

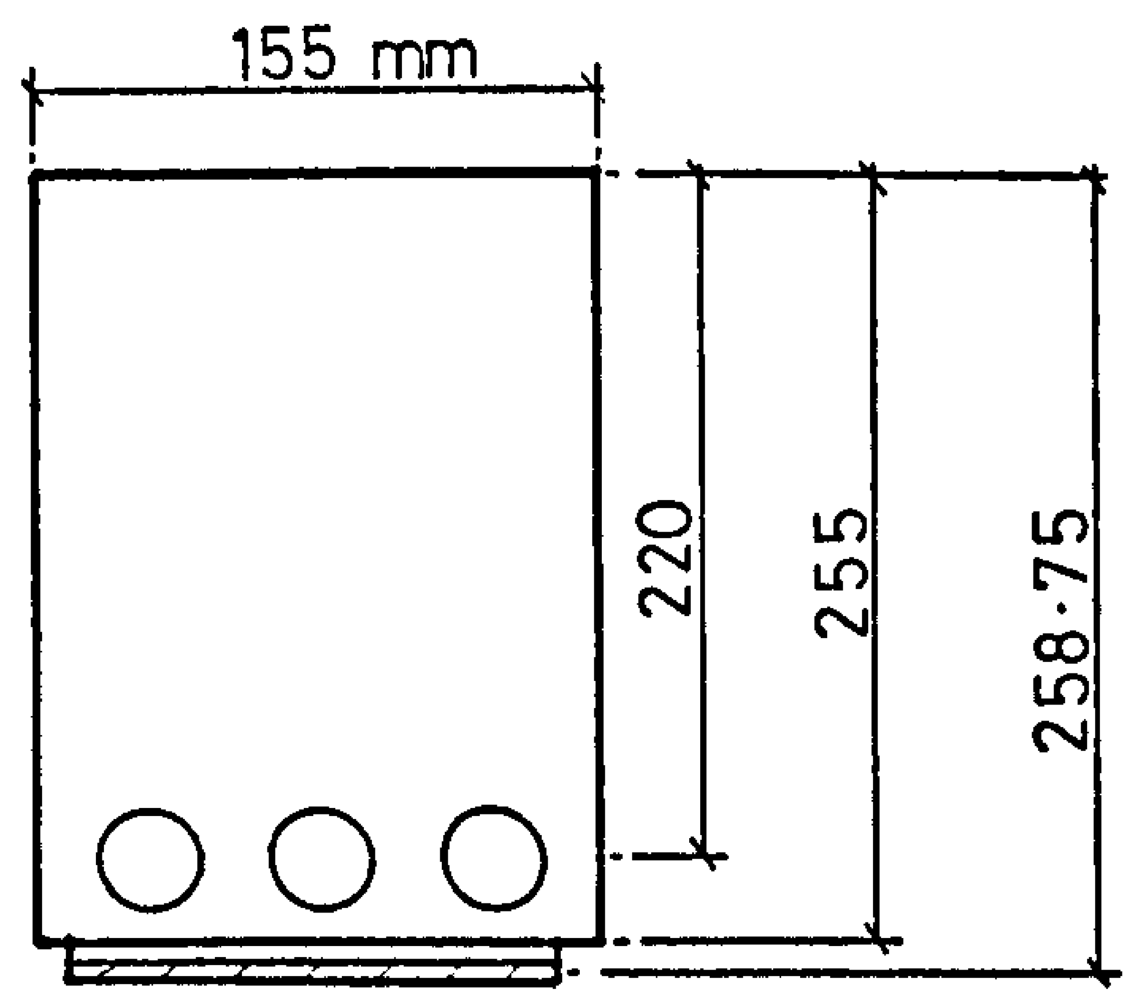

Plate thickness 1·5 mm

Glue thickness 3 mm

fcu 70·2 N/mm²

	Plate	Bar
fp =	275 N/mm²	470 N/mm²
ρ =	0·0047	0·0277
d =	258·75 mm	220 mm

Then the ultimate moment is given by

$$Mu = 275.0{\cdot}0047.155.258{\cdot}75^2 \left(1 - \frac{0{\cdot}83(0{\cdot}0047.275 + {\cdot}0277.470)}{70{\cdot}2}\right)$$

$$+ \; 470.0{\cdot}0277.155.220^2 \left(1 - \frac{0{\cdot}83(0{\cdot}0047.275 + 0{\cdot}0277.470)}{70{\cdot}2}\right)$$

$$= (\underset{\text{Plate}}{11{\cdot}14} + \underset{\text{Bars}}{81{\cdot}10}).10^6 \text{ Nmm}$$

$$= \underline{92{\cdot}24 \text{ kNm}}$$

(b) Strain Compatibility

The basic principle of strain compatibility is that for a given section, including the reinforcement, a neutral axis depth can be found so that the total compression force equals the total tension force; and hence the ultimate moment.

The following assumptions are made:

1. The strain distribution in the concrete in compression is derived from the assumption that plane sections before loading remain plane up to failure.

2. The resistance of concrete in tension is ignored.

3. The relationship between the stress and strain in the reinforcements are as shown in Figs. 3.8 and 3.9, found by experimental tests.

4. The relationship between the stress and strain in the concrete is the rectangular stress block with a maximum concrete compression strain of 0.0035, and a compressive stress of 0·60. fcu.

5. The relationship between the stress and strain in the glue is as shown in Fig. 3.4 found by experimental tests.

6. All material safety factors, γm, are equal to unity.

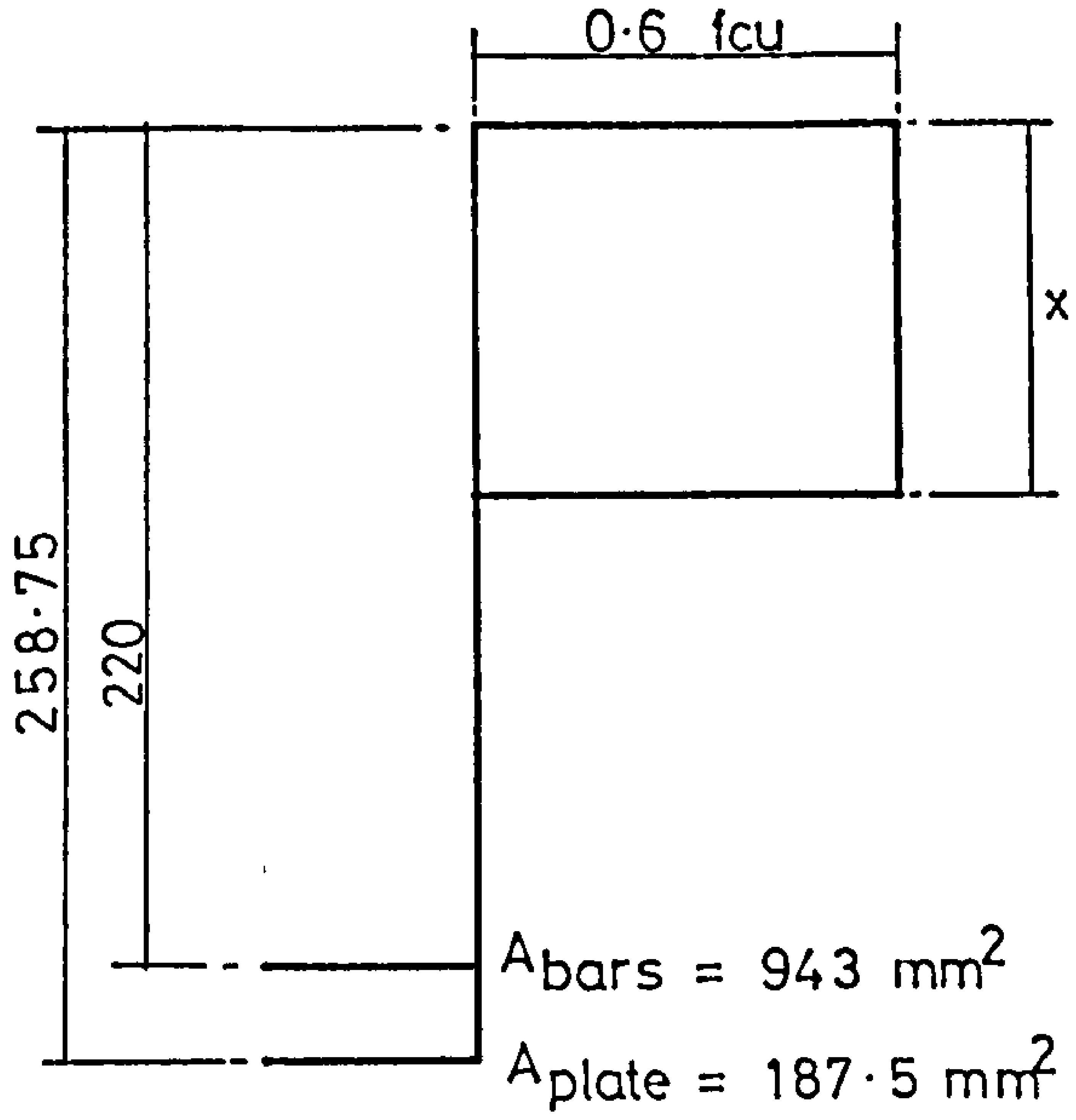

e.g. Beam 207

plate thickness 1·5 mm

glue thickness 3 mm

fcu = 70·2 N/mm^2

(i) <u>First it is assumed that no tensile contribution is made by the glue</u>

Guess f_{plate} = 250 N/mm^2 $\quad f_{bars}$ = 425 N/mm^2

Tensile force = Compressive force

250.187·5 + 425.943 = 0·6 fcu.155 x .

x = 75·74 mm

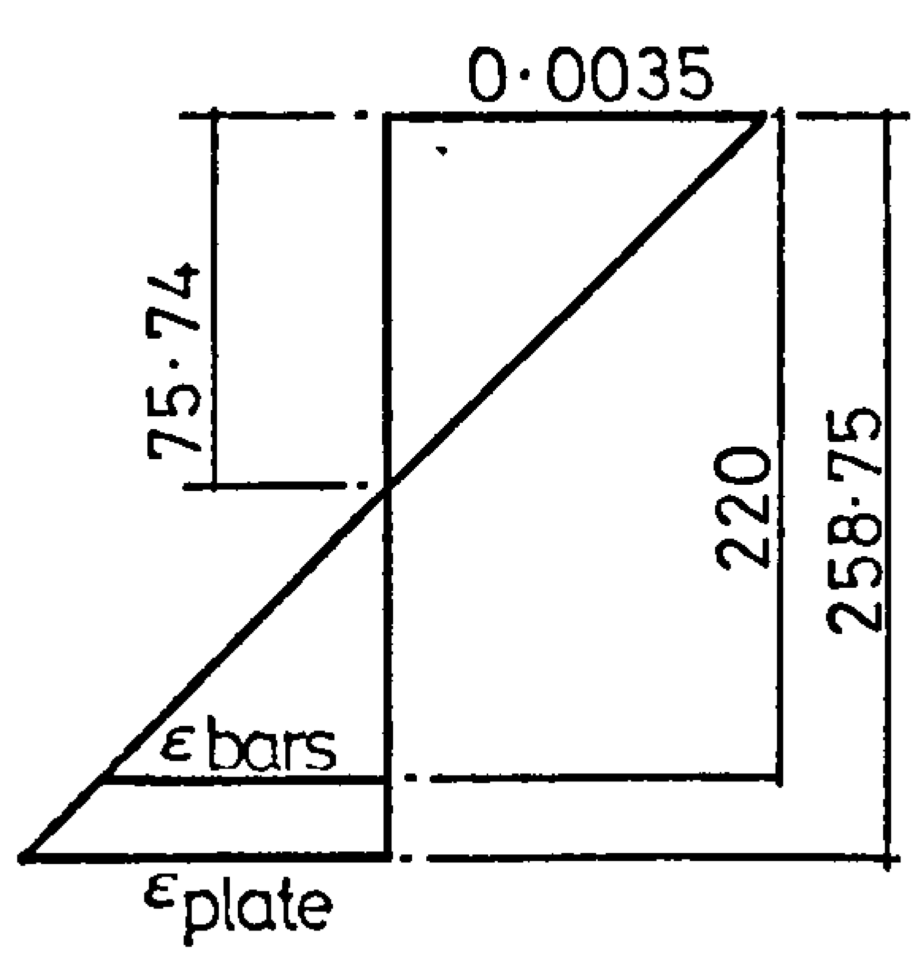

By strain compatibility:-

$$E_{bars} = \frac{220 - 75{\cdot}74}{75{\cdot}74} . {\cdot}0035 = {\cdot}0067$$

$$E_{plate} = \frac{258{\cdot}75 - 75{\cdot}74}{75{\cdot}74} . {\cdot}0035 = {\cdot}0085$$

From the experimental stress strain curves for the steel bar and plate, as shown in Figs. 3.8 and 3.9, the stresses corresponding to these strains are

f_{bars} 490 N/mm^2

f_{plate} 325 N/mm^2

The initial guess, therefore, was incorrect.

Try f_{plate} = 300 and f_{bars} = 490

Then 300.187·5 + 490.943 = 0·6 fcu. 155 x .

x = 79·39

Hence $E_{bars} = \frac{220 - 79{\cdot}39}{79{\cdot}39} . {\cdot}0035 = {\cdot}0062$

$E_{plate} = \underline{258{\cdot}75 - 79{\cdot}39} . {\cdot}0035 = {\cdot}0079$

From the experimental stress strain graphs:

$$\left.\begin{array}{l} f_{bars} = 490 \text{ N/mm}^2 \\ f_{plate} = 297 \text{ N/mm}^2 \end{array}\right\} \quad \text{O.K.}$$

The resistance moment is then found by taking moments about the centroid of the concrete stress block. $(z = d - \frac{x}{2} = d - \frac{79{\cdot}39}{2})$

$$Mu = 187{\cdot}5.300.(258{\cdot}75 - \frac{79{\cdot}39}{2}) + 943.490(220 - \frac{79{\cdot}39}{2})$$

$$Mu = \underline{95{\cdot}5 \text{ kNm}}$$

(ii) <u>Assuming the glue remains uncracked up to failure the force it imparts is included in the tensile component</u>

Assume $f_{glue} = 15 \text{ N/mm}^2$ $f_{plate} = 300 \text{ N/mm}^2$ $f_{rebar} = 490 \text{ N/mm}^2$

$$300.187{\cdot}5 + 490.943 + 15.375 = 0{\cdot}6 \text{ fcu}. 155 \text{ x}.$$

$\therefore \quad x = 80{\cdot}25$ mm

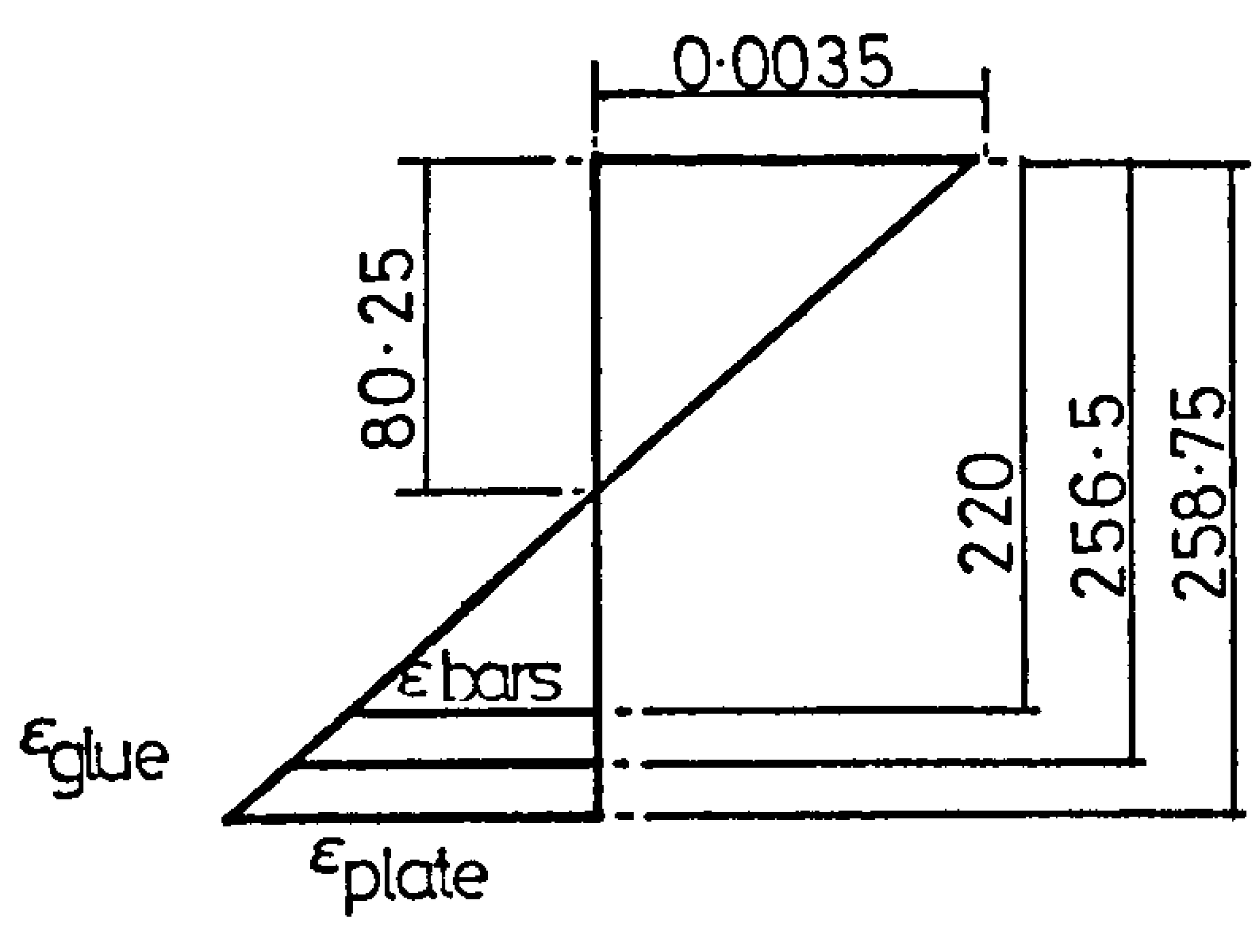

$E_{bars} = \frac{220 - 80{\cdot}25}{80{\cdot}25} . {\cdot}0035 = {\cdot}0061$

$E_{glue} = \frac{256{\cdot}5 - 80{\cdot}25}{80{\cdot}25} . {\cdot}0035 = {\cdot}0077$

$E_{plate} = \frac{258{\cdot}5 - 80{\cdot}25}{80{\cdot}25} . {\cdot}0035 = {\cdot}0078$

from experimental stress/strain graphs:-

$f_{rebar} = 490 \text{ N/mm}^2$

$f_{glue} = 14 \text{ N/mm}^2$

$f_{plate} = 297 \text{ N/mm}^2$

Then $$Mu = 187{\cdot}5.300 (258{\cdot}75 - \frac{80{\cdot}25}{2}) + 943.490 (220 - \frac{80{\cdot}25}{2}) + 15.375 (256{\cdot}5 - \frac{80{\cdot}25}{2})$$

$$= \underline{96{\cdot}6 \text{ kNm}}$$

The calculated ultimate loads are shown in Table 5.4 together with the experimental failure loads.

(c) Strain Compatibility

An alternative, and more refined method of calculation than in (b) is to use the stress distribution in the concrete as suggested by Hognestad, as shown below. (k_1, k_2, ε_c from Fig. 4.4-1, Reinforced and Prestressed Concrete - Kong and Evans.)

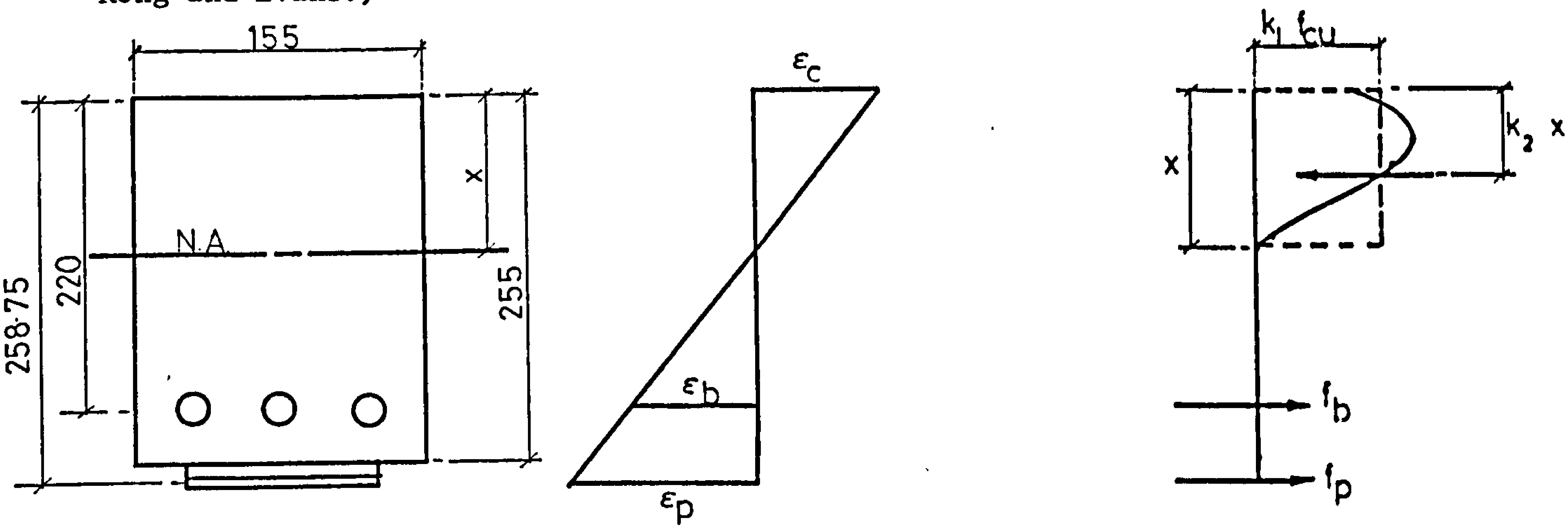

Beam 207

$$\varepsilon_b = \varepsilon_c \left(\frac{220 - x}{x}\right) \quad \text{and} \quad \varepsilon_p = \varepsilon_c \left(\frac{258{\cdot}75 - x}{x}\right)$$

$$k_1 . f_{cu} . b . x = A_p . f_p + A_b . f_b$$

Assume $x = 94$ mm   we also have: $f_{cu} = 70{\cdot}2$ N/mm^2

$f = 295$ N/mm^2 $k_1 = 0{\cdot}48$

$k_2 = 0{\cdot}41$

Then $0{\cdot}48.\ 70{\cdot}2.\ 155.\ 94 = 295.\ 187{\cdot}5 + 943.f_b$

$\therefore \quad f_b = 462$ N/mm^2

With $\varepsilon_c = 0{\cdot}0028$, $\varepsilon_b = 0{\cdot}0028 \left(\frac{220 - 94}{94}\right) = {\cdot}00375.$, $\varepsilon_p = {\cdot}00491$

From the experimental stress/strain curve, Fig. 3.8, the steel stress in the bars corresponding to this strain is 464 N/mm^2, and for the plate the stress is found from Fig. 3.9, 295 N/mm^2. $\therefore$ assumptions were OK. The ultimate moment is then given by:

$$M_u = 464.943\ (220 - 0{\cdot}41.94) + 295.187{\cdot}5\ (258{\cdot}75 - 0{\cdot}41.94)$$

$$= 91{\cdot}6 \text{KNm}$$

Similar calculations for beams 208 (3 mm plate) and 209 (6 mm plate) give values of 100·6 N/mm^2 and 120·1 N/mm^2. These differ from method (b) (i) by 2 to 4% only.

APPENDIX 5

CALCULATION OF DEFLECTIONS

(a) CP 110 Recommendations

This is dealt with in Appendix A of the code. In clause A.1 it states that in general it will be sufficiently accurate to assess the moments and forces at serviceability limit states by using an elastic analysis. When the deflections of reinforced concrete members are calculated there are a number of factors which are difficult to allow for but which have a considerable effect on the reliability of the result:

(a) support conditions

(b) precise loading conditions, especially long term

(c) extent of cracking.

The approach used is to assess the curvatures of sections under the appropriate moments and then calculate the deflections from the curvatures. The recommended procedure involves calculating the curvatures at successive sections along the beam and using numerical integration to compute the deflection. For calculating the curvatures clause A.2.2 gives a procedure which employs an appropriate set of assumptions depending on whether the section is cracked or uncracked. The test beams were all cracked at service load. The assumptions for this are straight forward and are illustrated diagrammatically in Fig. A.5.1.

(i) Strains are calculated on the assumption that plane sections before loading remain plane after loading.

(ii) The reinforcement is assumed to be elastic and its modulus of elasticity is taken as 200 kN/mm^2.

(iii) The concrete in compression is assumed to be elastic. Under short term loading, the modulus of elasticity E_c is used.

(iv) Stresses in the concrete in tension may be calculated on the assumption that the stress distribution is triangular having a value of zero at the neutral axis and a value of 1 N/mm^2 at the centroid of the tension steel.

To obtain a relationship between the bending moment and the curvature a force diagram is drawn and the bending moments taken. The equation for the

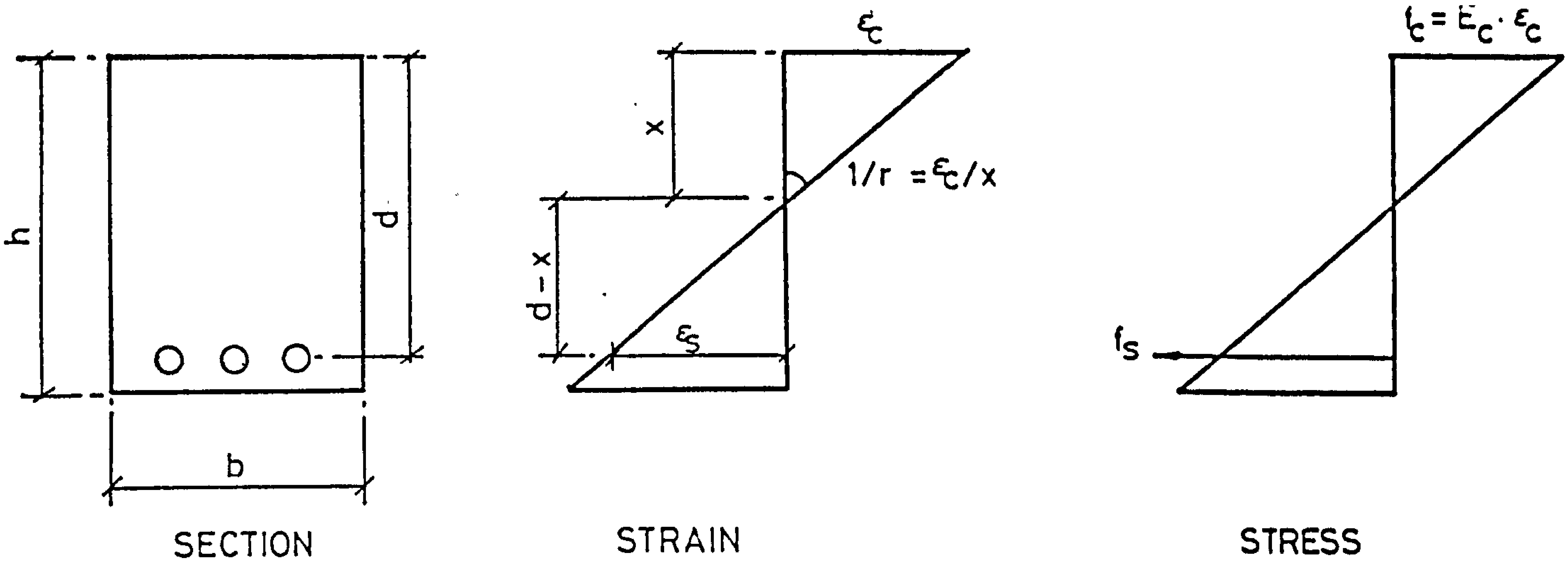

Compressive force = Tensile force

$$\frac{bx}{2} \cdot E_c \varepsilon_c = E_s \varepsilon_s A_s$$

but $\varepsilon_s = \varepsilon_c\left(\frac{d-x}{x}\right)$, $E_s / E_c = \alpha_e$ and $A_s / bd = \rho$

therefore $\frac{bx}{2} E_c \varepsilon_c = E_s \varepsilon_c \left(\frac{d-x}{x}\right) A_s$

or $x^2 = 2\alpha_e \rho d(d-x)$

then $x^2 + 2\alpha_e \rho dx - 2\alpha_e \rho d^2 = 0$

solving this quadratic equation gives: $x = -\alpha_e \rho d \pm d\sqrt{\alpha_e \rho(\alpha_e \rho + 2)}$

or $\frac{x}{d} = -\alpha_e \rho \pm \sqrt{\alpha_e \rho(2 + \alpha_e \rho)}$

also $z = d - \frac{x}{3} = d\left(1 - \frac{x}{3d}\right)$

and $I_e = \frac{bx^3}{12} + bx\left(\frac{x}{2}\right)^2 + A_s \alpha_e (d-x)^2$

or $\frac{I_e}{bd^3} = \frac{1}{3}\left(\frac{x}{d}\right)^3 + \alpha_e \rho \left(1 - \frac{x}{d}\right)^2$.

FIGURE A5·1 ELASTIC ASSUMPTIONS FOR CALCULATING CURVATURES neutral axis depth becomes rather complicated and a further assumption is made to simplify this. It is assumed that the neutral axis depth is calculated on the basis of zero stress in the concrete in the tension zone. This will slightly underestimate the neutral axis depth. Thus, the concrete in tension is ignored when calculating the neutral axis depth, but taken into account when calculating the resistance moment.

In the case of the plated beams the plate area has been added to the bar area and the effective depth is taken to their combined centroid.

EXAMPLE Beam 207

Glue thickness 3 mm $\quad E_c = 36$ kN/mm^2

Plate thickness 1·5 mm $\quad E_s = 200$ kN/mm^2

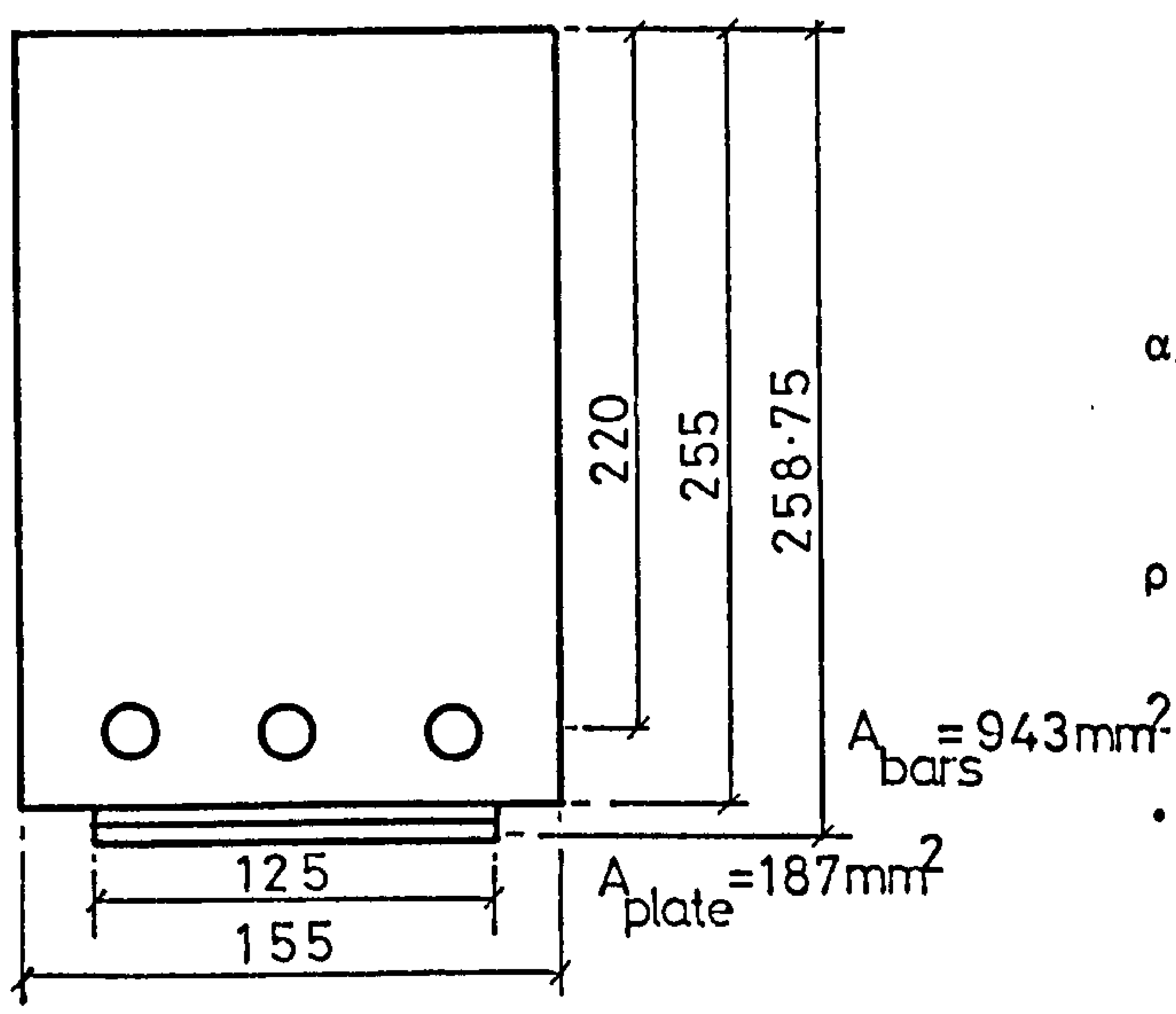

$$\alpha_e = \frac{200}{36} = 5.56$$

$$\rho = \frac{187 + 943}{155.226} = 3\cdot23.10^{-2}$$

$$\therefore \quad \alpha_e \cdot \rho = 0.179$$

From Fig. A.5.1 $\frac{x}{d} = -0\cdot179 + \sqrt{0\cdot179(2\cdot179)}$ Hence $x = 100\cdot6$ mm

and $\frac{I}{bd^3} = \frac{(0\cdot445)^3}{3} + 0\cdot179\ (1 - 0\cdot445)^2$ Hence $I = 1\cdot51.10^8$ mm^4

Next the resistance moment is calculated allowing for the tension stiffening of the concrete. As shown in Fig. A.5.2 the moment due to the concrete in tension is given by $\frac{fct.}{3} \cdot \frac{b(h - x)^3}{(d - x)}$

The deflections of the test beams were calculated at 130 KN load for comparison with experimental values. The applied moment $\frac{(W.L)}{6}$ corresponding to 130 KN load is 49·8 KNm.

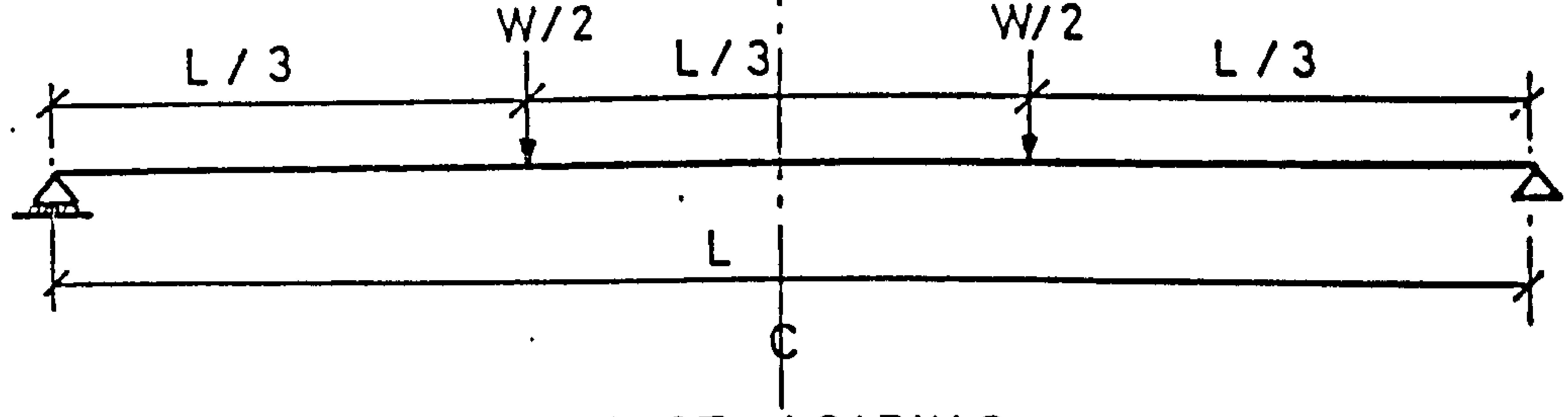

TYPICAL MODE OF LOADING

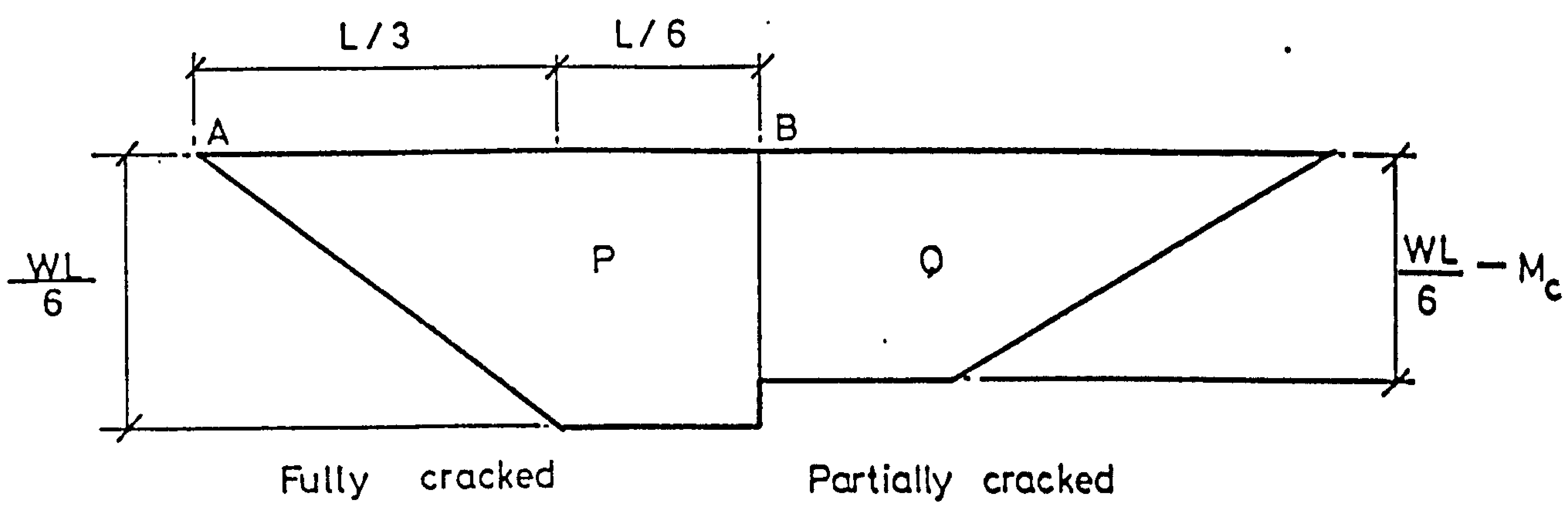

BENDING MOMENT DIAGRAM

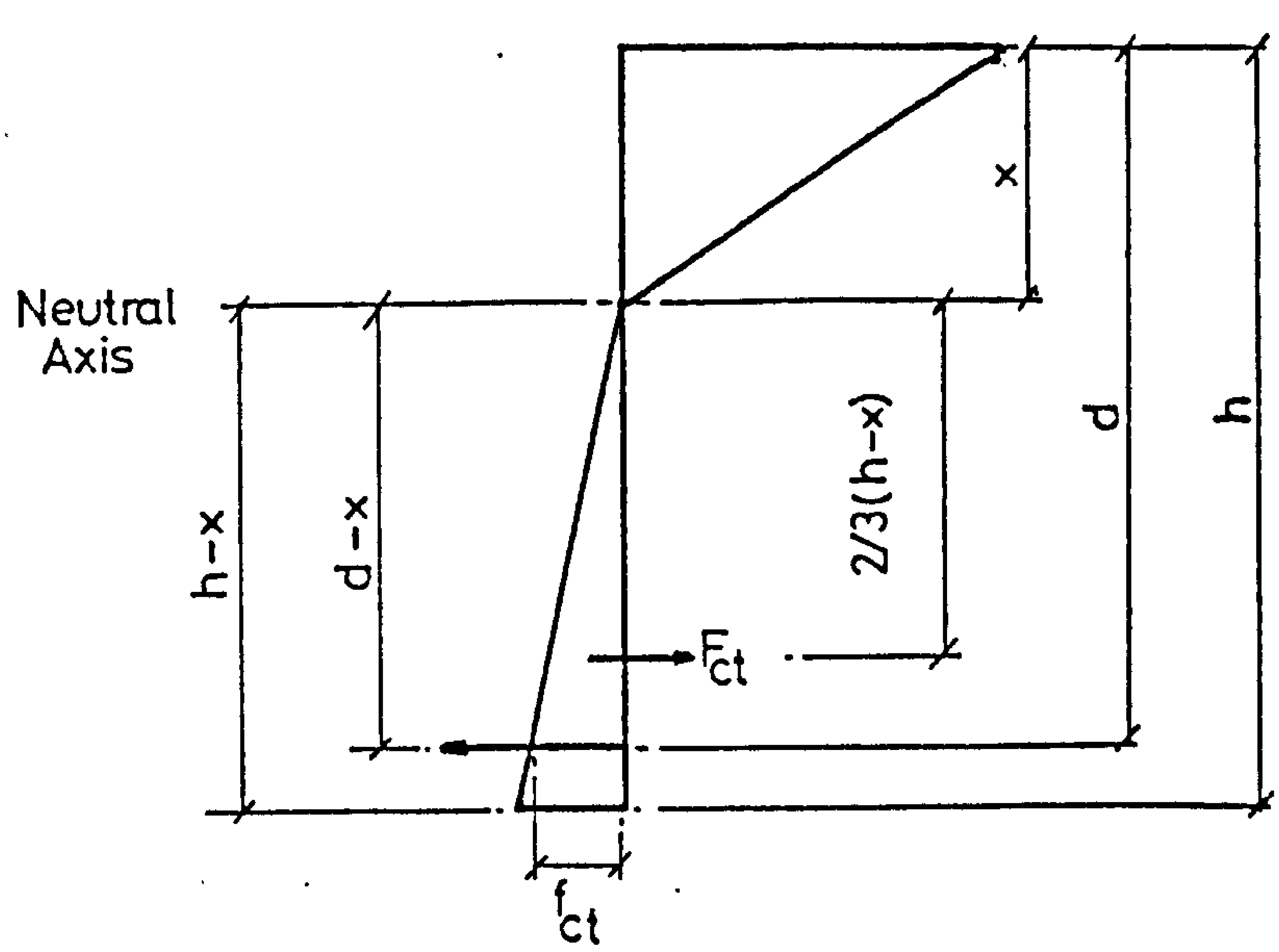

TENSILE CONCRETE

stress at reinforcement level = f_{ct}

stress at extreme fibre = $f_{ct}\dfrac{(h-x)}{(d-x)}$

force in tensile concrete = F_{ct}

$$F_{ct} = f_{ct}\frac{(h-x)}{(d-x)} \cdot b\frac{(h-x)}{2}$$

moment of tensile concrete about neutral axis = $F_{ct} \cdot 2/3\,(h-x)$

$$M_{ct} = f_{ct}\frac{b(h-x)^3}{3(d-x)}$$

FIGURE A5·2 BENDING MOMENT DUE TO THE CONCRETE IN THE TENSION ZONE

The resistance moment $= 49 \cdot 8 - \frac{1}{3} . 155 \frac{(255 - 100 \cdot 7)^3}{(226 - 100 \cdot 7)} . 10^{-6}$ KNm

$= 48 \cdot 3$ KNm

The curvature is then found from simple bending theory. $\frac{M}{I} = \frac{E}{R}$

Therefore $\frac{1}{R} = \frac{48 \cdot 3.10^6}{36.10^3.1 \cdot 51.10^8} = 8 \cdot 9.10^{-6}$ radians.

The deflection can then be found by the simplified approach recommended in clause A.2.3 from the equation $a = kl^2 \frac{1}{R}$.

Where K is a constant which depends on the loading and support conditions, and l is the effective span. The Code Handbook, in Table A3 gives values of K for various loadings and support conditions. In general the deflection of a beam is given by the formula $a = K_1 \frac{Wl^3}{EI}$, but also the bending moment, $M = K_2.W.l$.

For the test beams the loadings are symmetrically placed at the $\frac{1}{3}$ points of the span and the value of K_2 is $\frac{1}{6}$ or 0·167.

For the value of K_1 Macaulay's (81) method can be used as shown in Fig. A.5.3 and is equal to $\frac{23}{1296} = 0 \cdot 01775$.

Combining the equations containing K_1 and K_2: $a = \frac{K_1}{K_2} . \frac{l^2}{EI} . M$

or $K = \frac{0 \cdot 01775}{0 \cdot 1666} = 0 \cdot 1065$ as shown in Table A3 of the code.

Then the deflection for beam 207 is given by:

$a = 0 \cdot 1065 . 2300^2 . 0 \cdot 89.10^{-5} = 5 \cdot 0$ mm.

(b) ACI Recommendations

From the work performed by Branson (77) the effective moment of inertia is given by $I_e = \left(\frac{Mcr}{M}\right)^3 I^1_u + \left[1 - \left(\frac{Mcr}{M}\right)^3\right] . I^1_{cr}$.

The deflection is then given by $a = \frac{23}{1296} . \frac{Wl^3}{E_c I_e}$.

The same assumptions apply as for CP 110, i.e.:

(i) plane sections remain plane

(ii) reinforcement is elastic

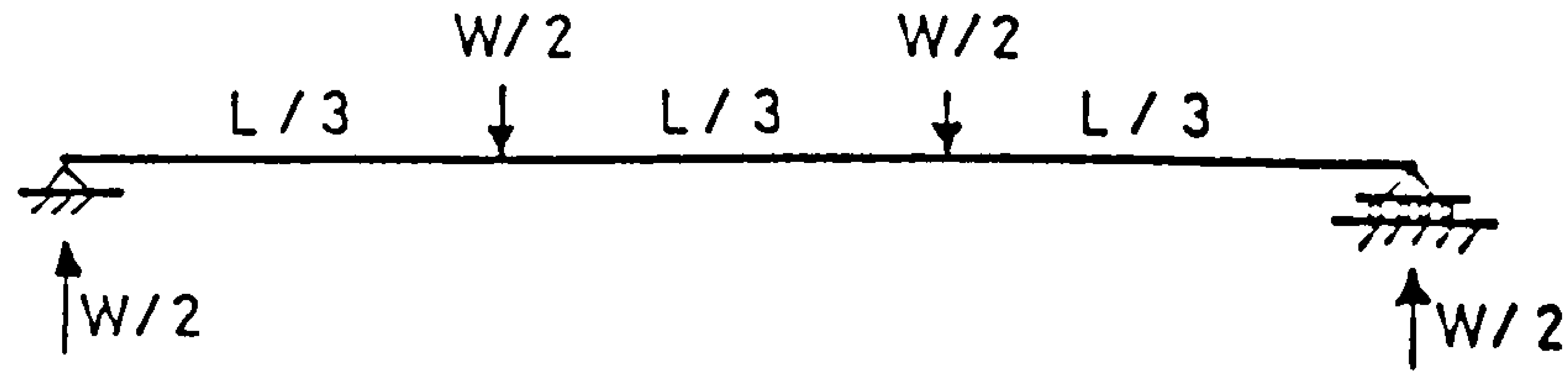

Convention (a) quantities within curly brackets are taken as zero if their value is negative.

(b) terms within curly brackets are integrated with respect to the terms within the brackets.

General expression for bending moment at distance x from the end.

$$M = EI\frac{d^2a}{dx^2} = -\frac{Wx}{2} + \frac{W}{2}\left\{x-\frac{L}{3}\right\} + \frac{W}{2}\left\{x-\frac{2L}{3}\right\}$$

$$\int M = EI\frac{da}{dx} = -\frac{Wx^2}{4} + \frac{W}{4}\left\{x-\frac{L}{3}\right\}^2 + \frac{W}{4}\left\{x-\frac{2L}{3}\right\}^2 + A$$

$$\iint M = EI\,a = -\frac{Wx^3}{12} + \frac{W}{12}\left\{x-\frac{L}{3}\right\}^3 + \frac{W}{12}\left\{x-\frac{2L}{3}\right\}^3 + Ax + B$$

Boundary conditions :

when $x = 0, \& L$ $\quad a = 0$

Therefore $B = 0$ and $-AL = -\frac{WL^3}{12} + \frac{W}{12}\left(\frac{2L}{3}\right)^3 + \frac{W}{12}\left(\frac{L}{3}\right)^3$

or $A = \frac{2WL^2}{36}$

Then:

$$EIa = -\frac{Wx^3}{12} + \frac{W}{12}\left\{x-\frac{L}{3}\right\}^3 + \frac{W}{12}\left\{x-\frac{2L}{3}\right\}^3 + \frac{2WL^2x}{36}$$

The central deflection:

when $x = \frac{L}{2}$

$$a = \frac{1}{EI}\left[-\frac{WL^3}{96} + \frac{W}{12}\left(\frac{L^3}{216}\right) + \frac{2}{3}\frac{WL^3}{24}\right]$$

or $\underline{a = \frac{23}{1296}\frac{WL^3}{EI}}$

FIGURE A5·3 CENTRAL DEFLECTION BY MACAULAY'S METHOD

(iii) concrete in compression is elastic.

EXAMPLE Beam 207

Mcr, the theoretical cracking moment, depends on the moment of inertia of the uncracked section (Fig. A.5.4) and the modulus of rupture which was determined by experiment - 5·56 N/mm^2.

$$\text{Thus Mcr} = \frac{2{\cdot}694.10^8.5{\cdot}56}{113{\cdot}83} = 13{\cdot}2 \text{ KNm.}$$

M, the moment under consideration = 49·8 kNm (130 kN load). The value of the cracked, transformed moment of inertia = $1{\cdot}54.10^8$ mm^4 (Fig. A.5.5). Hence the effective moment of inertia

$$= I_e = \left(\frac{13{\cdot}2}{49{\cdot}8}\right)^3 2{\cdot}694.10^8 + \left[1 - \left(\frac{13{\cdot}2}{49{\cdot}8}\right)^3\right] 1{\cdot}54.10^8 \text{ mm}^4$$

$$= 1{\cdot}561.10^8 \text{ mm}^4$$

$$\text{Then } a = \frac{23}{1296} \cdot \frac{130.10^3.2300^3}{36.10^3.1{\cdot}561.10^8}$$

$$= \underline{5{\cdot}0 \text{ mm}}$$

(c) CEB Recommendations

The deflections are calculated from considerations of whether the section is cracked or uncracked. In simply supported structures the deflections under short term loading may be calculated on the assumption that the stiffness in the cracked state = $E_s.A.z(d - x)$. Thus the total deflection is split into two parts, one applying before cracking and the other after.

Before cracking the curvature, $\frac{1}{r_1} = \frac{Mcr}{E_c I^1{}_u}$, notation as before

After cracking the curvature, $\frac{1}{r_2} = \frac{4}{3} \cdot \frac{(M-Mcr)}{E_s A_s z(d-x)}$

The deflection, a, is then given by $a = kl^2 \; \frac{1}{r_1} + \frac{1}{r_2}$

EXAMPLE Beam 207

Mcr as in ACI method	=	13·2 KNm
$I^1{}_u$ " " "	=	$2{\cdot}694.10^8$ mm^4
K as in CP 110 method	=	0·1065
x " " "	=	100·6 mm
z " " "	=	192·5 mm

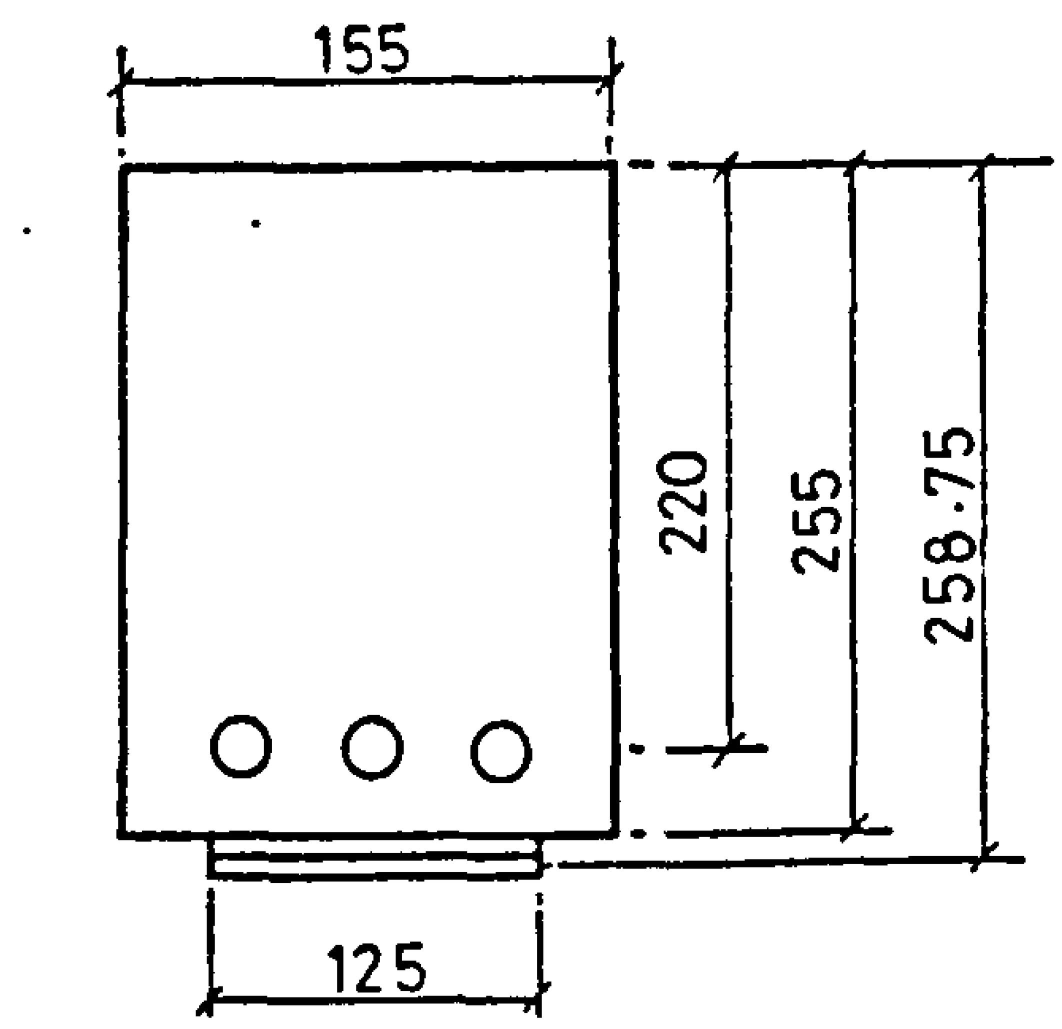

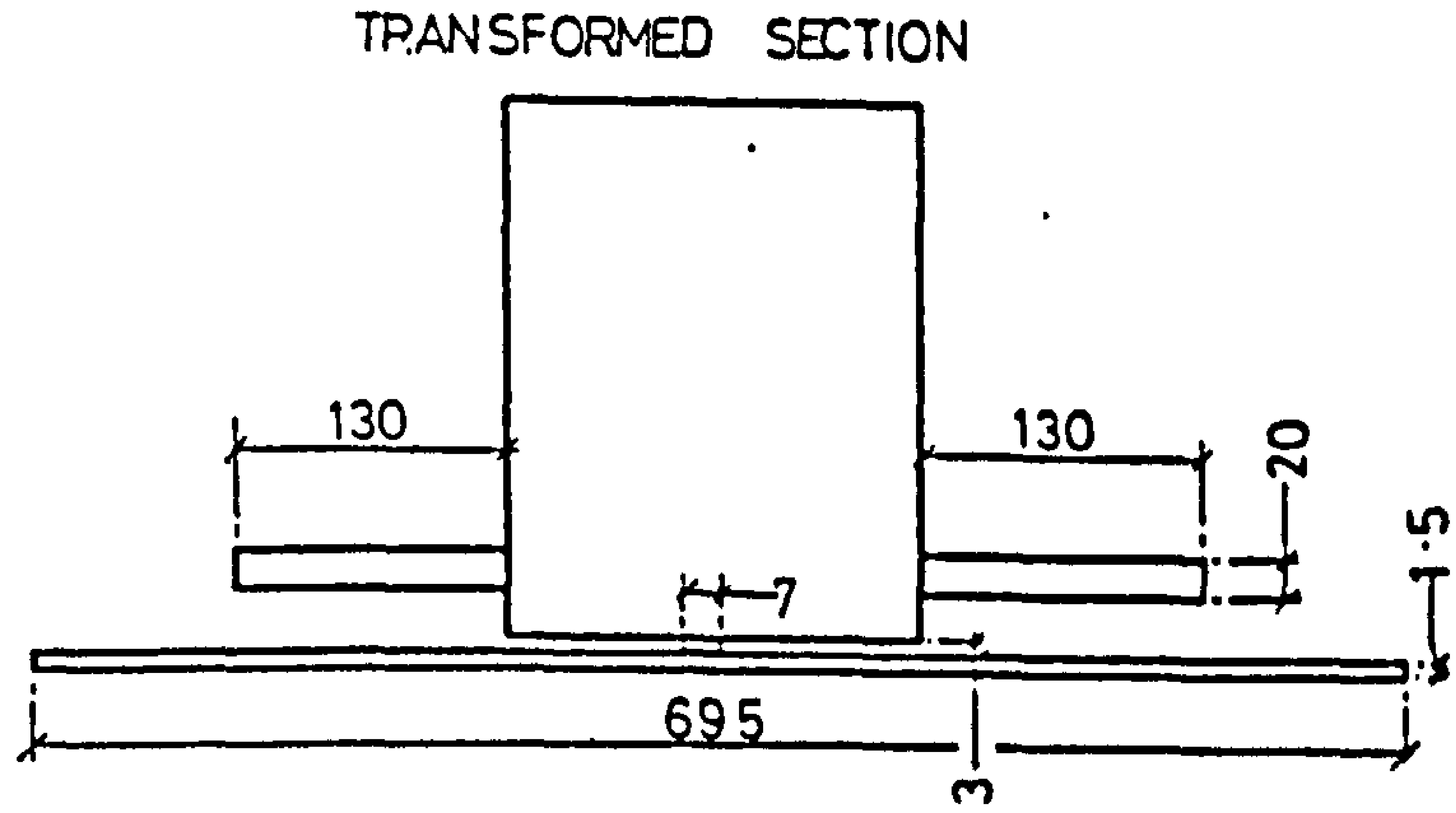

BEAM 207
area of bars 943 mm^2
area of plate 187 mm^2

E_{glue} 2·0 KN/mm^2
$E_{concrete}$ 36 KN/mm^2
E_{steel} 200 KN/mm^2

Neutral axis position - $\bar{x}$

$$\bar{x}(155.255 + 260.20 + 7.3 + 695.1{\cdot}5) = (155.\frac{255^2}{2} + 260.20.220 + 7.3.256{\cdot}5 + 695.1{\cdot}5.258{\cdot}75)$$

Hence $\bar{x}$ = 141·17mm.

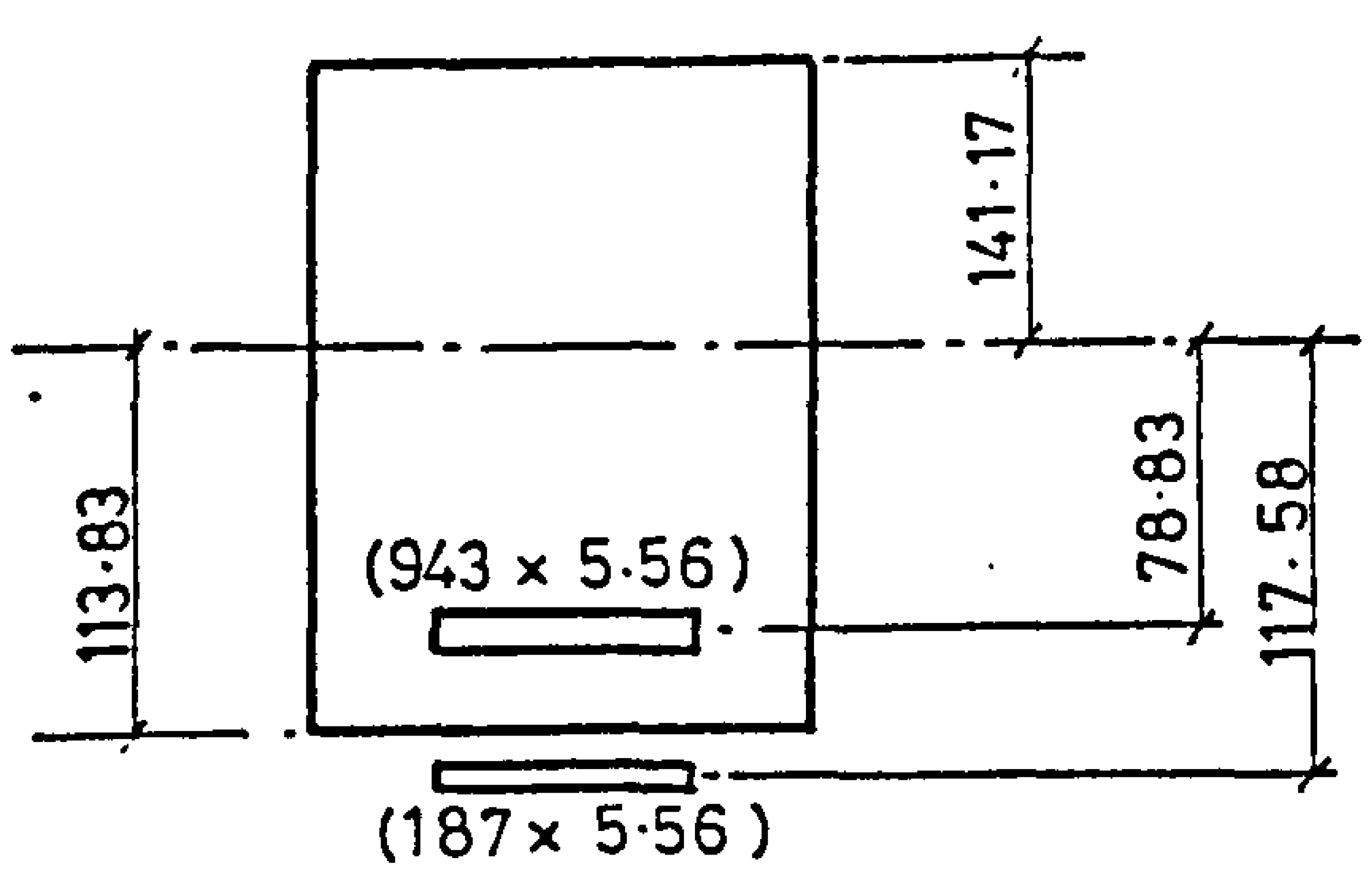

Moment of Inertia – taking moments about the Neutral Axis :

$$I = \frac{141{\cdot}17^3}{12}.155 + 155.141{\cdot}17.\left(\frac{141{\cdot}17}{2}\right)^2 = 1{\cdot}46.10^8\,mm^4 \text{ (concrete above N.A.)}$$

$$+ \frac{113{\cdot}83^3}{12}.155 + 155.113{\cdot}83.\left(\frac{113{\cdot}83}{2}\right)^2 = 0{\cdot}76.10^8 \text{ (concrete below N.A.)}$$

$$+ 943.5{\cdot}56.78{\cdot}83^2 = 0{\cdot}33.10^8 \text{ (steel bars, neglecting inertia about their own axis)}$$

$$+ 187.5{\cdot}56.117{\cdot}58^2 = 0{\cdot}14.10^8 \text{ (steel plate, =)}$$

+ glue negligible.

TOTAL I'_u = $2{\cdot}69.10^8\ mm^4$

FIGURE A5·4 MOMENT OF INERTIA OF UNCRACKED TRANSFORMED SECTION

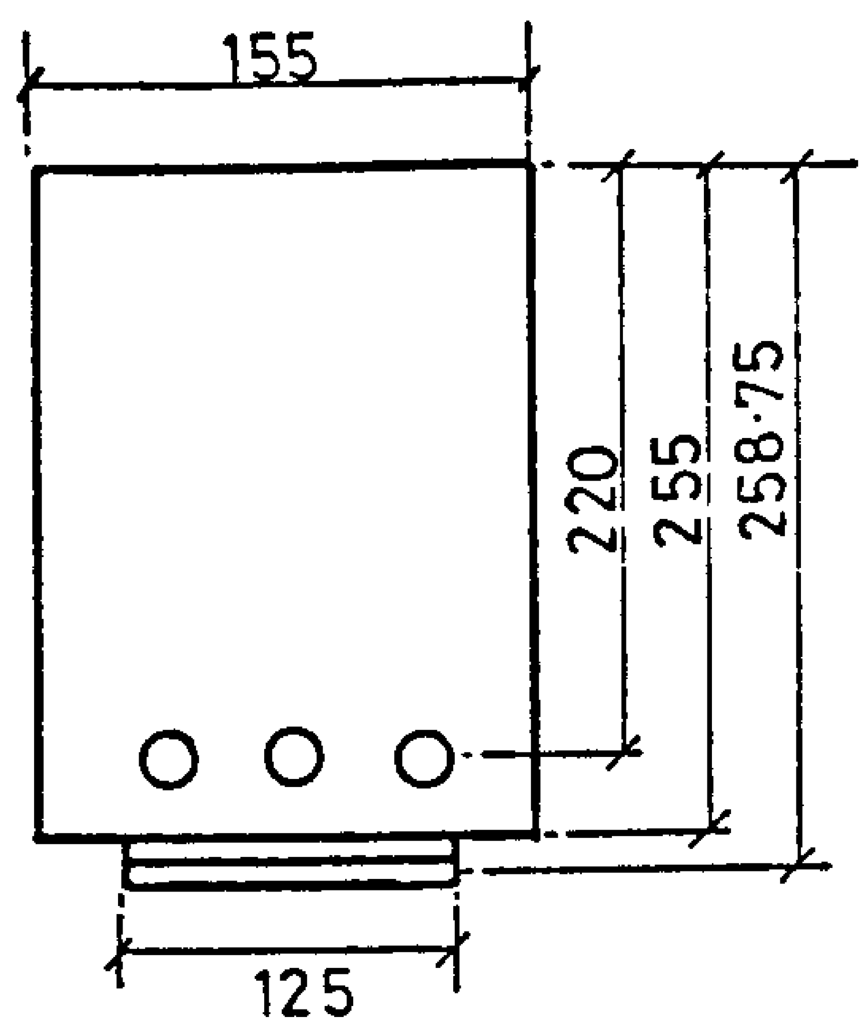

BEAM 207
area of bars 943 mm^2
area of plate 187 mm^2

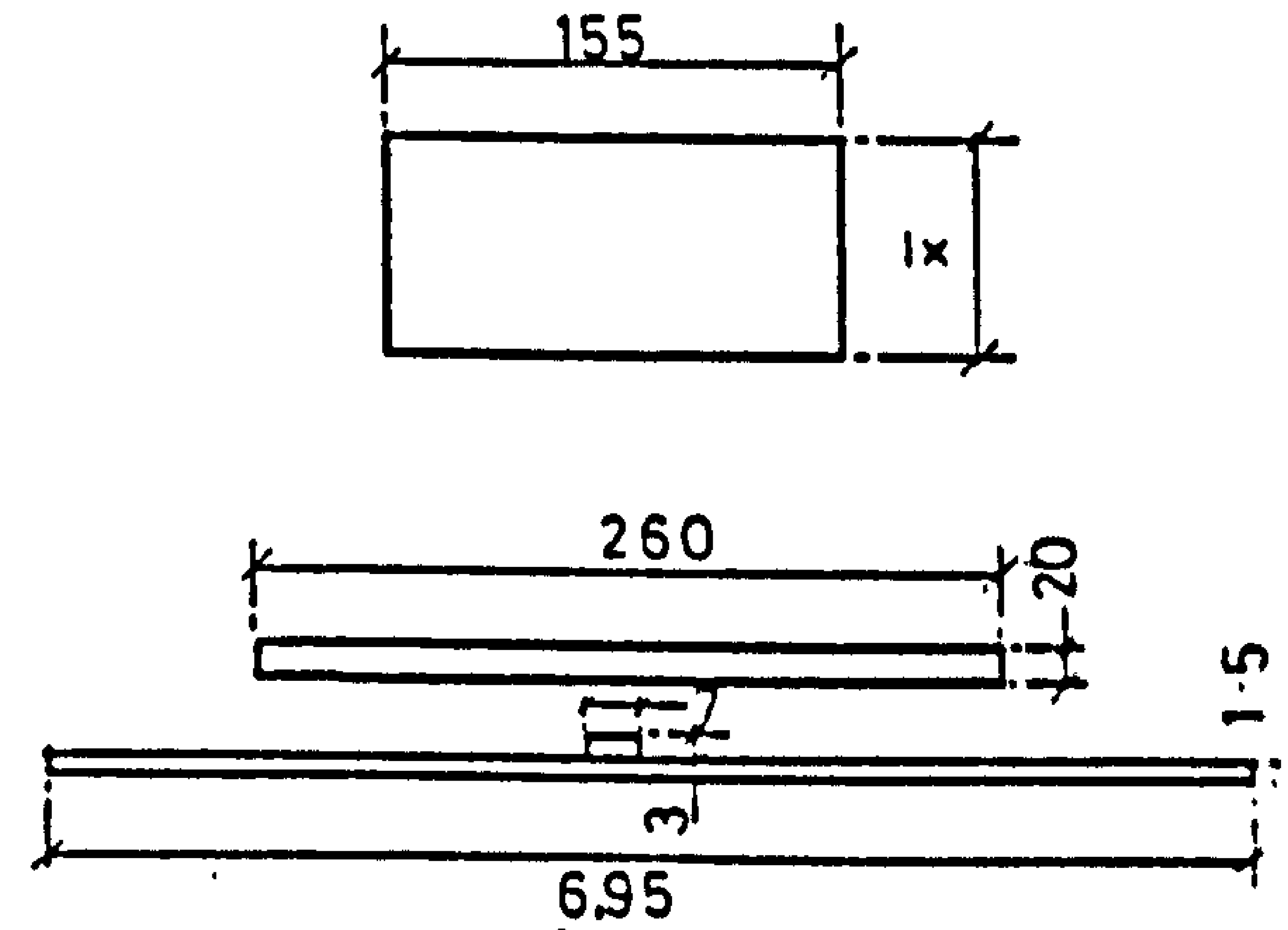

E_{glue} 2·0 KN/mm^2
$E_{concrete}$ 36 KN/mm^2
E_{steel} 200 KN/mm^2

Neutral axis position – $\bar{x}$

$$\bar{x}(155\bar{x} + 260.20 + 7.3 + 695.1\cdot5) = (155\frac{\bar{x}^2}{2} + 260.20.220 + 7.3.256\cdot5 + 695.1\cdot5.258\cdot75)$$

Hence $\bar{x} = 101\cdot15$ mm

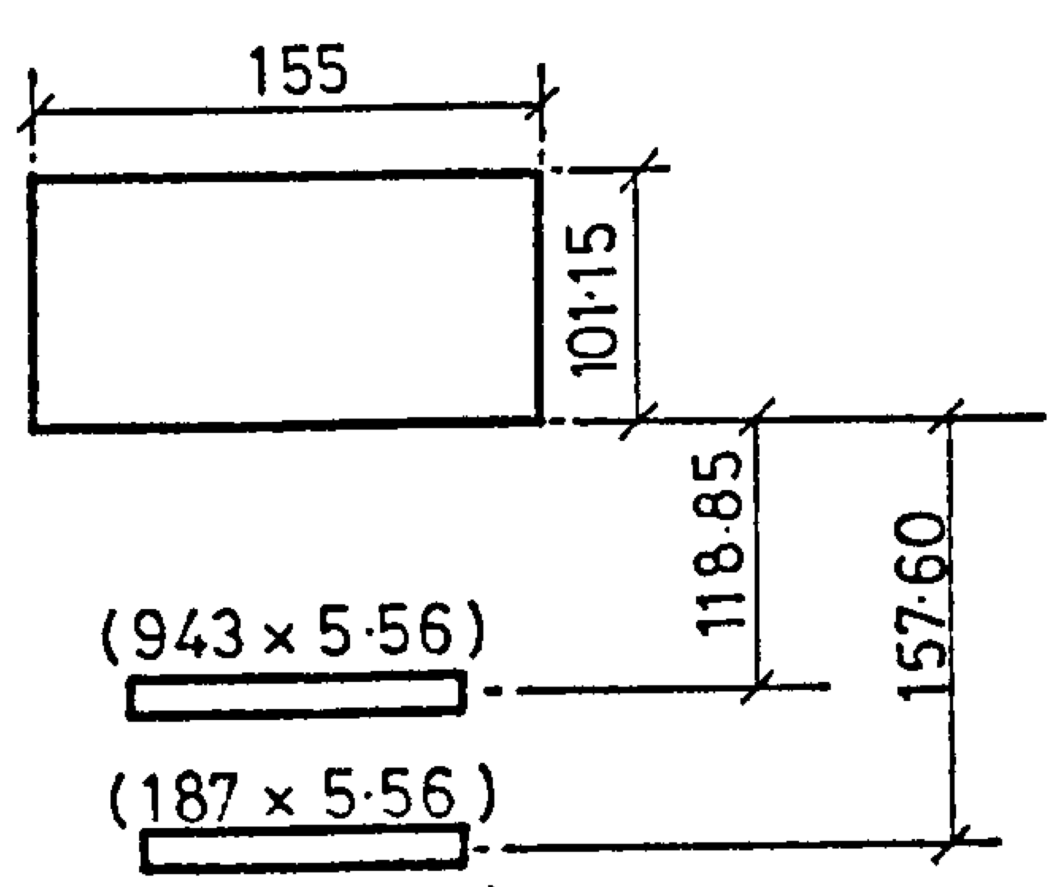

Moment of inertia:
taking moments about the Neutral Axis:

$I = 155\frac{101\cdot15^3}{12} + 155.101\cdot15(\frac{101\cdot15}{2})^2 = 0\cdot54.10^8\ mm^4$ (concrete)

$+ 943.5\cdot56.118\cdot85^2 = 0\cdot74.10^8$ (steel bars, neglecting Inertia about their own axis.)

$+ 187.5\cdot56.157\cdot60^2 = 0\cdot26.10^8$ (steel plate ")

+ glue negligible

TOTAL $I'_{cr} = 1\cdot54.10^8\ mm^4$

FIGURE A5·5 MOMENT OF INERTIA OF CRACKED TRANSFORMED SECTION

$$A_s = 943\ \text{(bars)} + 187\ \text{(plate)} = 1130\ \text{mm}^2$$

Hence

$$a = 0{\cdot}1065.2300 \left[\frac{13{\cdot}2.10^6}{36.10^3.2{\cdot}694.10^8} + \frac{4}{3}\,\frac{(49{\cdot}8 - 13{\cdot}2).\ 10^6}{2.10^5.1130.192{\cdot}5.125{\cdot}4} \right]$$

$$= \underline{5{\cdot}81\ \text{mm}}$$

APPENDIX 6

CALCULATION OF ROTATIONS

From basic bending theory $\frac{M}{I} = \frac{E}{R}$

where M = applied bending moment

I = moment of inertia of the section

E = Young's Modulus

$\frac{1}{R}$ = curvature at the section under consideration

The integral of the curvatures at each section along a beam produces the rotation. Hence the integral of $\frac{M}{EI}$ along the beam also gives the rotation. This is equivalent to the area under the bending moment diagram divided by EI, assuming a constant stiffness along the length of the beam. As in the calculation of deflections two cases must be considered, one before cracking occurs and the other after. Before cracking occurs the rotation =

$$\frac{\text{Area under Bending Moment Diagram}}{E_c \cdot I'_u}$$

where E_c = Young's Modulus of concrete, short term

and I'_u = uncracked, transformed moment of inertia.

In the second case the bending moment, resisted by the concrete in compression and the tension steel, is reduced by the moment resisted by the concrete in tension between the cracks. This is taken as, M_{ct},

$$M_{ct} = f_{ct} \frac{6}{3} \frac{(h-x)^3}{(d-x)} \qquad \text{Fig. A5.2}$$

The bending moments were calculated at four stages after cracking, up to failure, allowing for the tensile contribution of the concrete. The neutral axis positions found from the measured strain distributions were used and the effective depth was taken to the centroid of the steel bar and plate areas. The second moment of area was calculated at each stage using the same neutral axis positions. The rotations were then calculated as described above for a cracked section. Two values of tensile stress in the concrete were assumed. Firstly, f_{cr} = 1 N/mm^2 as recommended by CP110 and secondly, 3 N/mm^2. The latter value was not thought to be unreasonable as the modulus of rupture had an average value of 5.6 N/mm^2. A value of approximately half this did not seem too high.

EXAMPLE Beam 207

(i) Moments to be resisted by the section

Load (kN)	Moment $\left(\frac{WL}{6}\right) - M_{ct}$ (Nmm)		$f_{ct}=1\ N/mm^2$ (10^6)	$f_{ct}=3\ N/mm^2$ (10^6)
60	$\frac{60.2300.1000}{6} - f_{ct}.\frac{155}{3}\left(\frac{255-112}{226-112}\right)^3$	=	21·7	19·0
130	$\frac{130.2300.1000}{6} - f_{ct}.\frac{155}{3}\left(\frac{255-100}{226-100}\right)^3$	=	48·3	45·3
190	$\frac{190.2300.1000}{6} - f_{ct}\ \frac{155}{3}\left(\frac{255-90}{226-90}\right)^3$	=	71·1	67·7
250	$\frac{250.2300.1000}{6} - f_{ct}\ \frac{155}{3}\left(\frac{255-80}{226-80}\right)^3$	=	93·9	90·1

(ii) Moment of Inertia

The section is assumed to be cracked to some degree at all the load stages shown above. The neutral axis positions are as shown in the moment calculations, and concrete below the neutral axis is assumed to have no contribution to the moment of inertia, and ($\alpha_e = 5.56$).

Section

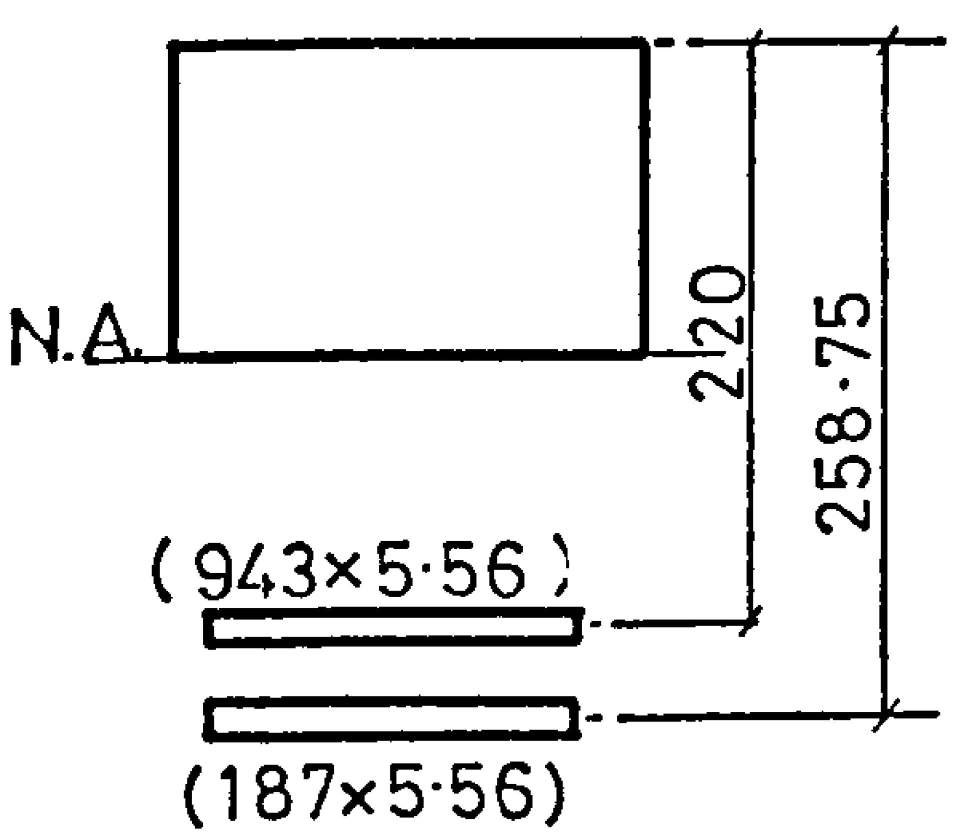

Load (kN)	Moment of Inertia (mm^4) (10^8)
60	$I = \frac{155.112^3}{12} + 155.112\left(\frac{112}{2}\right)^2 + 5243.108^2 + 1040.146{\cdot}75^2 = 1{\cdot}52$
130	$I = \frac{155.100^3}{12} + 155.100\left(\frac{100}{2}\right)^2 + 5243.120^2 + 1040.158{\cdot}75^2 = 1{\cdot}53$
190	$I = \frac{155.90^3}{12} + 155.90\left(\frac{90}{2}\right)^2 + 5243.130^2 + 1040.168{\cdot}75^2 = 1{\cdot}56$
250	$I = \frac{155.80^3}{12} + 155.80\left(\frac{80}{2}\right)^2 + 5243.140^2 + 1040.178{\cdot}75^2 = 1{\cdot}62$

neglecting the inertia of the steel bar and plates about their own axes.

(iii) Rotations - Area under B.M. diagram ÷ EI.

Load (kN)	Rotation (radians 10^4)		$f_{ct}=1\ N/mm^2$	$f_{ct}=3\ N/mm^2$
60	$\frac{2300}{3}.2.M \div 36000.1{\cdot}52.10^8$	=	61	53
130	$\frac{2300}{3}.2.M \div 36000.1{\cdot}53.10^8$	=	135	126
190	$\frac{2300}{3}.2.M \div 36000.1{\cdot}56.10^8$	=	195	186
250	$\frac{2300}{3}.2.M \div 36000.1{\cdot}62.10^8$	=	247	237

These rotations are given in Table 6.5. It is clear that at higher loads the predicted rotations are greatly exceeded. The main reason for this is that as cracking becomes more widespread and the concrete compressive strain increases the value assumed for E_c is not realistic.

APPENDIX 7

INTERFACIAL STRESSES

In this appendix an assessment is made of the bond stresses between the adhesive and plate and the shear stresses within the adhesive. It must be emphasised that the values should be treated qualitatively and that they in no way represent limiting or ultimate stresses. The beam tests were not designed to investigate such stress conditions but rather to study the flexural behaviour.

Bond Stresses

For concrete and steel to work in a beam it is necessary that stresses be transferred between the two materials. The term 'bond' can be used to describe the means by which slip, between the steel and concrete, is prevented or at least minimised. Wherever the tensile or compressive stresses in the reinforcing element change, bond stresses must act along their surface to produce this change.

Research on normal reinforced beams has shown that the bond stresses in a beam is neither uniform nor gradually varying from point to point. Rather, it has been found that very large bond stresses exist adjacent to cracks, essentially ultimate bond stresses, even at low loads. Very much smaller bond stresses exist close by on the same bar. Thus there is a practical problem as to how to describe, measure or evaluate such a fluctuating stress condition, and large bond stresses can exist in members at relatively low loads without signs of distress. Codes of Practice use two approximate methods to measure bond stress.

(a) Local Bond Stress

These are the shear stresses at the bar surface which prevent longitudinal movement of the bar in the concrete. Local bond failures are produced by large changes in the tensile force over a short length of bar. This change in tensile force is produced by a change in bending moment and the rate of change of bending moment is the shear force.

For plated beams the local bond stress at the plate/glue or concrete/glue interface is a horizontal shear stress given by

$$\frac{V.A.y}{I.b_p}$$

where A = area of plate or area (plate + glue),

b_p = width of plate,

V = shear force,

y = distance from the neutral axis to the section under consideration,

I = second moment of area of the cracked transformed section.

The results are given in Table A.7.1. The mean local bond stress near failure was 1.46 N/mm^2. CP110 limits the local bond stress in plain bars to 2.7 N/mm^2 (grade 40 concrete and above). These stresses are for the glue/plate interface.

(b) Anchorage Bond Stresses

This is the average bond stress over a particular length of bar. The removal of a bar from the concrete is resisted by shearing stresses, between the concrete and steel, which are assumed to be uniform along the length of the bar.

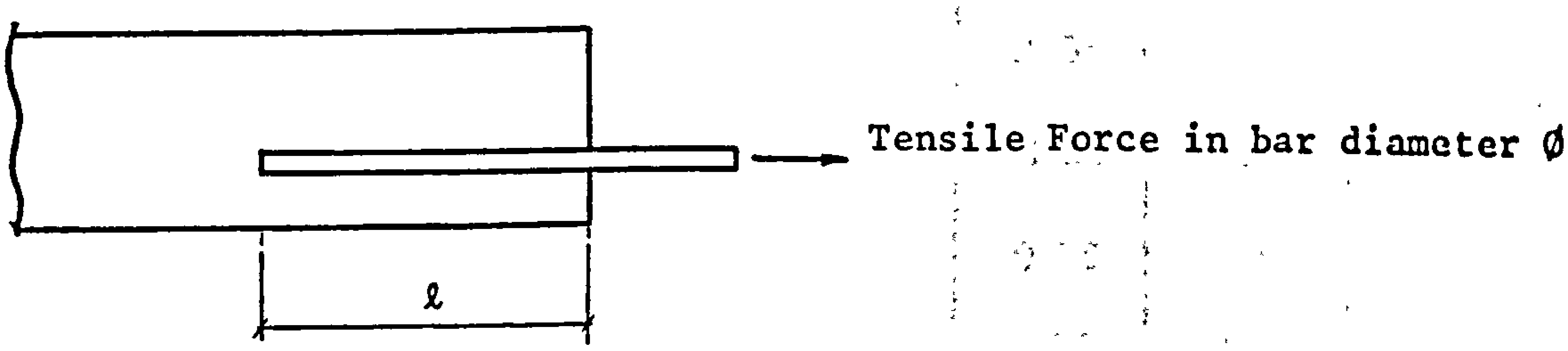

Considering the equilibrium of the forces at the ultimate limit state:

$$\frac{\pi}{4}\,\text{Ø}^2.f_u = \pi.\text{Ø}.f_{bs}.\ell$$

In CP110 f_u for the steel is limited to $\frac{f_y}{\gamma_m}$ to produce the allowable ultimate anchorage bond stresses. Certain experimentally determined limiting values are tabulated for different steel and concrete properties in Table 22 (CP110).

For evaluating the actual average anchorage bond stress between the plate and glue, in the test beams, a similar expression is used:

TABLE A 7·1 LOCAL BOND STRESSES IN PLATED BEAMS

BEAM NUMBER	GLUE mm THICKNESS	PLATE mm THICKNESS	SHEAR FORCE AT SERVICE LOAD kN	COMBINED CENTROID AT SERVICE LOAD mm	LOCAL BOND STRESS N/mm²	SHEAR FORCE AT ULTIMATE LOAD kN	COMBINED CENTROID AT ULTIMATE LOAD mm	LOCAL BOND STRESS N/mm²
203	1·5	1·5	65	226	0·55	125	226	1·05
204	1·5	3·0	65	231	0·89	125	231	1·70
205	1·5	6·0	65	238	1·23	95	238	1·80
207	3·0	1·5	65	226	0·55	125	226	1·05
208	3·0	3·0	65	231	0·90	125	231	1·72
209	3·0	6·0	65	238	1·24	95	238	1·81
210	3·0	6·0	65	238	1·24	95	238	1·81
216	6·0	1·5	65	226	0·57	125	226	1·09
217	6·0	3·0	65	231	0·90	125	231	1·74
218	6·0	6·0	65	238	1·24	95	238	1·81
219	6·0	6·0	65	238	1·24	95	238	1·81
220	3-8	1·5	65	226	0·55	125	226	1·05
221	3·0 (1)	1·5	65	226	0·55	125	226	1·05
222	3·0 (2)	1·5	65	226	0·55	125	226	1·05
223	3·0 (2)	1·5	65	226	0·55	125	226	1·05
224	3·0 (2)	3·0	65	231	0·90	125	231	1·74

(1) notched beam.
(2) precracked beams.

PLATE THICKNESS mm	MEAN SERVICE STRESS N/mm²	MEAN ULTIMATE STRESS N/mm²
1·5	0·55 (0·55)	1·05 (1·05)
3·0	0·90 (0·90)	1·72 (1·74)
6·0	1·24	1·81

Figures in brackets – precracked beams.

$$f_{bs} = f_p \cdot \frac{A_p}{A_c}$$

where f_p is the stress in the plate ($= \varepsilon_p . E_p$)

A_p is the cross section area of the plate ($= t_p \; b_p$)

A_c is the contact area between glue and plate ($= b_p \; \ell$)

ε_p, E_p, t_p and b_p are the strain, Young's Modulus, thickness and width, respectively, of the steel plate, and ℓ is the anchorage length.

Then,

$$f_{bs} = \varepsilon_p \; E_p \; \frac{t_p \; b_p}{b_p \; \ell}$$

For the test beams:

t_p = thickness of plate varies - 1.5 mm to 6 mm

b_p = width of plate constant - 125 mm

E_p = Young's Modulus 200,000 N/mm^2

ε = strain in the plate varies

ℓ = anchorage length is taken as the distance from the end of the plate to the loading point = 742 mm.

Substituting we have:

$$\underline{f_{bs} = 269 \; \varepsilon_p \; t_p}$$

Using the strains obtained by experiment at both working load and near ultimate load the anchorage bond stresses were calculated for beams with single layers of continuous plate. The results are given in Table A7.2.

The mean anchorage bond stress at the load stage prior to failure was 2.12 N/mm^2, and at service load it was 0.81 N/mm^2. The limiting values, at these load stages, given in CP110 for plain bars are 1.9 and 1.0 N/mm^2 respectively, (for concrete f_{cu} 40 N/mm^2 and above.)

(c) <u>Shear Stresses in the Glue</u>

Considering longitudinal forces on a short length of steel plate $\delta\ell$, the change in load corresponding to a change in strain of $\delta\varepsilon_p$ is given by:

$$\delta\varepsilon_p . E_p . b_p . t_p \quad \text{(Symbols as before)}$$

TABLE A 7·2 ANCHORAGE BOND STRESSES IN THE PLATED BEAMS

BEAM NUMBER	GLUE mm THICKNESS	PLATE mm THICKNESS	DESIGN SERVICE LOAD kN	PLATE STRAIN AT CENTRE microstrain	ANCHORAGE BOND STRESS N/mm²	ULTIMATE LOAD kN	PLATE STRAIN AT CENTRE microstrain	ANCHORAGE BOND STRESS N/mm²
203	1·5	1·5	130	1300	0·5	250	4900	2·0
204	1·5	3·0	130	1200	1·0	250	3700	2·9
205	1·5	6·0	130	650	1·0	190	1200	1·9
207	3·0	1·5	130	1300	0·5	250	4900	2·0
208	3·0	3·0	130	1100	0·8	250	3200	2·6
209	3·0	6·0	130	700	1·1	190	1350	2·2
210	3·0	6·0	130	650	1·0	190	1250	2·0
216	6·0	1·5	130	1100	0·4	250	4200	1·6
217	6·0	3·0	130	1000	0·8	250	2900	2·3
218	6·0	6·0	130	660	1·0	190	1200	1·9
219	6·0	6·0	130	750	1·2	190	1350	2·2
220	3–8	1·5	130	1200	0·5	250	4200	1·7
221	3·0 (1)	1·5	130	1300	0·5	250	4500	1·8
222	3·0 (2)	1·5	130	950	0·4	250	2900	1·2
223	3·0 (2)	1·5	130	700	0·3	250	2300	0·9
224	3·0 (2)	3·0	130	750	0·6	250	2400	1·9

(1) notched beam
(2) precracked beams

PLATE THICKNESS mm	MEAN SERVICE STRESS N/mm²	MEAN ULTIMATE STRESS N/mm²
1·5	0·49 (0·35)	1·19 (1·02)
3·0	0·87 (0·59)	2·58 (1·90)
6·0	1·07	2·00

Figures in brackets – precracked beams.

This must be balanced by a shear force in the resin which is given by:

$\tau.\delta\ell.b_p$ where τ = shear stress at the plate/glue interface.

$$\text{Hence } \tau = E_p.t_p.\frac{\delta\varepsilon_p}{\delta\ell}$$

In the limit $\tau = E_p.t_p.\frac{d\varepsilon_p}{d\ell}$ where $\frac{d\varepsilon_p}{d\ell}$ is the strain gradient.

This analysis has ignored the thickness of the glue and therefore assumes that the strain in the contact face of the steel is the same as the contact surface strain in the concrete.

It is evident that the glue will be subjected to high shear forces where the strain gradient is high. Such gradients occur where there is a sudden change in section, for example at the end of the plate, a joint in a plate or at a crack in the concrete. The strain gradients were measured at the plate ends for the test beams. However, the measured values of strain can only be an approximation to the local strains as they are based on average values over a finite length. Gauges of 6 mm length were used and in such a region of rapidly changing strain are not small enough to determine an accurate strain gradient. Nevertheless, the tests do give some indication of the order of magnitude of the shear stresses. The shear stresses are given in Table A7.3, for beams with single continuous layers of plate.

TABLE A·7·3 SHEAR STRESS IN THE GLUE LAYER AT THE END OF THE PLATE.

BEAM NUMBER	GLUE THICKNESS mm	PLATE THICKNESS mm	DESIGN SERVICE LOAD kN	STRAIN GRADIENT microstrain per mm	SHEAR STRESS N/mm²	ULTIMATE LOAD kN	STRAIN GRADIENT microstrain per mm	SHEAR STRESS N/mm²
203	1·5	1·5	130	2·4	0·7	250	5·4	1·6
204	1·5	3·0	130	1·8	1·1	250	4·4	2·6
205	1·5	6·0	130	1·4	1·7	190	3·0	4·1
207	3·0	1·5	130	2·6	0·8	250	6·6	2·0
208	3·0	3·0	130	2·0	1·2	250	5·5	3·3
209	3·0	6·0	130	1·3	1·6	190	3·8	4·6
210	3·0	6·0	130	1·8	2·2	190	3·6	4·3
216	6·0	1·5	130	2·7	0·8	250	8·5	2·6
217	6·0	3·0	130	2·2	1·3	250	6·0	3·6
218	6·0	6·0	130	1·5	1·8	190	4·0	4·8
219	6·0	6·0	130	2·0	2·4	190	4·2	5·0
220	3–8	1·5	130	3·7	1·1	250	8·2	2·5
221	3·0(1)	1·5	130	2·7	0·8	250	7·7	2·3
222	3·0(2)	1·5	130	2·0	0·6	250	6·5	2·0
223	3·0(2)	1·5	130	2·0	0·6	250	6·7	2·0
224	3·0(2)	3·0	130	1·2	0·7	250	4·4	2·6

(1) notched beam.
(2) precracked beams.

PLATE THICKNESS mm	MEAN SERVICE SHEAR STRESS N/mm²	MEAN ULTIMATE SHEAR STRESS N/mm²
1·5	0·85 (0·60)	2·18 (2·00)
3·0	1·43 (0·70)	3·18 (2·60)
6·0	1·72	4·56

Figures in brackets – precracked beams.

APPENDIX 8

CALCULATION OF CRACK WIDTHS

The crack widths were calculated by two methods:

a. British Standard Code of Practice CP110.

As with deflections an elastic analysis of the concrete section was used for calculating the stiffness. Any calculations to determine the moments and forces for deflections can also be used for cracking.

In Clause A.3.2 of the code, Equation 61 is given for determining the crack width

$$W_{cr} = \frac{3.\ a_{cr}.\ \varepsilon_m}{1 + 2\left(\frac{a_{cr} - C_{min}}{h-x}\right)}$$

At the level of reinforcement $a_{cr} = C_{min}$ hence the formula becomes:

$$W_{cr} = 3.\ a_{cr} \cdot \varepsilon_m$$

The average strain at the level of reinforcement, ε_m, is calculated from ε_1, the strain calculated ignoring the stiffening effect of the concrete in the tension zone, and then allowing for the tensile stiffening as shown by:

$$\varepsilon_m = \varepsilon_1 - \frac{1.2.b_t.h.\ (a'-x)\ .\ 10^{-3}}{A_s.(h-x).f_y}$$

The code states that the formula only applies if the strain in the tension reinforcement is limited to 0.8 f_y/E_s, and that when calculating strains the modulus of elasticity of the concrete should be taken as half the instantaneous value obtained from Table 1 in the code or by experiment. However, the proposed crack width formula gives a value which has a certain probability of being exceeded during the life of a structure. With repeated and sustained loadings, crack widths can increase over a period of time. To compute values for beams tested in the laboratory at an age of 28 days and loaded for only a few hours it is more reasonable to use the full elastic modulus of the concrete. Calculations were performed using both values, i.e. E_c and 0.5 E_c. The values given in brackets at the end of the calculations are for 0.5 E_c for comparison.

Beam 207   Glue thickness 3 mm

Plate thickness 1.5 mm

$$\alpha_e = \frac{200,000}{36,00} = 5.56$$

$$\rho = \frac{A_s}{bd}$$

d, the effective depth, is taken to the combined centroid of the plate and bars.

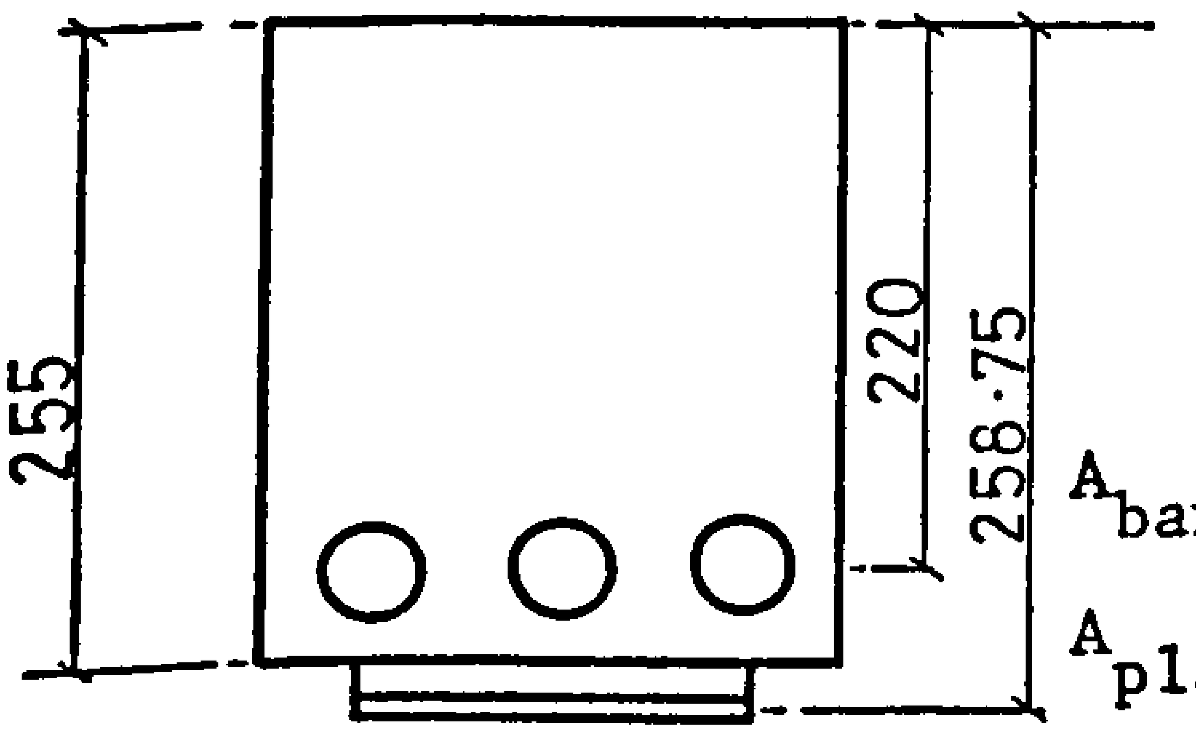

$A_{bars} = 943\ mm^2$

$A_{plate} = 187\ mm^2$

$$d.(943+187) = 220.943 + 187.158\cdot75$$

$$d = 226\ mm$$

$$\text{Thus } \rho = \frac{(187 + 943)}{155.226} = 0.032$$

$$\frac{x}{d} = \sqrt{\alpha e\cdot\rho(2+\alpha_e\rho)} - \alpha e.\rho$$

$$= 0.44 \qquad \text{Hence } x = 100\cdot5\ mm$$

$$\text{and} \quad Z = d - \frac{x}{3} = 192\cdot5\ mm$$

The crack widths are all calculated at 130 KN load which corresponds to a moment of 49·8 KNm.

The stress in the reinforcement (at the combined centroid) is given by:

$$f_s = \frac{M}{Z.A_s} = \frac{49\cdot8.10^6}{192\cdot5.1130} = 230\ N/mm^2$$

$$\text{Hence the strain, } \varepsilon_1, = \frac{230}{200000} = 0\ 00115.$$

Correcting for the tension stiffening of the concrete:

$$\varepsilon_m = 0\cdot00115 - \frac{1\cdot2.155.255.(226-100\cdot5).10^{-3}}{(187.250+943.410)(255-100\cdot5)}$$

$$= 0\cdot00107$$

The crack width is then given by:

$$W_{cr} = 3.a_{cr}.\varepsilon_m$$

For all the beams the cover to the bars; a_{cr}, is 27·5 mm.

Hence $W_{cr} = 3.\ 27{\cdot}5\ .\ 0{\cdot}00107$

$= 0{\cdot}088$ mm $(0{\cdot}093)$

For beams with 3 mm plate the values are $0{\cdot}074$ mm $(0{\cdot}079)$ and for beams with 6 mm plate the values are $0{\cdot}056$ mm $(0{\cdot}061)$.

The values are shown in Table 7.7.

b. American Concrete Institute.

The formula for crack width at the reinforcement level, as recommended by Gergely and Lutz (89) is given by:

$$W_{max} = \frac{0{\cdot}091\sqrt[3]{t_s.A}\ \ (f_s-5)\ .\ 10^{-3}}{1 + \frac{t_s}{h_1}} \qquad \text{(IMPERIAL UNITS)}$$

<u>Beam 207</u> Value E_c assumed.

The depth to the centroid of steel = 226 mm

Neutral axis depth = 100.5 mm

h_1, the distance from the neutral axis to the centroid of the tension steel $= 226 - 100{\cdot}5 = 125{\cdot}5$ mm.

For normally reinforced concrete beams $A = \frac{2b(h-d)}{\text{number of bars}}$

For the plated beams it is assumed that the concrete surrounding the plate is equal to that surrounding each bar, and that the plate is the same width as the beam.

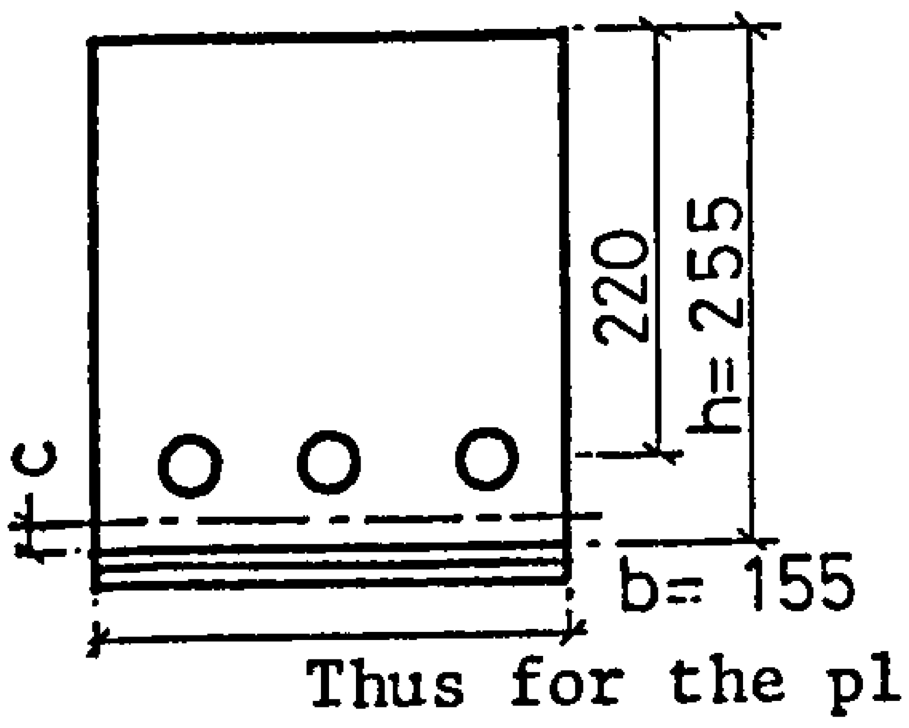

$$b.c = [\ 2(h-220) - c\ ]\,.\frac{b}{3}$$

$$\therefore\ c = \frac{(h-220)}{2}$$

$$\text{and } A = b.\ \frac{h-220}{2} = 2712 \text{ mm}^2$$

Thus for the plated beams, the thickness of plate is assumed not to affect A, but does affect the positions of the combined centroid of steel and hence x and d, which in turn affect h_1 and the steel stress, f_s.

As for CP110 $f_s = \frac{M}{zA_s} = 230$ N/mm^2

Converting to Imperial Units

t_s = 37·5 mm (to centre of bar) = 1.48 inches

A = 2712 mm = 4·2 in

f_s = 230 N/mm = 33·3 Kips/in

h_1 = 125·5 mm = 4·94 in

Then $$W_{max} = \frac{0{\cdot}091\ \sqrt[3]{1.48.4{\cdot}2}\ \ (33{\cdot}3 - 5).10^{-3}}{1 + \frac{1{\cdot}48}{4{\cdot}94}}$$

Hence W_{max} = 0·093 mm

The results are given in Table 7.7.

APPENDIX 9

STATISTICS

a. STANDARD DEVIATION. σ

When calculating the standard deviation of a set of numbers

$$\sigma = \sqrt{\frac{\Sigma_i \ (x_i - \bar{x})^2}{N}}$$

where N is the number of elements

$\bar{x}$ is the mean

b. COEFFICIENT OF VARIATION

This is taken as $\frac{\text{standard deviation}}{\text{mean}}$ $\frac{\sigma}{\bar{x}}$

c. LINEAR REGRESSION

In many disciplines it is desirable to express one variable in terms of another even though the variables are not necessarily analytical functions of each other. An accepted practice is to perform a least-squares regression which is designed to minimise the sum of the squares of the deviation of the actual data points from the straight line of best fit. In practice we are essentially constructing a plot of the variables, called a scatter diagram, and drawing the best straight line which uniformly divides the points. The result is a linear equation in the form $y = mx + b$.

It can be shown that the slope and y intercept are determined as follows:

$$m = \frac{\frac{\Sigma xi \Sigma yi}{N} - \Sigma xiyi}{\frac{(\Sigma xi)^2}{N} - \Sigma xi^2}$$

and $b = \bar{y} - m\bar{x}$

$$\bar{x} = \frac{\Sigma xi}{N}$$

$$\bar{y} = \frac{\Sigma yi}{N}$$

The degree of association between the two variables x and y is called the correlation, r.

where $r = m. \frac{\sigma_x}{\sigma_y}$ (σ = standard deviation)

In most applications it is advisable to select a degree of certainty that is desired when analysing a population of numbers. To facilitate this statisticians have constructed tables based on the areas under different portions of the normal curve. These tables are called 'Z' values and enable a prediction for the range of the mean value to a specific degree of certainty.

In the present case of cracking in the test beams, the relationship between the maximum and mean crack width is required.

$$W_{max} = W_{mean} + Z.\text{standard deviation.}$$

The experimental results from 24 test beams are used and from statistical tables this gives a factor of 2·5.

This gives:

$$W_{max} = W_{mean} + 2{\cdot}5.\ \sigma.$$

REFERENCES

1. A.C.I. COMMITTEE 403:
Guide for use of epoxy compounds with concrete.
Journal of the A.C.I., Volume 59, No. 9, September 1962, pp 1121-1142.

2. A.C.I. COMMITTEE 503:
Use of epoxy compounds with concrete.
Journal of the A.C.I., Volume 70, No. 9: part 2, September 1973, pp 614-645.

3. A.C.I.
Epoxies with concrete.
A.C.I. Special Publication, SP21, 1966.

4. E.W. BAUMAN, R.B. JACKSON and W.R. McCONNELL:
Guide for use of epoxy compounds with concrete - Discussion of paper by A.C.I. 403.
Journal of the A.C.I., Volume 59, No. 9, December 1962, pp 2015-2018.

5. R. HOUWINK and G. SALOMON:
Adhesion and Adhesives.
Volume 1 (1965) and Volume 2 (1967), 2nd edition,
Elsevier Publication Co., Amsterdam, London and New York.

6. H. LEE and K. NEVILLE:
Handbook of epoxy resins.
McGraw Hill Book Company, New York, Toronto, London, 1957.

7. B. TREMPER:
Repair of damaged concrete with epoxy resins.
Journal of the A.C.I., Volume 57, August 1960, pp 173-182, 1187-9.

8. F.P. BRUINS:
Epoxy resin technology.
Interscience Publishers, New York, 1968.

9. R. GAUL and N. APTON:
Epoxy adhesives in concrete construction.
Civil Engineering (New York), Volume 29, No. 11, 1959, pp 50-52.

10. C.M. WAKEMAN, H.E. STOVER and E.N. BLYE:
Glue for concrete repair.
A.S.T.M. Bulletin, Volume 2, No. 2, 1962, pp 93-97.

11. J. CIESIELSKI:
Reinforcement of reinforced concrete beams by epoxy resin injection.
RILEM Symposium - Synthetic Resins in Building Construction - Paris 1967.

12. R. GUTTMAN:
Concise guide to structural adhesives.
Reinhold Publishing Corporation, New York, 1961.

13. R.P. JOHNSON:
Glued joints for structural concrete.
Structural Engineer, Volume 41, No. 10, October 1963, pp 313-321.

14. M. LEVY:
The use of adhesives in the bonding and repair of precast products.
Civil Engineering, Volume 56, 1961, pp 333-5, 495-6.

15. R.P. JOHNSON:
Creep tests on glued joints.
Proceedings of Conference on 'Industrialised Building and the Structural Engineer', Institution of Structural Engineers, 1967, pp 143-147.

16. B. TAYLOR:
The effect of vibration on creep of glued concrete joints.
Research Project, Cambridge University Engineering Laboratory, 1965.

17. J.D. KREIGH:
The use of epoxy resin in reinforced concrete - Dynamic tests.
Engineering Research Laboratories, University of Arizona, August 1963.

18. T. O'BRIEN:
Jointing structural precast concrete units with resin adhesives.
RILEM Symposium, Sythetic Resins in Building Construction, Paris 1967.

19. P.W. ABELES:
Investigation of composite prestressed concrete beams comprising precast members glued together by means of resins.
Materials and Structures, Volume 1, No. 1, Jan.-Feb. 1968, pp 33-36

20. R.P. JOHNSON:
The properties of an epoxy mortar and its uses for structural joints.
Structural Engineer, Volume 48, No. 6, June 1970, pp 227-232

21. M.L. BATCHELAR:
Epoxy resin materials as structural adhesives.
M. Eng. report, University of Canterbury, New Zealand, 1973.

22. J. MOAR:
The strength, creep and durability of epoxy jointed concrete members.
PhD thesis, University of New South Wales, Australia, 1974

23. V. GORGOL:
Epoxy resin finish of the grandstands of Paris sports stadium.
RILEM Symposium, Synthetic Resins in Building Construction, Paris 1967.

24. A. HALLQUIST:
An investigation on epoxy and polyester resin mortars as a jointing material.
RILEM Symposium, Synthetic Resins in Building Construction, Paris 1967.

25. CIBA GEIGY:
Araldite Bonding.
Instruction Manual A15g, August 1971.

26. I.P. SHUE FAI:
Structural applications of epoxy resin adhesives.
National Roads Board of New Zealand, RRU Bulletin No. 29, 1974.

27. R. SHAW:
Epikote resins in civil engineering applications - recent developments.
Shell Research Ltd., Report ERLP/64, 1971.

28. A.R. CUSENS and D.W. SMITH:
A study of epoxy resin adhesive joints in shear.
Structural Engineer, Volume 58A, No. 1, January 1980

29. C. CARON:
Synthetic Resins. Laboratory tests applied to resins injection.
RILEM Symposium, Synthetic Resins in Building Construction, Paris 1967.

30. R. VOLKERSEN:
Stress distribution in adhesive joints.
Luftfahrtforsch, Volume 15, No. 31, 1938.

31. M. GOLAND and E. REISSNER:
Stress distribution in adhesive joints.
Journal of Applied Mechanics, Volume 1, No. 1, 1944, pp A.17.

32. R.W. CORNELL:
Stress distribution in adhesive joints.
Journal of Applied Mechanics, Volume 20, 1953, p. 355.

33. G.R. WOOLEY and D.R. CARVER:
Stress distribution in bonded lap joints.
Aircraft, Volume 8, No. 10, 1971, p. 817.

34. S. AMIJIMA, T. FUJII and A. YASHIDA:
Two dimensional stress analysis of adhesive bonded joints.
20th Japan Congress on Materials Research, 1977.

35. D. MYLONAS:
Critical comparison of theories of stress distribution in adhesive joints.
PhD. thesis, University of London, 1949.

36. Y. GILIBERT, J.P. DELMAS and C. COLLOT:
Contribution to the study of plated concrete.
RILEM Bulletin, No. 41, 1974, pp 319-327.

37. Y. GILIBERT and C. COLLOT:
Contribution to the study of adhesion between steel and adhesive as a function of the micro-geometric properties of the roughened surface.
RILEM Bulletin, No. 48, 1975

38. K.W. ALLEN:
Strength and Structure - Aspects of adhesion. Volume 1.
University of London Press Ltd., London 1965.

39. C.V. CAGLE:
Adhesives Bonding.
McGraw Hill Book Company, New York 1968.

40. D.R. SMITH:
How to prepare the surface of metals and non metals for adhesive bonding.
Adhesives Ages, March 1967.

41. J. OLSEN:
The industrial adhesives plausibility gap.
Adhesives Age, January 1975.

42. J. SHIELDS:
Adhesives Handbook.
Newness Butterworth, London 1976.

43. C.W. JENNINGS:
Surface Roughness and bond strengths of adhesives.
Journal of Adhesion, Volume 4, 1972.

44. E.B. RAMEL:
Analytical and experimental studies of adhesive bonded beams and plates.
PhD thesis, University of Dundee, 1976.

45. N.J. DELOLLIS:
Adhesion theory and review. Handbook of adhesive bonding.
McGraw Hill Book Company, New York 1973.

46. R. BUCK and J. HOCKNEY:
Immersion tests on lap shear specimens.
Aspects of Adhesion, Volume 7, 1973, pp243-252.

47. A.J. KINLOCH and R.A. GLEDHILL:
Environmental failure of structural adhesive joints.
Journal of Adhesion, Volume 6, 1974, pp315-330.

48. PAPER E2:
Adhesive joints in primary structures.
Conference on Joints in Structures - Sheffield University, Institution of Structural Engineers.

49. C. McNICHOLAS:
A critical study of joints in aluminium alloy.
PhD. thesis, University of Salford, 1969.

50. L.J. TABOR:
Effective use of epoxy and polyester resins in civil engineering structures.
CIRIA Report 69.
Construction Industry Research and Information Association, London, January 1978, pp 221-225

51. ANON:
Research on strengthening of bridges.
Proceedings of Annual Meeting of Civil Engineering, Tokyo, Ministry of Construction, November 1975.

52. ANON:
'M5 shrinkage cracks - traffic restricted.'
New Civil Engineer, No. 62, October 1973, pp 21.

53. T. SOMMERARD:
'Swanley's steel plate patch up'
New Civil Engineer, No. 247, June 1977, pp 18.

54. J. BRESSON:
New research and applications of adhesive joints in composite construction.
Annales de l'Institut Technique du Bâtiment et des Travaux Publics.
Supplement No. 278, February 1971.

55. J. BRESSON:
The strengthening, by bonded reinforcement, of the underpass of the CD 136 to the autoroute du Sud.
Annales de l'Institut Technique du Bâtiment et des Travaux Publics.
Supplement No. 297, September 1972.

56. M. LADNER and FLÜELER:
Tests on reinforced members with glued reinforcement.
Schweizerische Bauzeitung, May 1974, pp 463-479

57. W. FRANKE:
The employment of epoxy resins for reinforcing prefabricated water storage tanks made of prestressed concrete members.
RILEM Symposium, Synthetic Resins in Building Construction, Paris 1967.

58. R. L'HERMITE:
Use of bonding techniques for reinforcing concrete and masonry structures.
Materials and Structures, Volume 10, No. 56, 1977, pp 85-89.

59. R. L'HERMITE and J. BRESSON:
Concrete reinforced with glued plates.
RILEM Symposium, Synthetic Resins in Building Construction, Paris 1967, pp 175-203.

60. C.A.K. IRWIN:
The strengthening of concrete beams by bonded steel plates.
TRRL Report SR 160 UC, 1978.

61. M.B. MACDONALD
The flexural behaviour of concrete beams with bonded external reinforcement.
TRRL Report SR 415, 1978.

62. ANON:
The strengthening of concrete structures by bonded external reinforcement
Long term exposure tests.
TRRL Leaflet 627, 1978.

63. S.K. SOLOMON, D.W. SMITH and A.R. CUSENS:
Flexural tests on steel-concrete-steel sandwiches. Vol. 28:94
Magazine of Concrete Research, March 1976, pp 13-20.

64. R.P. JOHNSON and C.J. TAIT:
Unpublished Work. 1979.

65. C.H. LERCHENTHAL:
Bonded steel reinforcement for concrete slabs.
RILEM Symposium, Synthetic Resins in Building Construction, Paris 1967, pp 165-173.

66. R. CIRODDE:
Techniques of glued assembly.
RILEM Symposium, Synthetic Resins in Building Construction, Paris 1967, pp 47-59.

67. C.J. FLEMING and G.E.M. KING:
The development of structural adhesives for three original uses in South Africa.
RILEM Symposium, Synthetic Resins in Building Construction, Paris 1967.

68. S. KAIFASZ:
Concrete beams with external reinforcement bonded by glueing - preliminary investigation.
RILEM Symposium, Synthetic Resins in Building Construction, Paris 1967.

69. M. LADNER:
Field measurement on subsequently strengthened concrete slabs.
ACI Special Publication, SP 55, 1978, pp 481-492.

70. S.K. SOLOMON and L.K. GOPALANI:
Flexural tests on concrete beams externally reinforced by steel sheet.
The Indian Concrete Journal, Volume 53, No. 9, September 1979, pp 249-253.

71. A. BOUDERBALAH:
Strengthening of existing concrete beams by the use of glued steel plates.
M. Eng. dissertation, University of Sheffield, September 1978.

72. T. ANG:
The strengthening of reinforced concrete beams using glued steel plates.
M. Eng. dissertation, University of Sheffield, September 1979.

73. R.N. SWAMY and R. JONES:
Unpublished work.

74. Plastics Engineering Handbook, 3rd Edition.
Reinhold, New York 1960.

75. A.O. KAEDING:
Structural use of polymers in concrete.
Proceedings Second International Congress on Polymers in Concrete.
University of Texas, Austin, October 1978, pp 9-23.

76. W.W. YU and G. WINTER:
Instantaneous and long-term deflections of reinforced concrete beams under working loads.
ACI Journal, Proceedings, Volume 57, No. 1, July 1960, pp 29-50.

77. D.E. BRANSON:
Instantaneous and time-dependent deflections of simple and continuous reinforced concrete beams.
Report No. 7, Part 1, Alabama Highway Research Bureau of Public Roads, August 1963, 78 pp.

78. Comité European du Beton
Recommendations for an international code of practice for reinforced concrete.
Cement and Concrete Association, 1964.

79. A.W. BEEBY and J.R. MILES:
Proposals for the control of deflection in the New Unified Code.
Concrete Journal, Volume 3, No. 3, March 1969, pp 101-110.

80. R.F. STEVENS:
Deflections of reinforced concrete beams.
Proceedings of ICE, Volume 53, September 1972, pp 207-224.

81. W.H. MACAULAY:
Note on the deflection of beams.
Messenger of Mathematics, Volume 48, 1919, p 129.

82. A.W. BEEBY:
A note on an aspect of the variability of deflections.
Cement and Concrete Association, paper for publication, April 1974, pp 1-16.

83. V.E. MURASHEV:
Theory of appearance and opening of cracks, computation of rigidity of reinforced concrete members.
Stroitelnaya Promishlenost (Moscow) 1940, p 11.

84. A.W. BEEBY:
Short term deformations of reinforced concrete members.
Cement and Concrete Association, Technical Report, TRA 408, London, March 1968.

85. Comité European du Beton (CEB)
International recommendations for the design on construction of concrete structures.
Cement and Concrete Association 1970, pp 1-80.

86. CP110. The structural use of concrete.
British Standards Institution, London 1972.

87. H.A. SAWYER:
Elastic-plastic design of single span beams and frames.
American Society of Civil Engineers, Proceedings, Volume 81, Dec. 1955, pp 1-29.

88. A.L.L. BAKER:
The Ultimate Load Theory - applied to the design of reinforced and prestressed concrete frames.
Concrete Publications, London 1956.

89. P. GERGELY and L.A. LUTZ:
Maximum crack width in reinforced concrete flexural members.
Proceedings of the Symposium of Causes, Mechanism and Control of Cracking in Concrete.
American Concrete Institute, SP 20, Detroit 1968, pp 87-117

90. J.M. ILLSTON and R.F. STEVENS:
Internal Cracking in Reinforced Concrete.
Concrete Journal, Volume 7, July 1972, pp 28-31.

91. G.D. BASE et al:
An investigation of the crack control characteristics of various types of bars in reinforced concrete.
Cement and Concrete Association, Report No. 18, Parts 1 and 2, Dec. 1966, 44, 32 pp.

92. A.W. BEEBY:
Suggested recommendations to the crack prediction formula in the 1970 CEB Recommendations.
CEB Bulletin D'Information, March 1973.

93. B.B. BROMS:
Crack width and crack spacing in reinforced concrete members.
American Concrete Institute Journal, Volume 62, No. 10, Oct. 1965, pp 1230-1246.

94. E. HOGNESTAD:
High strength bars as concrete reinforcement, Part 2, control of flexural cracking.
Journal of the PCA Research and Development Labs., Volume 5, No. 1, Jan. 1963, pp 15-38.

95. J. FERRY-BORGES:
Cracking and deformability of reinforced concrete beams.
Publications, Association International des Ponts et Charpentes, 26, 1966.

96. A.P. CLARK:
Cracking in reinforced concrete flexural members.
ACI Journal, Proceedings, Volume 52, No. 8, April 1956, pp 851-862.

97. A.W. BEEBY:
A study of cracking in reinforced concrete members, subjected to pure tension.
Cement and Concrete Association Technical Report No. 42,468, June 1972, 24 pp

98. A.H. MATTOCK:
The strength of singly reinforced beams in bending.
Session B, Paper 1, Symposium on the Strength of Concrete Structures.
Cement and Concrete Association, London 1956, pp 77-100.